FIELD AND LABORATORY PERFORMANCE EVALUATION OF SPREAD FOOTINGS

FINAL REPORT

OHIO DEPARTMENT OF TRANSPORTATION and
FEDERAL HIGHWAY ADMINISTRATION

Principal Investigators:
Shad M. Sargand
Glenn A. Hazen

Project Research Engineer:
Teruhisa Masada

OHIO RESEARCH INSTITUTE FOR TRANSPORTATION AND THE ENVIRONMENT
CIVIL ENGINEERING DEPARTMENT
OHIO UNIVERSITY

February 1999

1. Report No.	2. Government Accession No.	3. Recipient's Catalog No.
FHWA/OH-98/017		

4. Title and Subtitle	5. Report Date
FIELD AND LABORATORY PERFORMANCE EVALUATION OF SPREAD FOOTINGS	December, 1997
	6. Performing Organization Code
	8. Performing Organization Report No.
7. Author(s)	10. Work Unit No. (TRAIS)
Shad M. Sargand, Glenn A. Hazen	
9. Performing Organization Name and Address	11. Contract or Grant No.
Ohio University Department of Civil Engineering Athens, OH 45701	State Job No. 14457(0)
	13. Type of Report and Period Covered
	Final Report
12. Sponsoring Agency Name and Address	14. Sponsoring Agency Code
Ohio Department of Transportation 25 S. Front St. Columbus, OH 43215	

15. Supplementary Notes

Prepared in cooperation with the U.S. Department of Transportation, Federal Highway Administration

16. Abstract

The performance of five highway bridge structures, located in Ohio and supported by spread footings on cohesionless soils or cohesive soils, was monitored in the field throughout construction and under service conditions. The performance of these structures was also examined through centrifuge modeling in the laboratory. Factors used in evaluating these bridges were overall settlement, tilting of abutment walls/pier columns, and pressure distribution under the footings. Field and experimental measurements were then compared against estimates made by selected geotechnical methods.

None of the spread footings in these five bridge structures experienced an average settlement of more than two inches prior to service load application. Contact pressure monitored at the footing/bearing soil interface in the field remained less than 2.9 tsf (40 psi) and was generally close to the theoretical estimate. Poorer agreement resulted between the measured and predicted abutment wall tilting. None of the six geotechnical methods for predicting settlement of footings on cohesionless soils was accurate in all cases. The method proposed by Hough appeared to be the best. Standard methods used to estimate immediate and time dependent consolidation settlements were reasonably accurate when compared to field data. Centrifuge testing techniques provided settlement results superior to those predicted by any of the six geotechnical methods. One limitation of centrifuge testing, however, is the simulation of complex subsurface conditions in the laboratory.

17. Key Words	18. Distribution Statement
spread footing; field performance; settlement; tilting; highway bridge; laboratory modeling; contact pressure	No Restrictions. This document is available to the public through the National Technical Information Service, Springfield, Virginia 22161

19. Security Classif. (of this report)	20. Security Classif. (of this page)	21. No. of Pages	22. Price
Unclassified	Unclassified		

ACKNOWLEDGMENTS

This investigation was sponsored by the Federal Highway Administration (FHWA) and the Ohio Department of Transportation (ODOT). The authors express their appreciation to Richard L. Engel of ODOT for his assistance and guidance throughout the study. The authors are also grateful to Baimin Mao, Ram Yalamanchili, Sedtha Mahasantipiya, and Chatchawahn Payoongwong for providing valuable assistance both in the field and in the laboratory.

Table of Contents

List of Tables

List of Figures

Chapter 1

Introduction

1.1 General Statement

Traditionally, highway bridge structures have been supported by one of two conservative foundation types to assure their long term serviceability: (1) shallow spread footings on bedrock, and (2) pile foundations that rely on end bearing. Type (1) is applicable only at sites where the depth to bedrock is very limited. Since such sites are not commonly encountered, type (2) is frequently specified for bridge construction. Pile foundations have a lower maintenance cost, although their initial costs are higher than those for spread footings. The selection of a foundation type depends upon the design loads, subsurface exploration data, predicted settlement and other behavior, and the relative cost associated with each type. Given that a few foundation types satisfy all of the design considerations, bridge design engineers obviously select the most economical option. Being the most basic (or the simplest) foundation type, the spread footing usually costs less than the other types (deep foundations) at the time of construction. Long term maintenance costs are difficult to estimate in most cases.

With the recent trend within government to reduce expenditures and the need to maintain an aging infrastructure, the use of shallow depth spread footings on soils has become worth considering for bridges where subsoil conditions are suitable and scouring is not a problem. For example, sites consisting largely of granular (non-plastic) soils may be good candidates for utilizing spread footings since granular soils tend to deform almost instantaneously with little time-dependent movement. Sites consisting of stiff, over-consolidated cohesive soils may also be suitable for the spread footing use. In order to justify such alternatives, a detailed collection of case histories must be established

to gain more experience and confidence. The understanding of settlement and other behaviors of spread footing foundations under various loading and environmental conditions, supplemented by comprehensive field and laboratory studies, are essential in encouraging their use in highway bridge structures. Currently, there is a severe lack of published data on the field performance of spread footing foundations for highway bridges.

There are geotechnical formulas, based on theories and empirical observations, available for the assessment of bearing capacity, settlement, and tilting of spread footings. However, the validity of these formulas has not been fully examined in light of actual field experience. Bridge designers tend to select more conservative pile foundations because of a lack of confidence in these formulas. Further verification of the equations should contribute to an increased use of spread footing foundations.

In the field of geotechnical engineering and related fields, the centrifuge modeling technique has been applied to a wide variety of topics such as slope stability, performance of footings and piles, seepage flow, and solute transport. Laboratory results obtained with this equipment have been quite valuable in understanding and predicting performance observed in the field.

This report presents findings recently made by researchers at Ohio University on the field and laboratory performance of five highway bridges with spread footing foundations for the Ohio Department of Transportation and the Federal Highway Administration.

1.2 Objectives of Research

The objectives of the current investigation were as follows:

- To develop a comprehensive instrumentation plan for monitoring the field performance of

spread footing foundations for highway bridges.

- To instrument spread footing foundations at five highway bridge construction sites. To monitor field performance of the bridge foundations frequently during construction stages and under service load application. Present all the data in a manner that is consistent with the data base requirements of FHWA and ODOT.
- To perform laboratory simulated model studies of the spread footing foundations in the centrifuge environment.
- To examine reliability of selected empirical design equations available in the literature for estimating average vertical settlement by comparing them with the field observations and measurements.

1.3 Outline of Research

Chapter 2 is devoted to a review of relevant literature. First, the current state of the use of shallow foundation (spread footings) in highway bridge construction is discussed. Then, the historical development of a variety of settlement prediction methods is traced for spread footings on cohesionless soil. For spread footings on cohesive soils, available methods are briefly summarized. Results from a limited number of case histories are summarized with some discussion on past accomplishments in the area of laboratory studies, focusing on the centrifuge modeling technique.

Chapter 3 describes in detail information regarding the bridge structure, spread footing foundation, and general subsurface condition encountered at each of the five project sites in Ohio. This chapter also presents a description of the field instrumentation methods and actual construction sequences/practices observed in the field, as well as basic laboratory test results on representative

soil samples recovered from each site.

Chapter 4 reports and discusses the field measured performance of spread footings at the five bridge project sites. Data are presented in terms of overall settlement differential settlement, magnitude and distribution of contact pressure at the footing/bearing soil interface, degree of tilting of abutment walls/pier columns, and other measurements taken throughout different construction stages and under service load conditions.

Chapter 5 presents a brief description of commonly used empirical and semi-empirical geotechnical design formulas for estimating the settlement and bearing capacity of spread footing foundations. Predictions from these formulas are compared to the actual performance of the spread footings measured at each site, and qualitative discussions on the validity or accuracy of the empirical methods are drawn.

Chapter 6 deals with the centrifuge modeling technique. After the background of centrifuge modeling is presented, a detailed description of the laboratory method developed specifically for simulating the field behavior of spread footings is provided. The second section of this chapter reports results of the laboratory centrifuge modeling tests for each site. Discussions are developed by comparing the centrifuge modeling results to actual field measurements and predictions of selected empirical formulas.

Finally, Chapter 7 provides a summary of the project and conclusions drawn from all laboratory and field observations. Recommendations and possible items for implementation are presented to understand and promote the use of spread footing foundations where applicable.

Chapter 2

Review of Relevant Literature

2.1 Introduction

Wahls (1) prepared a synthesis report on the state of shallow foundation use for highway structures for the Transportation Research Board in 1983. He reported that shallow foundations on soil had been used successfully for highway bridges in only a few states. For example, in Washington, more than 30 bridges were constructed with one or more abutments or piers supported on shallow spread footings per year. New York and Connecticut were the other states which utilized shallow foundations. Despite the success in these few states, there still exists a reluctance to utilize spread footings for highway bridges elsewhere. Often, spread footings are only considered if they can be placed on bedrock. He attributed this negative trend to four sources - (1) AASHTO bridge specifications; (2) severe restrictions on the tolerable movement designated by bridge engineers; (3) a general view that predicted performance of spread footings on soil involves less reliability; and (4) a lack of comprehensive data for successful cases in other geographical areas. The AASHTO specifications state that "piling shall be considered when footings cannot, at reasonable expense, be founded on rock or other solid foundation material". There have been no AASHTO guidelines on the tolerable movement of bridges supported by spread footings. However, performance limits are generally accepted to be a maximum 1 inch differential settlement and a 2 inch total settlement (1). Among various factors which influence the accuracy of the performance prediction models, the properties of subsurface soils may bring the largest source of uncertainty. Adequate evaluation of subsurface conditions is a key in enhancing the reliability of performance prediction models.

2.2 Spread Footings on Cohesionless Soils

A footing resting on cohesionless soil settles immediately under load, due to volume change and distortion in the soil. There have been a number of investigations on the assessment of spread footing behavior on cohesionless soils. Several analytical and empirical methods of predicting settlement and bearing capacity using Standard Penetration Test (SPT) or Cone Penetration Test (CPT) data are discussed briefly in the following paragraphs.

The settlement of foundations on cohesionless soil was studied by Terzaghi and Peck (2). They proposed a formula based on the interpretation of data from plate loading tests and field observed settlement. They identified the relationship between settlement and the density variations of the subsoil and recommended extensive plate load tests if erratic variations of density of soil were observed. They provided a design chart for estimating allowable soil pressure for footings on sand based on Standard Penetration Tests (SPT).

Peck, Hanson and Thornburn (3) published a set of empirical design charts which provide allowable maximum bearing stress to induce a 1 inch settlement of shallow footings on sand under a wide range of the SPT-N values. They also presented a formula to correct the SPT-N values for cases in which the soil is a fine sand with some silt and located below the groundwater table. Their findings were based on the original Terzaghi and Peck method.

Hough (4) proposed a method of predicting footing settlement similar to the method used for estimating consolidation settlement of clay. He used an empirical relationship to correlate the bearing capacity index to the SPT-N value corrected for overburden pressure.

Alpin (5) studied the settlement equation proposed by Terzaghi and Peck (2) and attempted to correlate the SPT-N value with the settlement of a loaded footing area of one square foot. He

implemented the concept of "Modulus of subsurface reaction" to the equation and modified the SPT-N value for overburden pressure as suggested by Gibbs and Holtz (6).

DeBeer (7) studied the estimation of settlement of footings on sand by a semi-empirical method based on results obtained from Cone Penetration Tests (CPT). In this method, an empirical relationship between the compressibility and cone resistance was used. He concluded that methods based on CPT were more reliable than methods based on SPT test results.

Meyerhof (8) reviewed both Terzaghi and Peck, and DeBeer methods of calculating the settlement of footings. He compared predicted values with experimental results and supported the view that both methods yield rather conservative estimates of settlement and corresponding bearing pressure. Further, he concluded that the allowable bearing pressure could be increased by as much as 50%. In his study, he assumed that the effect of water table is represented in the SPT-N values and, therefore, did not use a correction factor for this parameter.

Peck and Bazaraa (9) concluded from settlement measurements of field tests that the Terzaghi and Peck method is too conservative. Three modifications were proposed: 1) use the Gibbs and Holtz method to correct SPT-N values; 2) adjust the allowable pressure by 50%, 3) ignore the groundwater table. Subsequently, Bazaraa (10) developed a relation from field data to correct the SPT-N values for the effect of overburden pressure.

D'Appolonia, et al., (11) obtained settlement data from about 300 spread footings on fine dune sand and compared the data statistically with available settlement methods. He estimated settlement based on SPT data, plate load test data, and laboratory (triaxial and odometer) test results, using available geotechnical techniques. Subsequently, D'Appolonia and his associates (12) proposed a method to calculate settlement based on elastic theory assuming linear, homogeneous,

and isotropic material. In this method, the modulus of compressibility was determined from SPT values.

Schmertmann (13) proposed a procedure based on linear, elastic, half-space theory. The method is simple and may be computed in the field. The static cone bearing capacity profile was correlated to the elastic modulus of sand. The distribution of the strain influence factor was approximated to a triangular shape. Results were shown to be accurate in a variety of situations.

Leonards and Frost (14) suggested an improvement to the Schmertmann method by incorporating the effect of over-consolidation in reducing the compressibility of soils.

Oweis (15) presented an elastic model based on results of plate load tests at locations where SPT-N values were known. Predicted settlement showed good accuracy when compared to the recorded values. However, he suggested further review of the method with additional case histories to confirm its validity.

Burland and Burbridge (16) established an empirical relationship among average SPT blow count, width of footing, and modulus of subgrade compressibility, through regression analyses of more than 200 settlement cases of spread footing foundation on sand.

Bowles (17) used the Boussinesq stress profile to calculate foundation settlement by adjusting the settlement influence factors as computed by Steinbrennmer (18). A reduced influence depth was incorporated and empirical relations were obtained for the elastic modulus.

2.3 Spread Footings on Clay

The settlement of spread footings on cohesive soil is more complicated than that on cohesionless soil. However, a review of available literature reveals that procedures to predict

settlement have been relatively standardized in this case. Immediate settlement, which takes place upon load application, is a result of volume reduction and distortion in unsaturated clays and a result of distortion only in saturated clays. Elastic theory can be applied to estimate immediate settlement. Consolidation settlement, which takes place gradually over time, is due to consolidation of clay and involves plastic deformation accompanied by dissipation of excess pore water pressure. Theory developed by Terzaghi (2) is applied to predict consolidation settlement. It is essential that laboratory tests are performed on high-quality soil specimens to derive soil properties necessary for proper application of the theory.

2.4 Field Surveys

Keene (19) studied seven case histories of spread footing uses in Connecticut in identifying major factors that influence movement. Some cases showed post-construction settlement of 2 to 3 inches without any damage to the bridge structures. He stressed the importance of "staged" construction, in which footings are allowed to settle under the load of approach embankment prior to placement of the superstructure.

Walkinshaw (20) reviewed field performance data on 35 bridges supported by spread footings in the western states. He stated that poor riding quality resulted when vertical settlement exceeded 2.5 inches.

Grover (21) made the following conclusions based on a review of 80 bridges in Ohio:

Abutment settlement	= less than 1 inch	Tolerable.
	= 2 to 3 inches	Noticeable to drivers, but not severe enough to cause structural damage.
	= more than 4 inches	Objectionable to drivers and severe enough to cause structural damage.

Bozozuk (22) examined the 1975 survey data obtained by TRB Committee A2K03. He realized that equally large movements were reported also for bridges supported on piles. He plotted the survey data for both the spread footings and deep foundations. According to these figures, tolerable movements are set at 3.9 inches (or 100 mm) (vertical) and 2 inches (or 50 mm) (horizontal) for all types of bridges, including those on spread footings, friction piles, and end-bearing piles.

There has been a recent comprehensive field study by Gifford, et al., (23) on a long term study of the settlement of 21 bridge spread footings constructed on cohesionless soils. In this report, available methods of settlement estimations were extensively documented. Authors selected five methods for predicting settlement and compared the results with the field observations. Recommendations for the design were provided based on the findings. In their study, tilting of the abutments and contact pressure under the footings were also measured in addition to the settlement.

DiMillio (24) surveyed the condition of 148 highway bridges supported by spread footings on compacted fill in the state of Washington. His inspection included the structural condition of the bridges and the approach pavements. All bridges inspected were in good condition and none exhibited any safety or serious functional problems. He also investigated 28 selected bridges in detail for foundation movement and found that the bridges could easily tolerate differential settlement of 1 to 3 inches without serious distress. He estimated through cost analyses that spread footings were 50 to 60% less expensive than pile foundations.

The tolerable movement of bridges was extensively studied by Moulton, et al., (25). He reviewed data on movements and damages for 204 bridges on both spread footings and pilings. This study revealed that the average vertical movement of abutments was in excess of 4 inches, regardless

of the foundation type, and the average horizontal movement was larger than 2.5 inches. Out of 171 bridges for which damage reports were filed, only 63 actually experienced intolerable movements. Based on these findings, a set of tolerable movement criteria was established for vertical and horizontal movements, and angular distortion.

Baus (26) monitored the settlement of 12 spread footings at 3 highway bridge construction sites in South Carolina. Data were collected during construction and the first several months under traffic loading. The amount of overall settlement varied from 0.38 to 2.15 inches, while the estimated total load varied from 495 to 678 kips. Maximum settlement measured in the field was compared to predictions from six geotechnical methods (Alpin, Hough, Meyerhof, Peck and Bazaraa, Buismann and DeBeer, and Schmertmann) for each footing. He concluded that the Peck and Bazaraa method provided the best settlement predictions.

2.5 Laboratory Investigations

In geotechnical engineering, the use of centrifuge modeling has increased rapidly over the last three decades, because of its simplicity and unique ability to closely simulate the actual prototype structure. The concept of centrifuge modeling has been applied to a wide range of subjects such as stability of soil structures, forces on piles, responses of soil structures to dynamic loading, measurement of hydraulic conductivity of soils, and solute transport in soils. However, a very limited number of centrifuge model studies have been reported for spread footing structures on cohesionless soil. Gemperline (27) carried out a series of simulated model tests of shallow spread footing foundations for load-displacement behavior. He analyzed single and coupled effects of variables on the load-displacement response and maximum bearing pressure. His model tests

showed that coupled effects were substantial when predicting settlement.

Ovesen (28) conducted a series of bearing capacity tests of circular footings on sand with a centrifuge device. After examining load-settlement data from three (30G, 51G, and 79G) models and similar test results obtained by other researchers, he observed that the centrifuge models built to the length scale of $(1/n_1)$ and $(1/n_2)$ yield the same bearing capacity behavior for the case where $1 \leq (n_1/n_2) \leq 3$.

Cenepa, et al., (29) briefly presented a case study of field and centrifuge model test results on square footings on sand. They stated that a good agreement was obtained between the field and model test results for load-settlement curves, creep rates, and ultimate bearing pressures. Pu and Ko (30) reported a study in which centrifuge experimental determinations were made on bearing capacity of spread footings on sand. Fujii, et al., (31) attempted centrifuge model tests to make a direct comparison with large scale field loading tests on a footing with an uneven base on a slope. They observed a remarkable agreement between the model test and field test results in terms of ultimate bearing capacity. Disturbance of the soil samples was responsible for the less remarkable agreement on settlement.

Chapter 3

Descriptions of Subgrade Conditions, Bridge Structures, and Field Instrumentation

3.1 General

In this study, a total of five highway bridge structures, supported by spread footings, were instrumented and monitored during construction and under service loads. These structures were built in different regions in Ohio as part of a major highway construction project or as a replacement for an old deteriorating structure. Table 3.1 lists the location and basic design parameters for these bridge structures. Subsurface conditions encountered at each site are summarized in Table 3.2. Tables 3.3 and 3.4 summarize the construction history and overall instrumentation plan (summarized in Figure 3.1) for each bridge structure, respectively.

3.2 Performance Criteria and Field Instrumentation Methods

In this investigation, four parameters were used to evaluate the field performance of the selected bridge structures. They were overall average settlement, differential settlement, tilting/overturning of the abutment walls and pier columns, and magnitude and distribution of the contact pressure at the base of the footings. The same parameters were used to evaluate the use of spread footings in a previous study by Gifford, et al., (23).

Overall settlement was typically monitored at a minimum of two locations on each foundation, as shown in Figure 3.2. For rectangular pier foundations, the settlement point was established either near the center or near each of the four corners. Monitoring points were installed into the footing when concrete was placed during construction (See Figure 3.3). As soon as the

Table 3.1 Design Parameters of Five Bridge Structures

Item	Bridge A	Bridge B	Bridge C	Bridge D	Bridge E
No. of Spans	One	Two	One	Six	Nine
Max. Span Length (ft.)	61.86	124.	22.0	76.33	86.17
Combined Area of Spread Footings ($ft.^2$)	4,984 (divided over 6 panel sections)	1,952 (divided over 3 footings)	389 (divided over 2 footings)	2,528 (divided over 10 footings)	3,633 (divided over 16 footings)
Width of Footing	12.0 - 16.0	16.75	4.0	7.5 - 10.5	11.0 - 15.0
Thickness of Footing	3.0 - 3.25	3.25 - 3.5	2.0	2.5	3.0 - 3.25
Keyway Construction	Yes	Yes	No.	No.	Yes @ abut.
Height of Abutment Wall (ft.)	15.3	16.0 - 17.6	10.0	4 - 5	16.5 - 26.9
Width of Bridge Deck (ft.)	130.0	57.2	N/A	72.0	52.0
Superstructure : Beams Concrete	 3.66 kips/ft. 7.11 kips/ft.	 2.91 kips/ft. 9.87 kips/ft.	N/A (25" of soil and pavement layers above culvert)	 12.9 kips/ft. 8.63 kips/ft.	 12.0 kips/ft. 4.0 kips/ft.
Projected ADT (Year)	81,324 (2004)	9,065 (2010)	8,300 (2010)	20,531 (2012)	47,189 (2011)

(Notes) 1. Bridge C = Three-Sided, Flat-Topped, Concrete Box Culvert.
2. Bridge D information presented here is for the portions that were constructed entirely new from the foundation to the deck.
3. Bridge D construction includes two abutments supported by piles.

Table 3.2 Summary of Typical Subsurface Conditions Encountered

Item \ Structure	Bridge A	Bridge B	Bridge C	Bridge D	Bridge E
No. of Soil Borings	5	2	2	11	10
Dominant Soil Types Encountered	A - 2 - 4 A - 4 a, 4b	A - 4 a A - 6 a	A - 4 a, 4b	A - 6a, 6b A - 4 a	A - 6a, 6b A - 7- 6
Depth to Bedrock (ft.)	Not Rechached within 42.5 ft.	Not Rechached within 28.0 ft.	Not Rechached within 45.5 ft.	0.0 - 20.0 ft. below Bottom of Footings.	Varied from 10.0 ft. (Rear Abutment) to More Than 80 ft. (Forward Abutment).
Depth to Groundwater Table (ft.)	Not Rechached within 42.5 ft.	Not Rechached within 28.0 ft.	6.3 ft. above Bottom of Footings.	Not Found before Reaching Bedrock	Not Found before Reaching Bedrock
Plasticity Index (PI) : - Range - Average	2 - 15 4	3 - 18 7	NP NP	8 - 21 14	4 - 30 17
SPT-N Value (blows/ft.) * Typical Data	11 @ 0' Depth	49 @ 0' Depth	14 @ 0' Depth	37 @ 0' Depth	13 @ 0' Depth
	18 @ 10' Depth	50 @ 5' Depth	20 @ 10' Depth	36 @ 5' Depth	31 @ 10' Depth
	100+ @ 20' Depth	67 @ 10' Depth	11 @ 20' Depth	24 @ 10' Depth	30 @ 20' Depth
	100+ @ 30' Depth	45 @ 10' Depth	21 @ 30' Depth	38 @ 15' Depth	30 @ 30' Depth

(Notes) 1. Depth to Bedrock = Measured from the bottom of the footings.
2. Depth to Groundwater Table = Measured from the bottom of the footings.
3. "NP" = Soil Non-plastic.
4. SPT-N Values = Presented in terms of the depths below the bottom of the footings.

Table 3.3 Summary of Construction Records

Stages \ Structure	Bridge A	Bridge B	Bridge C	Bridge D	Bridge E
Start Bridge Construction Work	12 - 06 - 89	10 - 11 - 90	10 - 16 - 91	6 - 04 - 93	3 - 13 - 94
Finish Construction of Footings	1 - 31 - 90	12 - 13 - 90	10 - 24 - 91	7 - 29 - 93	4 - 5 - 94 (I) 9 - 18 - 94 (II)
Finish Construction of Abutment Walls, Pier Columns & Caps (or Place Box Culverts)	3 - 03 - 90	1 - 28 - 91	11 - 08 - 91	8 - 16 - 93 (I) 8 - 9 - 93 (II)	5 - 13 - 94 (I) 10 - 2 - 94 (II)
Finish Backfilling behind Abutments (or over Box Culvert)	5 - 18 - 90	5 - 10 - 91	11 - 24 - 91	8 - 30 - 93	6 - 22 - 94 (I) 11 - 6 - 94 (II)
Place Beams for Bridge Deck	3 - 26 - 90	2 - 13 - 91	N/A	9 - 17 - 93 (I) 10 - 20 - 93 (II)	7 - 1 - 94 (I) 11 - 6 - 94 (II)
Open Bridge to Live Loads	12 - 11 - 90	7 - 03 - 91	12 - 01 - 91	10 - 23 - 93 (I) 6 - 28 - 94 (II)	8 - 6 - 94 (I) 7 - 1 - 95 (II)

(Note) Roman numerals refer to applicable construction phase.

Table 3.4 Summary of Overall Field Instrumentations

Instrumentation \ Structure	Bridge A	Bridge B	Bridge C	Bridge D	Bridge E
No. of Settlement Monitoring Points: - Original	18	14	6	61	60
- Alternate	0	6	6	0	0
No. of Pressure Cells	6	0	2	19	20
No. of Tilting Measurement Locations	8	8	2	20	15
Others	2 Settlement Monitoring Stations for Footing Heel	N/A	N/A	N/A	Tilting of Column also Measured in Transeverse Direction.

(Notes) 1. Bridge C = Three-Sided, Flat-Topped, Concrete Box Culvert.
2. Bridge D information presented here is for the portions that were constructed entirely new from the foundation to the deck.
3. Bridge D construction includes two abutments supported by piles.

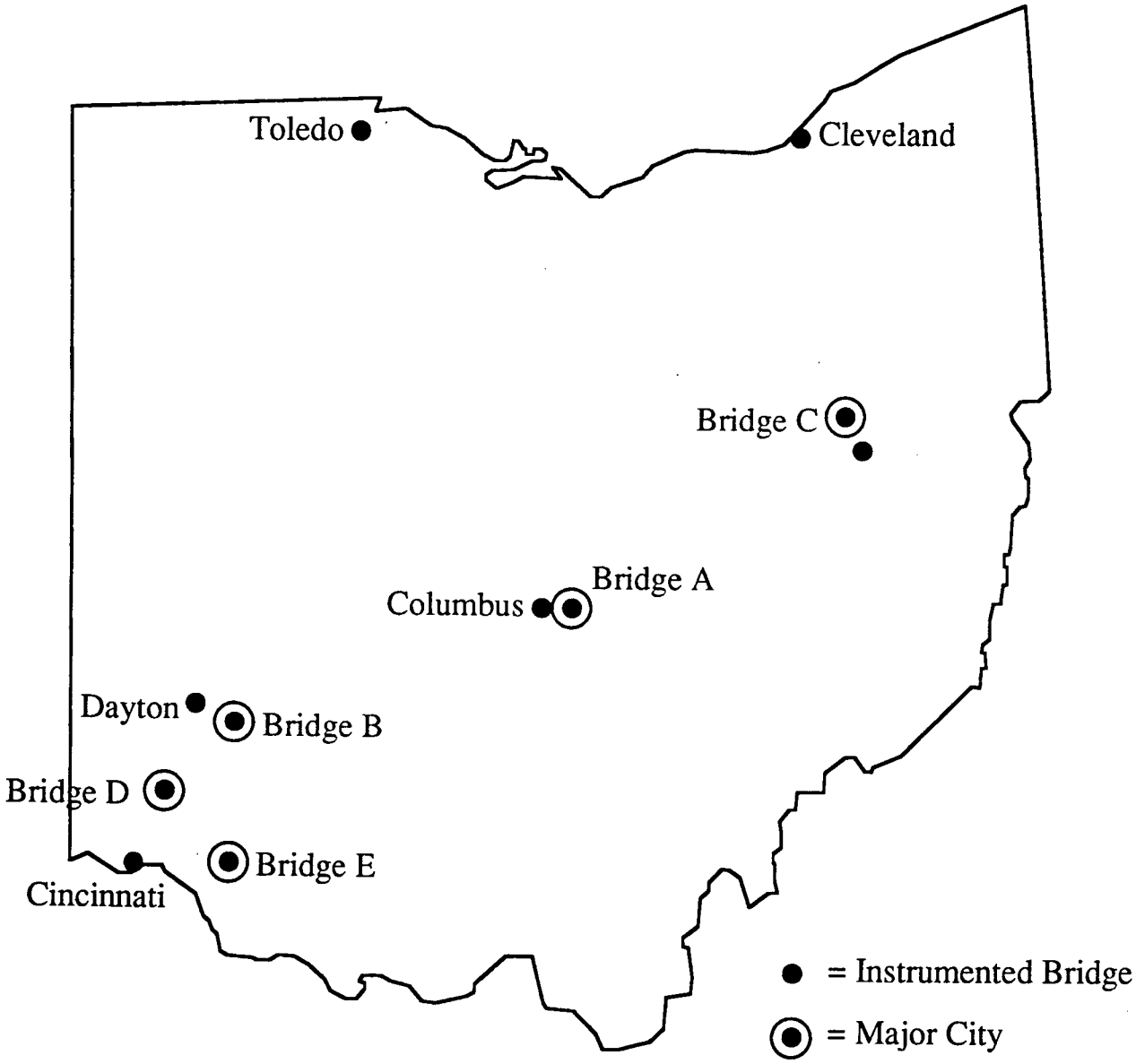

Figure 3.1 General Location of Five Spread Footing Supported Highway Bridges Instrumented and Monitored in Ohio

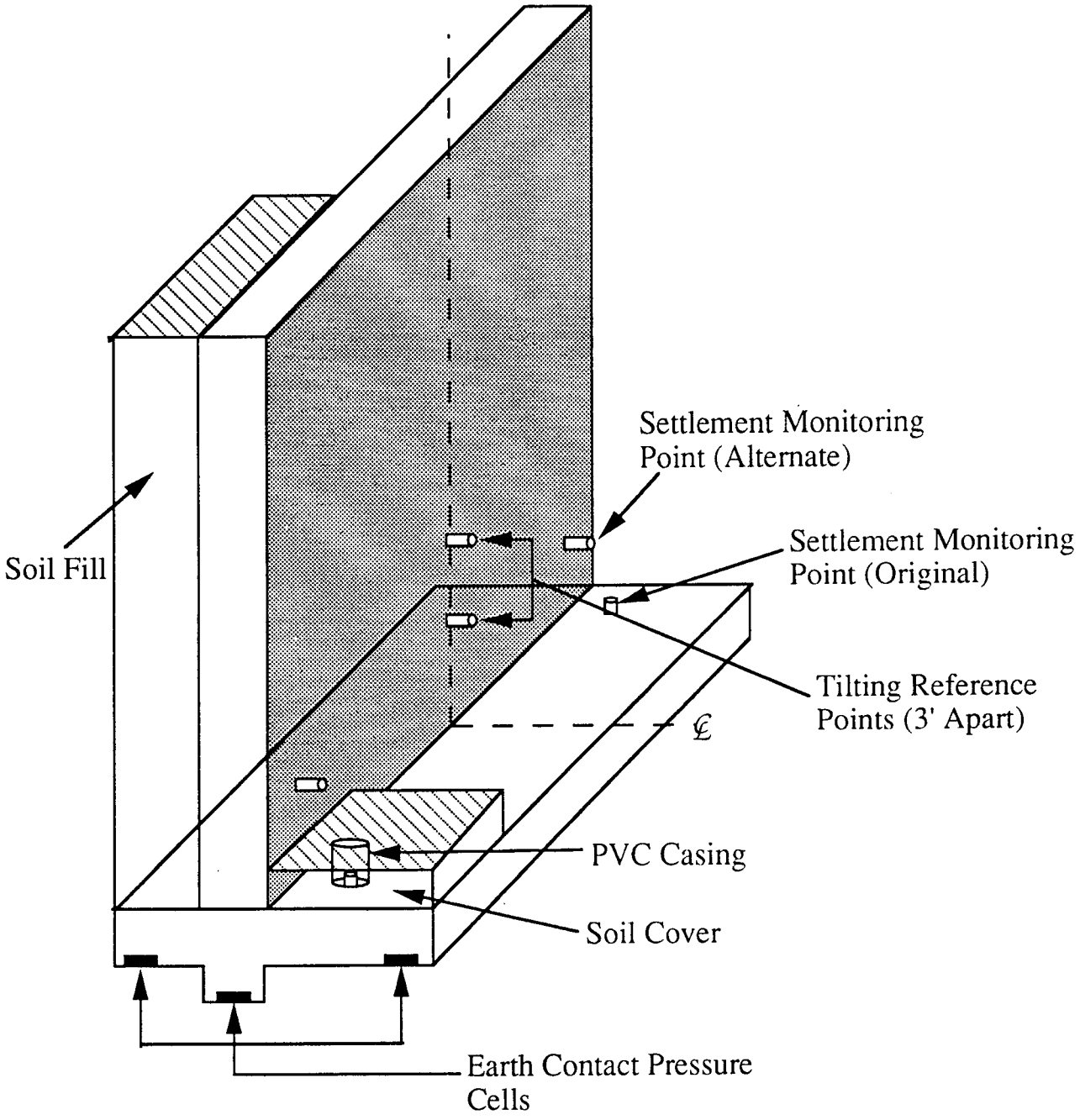

Figure 3.2 Basic Instrumentation Schemes for Highway Bridge Abutment Structure

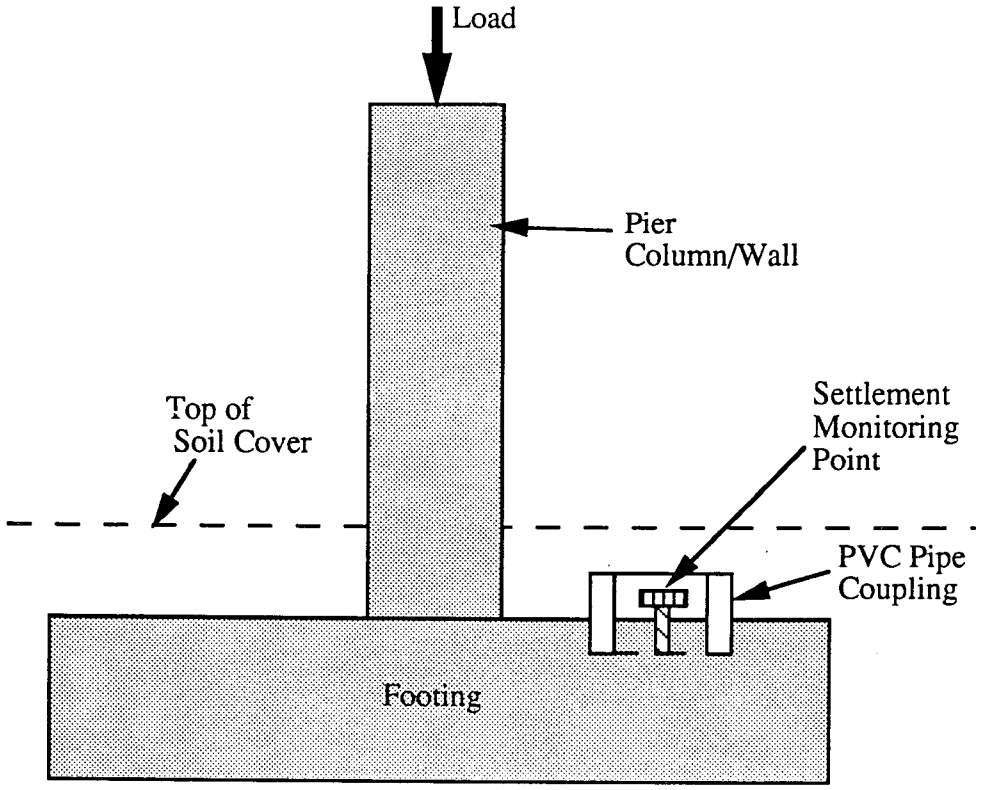

(a) General View of Settlement Reference Points Installation

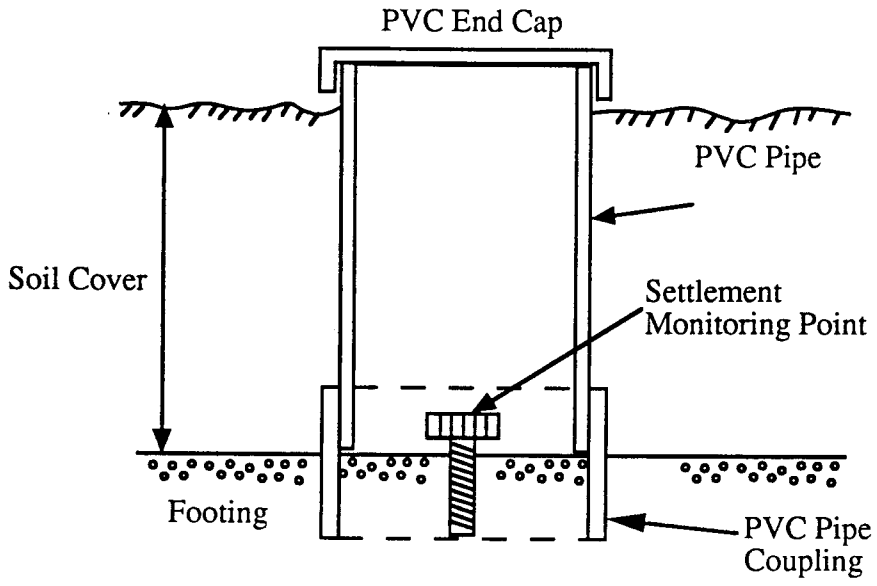

(b) Details of PVC Pipe Installation

Figure 3.3 Typical Settlement Monitoring Point Installation Details

footing concrete set over night, initial elevations were established at these monitoring points with reference to a few bench marks existing within the construction site. A Topcon AT-F2 auto level and a K&E level rod with a target were used to perform this conventional optical level surveying. Elevation changes were then monitored during the various stages of construction. Mathematically, settlement is expressed through,

$$S_i = 12 * (H_o - H_i) \qquad \text{Eq. (3.1)}$$

where S_i = settlement at the i-th construction increment (inches); H_o = initial elevation with reference to the bench mark elevation (feet); and H_i = elevation at the i-th construction increment with reference to the bench mark elevation (feet).

As construction progresses, the footing eventually will be covered with soil. In order to continue monitoring the settlement, one of two approaches was taken in the field (see Figures 3.2 and 3.3). In the first approach, which applied to relatively shallow final cover conditions, a 6 inch diameter PVC casing was installed at each monitoring point before placement of the soil cover to maintain direct access to the point. In an alternate approach for deep soil cover cases, a new monitoring point was installed on the abutment wall/pier column at a height slightly above the specified soil cover thickness and referenced to the original point. Once reliable survey data were established for each footing, differential settlement could be determined simply by taking the difference in the elevation readings among the monitoring points.

To monitor the contact pressure distribution at the footing/bearing soil interface, typically three pressure cells were installed across the base of the abutment foundation, as shown in Figures 3.2 and 3.4. For pier footings, one, two, or four pressure cells were installed underneath, depending

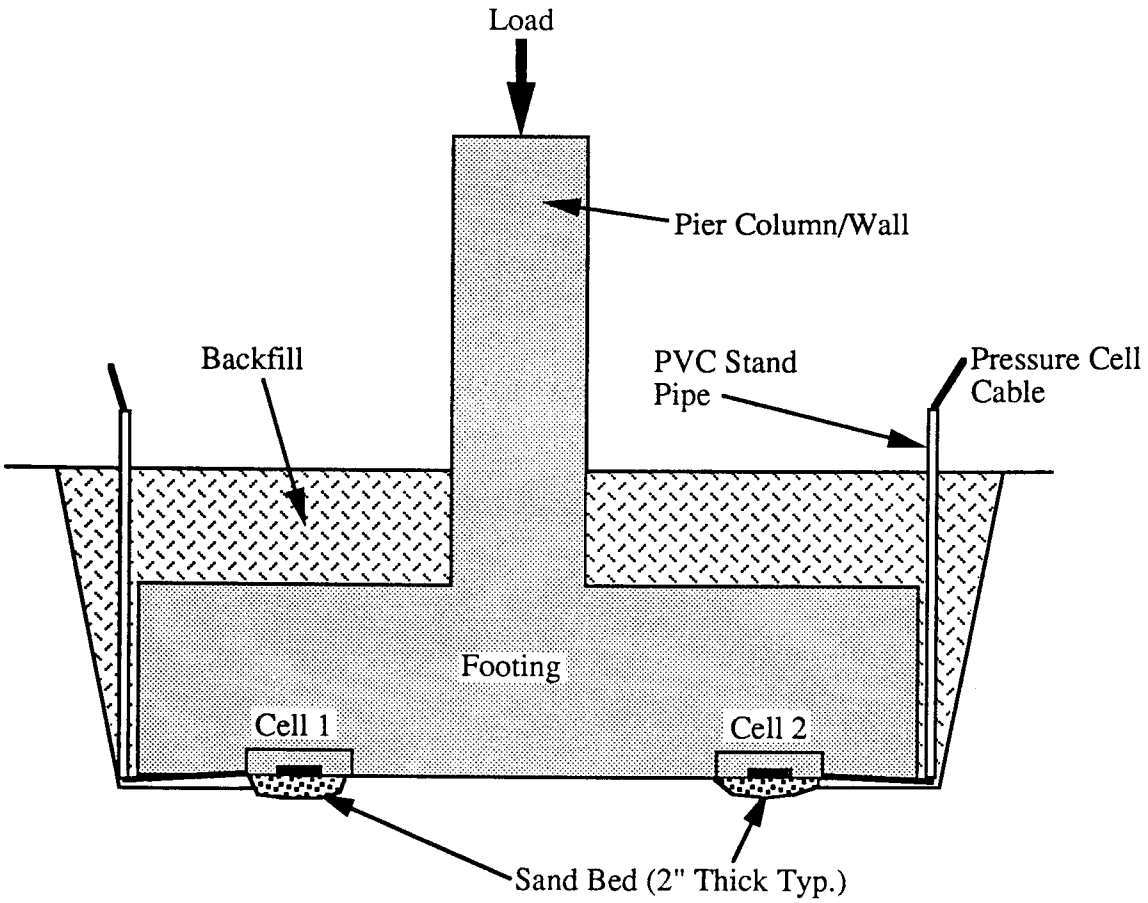

(a) General View of Pressure Cell Installation at Footing Base

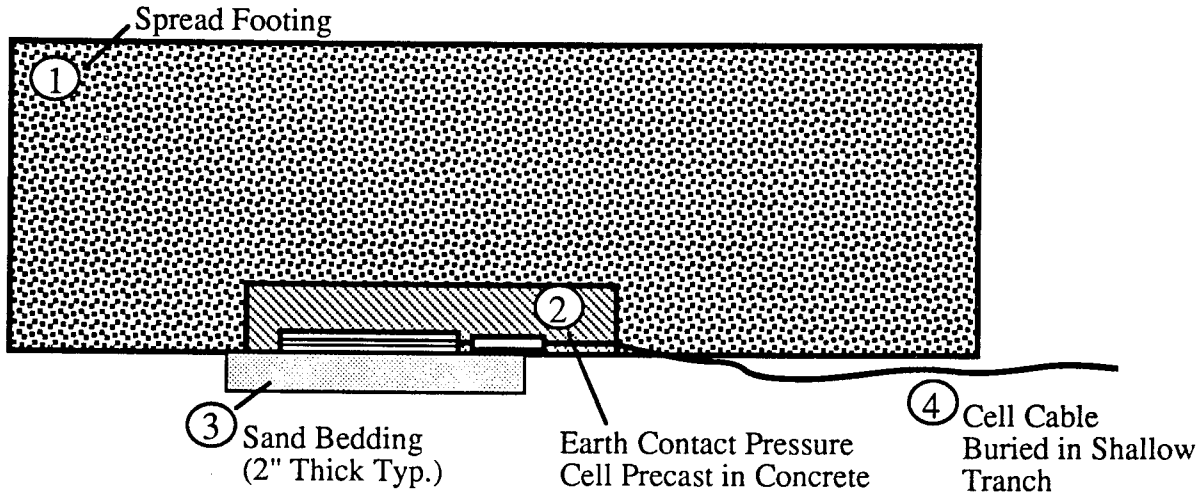

(b) Close-Up View of Pressure Cell Installation

Figure 3.4.(a) Typical Earth Contact Pressure Cell Installation Details at Pier Footing

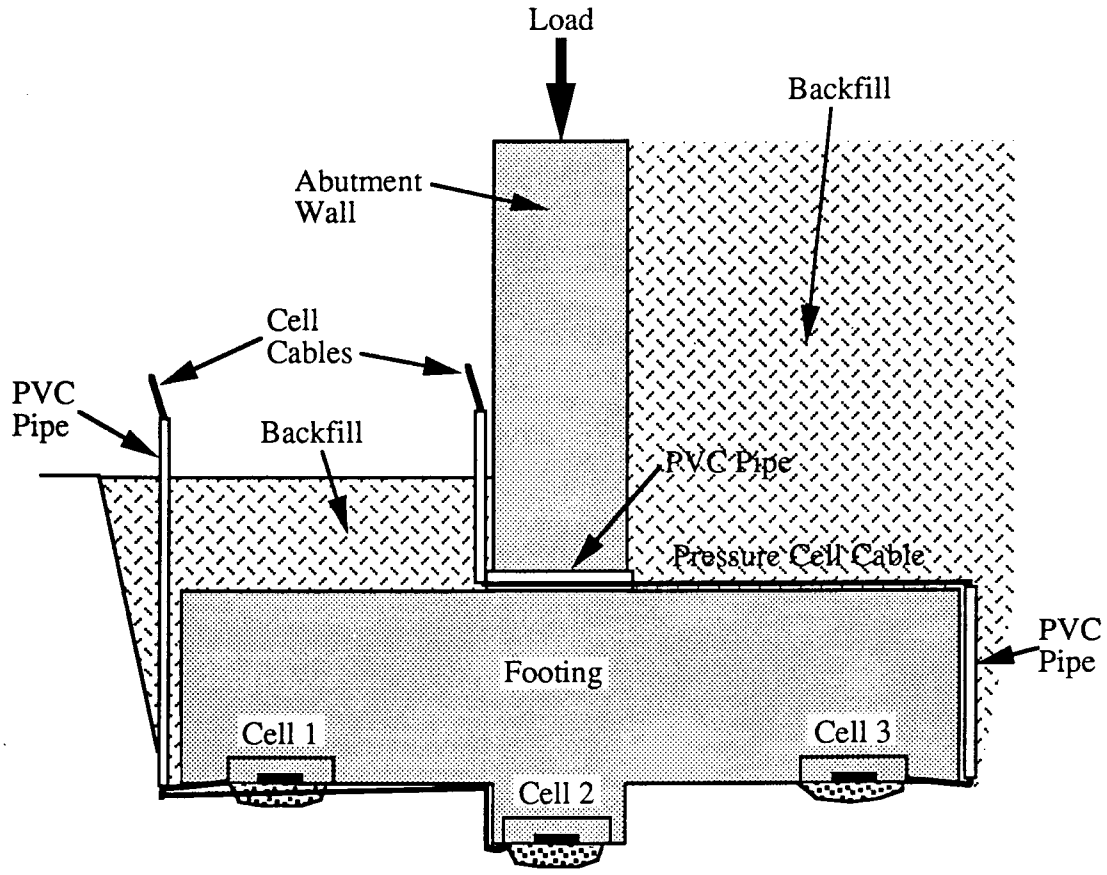

(c) Pressure Cell Installation at Phase I Abutment Foundation

Figure 3.4.(b) Typical Earth Contact Pressure Cell Installation Details at Abutment Structure

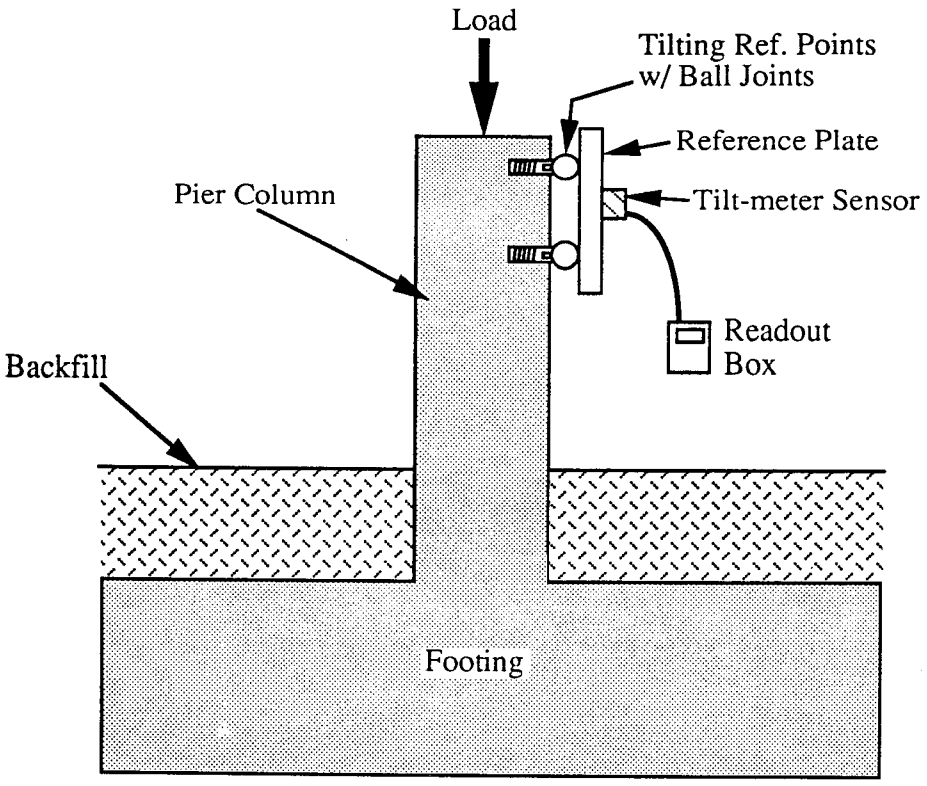

(a) General View of Tilting Measurement Station

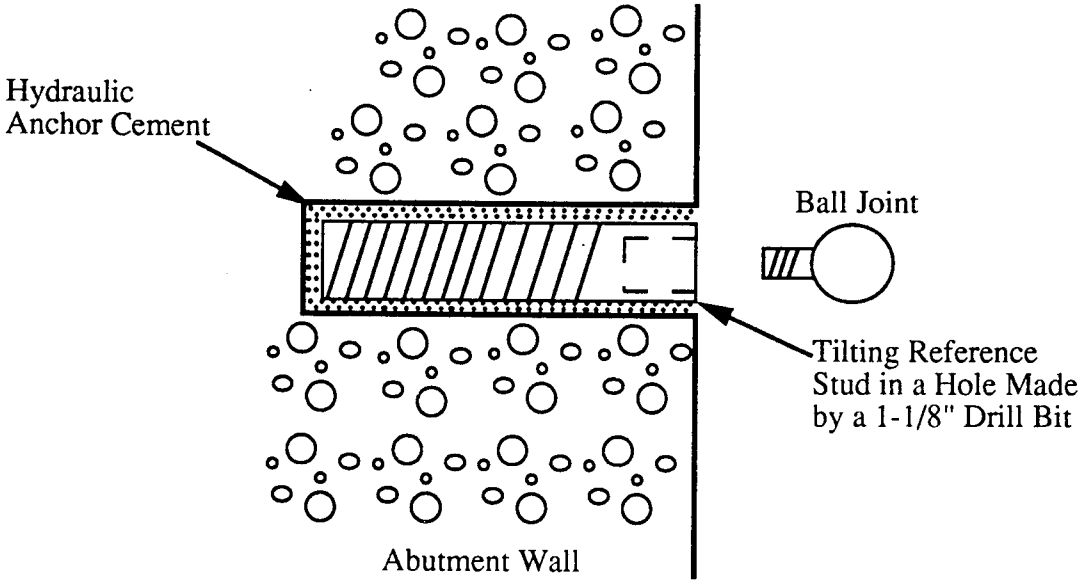

(b) Close-Up View of Reference Stud Installation

Figure 3.4.(c) Typical Instrumentation Details for Tilting Reference Point

on the situation. The pressure cells selected were the vibrating wire transducer type, manufactured by GEOKON, Inc. (New Hampshire). Contact pressure can be computed from the raw pressure cell readings by Equation 3.2, as follows.

$$P_i = C*(R_o - R_i) + K*(T_o - T_i) \qquad \text{Eq. (3.2)}$$

where P_i = contact pressure at the i-th construction increment (psi); C = main calibration factor (psi/digit); R_o = initial transducer reading (digit); R_i = transducer reading at the i-th construction increment (digit); K = temperature correction factor (psi/°C rise); T_o = initial temperature(°C); and T_i = temperature at the i-th construction increment (°C).

Data supplied by the manufacturer was used to convert electric resistance readings from the cell transducer to pressure values. The pressure cells typically had a 0 to 100 psi (0 to 7.2 tsf) range with a sensitivity of $\pm$ 0.1 psi. Prior to installation in the field, each cell was cast in a 12 inch x 24 inch x 3 inch concrete block with its sensitive surface exposed on the surface. This arrangement was made so the cells would not be disturbed easily during concrete placement and would become an integral part of the footing. In the field, the cells were placed with the sensitive surface facing down against a 2 to 3 inch thick, fine sand bedding layer to prevent the so-called "bridging" effect (see Figures 3.4a and 3.4b). Prior to placement, each cell was calibrated carefully in the laboratory to yield an accurate value of the main calibration factor C. In the flexible loading test, a special calibration chamber equipped with a very flexible (silicone rubber) membrane was utilized for applying uniform pressure (see Figure 3.5a). The cell was installed in the chamber under conditions simulating a field environment. In the rigid loading test, each pressure cell was loaded against a 2 to 3 inch thick fine sand layer underneath a stiff steel plate, as shown in Figure 3.5b. These two tests

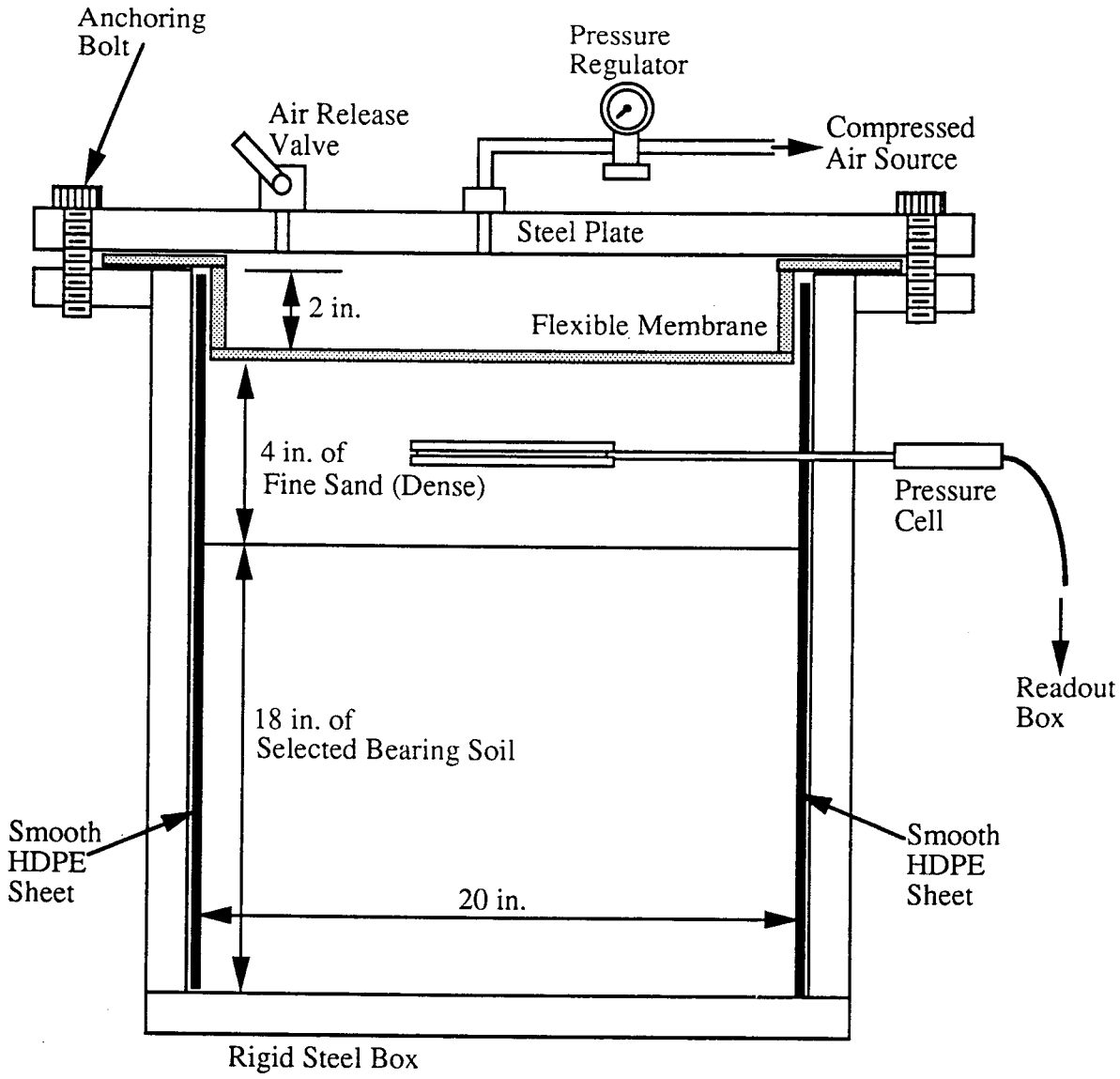

Figure 3.5. (a) Typical Pressure Cell Calibration Test Setup
(Using a Flexible Membrane)

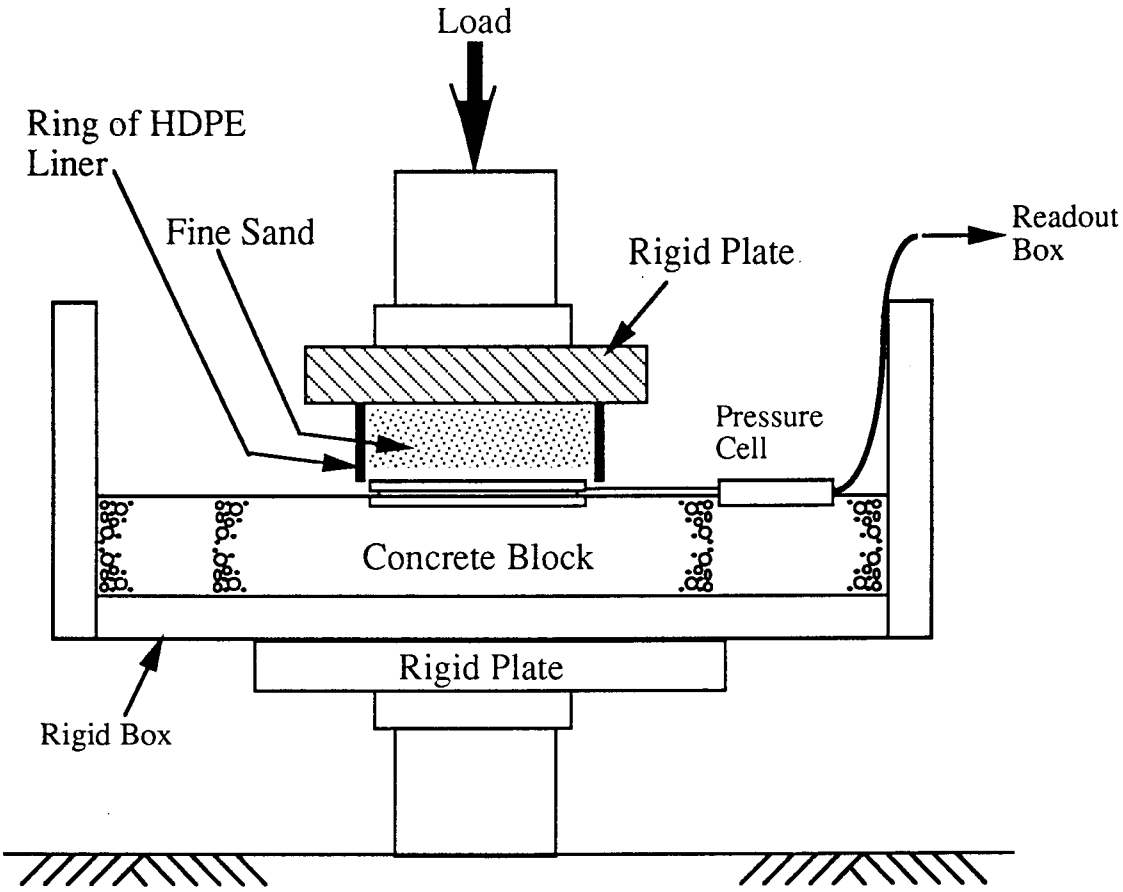

Figure 3.5.(b) Typical Pressure Cell Calibration Test Setup (Using a Rigid Plate)

were devised to simulate two extreme boundary conditions for the sensitive face of the pressure cell. On the average, the C value resulting from the rigid loading set-up was about 70 percent of that under the flexible loading, and the flexible loading produced C values which were very close to the manufacturer's values. The other calibration factor K was independent of installation conditions, so the values given by the manufacturer were accepted.

Tilting/overturning of the abutment wall/pier column was monitored at the center of these vertical members, as seen in Figure 3.2. The instrument used for this purpose was a single servo-accelerometer tilt sensor system developed by Slope Indicator (Seattle, WA). Tilting was determined from readings by the following equation (3.3).

$$\theta = \sin^{-1}[((Diff)/4)x10^{-4}] \qquad \text{Eq. (3.3)}$$

where θ = tilt angle (rad.); and (Diff) = difference in two tiltmeter readings taken on the (+) and (-) sides of the sensor (digit).

The tiltmeter had a range of $\pm 30°$ with a sensitivity of $\pm 0.0028°$. As shown in Figure 3.4c, two stainless steel reference points were installed as soon as forms of the abutment wall/pier column were removed. These points were approximately 3 feet apart, permanently grouted into the abutment wall/pier column, and the sensor was placed against them through a brass tilt reference plate.

3.3 Bridge A

Bridge A was a single-span, composite steel bridge structure with a reinforced concrete deck. It was constructed over Nelson Road in Columbus, Ohio as part of I-670 which connects the downtown to Port Columbus in Franklin County. The new bridge was built at a 57° 9' 13" skew

angle. Its span length was 61.86 feet from bearing to bearing, and the width of the bridge deck was 130 feet The abutment structure on each end was divided into three panel sections through contraction joints. The width of the footings varied from 12 to 16 feet, and the footing thickness was 3.0 to 3.25 feet A 3 feet wide, 2 feet deep key was provided for each footing section to enhance its resistance against horizontal sliding. The height of the new deck above Nelson Road was a minimum of 15.31 feet. Projected ADT for the year 2004 is 81,324. Figure 3.6 illustrates some of these basic features of the bridge foundation/abutment design, and Figure 3.7 presents a typical design of the abutment wall/footing at this site. This new bridge structure was built adjacent to an abandoned retaining wall structure for an old railroad overpass. Panels "C" and "F" were constructed about 3 feet in front of this retaining wall. Figure 3.8 shows photographs of the bridge taken in the field.

A total of five soil borings were placed in the bridge construction area. They were designated as Borings F-1 through F-5. Variations in the subsurface soil conditions did not differ significantly among the five holes. Appendix A presents a boring location plan (see Figure A.1) and data from these borings (Tables A.1 through A.4). The data indicted that the soil below the footing, typically classified as A-2-4, A-4-a, or A-4-b, mostly had a plasticity index value of less than 3 or 4 down to a depth of 20.5 feet below the footing, which is below the zone of influence. Under the upper granular soil layers was a cohesive glacial till material and a perched groundwater table at 7.8 to 9.5 feet below the footing base. SPT-N values increased with depth and rage from 9 to 100+ in granular soil and from 66 to 100+ in the glacial till. The typical SPT-N value range was from 20 to 80 in the granular layers and from 60 to 100 in the glacial till material. Figure 3.9 shows changes in the average SPT-N value with respect to the depth below the footing at Boring F-1 (located near Panel

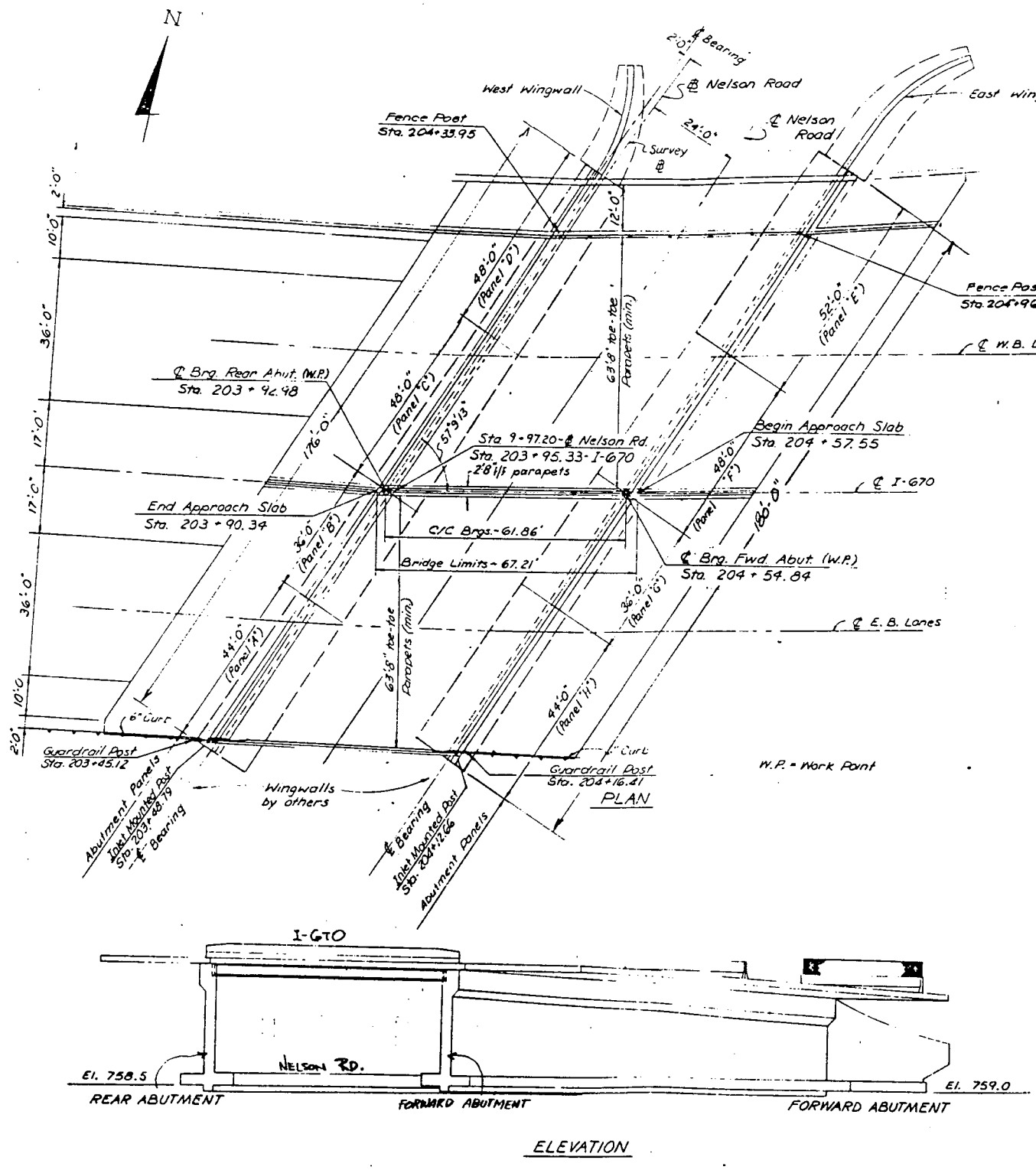

Figure 3.6 Overall Design Details of Bridge A Structure

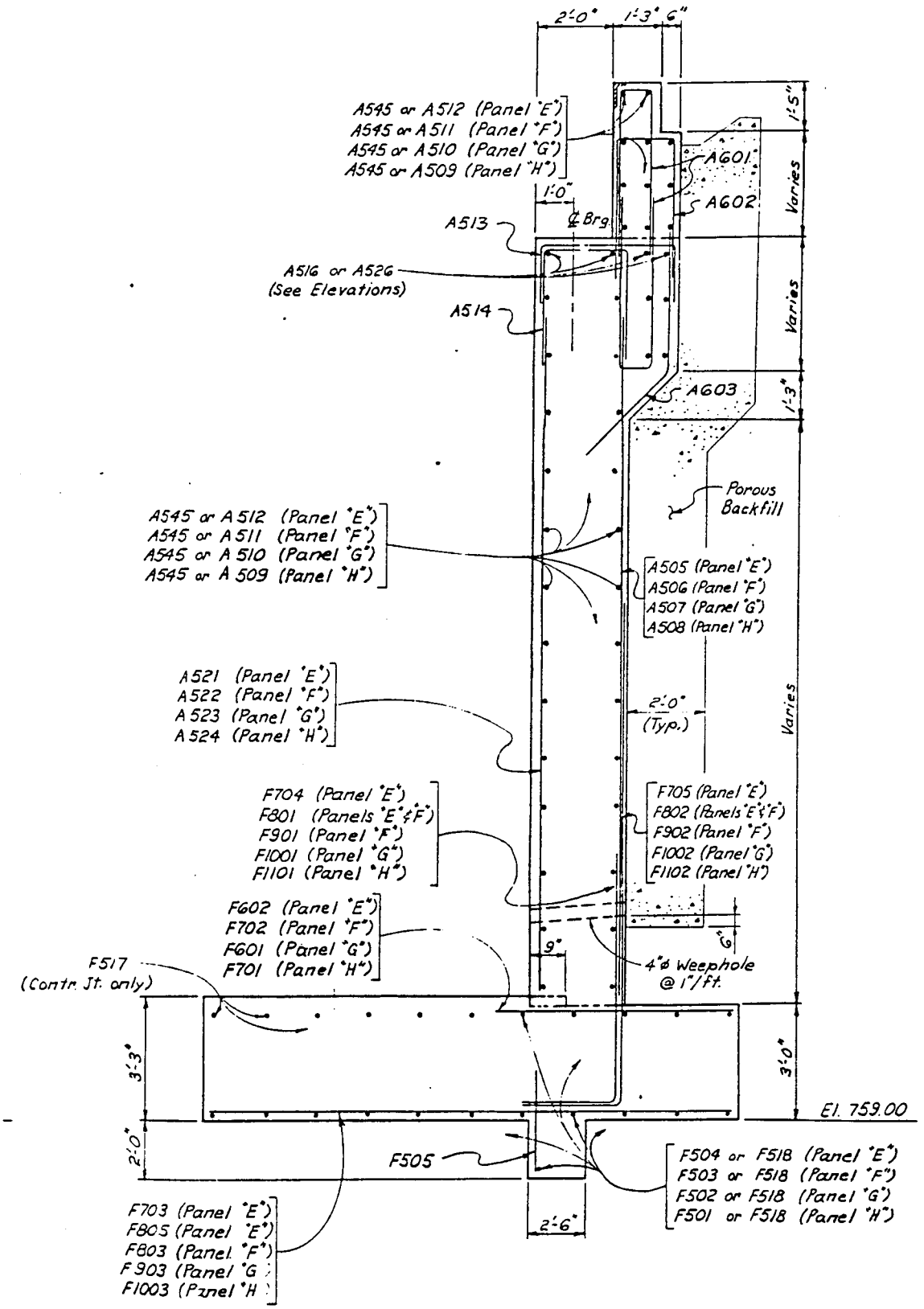

Figure 3.7 Typical Cross-sectional design details of Abutment/Footing (Bridge A)

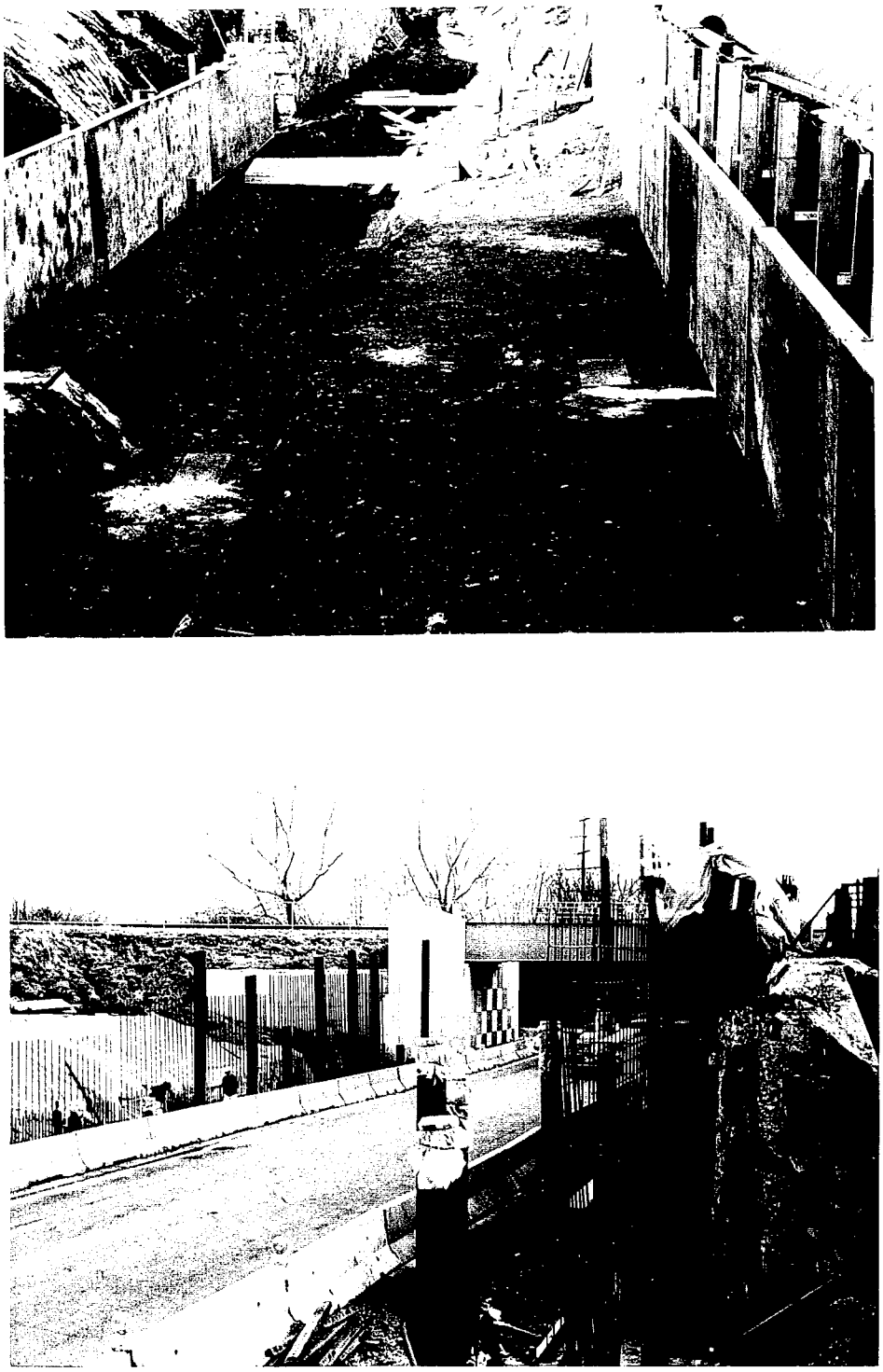

Figure 3.8 Pictures of Bridge A and Its Foundations During Construction

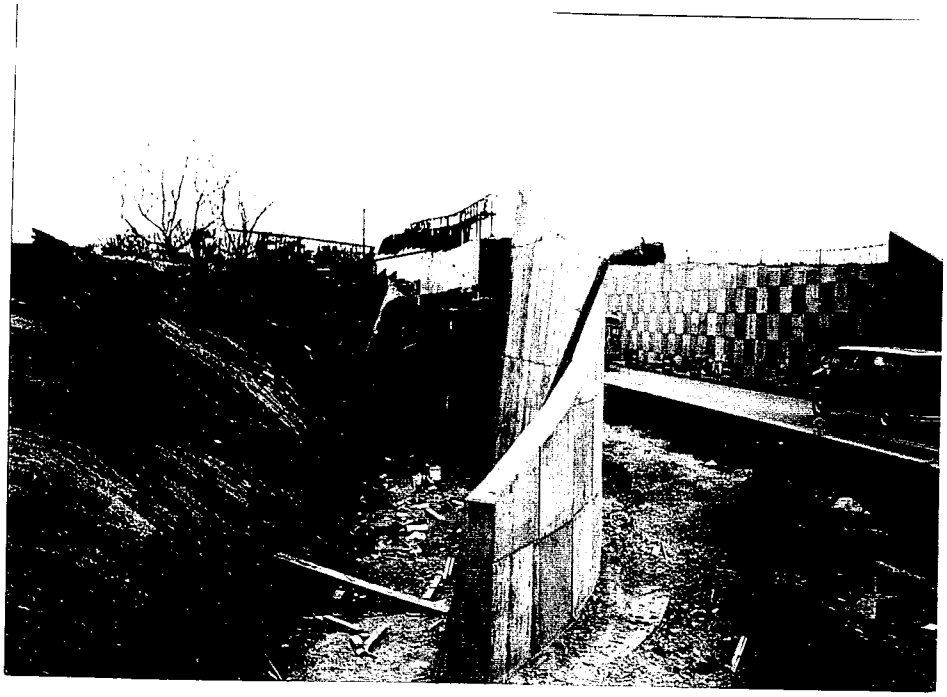

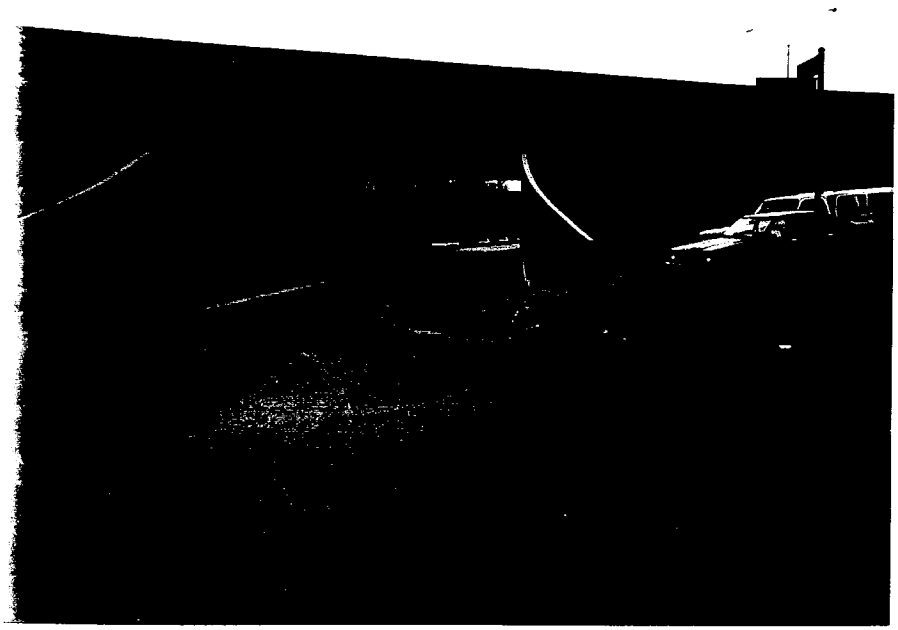

Figure 3.8 Pictures of Bridge A and Its Foundations During Construction

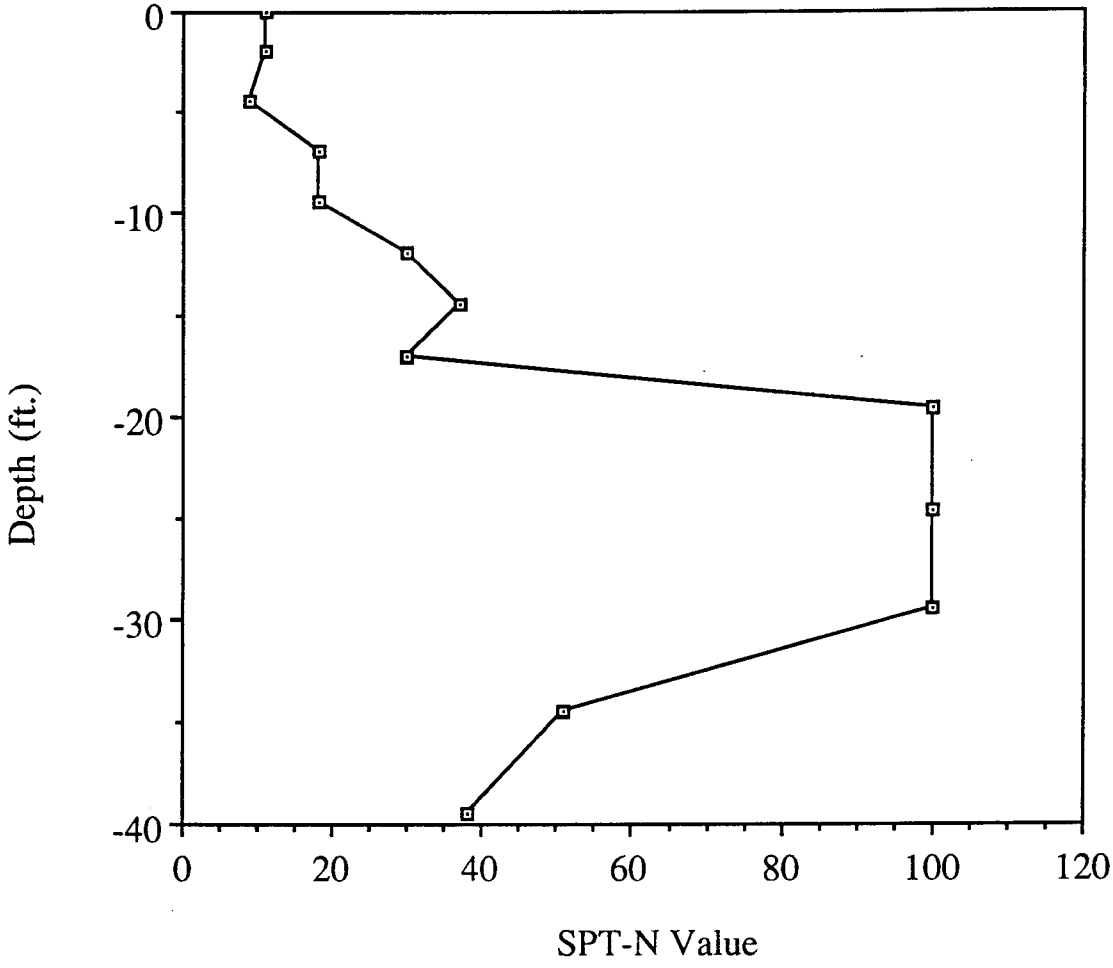

Figure 3.9 Variations of SPT-N Value with Depth Below Footing at Boring F-1 (Bridge A)

"G/H" footing). Similar plots of depth vs. SPT-N for the other four bore holes are provided in Figures A.2 through A.5, Appendix A. The SPT-N value increased from about 40 to 100+ in the zone more than 10 feet below the footing bottom elevation. The bearing granular material typically had a dry density of 98 pcf and an internal friction angle of 44 degrees.

Initial excavation started on both sides of Nelson Road around December 6, 1989. Since then, the structure has gone through seven major stages until its completion and opening to the general highway traffic on December 11, 1990, 363 days after completion of the first footing. Table 3.5 notes significant construction milestones observed on this bridge. As indicted in the table, the superstructure frame was placed when backfilling was nearly completed on the west side and half-way finished on the east side. Soil used in backfilling behind abutment walls consisted of a sandy clay material transported from another site. A representative sample provided the following basic geotechnical properties:

-Maximum dry density = 111.1 pcf

-Optimum moisture content = 13.5%

-Liquid limit = 26%; Plasticity index = 9.8%

This material was spread and compacted in 8 to 10 inch lifts to a minimum 95 percent of the maximum Proctor dry density by a self-propelled segmented roller. The final height of the backfill material was about 21 to 27 feet above the top of the footings. Laboratory direct shear tests provided an internal friction angle of 33.3 degrees for this soil. The contractor placed ODOT #304 crushed limestone in 12 inch lifts and compacted it over the heel section of the footings, using a self-propelled vibro-plate. The final thickness of this sidewalk area backfill was between 1.5 and 3.0 feet

Figure 3.10 summarizes the instrumentation plan implemented for Bridge A. Although all

Table 3.5 Detailed Construction Records on Bridge A

Date	No. of Days Elapsed	Description of Construction Activities
12-06-89	0	Initiation of construction.
12-13-89	7	Panel "A/B" footing placed.
12-18-89	12	Panel "C" footing placed.
12-28-89	22	Panel "D" footing placed.
01-12-90	37	Abutment wall constructed at Panel "A/B" footing.
01-19-90	44	Panel "G/H" footing placed.
01-24-90	49	Panel "F" footing placed. Abutment wall constructed at Panel "C" footing.
01-31-90	56	Panel "E" footing placed.
02-12-90	68	Abutment wall constructed at Panel "D" footing.
02-21-90	77	Backfilling started behind Panel "A/B" abutment wall.
03-03-90	87	Abutment wall constructed at Panel "E", "F", and "G/H" footings. Backfilling completed behind Panel "A/B" through "D" abutment walls.
03-26-90	110	Girder beams placed across span.
05-18-90	163	Backfilling completed behind Panel "E" through "G/H" abutment walls.
05-31-90	176	Concrete slab placed for the deck construction.
12-11-90	369	Bridge opened to general traffic.
09-15-91	643	Temperature effect on abutment wall tilting monitored.

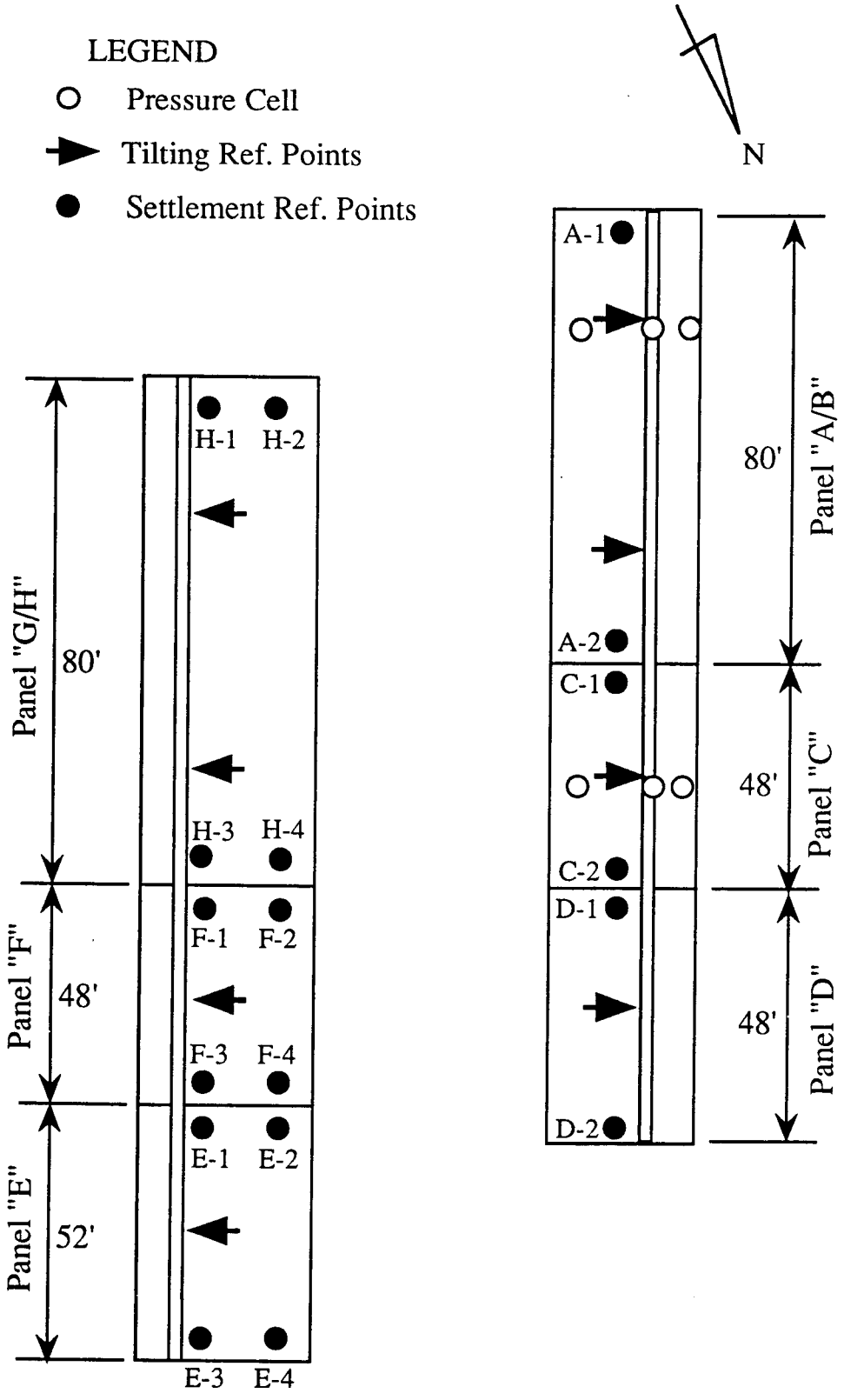

Figure 3.10 Overall Field Instrumentation Plan (Bridge A)

panel structures were instrumented to monitor settlement and tilting, the instrumentation efforts were mostly concentrated on Panels "A" and "C" to evaluate the influence of the old retaining wall structure (which existed behind Panel "C" abutment wall) on the performance of the new structure. Three pressure cells were installed across the base of the footing at the centerline of the two panel locations (see Figure 3.10). They all had a range of 0-500 psi with a sensitivity of $\pm$ 1.25 psi. Cables from these pressure cells were directed into a compact manhole located at the center of each panel. Overall foundation settlement was monitored at two points located near the edge of the footing for Panels "A" through "D". At panels "E" through "H", a total of four monitoring points were installed on the footing so that both average and differential settlement information could be obtained. Figure 3.10 illustrates the general location plan for the settlement monitoring points. These monitoring points were protected by 6 inch diameter PVC casings during and beyond the construction phases. Level surveys were conducted often with respect to the permanent bench mark used by the contractor and the temporary bench mark installed by Ohio University personnel. Settlement of the heel section of the foundations was monitored at the center of Panels "A" and "C" by installing a PVC pipe horizontally over the top of the footing. The mouth of these PVC pipes was fed into the compact manhole. Tilting of the abutment wall was monitored at the center of each panel structure, as shown in Figure 3.10. Field performance was monitored until June 15, 1991 (about 6 months beyond the bridge opening).

3.4 Bridge B

Bridge B was a two-span bridge supported by two large abutment/wingwall structures at the ends and by a pier foundation in the center. Each span was about 124 feet from bearing to bearing,

and the width of the bridge deck was about 57 feet The bridge was constructed to carry U.S. Rt. 68 over U.S. Rt. 35, as part of a major extension project for U.S. Rt. 35, just south of the city of Xenia, in Greene County, Ohio. Design of the bridge deck was similar to that of Bridge A. The bridge was built in parallel, next to the old U.S. Rt. 68 embankment. The abutment structure at each end was U-shaped, having wingwalls to contain the backfill soil for the approach section. Within each abutment structure, only the wall section had contraction joints. The central pier structure consisted of three piers and a pier cap. The current ADT is about 6,500, while the ADT for the year 2010 is projected to be 9,065. Figure 3.11 illustrates some of the basic features of the bridge foundation/abutment design. The two abutment footings were a stepped type to conform to the sloping grade. Photographs of this structure are shown in Figure 3.12.

The bridge construction site is located on a rolling portion of the Mississippi Valley Plain, in an area where deep glacial and valley deposits overlie bedrock of Siluarian Age. One test boring was placed to a 52 to 56 feet depth in each abutment construction area. Their locations are shown in Figure A.6 in Appendix A. The borings encountered intervals of loose to extremely dense unstratified sand, silt and clay containing various amounts of gravel. Soil density increased with depth. No bedrock surface was reached in either of the borings. Free water was observed in both borings. Tables A.5 and A.6 in Appendix A presents a summary of the soil boring data, and variation of the SPT-N value is plotted with respect to depth below the footing in Figures 3.13 and 3.14.

Construction of the foundations proceeded from the cental pier to Abutment No. 1 (south abutment) to Abutment No. 2 (north abutment). Table 3.6 summarizes the construction sequence and time schedule data. Six major construction stages can be identified in the table. Initial excavation started for the central pier foundation around October 11, 1990. By February 2, 1991

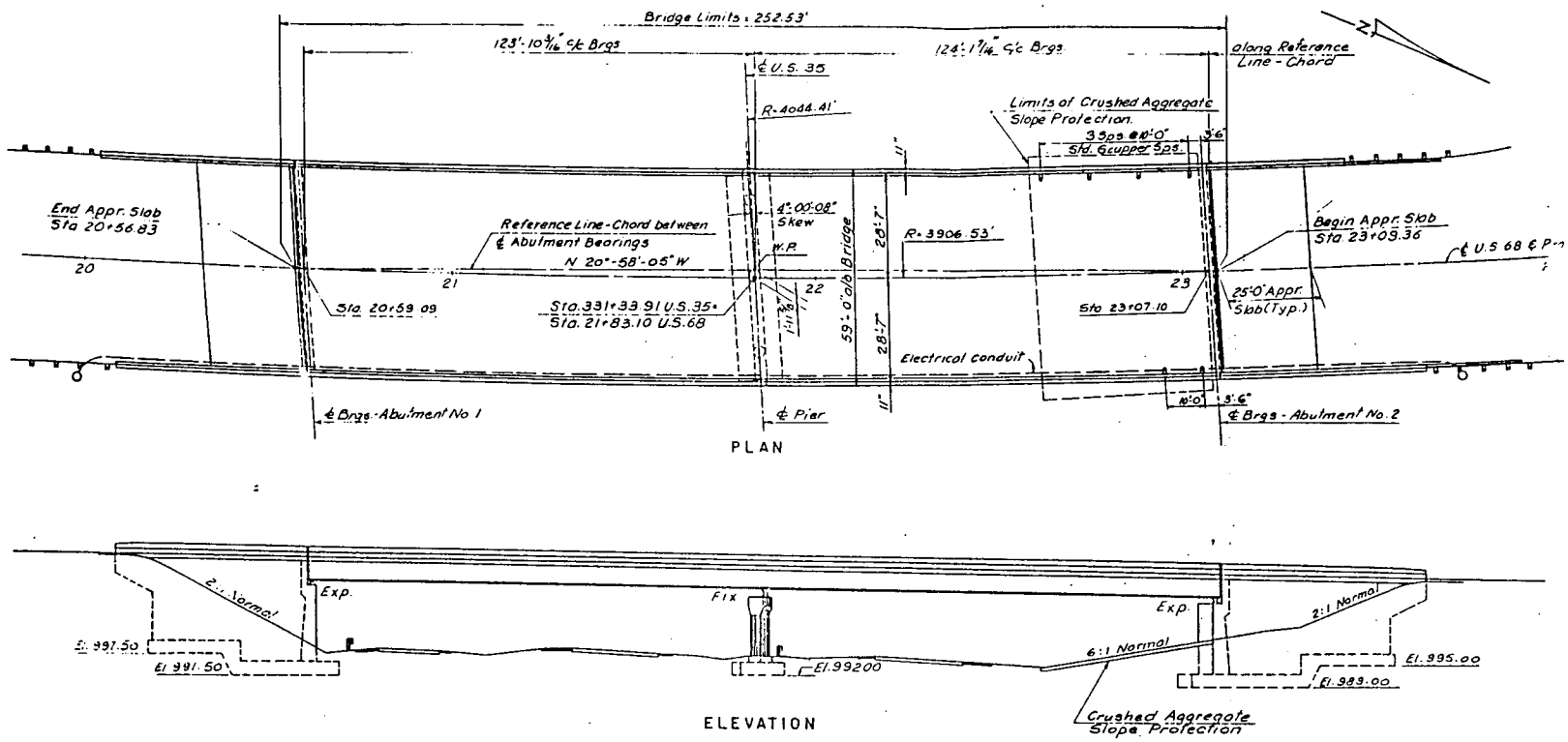

Figure 3.11 Typical Cross-sectional design details of Abutment/Footing (Bridge B)

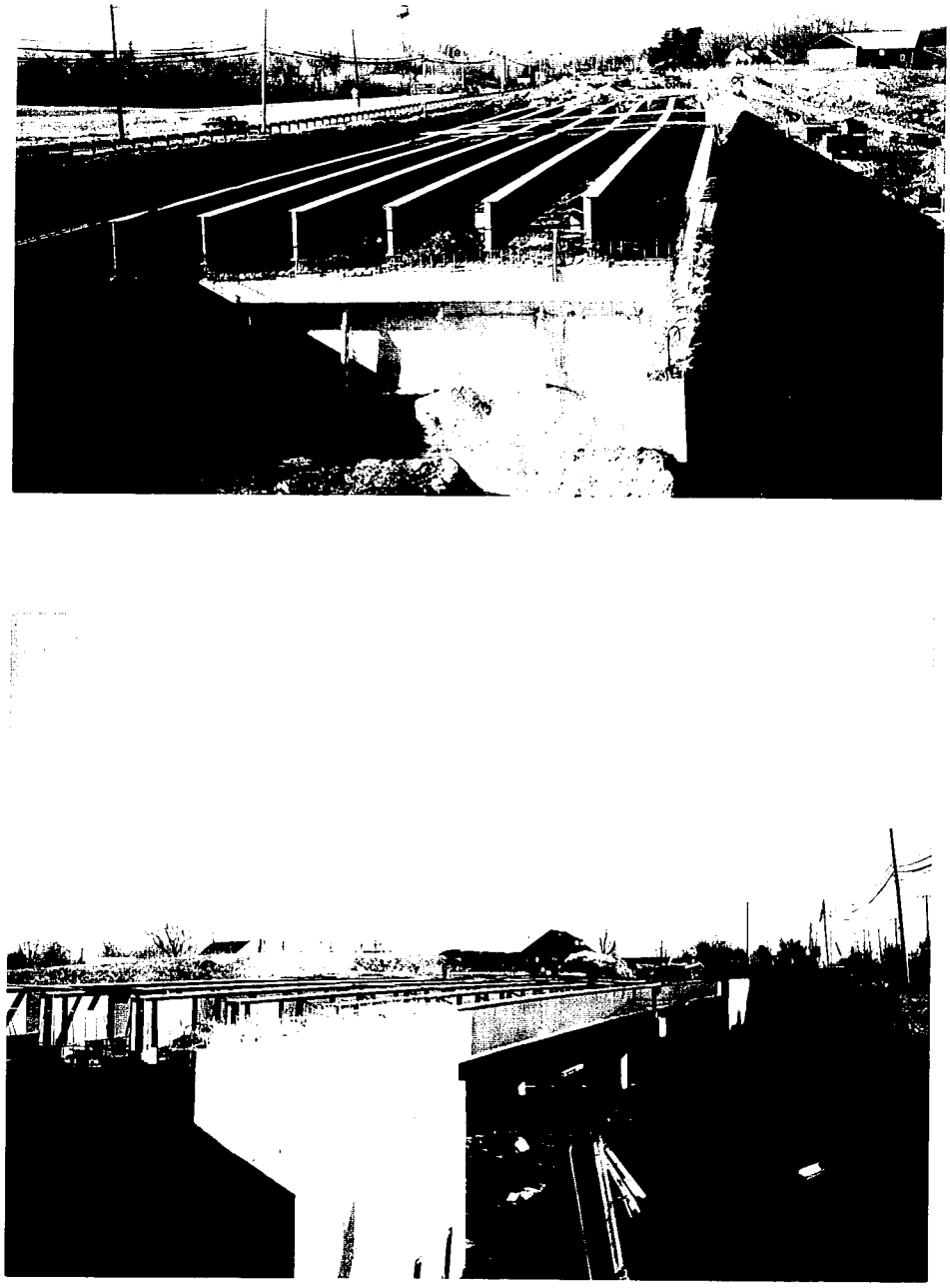

Figure 3.12 Pictures of Bridge B and Its Foundations During Construction

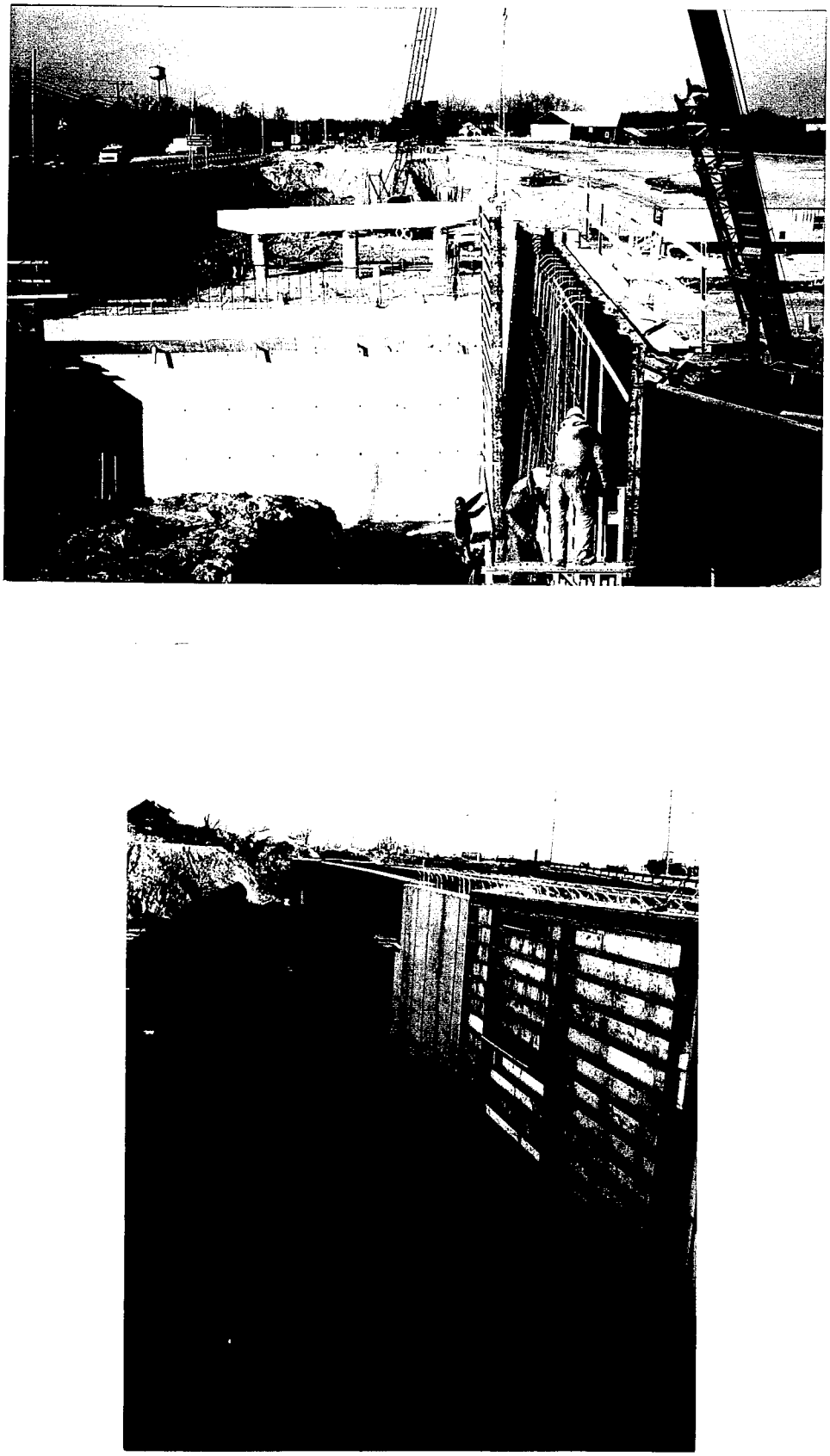

Figure 3.12 Pictures of Bridge B and Its Foundations During Construction

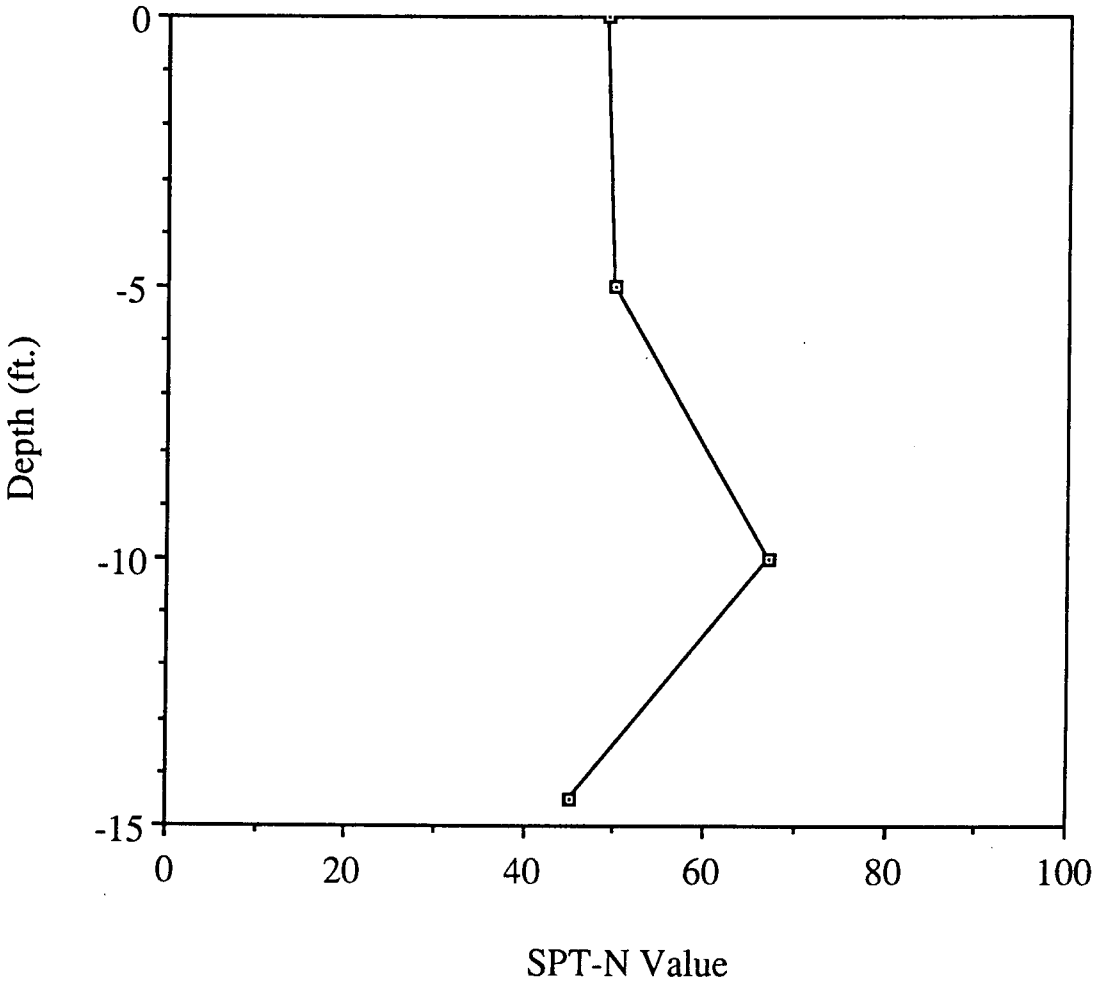

Figure 3.13 Variations of SPT-N Value with Depth Below Footing at Boring B-1 (Bridge B)

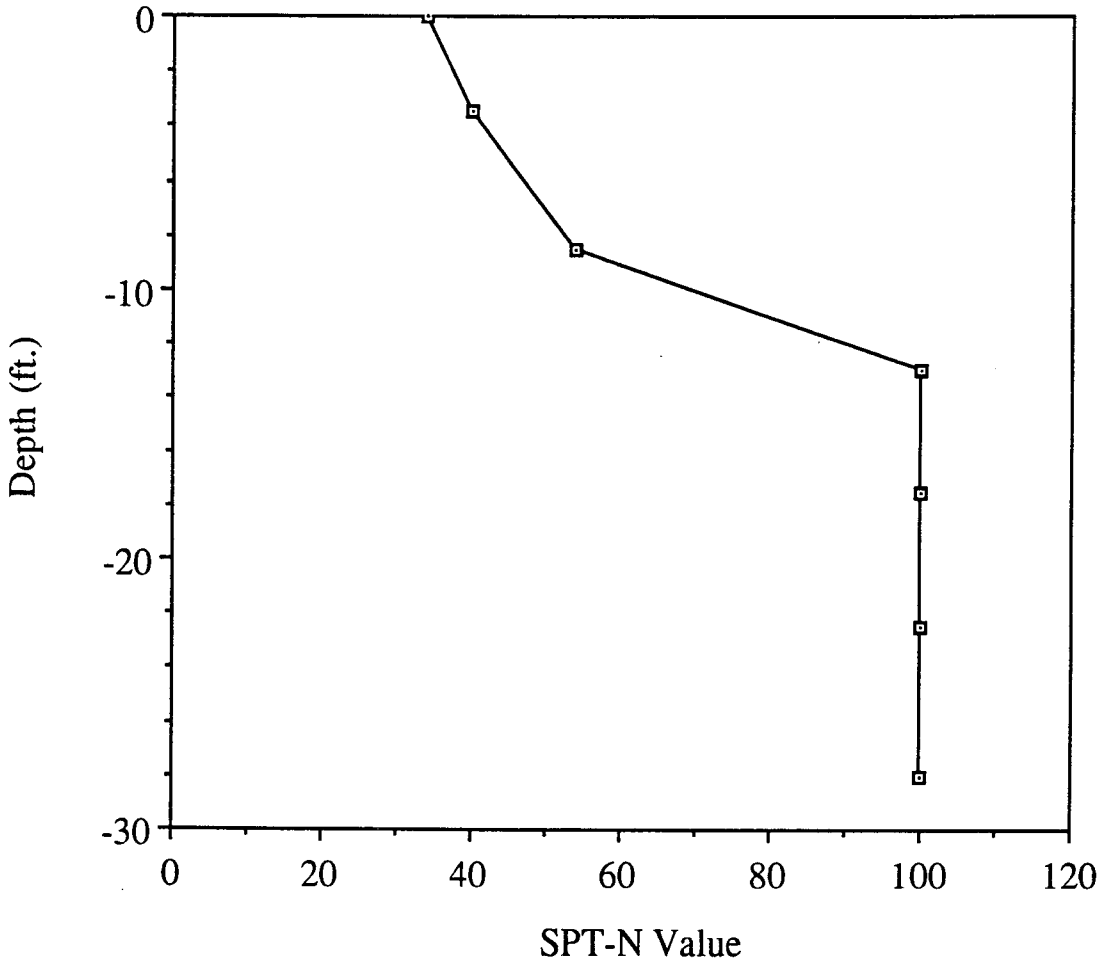

Figure 3.14 Variations of SPT-N Value with Depth Below Footing at Boring B-6 (Bridge B)

Table 3.6 Detailed Construction Records on Bridge B

Date	No. of Days Elapsed	Description of Construction Activities
10-11-90	0	Central Pier foundation placed.
10-15-90	4	Three pier columns constructed at Central Pier footing.
10-19-90	8	Pier cap placed on the columns and the pier footing backfilled.
11-02-90	22	Abutment No. 1 foundation placed.
11-21-90	41	Front wall was constructed at Abutment No. 1 footing.
12-13-90	63	Abutment No. 2 foundation placed.
01-03-91	84	West wingwall constructed at Abutment No. 1 footing.
01-15-91	96	Front wall placed at Abutment No. 2 foundation.
01-28-91	109	East wingwall built at Abutment No. 1 footing.
02-07-91	119	Construction of Abutment No. 2 completed.
02-12-91	124	Six girder beams placed across Abutment No. 1 and Central Pier.
02-13-91	125	Six girder beams placed across Abutment No. 2 and Central Pier.
04-02-91	173	Backfilling operation started behind Abutment No. 2.
04-12-91	183	Backfilling operation began behind Abutment No. 1.
04-18-91	189	Concrete slab placed as part of bridge deck construction.
05-10-91	211	Backfilling work completed behind Abutment Nos. 1 and 2.
06-12-91	244	Asphalt layer placed over concrete deck surface.
07-03-91	265	Bridge opened to general traffic.

(after 113 days) all the foundation structures were constructed. Backfilling behind the abutments began on April 2, 1991. The I-beam frame for the superstructure was placed on February 11, 1991 (after 122 days), even before the backfilling operation started for both abutments. This was one of a few major differences in construction practices observed between the Bridge A and Bridge B sites. Bridge B was opened to the general highway traffic on July 3, 1991, 242 days after the construction of the central pier foundation. Soil encountered under the abutment footings was taken to the ORITE laboratory and provided the following basic geotechnical properties:

-Maximum dry density = 111.1 pcf

-Optimum moisture content = 13.5%

-Liquid = 26.0%; Plasticity index = 9.8%

-Angle of internal friction = 34.4 degrees

Figure 3.15a through 3.15c summarize the instrumentation plan implemented for Bridge B. The instrumentation plan was developed to mainly monitor the overall settlement and degree of tilting for the two abutments and the central pier. Pressure cells were not installed under the footings at this site. Overall settlement was monitored at a minimum of three points each for Abutments No. 1 and No. 2, and at four points on the central pier foundation. Alternate settlement monitoring points had to be established for the two abutment structures in early 1991, since relatively deep fill was placed over their toe sections. Field performance data were collected until August 11, 1991, about one month after the bridge opening.

3.5 Bridge C

Bridge C, constructed on U.S. Rt. 39 just west of the city of Dover in Tuscarawas County,

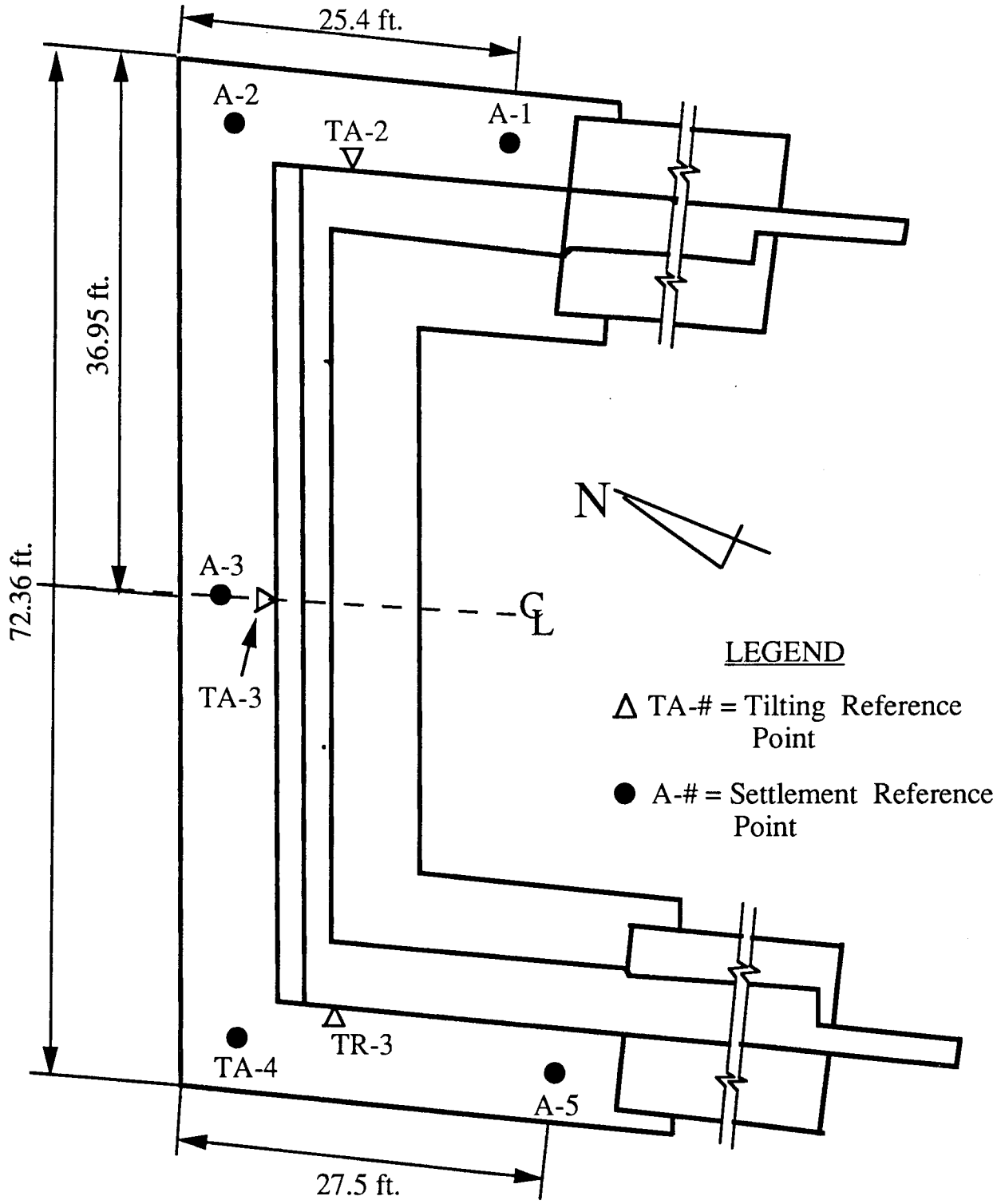

Figure 3.15.(a) Overall Field Instrumentation Plan for Abutment No. 1 (Bridge B)

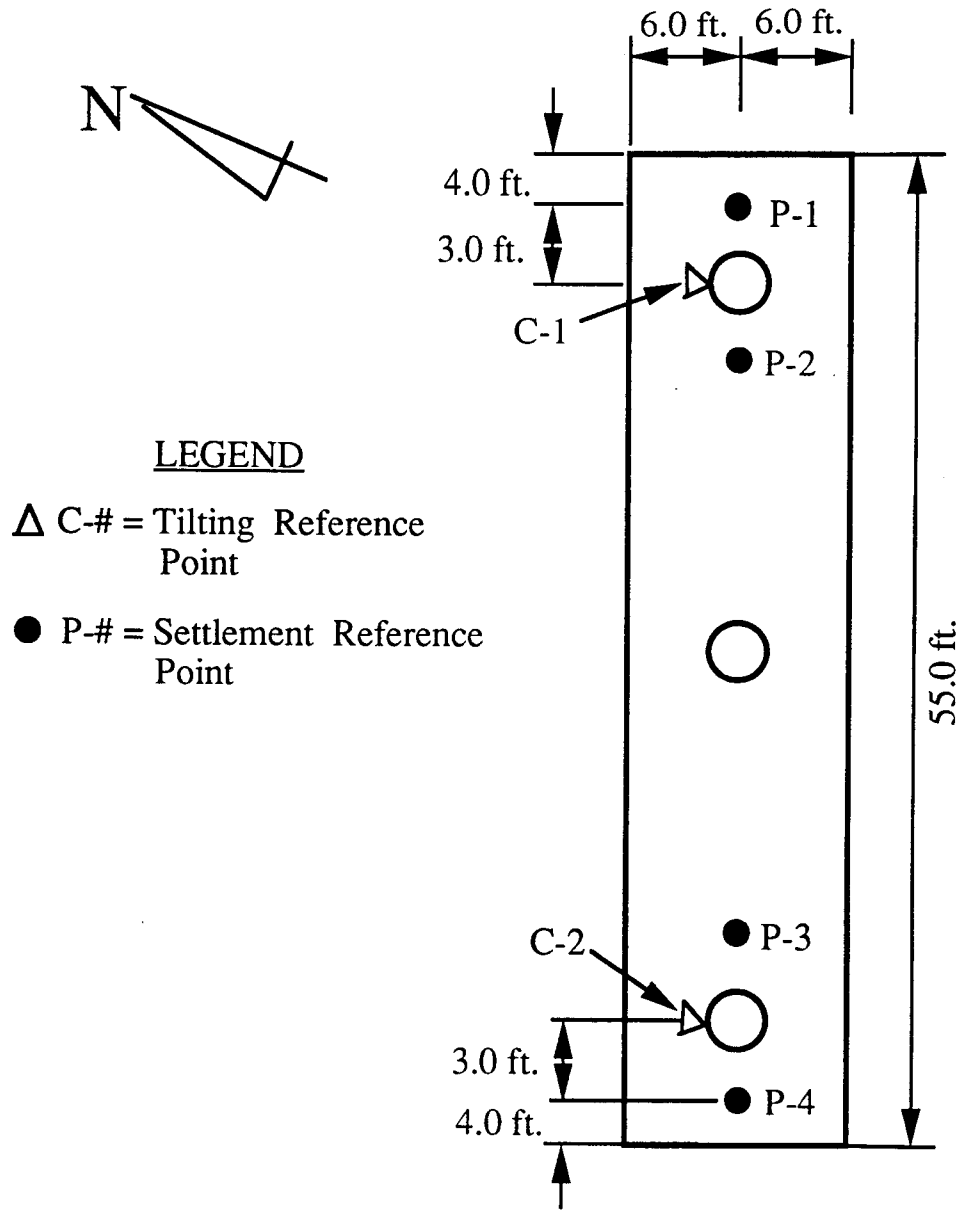

Figure 3.15.(b) Overall Field Instrumentation Plan for Central Pier (Bridge B)

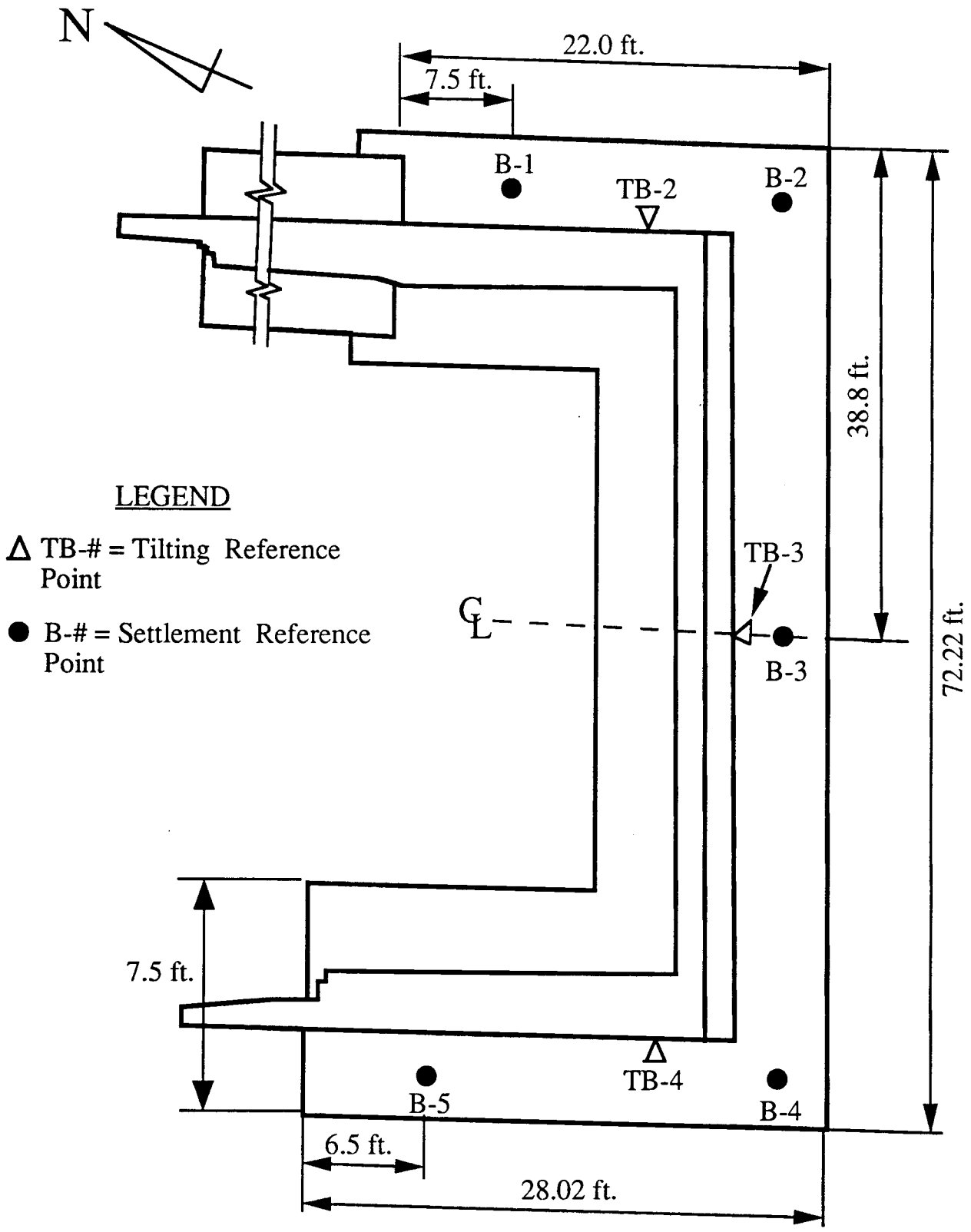

Figure 3.15.(c) Overall Field Instrumentation Plan for Abutment No. 2 (Bridge B)

Ohio, was a three-sided, flat-topped, concrete box culvert structure. This spread-footing-supported box culvert was installed to replace an old stone arch and to provide an improved drainage way for the Brandywine Creek. The rise and span dimensions of the culvert were 10 feet and 22 feet, respectively. The culvert was built skew at a 15° angle with respect to the line perpendicular to the roadway centerline. A total of ten prefabricated, three-sided box sections were placed in a key way at the top of a 4 feet wide by 2 feet thick footing on both sides. Current ADT is reported to be 5,690, and is expected to rise to 8,300 by the year 2010. Figure 3.16 presents photos of the structure during construction.

Two soil borings, B-1 and B-2, were made in the vicinity of the culvert construction area. Their locations are shown in Figure A.7, Appendix A. According to available geological data, the site is located in the highly bisected and glaciated portion of the Alelghent Plateau Region. It is on a broad floodplain of Brandywine Creek, in an area where deep glacially derived material and alluvial deposits overlie bedrock of Pennsylvanian age. Tables A.7 and A.8 in Appendix A summarize soil boring log data. Both borings encountered basic silts and sands. Figures 3.17 and 3.18 show changes in the average SPT-N value with respect to depth below the footing. SPT-N values ranged from 3 at the surface to about 40 at the bottom of the borings. The blow counts also increased with depth. Boring B-1, placed near the rear abutment, penetrated to a depth of 56.5 feet and terminated when the SPT-N value was exceeding 30. Boring B-2, placed near the forward abutment, penetrated to a depth of 61.5 feet Bedrock was not encountered in either of the borings. A representative sample of the silty-sandy bearing soil was taken to the ORITE soils laboratory and some basic tests were performed to obtain the following geotechnical properties:

-Soil classification = ML-CL (Unified Soil Classification), A-4 (AASHTO)

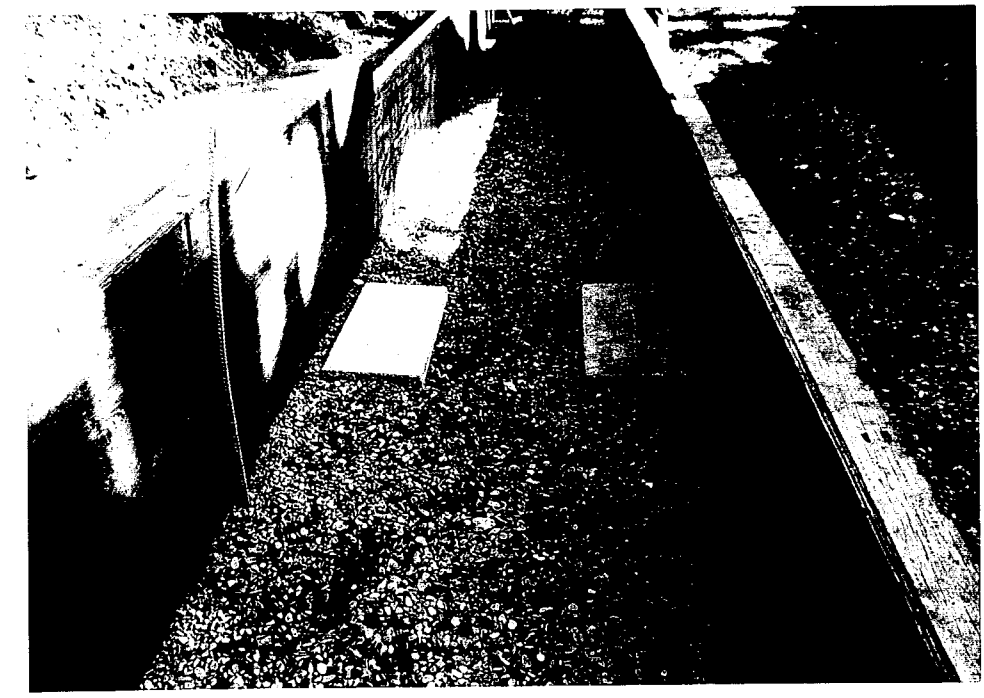

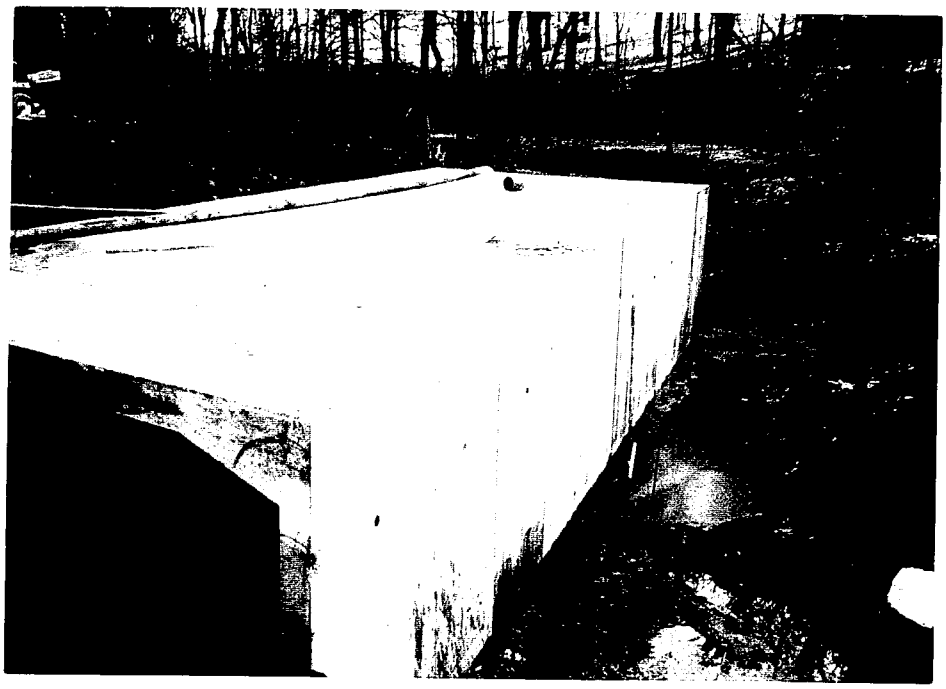

Figure 3.16 Pictures of Bridge C and Its Foundations During Construction

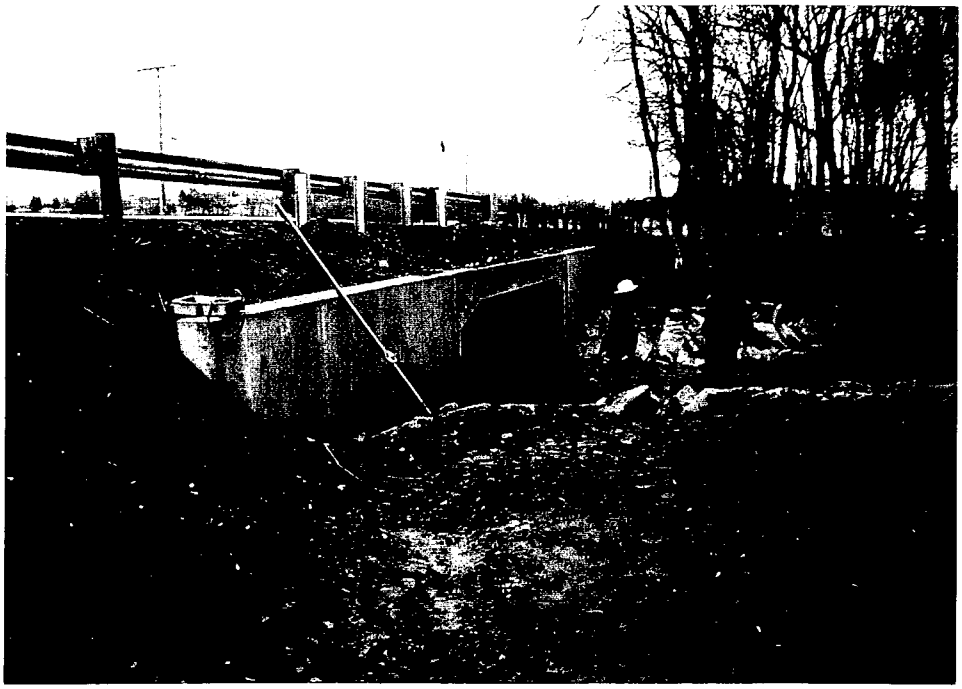

Figure 3.16 Pictures of Bridge C and Its Foundations During Construction

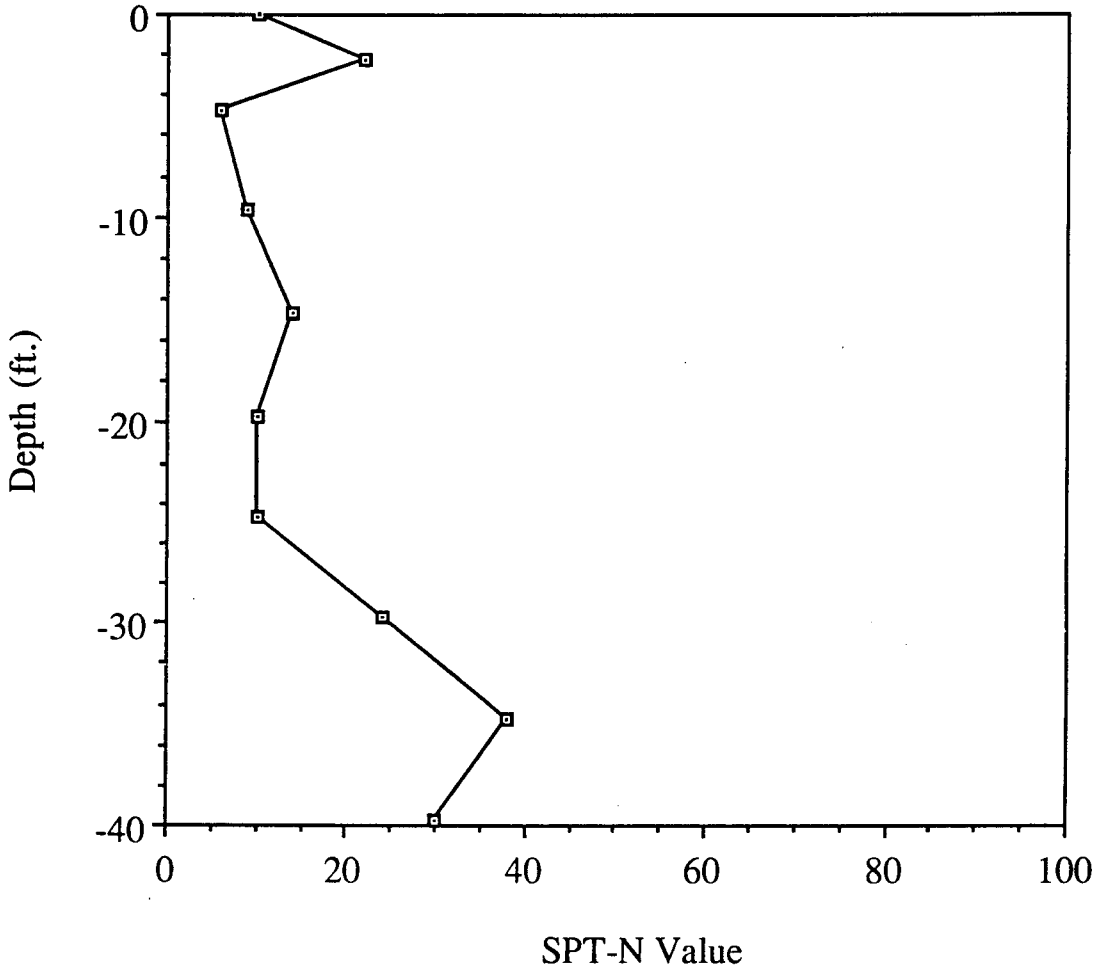

Figure 3.17 Variations of SPT-N Value with Depth Below Footing at Boring B-1 (Bridge C)

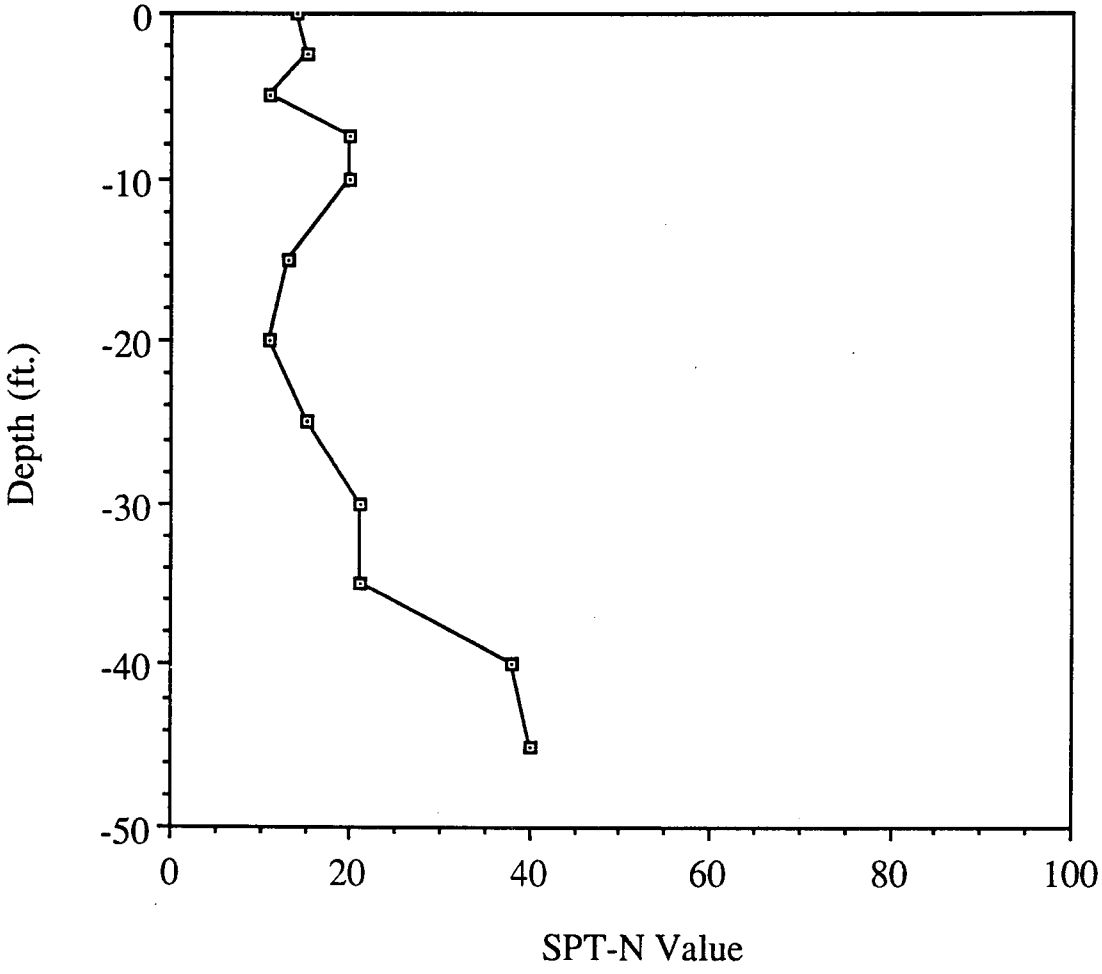

Figure 3.18 Variations of SPT-N Value with Depth Below Footing at Boring B-2 (Bridge C)

-Liquid limit = 26.5%; Plasticity index = 9.7%

-Angle of internal friction = 37.5 degrees; Cohesion = 2.6 psi

-Maximum dry density = 103.7 pcf

-Optimum moisture content = 16.2%

The construction of the box culvert was conducted in a single phase. The total amount of time spent between the initiation of footing construction to completion and service load application was only about 50 days. Table 3.7 summarizes key information regarding sequences and the time schedule of construction. Five major stages existed for this structure. Specifications called for placing a 24-inch thickness of ODOT #57 stone below each footing. A total of 35 cubic yards of concrete was poured for each footing. The weight of each prefabricated box section was 20 tons, and these sections were placed on the footings according to the order shown in Figure 3.19. Once all the culvert sections were placed, the key was grouted and wingwalls were constructed. Granular backfill was tamped into the space between the culvert and the excavated cut slope up to the top of the culvert. Then additional layers were placed above the culvert. Figure 3.20 shows the description and thickness of these layers.

Figure 3.21 depicts the overall instrumentation plan implemented for Bridge C. To evaluate the magnitude and distribution of contact pressure at the footing/soil interface, two pressure cells - one at the toe and the other at the heel - were installed across the base of the west footing at the centerline (Figure 3.23a). Only two cells were required because the footing width was 4 feet The cells had a pressure range of 0-150 psi with a sensitivity of $\pm$ 0.75 psi. A specially made geofabric pocket containing fine sand was placed in coarse granular bedding layer underneath each pressure cell. Overall settlement of the foundations was monitored at three monitoring points per footing.

Table 3.7 Detailed Construction Records on Bridge C

Date	No. of Days Elapsed	Description of Construction Activities
10-16-91	0	Initial excavation finished.
10-17-91	1	24-in. thick ODOT #57 stone layer placed in footing construction areas.
10-18-91	2	West footing constructed.
10-24-91	8	East footing constructed.
11-08-91	24	All ten box culvert sections placed on top of footings.
11-10-91	26	Backfilling work began on both sides of the culvert. Head wall construction was also started.
11-15-91	31	Backfill height reached the top of culvert.
11-23-91	39	Headwalls completed at both ends.
11-24-91	40	Backfilling work completed. Final height of cover 43 inches over the top of culvert.
11-25-91	41	Paving operations began.
12-01-91	47	Bridge opened to general traffic.

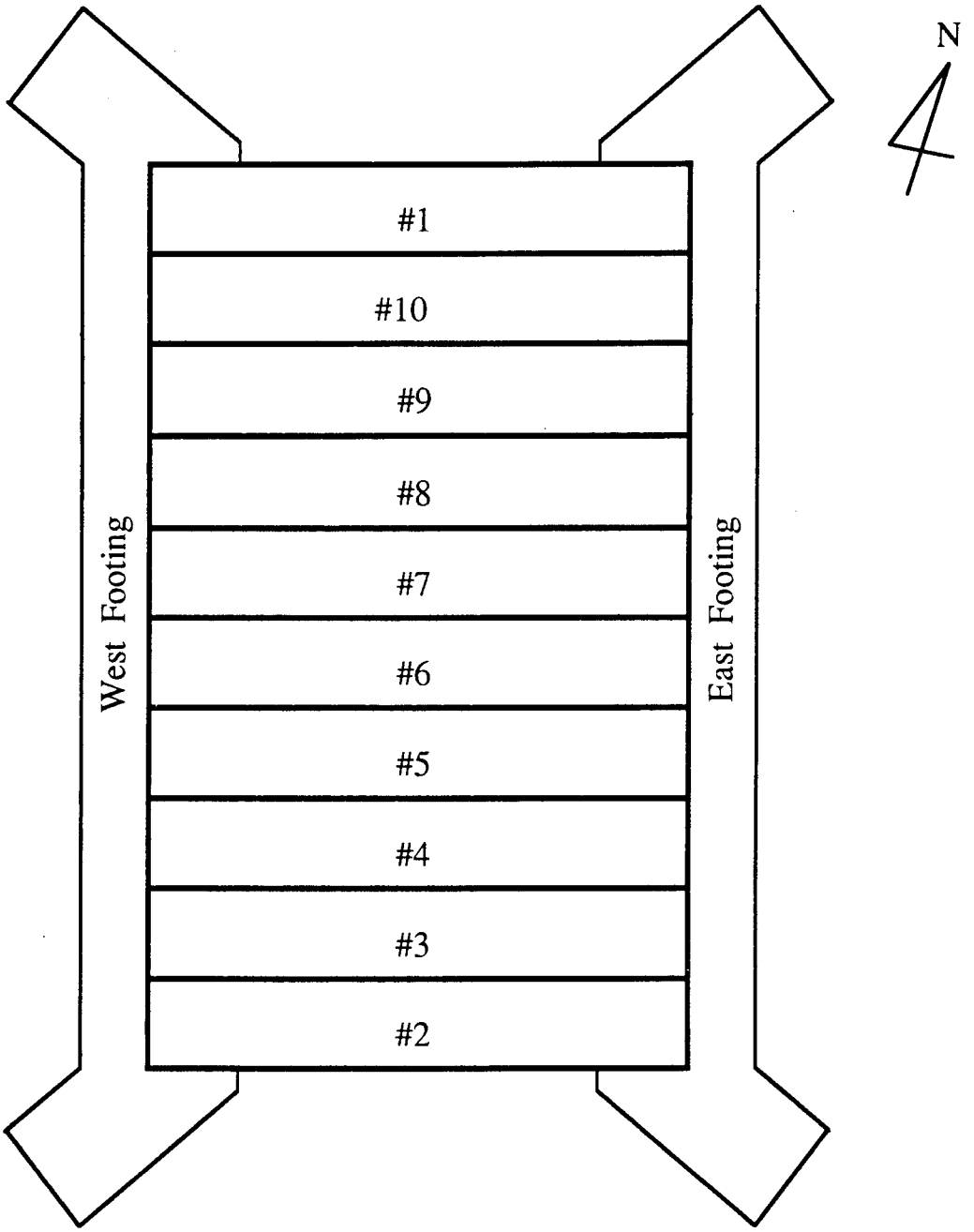

Figure 3.19 Sequence of Box Culvert Placement Over Footings (Bridge C)

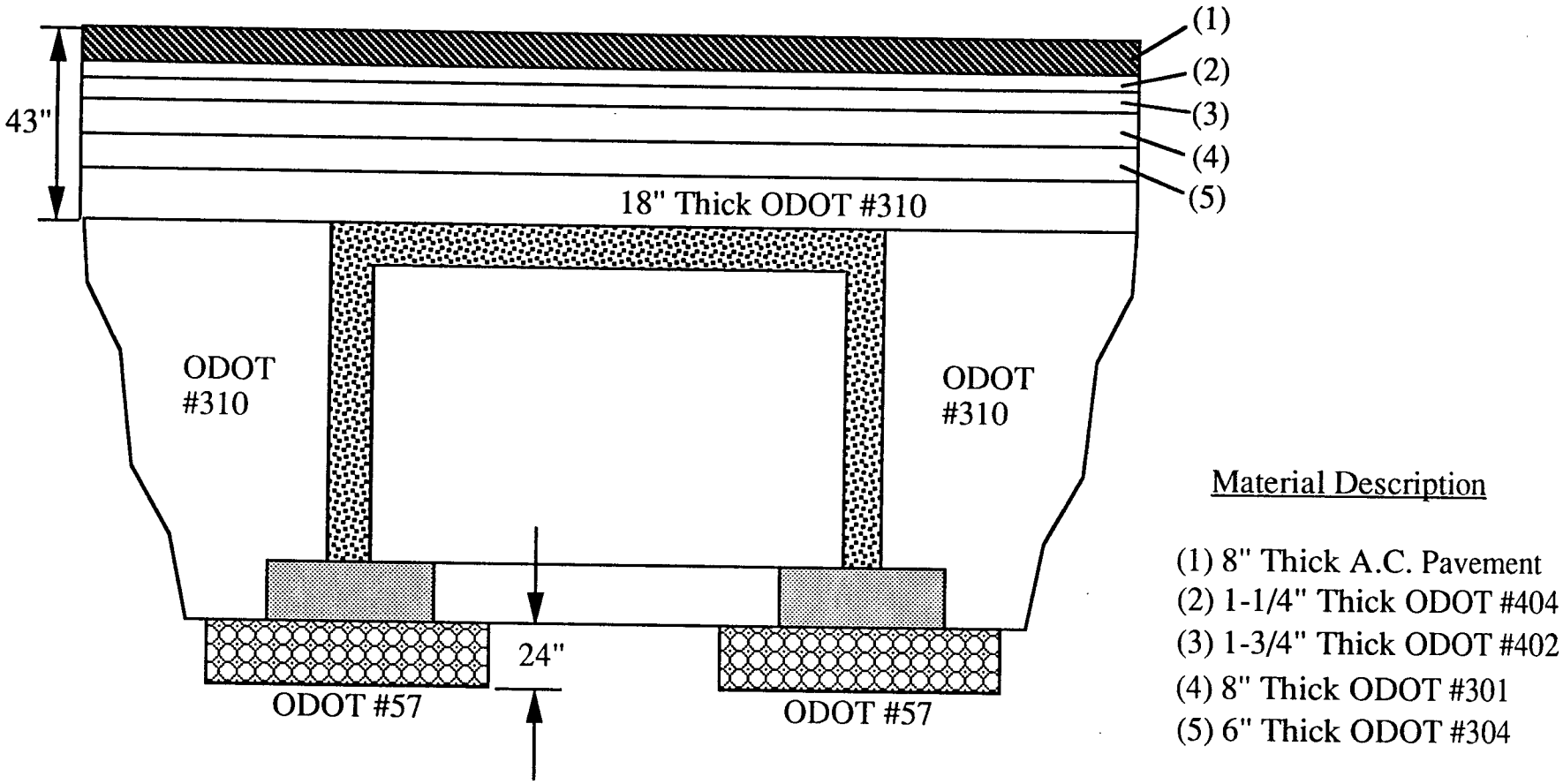

Figure 3.20 Field Backfilling of Box Culvert (Bridge C)

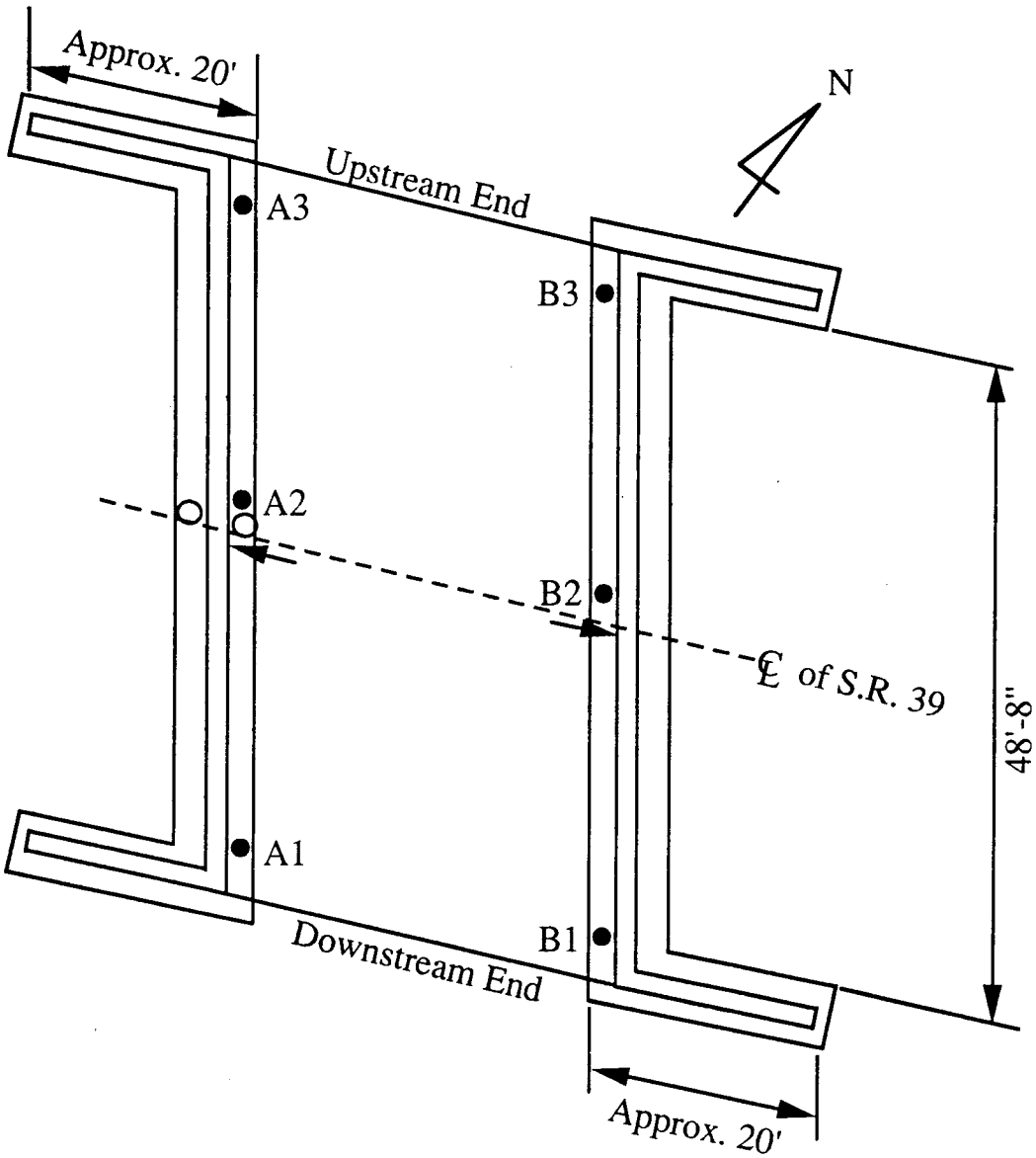

LEGEND

- ● Settlement Reference Point
- ○ Earth Contact Pressure Cell (Under the Footing)
- ◄ Tilting Reference Points

Figure 3.21 Overall Field Instrumentation Plan (Bridge C)

They were originally installed directly on the footing. Because the footing would be 4 to 4.5 feet under the normal creek water level, alternate monitoring points were established on the culvert interior wall at a height of 5 feet above the top of the footings (see Figure 3.22). All survey work was performed with respect to a permanent bench mark used by ODOT and the contractor. During placement of the box culvert sections, a profilemeter was utilized to monitor settlement of the west footing. Tilting/overturning of the culvert wall was measured at monitoring points installed on each side of the centerline, as shown in Figures 3.23b. Field performance was monitored until June 20, 1992, about seven months beyond the bridge opening.

3.6 Bridge D

Bridge D, constructed over I-75 in Butler County, Ohio, was a six-span, composite deck bridge structure associated with the widening of Taylorsville Road. This new bridge had a width of 72 feet and a total length of 414.7 feet (bearing to bearing). It maintained the same skewness (21° 30' L.F.) of the previous bridge. The longest span dimension was 76.3 feet The superstructure of the bridge was supported by two abutments on piles and twenty-five spread footings, of which fifteen were relatively small size, pre-existing square footings. This arrangement was a result of a construction plan in which all of the pier foundations of the old bridge were saved below the pier caps and additional pier foundations were added on both north and south sides to widen the deck width. The abutments of the previous bridge structure were removed completely. New abutments were to be supported by HP10 x 42 piles. General layout of the foundations for the new bridge is given in Figure 3.25, and pictures of the bridge structure are shown in Figure 3.24. The ADT was reported to be 13,925 in 1992 and projected to be 20,531 by the year 2012.

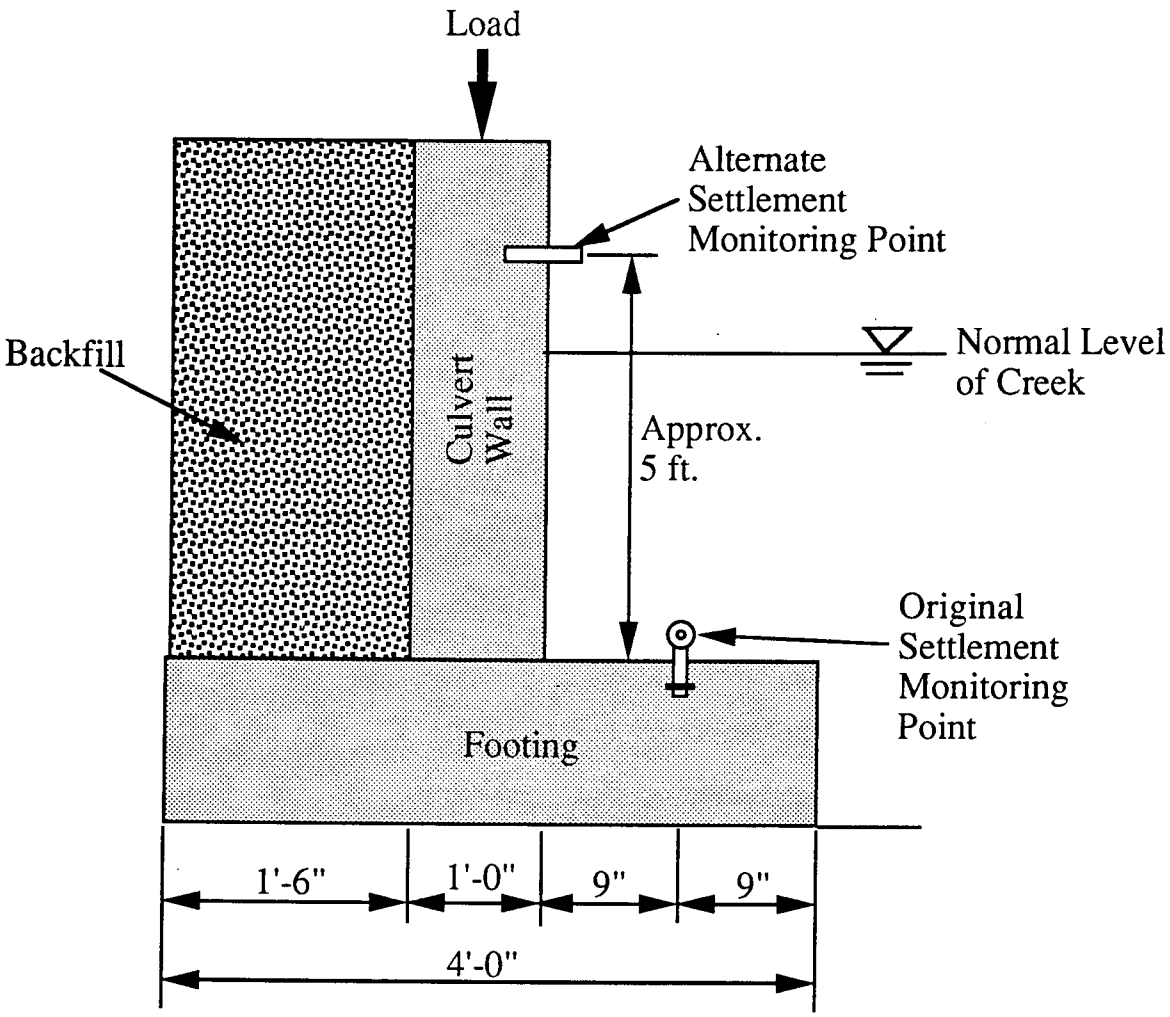

Figure 3.22 Typical Settlement Monitoring Point Installation Details (Bridge C)

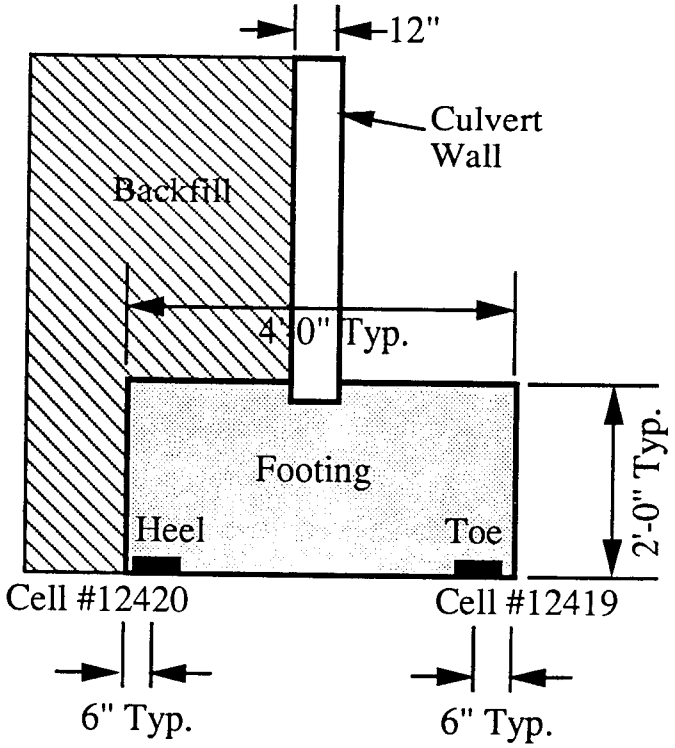

(a) General Location of Pressure Cell Installation

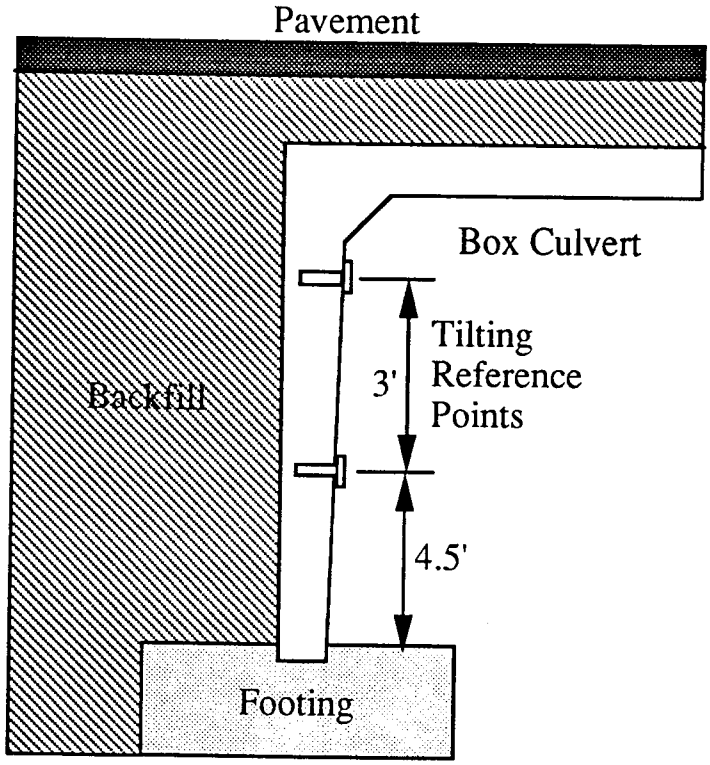

(b) General Location of Tilting Reference Points

Figure 3.23 Detailed Pressure Cell and Tilting Reference Point Installations (Bridge C)

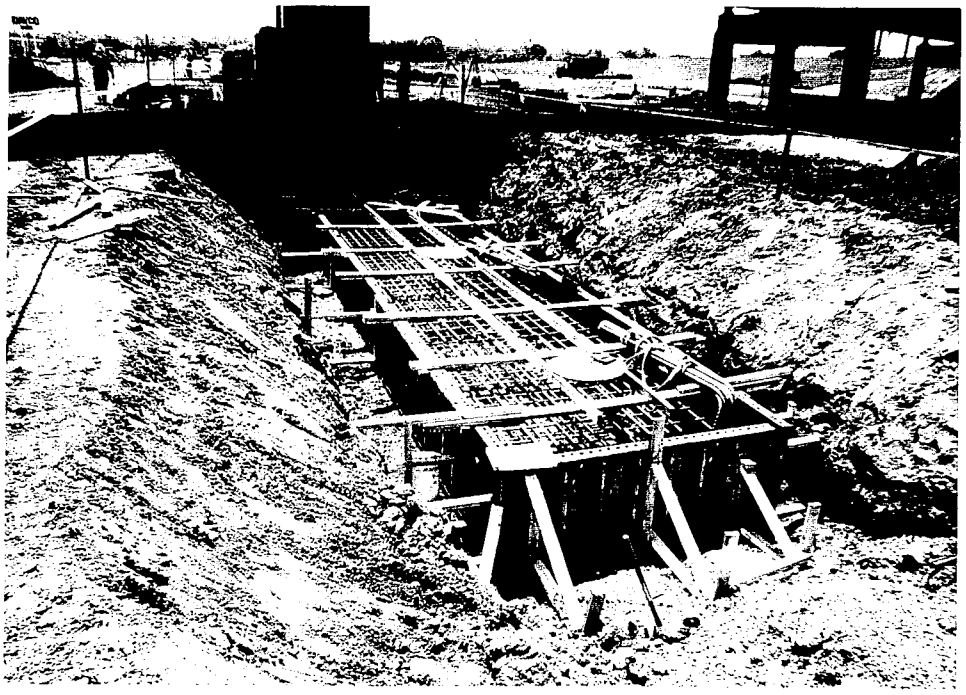

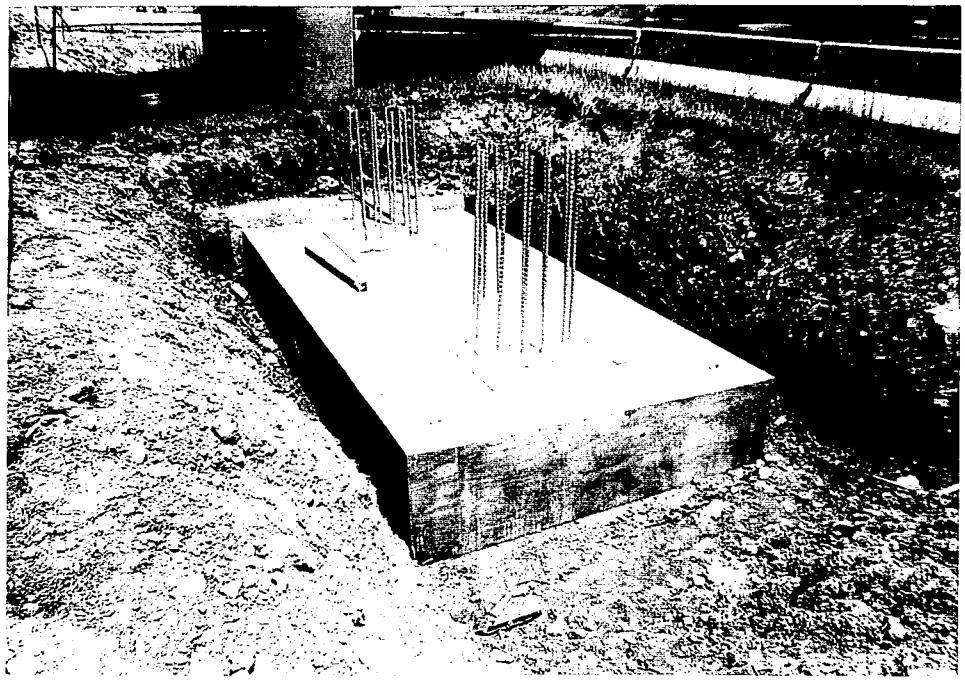

Figure 3.24 Pictures of Bridge D and Its Foundations During Construction

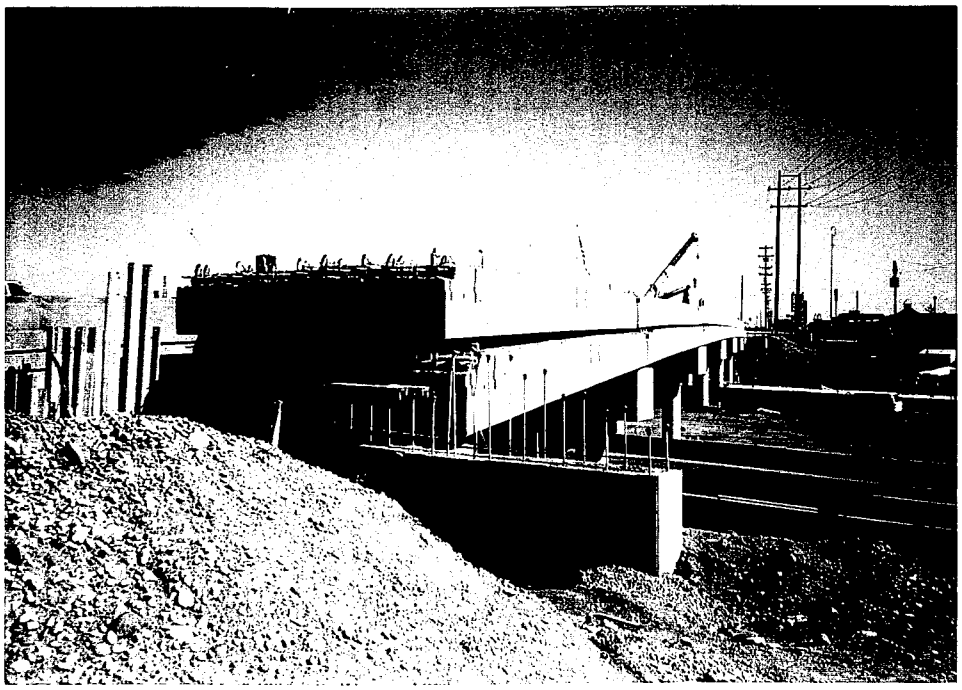

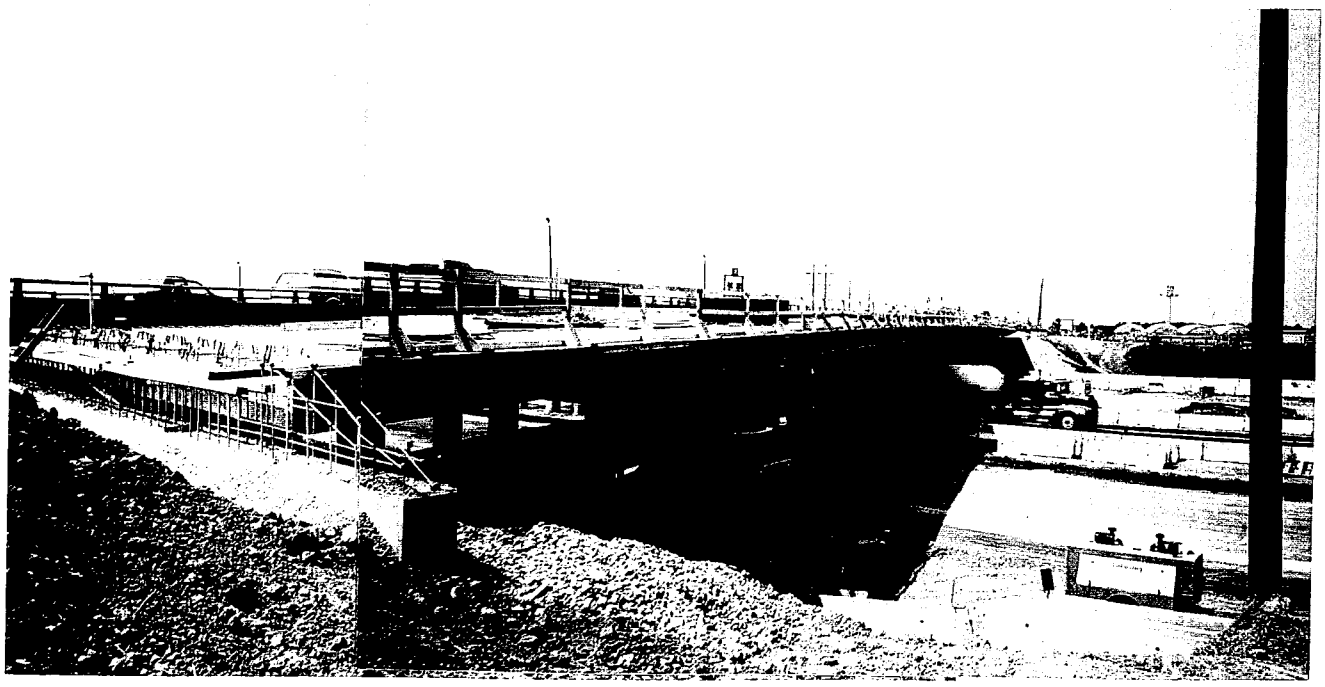

Figure 3.24 Pictures of Bridge D and Its Foundations During Construction

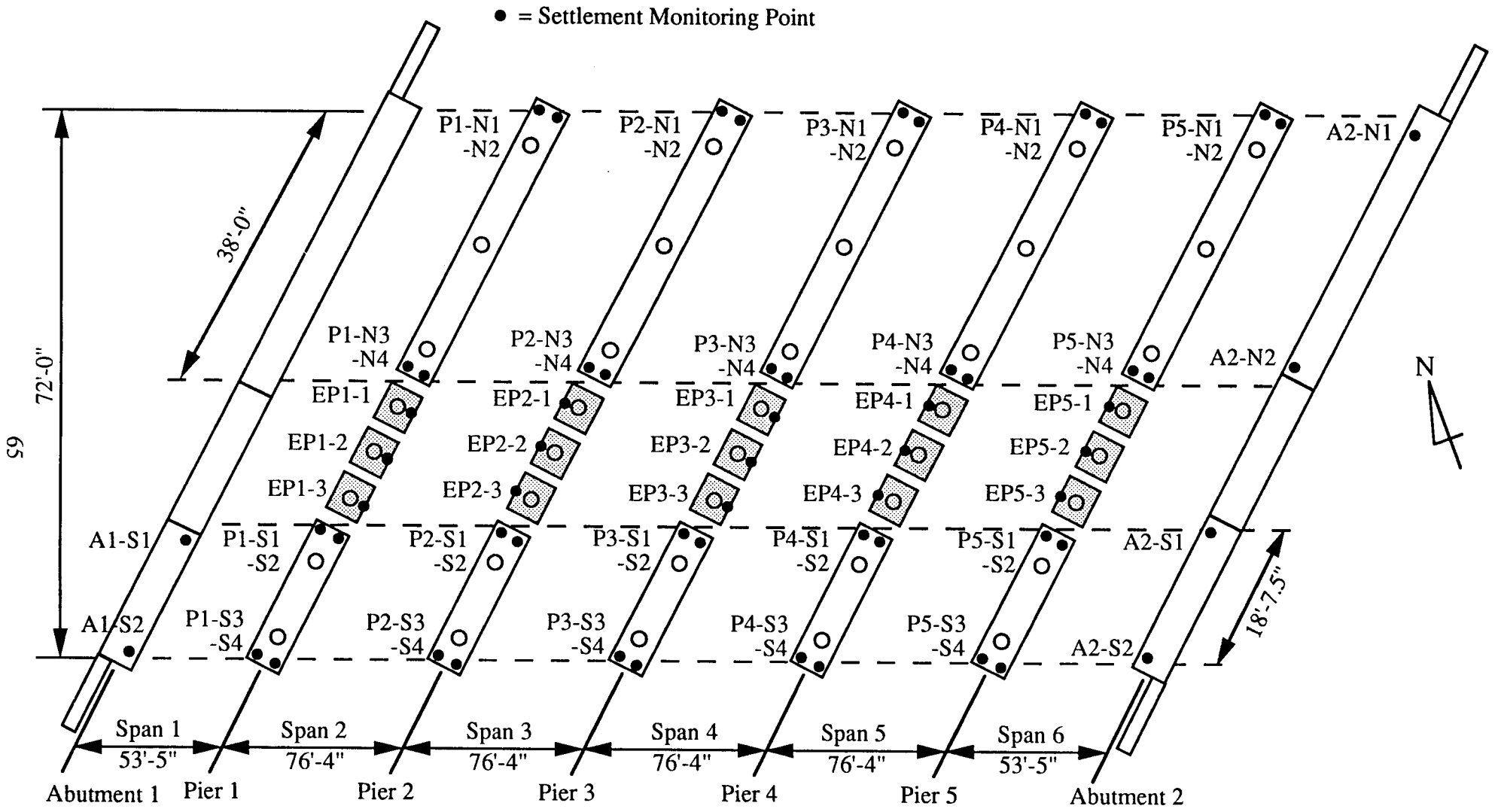

Figure 3.25.(a) Settlement Monitoring Location Plan for Bridge D

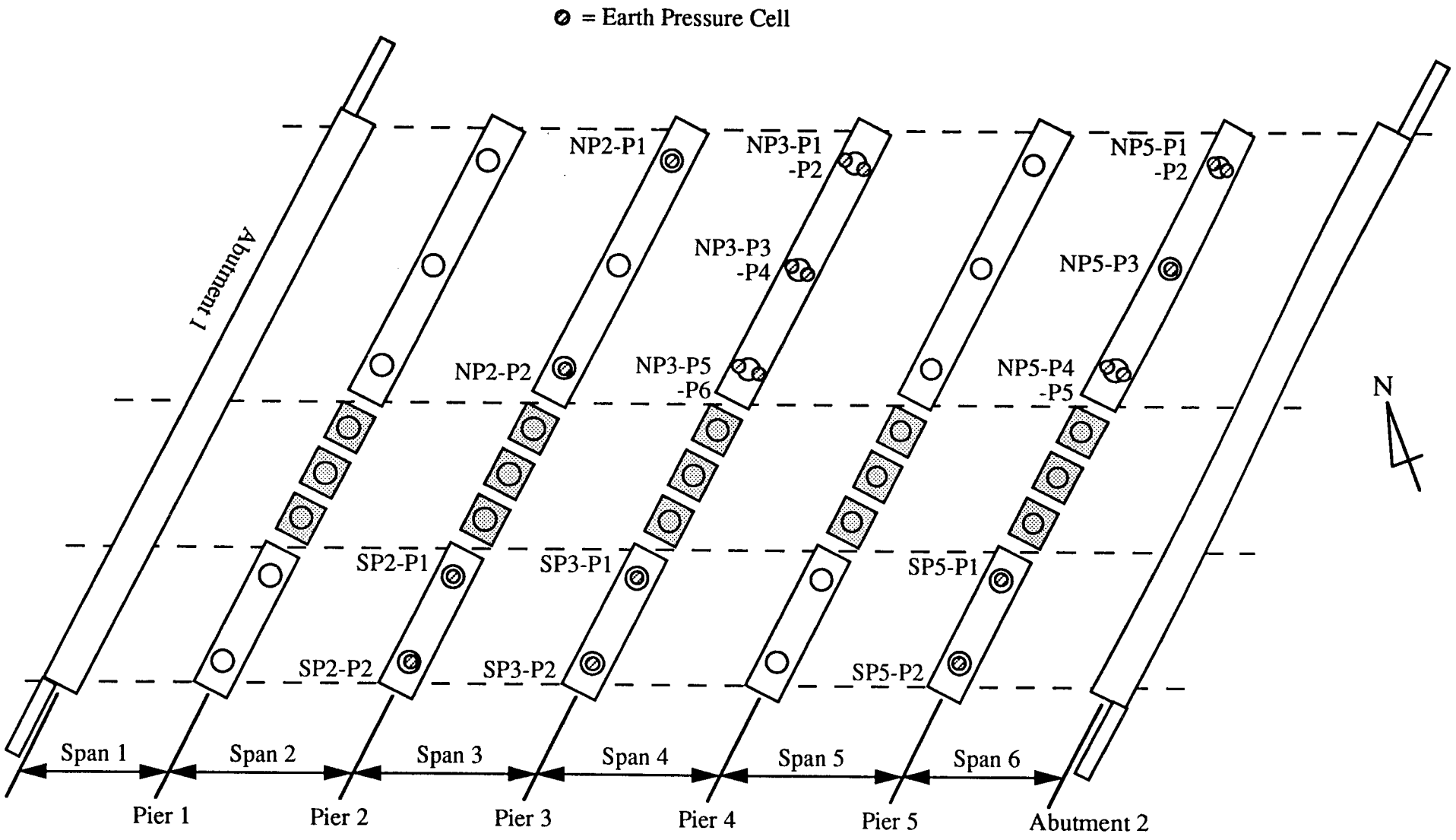

Figure 3.25.(b) Pressure Cells Location Plan for Bridge D

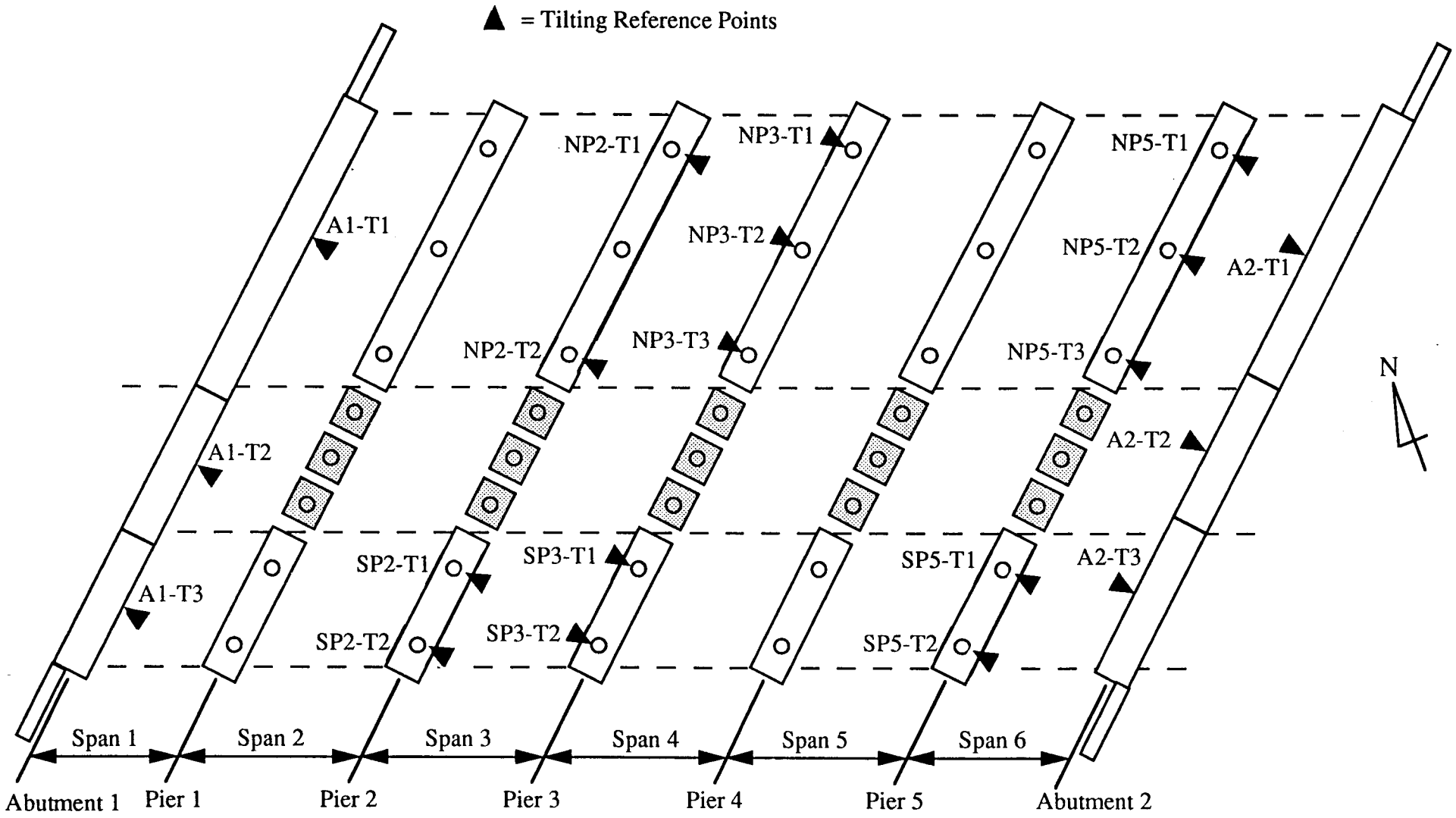

Figure 3.25.(c) Tilting Station Location Plan for Bridge D

Originally, five soil borings (B-1 through B-5) were placed at the site. Their general locations are shown in Figure A.8 (Appendix A). Soils encountered in these borings were cohesive and classified typically as A-6-a or A-6-b according to the AASHTO soil classification system. In the area of Pier 3, soils classified as A-4-a were found from a depth of 0 to 11 feet below the footing bottom. According to the boring logs, the depth to bedrock (or the depth where the SPT-N value became 100+) increased from Pier 1 to Pier 5 (from west to east). Bedrock was about 4 feet deep under Pier 1, 5 feet deep under Pier 2, and 15.5 feet deep under Pier 3. No bedrock was found within 28 feet depth in the Pier 4, Pier 5, and Abutment 2 (East Abutment) areas. The SPT-N value ranged from 30 to 60 at B-1 (near the Pier 1 area), 30 to 57 at B-3 (at the Pier 3 area), 34 to 73 at B-4. Tables A.8 through A.12 are the boring logs for these bore holes, and plots of depth vs. SPT-N value are given in Figures A.8 through A.12.

A large discrepancy in the depth to bedrock between the original boring logs and actual site conditions was realized when the excavations for spread footing construction began. The depth to bedrock was measured to be less than 5 feet below the bottom of footings in the Pier 4 and 5 areas.

Basic properties (natural moisture content, Atterberg limits) of the soils are summarized in the soil boring logs in Appendix A. Additional laboratory tests performed by the ODOT included unconfined compression tests and consolidation tests. The unconfined compression tests were conducted on soil samples recovered from Boring B-2 at a depth of 1 feet below the footing and from Boring B-4 at depths 10 feet and 16 feet below the footing. Unconfined compression strength resulted from these tests were 1.54, 3.58, and 4.0 tsf, respectively. A soil sample obtained from Boring B-3 at the footing base elevation was subjected to the standard consolidation test. Test results revealed that the soil was over-consolidated with a preconsolidation pressure of 2,000 psf.

The void ratio was 0.36, the average value of coefficient of consolidation (c_v) was 0.22 feet^2/day, and the compressibility index (C) was 0.024 based on the e-p plot.

Construction of the Phase I foundation on the north side of the old, narrow bridge structure progressed in parallel with construction of the Phase II foundation on the south side beginning the first week of June, 1993. By the end of August, 1993, all of the Phase I foundations were in place, and nine composite beams were set over each span. These beams weighed about 33 tons each. The superstructure deck of the Phase I bridge was paved with 270 cubic yards of concrete on September 17, and service load was introduced on October 23, 1993 (after 141 days). While traffic was diverted through the Phase I section of the new bridge, the deck of the old bridge was demolished and the foundations on the south side were preloaded under two layers of the composite beam from August 19, 1993 to February 14, 1994. Pier caps of the old bridge foundations were removed and replaced with new caps. Composite beams in the second layer were moved to the center section on February 14, 1994. The deck in Phase II was paved using 538 cubic yards of concrete between May 11 and June 3, 1994. Table 3.8 summarizes construction events and time schedule data. The bridge was opened to traffic on June 28, 1994, about 13 months after construction of the first Phase I pier foundation.

Figure 3.25a through 3.25c illustrates the instrumentation plan applied to Bridge D. A summary is given in Table 3.9. Pier 2, 3, and 5 foundations received more instrumentation. Four settlement monitoring points were established on each of the new pier foundations, while only one point was set near the center of each of the footings of the previous bridge. Pressure cell and tilting station installations concentrated mainly on the foundations of Pier 2, 3, and 5. In order to compare the field performance between spread footings and pile foundations, a limited amount of data were

Table 3.8.(a) Detailed Construction Records on Bridge D (Phase I)

Date	No. of Days Elapsed	Description of Construction Activities
06-04-93	0	Pier 3 and 4 footing areas excavated.
06-08-93	4	Pier 4 footing constructed.
06-10-93	6	Pier 3 footing constructed.
06-11-93	7	Pier 2 and 3 footings concreted.
06-14-93	10	Pier 2 footing constructed
06-16-93	12	Columns constructed at Pier 4 footing.
06-17-93	13	Columns placed at Pier 3 footing.
06-18-93	14	Pier 1 footing constructed. Columns placed at Pier 2 footing.
06-24-93	20	Pier 4 footing backfilled.
06-29-93	25	Pier cap constructed at Pier 4 footing.
06-30-93	26	Columns constructed at Pier 1 footing.
07-01-93	27	Pier cap constructed on top of Pier 3 footing.
07-07-93	33	Pier 3 footing backfilled.
07-12-93	38	Pier cap constructed at Pier 2 footing.
07-22-93	48	Pier cap constructed at Pier 1 footing. Pier 1 and 2 footings backfilled.
07-29-93	55	Pier 5 footing constructed.
08-02-93	59	Columns placed at Pier 5 footing.
08-13-93	70	Composite beams placed over Spans 3 and 4 (between Piers 2 and 3 and between Piers 3 and 4).
08-16-93	73	Pier cap constructed at Pier 5 footing.

Table 3.8.(a) Detailed Construction Records on Bridge D (Phase I) - cont'd

Date	No. of Days Elapsed	Description of Construction Activities
08-19-93	76	Composite beams placed over Spans 1 and 2 (between Abutment No.1 and Pier 1 and between Piers 1 and 2).
08-25-93	82	Composite beams placed over Spans 6 (between Pier 5 and Abutment No. 2).
08-30-93	87	Pier 5 footing backfilled.
08-31-93	88	Composite beams placed over Span 5 (between Piers 4 and 5).
09-17-93	105	Concrete placed as part of bridge deck construction.
10-23-93	141	Bridge opened to general traffic.

Table 3.8.(b) Detailed Construction Records on Bridge D (Phase II)

Date	No. of Days Elapsed	Description of Construction Activities
06-08-93	4	Pier 4 footing area excavated.
06-09-93	5	Pier 4 footing constructed.
06-11-93	7	Pier 2 and 3 footings constructed.
06-22-93	18	Columns built at Pier 2, 3, and 4 footings.
06-29-93	25	Pier 1 footing constructed.
07-07-93	33	Columns constructed at Pier 1 footing. Pier caps built at Pier 3 and 4 footings.
07-08-93	34	Pier 4 footing backfilled.
07-09-93	35	Pier 3 footing backfilled.
07-15-93	41	Pier cap placed at Pier 2 footing.
07-22-93	48	Pier 1 and 2 footings backfilled.
07-27-93	53	Pier cap placed at Pier 1 footing.
07-29-93	55	Pier 5 footing constructed.
08-02-93	59	Columns constructed at Pier 5 footing.
08-09-93	66	Pier cap constructed at Pier 5 footing columns.
08-19-93	76	Composite beams (first layer) placed over Spans 3 and 4 (between Piers and 3 and between Piers 3 and 4).
08-25-93	82	Composite beams (first layer) placed over Spans 1 and 2 (between Abutment No. 1 and Pier 1 and between Piers 1 and 2).
08-30-93	87	Pier 5 footing backfilled.
10-20-93	138	Composite beams (first layer) placed over Spans 5 and 6 (between Piers 4 and 5 and between Pier 5 and Abutment No. 2).

Table 3.8.(b) Detailed Construction Records on Bridge D (Phase II) - cont'd

Date	No. of Days Elapsed	Description of Construction Activities
10-20-93	138	Additional composite beams (second layer) placed over Spans 1 through 6.
02-14-94	255	Composite beams (second layer) removed over Span 1.
02-16-94	257	Composite beams (second layer) removed over Span 2.
02-19-94	260	Composite beams (second layer) removed over Span 3.
02-21-94	262	Composite beams (second layer) removed over Span 4.
02-23-94	264	Composite beams (second layer) removed over Span 5.
02-25-94	266	Composite beams (second layer) removed over Span 6.
06-03-94	391	Concrete paving completed on the deck.
06-18-94	406	Entire bridge (Phases I and II) opened to general traffic.

(Note) Modifications of the pier caps on the pre-existing footings were done between 11-23-93 and 01-26-94.

Table 3.9 Amount of Instrumentations per Foundation (Bridge D)

Location		No. of Sensors to Monitor :		
		Settlement	Contact Pressure	Tilting
Abutment No. 1	North	2	0	1
	Center	0	0	0
	South	2	0	1
Pier 1	North	4	0	0
	Old	3	0	0
	South	4	0	0
Pier 2	North	4	2	2
	Old	3	0	0
	South	4	2	2
Pier 3	North	4	6	3
	Old	3	0	0
	South	4	2	2
Pier 4	North	4	0	0
	Old	3	0	0
	South	4	0	0
Pier 5	North	4	5	3
	Old	3	0	0
	South	4	2	2
Abutment No. 2	North	2	0	1
	Center	0	0	0
	South	2	0	1
TOTAL		43	19	18

obtained from the monitoring points established on the abutments. Three bench marks, including the one used by the contractor, were used in all level survey work. Field performance data were collected until July 21, 1994, about one month beyond the opening of the entire bridge.

3.7 Bridge E

This bridge, having nine spans, was the longest of the five bridges examined in this study. It was constructed in two phases to replace an aging bridge structure which had existed since 1930 on State Route 32 over Consolidation Rail and State Route 35, in southeast Cincinnati, Hamilton County, Ohio. This construction was initiated due to the poor condition of the existing bridge structure. The new bridge had a width of 54 feet and an overall length of 670 feet (bearing to bearing). The longest span dimension was 86.2 feet. It was supported by eight composite pier foundations and two abutments. Each of these foundations was partitioned into Phase I (south side) and Phase II (north side). The Phase I section of the bridge was built parallel to the existing bridge on the south side. Once traffic was diverted to the Phase I bridge section, demolition of the old bridge took place. Construction of Phase II foundations, except for the rear abutment, involved placement of 42-inch diameter, 18-feet long drilled pier shafts along the north edge. This was done to protect an existing brick sewer line by transferring the load to soils below the line. Figure 3.29 illustrates a layout of foundations for the new bridge. General views of the new bridge structure are shown in the pictures in Figure 3.26. The ADT was reported to be 35,234 in 1991 and projected to be 47,189 by the year 2011.

The site lies on the northern end of the Cincinnati Arch, the major structural feature of western Ohio, and the drainage basin of the Little Miami River. Soils are glacial moraine of the

Figure 3.26 Pictures of Bridge E and Its Foundations During Construction

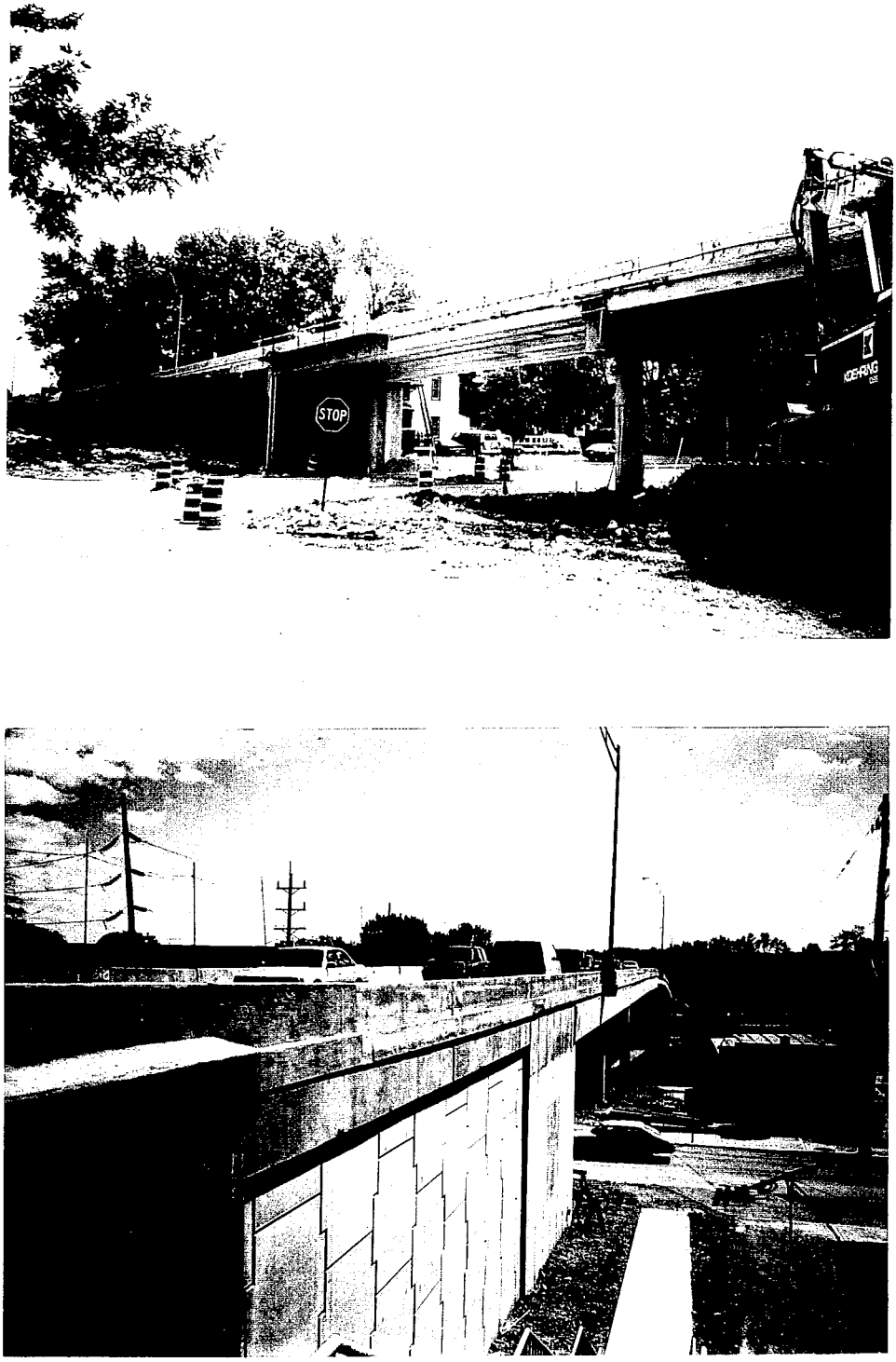

Figure 3.26 Pictures of Bridge E and Its Foundations During Construction

Illinoisan and Wisconsin ages. The uppermost portion of the bedrock is composed of alternating strata of blue-gray limestone and blue to dark blue shales of the Upper Ordovician Cincinnati series. The limestone is generally coarse in texture and highly fossiliferous. The shale is weathered, soft, and calcareous.

Ten borings, designated as Borings H-1 through H-4 and H-6 through H-11, were placed in the bridge construction area to depths ranging from 40 feet to 95 feet at this site. Logs for these boreholes are included in Appendix A (Tables A.13 through 22). A few different soil types were encountered in these boreholes. The dominant soil type was a silty clay soil and classified as A-7-6, A-6-a, or A-6-b, according to the AASHTO system. In the rear abutment area, soils classified as A-2-7 and A-1-b were detected over the bedrock. A similar granular soil, A-1-a or A-1-b, was found below the clayey soil at a depth 15 to 20 feet between the forward abutment and Pier 2. The depth to bedrock below the bottom of the new foundation was 9.3 feet at the rear abutment, 8.7 ft, at Pier 1, 16.7 feet at Pier 2, 33 feet at Pier 3, 79.5 feet at Pier 5, and 75.5 feet at the forward abutment. No bedrock was reached within 85 feet depth between Pier 6 and Pier 8. An estimated soil profile is drawn for the entire site are in Figure 3.27. No groundwater was encountered in Borings H-1 through H-7 (between the rear abutment and Pier 6). Water was found in the granular soil, Type A-1-a, about 30 feet below the footing bottom elevation at Piers 7 and 8. The SPT-N value ranged from 5 to 100+ at Boring H-1 (near the rear abutment), 9 to 100 + at Boring H-2 (near Pier 1), 7 to 100 + at Boring H-3 (near Pier 2), 9 to 32 at Boring H-4 (near Pier 3), 8 to 56 at Boring H-6 (near Pier 5), 6 to 76 at Boring H-7 (near Pier 6), 4 to 77 at Boring H-8 (near Pier 7), 6 to 21 at Boring H-9 (near Pier 8), and 6 to 51 at Boring H-10 (near forward abutment). Figures A.13 through A.22 in Appendix A plot variations of SPT-N values with depth below the footings. Due to the presence of

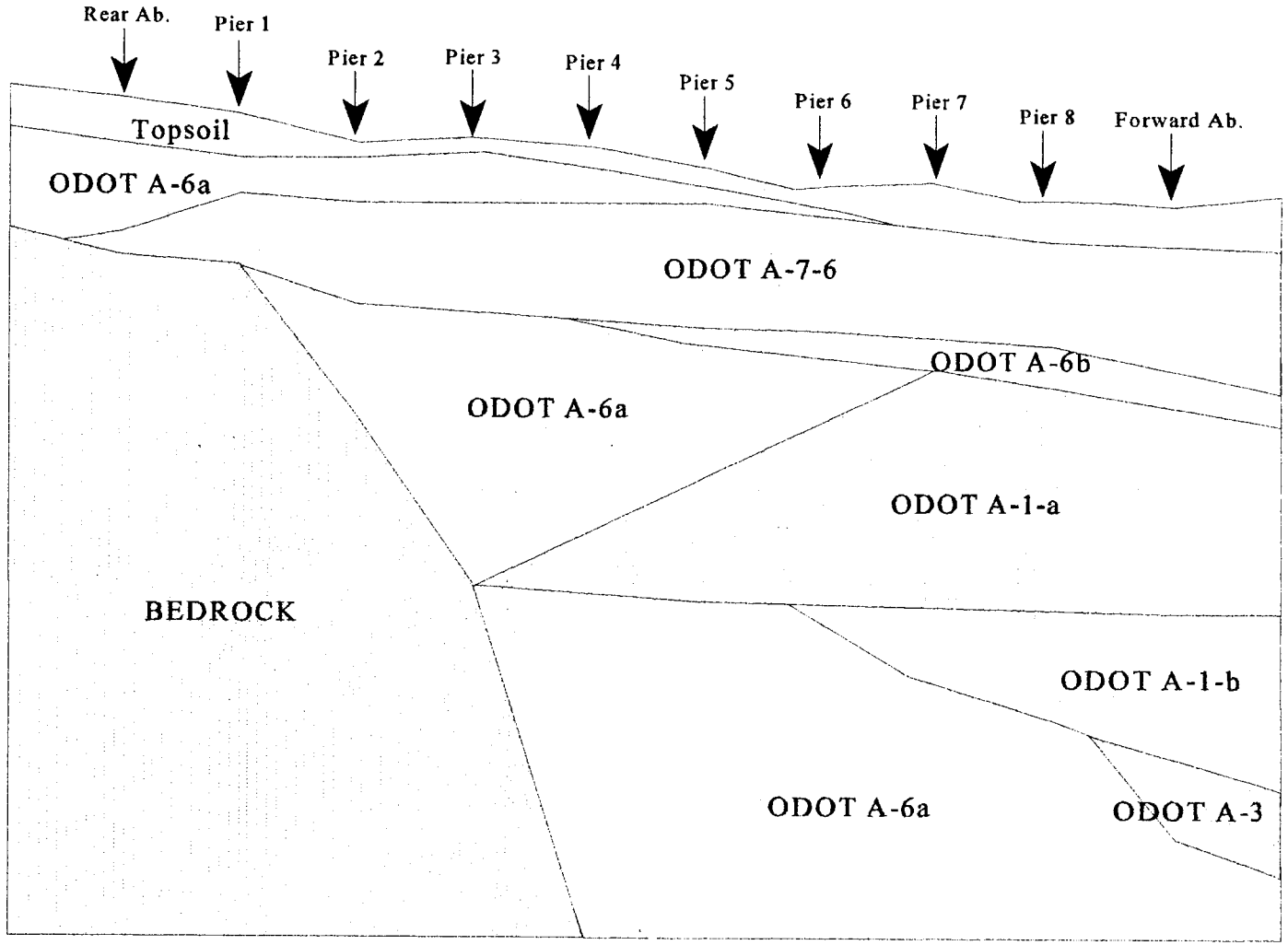

FIGURE 3.27 General Soil Profile at Bridge E Site

the adjacent sewer and the soft soils in some of these borings, a consultant was reluctant to recommend using spread footings at this site. Their estimated maximum settlements under the dead and service loads were 1.5 inch (total) and 0.5 inch (differential).

Construction work for the new bridge began in mid-March, 1994. It was divided into two phases to maintain traffic during construction. The gap between the Phase I and Phase II footings varied from 3 inch (equaling the thickness of contraction joint material) at both abutments and Piers 3 and 4 to 3.25 feet at Piers 1, 2, and 5 through 8. Phase I foundations were constructed on the south side of the existing bridge from March to May 24, 1994 while traffic was maintained. During the Phase I footing construction, the bearing soil layer received different treatment prior to concreting. For example, the top 2 to 3 inches of soil was replaced with a compacted crushed limestone (meeting ODOT #305 gradation specifications) layer in the Phase I-Pier 8 and forward abutment footing construction areas. In the Phase I-Pier 3 and 5 footing areas, old concrete footings were unearthed during excavation. These extended to depths of 2.0 to 2.5 feet below the planned bottom elevations of the new footings. These foundations were fully removed, and concrete with no reinforcements was poured to fill the cavities up to the bottom elevations of the new footings. Boundaries of the unreinforced concrete layer extended beyond all four edges of the new footings no top, covering an area of 16 feet by 30 feet at Pier 3 and 21 feet by 28 feet at Pier 5. A similar situation was encountered in the Phase I-rear abutment construction zone, and the same remedial measures were taken there as well. However, the unreinforced concrete was placed inside panels outlining the edges of the planned new footing. The base concrete was poured in a manner such that it would have a key way open through it. At Pier 1, a small pocket of very weak, organic soil was found within the north half of the footing construction area. This soil was removed and replaced with concrete. The

unreinforced concrete layer was fully contained inside the outline of the new footing. At Pier 1, crushed limestone material was compacted to fill in a void created by removing an old foundation. Figure 3.28 illustrates each of these special cases of treating the bearing layers in the Phase I construction side.

Starting from May 25, 1994, concrete box beams were placed across each span of the Phase I bridge. On July 15, 1994, 378 and 194 cubic yards of concrete were placed for the deck and parapets. At the completion of the Phase I bridge deck construction on August 6, 1994 (after about five months), traffic was moved to the new bridge. Both foundations and superstructure of the old bridge were then removed entirely. Construction of the Phase II foundations lasted from early September to October, 1994. A sandy soil, meeting the specifications of ODOT #310 was used to backfill behind the abutments. Table 3.10 summarizes the construction sequence and time schedule data for Bridge E.

Figures 3.29a through 3.29c present the overall instrumentation plan implemented on Bridge E, with instrumentation installed on each footing structure summarized in Table 3.11. The Phase I side received more instrumentations than the Phase II side because these foundations were all simple spread footings (no drilled pier shafts were tied in). Although every foundation received at least one settlement monitoring point, most of the instrumentation efforts were made on Pier 1 (Phase I), Pier 3 (Phase I), Pier 6 (Phase I), Pier 8 (Phase I), and the Phase I abutments. Location of the four pressure cells at Pier 8 differ from the original symmetric layout because of an error surveyors made in staking out the area (the error was discovered just prior to concreting, and panels were moved at the last minute). Figure 3.30 compares the original and final pressure cell installation plan for the pressure cells under Pier 1 (Phase I). Under Pier 3 and rear abutment (Phase I) footings,

* Footing on In-Situ Clay Soil : Pier 4, Pier 6, Pier 7

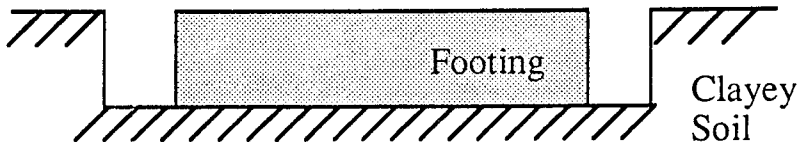

* Footing on Compacted 3"-4" Crushed Limestone Layer:
Forward Abutment, Pier 1, Pier 8

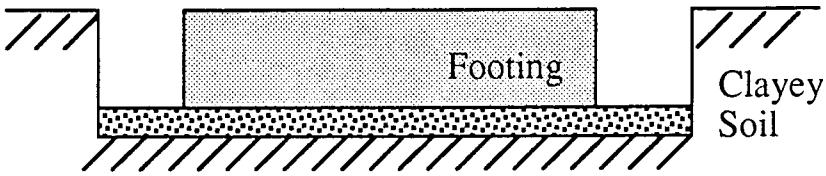

* Footing on Unreinforced Concrete Slab :
Pier 3, Pier 5, Rear Abutment

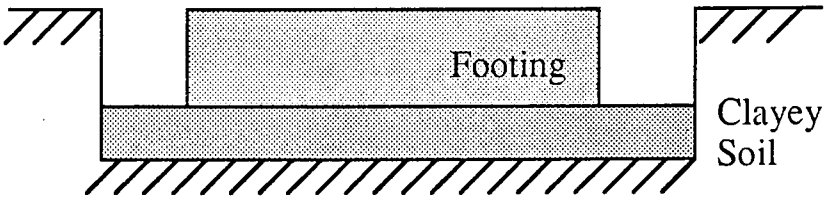

* Footing Partially on Unreinforced Concrete Slab : Pier 2

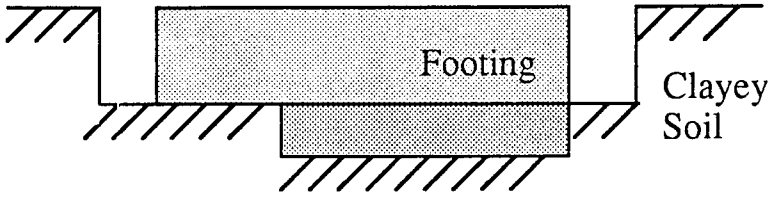

Figure 3.28 Different Practices Observed in Preparing Top of Bearing Layer for Phase I Foundations (Bridge E)

Table 3.10.(a) Detailed Construction Records on Bridge E (Phase I)

Date	No. of Days Elapsed	Description of Construction Activities
03-10-94	0	Initiation of construction work.
03-14-94	4	Forward Abutment and Pier 8 foundation construction areas excavated.
03-16-94	6	Pier 8 footing placed.
03-17-94	7	Forward Abutment foundation placed.
03-18-94	8	Pier 6 and 7 footings placed.
03-23-94	13	Pier 3 footing constructed.
03-25-94	15	Pier 5 footing placed. Columns placed at Pier 8 footing.
03-28-94	18	Forward Abutment wall constructed.
03-29-94	19	Columns placed at Pier 5 footing.
03-31-94	21	Rear Abutment foundation placed.
04-01-94	22	Pier 7 columns constructed.
04-04-94	25	Pier 2 footing constructed.
04-05-94	26	Pier 1 footing constructed.
04-06-94	27	Pier 6 columns placed.
04-07-94	28	Pier 5 footing backfilled. Cap for Pier 8 columns placed.
04-13-94	34	Columns placed at Pier 2 footing. Cap for Pier 5 structure placed.
04-14-94	35	Wall constructed at Pier 3 footing.
04-19-94	40	Cap for Pier 7 columns placed.
04-21-94	42	Rear Abutment wall constructed.
04-22-94	43	Cap for Pier 6 columns placed.
04-26-94	47	Pier 1, 2, and 8 footings backfilled.
04-29-94	50	Cap for Pier 1 columns placed.

Table 3.10.(a) Detailed Construction Records on Bridge E (Phase I)

Date	No. of Days Elapsed	Description of Construction Activities
03-10-94	0	Initiation of construction work.
03-14-94	4	Forward Abutment and Pier 8 foundation construction areas excavated.
03-16-94	6	Pier 8 footing placed.
03-17-94	7	Forward Abutment foundation placed.
03-18-94	8	Pier 6 and 7 footings placed.
03-23-94	13	Pier 3 footing constructed.
03-25-94	15	Pier 5 footing placed. Columns placed at Pier 8 footing.
03-28-94	18	Forward Abutment wall constructed.
03-29-94	19	Columns placed at Pier 5 footing.
03-31-94	21	Rear Abutment foundation placed.
04-01-94	22	Pier 7 columns constructed.
04-04-94	25	Pier 2 footing constructed.
04-05-94	26	Pier 1 footing constructed.
04-06-94	27	Pier 6 columns placed.
04-07-94	28	Pier 5 footing backfilled. Cap for Pier 8 columns placed.
04-13-94	34	Columns placed at Pier 2 footing. Cap for Pier 5 structure placed.
04-14-94	35	Wall constructed at Pier 3 footing.
04-19-94	40	Cap for Pier 7 columns placed.
04-21-94	42	Rear Abutment wall constructed.
04-22-94	43	Cap for Pier 6 columns placed.
04-26-94	47	Pier 1, 2, and 8 footings backfilled.
04-29-94	50	Cap for Pier 1 columns placed.

Table 3.10.(b) Detailed Construction Records on Bridge E (Phase II)

Date	No. of Days Elapsed	Description of Construction Activities
08-26-94	169	Pier 5 and Forward Abutment foundations in place.
08-27-94	170	Pier 6 and 8 footings constructed.
09-01-94	175	Pier 4 and 7 footings constructed. Columns placed at Pier 5 footing.
09-02-94	176	Columns constructed at Pier 8 footing.
09-07-94	181	Pier 2 footing constructed.
09-08-94	182	Rear abutment foundation placed.
09-09-94	183	Columns for Pier 2 structure placed.
09-10-94	184	Pier cap constructed at Pier 5 footing.
09-12-94	186	Forward Abutment wall built.
09-18-94	192	Pier 1 and 3 footings constructed. Columns constructed at Pier 4, 6, and 7 footings. Pier cap placed at Pier 2 and 8 footings. Pier 2, 5, and 8 footings backfilled.
09-23-94	197	Pier cap constructed at Pier 7 footing.
09-25-94	199	Rear Abutment wall constructed. Columns placed at Pier 1 footing. Pier 4, 6, and 7 footings backfilled. Toe section of Forward Abutment backfilled.
09-28-94	202	Pier cap placed at Pier 6 footing.
10-02-94	206	Wall constructed at Pier 3 footing. Pier cap constructed at Pier 1 foundation. Pier 3 footing backfilled.
10-08-94	212	Concrete box beams placed over Span 9 (between Piers 8 and Forward Abutment).
10-10-94	214	Concrete box beams placed over Span 8 (between Piers 7 and 8).

Table 3.10.(b) Detailed Construction Records on Bridge E (Phase II) - cont'd

Date	No. of Days Elapsed	Description of Construction Activities
10-11-94	215	Pier 1 footing backfilled.
10-12-94	216	Concrete box beams placed over Span 7 (between Piers 6 and 7).
10-14-94	218	Concrete box beams placed over Span 6 (between Piers 5 and 6).
10-16-94	220	Concrete box beams placed over Span 5 (between Piers 4 and 5). Toe section of Rear Abutment backfilled.
10-18-94	222	Concrete box beams placed over Span 4 (between Piers 3 and 4).
10-20-94	224	Concrete box beams placed over Span 3 (between Piers 2 and 3).
10-22-94	226	Concrete box beams placed over Span 2 (between Piers 1 and 2).
10-24-94	228	Concrete box beams placed over Span 1 (between Rear Abutment and Pier 1).
11-06-94	241	Backfilling behind Rear Abutment completed.
03-23-95	379	Bridge deck paved.
05-17-95	434	Backfilling behind Forward Abutment completed.
07-01-95	479	Entire bridge opened to traffic.

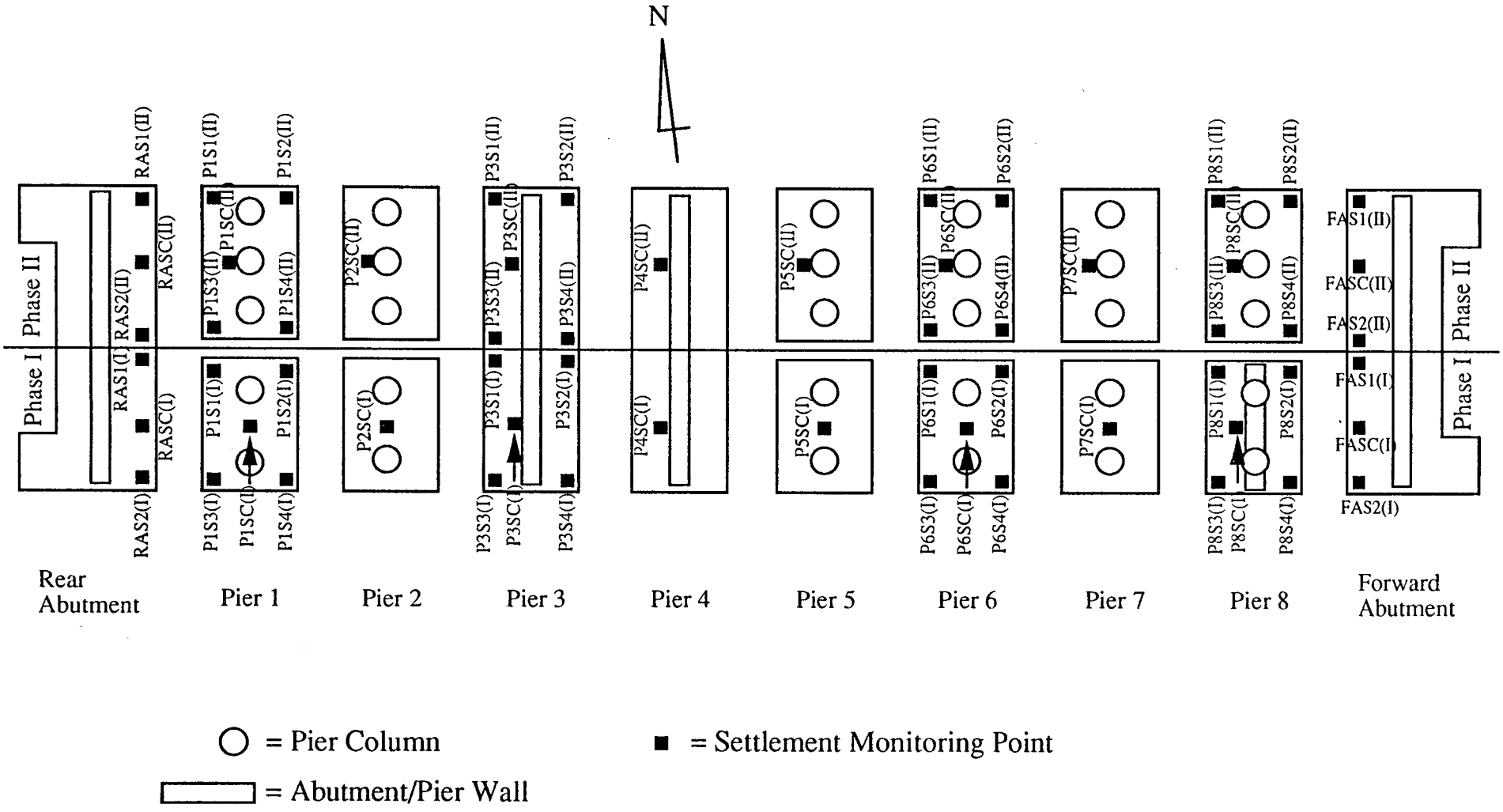

Figure 3.29.(a) Settlement Monitoring Points Location Plan (Bridge E)

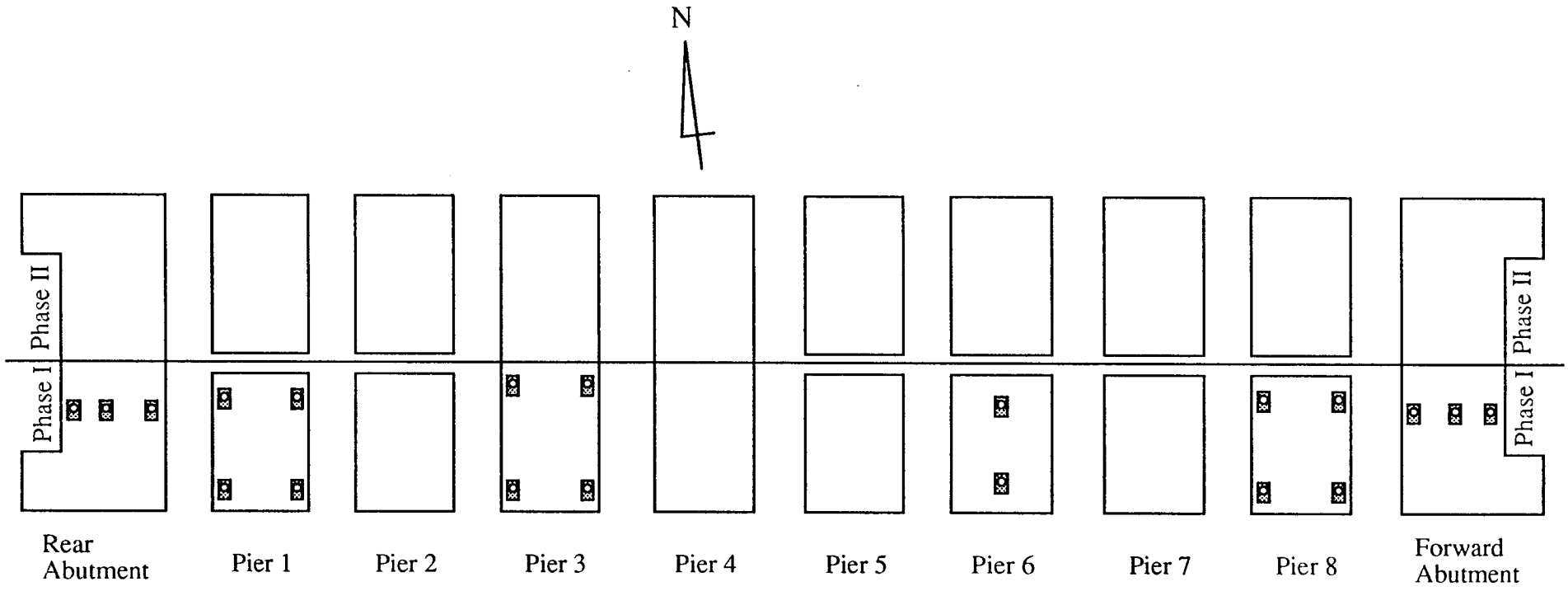

Figure 3.29.(b) Contact Pressure Cell Location Plan (Bridge E)

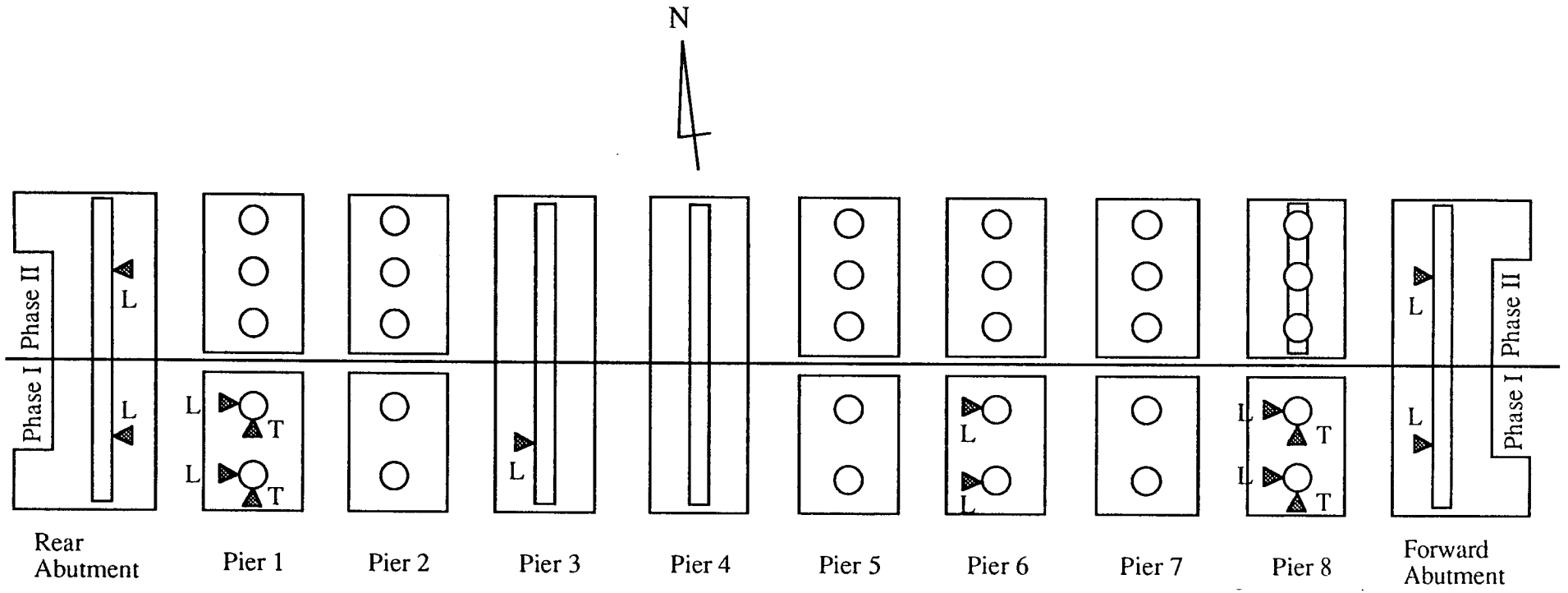

Figure 3.29.(c) Tilting Measurement Stations Location Plan (Bridge E)

Table 3.11 Amount of Instrumentations per Foundation (Bridge E)

Location		No. of Sensors to Monitor :		
		Settlement	Contact Pressure	Tilting
Rear Abutment	Phase I	3	3	1
	Phase II	3	0	1
Pier 1	Phase I	5	4	4
	Phase II	5	0	0
Pier 2	Phase I	1	0	0
	Phase II	1	0	0
Pier 3	Phase I	5	4	1
	Phase II	5	0	0
Pier 4	Phase I	1	0	0
	Phase II	1	0	0
Pier 5	Phase I	1	0	0
	Phase II	1	0	0
Pier 6	Phase I	5	2	2
	Phase II	5	0	0
Pier 7	Phase I	1	0	0
	Phase II	1	0	0
Pier 8	Phase I	5	4	4
	Phase II	5	0	0
Forward Abutment	Phase I	3	3	1
	Phase II	3	0	1
TOTAL		60	20	15

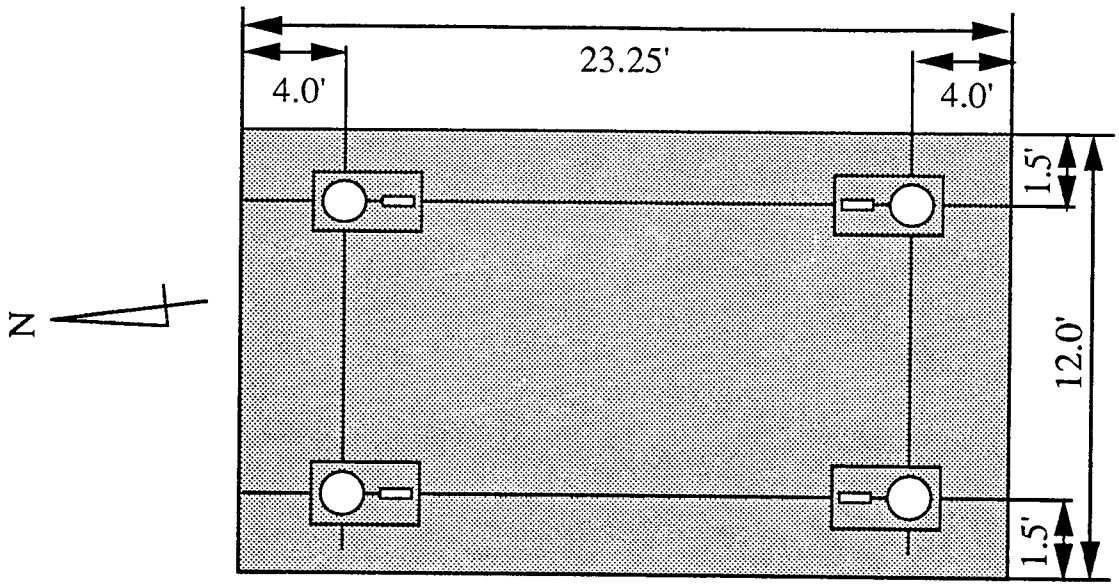

(a) Original Pressure Cell Location Plan

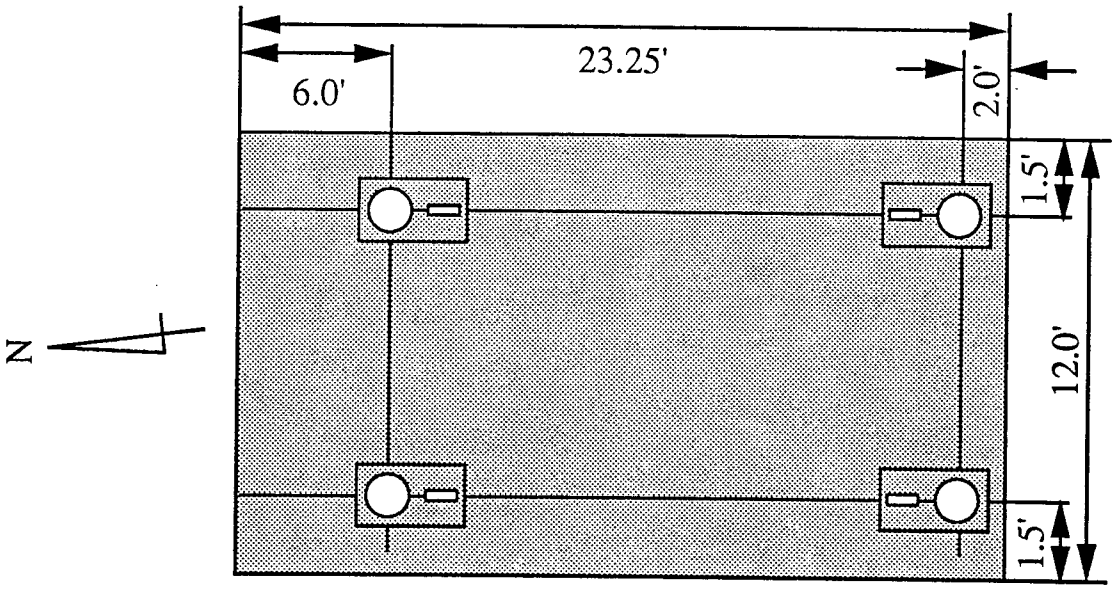

(b) Actual Pressure Cell Locations in Field

Figure 3.30 Changes in Pressure Cell Location Plan for Pier 8 (Phase I) -- Bridge E

pressure cells were installed at the base of the unreinforced concrete layer. One new aspect of tilt monitoring introduced at this site was installation of stations in the transverse directions of the bridge, as well as those in the usual longitudinal direction. Field performance was monitored until September 29, 1995, about three months beyond the opening of the entire bridge structure.

Chapter 4

Field Measured Performance

4.1 General

This chapter presents field monitored performance of the five spread footing supported bridge structures in terms of each of the performance criteria identified in Section 3.2. Field performances are presented in many graphical plots against the construction stages instead of the elapsed time, so that impact of each construction phase can be easily identified. Each discussion points out similar and/or contrasting behaviors exhibited among the foundations. Comparison of the field monitored data with predictions of theoretical/empirical formulas will be provided in Chapter 5.

4.2 Overall Settlement

Overall settlement was monitored from the time the footing was constructed to the time service load was applied. Figures 4.1 and 4.6 present average settlement of all the footings of Bridge A structure. Figures 4.7 through 4.9 plot average settlement versus construction stage for the three foundations of Bridge B. Settlement performance of the Bridge C footing is shown in Figures 4.10 and 4.11. Figures 4.12 through 4.24 are dedicated to present settlement behaviors of the Bridge D foundations. Finally, similar plots showing settlement performance of the Bridge E foundations are attached in Appendix B.

At the Bridge A construction site, average overall settlement of the foundations ranged from 0.4 to 1.5 inches. A review of the plots indicates that the footings located on the south side had greater settlement. This can be supported by the fact that the SPT-N values were slightly lower in

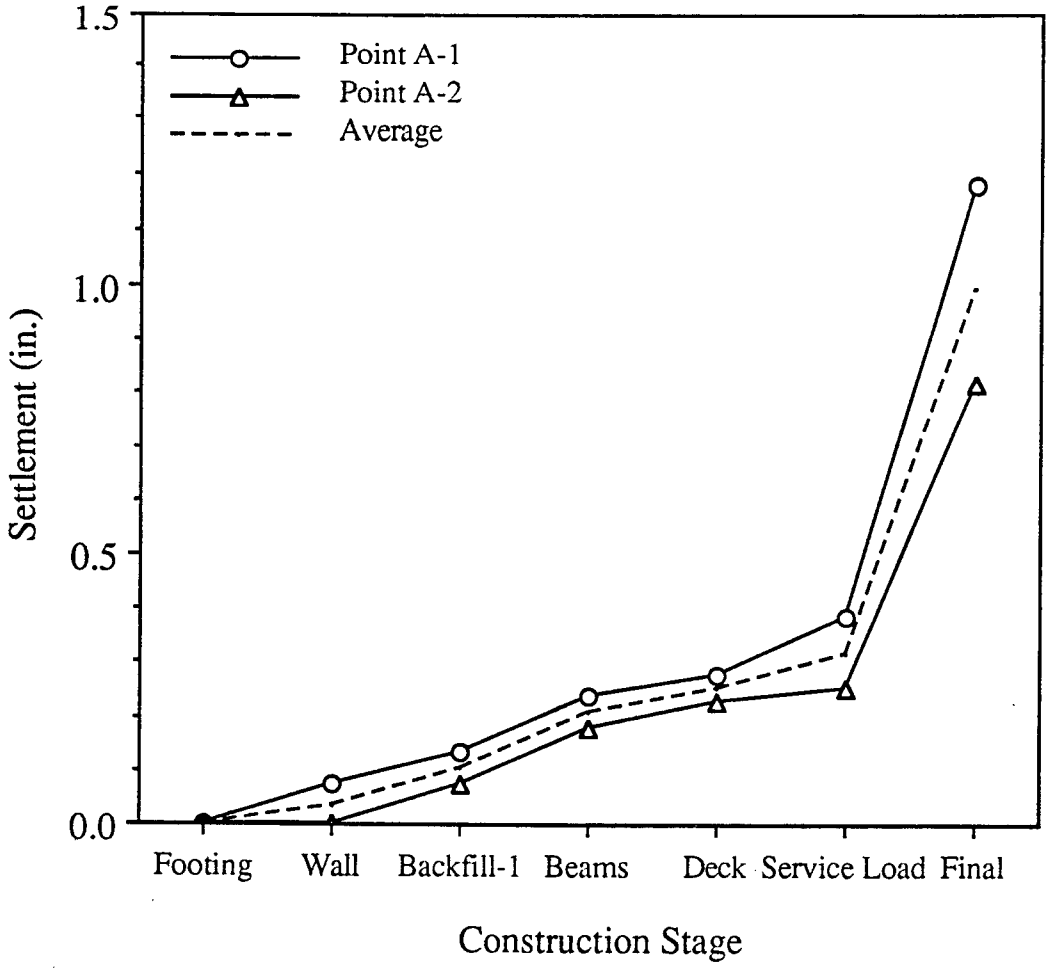

Figure 4.1 Settlement Performance of Panel "A/B" Footing (Bridge A)

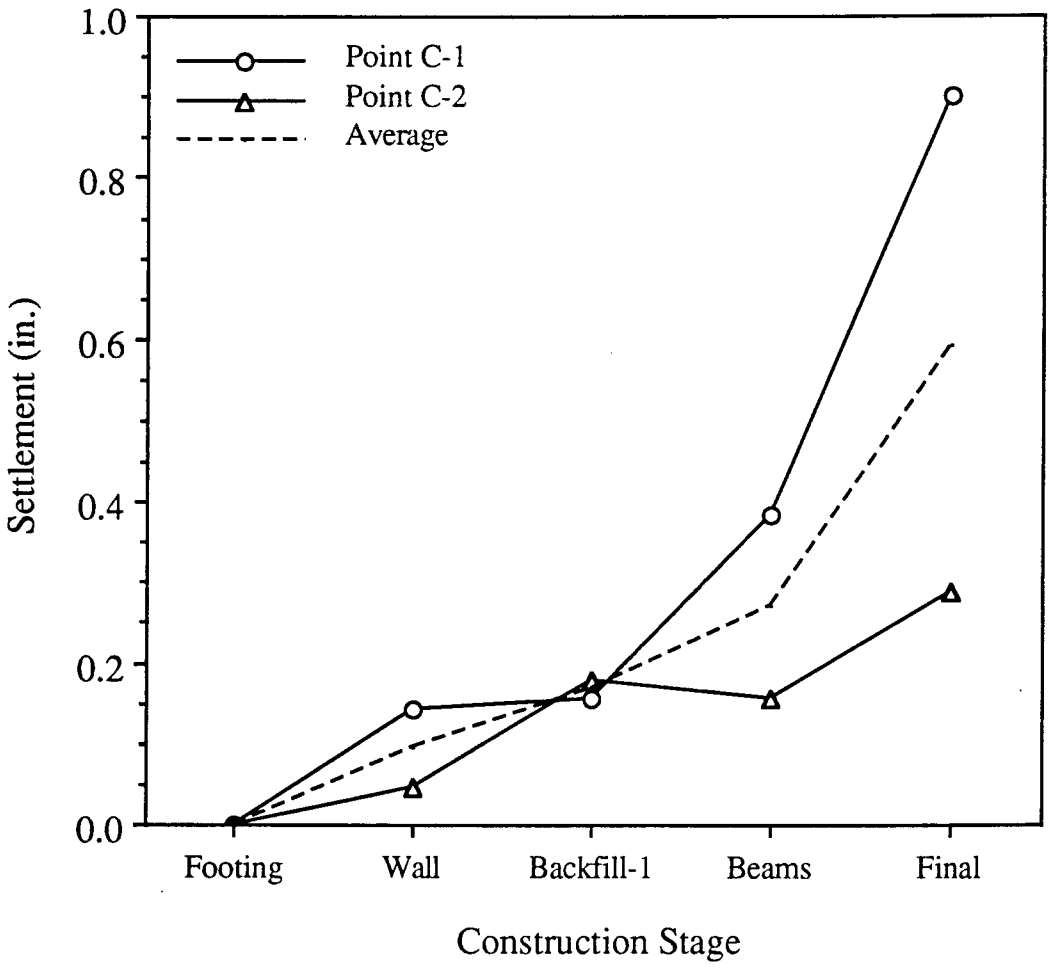

Figure 4.2 Settlement Performance of Panel "C" Footing (Bridge A)

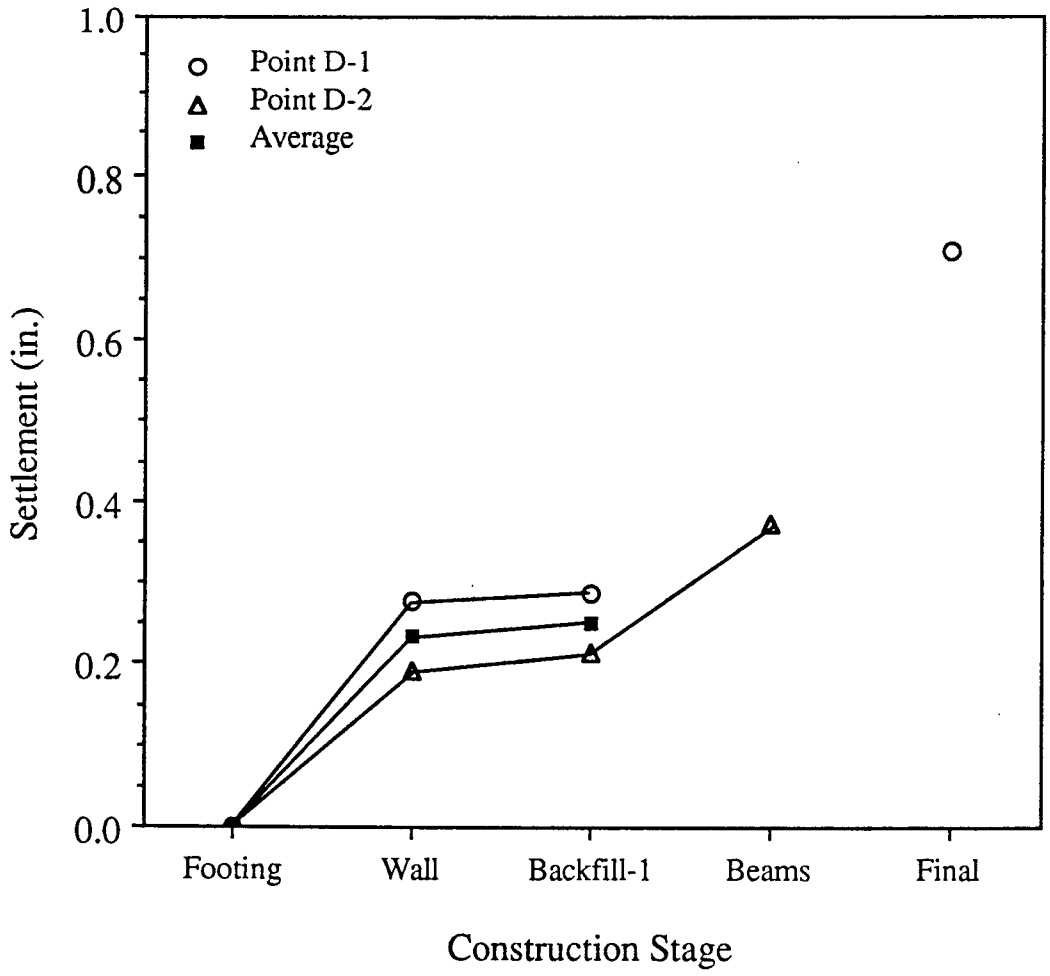

Figure 4.3 Settlement Performance of Panel "D" Footing (Bridge A)

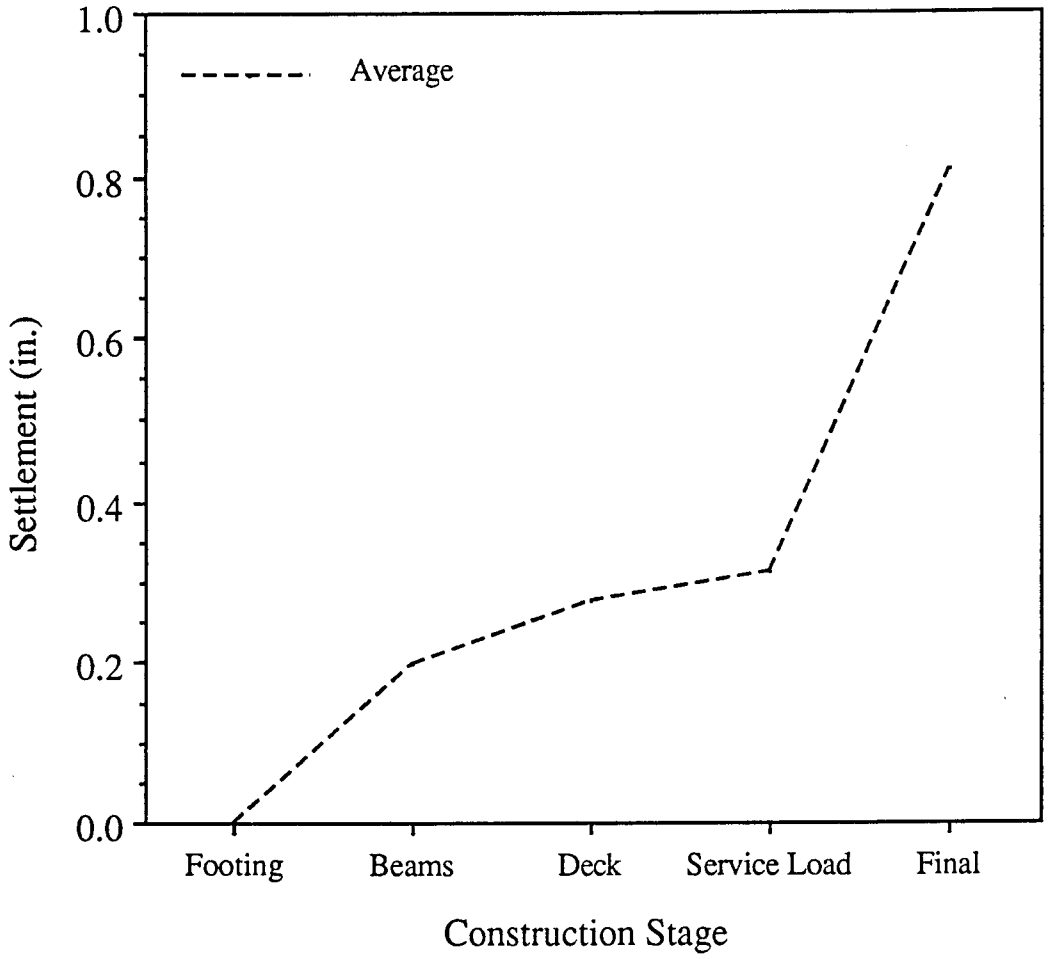

Figure 4.4 Settlement Peformance of Panel "E" Footing (Bridge A)

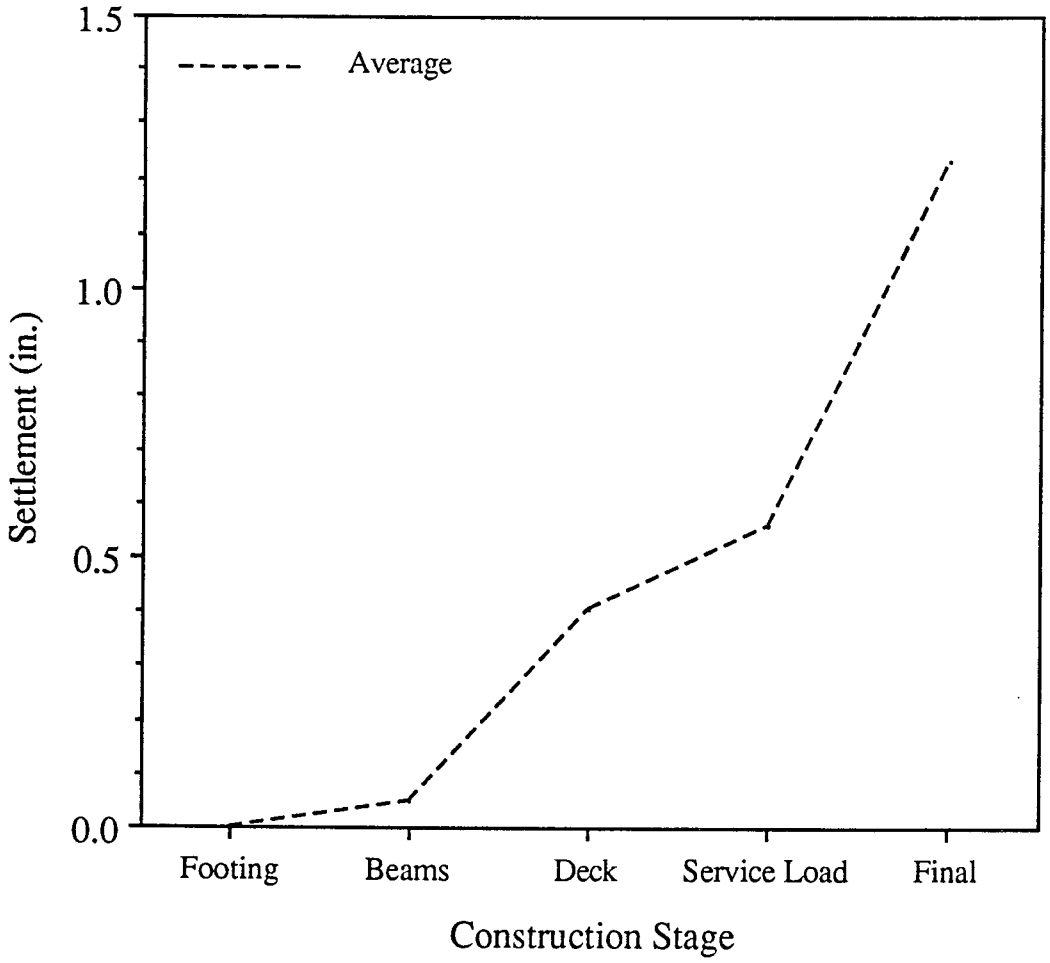

Figure 4.5 Settlement Performance of Panel "F" Footing (Bridge A)

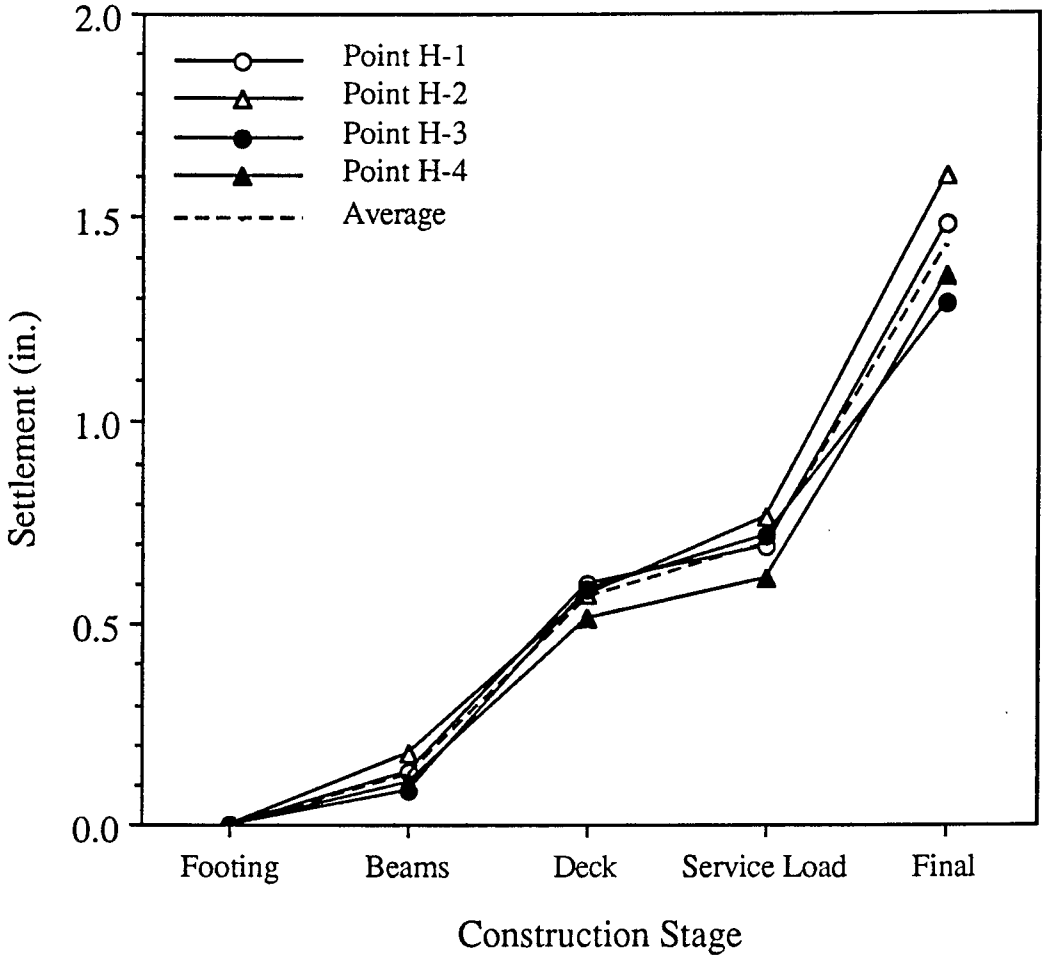

Figure 4.6 Settlement Performance of Panel "G/H" Footing (Bridge A)

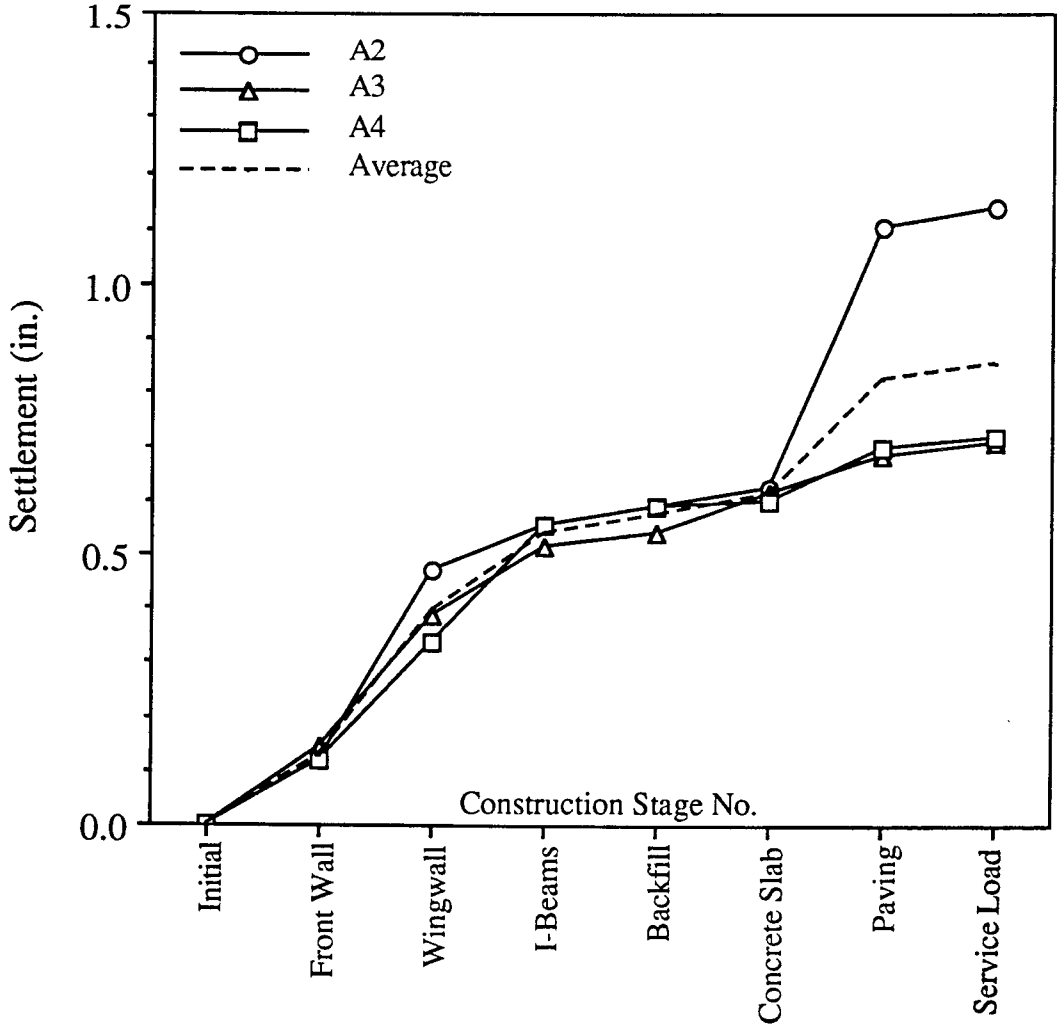

Figure 4.7 Settlement Performance of Abutment No. 1 Foundation (Bridge B)

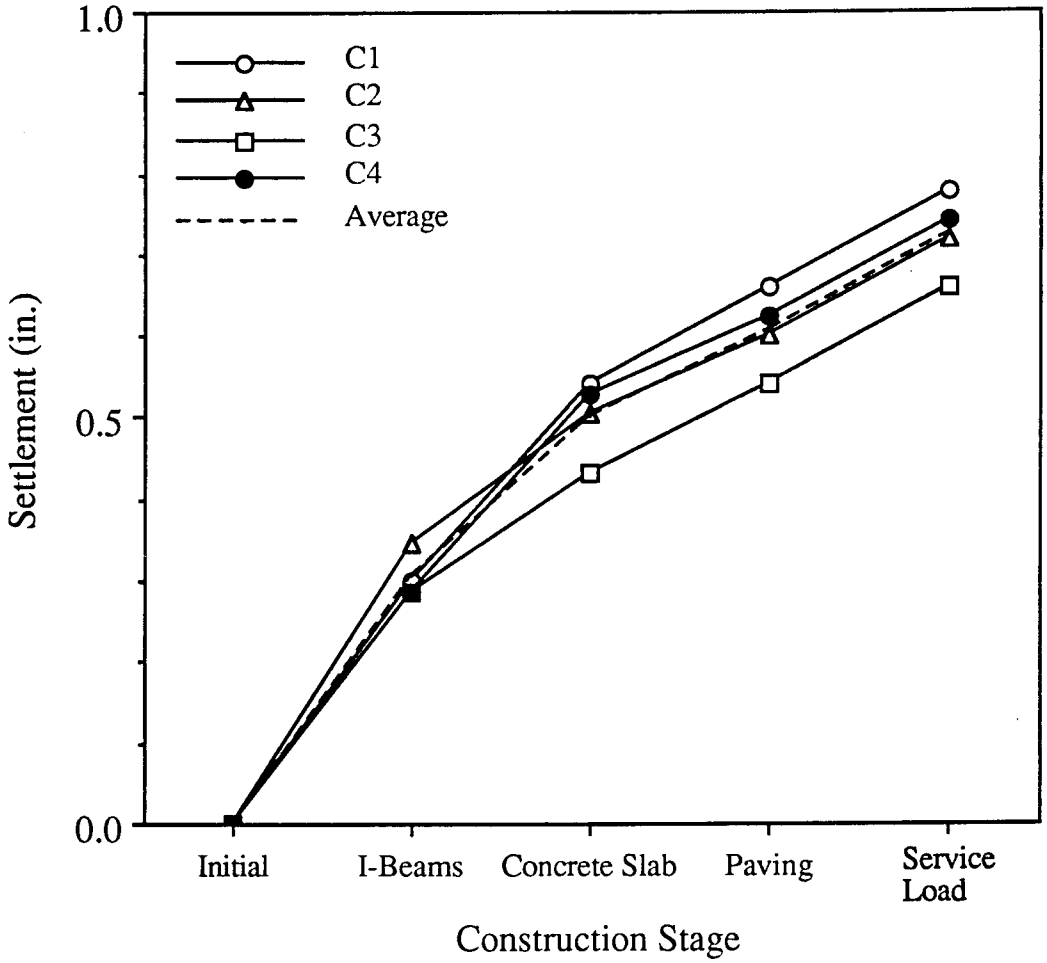

Figure 4.8 Settlement Performance of Central Pier Foundation (Bridge B)

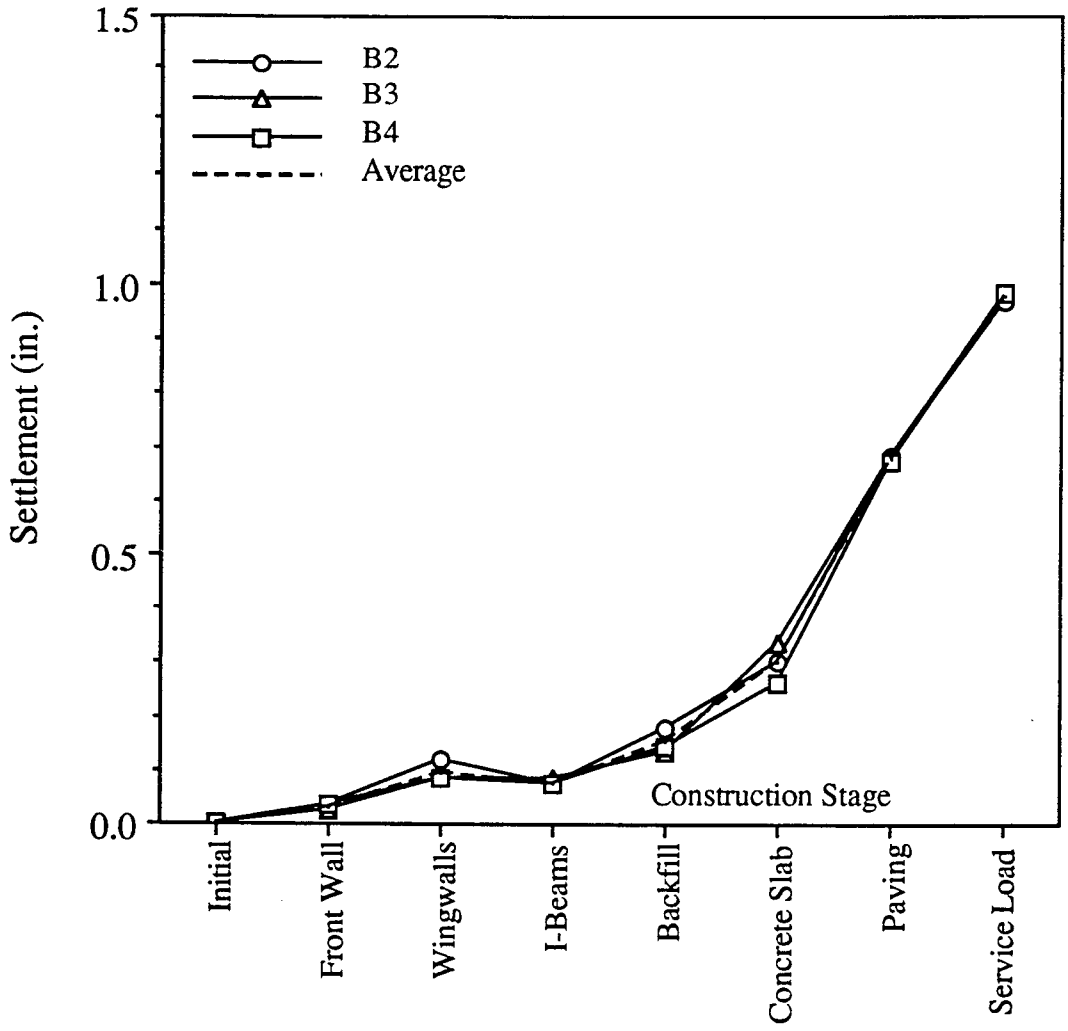

Figure 4.9 Settlement Performance of Abutment No. 2 Foundation (Bridge B)

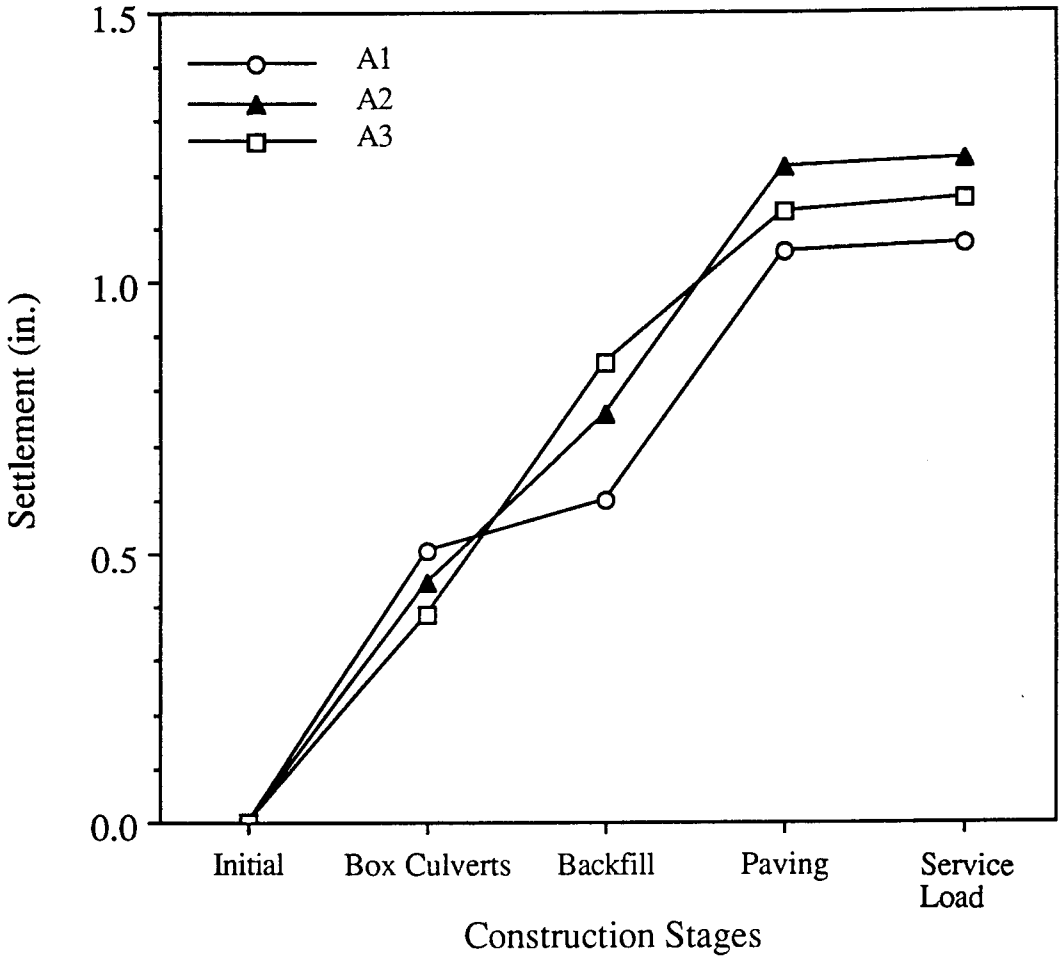

Figure 4.10 Settlement Performance of West Footing (Bridge C)

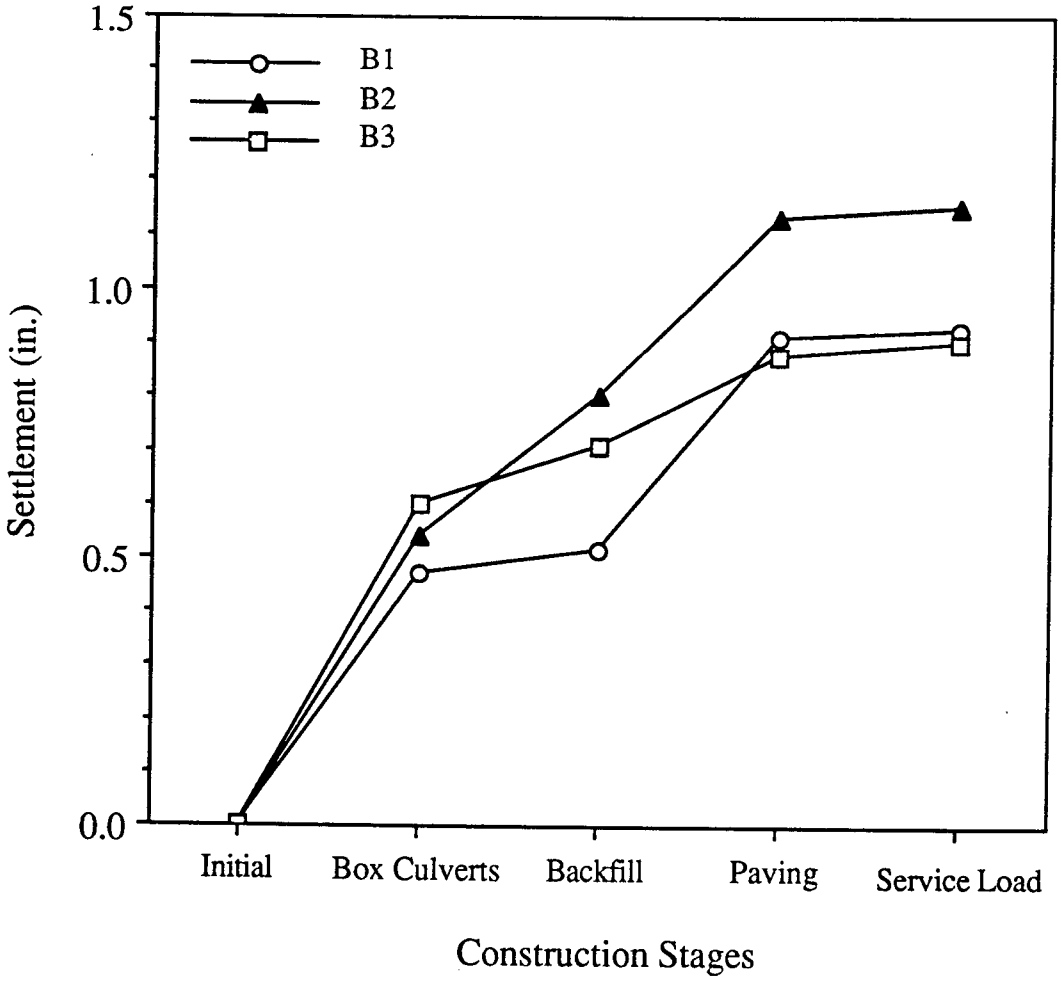

Figure 4.11 Settlement Performance of East Footing (Bridge C)

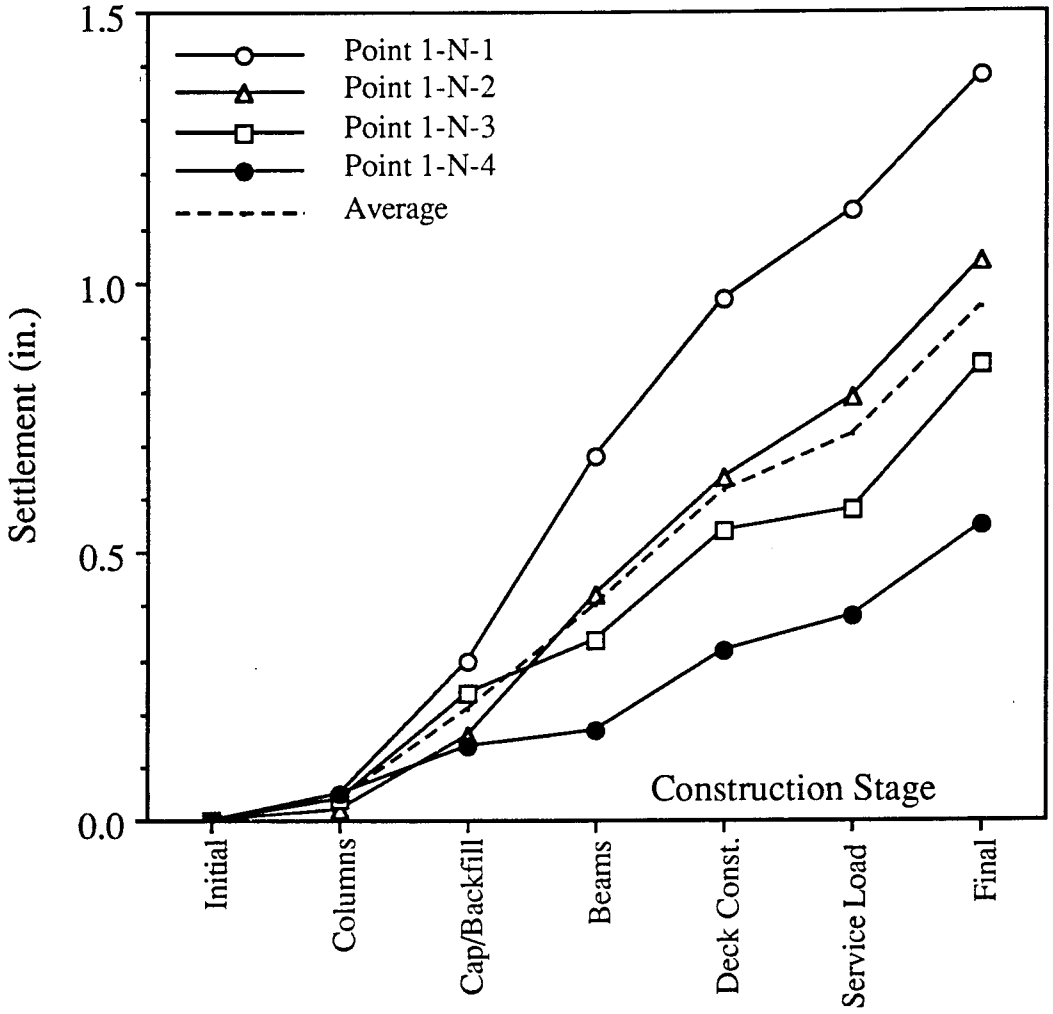

Figure 4.12 Settlement Performance of Pier 1 - North Footing (Bridge D)

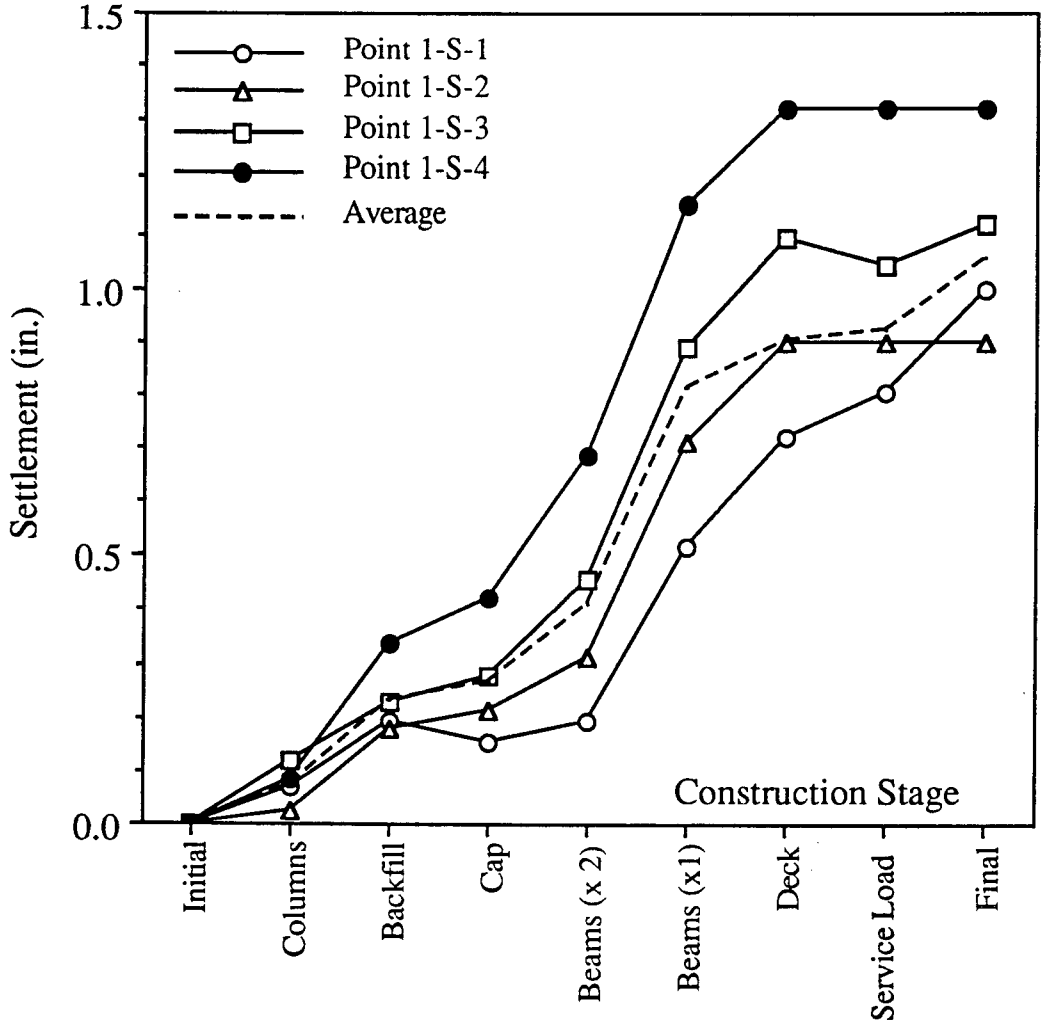

Figure 4.13 Settlement Performance of Pier 1 - South Footing (Bridge D)

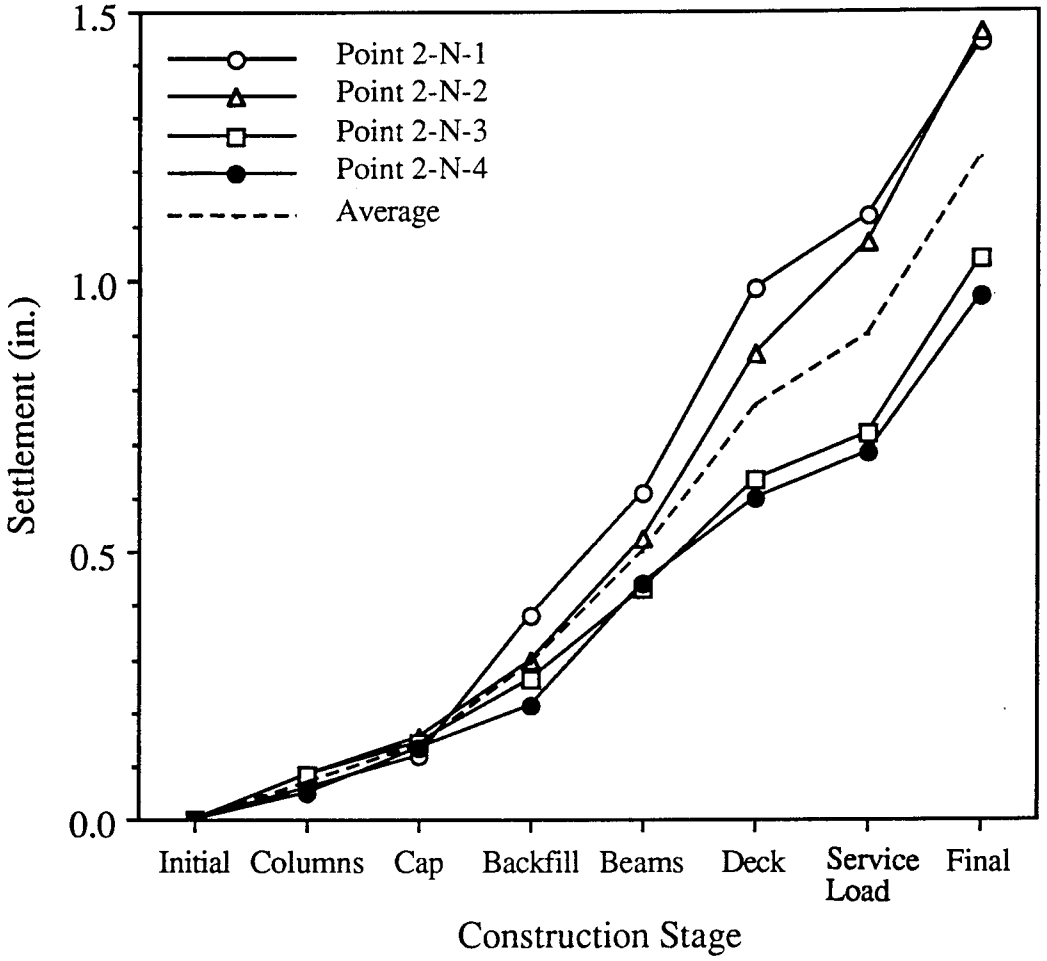

Figure 4.14 Settlement Performance of Pier 2 - North Footing (Bridge D)

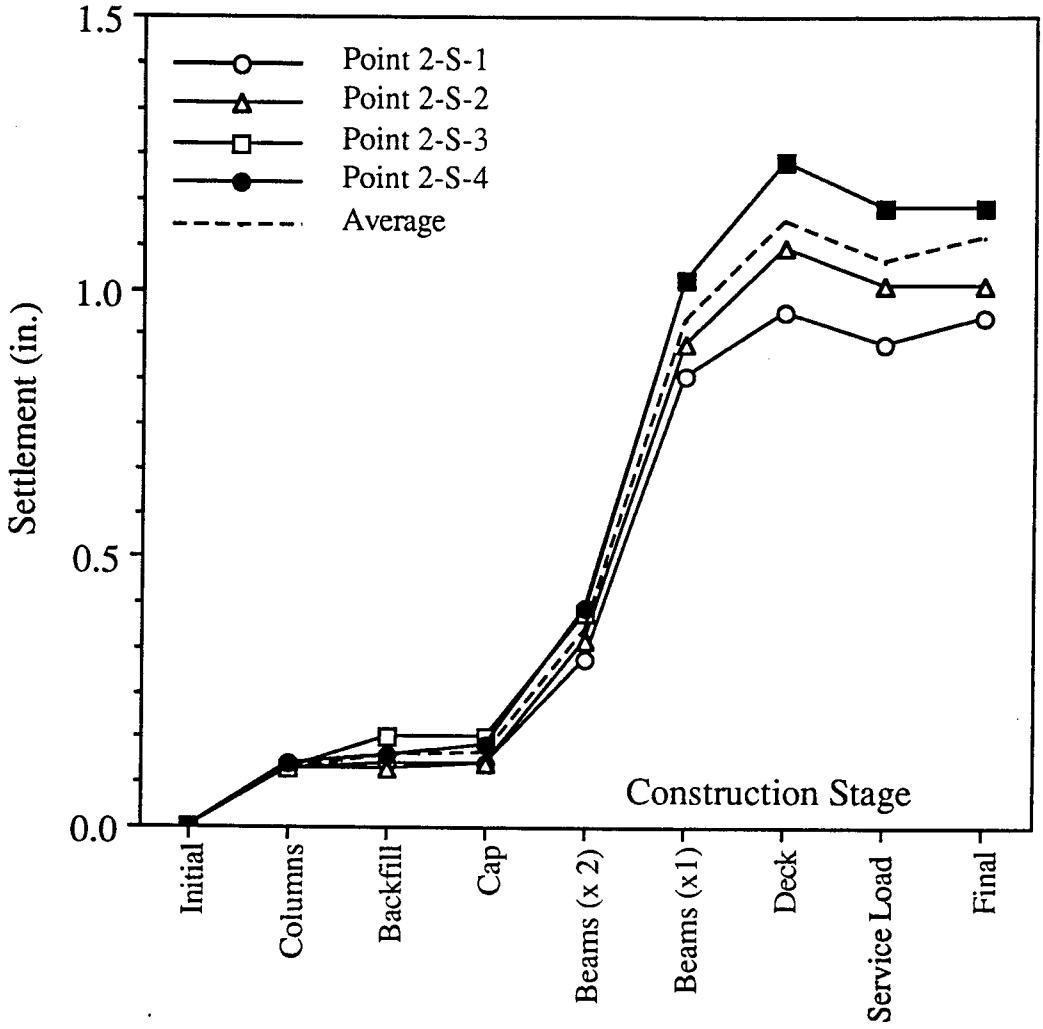

Figure 4.15 Settlement Performance of Pier 2 - South Footing (Bridge D)

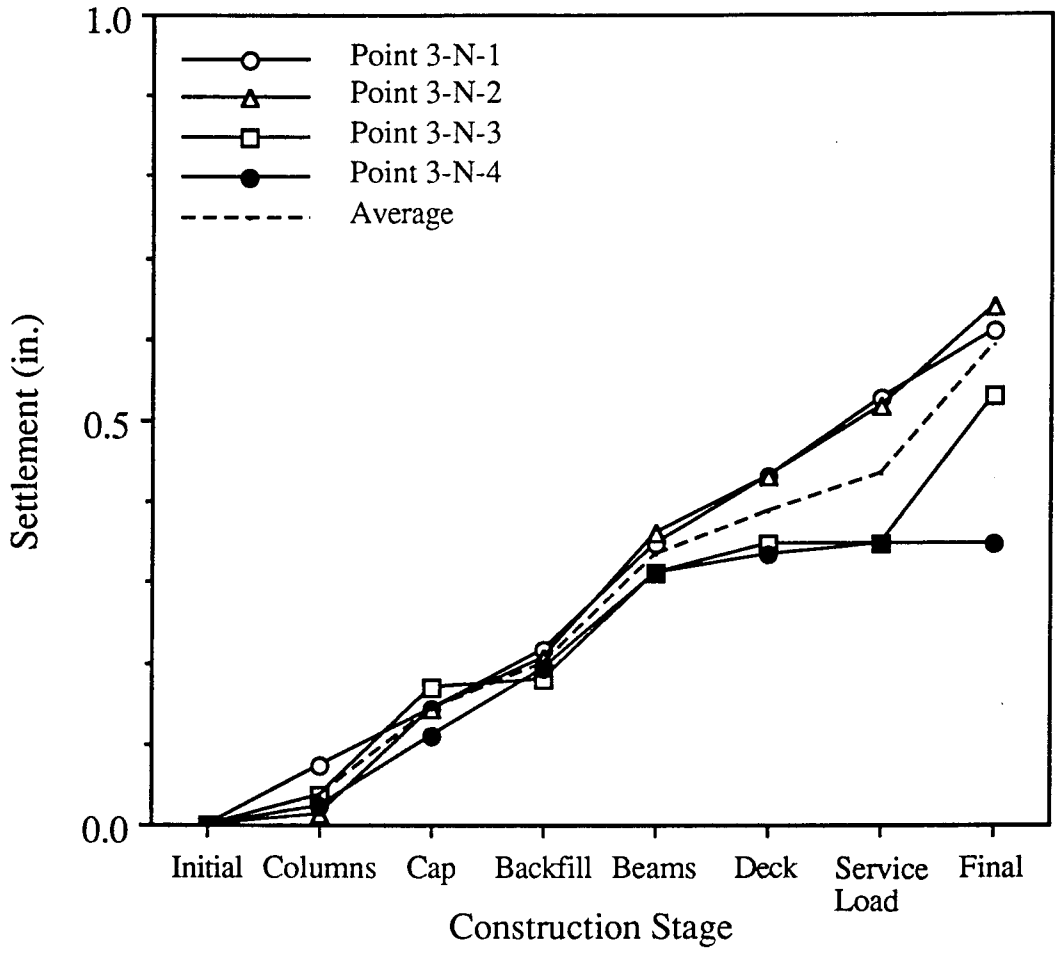

Figure 4.16 Settlement Performance of Pier 3 - North Footing (Bridge D)

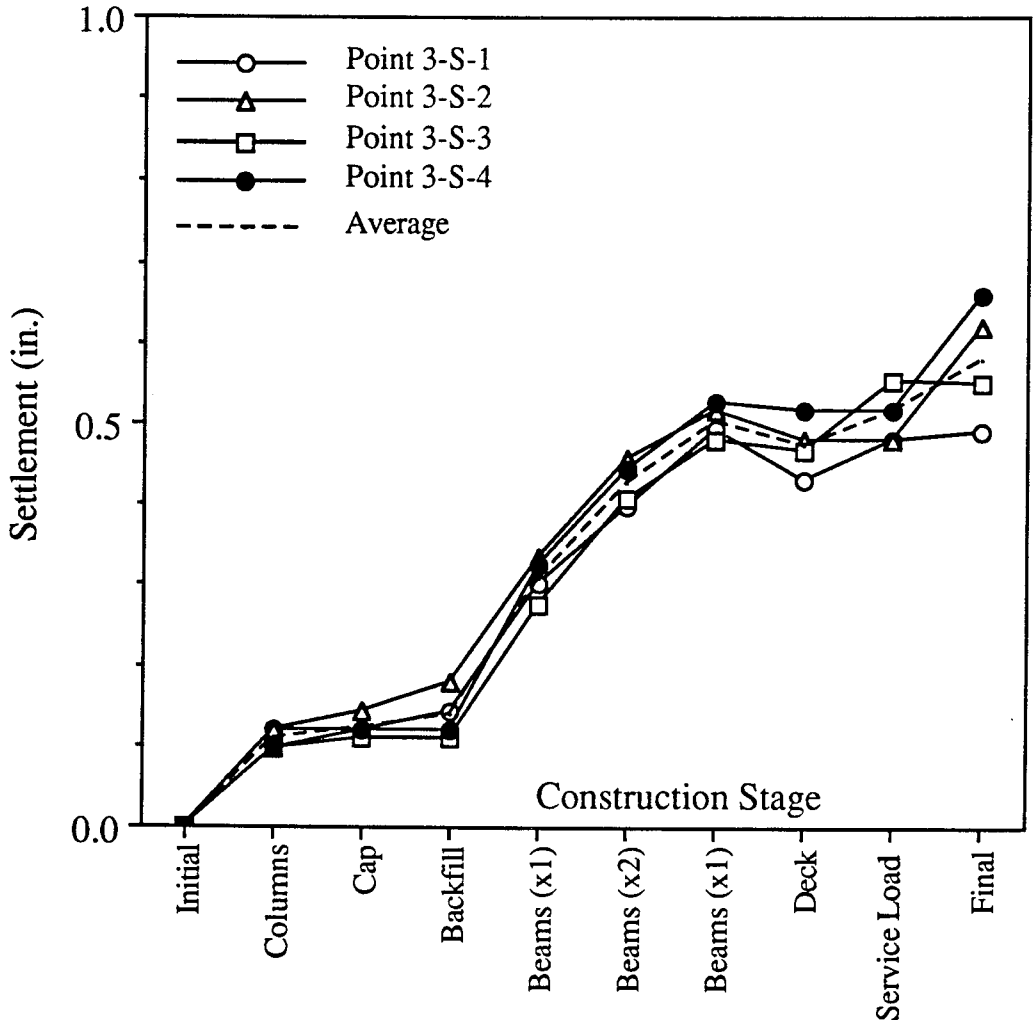

Figure 4.17 Settlement Performance of Pier 3 - South Footing (Bridge D)

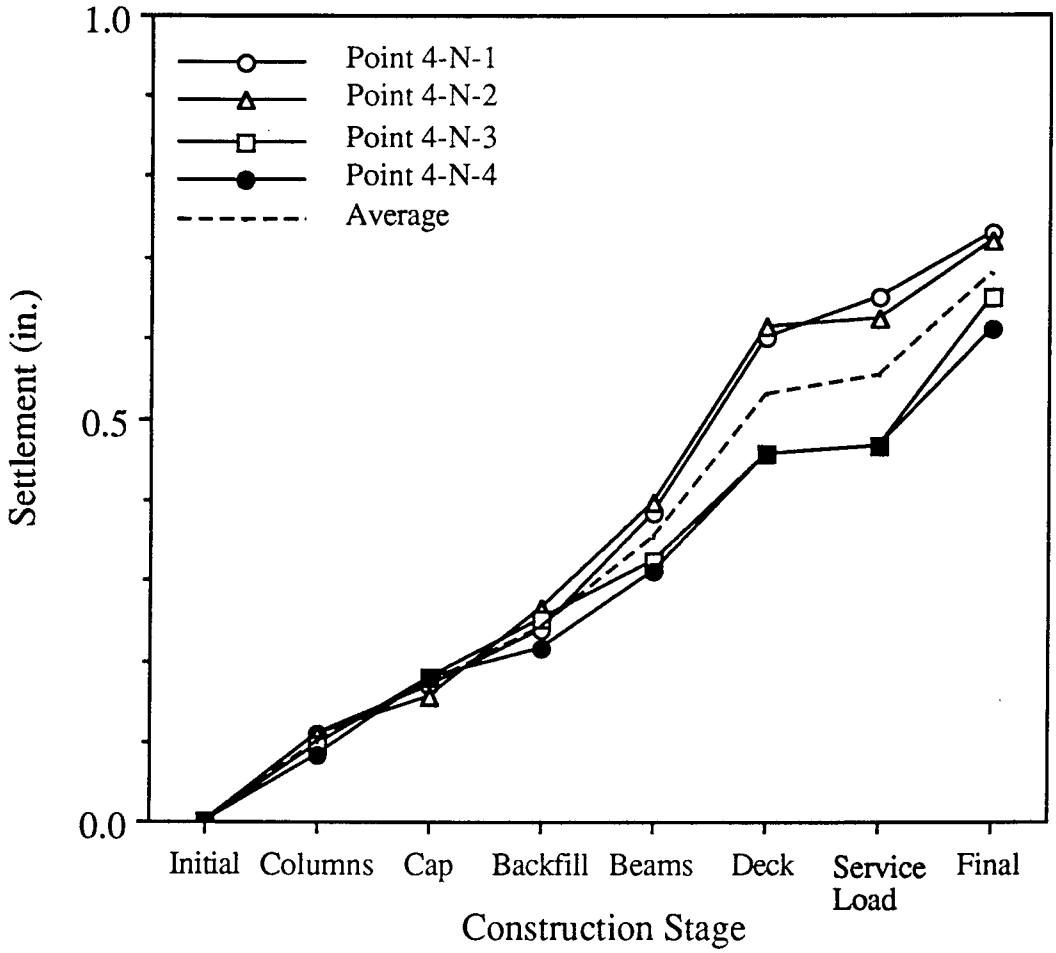

Figure 4.18 Settlement Performance of Pier 4 - North Footing (Bridge D)

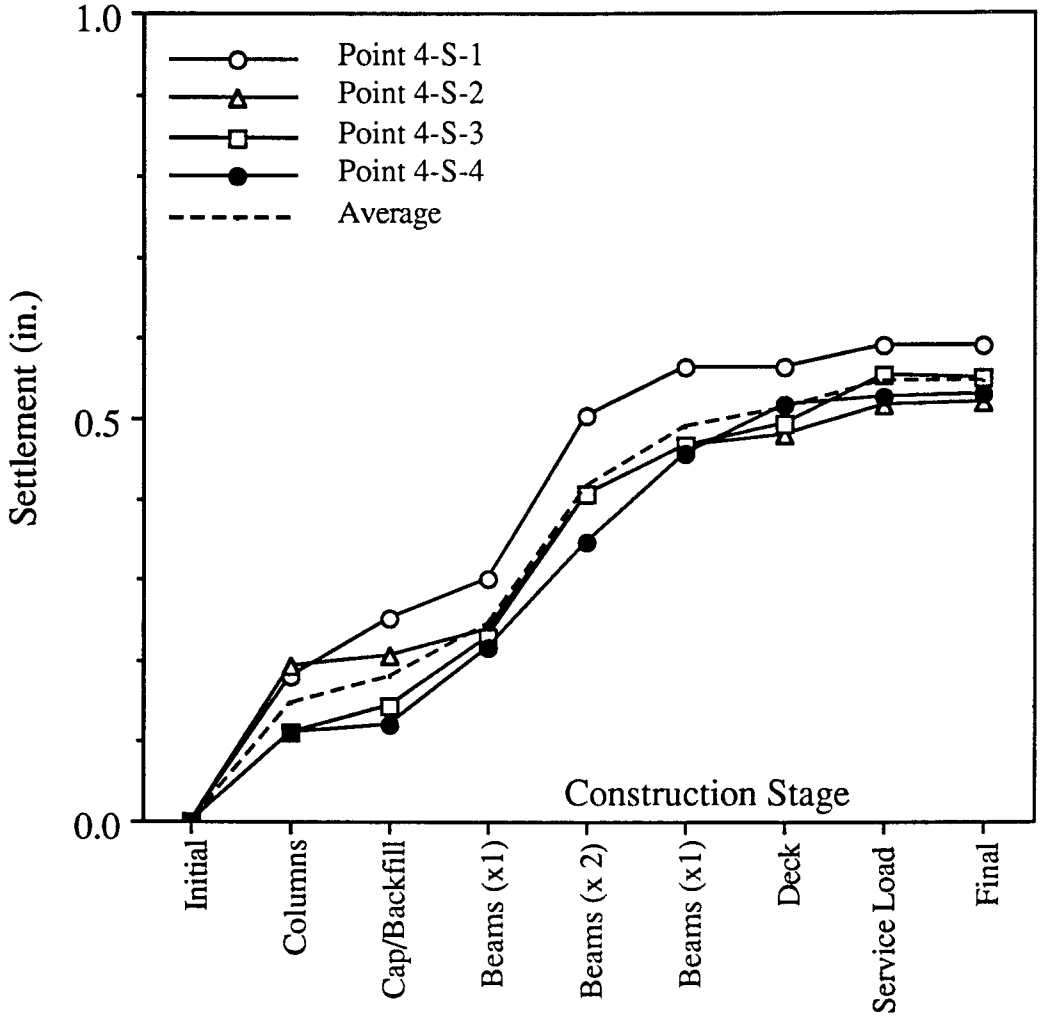

Figure 4.19 Settlement Performance of Pier 4 - South Footing (Bridge D)

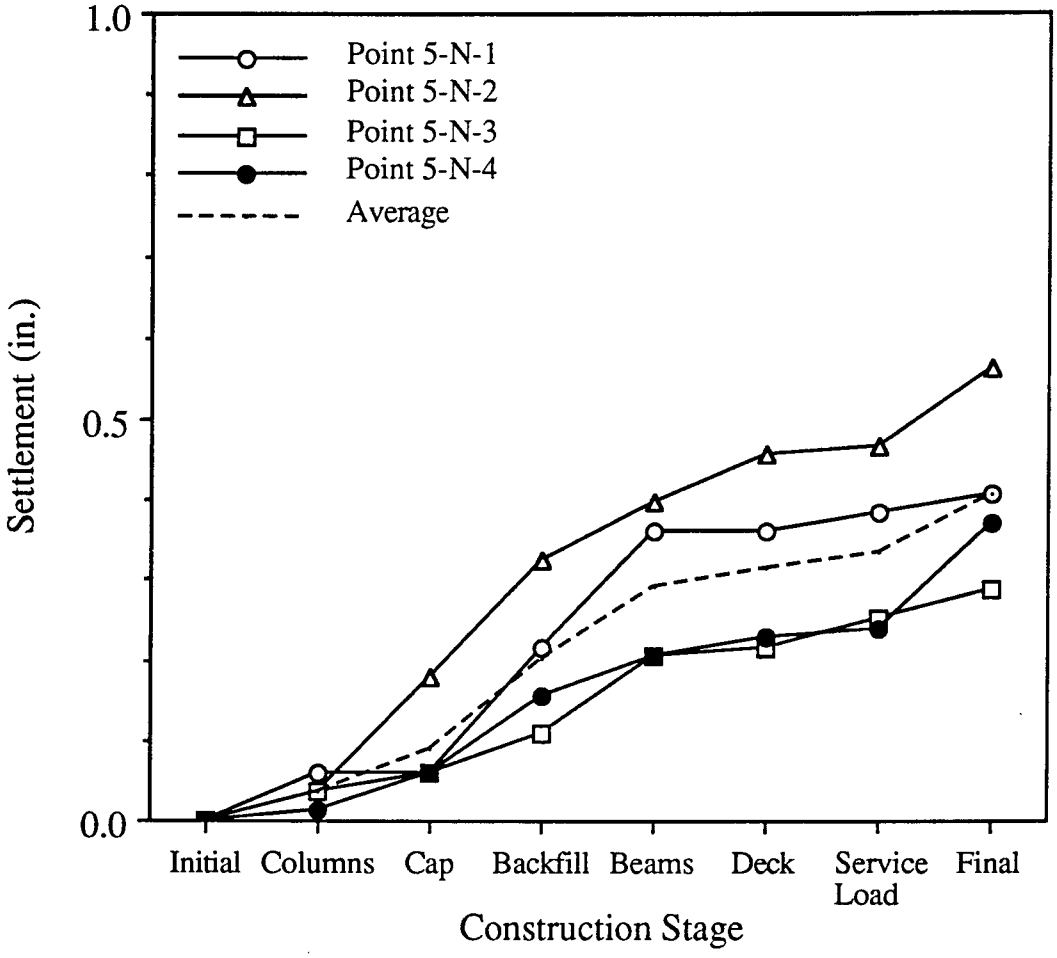

Figure 4.20 Settlement Performance of Pier 5 - North Footing (Bridge D)

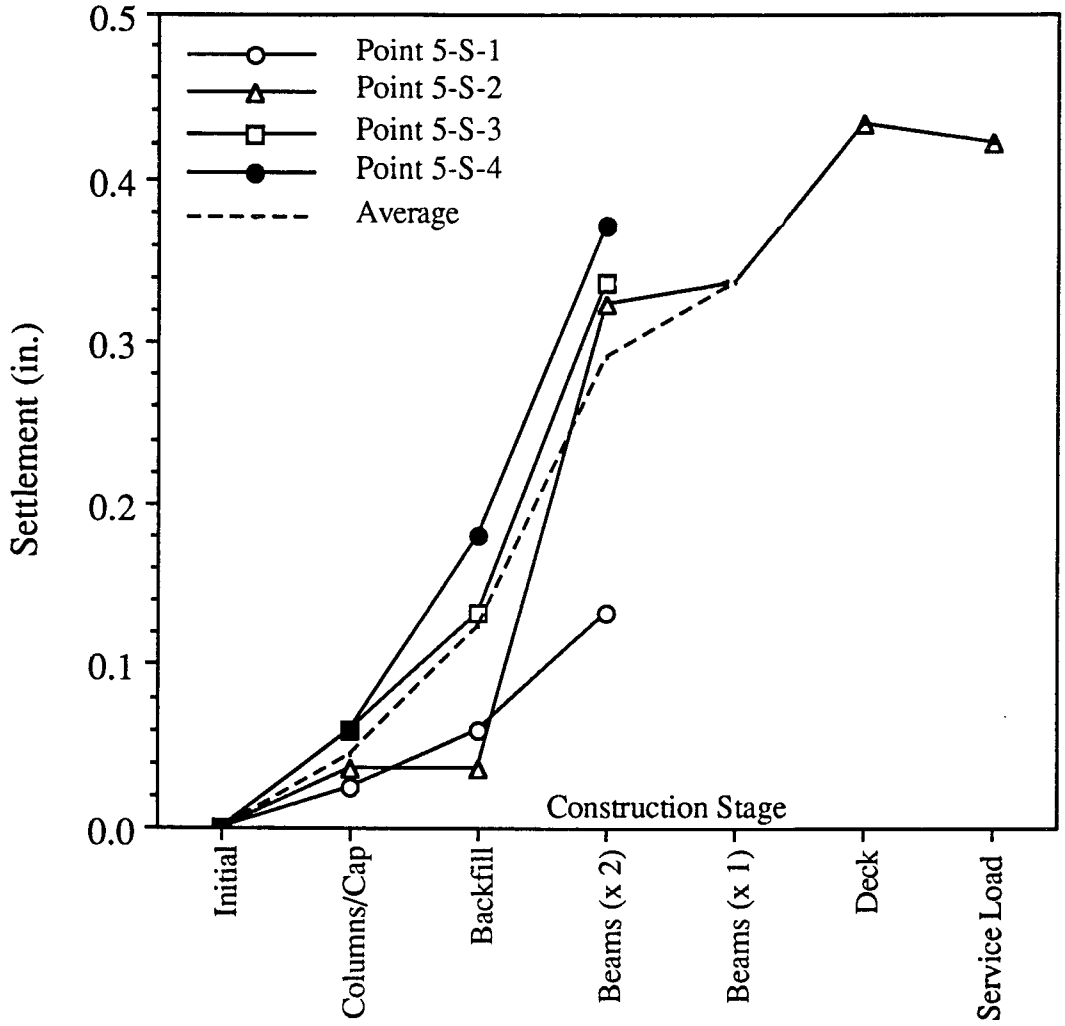

Figure 4.21 Settlement Performance of Pier 5 - South Footing (Bridge D)

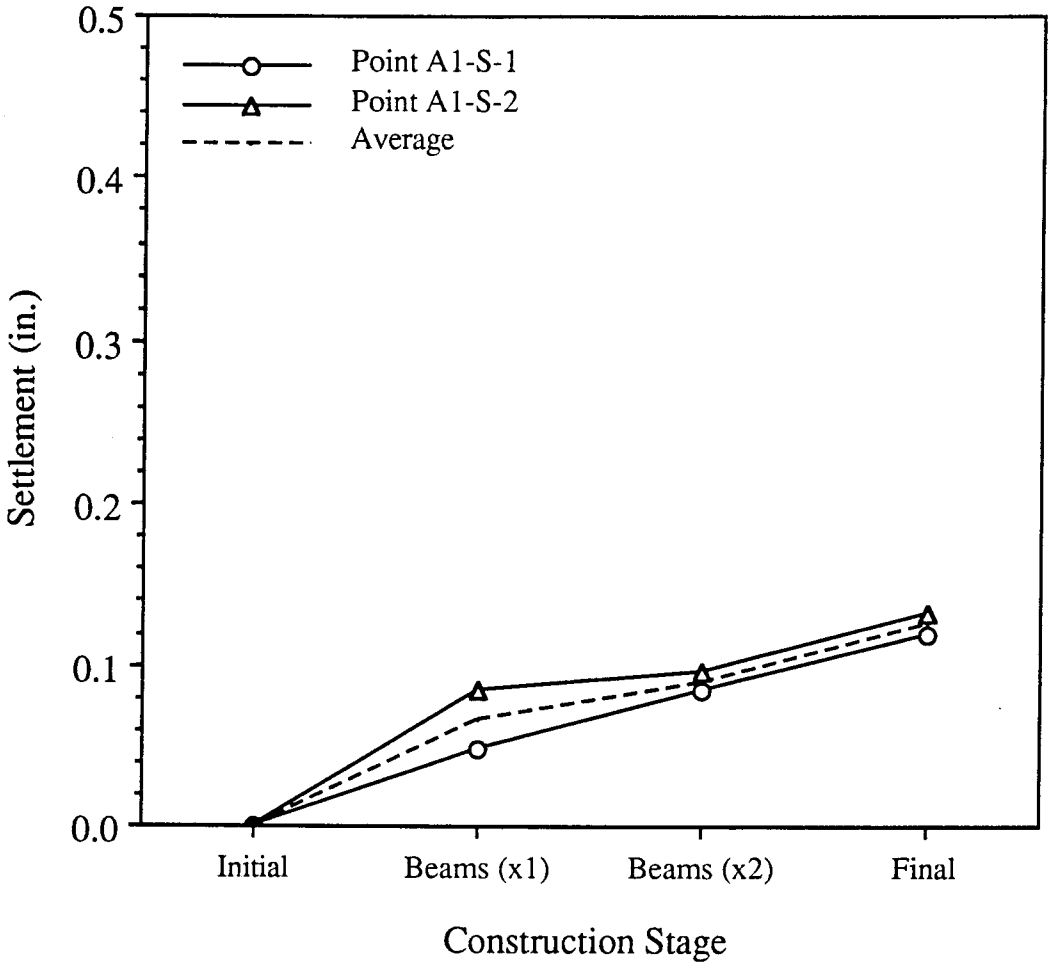

Figure 4.22 Settlement Performance of Abutment No. 1 Foundation (Bridge D)

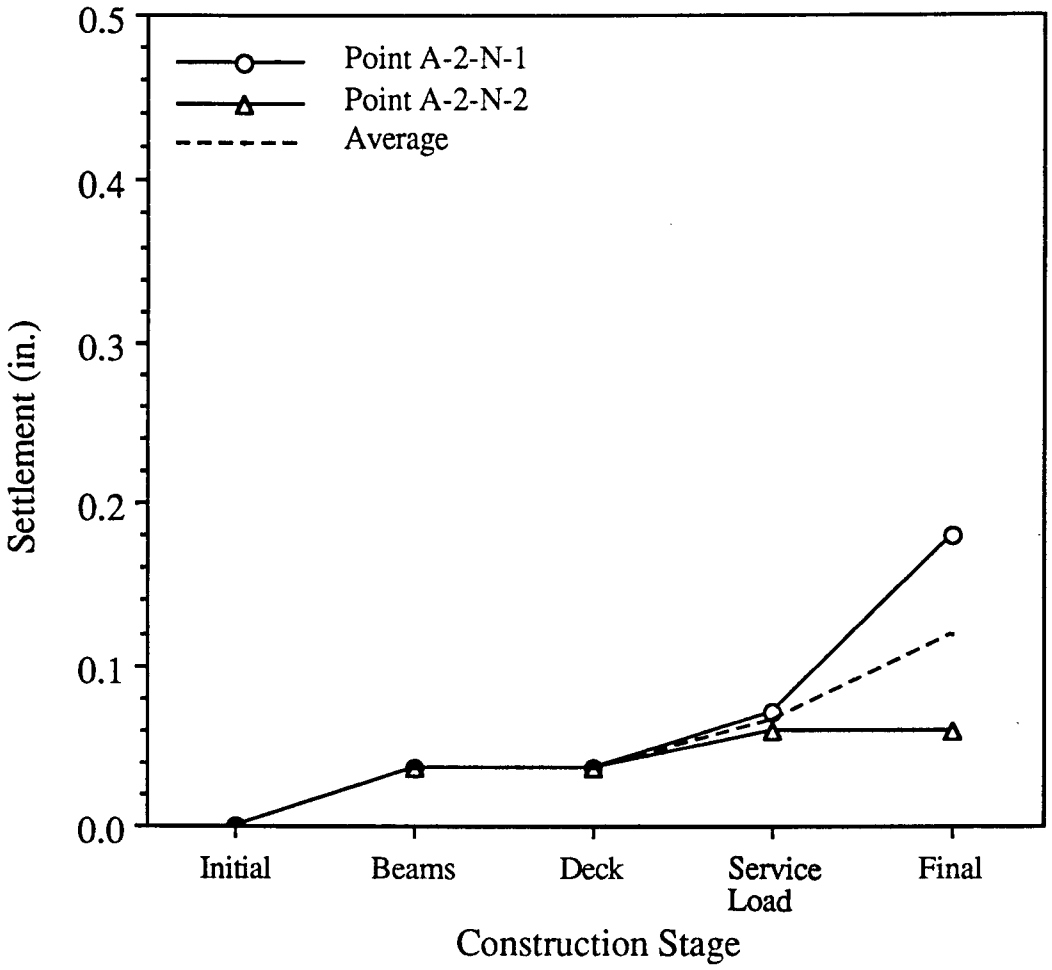

Figure 4.23 Settlement Performance of Abutment No. 2 - North Foundation (Bridge D)

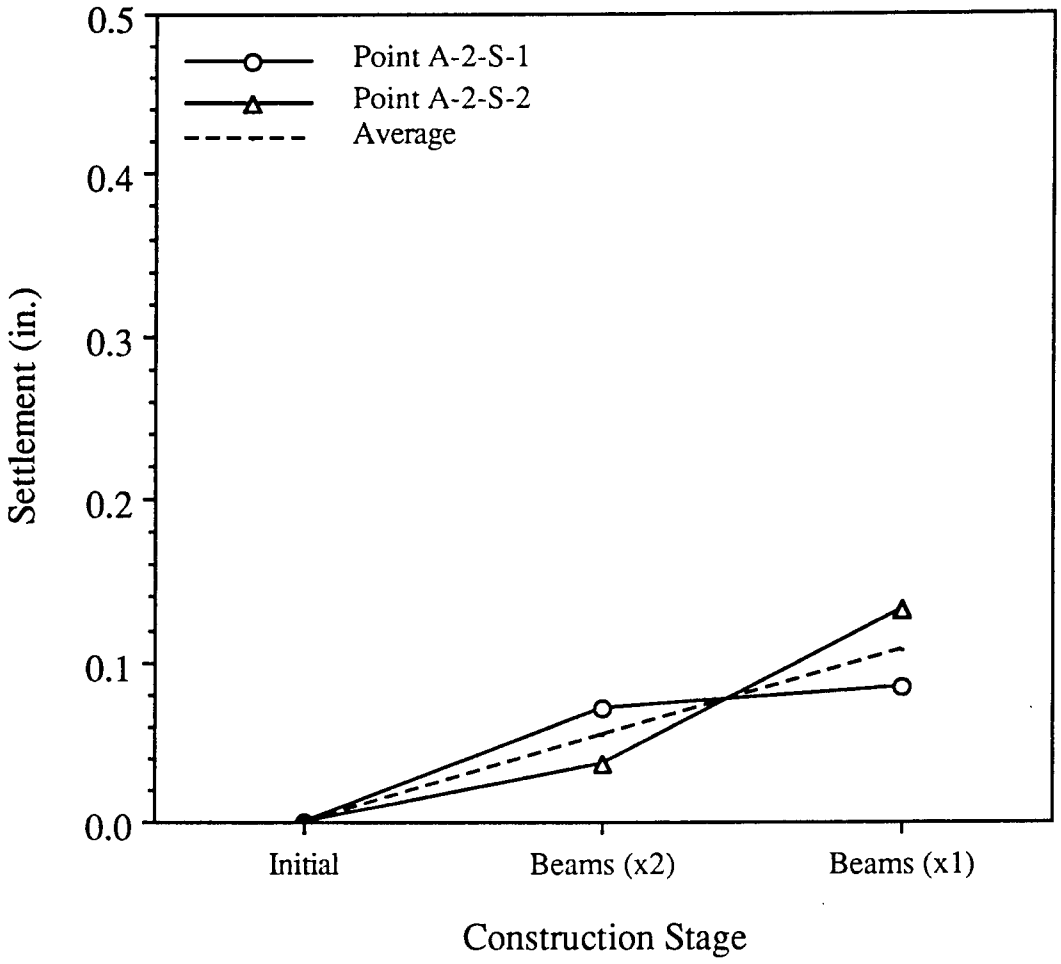

Figure 4.24 Settlement Performance of Abutment No. 2 - South Foundation (Bridge D)

the south part of the construction area (see Appendix A). Prior to the service load application, the average settlement was 0.25 inch for Panel "A/B" footing and 0.11 inch for Panel "C" footing. Settlement of Panel "C" structure, built next to an old retaining wall, was about a half of the settlement of Panel "A/B" footing. Average post-deck settlement was about 0.7 inch for Panel "A/B" footing and about 0.3 inch for Panel "C" footing. Post deck settlement constituted on the average about 46% of the total settlement at this site. In monitoring settlement of Bridge A footings, the original points were protected inside 6 inch diameter PVC casings (as shown in Figures 3.2 and 3.3) and utilized continuously after backfilling of the toe section of the footing.

At the Bridge B construction site, average total settlement of the foundations ranged from 0.7 to 1.0 inch. Central Pier experienced slightly less settlement than the abutment foundations. Overall shape of the settlement performance curve is concave downward for both Abutment No. 1 and Central Pier and concave upward for Abutment No. 2. Construction stages which had a greater impact on the settlement performance were abutment wall and deck constructions for the Abutment Nos. 1 and 2 foundations and I-beam placement for the Central Pier footing. Post-deck settlement constituted on the average about 38% of the total settlement at this site.

At the Bridge C construction site, average total settlement of the footings ranged from 1.0 to 1.2 inches. Amount of settlement prior to service load application for Bridge C was relatively uniform between the east and west footings at 0.9 to 1.1 inches, of which about 50% occurred after placing the box culvert sections. Within each footing, the maximum settlement was detected under the centerline of the roadway. Figures 4.10 and 4.11 show that the box culvert placement had more impact on the settlement performance than any other construction stages. Settlement stabilized beyond the paving operations.

At the Bridge D construction site, average total settlement of the spread footing foundations ranged from 0.4 to 1.2 inches for the Phase I (north side) footings. Average total settlement of the Phase II (south side) foundations ranged from 0.4 to 1.1 inches. Abutment structures supported by piles experienced less than 0.1 inch overall settlement. The small settlement value was found to be close to elastic shortening of the H-piles under the applied load. Footings located on the west side (closer to Abutment No. 2) experienced less settlement, since the bedrock approached the ground surface toward the west. A review of Figures 4.12 through 4.21 reveals that combined effect of the two construction stages of beam placement and deck construction induced about 37% of the total settlement for the Phase I footings. Post-deck settlement constituted on the average about 31% and 10% of the total settlement for Phase I and Phase II foundations, respectively.

At the Bridge E construction site, average total settlement of the Phase I spread footing foundations ranged from 0.2 to 1.4 inches. Average total settlement of the Phase II foundations ranged from 0.1 to 0.6 inches. These differences can be explained by the fact that the Phase II foundations included drilled pier shafts along the north side edge and the Phase I foundations were subjected to loads over longer periods of time. A review of Figures B.1 through B.20 (in Appendix B) reveals that total settlement was similar among the Phase I footings regardless of the type of treatment the top of the bearing layer received prior to placement of concrete (see Figure 3.30). The construction stage which had a greater impact on the settlement performance was placement of the concrete box beams. It is interesting to note that in some cases the Phase II construction activities appeared to induce additional settlement on the Phase I foundations (see Figure B.1). The Phase I and II foundations were positioned very close to each other at this site. Post-deck settlement constituted on the average about 24% and 20% of the total settlement for Phase I and Phase II

foundations, respectively.

In summary, no spread footing experienced average settlement of more than 2 inches during the duration of this study. The average total settlement was 0.92 inch for Bridge A, 0.88 inch for Bridge B, 1.05 inches for Bridge C, 0.76 inch for Bridge D (excluding the abutments), 0.60 inch for Bridge E (Phase I) and 0.28 inch for Bridge E (Phase II). If a basic statistical analysis is performed with all the data, the mean and standard deviation of the average total settlement will be 0.66 and 0.359, respectively. No significant differential settlement was observed in any case. Maximum total settlement of about 1.25 inches was recorded for Panel "F" of Bridge A and Pier 2 (Phase I) of Bridge D. Table 4.1 gives a summary of the settlement performance exhibited by the foundations of the five bridges.

4.3 Contact Pressure

Contact pressure at the foundation/bearing layer interface was monitored from the time the footing was constructed to the time service load was applied. Figures 4.25 and 4.26 present the data obtained at the Bridge A site. No contact pressure data existed for the Bridge B structure, since there was not a sufficient preparation time to procure and calibrate pressure cells for this project. Data obtained for the Bridge C footings are shown in Figures 4.27 and 4.28. Figures 4.29 through 4.34 are dedicated to present contact pressure data recorded under the Bridge D foundations during construction, and similar plots showing contact pressure under the Bridge E foundations are attached in Appendix B. In some of these plots, two field response curves were plotted against the major construction stages. One of them, labeled "flexible", resulted from applying a calibration constant in Eq. 3.2 obtained by performing tests in a special calibration chamber shown in Figure 3.5a. The

Table 4.1 Summary of Field Monitored Performance Data

Structure		Ave. Settlement (in.)			Maximum Average Contact Pressure (tsf)	Tilting (deg.)
		Total	Postdeck	After Culvert Placement		
Bridge A	Panel "A & B"	1.00	0.70 (70.0 %)		1.4 to 2.1	Within ± 0.15
	Panel "C"	0.59	0.30 (50.0 %)		1.6 to 2.0	-0.20 to 0
	Panel "D"	0.43	0.02 (4.7 %)		0.7 to 1.0	Within ± 0.10
	Panel "E"	0.81	0.58 (71.6 %)			Within ± 0.10
	Panel "F"	1.23	0.80 (65.0 %)			-0.20 to 0
	Panel "G & H"	1.43	0.77 (53.8 %)			Within ± 0.15
Bridge B	Abut. No. 1	1.09	0.48 (44.0 %)			Within ± 0.02
	Central Pier	0.73	0.23 (31.5 %)			-0.20 to 0.05
	Abut. No. 2	1.00	0.68 (38.9 %)			Within ± 0.03
Bridge C	West Footing	1.13		0.69 (61.1 %)	1.7 to 2.3	0 to 0.3
	East Footing	0.97		0.44 (45.4 %)		0 to 0.3
Bridge D	Abut. No. 1	0.09	—			
	Pier 1 - North	0.96	0.34 (35.4 %)			
	Pier 1 - South	1.06	0.15 (14.2 %)			
	Pier 2 - North	1.23	0.46 (37.4 %)		0.7 to 1.0	-0.07 to 0
	Pier 2 - South	1.10	0.07 (6.4 %)		1.1 to 1.5	Within ± 0.02
	Pier 3 - North	0.59	0.21 (35.6 %)		3.1 to 4.4	-0.04 to 0.02
	Pier 3 - South	0.58	0.11 (19.0 %)		1.6 to 2.3	Within ± 0.01
	Pier 4 - North	0.68	0.15 (22.1 %)			
	Pier 4 - South	0.55	0.04 (7.3 %)			
	Pier 5 - North	0.41	0.09 (22.0 %)		1.6 to 2.3	-0.07 to 0
	Pier 5 - South	0.43	0.02 (4.7 %)		0.7 to 1.0	-0.07 to 0
	Abut. No. 2	0.08	—			0 to 0.03

(Note) North = Phase I, South = Phase II for Bridge D

Table 4.1 Summary of Field Monitored Performance Data (cont'd)

Structure		Ave. Settlement (in.)		Maximum Average Contact Pressure (tsf)	Tilting (deg.)	
		Total	Postdeck		Longitudinal	Transverse
Bridge E	Rear Abut. - I	1.39	0.51 (36.7 %)	3.0 to 4.3	0 to 0.1	
	Rear Abut. - II	0.35	0.03 (8.6 %)		-0.02 to 0.03	
	Pier 1 - I	0.77	0.20 (26.0 %)	2.8 to 4.0	-0.05 to 0	0 to 0.10
	Pier 1 - II	0.60	0.03 (5.0 %)			
	Pier 3 - I	0.56	0.28 (50.0 %)	1.4 to 2.0	Within $\pm$ 0.08	
	Pier 3 - II	0.31	0.04 (12.9 %)			
	Pier 4 - I	0.58	0.11 (19.0 %)			
	Pier 4 - II	0.13	0.02 (15.4 %)			
	Pier 5 - I	0.19	0.04 (21.1 %)			
	Pier 5 - II	0.12	0.05 (41.7 %)			
	Pier 6 - I	0.39	0.06 (15.4 %)	1.8 to 2.5	-0.05 to 0	
	Pier 6 - II	0.30	0.05 (16.7 %)			
	Pier 7 - I	0.43	0.07 (16.3 %)			
	Pier 7 - II	0.23	0.05 (21.7 %)			
	Pier 8 - I	0.55	0.04 (7.3 %)	0.6 to 0.9	-0.10 to 0.05	-0.05 to 0.10
	Pier 8 - II	0.28	0.08 (28.6 %)			
	Forw. Abut. - I	0.50	0.10 (20.0 %)		0 to 0.05	
	Forw. Abut. - II	0.22	0.06 (27.3 %)		0 to 0.12	

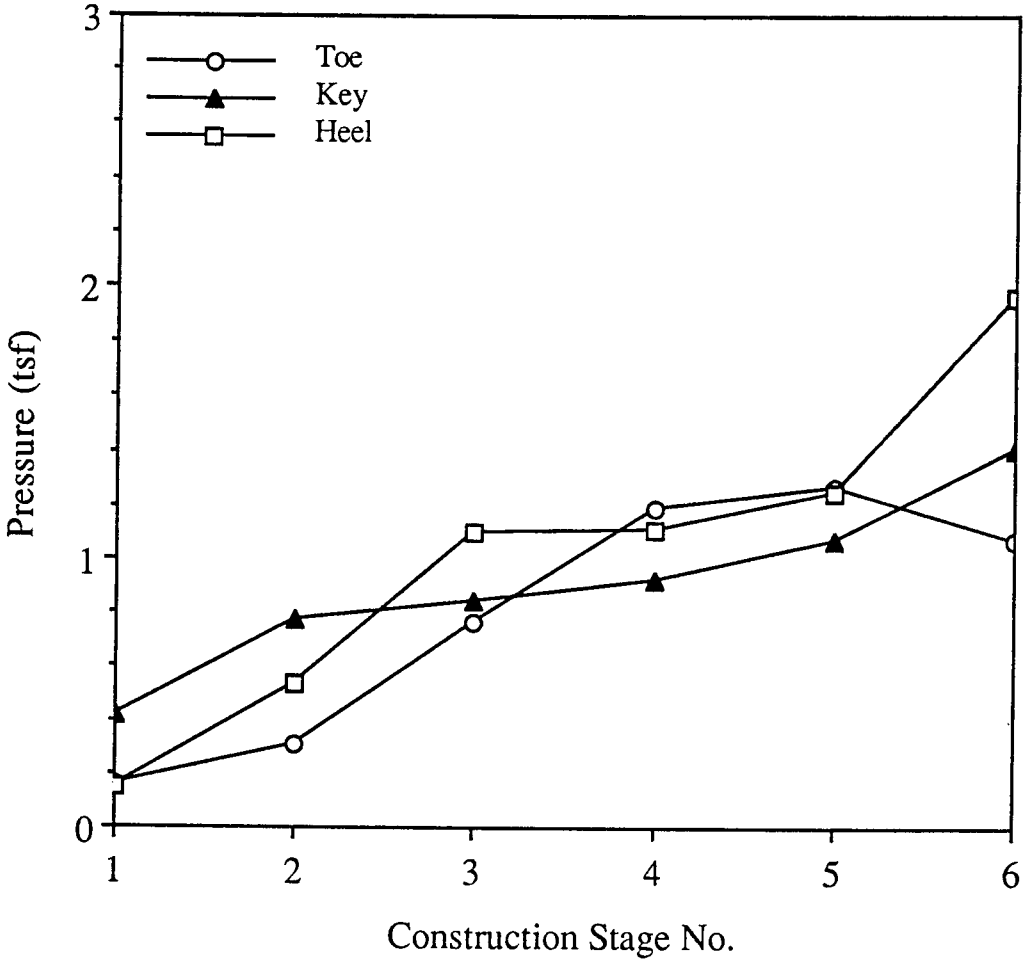

Figure 4.25 Contact Pressure Under Panel "A/B" Footing (Bridge A)

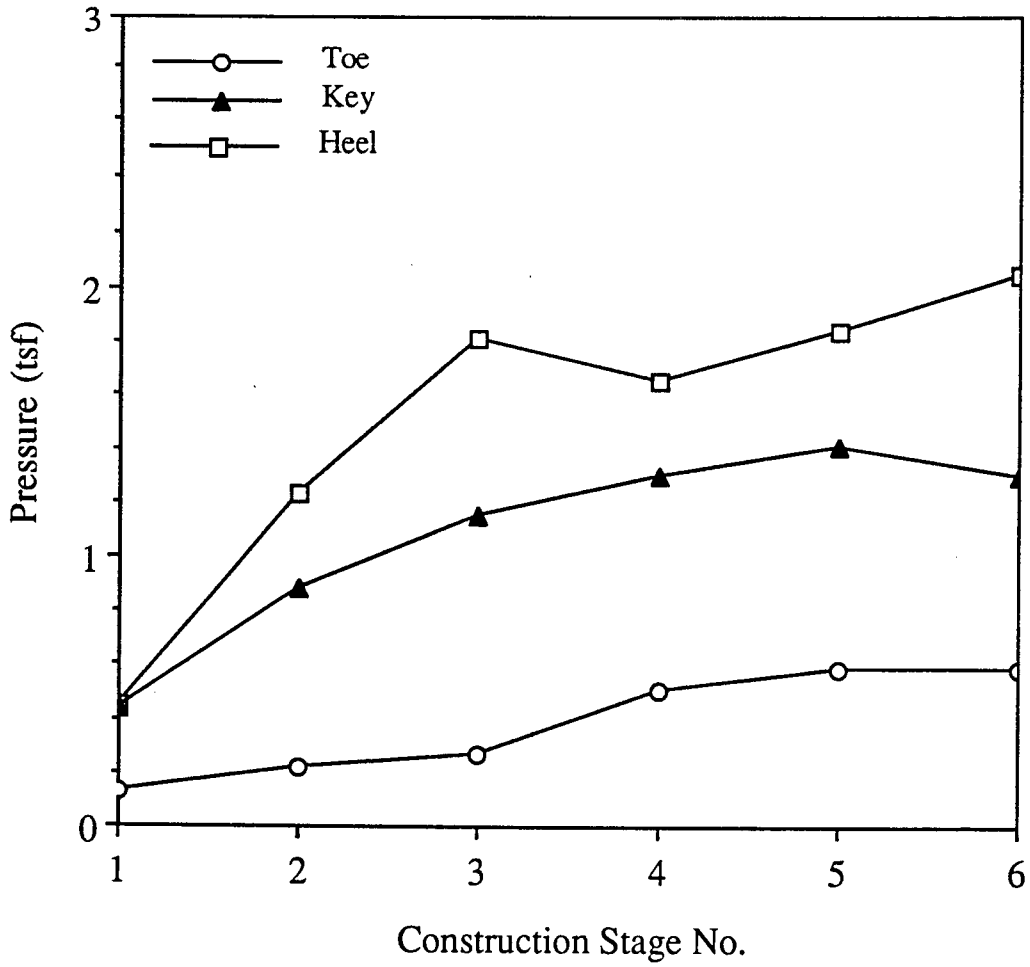

Figure 4.26 Contact Pressure Under Panel "C" Footing (Bridge A)

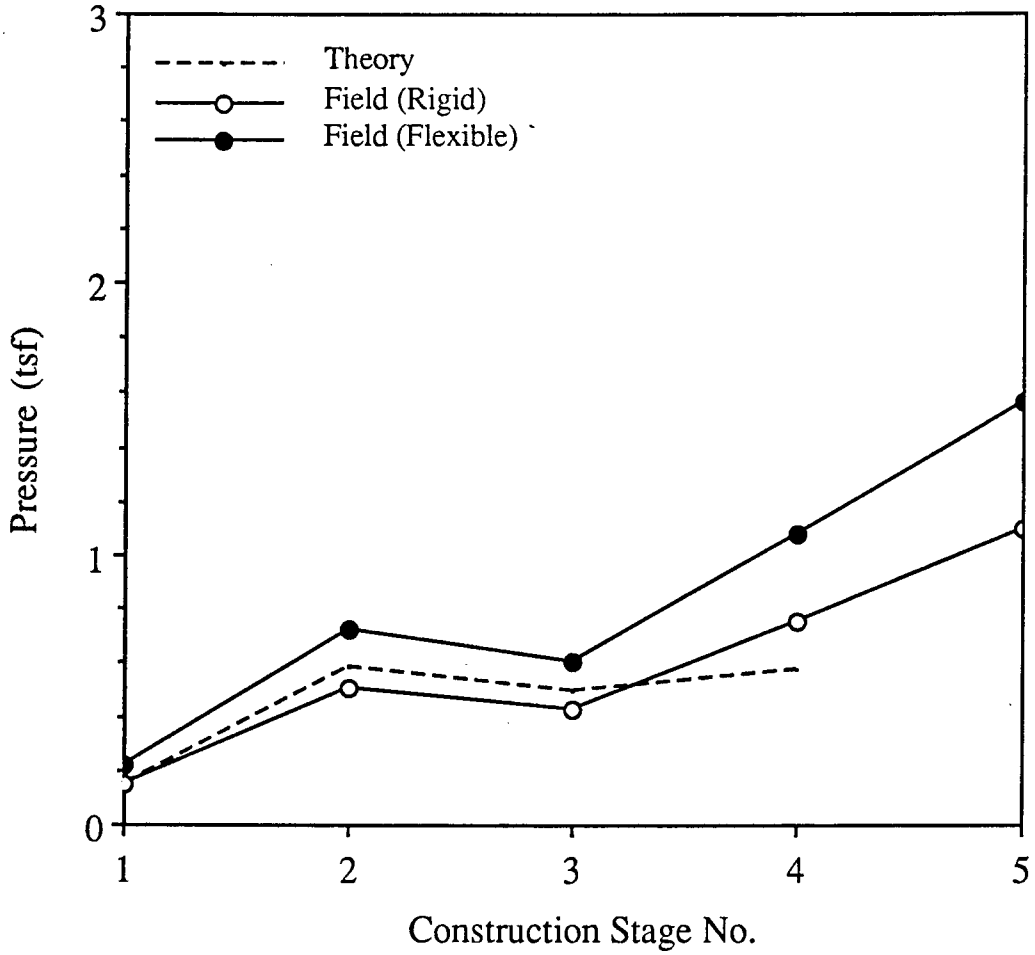

Figure 4.27 Contact Pressure at Heel of West Footing (Bridge C)

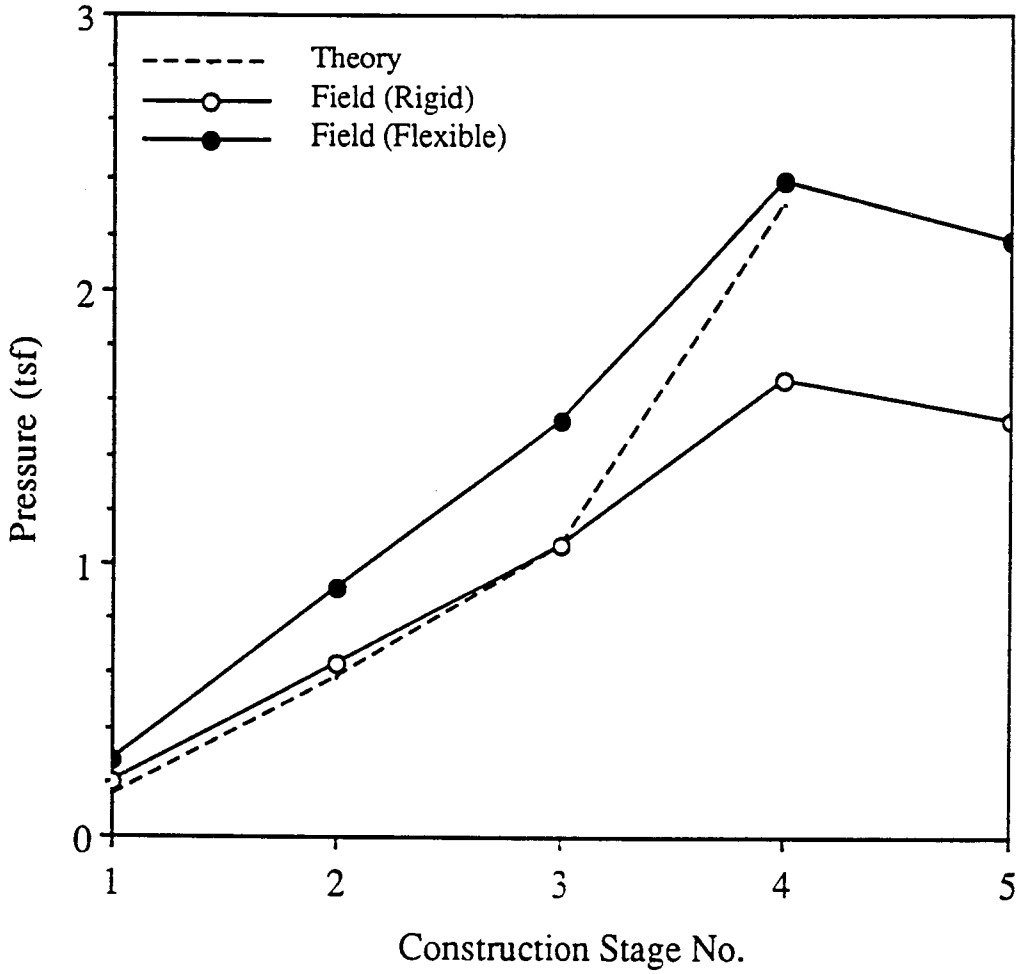

Figure 4.28 Contact Pressure at Toe of West Footing (Bridge C)

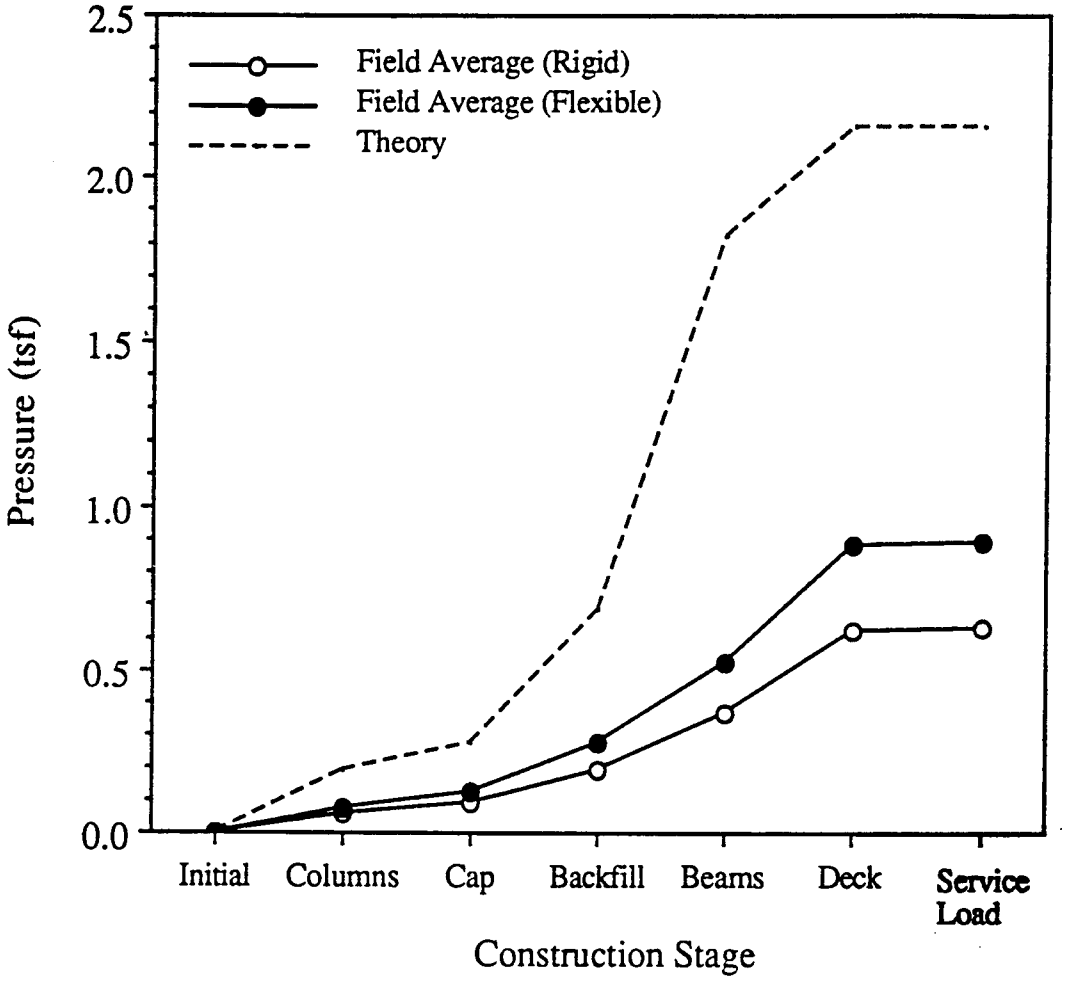

Figure 4.29 Contact Pressure Under Pier 2 - North Footing (Bridge D)

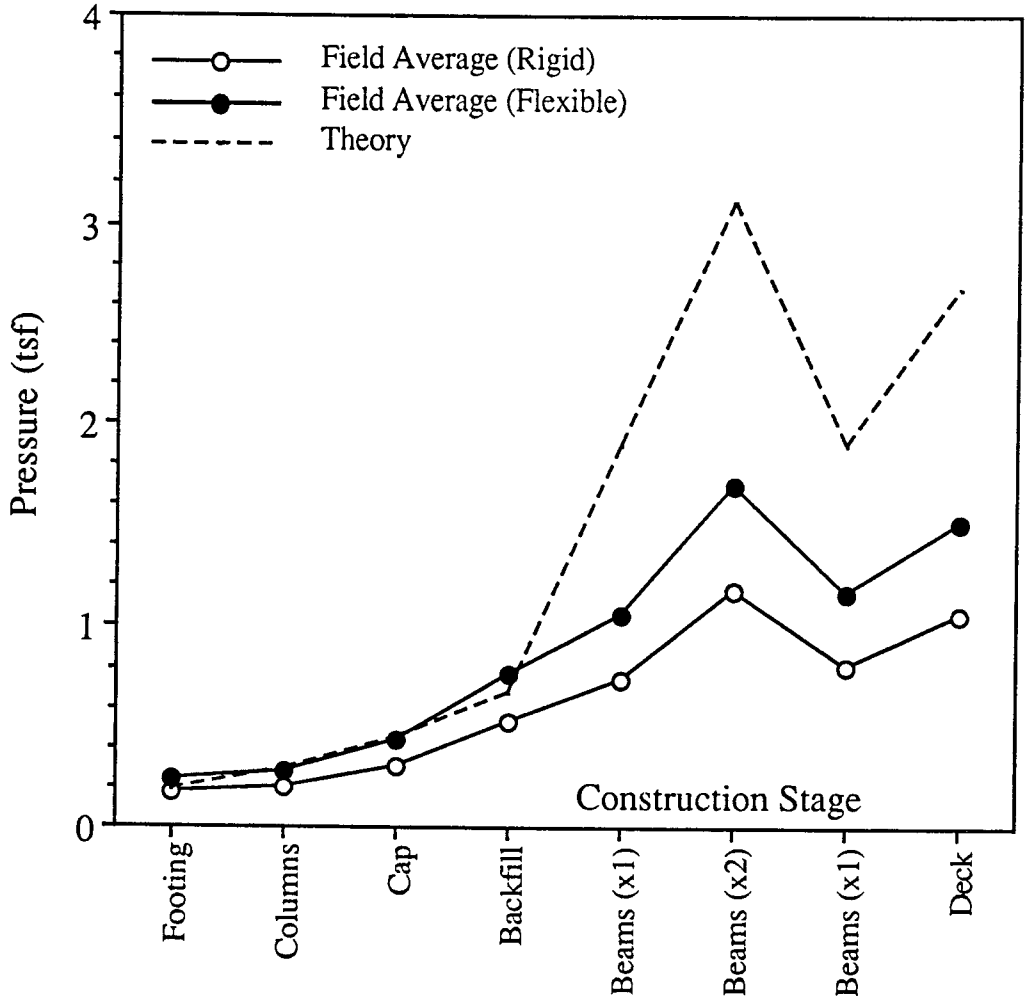

Figure 4.30 Contact Pressure Under Pier 2 South Footing (Bridge D)

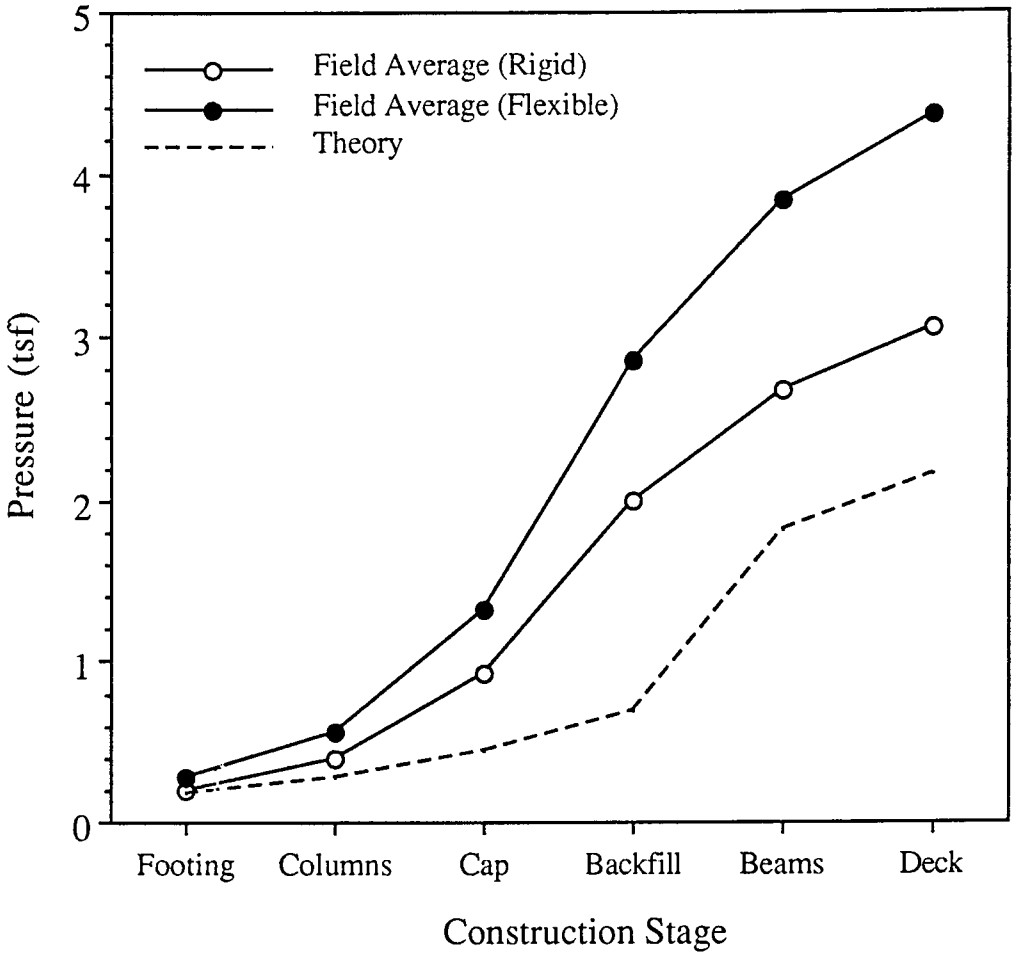

Figure 4.31 Contact Pressure Under Pier 3 - North Footing (Bridge D)

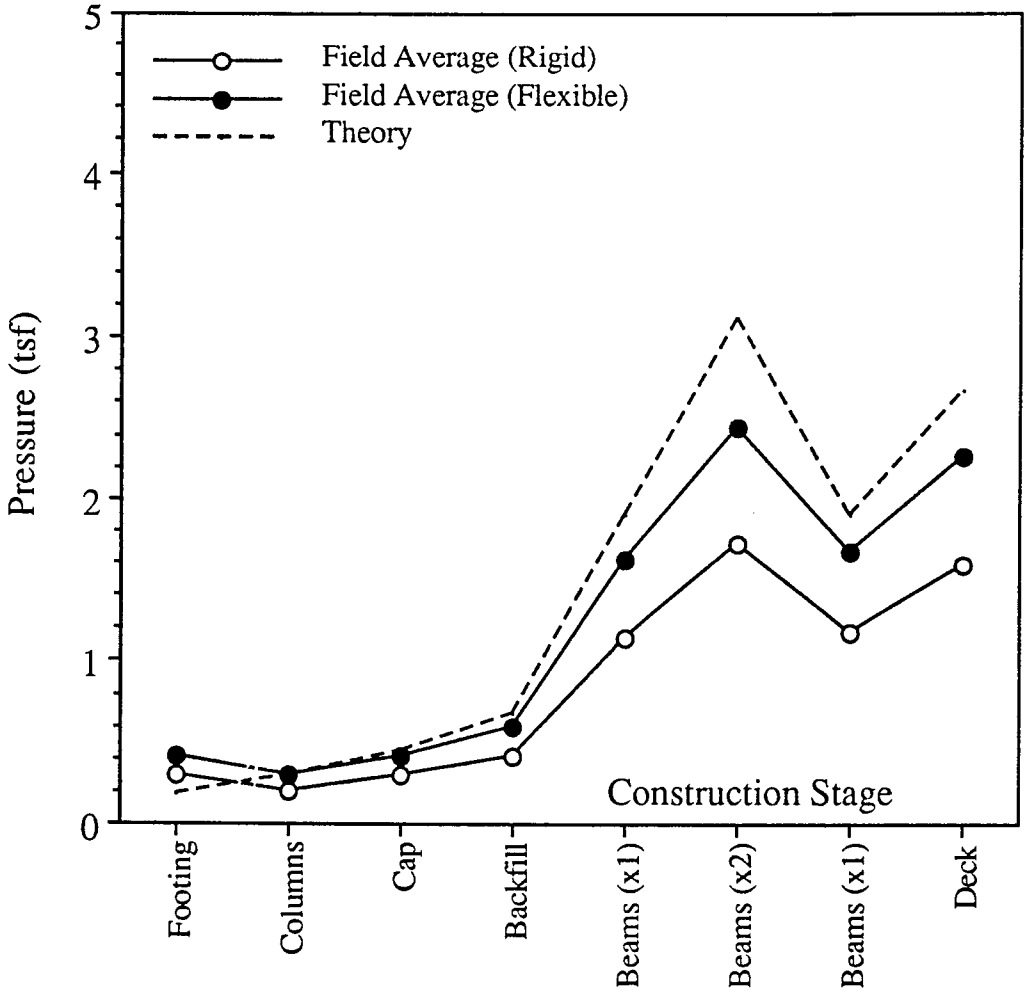

Figure 4.32 Contact Pressure Under Pier 3 - South Footing (Bridge D)

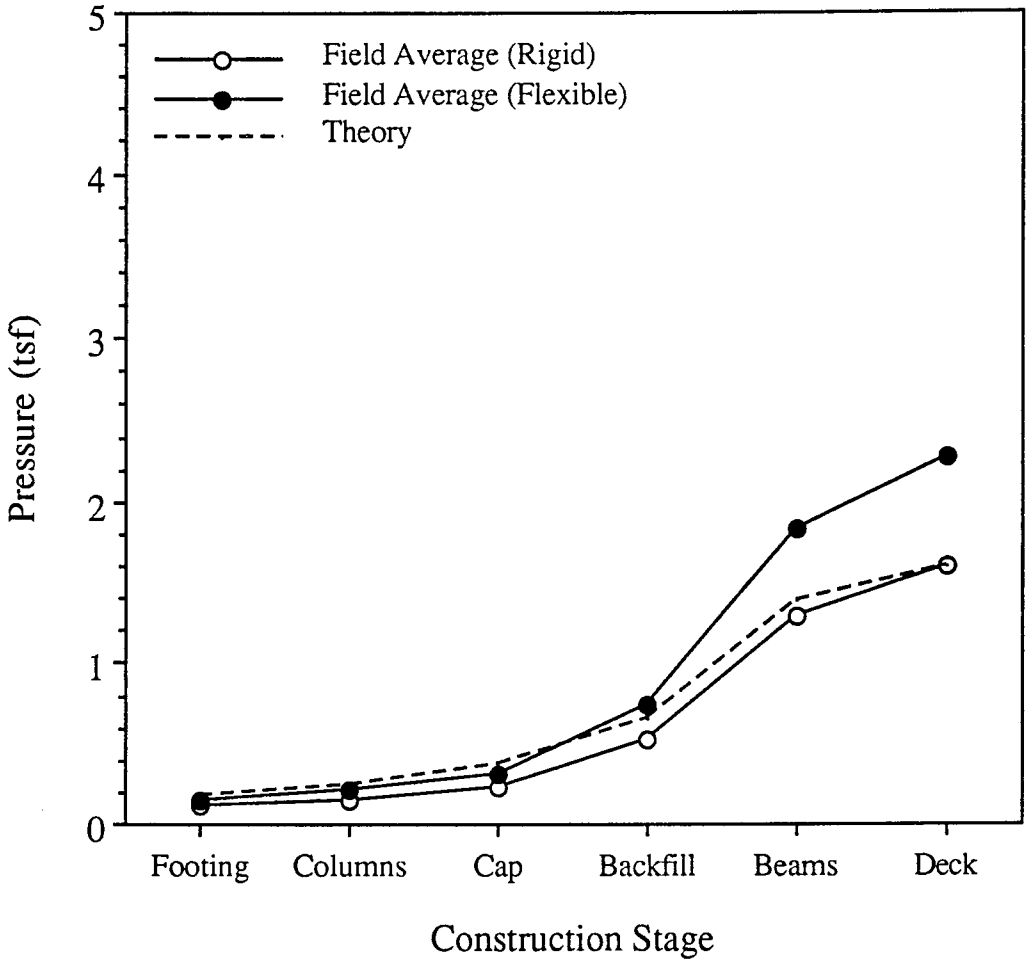

Figure 4.33 Contact Pressure Under Pier 5 - North Footing (Bridge D)

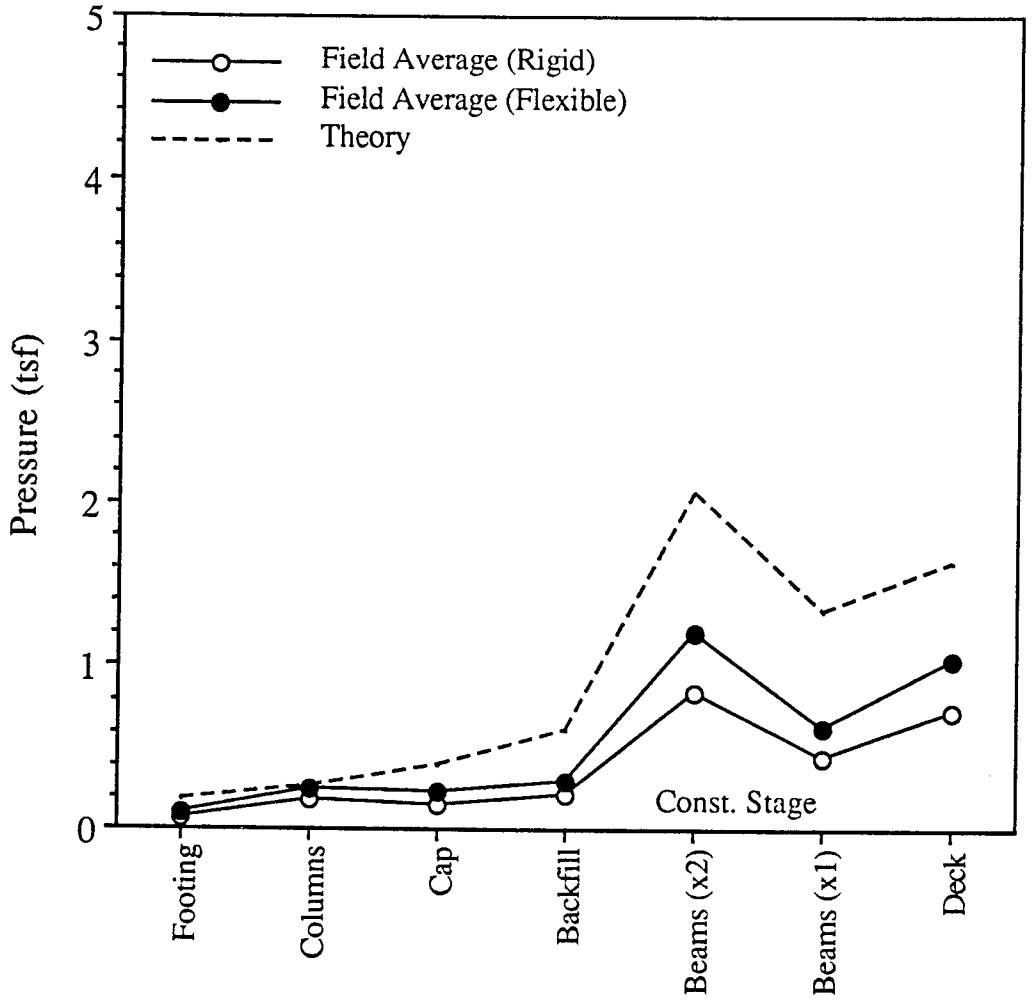

Figure 4.34 Contact Pressure Under Pier 5 - South Footing (Bridge D)

second curve, labeled "rigid", was generated by applying another calibration constant established from the test set-up of Figure 3.5b.

The contact pressure at the base of the footing was expected to vary widely during construction phases because of change in the magnitude and location of the resultant force within the Kern limit. The pressure of the toe, key, and heel should all increase when the footing is placed and when the abutment wall is placed on top of the footing. However, when backfilling operation begins behind the abutment wall, depending on the type of lateral pressure developing, pressure at either toe to heel may decrease. Figures 4.25a through 4.26c present field monitored contact pressure data at toe, key, and heel of Panel "A/B" and "C" footings of the Bridge A structure. Pressure values in these figures were obtained by applying the calibration factor C for the flexible loading condition. Construction stages are numbered as: 1 = footing construction; 2 = abutment wall construction; 3 = backfilling behind abutment wall; 4 = placement of girder beams; 5 = completion of composite deck construction; and 6 = service load. Under Panel "A/B" foundation, the contact pressure varied within a 0.2 to 2.0 tsf range. Maximum contact pressure detected prior to service load application was about 1.25 tsf (17.4 psi) near the toe, 1.4 tsf (19.4 psi) in the keyway, and 2.0 tsf (27.8 psi) near the heel. In early construction stage, the pressure was the largest under the keyway. As the construction progressed, the pressure near the toe and/or heel became larger than that at the key. Backfilling behind the abutment appeared to be more influential than the other stages on the magnitude of pressure. Near the end of data collection, the pressure near the toe decreased, while the pressure near the heel increased. This may be implying that the foundation tilted toward the backfill. Under Panel "C" foundation, the contact pressure fluctuated below 1.8 tsf (25 psi). Maximum pressure prior to service load application was 0.6 tsf (8.3 psi) near the toe, 1.4 tsf (19.4

psi) in the key, and 1.8 tsf near the heel. Very little redistribution of contact pressure was observed during various construction stages. Throughout the construction stages, ranking (in a descending order) among the three pressure measurements remained unchanged - (1) heel, (2) key, and (3) toe.

Figures 4.27 and 4.28 show the contact pressure data obtained under West Footing at the Bridge C site. Field curves based on the flexible load application method yielded higher pressure responses in all three cases, since this method resulted in higher calibration constant values. The construction stages are defined as: 1 = footing construction; 2 = placement of box culvert sections; 3 = backfilling; 4 = paving; and 5 = service load. Most of the following discussions are made focusing on the "Field (Flexible)" curves. Maximum pressure prior to service load application was 2.4 tsf (33.3 psi) near the toe, and 1.1 tsf (15.3 psi) near the heel. Pressure was distributed uniformly up to the end of the second construction stage. When the backfilling operation started, the pressure at the toe kept increasing while the pressure at the heel decreased. The pressure at the heel stayed lower than that at the toe during the remaining construction stages. This suggests that the footing was tilting toward the toe.

Figures 4.29 through 4.34 show the contact pressure data obtained under selected footings at the Bridge D site. Construction stages are clearly defined in each figure. Again, most of the following discussions are made focusing on the "Field (Flexible)" curves. The contact pressure measured at this site generally stayed well below 3.0 tsf (41.7 psi). Under Pier 3-North (Phase I) footing, however, the average contact pressure increased to about 4.4 tsf (61.1 psi). The field pressure readings remained relatively low under the Pier 2 (Phase I) footing, since ample time was not available for the pressure cell installation. Field readings for the Phase II (Phase II) footings responded well to the sixth construction stage, removal of the second layer beams, and through

reduction in pressure.

Figures B.21 through B.26 (Appendix B) present the contact pressure data obtained under selected foundations at the Bridge E site. All contact pressures remained well below 3.6 tsf (50 psi) except for the readings at the key of Rear Abutment (Phase I) which went as high about 5.2 tsf (72 psi). At both abutment foundations the pressure was higher near the heel than near the toe. Pressure near the toe of the Rear Abutment foundation was reduced to 0.07 tsf (1 psi) or less when backfilling was completed behind the abutment wall. This may indicate that the foundation tilted toward the backfill under the weight of the backfill. According to the field measured data, the pressure distribution was not as uniform as expected under the spread footings. For example, pressure was higher on the east side of the Pier 1 (Phase I) footing. Contact pressure readings under foundations, which were treated with unreinforced concrete pads underneath, were considerably less than those which rested directly over the soils. This can be seen by comparing Figure B.21 to Figure B.26 and Figure B.22 to Figure B.23. Figure B.56, along with Figure 3.29, shows that the bearing pressure becomes substantially less at the edge of the footing.

The average maximum contact pressure was about 1.9 tsf (26.4 psi) for Bridge A, 2 tsf (27.8 psi) for Bridge C, 2.5 tsf (34.7 psi) for Bridge D - Phase I, 1.8 tsf (25 psi) for Bridge D - Phase II, and 2.0 tsf (28.3 psi) for Bridge E - Phase I. The highest maximum contact pressure of about 5.2 tsf (72.3 psi) was recorded in the key of the Rear Abutment foundation (Phase I) at the Bridge E site. These field contact pressure values were all well below allowable bearing capacity of the bearing soils in the influence zones. Based on the SPT data available at each site, average allowable bearing capacity of the bearing soils in the influence zones were estimated to vary from 5.8 tsf (80.6 psi) at the Bridge A site to 10.6 tsf (147 psi) at the Bridge D site. Table 4.1 gives a summary of the contact

pressure data for the foundations of the five bridges.

4.4 Tilting of Abutment Walls and Pier Columns

Factors which are generally considered to contribute to tilting of the abutment walls are geometry of the abutment structure, forces induced by backfilling and deck construction, rigidity of the wall to foundation connection, and spatial variability in properties of the bearing soil. On the pier columns, rotational movement may be also driven by the uneven span dimensions. Tilting of the abutment walls and pier columns was expected to be small. Figures 4.35 through 4.41 and 4.43 through 4.48 present field monitored tilting data for the walls/columns of the Bridges A, B, C, and D structures. Tilting performance plots of the pier columns and abutment walls at the Bridge E site are shown in Figures B.27 through B.34 in Appendix B. In any of these plots prepared for the abutment wall, a relative change in angle in the negative direction indicates that the wall has rotated away from the backfill behind the wall.

From Figures 4.35 and 4.37, it is evident that the backfilling operation made the abutment walls of Bridge A tilt away from the backfill. Panel "C" section, which was constructed in front of the old retaining wall structure, experienced as much tilting (0.1 degree) as Panel "A" section. Presence of the retaining wall structure did not have any significant effect on the abutment wall tilting. When the toe section of these footings was covered with soil thereafter, reversal in wall tilt direction was recorded. When additional loads were imposed through construction of the bridge deck, the abutment walls started tilting again away from the backfill. Before the completion of the bridge deck construction, the rate of tilting stabilized, except at the Panel "C" abutment wall. Together, the contact pressure and abutment wall tilting data may be able to show if the overall

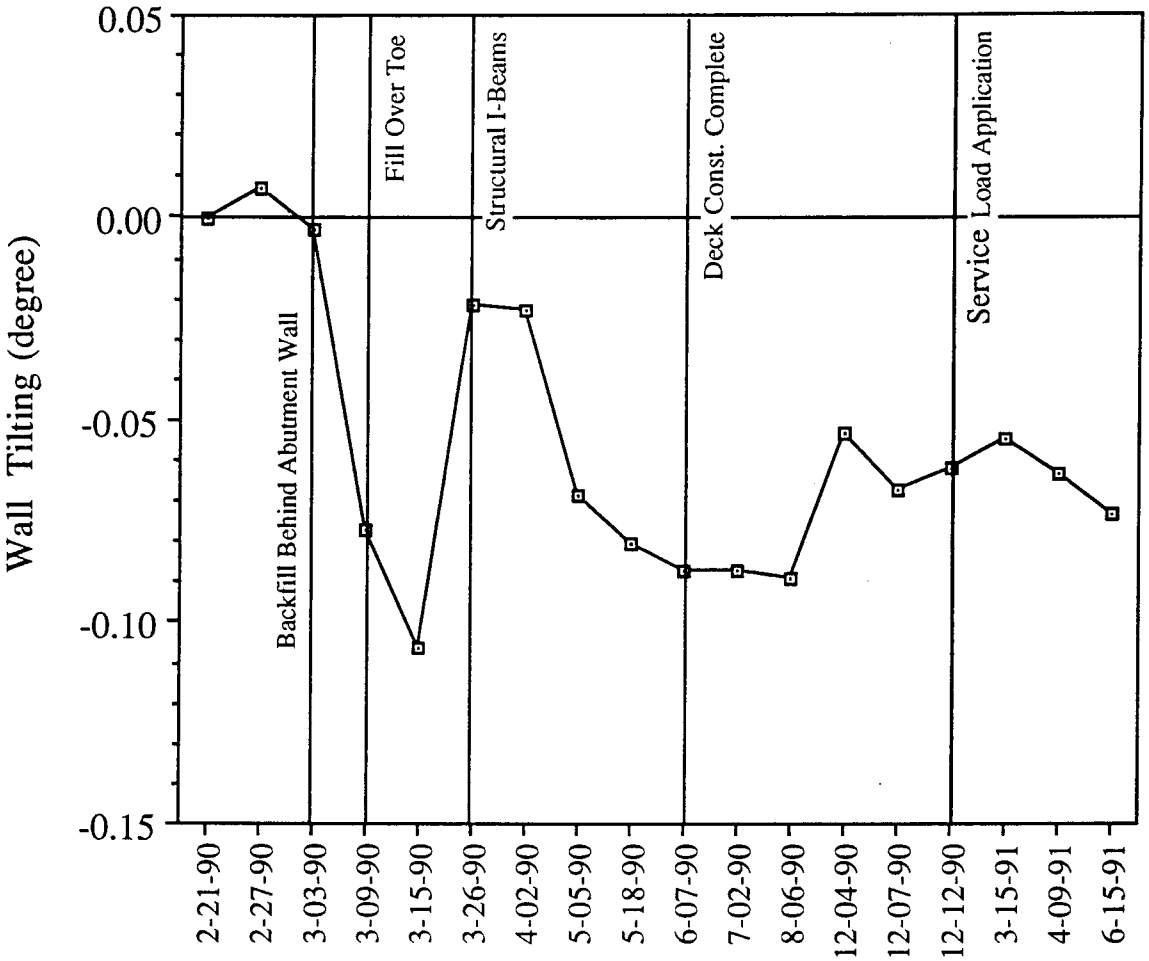

Figure 4.35 Tilting of Panel "A" Abutment Wall
(Bridge A)

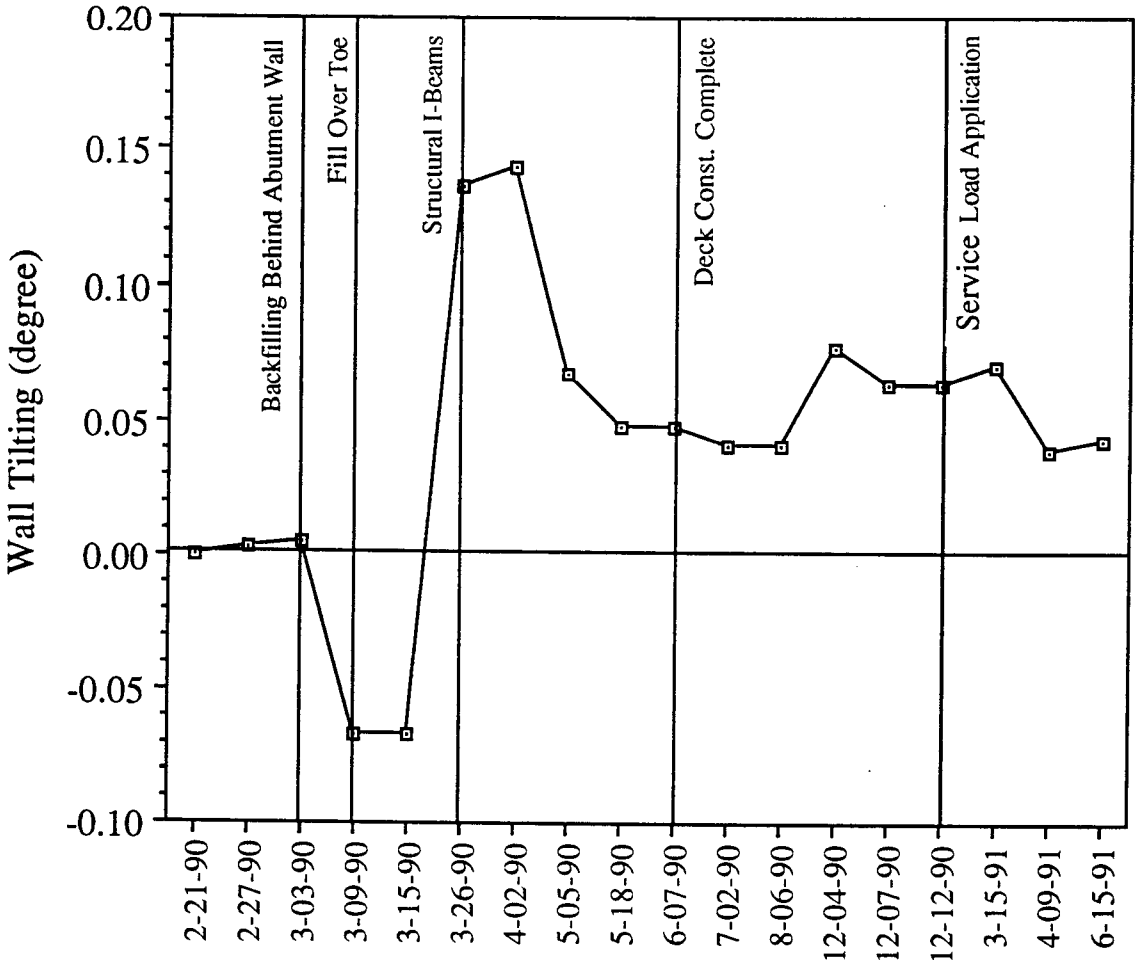

Figure 4.36 Tilting of Panel "B" Abutment Wall
(Bridge A)

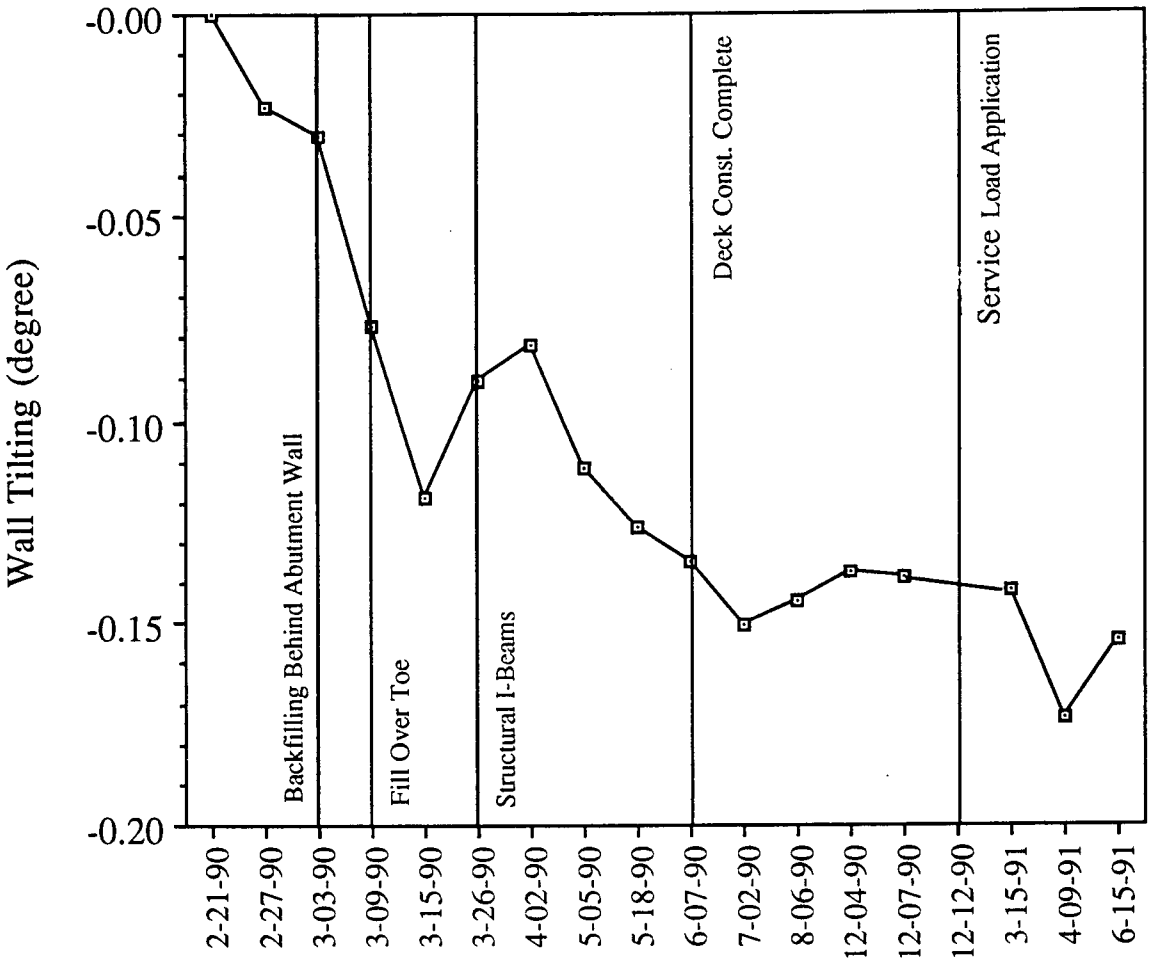

Figure 4.37 Tilting of Panel "C" Abutment Wall
(Bridge A)

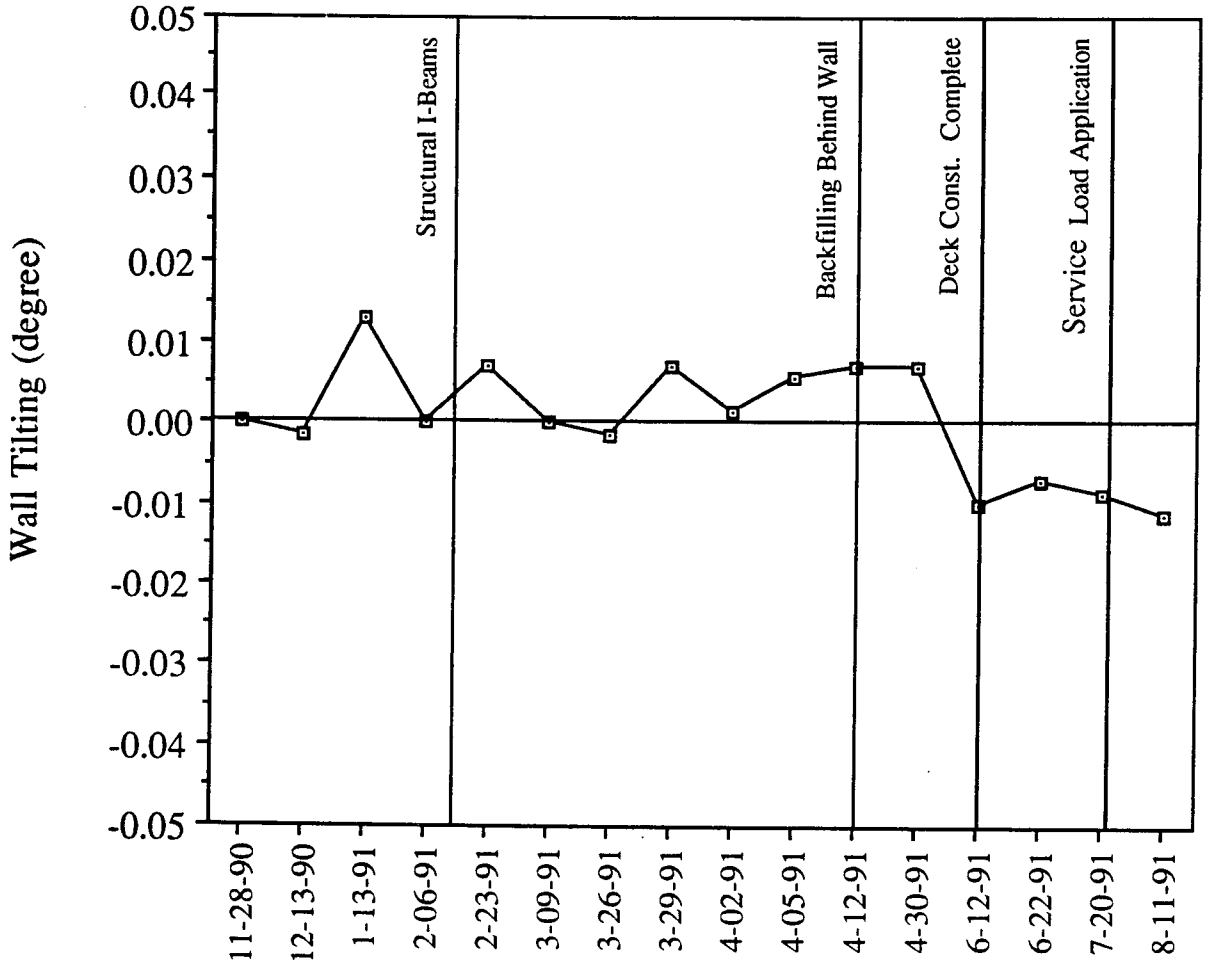

Figure 4.38 Tilting of Abutment No. 1 Front Wall (Bridge B)

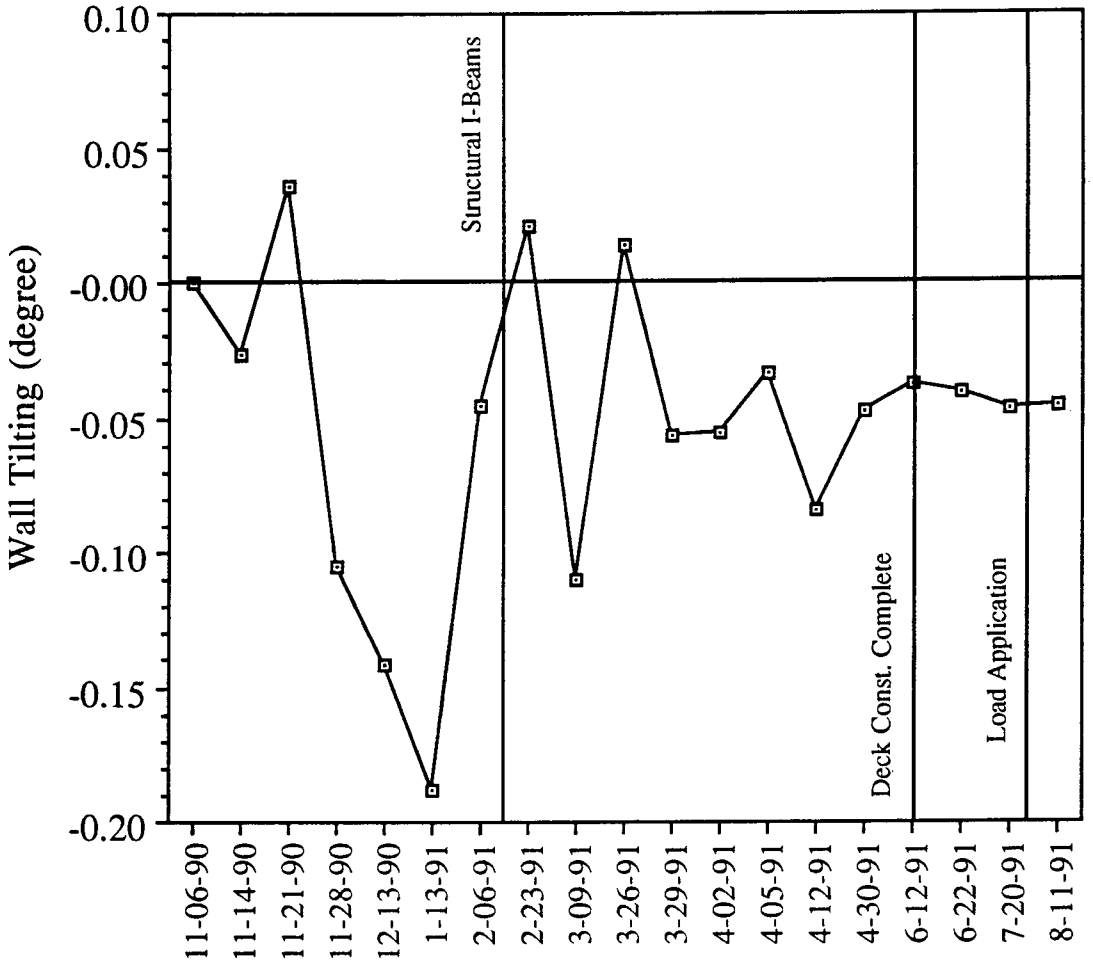

Figure 4.39 Tilting of Central Pier Foundation Columns (Bridge B)

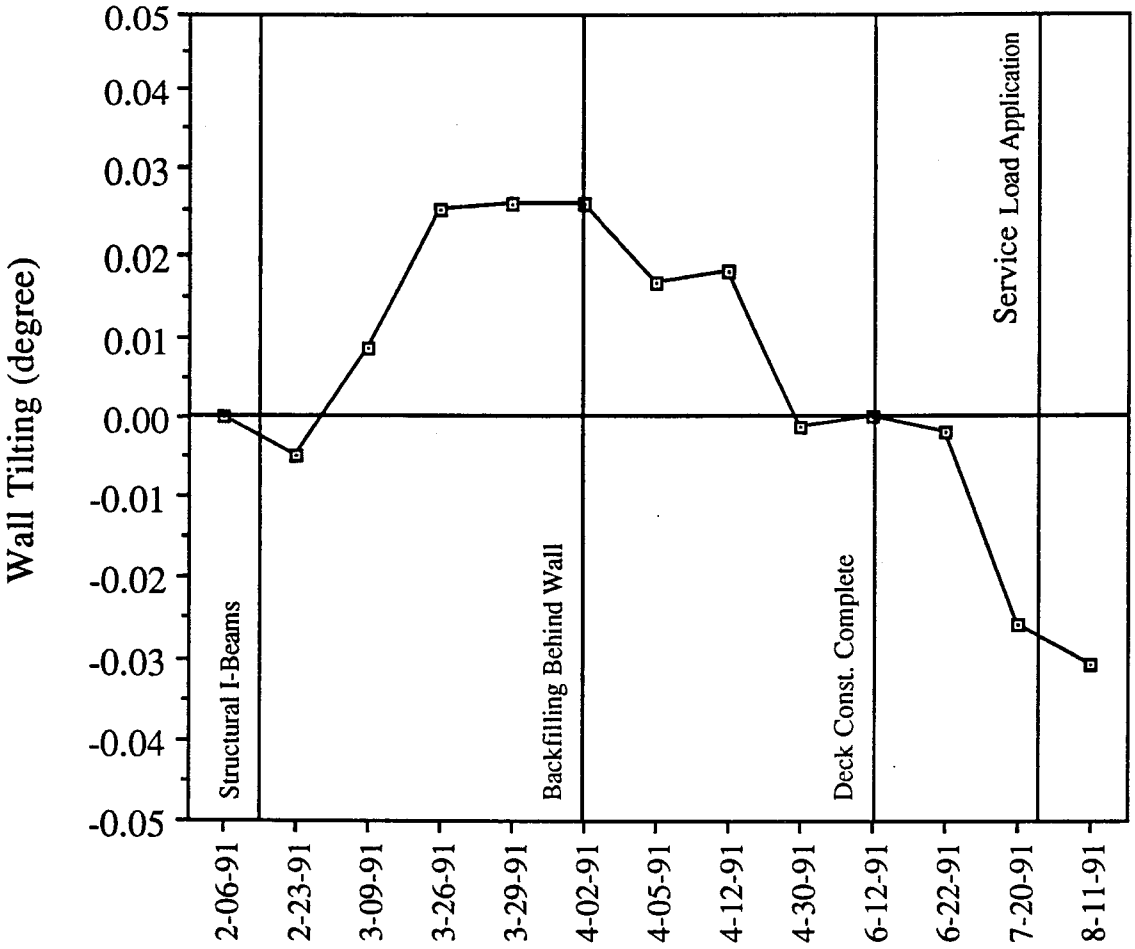

Figure 4.40 Tilting of Abutment No. 2 Front Wall
(Bridge B)

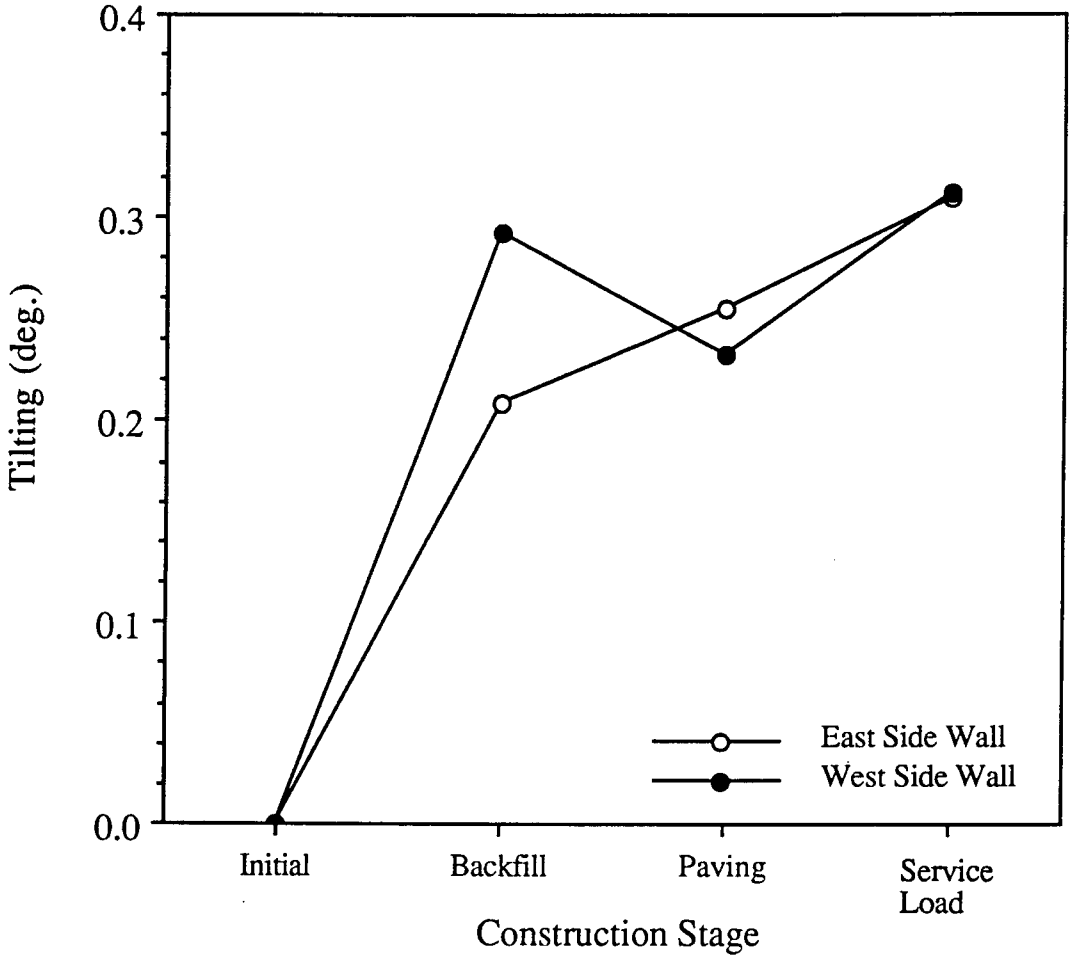

Figure 4.41 Tilting of Box Culvert Walls (Bridge C)

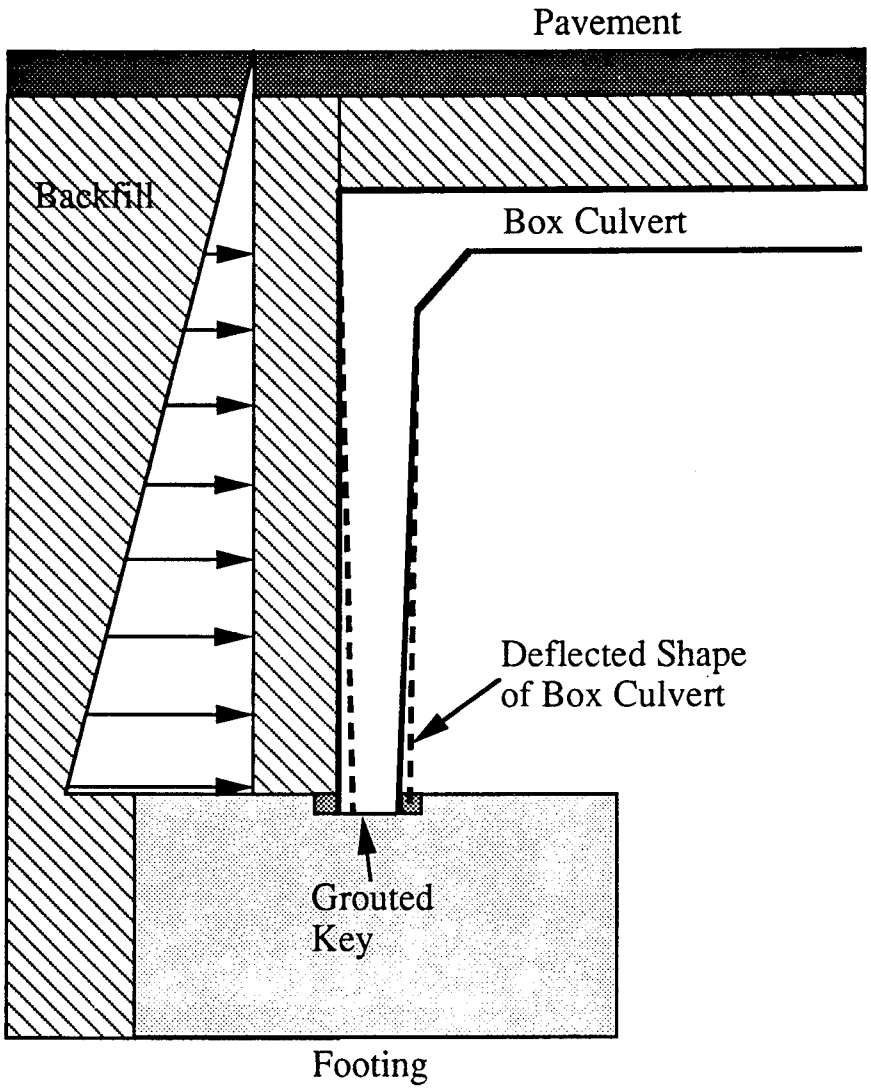

Figure 4.42 Inward Lateral Movement of Culvert Wall

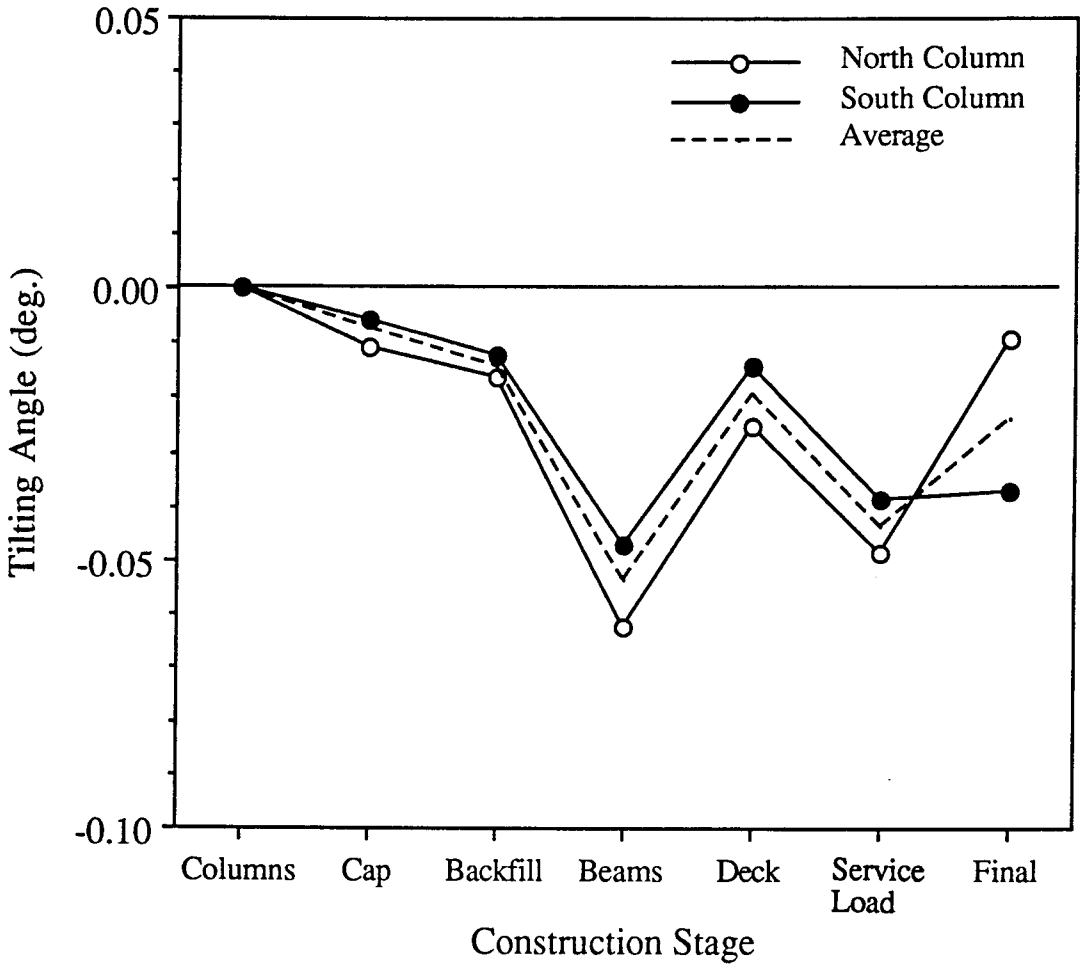

Figure 4.43 Tilting Performance of Pier 2-North Footing Columns (Bridge D)

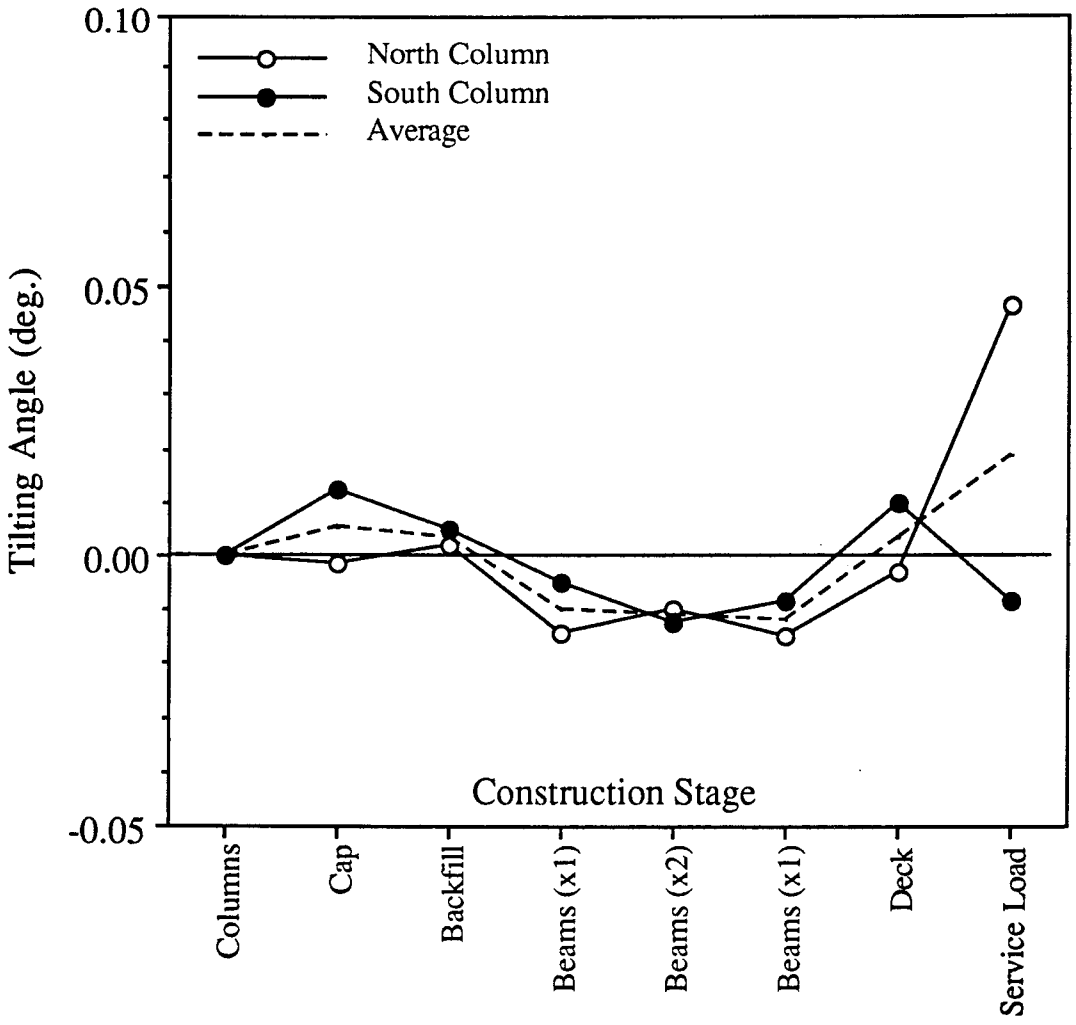

Figure 4.44 Tilting Performance of Pier-2 South Footing Columns (Bridge D)

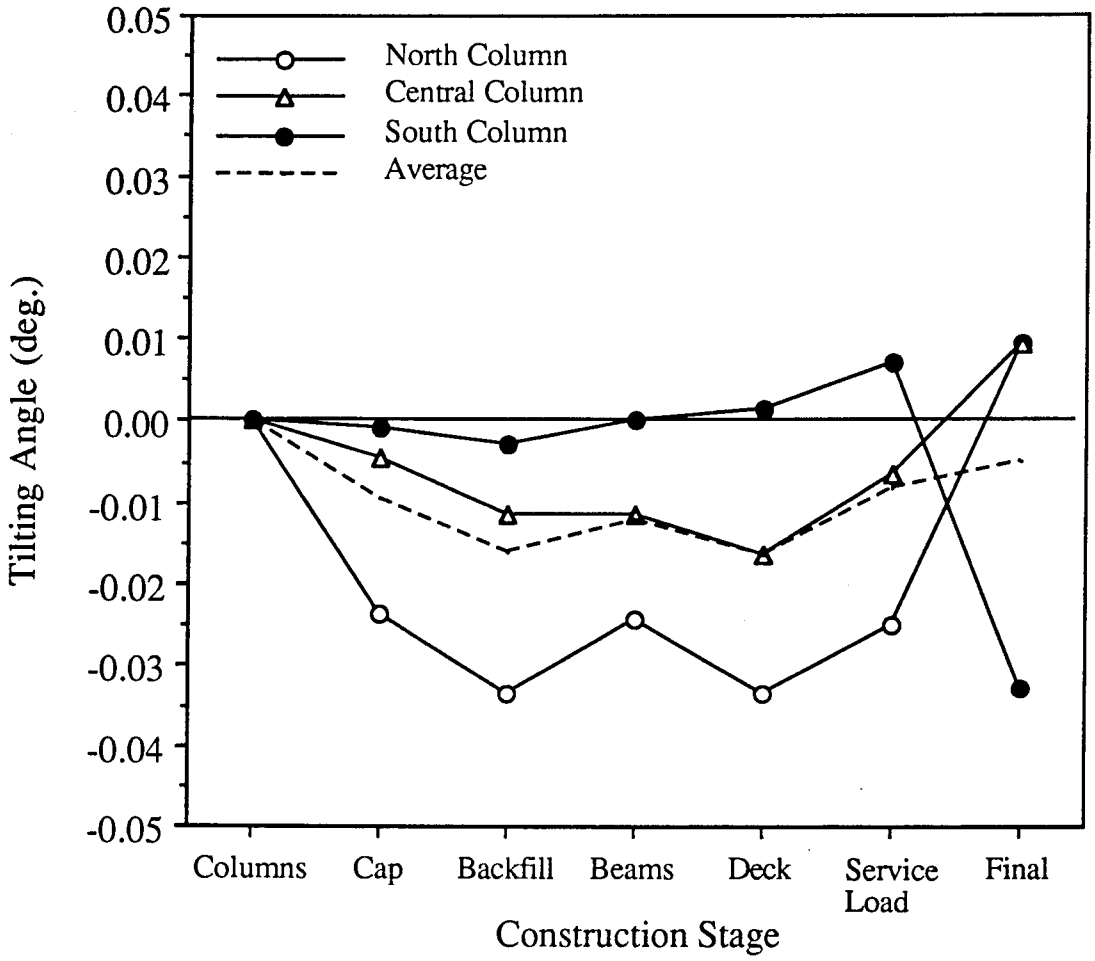

Figure 4.45 Tilting Performance of Pier 3-North Footing Columns (Bridge D)

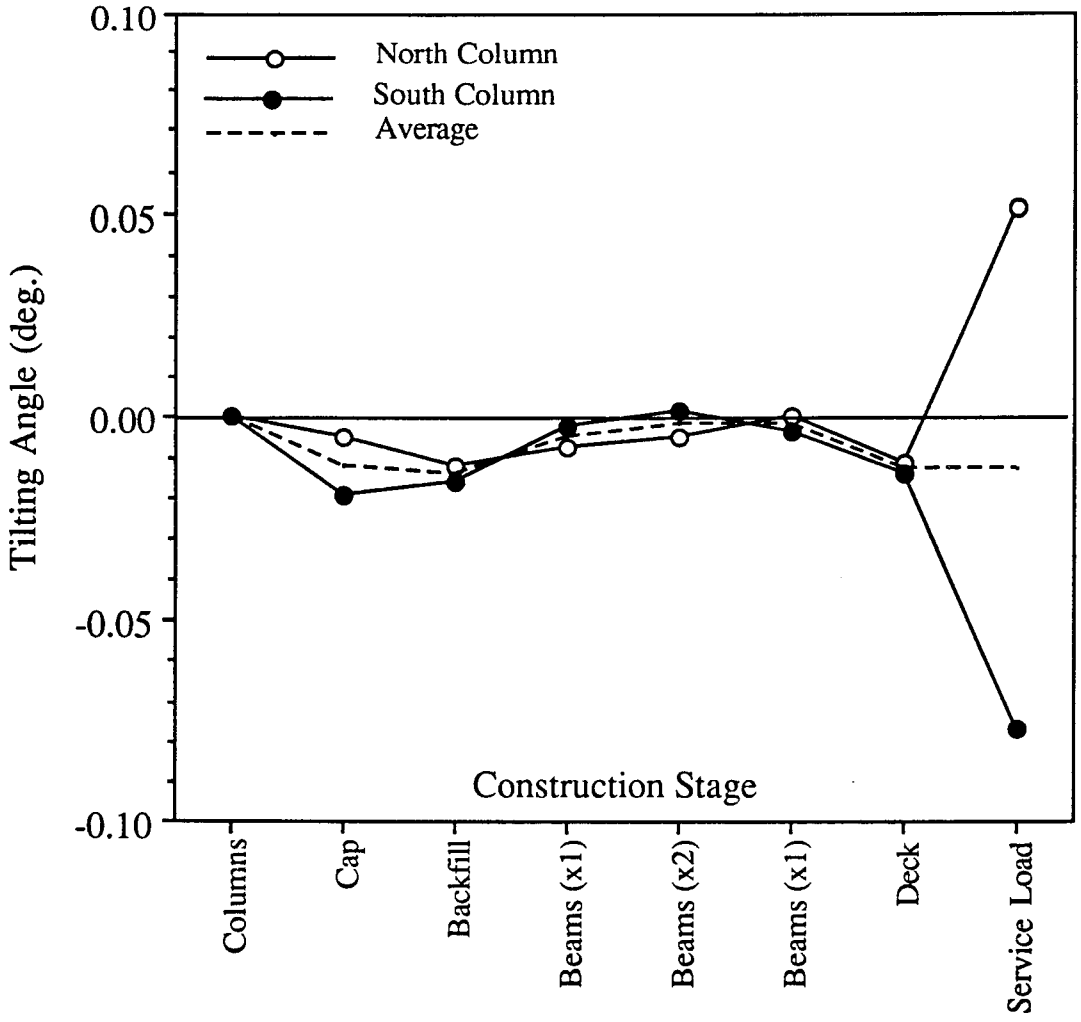

Figure 4.46 Tilting Performance of Pier 3-South Footing Columns (Bridge D)

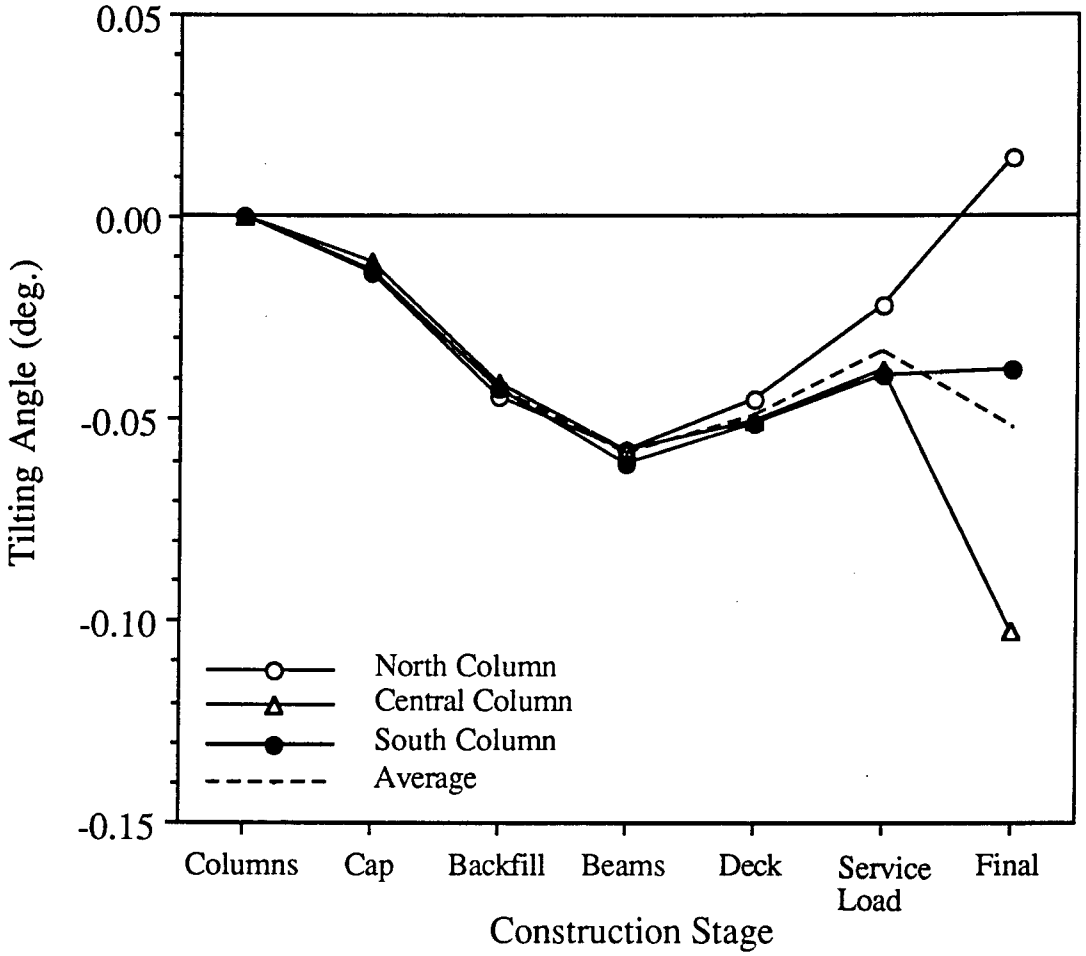

Figure 4.47 Tilting Performance of Pier 5-North Footing Columns (Bridge D)

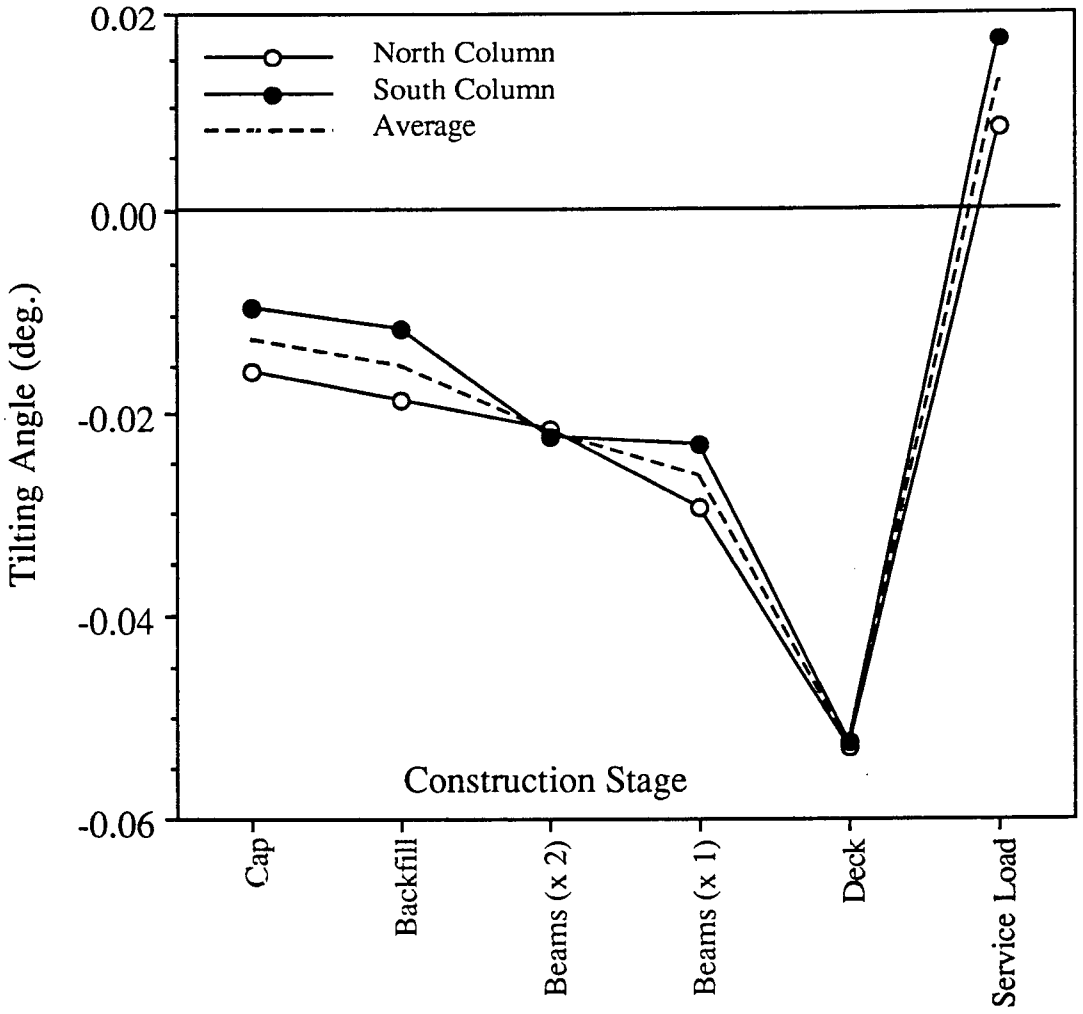

Figure 4.48 Tilting Performance of Pier 5-South Footing Columns (Bridge D)

abutment wall/footing behaves as a rigid structure. At Panels "A" and "C", the pressure at the toe decreased and the pressure at the heel increased when the abutment wall was rotating away from the backfill during the backfilling stage. This observation indicates that this type of structure may not be considered truly rigid.

According to Figures 4.38 and 4.40, the front walls of Abutment No. 1 and Abutment No. 2 at Bridge B site hardly tilted throughout the construction stages. For Abutment No. 1 wall, the tilt reading fluctuated within $\pm$ 0.01 degree. Slightly larger range in tilting of $\pm$ 0.03 was recorded for the wall of Abutment No. 2. In both cases, the abutment wall rotated away from the backfill during the backfilling process. However, the columns of Central Pier experienced up to almost -0.2 degree tilting, showing no clear trend (Figure 4.39).

Culvert walls at Bridge C site behaved differently during backfilling. As shown in Figure 4.41, the walls rotated toward the backfill by 0.2 to 0.3 degree. This is understandable, for the three-sided box culvert sections were simply placed and grouted in the key way at the top of the strip footings. This formed a very loose connection between the culvert wall and the footing. As the culvert was backfilled, earth pressure was developed against the culvert wall such that it increased with depth. Since the culvert was a frame structure, the upper portion had little horizontal movement, while the lower portion was pushed inward due to the loose connection subjected to larger lateral pressure. Such an inward lateral movement at the bottom showed up as if the whole structure had tilted toward the backfill. Figure 4.42 illustrates such a behavior.

According to Figures 4.43 through 4.48, range of tilting measured at Bridge D site was within $\pm$ 0.1 degree. There appears to be no correlation between the construction stages and the actual tilting behaviors observed for the pier foundations. For the Pier 2 (Phase I) and Pier 5 (Phase II)

columns, beam placement and deck construction had larger contributions than other construction stages. However, for the other columns shown, the tilting performance was more pronounced during the service load application period.

According to Figures B.27 and B.34, range of tilting of the pier columns and abutment walls detected at the Bridge E site was within $\pm$ 0.12 degree. All the abutment walls rotated slightly toward the backfill except for the Phase II forward abutment wall. The Phase I abutment walls tilted more than the Phase II abutment walls. Figures B.27 and B.28 show that tilting of the pier foundation columns in the transverse direction was as much as that in the longitudinal direction.

In summary, maximum tilting of pier columns and abutment walls was measured to be well within $\pm$ 0.3 degree of all five bridge sites. The average absolute maximum tilting (in the longitudinal direction) was 0.2 degree for Bridge A, 0.2 degree for Bridge B, 0.3 degree for Bridge C, 0.07 degree for Bridge D, and 0.12 degree for Bridge E (Phase I). If a basic statistical analysis is performed with all the data, the mean and standard deviation of the average maximum tilting will be 0.66 and 0.359, respectively. The largest tilting of about 1.25 degree was recorded at... Table 4.1 gives a summary of the tilting performance exhibited by the pier columns and abutment walls (or culvert walls) of the five bridges.

Effect of the construction activity was easier to observe on the tilting behavior of the abutment walls than on that of the pier columns. Tilting of the pier structures appeared to be induced by variations in the span dimensions and spatial variability in the properties of the bearing soil layers. According to the field data obtained at the Bridge E site, tilting of the pier columns in the transverse direction was about the same order of magnitude as that in the longitudinal direction.

4.5 Other Field Monitored Performance

On September 15, 1991, a special investigation was conducted at the site of Bridge A. The goal of the investigation was to collect field data to draw a general conclusion on the effect of daily temperature fluctuation on the tilting of the spread footing supported bridge abutment wall. Field readings of wall tilting and concrete surface temperature were taken using the Sinco Tiltmeter system and general purpose laboratory thermometer at 7 a.m., 9 a.m., 12 p.m., 1 p.m., 2 p.m., and 3 p.m. Weather was mostly sunny with no precipitation, and the temperature at the concrete surface exposed to the sunlight near the bridge varied from 70 to 103°F (21.1 to 39.4°C).

Figures 4.49 through 4.55 present results of the temperature effect investigation. In these plots, the following sign conventions were used to indicate the direction of the wall rotation:

"+" value....Rotation toward the backfill behind the abutment wall

"-" value....Rotation away from the backfill behind the abutment wall

Although additional studies are suggested, it is observed that increase in the ambient temperature had a tendency to induce a small amount of rotation of the abutment wall in the direction toward the backfill.

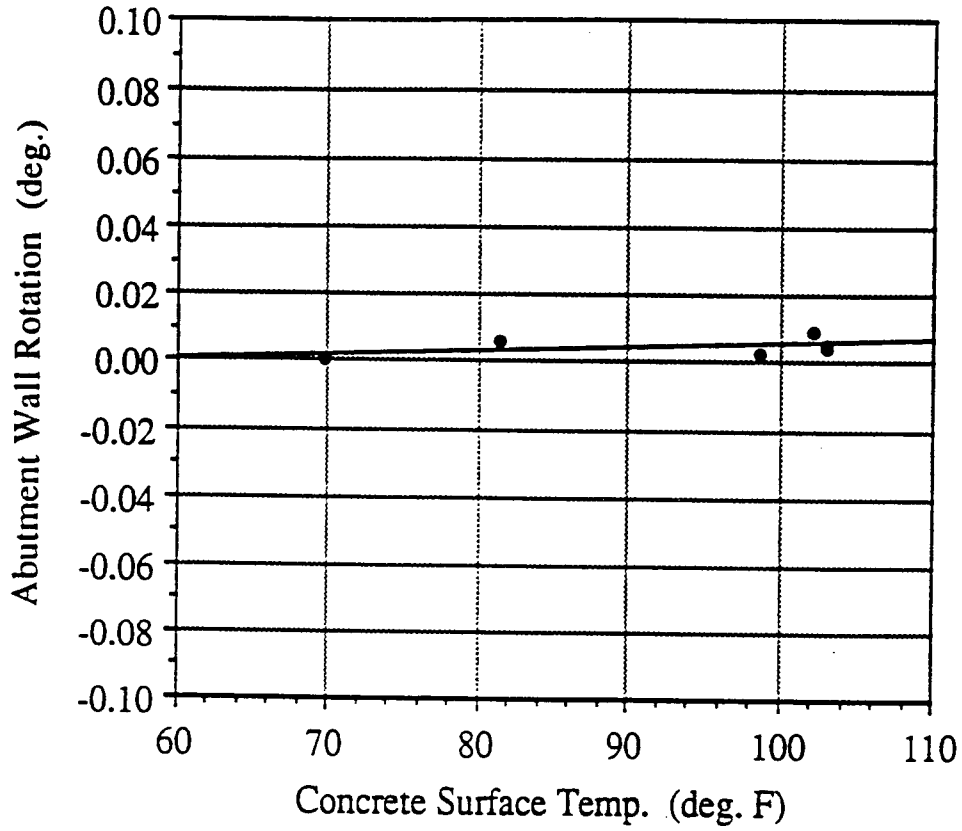

Figure 4.49 Temperature Influence on Panel "A" Abutment Wall Rotation (Bridge A)

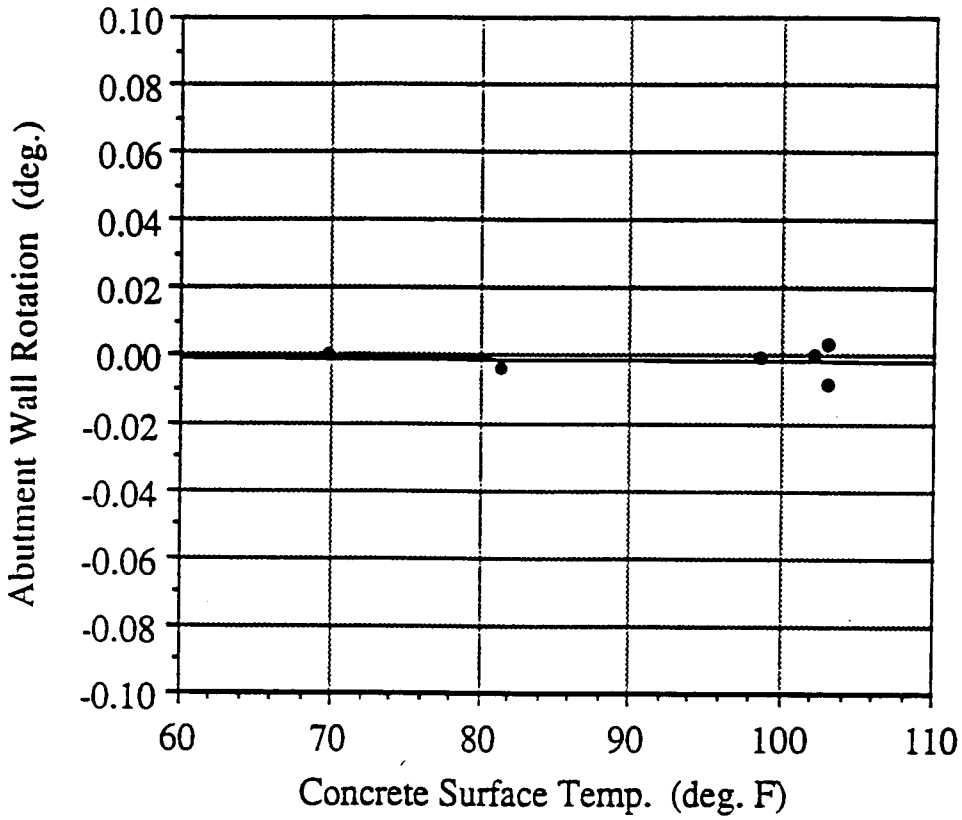

Figure 4.50 Temperature Influence on Panel "B" Abutment Wall Rotation (Bridge A)

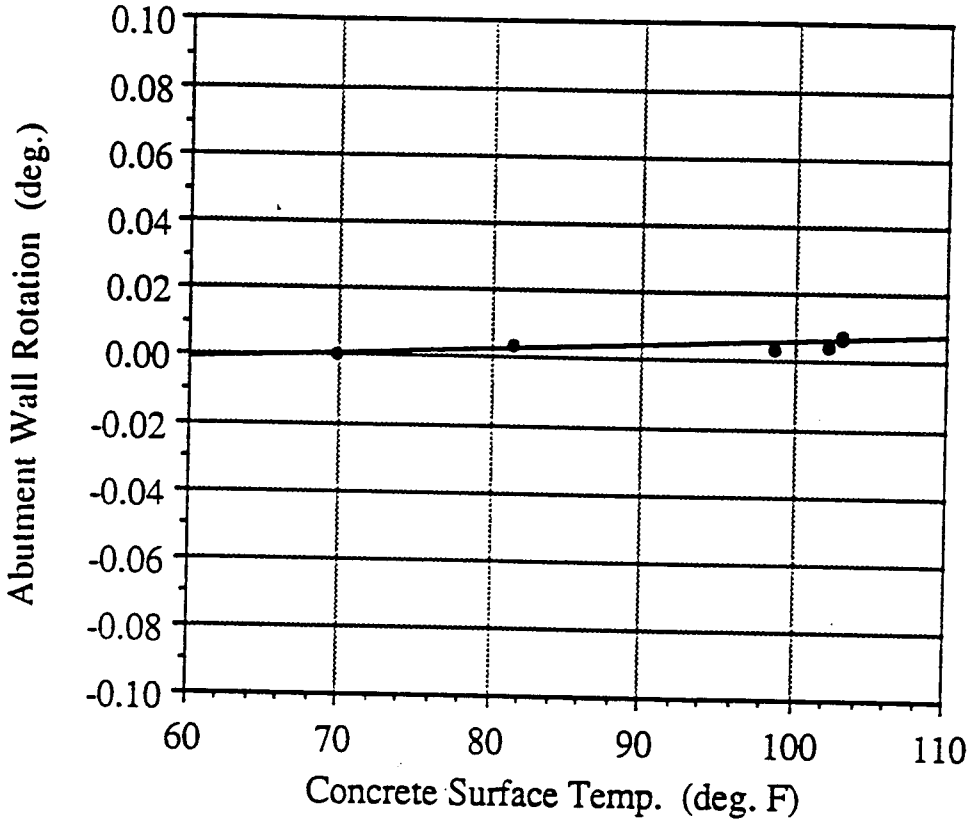

Figure 4.51 Temperature Influence on Panel "C" Abutment Wall Rotation (Bridge A)

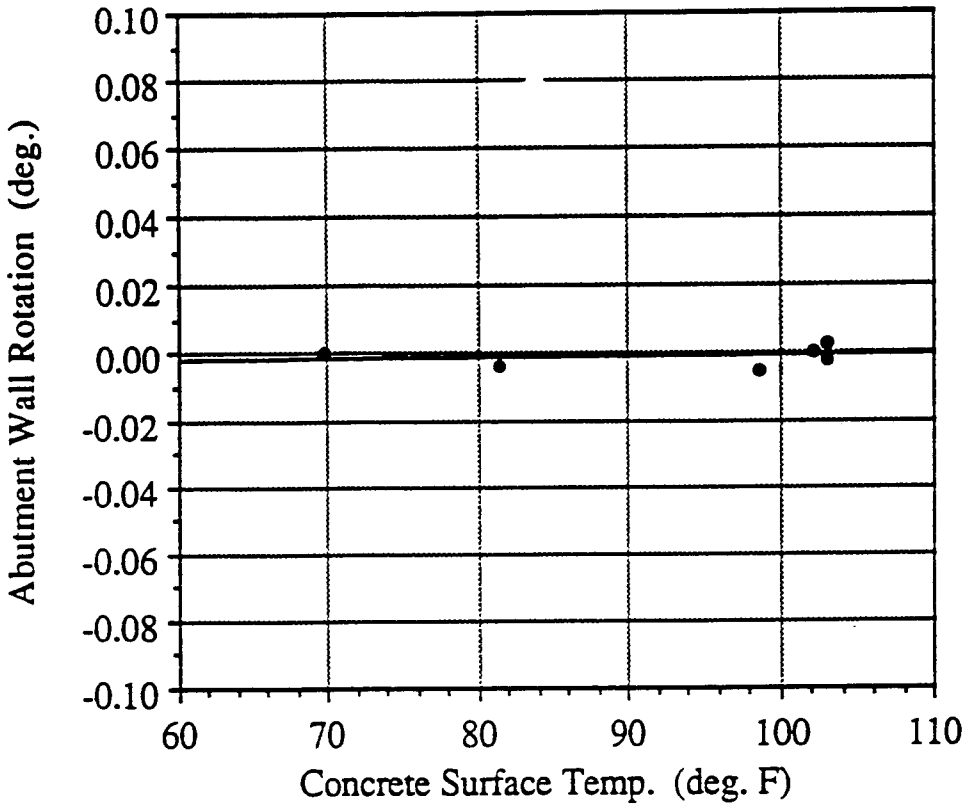

Figure 4.52 Temperature Influence on Panel "E" Abutment Wall Rotation (Bridge A)

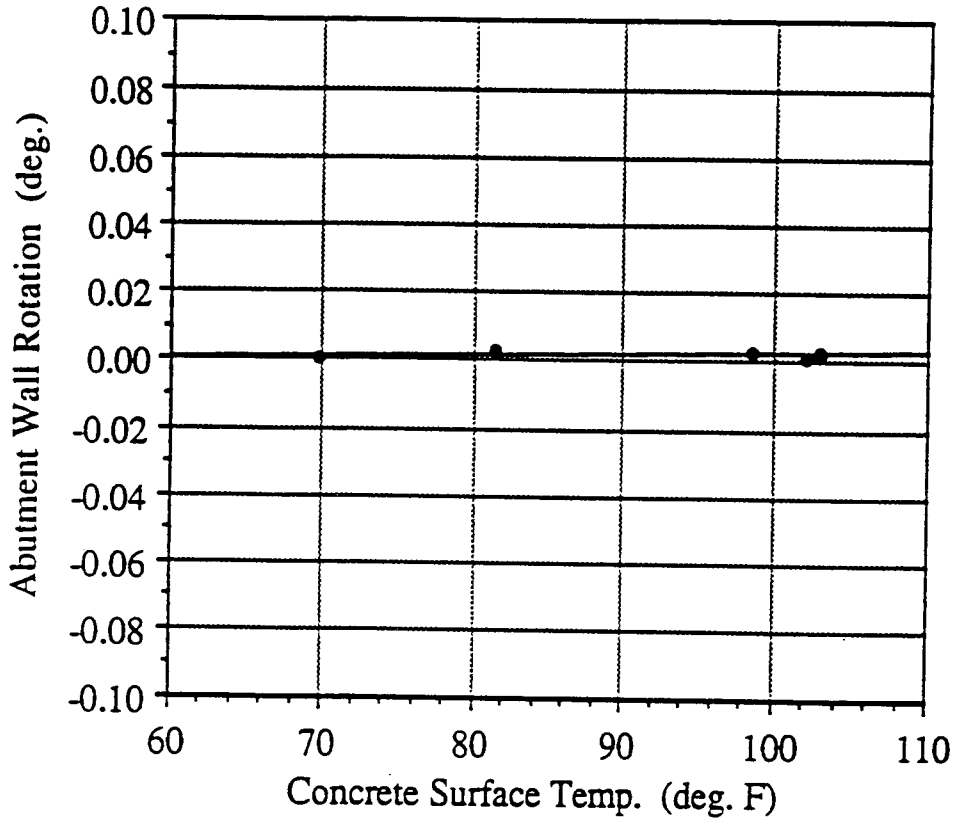

Figure 4.53 Temperature Influence on Panel "F" Abutment Wall Rotation (Bridge A)

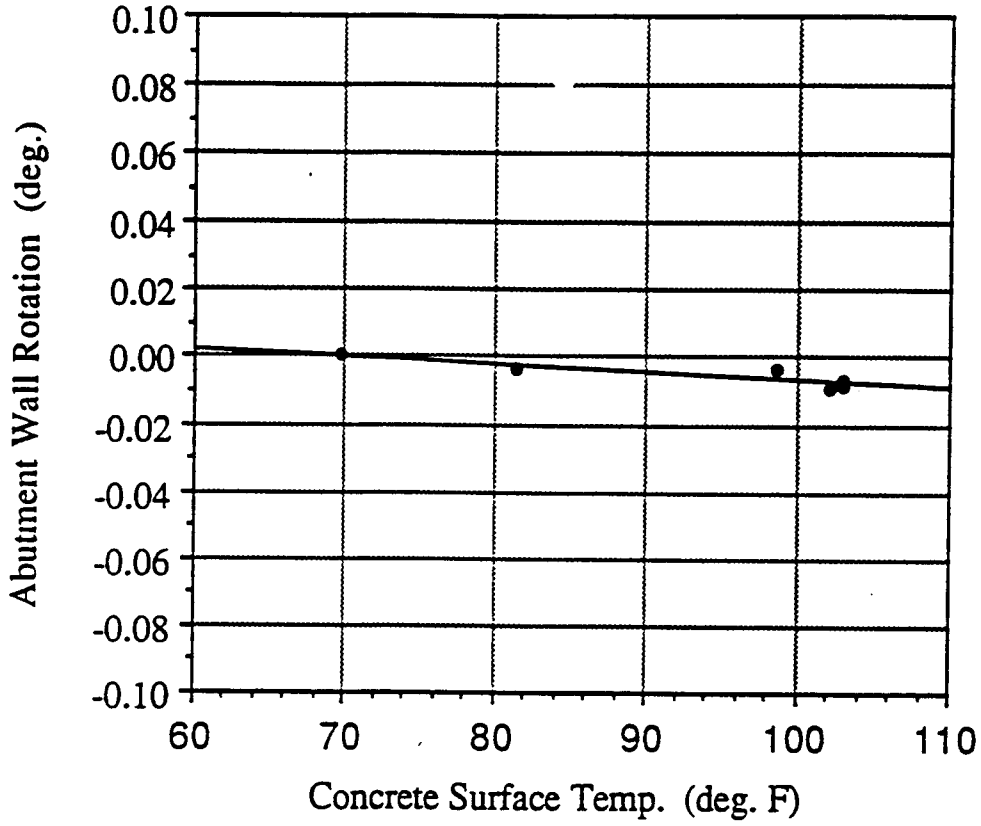

Figure 4.54 Temperature Influence on Panel "G" Abutment Wall Rotation (Bridge A)

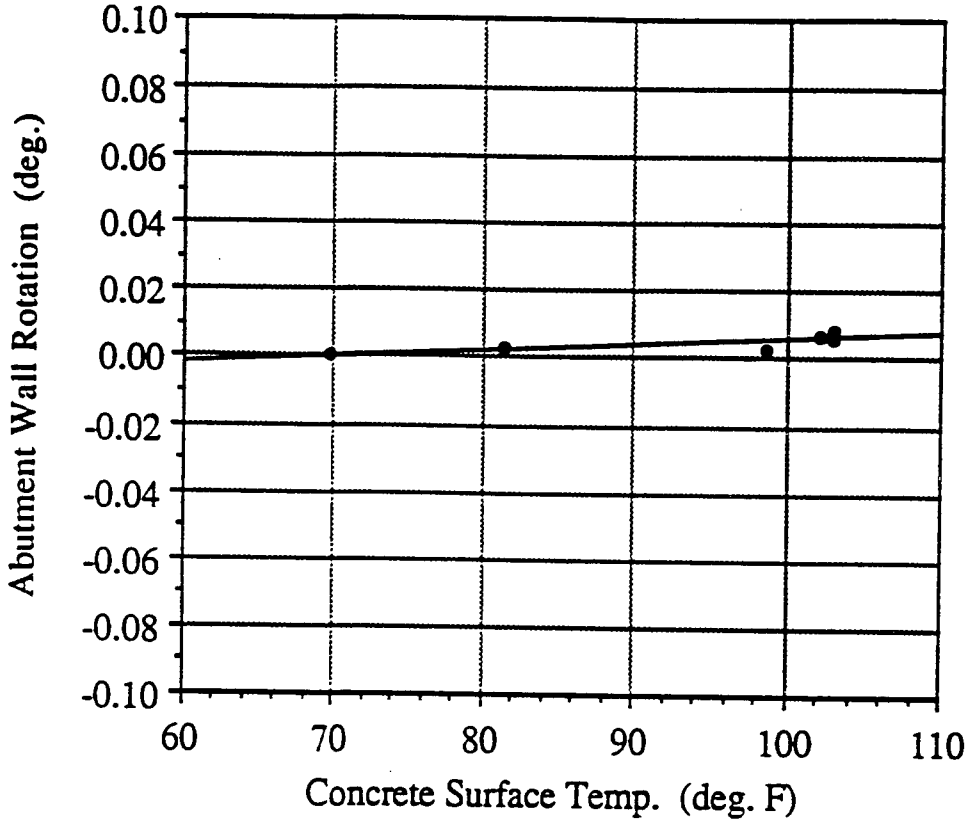

Figure 4.55 Temperature Influence on Panel "H" Abutment Wall Rotation (Bridge A)

Chapter 5

Geotechnical Methods and Their Predictions

5.1 Introduction

Three essential considerations in designing spread footings for highway bridges are bearing pressure, overall settlement, and differential settlement. Obviously, contact pressure at the footing/ bearing soil interface must be less than the allowable bearing pressure for the soil strata in the loaded area to prevent shear failure of the soil. Overall or uniform settlement must not exceed the limit which will affect integrity of the superstructure and safety of drivers. Also, the amount of differential settlement must be within the tolerable range for a given structure to prevent structural damage to the bridge deck and abutments/wingwalls. In general, the bearing pressure is a less significant controlling factor than the other two. In other words, the load which results in tolerable overall and differential settlement of the structure will normally provide adequate factor of safety against shear failure of the bearing soil strata.

There are theoretical/empirical methods developed over the past years to estimate contact pressure, bearing capacity of soils, abutment wall tilting, and settlement for spread footings. Especially, for settlement estimation, there are more than several methods to choose from, and their nature varies from empirical to theoretical (elasticity, one-dimensional compression). This chapter presents a compilation of geotechnical methods which are useful for design and analysis of spread footings on cohesionless and cohesive soils. Comparisons between field monitored performance and predictions by these methods follow the descriptions of the methods.

5.2 Contact Pressure and Distribution

Theoretical distribution of the contact pressure at the base of the footing was computed with overturning moment in consideration. The formula given below assumes that the footing is a rigid structure,

$$q = \frac{P}{A} \pm \frac{M}{S} \qquad \text{Eq. (5.1)}$$

where q = contact pressure at footing/soil interface; P = dead load on footing (including the self weight); A = footing base area; M = overturning moment; and S = section modulus.

Using this equation, the maximum and minimum pressures acting at the heel and toe can be determined. Also, the pressure at other locations between the tow and heel can be obtained by assuming that the contact pressure varies linearly between the edges. This is a crude approximation of the realistic case. Actual pressure distribution is known to be nonlinear and its magnitude, especially at the corner, is influenced by the flexibility of the footing and type of the bearing soil. In addition, calculation of M requires estimation of the lateral earth pressure, which is indeterminate between K_a and K_o. In application of the above formula, the minimum earth pressure coefficient K_a was assumed to exist behind the wall in all cases and determined based on the internal friction angle (Φ) of the soil retained by the abutment wall.

Figures 5.1 through 5.3 present a comparison between field data and theoretical results at toe, key, and heel of the Panel "A/B" footing of Bridge A. Construction stages are numbered as: 1 = footing construction; 2 = abutment wall construction; 3 = backfilling behind abutment wall; 4 = placement of girder beams; 5 = deck construction; and 6 = service load application. Additional stress induced by the service load application was assumed to be equal to 10% of the total load that

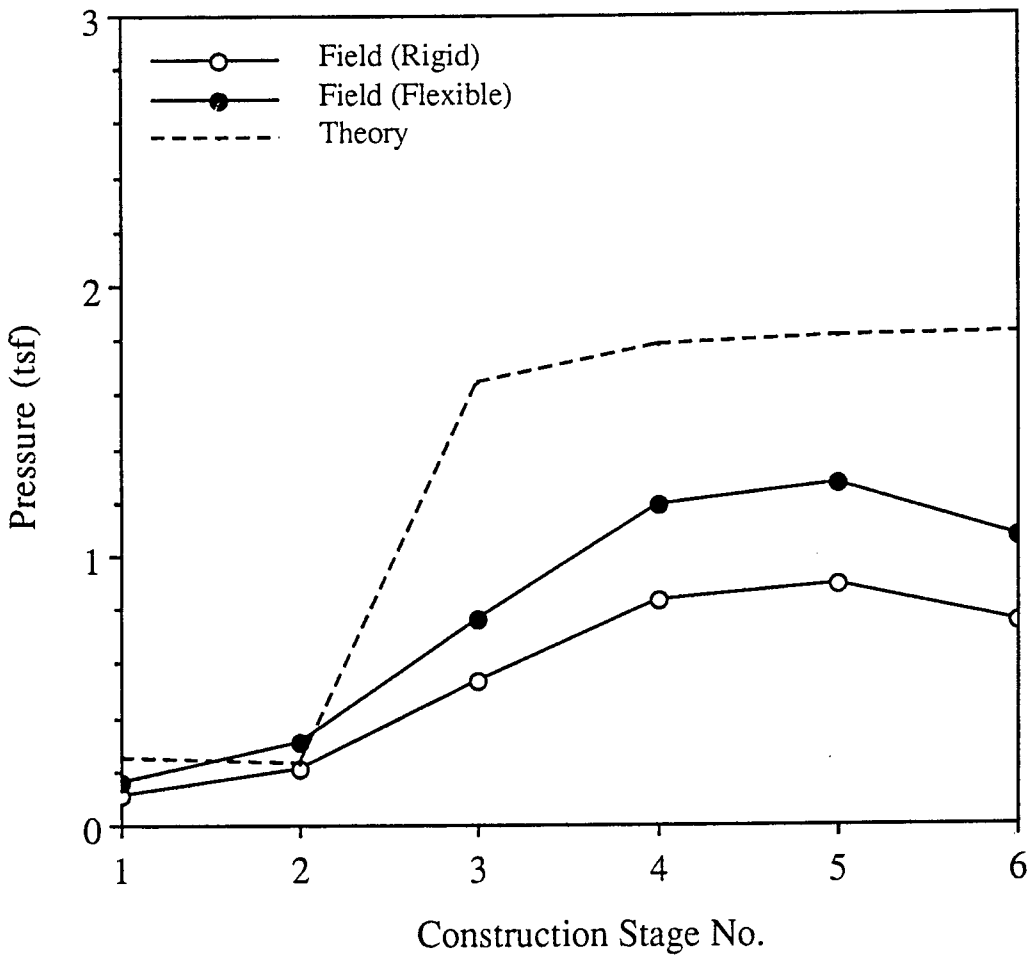

Figure 5.1 Contact Pressure Near Toe of Panel "A/B" Footing (Bridge A)

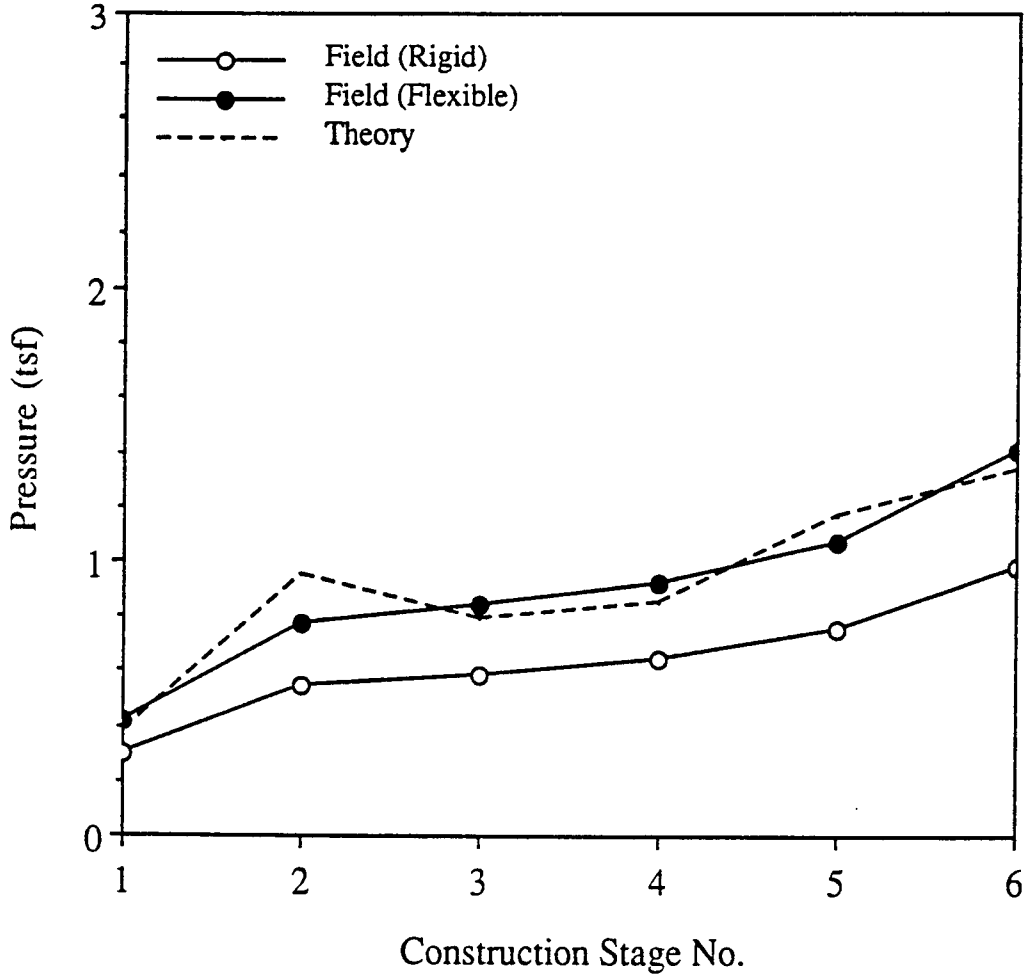

Figure 5.2 Contact Pressure at Key of Panel "A/B" Footing (Bridge A)

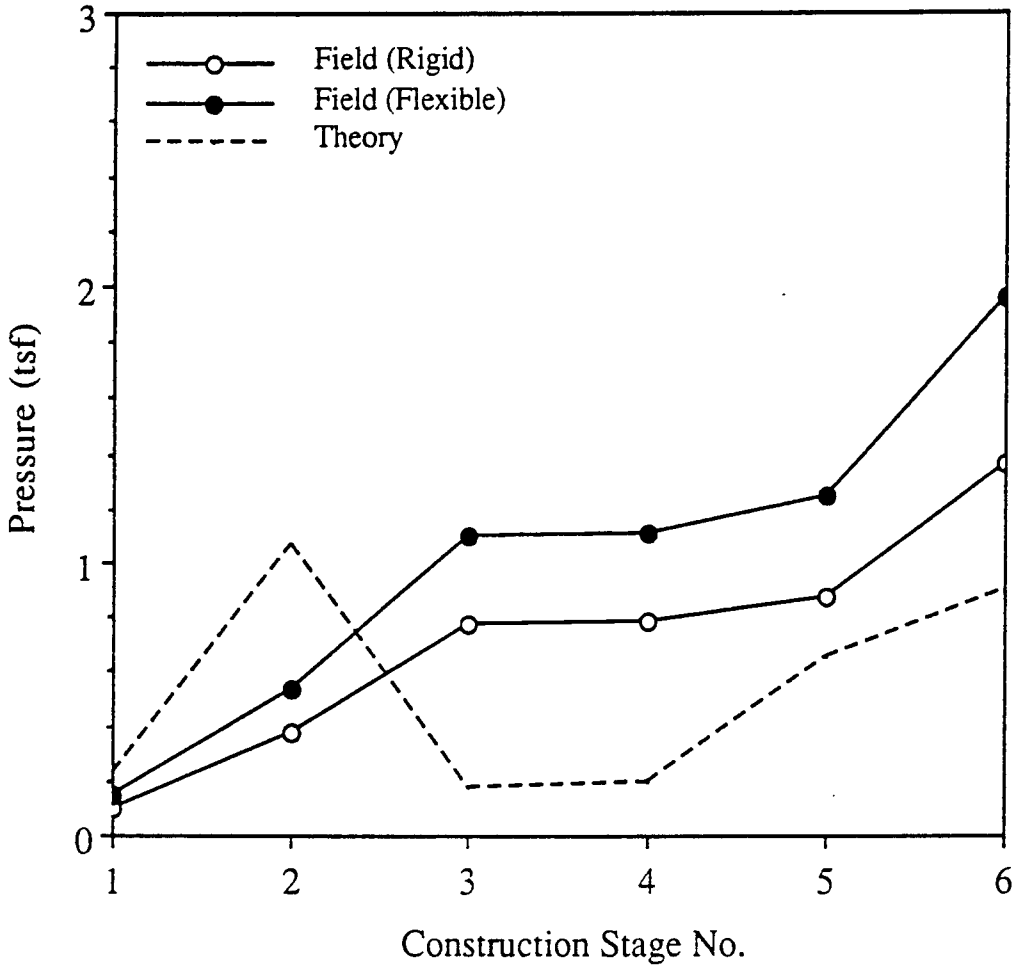

Figure 5.3 Contact Pressure Near Heel of Panel "A/B" Footing (Bridge A)

existed at the end of construction (stage 5). This was believed to be a very conservative approach. Generally, a good agreement was observed between the theory and field values (based on a calibration factor under flexible loading) at the key of the Panel "A/B" footing. However, level of agreement is poor near the toe and heel. The curves connecting the field data points are smoother, and mostly the difference between the field and theoretical values was less than 0.5 tsf (6.9 psi). Theoretical computations show that backfilling operation induces the largest change in the bearing pressure distribution. However, in the field the pressure did not redistribute much in response to the backfilling. Mostly the theoretical pressure fluctuated above the field values near the toe and below the field values near the heel.

Figure 5.4 plots only the theoretical contact pressure for Abutment No. 1 footing of Bridge B, since no pressure cells were installed for this bridge (see Section 4.3 for explanation). Construction stages indicated in the figure for Bridge B are set up as: 1 = footing construction; 2 = abutment wall construction; 3 = placement of beams; 4 = backfilling behind abutment wall; 5 = deck construction; and 6 = service load application. According to the theoretical computations, the fourth stage is considered to induce more pressure than any other stage.

Figure 4.27 and 4.28 show the footing/bearing soil contact pressure data from the Bridge C site. Construction stages are set as: 1 = footing construction; 2 = placement of box culvert sections; 3 = backfilling next to and above culvert; 4 = paving; and 5 = service load application. The theoretical pressure stayed very close to the field curve, based on the calibration test setup of Figure 3.5b, up to the third stage at both the heel and toe locations for this structure. Beyond the third stage, the theoretical pressure approached the field curve resulting from the flexible loading condition (see Figure 3.5a) at the toe of west footing.

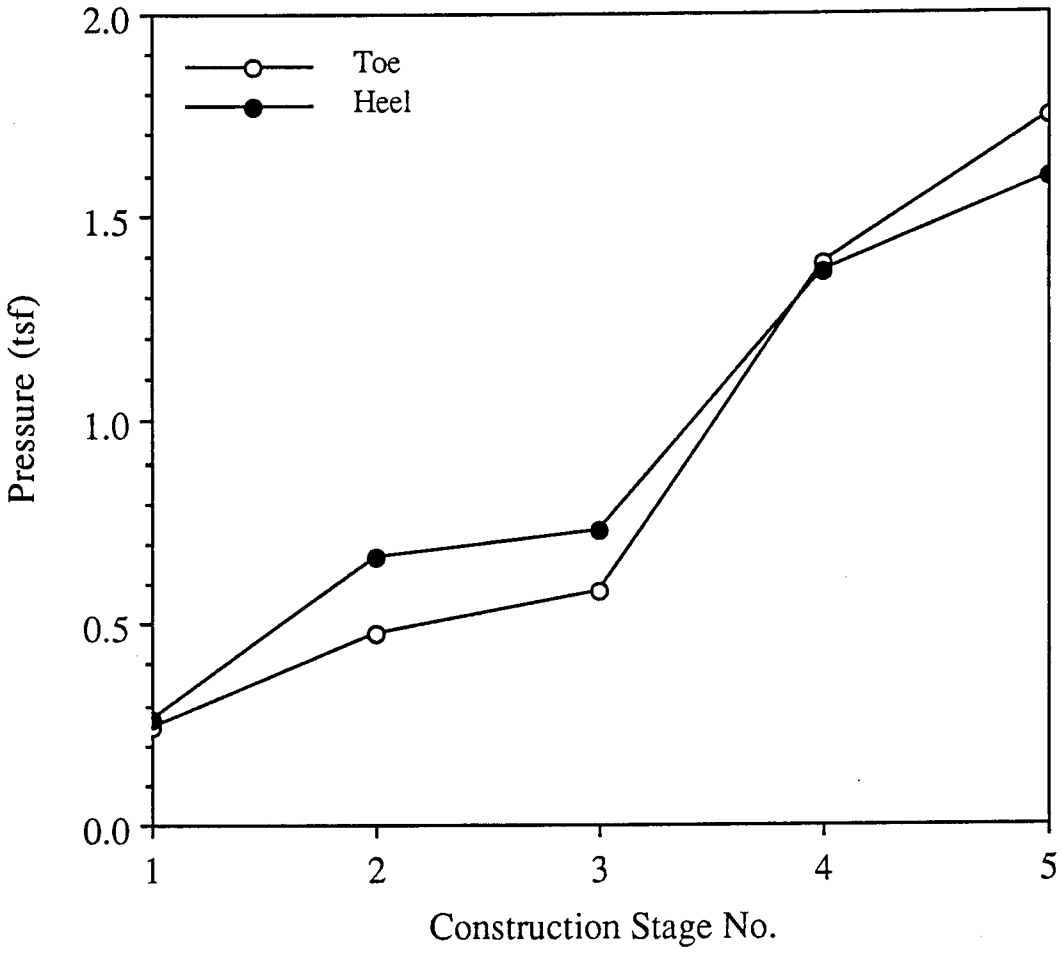

Figure 5.4 Theoretical Contact Pressure Under Abutment No. 1 (Bridge B)

Similar comparisons between the theoretical and field average contact pressure are made for Bridge D foundations in Figures 4.29 through 4.34. In all of these plots general shape of the field curves is very similar to that of the theory. Agreement between the theory and field responses is very poor under the Pier 2 (Phase I) footing, since the pressure cells were not installed properly as stated previously in Section 4.3 (see Figure 4.29). In the other figures, agreement is generally good between the theory and the field values up to the third stage. The best case is observed for the Pier 5 (Phase I) footing. No definite trend can be found in the correlations among the theoretical, field (flexible loading), and field (rigid loading) curves.

Figures B.54 through B.59 in Appendix B show both theoretical and average field values for the selected Bridge E (Phase I) foundations. The field curve in each figure is based on the calibration constant which resulted from the "rigid" loading case. The field curve, based on the "flexible" loading, would be located at 30 to 40% above the field curve shown in these figures. According to Figure B.54, the theoretical estimate overpredicted the field readings near the heel, but underpredicted the field responses at the key and toe. In Figures B.56 through B.59, the theoretical computations consistently resulted in higher pressure.

5.3 Tilting Estimation

Tilting of the abutments may be estimated using a method described by Bowles (34), which was developed by Tettinek and Matl (35) and Taylor (36). In this method, the static rotation of the footing is expressed as,

$$\tan\theta = \frac{1-\mu^2}{E_s} \cdot \frac{M}{B^2 L} \cdot I_\theta \qquad \text{Eq. (5.2)}$$

where μ = Poisson's ratio; E_s = Young's modulus (psi); M = overturning moment resisted by base dimension B (lb.-in./in.); B, L = footing base width, length (inches); and I_θ = influence factor which depends on the ratio (L/B) and flexibility of the footing base.

The factor I_θ accounts for the influence of (L/B) ratio and rigidity. Its value can be obtained from Table 5.1, which was prepared originally by Tettinek and Matl (35) and later by Taylor (36). Obviously, the factor I_θ takes a larger value if the footing behaves as a rigid slab. Table 5.2 lists a typical range of E_s for selected soils. According to a standard guideline (37), a wall deflection must be equal to 0.005 times the height to develop the Rankine's active earth pressure condition. This criteria is equivalent to 0.3 degree rotation away from the backfill.

Theoretical rotation was made with Poisson's ratio of 0.3, the I_θ value for flexible foundation (from Table 5.1) to be conservative, and a mid-range of E_s value for corresponding soil type found in Table 5.2. Soil type was identified with the aid of Table 5.3. Overturning moment for each abutment wall was determined assuming that the Rankine's active pressure condition exists behind the wall. In the field, tilting measurement was only possible after the abutment wall and/or pier columns were constructed. Theoretical tilting was computed under later construction stages with relation to the stage in which tilting measurements began.

Figure 5.5 through 5.7 compare the field monitored tilting with predictions of Eq. 5.2 for the abutment walls at the first three bridge construction sites. Construction stages are numbered for Panel "A" of Bridge A as: 2 = abutment wall construction; 3 = backfilling behind abutment wall; and

Table 5.1 Influence Factor I_θ to Compute Footing Rotation [34]

L/B	Flexible	Rigid
0.10	1.045	1.59
0.20	1.60	2.42
0.50	2.51	3.54
0.75	2.91	3.94
1.00 (circle)	3.15 (3.00)	4.17 (5.53)
1.50	3.43	4.44
2.00	3.57	4.59
3.00	3.70	4.74
5.00	3.77	4.87
10.0	3.81	4.98
100.	3.82	5.06

Notes : * For Rigid: $I_\theta = 16/[\pi(1+0.22B/L)]$
* For Circle: B = diameter.

Table 5.2 Typical Range of E_s for Selected Soils [34]

Soil		Range of E_s (ksf)
Clay	Very Soft	50 to 250
	Soft	100 to 500
	Medium	300 to 1,000
	Hard	1,000 to 2,000
	Sandy	500 to 5,000
Glacial Till	Loose	200 to 3,200
	Dense	3,000 to 15,000
	Very Dense	10,000 to 30,000
Sand	Silty	150 to 450
	Loose	200 to 500
	Dense	1,000 to 1,700
Sand & Gravel	Loose	1,000 to 3,000
	Dense	2,000 to 4,000
Silt		40 to 400
Shale		3,000 to 300,000

Table 5.3 Consistency of Soils [34]

(a) Consistency of Saturated Cohesive Soils

Consistency	Age	N'_{70}	q_u (kPa)	Remarks
Very Soft	Young (NC)	0 to 2	< 25	Squishes between fingers when squeezed
Soft	Young (NC)	3 to 5	25 to 50	Very easily deformed by squeezing
Medium	Young (NC)	6 to 9	50 to 100	
Stiff	Aged (OC)	10 to 16	100 to 200	Hard to deform by squeezing
Very Stiff	Aged (OC)	17 to 30	200 to 400	Very hard to deform by squeezing
Hard	Aged (OC)	> 30	> 400	Nearly impossible to deform by hand

Notes : 1. "NC" = normally consolidated ; "OC" = overconsolidated.
2. Blow counts are for a guide --- in clay "exceptions to the rule" are very common.

(b) Descriptions of Granular Soils

Description		Very loose	Loose	Medium	Dense	Very Dense
Relative density (D_r)		0	0.15	0.35	0.65	0.85
SPT N'_{70} :	fine	1-2	3-6	7-15	16-30	
	medium	2-3	4-7	8-20	21-40	> 40
	coarse	3-6	5-9	10-25	26-45	> 45
ϕ :	fine	26-28	28-30	30-34	33-38	
	medium	27-28	30-32	32-36	36-42	< 50
	coarse	28-30	30-34	33-40	40-50	
γ_{wet} (kN/m^3)		11-16	14-18	17-20	17-22	20-23

Notes : 1. SPT value is at about 6 m depth.
2. $\phi = 28° + 15° * D_r$ (+ 2°)

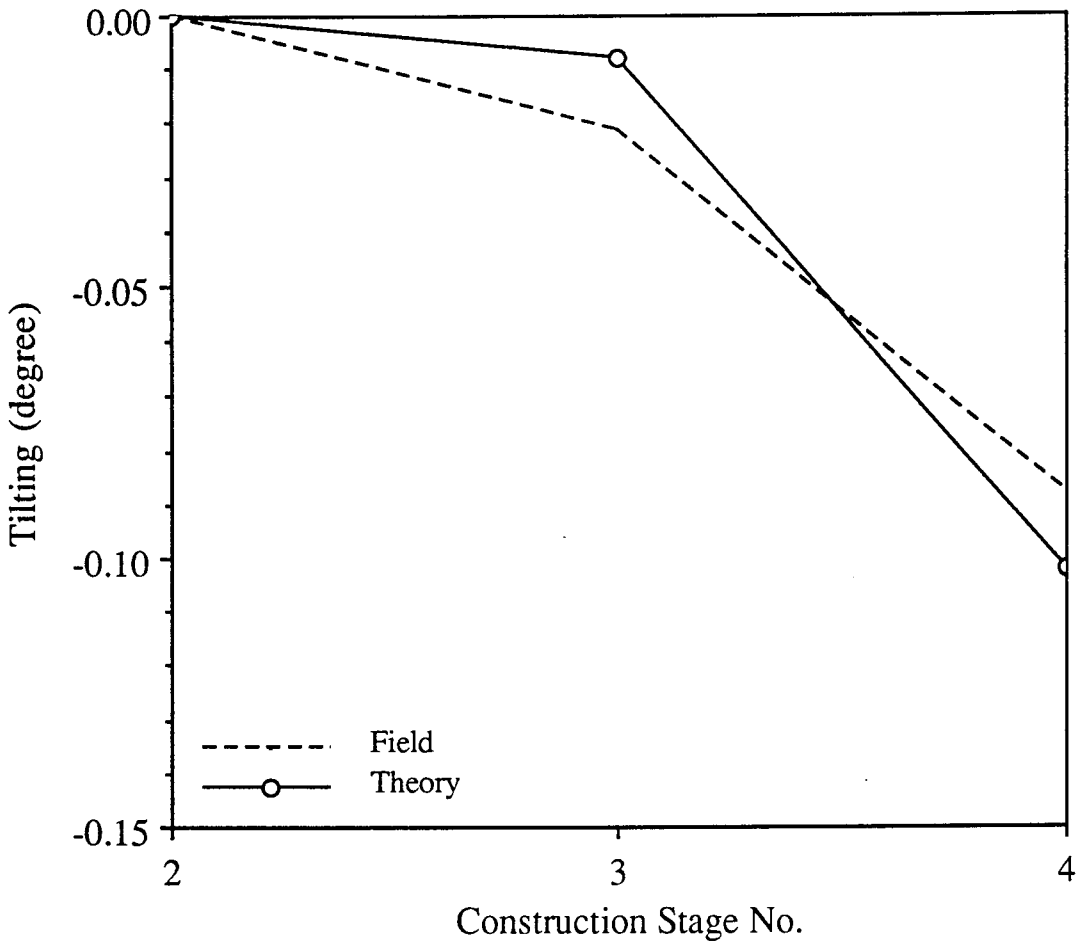

Figure 5.5 Comparison of Field and Theoretical Panel "A/B" Abutment Wall Tilting (Bridge A)

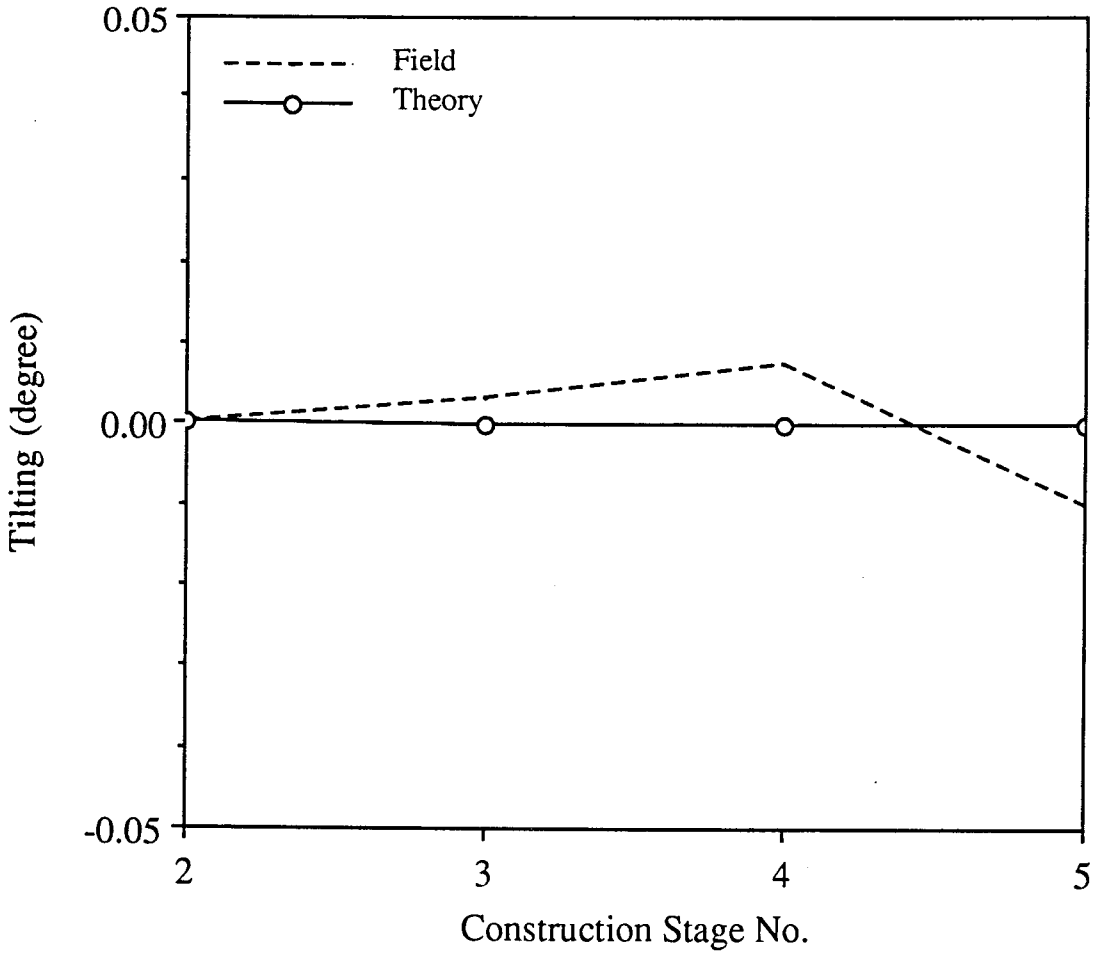

Figure 5.6 Comparison of Field and Theoretical Abutment No. 1 Front Wall Tilting (Bridge B)

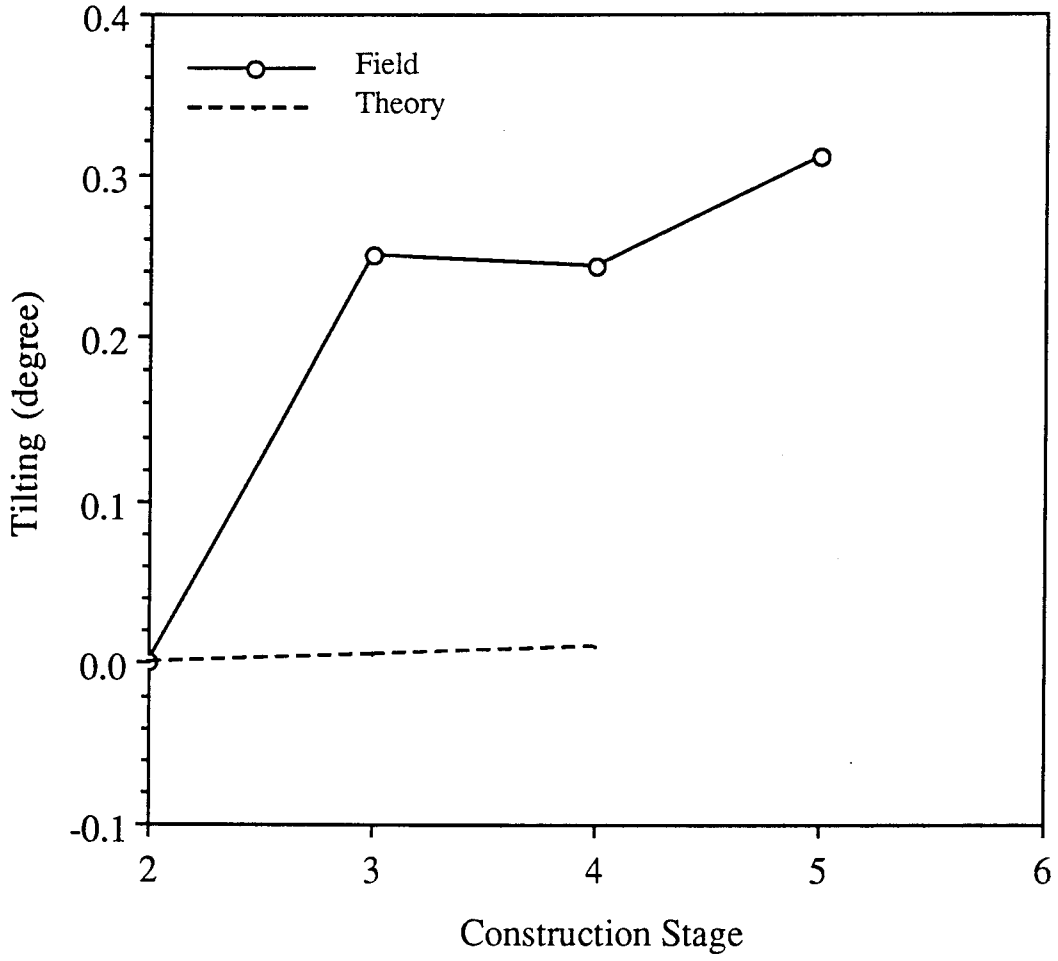

Figure 5.7 Tilting of Culvert Wall - Comparison Between Theory and Field Data (Bridge C)

4 = placement of girder beams and deck construction. For Abutment No. 1 of Bridge B, construction stages are numbered as: 2 = abutment wall construction; 3 = placement of beams; 4 = backfilling behind abutment wall; and 5 = deck construction. For Bridge C, construction stages are numbered as: 2 = placement of box culvert sections; 3 = backfilling next to and over culvert; 4 = paving; and 5 = service load application. Good agreement is seen for Panel "A" abutment wall (Bridge A) and the front wall of Abutment No. 1 structure (Bridge B). The theory predicted that the Panel "A" wall would continue to rotate away from the backfill, and the same trend was seen in the field. The front wall of Abutment No. 1 (Bridge B) was supposed to tilt slightly toward the backfill initially and then away from the backfill after the fourth stage, but in the field the wall kept rotating toward the backfill. Actual field tilting was much larger than the predicted for the side wall of the box culvert (Bridge C). This may be due to the way the culvert was set on top of the strip footings.

Tilting of Bridge D pier columns was estimated to be zero for Pier 2, 3, and 4 foundations, since the span 2, 3, and 4 dimensions were equal (no factor existed to create overturning moment). However, Pier 1 and 5 foundations were predicted to tilt slightly away from the abutment because of unequal span dimensions between Spans 1 (53'-5") and 2 (76'-4") and Spans 5 (76'-4") and 6 (53'-5"). In reality, columns of Pier 2 through 4 foundations rotated slightly in the field (see Figures 4.43 through 4.48). Figures 5.8 and 5.9 compare the field rotation angles of the Pier 5 - North, South (or Phases I and II) foundations with the theoretical estimates. Parameter values used for the theoretical computations were E_s (1,000 ksf) and μ (0.3). In these plots, the field values were typically more than 10 times as large as the theoretical estimates.

Plots in Appendix B (Figures B.60 through B.67) show both theoretical and average field tilting for the selected Bridge E Phase I and II foundation walls and columns. Overall, somewhat

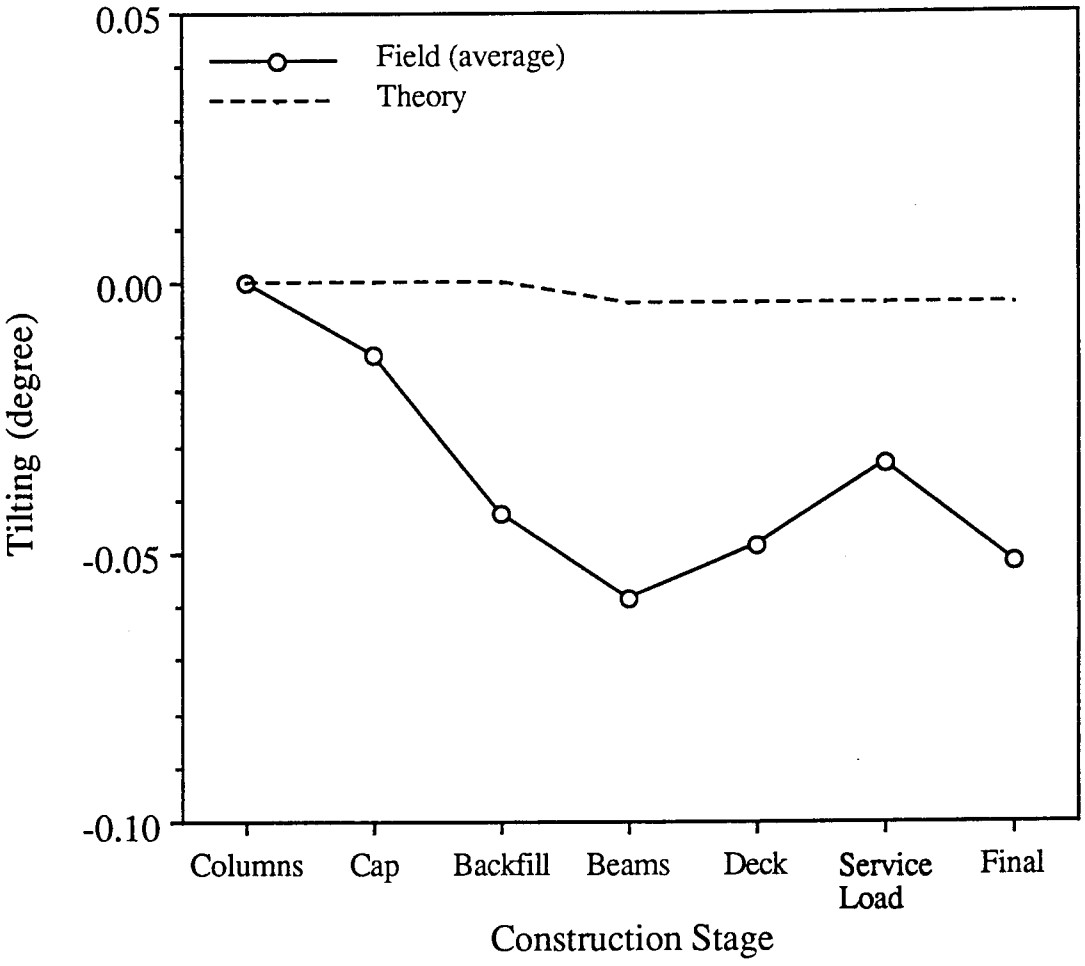

Figure 5.8 Tilting of Pier 5 - North Footing Columns - Comparison Between Theory and Field Data (Bridge D)

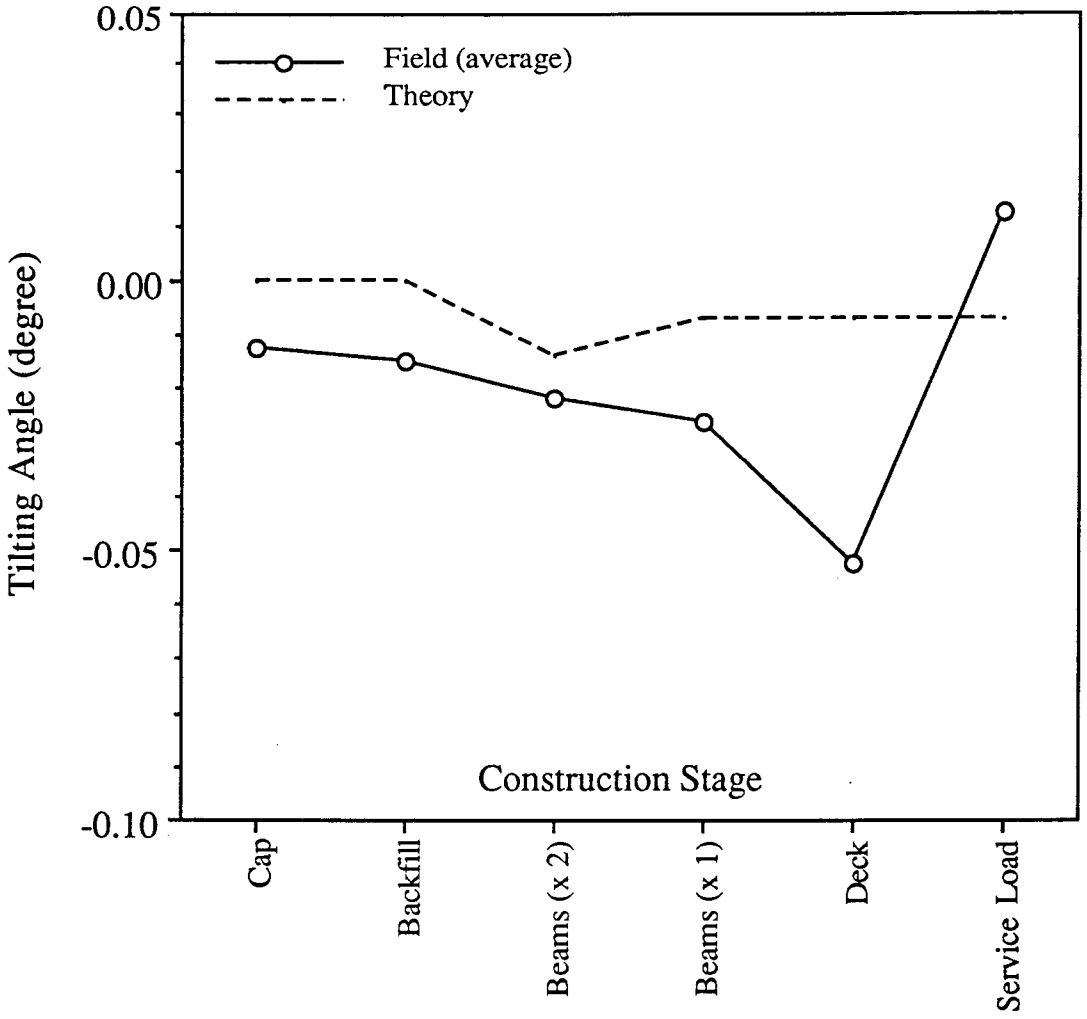

Figure 5.9 Tilting of Pier 5 - South Footing Columns - Comparison Between Theory and Field Data (Bridge D)

better agreement resulted between theoretical estimates and field data for tilting of pier columns than for tilting of abutment walls. All of the abutment walls, except for the forward abutment (Phase II) rotated slightly toward the backfill, while the theory based on the active pressure concept predicted the opposite.

5.4 Selection and Classification of Settlement Estimation Methods

5.4.1 Settlement of Footings on Cohesionless Soils

Currently, there are at least several geotechnical methods available to estimate settlement of footings on sand. These methods can be classified into three major categories based on their fundamental approaches. The first category is the empirical method, the second is the method related to the elasticity theory, and the third is the method based on the one-dimensional compression theory.

In this study, six methods were selected to be compared against the field and experimental settlement results. They are:

Method #1 Terzaghi and Peck Method (2)

Method #2 Peck and Bazaraa Method (9)

Method #3 Schmertmann Method (3)

Method #4 D'Appolonia Method (12)

Method #5 Hough Method (4); and

Method #6 Burland Method (6).

Methods #1, #2, and #6 belong to the first category. Method #3 is a semi-empirical approach based on CPT data. Method #4 is based on the elastic theory using the SPT data to estimate soil modulus.

Method #5 relies on the one-dimensional compression theory. Therefore, selection of these methods will enable a comprehensive evaluation of the methods based on vastly different concepts.

Method #1 is the simplest and expected to predict an upper limit for settlement of spread footings on sand. Contact pressure, SPT-N value, and footing width are input parameters, and it applies correction factors due to groundwater table and embedment depth. Method #2 is the modification of Method #1, which is also intended for use for spread footings on sand. It requires a correction on the average SPT-N value, and its method of determining the embedment correction factor is different from that of Method #1. Method #3 defines settlement as a function of net contact pressure, thickness, and modulus of soil layer and three influence factors (see Table 5.4). This is the only method which requires a conversion of SPT data to CPT data. Method #4 is also limited to footings on cohesionless soils and incorporates influence factors due to embedment and compressible strata, average applied pressure, footing width, and modulus of compressibility in estimating settlement. The modulus of compressibility is obtained through the average SPT-N value. Method #5 involves calculation of settlement within each soil layer, which depends on bearing capacity index, layer thickness, and overburden pressure. Method #6 is the only one which can be applied to both normally consolidated and over-consolidated soils. Settlement is defined as a function of applied pressure, footing width, and compressibility index. Calculated settlement is corrected for footing shape, sand layer thickness, and time factor. Compressibility index is determined after the depth of influence is estimated. Table 5.4 summarizes a brief description of the six geotechnical settlement estimation methods. Readers should consult the referred technical papers for more detailed information on these methods.

Table 5.4 Equations of Selected Settlement Estimation Methods for Footings on Cohesionless Soils

Burland Method:

$$S = f_s f_l f_t \left\{ \left(q' - \tfrac{2}{3}\sigma'_{vo} \right) B^{0.7} I_c \right\}$$

f_s = shape correction factor
f_l = correction factor for sand layer thickness
f_t = correction factor for time

q' = average gross effective applied pressure (kN/m^2)
σ'_{vo} = maximum previous effective overburden pressure (kN/m^2)
B = footing width (m)
I_c = compressibility index

D'Appolonia Method:

$$S = \mu_o \mu_1 \frac{qB}{M}$$

μ_o = embankment influence factor
μ_1 = compressive strata influence factor
q = average applied bearing pressure (tsf)
B = footing width (m)
M = modulus of compressibility (tsf)

Hough Method:

$$S = \sum_0^z \left(\frac{1}{C}\right) \Delta Z \log\left(\frac{\overline{\sigma}_{vo} + \Delta\overline{\sigma}_v}{\overline{\sigma}_{vo}} \right)$$

C = bearing capacity index
ΔZ = layer thickness (ft.)
$\overline{\sigma}_{vo}$ = initial effective overburden pressure at mid-height of layer (ksf)
$\Delta\overline{\sigma}_v$ = change in effective vertical stress at mid-height of layer (ksf)

Terzaghi-Peck Method:

$$S = C_w C_D \left(\frac{3P}{N}\right)\left(\frac{2B}{B+1}\right)^2$$

C_w = groundwater correction factor
C_D = embankment correction factor
P = applied bearing pressure (tsf)
N = SPT blow count
B = footing width (ft.)

Peck-Bazaraa Method:

$$S = C_w C_d \left(\frac{2q}{N_B}\right)\left(\frac{2B}{B+1}\right)^2$$

C_w = groundwater correction factor
C_d = embankment correction factor
q = applied bearing pressure (tsf)
N_B = corrected SPT N-value
B = footing width (ft.)

Schmertmann Method:

$$S = C_1 C_2 \Delta P \sum_0^{2B} \left(\frac{I_z \Delta Z}{E_s}\right)$$

C_1 = embankment correction factor
C_2 = creep correction factor
ΔP = net bearing pressure
I_z = strain influence factor
ΔZ = thickness of layer having a constant Es
E_s = soil modulus
B = footing width (ft.)

5.4.2 Settlement of Footings on Cohesive Soils

As indicated in Section 2.3, the settlement prediction methods for footings on cohesive soils have been more unified. The methods are normally divided into two areas: 1) method for immediate settlement based on elastic theory; and 2) method for time-dependent consolidation settlement based on Terzaghi consolidation theory. Method 1 is based on integration of Boussinesq's solutions under a point load applied to homogeneous, isotropic, linearly-elastic, and half-space.

According to Janbu, et al., (38), the following formula can be used to estimate the elastic settlement,

$$S_e = (\frac{qB}{E_s}) I_o \cdot I_1 \qquad \text{Eq. (5.3)}$$

where S_e = elastic settlement (inches); q = average bearing pressure (psi); B = footing base width; E_s = Young's modulus of soil (psi); I_o = influence factor due to (D/B) ratio; I_1 = influence factor due to (H/B) ratio; D = depth of embedment; and H = stratum depth.

Typical range of the E_s value can be estimated from Table 5.2, given that relative consistency of the clayey soil is determined from Table 5.3 based on the SPT-N value. Values of I_o and I_1 are obtained from Figure 5.10.

Time dependent, consolidation (primary) settlement is computed from (39):

$$S_c = \sum_i \left[\frac{C}{1+e_o} \log \left(\frac{p_{o(i)} + \Delta p_{(i)}}{p_{o(i)}} \right) \right] \qquad \text{Eq. (5.4)}$$

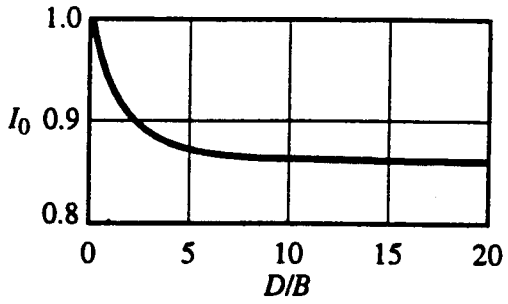

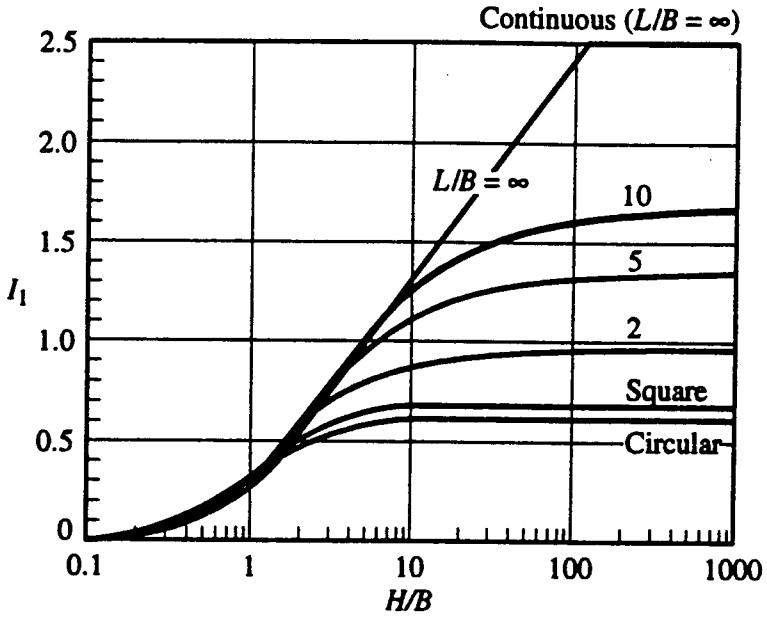

Figure 5.10 Influence Factors I_0 and I_1

where S_c = primary consolidation settlement; C = compression index; H_i = thickness of the i-th layer; e_o = initial void ratio; $p_{o(I)}$ = average initial vertical effective stress in the i-th layer; and Δp = average increase in vertical effective stress in the i-th layer due to load.

In the past, a few different empirical formulas were proposed to estimate compression index (C):

$$C = 0.007(LL - 10) \quad \textit{by Terzaghi and Peck}(2) \qquad \text{Eq. (5.5a)}$$

$$C = 0.2343(LL/100)G_s \quad \textit{by Nagaraj and Murty}(40) \qquad \text{Eq. (5.5b)}$$

$$C = 0.141 G s^{1.2}\left(\frac{1+e_o}{G_s}\right)^{2.38} \quad \textit{by Rendon - Herrero}(41) \qquad \text{Eq. (5.5c)}$$

where LL = liquid limit (%); G_s = specific gravity; and e_o = initial void ratio.

Equation 5.4 provides ultimate settlement due to primary consolidation, given a sufficient time to allow 100% of the consolidation. In order to determine the degree of consolidation that has taken place within a given period, time rate of consolidation must be estimated. According to the traditional method (39), this is done through a non-dimensional time factor:

$$T_v = \frac{c_v \cdot t}{H^2} \qquad \text{Eq. (5.6)}$$

where T_v = time factor; t = time elapsed; c_v = coefficient of consolidation; and H = maximum length of drainage path in the field.

The coefficient of consolidation is usually computed based on a plot from a laboratory one-dimensional compression test (39):

$$c_v = \frac{0.197 D^2}{t_{50}} \qquad \text{Eq. (5.7)}$$

where D = length of drainage path of the laboratory test specimen; t_{50} = time for 50% consolidation (obtained graphically on the plot of deformation dial gage readings vs. log of time or square root of time).

In the absence of laboratory test data, approximate value of the coefficient of consolidation may be obtained from a table prepared by Terzaghi and Peck (2),

c_v (ft^2/year)	= 20 to 360	for liquid limit of 30%	
	= 18 to 230	for liquid limit of 40%	
	= 8 to 150	for liquid limit of 50%	Eq. (5.8)
	= 5 to 90	for liquid limit of 60%	
	= 3 to 58	for liquid limit of 70%	
	= 2 to 36	for liquid limit of 80%	

The degree of consolidation, U (%), is then back-calculated from (39):

$$T_v = \frac{\pi}{4}\left(\frac{U(\%)}{100}\right)^2 \quad for\ U = 0\ to\ 60\% \qquad \text{Eq. (5.9a)}$$

$$T_v = 1.781 - 0.933 \log(100 - U\%) \quad for\ U > 60\% \qquad \text{Eq. (5.9b)}$$

Once the degree of consolidation is known, then the total settlement (S_t) due to elastic distortion and consolidation in a given time frame is simply obtained by,

$$S_t = S_e + S_c[U(\%)/100] \qquad \text{Eq. (5.10)}$$

5.5 Settlement Predicted by Geotechnical Methods

5.5.1 Footings on Cohesionless Soils (Bridges A through C)

Figures 5.11 through 5.13 present comparisons among the field settlement and predictions of the six geotechnical methods for the first three bridges (Bridges A through C). In Figure 5.11 (for Bridge A), the construction stages are numbered as: 1 = footing construction; 2 = abutment wall construction; 3 = backfilling; and 4 = bridge deck placement. In figure 5.12 (for Bridge B), the stages are defined as: 1 = footing construction; 2 = front abutment wall construction; 3 = placement of structural I-beams; 4 = backfilling; and 5 = construction of concrete deck. In Figure 5.13 (for Bridge C): 1 = footing construction; 2 = placement of box culvert sections; 3 = backfilling; and 4 = paving. In each figure, the field measured settlement was plotted against results from the six methods as well as the average of the six methods.

Figure 5.11 indicates that the predictions by Hough and D'Appolonia methods were equally closest to the actual field settlement up to the end of backfilling and beyond backfilling the field measurement converged to the Peck-Bazaraa method prediction. Schmertmann and Terzaghi-Peck Methods overpredicted the settlement. The average settlement yielded from the six methods remained more than twice as large as the actual field values.

For Abutment No. 1 of Bridge B (Figure 5.12), the most geotechnical methods underpredicted settlement. The only method which predicted relatively close to the actual was the method by Schmertmann. However, even this method resulted in much smaller settlement up to the third construction stage.

According to Figure 5.13, Hough Method slightly underestimated and Schmertmann Method overestimated the field settlement of the box culvert (Bridge C). All the other methods predicted

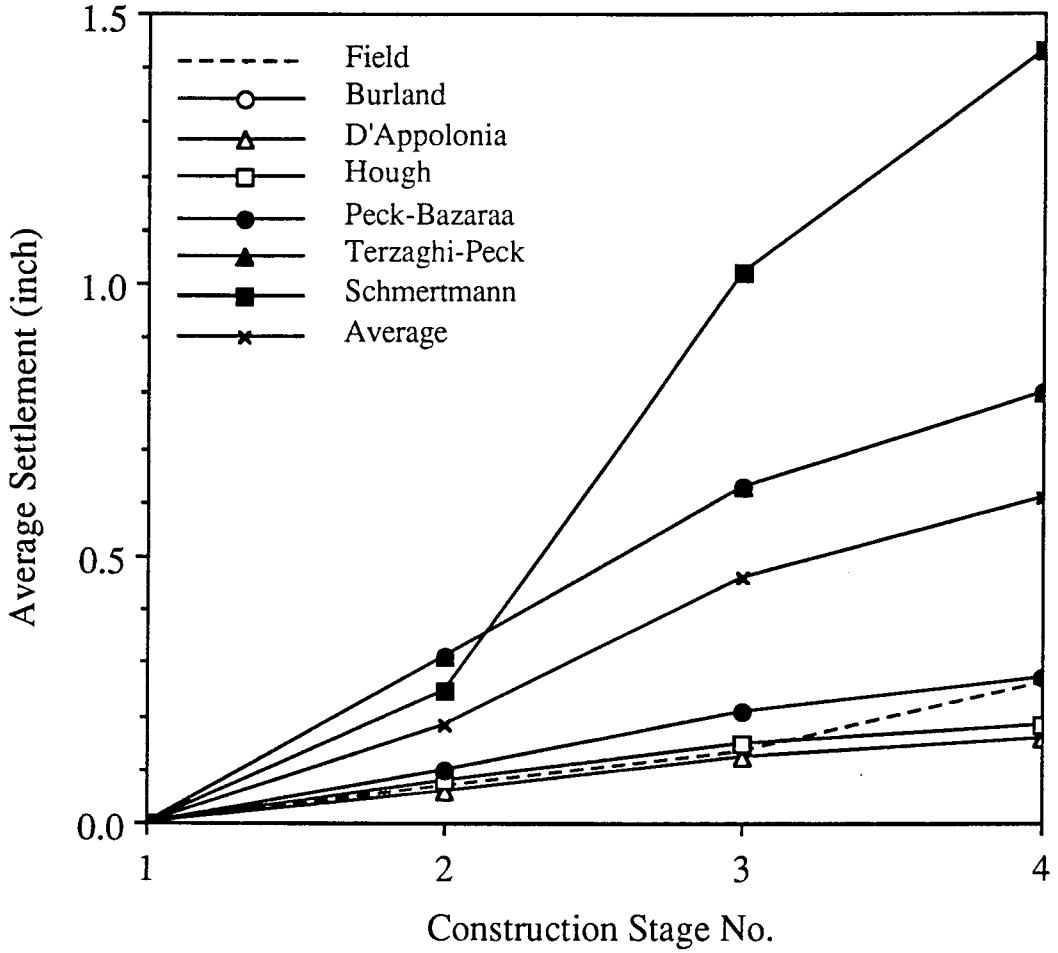

Figure 5.11 Comparison of Field Settlement and Geotechnical Method Predictions for Panel "A/B" Footing (Bridge A)

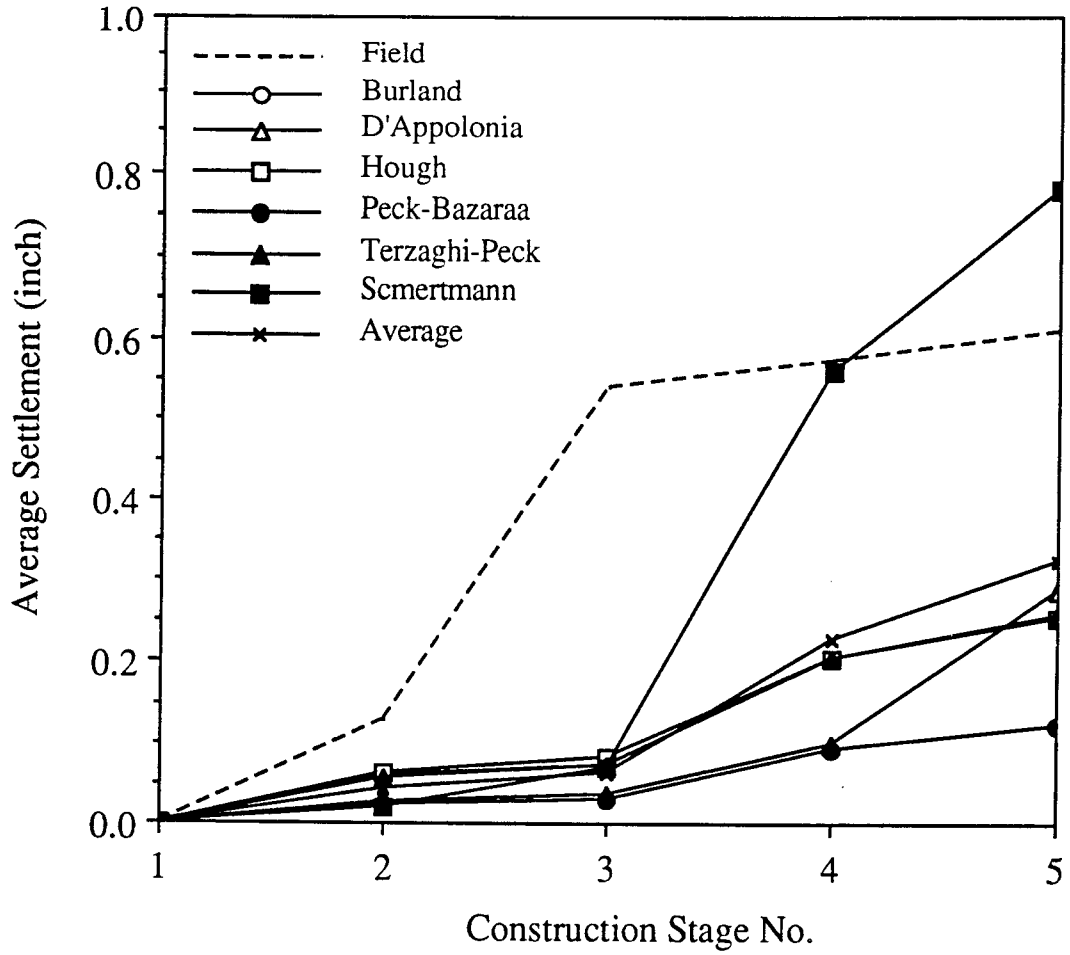

Figure 5.12 Comparison of Field Settlement and Geotechnical Method Predictions for Abutment No. 1 Footing (Bridge B)

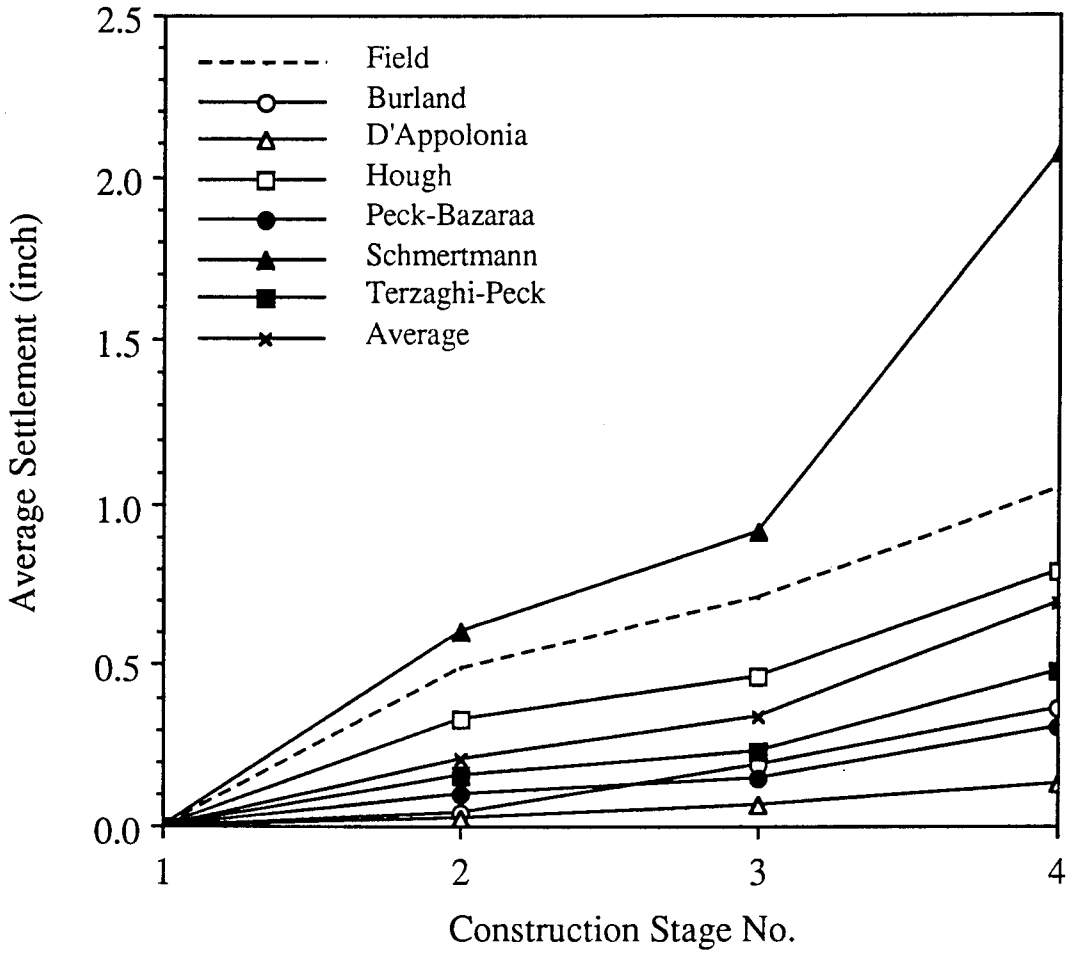

Figure 5.13 Comparison of Field Settlement and Geotechnical Method Predictions for Box Culvert West Footing (Bridge C)

about or less than a half of the actual.

Based on the above case-by-case comparisons, it is somewhat difficult to generalize which geotechnical method is the most promising for predicting spread footing performance on sands. Not only soundness of the underlining concept, but also quality of the SPT data and spatial variability of soil properties influence the level of agreement any method demonstrates against the field measurement. However, some conclusions can be extracted from the three cases. First, none of the six methods was successful in predicting settlement closely through the entire construction stages and beyond. Second, Burland and Terzaghi-Peck Methods yielded very similar predictions which were far from the actual. Third, predictions by Schmertmann Method were always the largest. Fourth, the best prediction of the field settlement was observed when Peck-Bazaraa Method was applied to Panel "A/B" of Bridge A. Lastly, D'Appolonia Method consistently underestimated the field settlement. Based on the overall average performance summarized on Table 5.5, Hough Method appears to be the most consistent in estimating the actual settlement with relatively reasonable accuracies.

Somewhat different conclusions were reached in previous studies. Baus (26) selected six settlement prediction methods (by Alpin, Hough, Meyerhof, Peck-Bazaraa, Buisman-DeBeer, and Schmertmann) and compared their estimates again the maximum field settlement monitored at nine spread footing locations. A summary of his results are presented in Table 5.6. Peck-Bazaraa Method, as well as Hough Method, provided the best settlement predictions. In a study documented in (23), six methods (Burland-Burbridge, D'Appolonia, Hough, Peck-Bazaraa, Peck-Bazaraa-Ladd, Schmertmann) were selected to be compared with the field measured settlement for twenty one bridges on spread footing. Some of their results are summarized in Table 5.7. They concluded that

Table 5.5 Comparisons Among Six Geotechnical Methods

Construction Stage No.	Settlement Ratio = (Estimate/Field) :					
	Burland	D'Appolonia	Hough	Peck-Bazaraa	Terzaghi-Peck	Schmertmann
Panel "A" - Bridge A						
1						
2	4.429	0.814	1.143	1.429	4.429	3.571
3	4.773	0.939	1.129	1.591	4.758	7.727
4	3.030	0.595	0.693	1.030	3.030	5.417
Abutment No. 1 - Bridge B						
1						
2	0.453	0.219	0.500	0.188	0.445	0.156
3	0.135	0.067	0.156	0.057	0.135	0.130
4	0.356	0.175	0.356	0.159	0.354	0.977
5	0.413	0.469	0.415	0.198	0.418	1.275
Bridge C						
1						
2	0.082	0.045	0.674	0.208	0.320	1.222
3	0.262	0.094	0.648	0.210	0.325	1.287
4	0.349	0.126	0.752	0.290	0.452	1.975
Average	1.428	0.354	0.647	0.536	1.467	2.374
Std. Dev.	1.883	0.329	0.315	0.581	1.852	2.475
Maximum	4.773	0.939	1.129	1.159	4.758	7.727
Minimum	0.082	0.045	0.156	0.057	0.135	0.130

Table 5.6 Results Obtained by Baus [27]

Method	Settlement (in.) of Foooting :			
	No. 1	No. 2	No. 3	No. 4
Field	0.51	0.62	0.38-0.59	2.03-2.15
Alpan (1)	0.42	0.21	0.25	0.21
Hough (2)	1.66	1.19	1.11	2.28
Meyerhof (3)	1.88	0.46	0.69	0.75
Peck-Bazaraa (4)	0.49	0.35	0.48	0.52
Buisman-De Beer (5)	1.64	1.57	1.30	N/A
Schmertmann (6)	1.88	1.81	1.10	N/A

Method	Settlement (in.) of Foooting :			
	No. 5	No. 6	No. 7	No. 8
Field	0.55	N/A	1.04	0.73
Alpan (1)	0.53	0.39	0.17	0.17
Hough (2)	1.11	1.07	1.06	0.88
Meyerhof (3)	1.10	0.97	0.71	0.56
Peck-Bazaraa (4)	0.87	0.68	0.50	0.39
Buisman-De Beer (5)	1.22	0.47	0.68	0.47
Schmertmann (6)	0.66	0.19	0.65	0.43

Table 5.7 Results Obtained by Gifford et al. [23]

Spread Footing	Ratio of (Calculated/Measured) for Settlement :					
	Burland-Burbridge	D'Appolonia	Hough	Peck-Bazaraa	Peck-Bazaraa w/ Ladd	Schmertmann
S1	0.86	1.86	2.14	0.83	1.23	2.26
S2	0.18	0.58	1.40	0.24	0.24	2.76
S3	0.14	0.32	1.29	0.20	0.30	0.91
S4	0.51	0.76	1.92	0.47	0.70	0.61
S5	0.93	0.62	1.61	0.69	1.00	0.49
S6	0.81	1.19	1.45	0.40	0.57	1.24
S7	0.31	0.31	0.66	0.49	0.74	0.30
S8	0.50	0.93	2.14	0.57	0.86	1.07
S9	0.42	0.77	2.04	0.62	0.92	0.69
S10	0.31	0.79	1.38	0.55	0.83	1.00
S11	0.24	1.16	1.88	0.64	0.96	1.44
S14	0.87	1.24	2.76	1.09	1.52	0.89
S15	4.74	2.18	4.29	4.00	15.74	4.62
S16	0.74	1.70	3.22	0.74	1.09	1.13
S17	0.52	1.05	1.86	0.64	0.93	0.91
S19	0.78	0.12	0.40	0.08	0.12	0.05
S20	0.84	0.77	1.64	0.33	0.50	1.89
S21	0.67	1.22	1.83	1.13	1.70	0.63
S22	0.97	0.92	2.11	0.52	0.77	2.33
S23	0.72	0.97	1.62	0.54	0.80	1.67
S24	1.29	1.29	2.18	0.89	1.32	2.29

three methods (Burland-Burbridge, D'Appolonia, and Peck-Bazaraa) typically underpredicted settlement, while the other two (Hough and Schmertmann) typically overpredicted. The most accurate method was the one by D'Appolonia, and Burland-Burbridge method came second. Hough method turned out to be the least accurate of the six. These differences stemmed from inherent differences in the subsurface and other conditions between this and other studies.

5.5.2 Footings on Cohesive Soils (Bridges D and E)

Figure 5.14 through 5.21 and B.35 through B.53 (in Appendix B) compare average field settlement and theoretical predictions from Eq. 5.10 for the selected foundations of Bridges D and E. For computing theoretical settlement, original soil boring log data and laboratory soil test results were incorporated as much as possible (see Chapter 2). Whenever C and C_v values were not readily available, empirical relationships, such as Eqs. 5.5b and 5.8, were applied. Generally, good agreement resulted between the average field and theoretical settlement for the Pier 1 and 2 foundations of Bridge D. However, as seen in Figure 5.18 through 5.21, agreement became poorer under later construction stages for Pier 3 and 5 foundations. This was believed to be due to increasing discrepancies detected between the original boring log data and actual site conditions in the eastern half of the bridge construction area.

In figures B.37, B.38, and B.40 through B.42, the field settlement curve is located between the elastic settlement curve, theoretical lower limit, and the (elastic + consolidation) curve, theoretical upper limit. The theory significantly overpredicted settlement behaviors of the Phase II foundations. This was expected since the theoretical estimates were made by neglecting the presence of the drilled pier shafts.

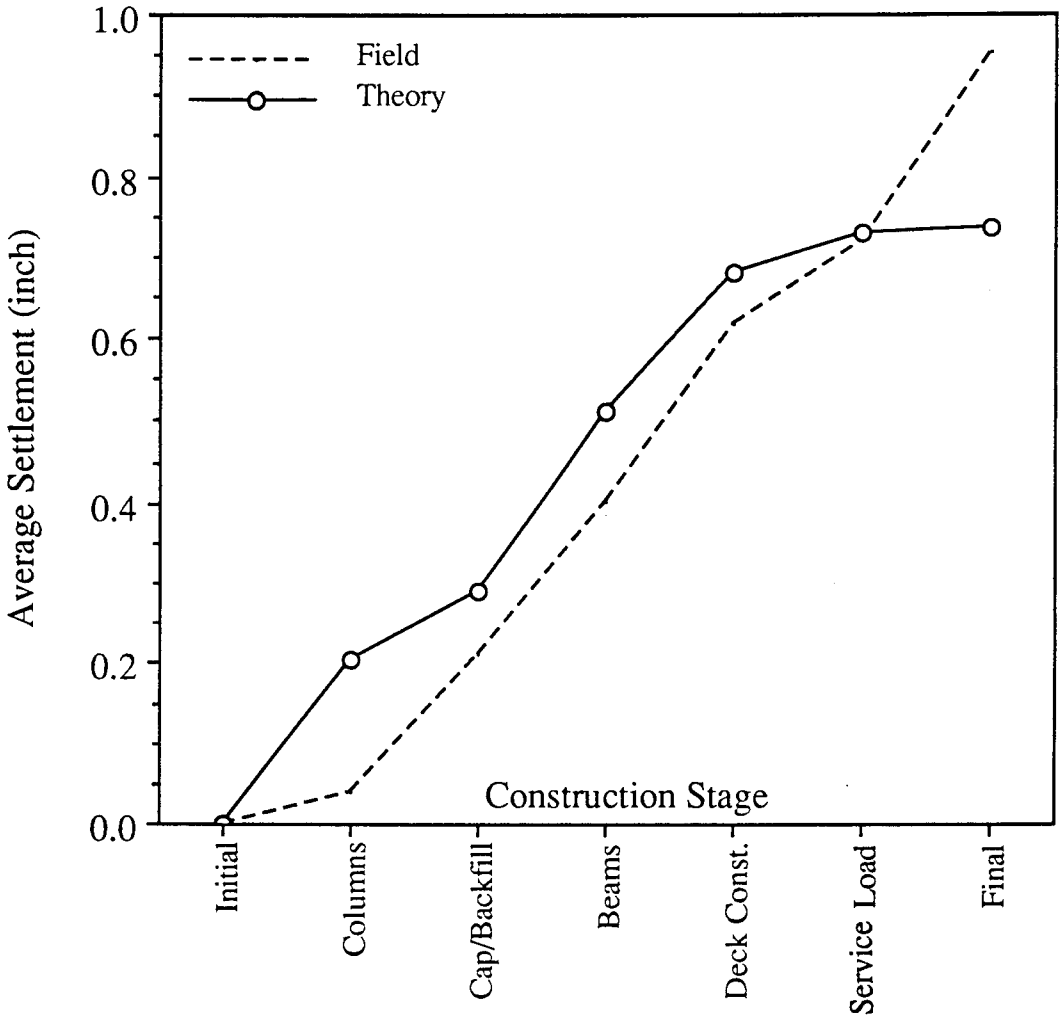

Figure 5.14 Comparison Between Field Average and Theoretical Settlement for Pier 1-North Footing (Bridge D)

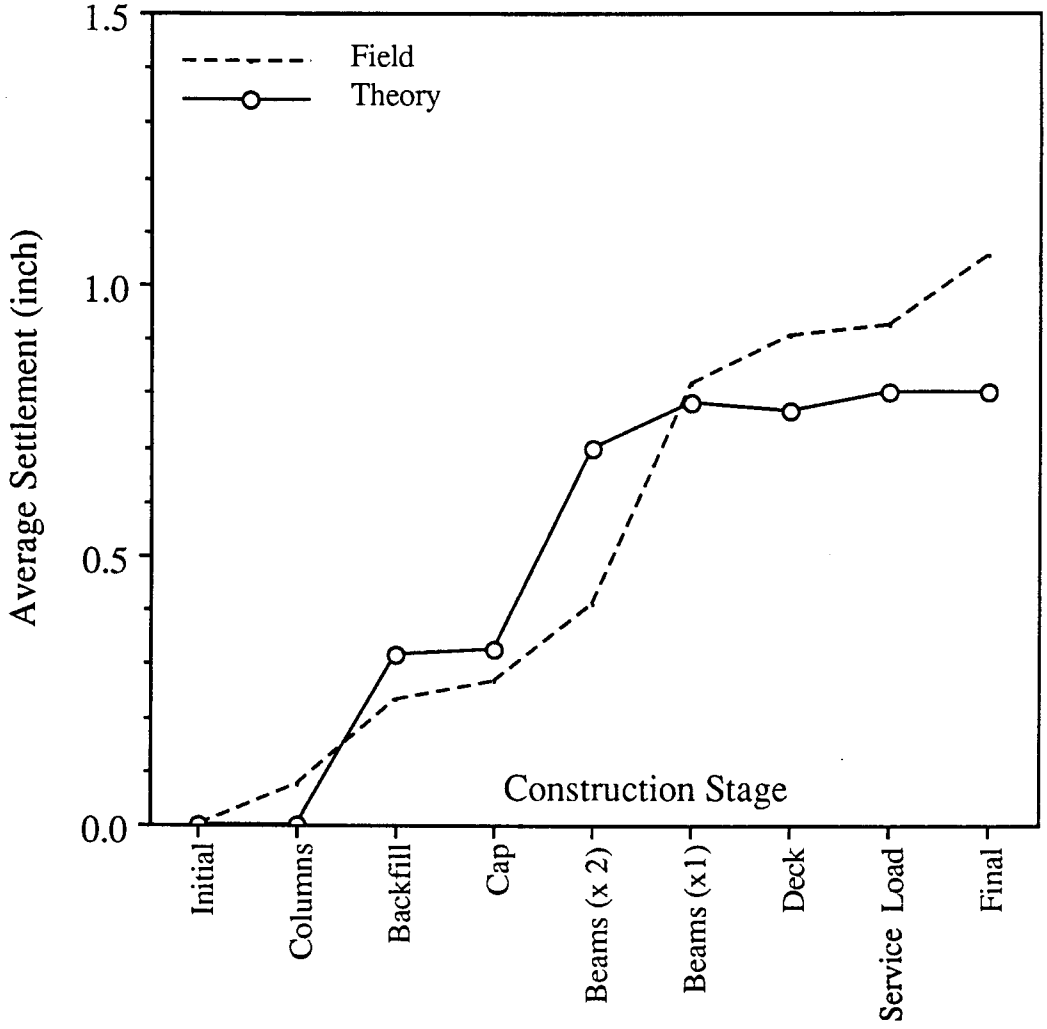

Figure 5.15 Comparison Between Field Average and Theoretical Settlements for Pier 1-South Footing (Bridge D)

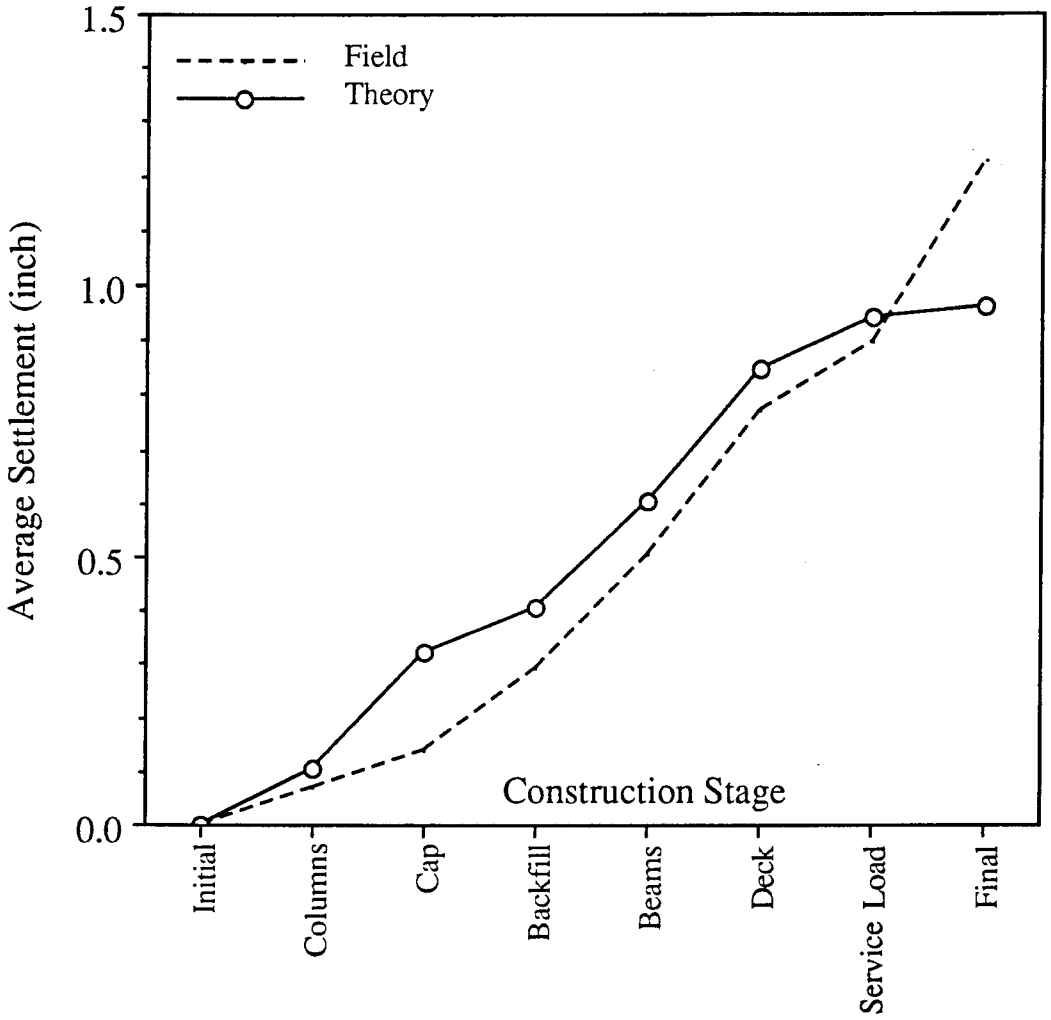

Figure 5.16 Comparison Between Field Average and Theoretical Settlements for Pier 2-North Footing (Bridge D)

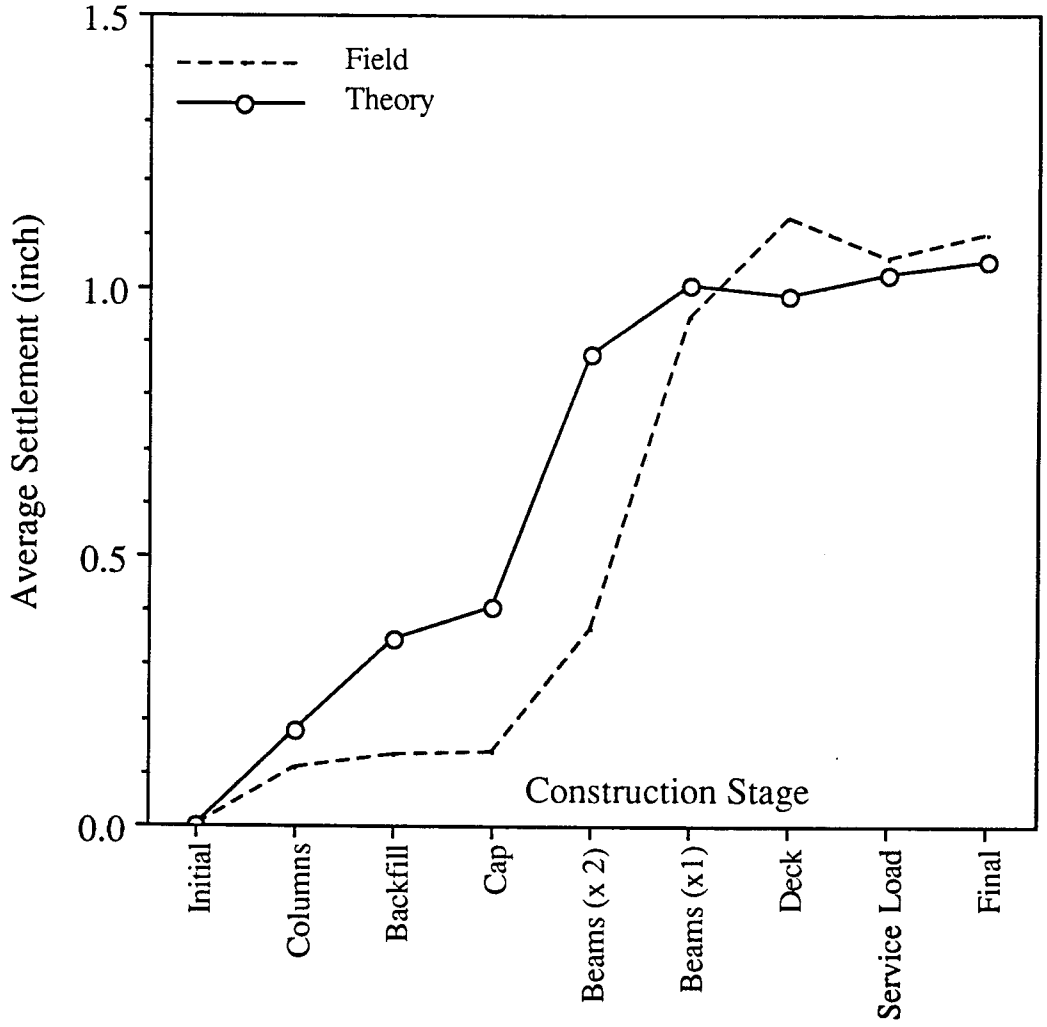

Figure 5.17 Comparison Between Field Average and Theoretical Settlements for Pier 2-South Footing (Bridge D)

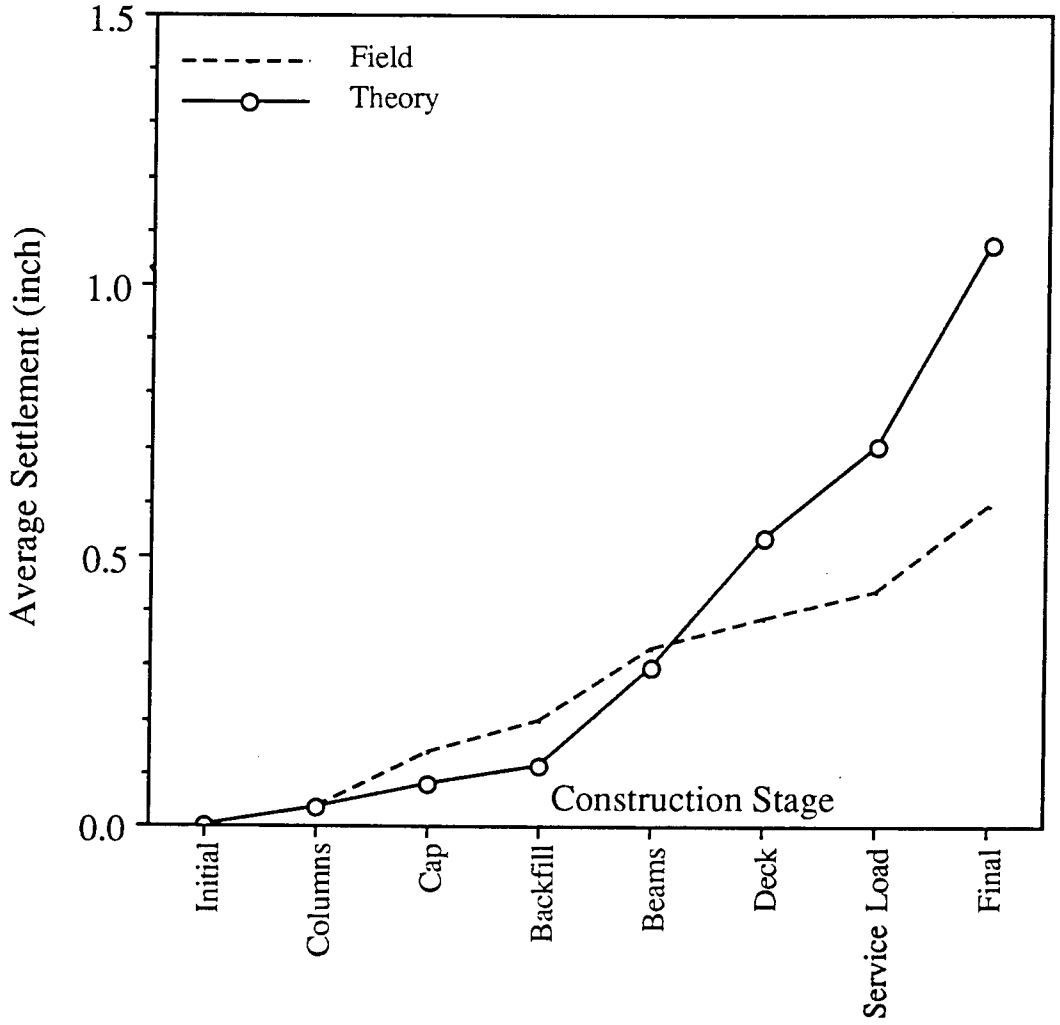

Figure 5.18 Comparison Between Field Average and Theoretical Settlements for Pier 3-North Footing (Bridge D)

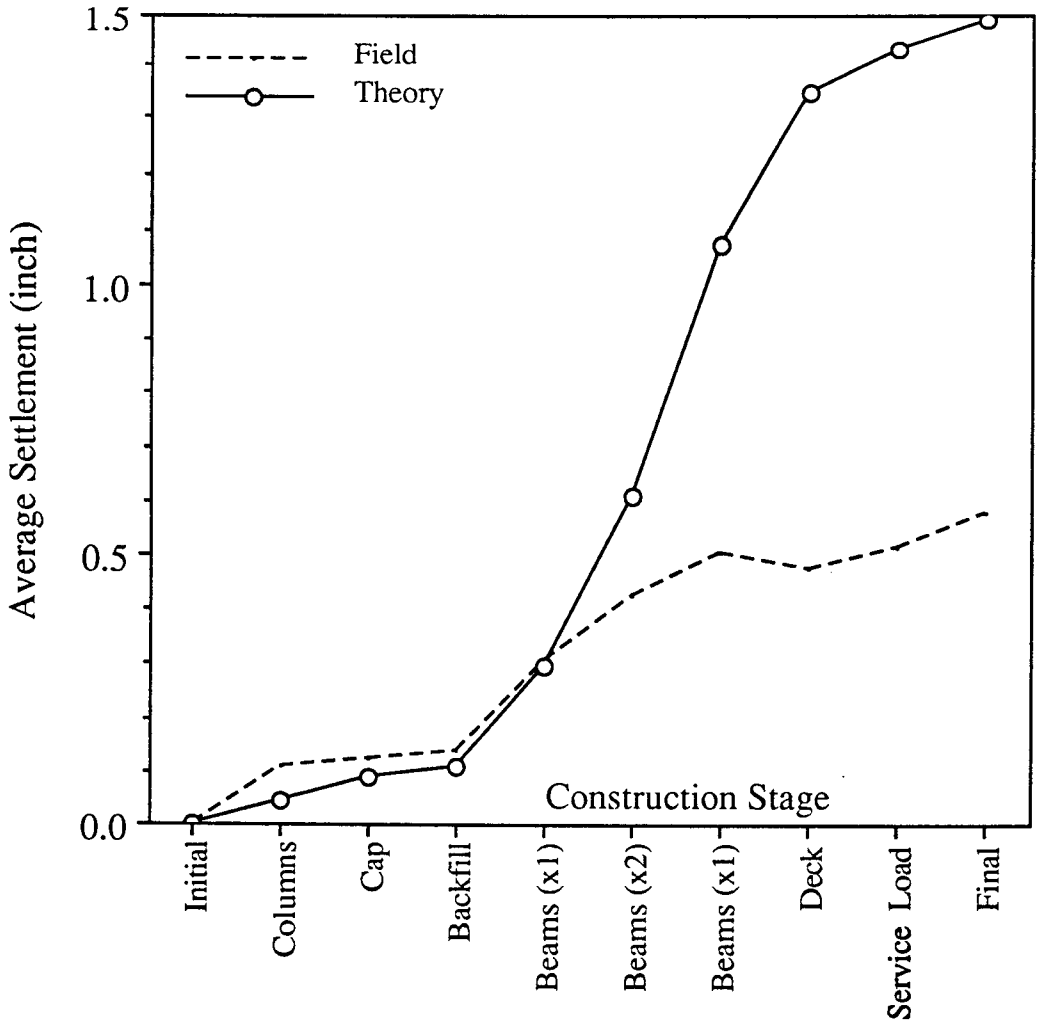

Figure 5.19 Comparison Between Field Average and Theoretical Settlements for Pier 3-South Footing (Bridge D)

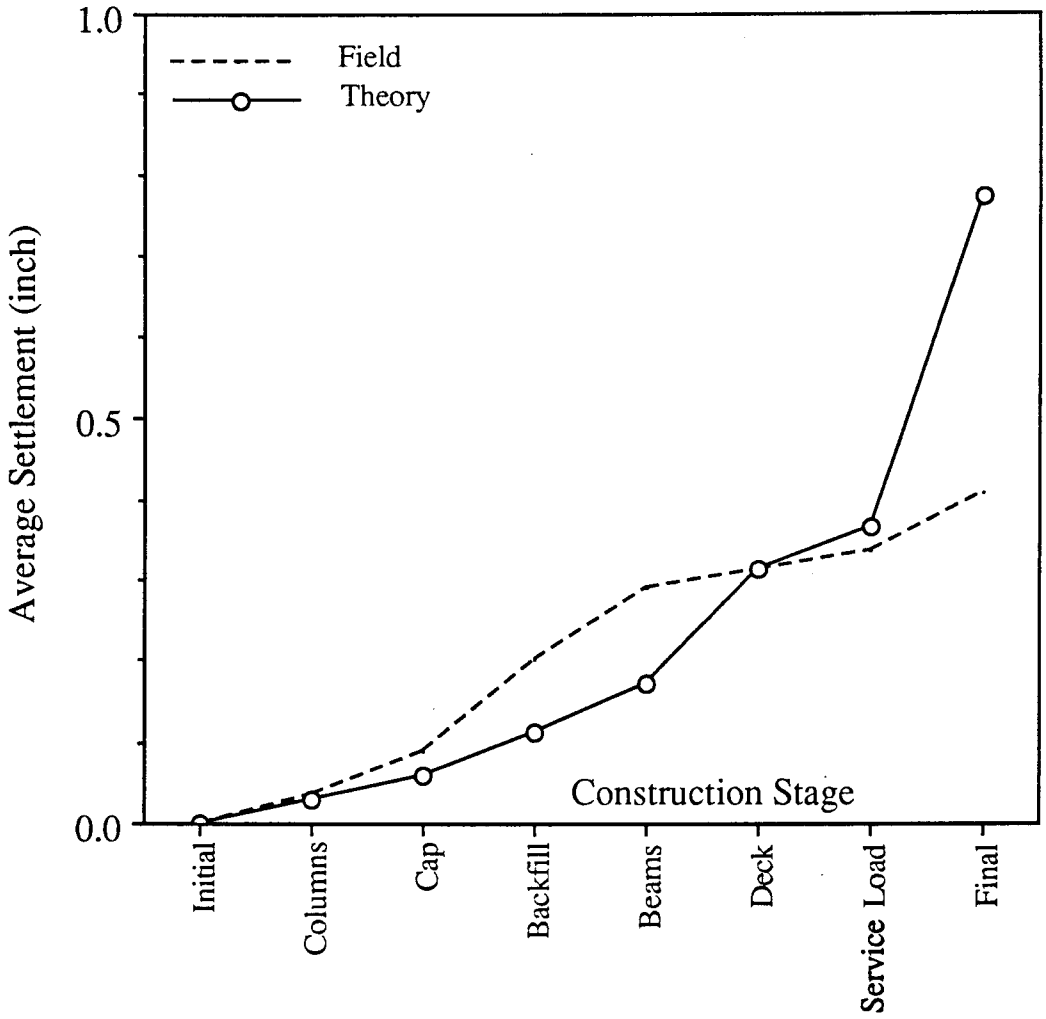

Figure 5.20 Comparison Between Field Average and Theoretical Settlements for Pier 5-North Footing (Bridge D)

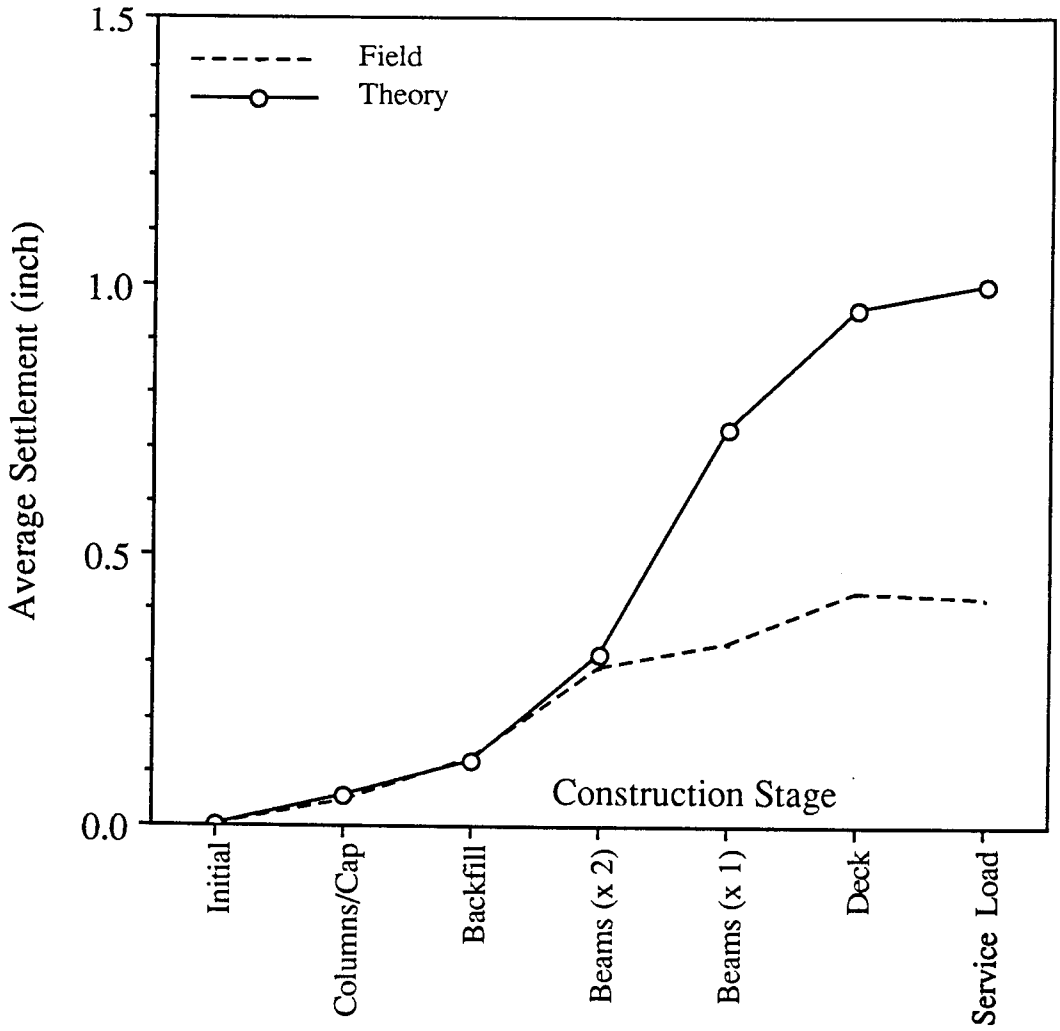

Figure 5.21 Comparison Between Field Average and Theoretical Settlements for Pier 5-South Footing (Bridge D)

Chapter 6

Centrifuge Modeling

6.1 Concept of Centrifuge Modeling

In recent years, researchers in the geotechnical engineering field have shown an increasing desire to study the behavior of structures and soil masses through the application of laboratory models. This is due to the fact that an extensive investigation with the full scale field prototype is in most cases difficult, cost prohibitive, and risk oriented. Also, actual behavior/phenomenon of concern is often too complicated for any empirical or mathematical (or numerical) method to accurately predict. One powerful technique developed in the past, which may be useful in predicting behavior of the full scale model, is called "centrifuge modeling" and involves utilization of a high intensity gravitational acceleration in the centrifuge environment. In this method, first a model of the prototype is made with a uniform scaling factor of (1/n). Then, the model is subjected to a centrifugally created artificial gravity field of (n) times the normal gravitational field. By applying the scaling relations, various parameters defining performance of the model is transformed to those of the prototype. For example, for the (1/n) model subjected to (n) x G gravitational field, stress level will be the same as that in the prototype and its deformation state will be scaled down by the factor (1/n). Table 6.1 summarizes the scaling relations. These scaling factors can be obtained through dimensional analysis applied to governing equation or solution in each category. In the art of centrifuge modeling, the concept of "modeling of models" is important. Influence of the normal gravity is considered to become less as the scaling factor (n) gets larger. Results obtained with one scaling factor must be checked by performing similar tests under a few different scaling factors.

As it is evident in Section 2.4, in the past centrifuge modeling of spread footing foundations

Table 6.1 Scaling Relations for Centrifuge Testing

Quantity		Prototype	(1/n) Model
Linear Dimension		1	(1/n)
Area		1	$(1/n)^2$
Volume		1	$(1/n)^3$
Time	dynamic	1	(1/n)
	hydrodynamic	1	$(1/n)^2$
	viscous flow	1	1
Velocity		1	n
Acceleration		1	$(n)^2$
Mass		1	$(1/n)^3$
Force		1	$(1/n)^2$
Energy		1	$(1/n)^3$
Stress		1	1
Strain		1	1
Density		1	1
Frequency		1	n

focused mainly on bearing capacity (failure). Its application to simulation of settlement performance of the spread footing has been limited. In the current investigation, efforts were made to evaluate general ability of the centrifuge modeling technique to simulate the actual field settlement performance of spread footing.

Centrifuge modeling of spread footing performance can be achieved by first placing soil obtained from the actual site inside a centrifuge model basket. Maximum grain size needs to be properly scaled down properly, and the soil must be compacted in layers to meet the average in-situ moisture and density conditions. Then, a properly scaled down model of a spread footing structure can be positioned over the soil. In order to simulate different stages during construction, the position of the load application is adjusted. A minimum of two LVDTs (linear variable differential transformers) are secured on the side walls of the basket. After reaching a predetermined gravity field, hydraulic pressure is applied in increments up to a level which simulates a resultant force existing in the specific stage. The LVDT readings are taken during the load application to obtain scaled down settlement data. When the soil used in the centrifuge test is cohesionless, the LVDT readings can be recorded as soon as they become relatively stable under each load increment. If the soil used in the test is cohesive, a certain time must elapse before recording the LVDT readings. The time rate of consolidation is governed by Eq. (5.8), the scaling factor for time is equal to $(1/n)^2$. This acceleration of time is another advantage the centrifuge technique can offer. For example, a three month period in the field will be equivalent to a duration of about 52 minutes for a model having a scaling factor of 50.

6.2 Centrifuge Modeling of Bridge A Footing

To simulate performance of Bridge A - Panel "A" footing, footing models in three different scaling factors (1/40, 1/50, and 1/60) were constructed and exposed to a high intensity gravitational acceleration field. The centrifuge system utilized in the study was designed and manufactured by Genisco Technology. The system components are a symmetrical rotating arm assembly, triangular mounting platform, integral slip ring, motor, circular enclosure, electronic assembly, and control console. The maximum rotational speed it can achieve is 400 RPM. It holds a mass of up to 45.36 kg (100 lb.) at a distance of 1.36 m (4.46 feet) from its rotational axis and produces a maximum acceleration of 200 G. The dimensions of the swing basket container, in which a model can be set up, are 6 inches (W) by 16 inches (L) by 11.5 inches (H). For each scaling factor, the following formula was applied to determine a rotational velocity which will achieve a desired level of gravitational field:

$$N = \sqrt{\frac{G}{C_1 \cdot R}} \qquad \text{Eq. (6.1)}$$

where N = rotational velocity (rpm); G = model scaling factor; C_1 = calibration constant = 28.416 x 10^{-6}; and R = radius = 42 inches.

Each model was placed on top of the bearing soil material obtained from the actual site, which had been regraded (stones retained on No. 4 sieve removed) and recompacted, inside the swing basket. A hydraulic loading ramp was mounted vertically to the scaled footing model. Two (2) LVDTs were attached to a rigid load frame above the model to monitor its differential movement in the direction of loading during tests. The concept of "modeling of models" was applied among

these models in examining consistency in their behavior in spite of the scaling and boundary effects. Figure 6.1 presents a schematic of the centrifuge test model set-up.

Except for the first construction stage (construction of footing), the prototype structure was subjected to overturning moment which would create non-uniform contact pressure distribution at the base of the footings. In order to model different construction stages, the eccentricity of resultant load was computed and the magnitude and the position (with respect to the centerline of the footing model) of the hydraulic load were adjusted accordingly. For these tests under eccentric loading conditions, the two LVDTs were positioned so that not only overall settlement, but tilting, could be monitored. Once the LVDT readings were recorded, they were transformed back to settlement of a prototype using the following equation:

$$S = (V_o - V) \cdot C_3 \cdot G \tag{6.2}$$

where S = settlement of prototype footing (inches); V_o = initial LVDT output voltage (volt); V = subsequent LVDT output voltage (volt); C_3 = calibration factor of LVDT being used (inch/volt); and G = model scaling factor.

A total of thirty one experiments were performed, among which eight were with the 40 G model, eight with the 60 G model, and fifteen with the 50G model. Results of the centrifuge tests for Panel "A/B" footing of Bridge A are presented against the field results in Figure 6.2. Settlement responses of Panel "A/B" footing are summarized in Table 6.2. Definitions of the construction stages shown in the figure are the same as those used in Chapter 4: 1 = footing construction; 2 = abutment wall construction; 3 = backfilling behind abutment wall; and 4 = completion of composite deck construction. All three centrifuge models exhibited a similar settlement behavior, having about

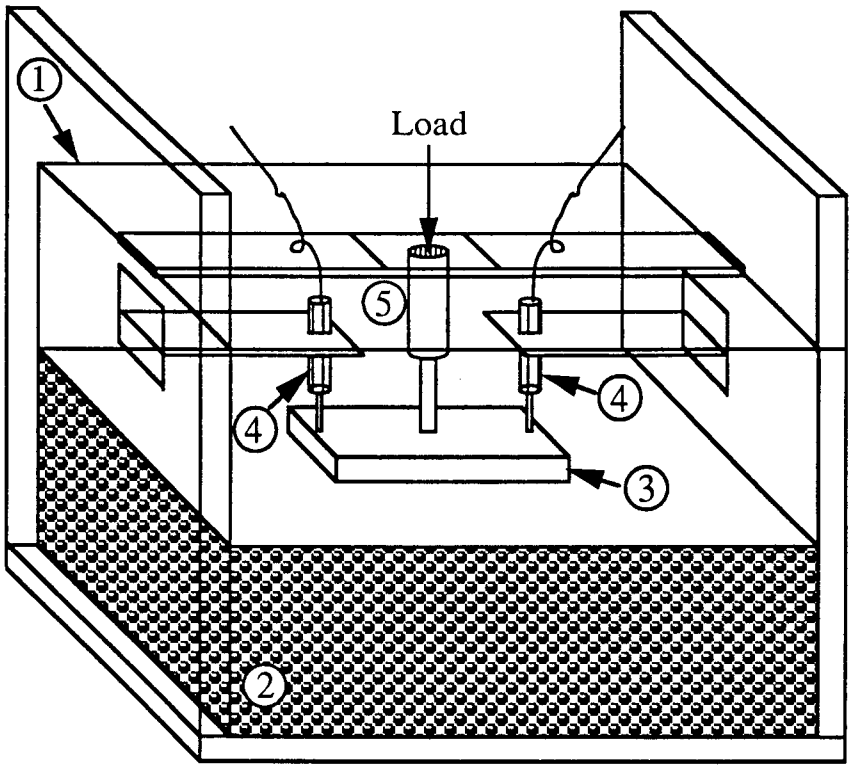

① Centriguge Box
② In Situ Soil
③ Scaled-down Spread Footing Model
④ LVDT
⑤ Hydraulic Piston

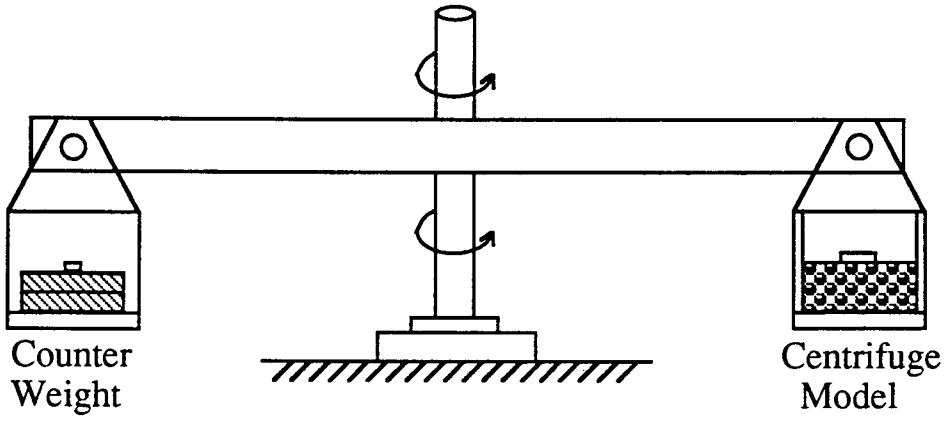

Figure 6.1 Typical Set-Up for Laboratory Centrifuge Modeling Test

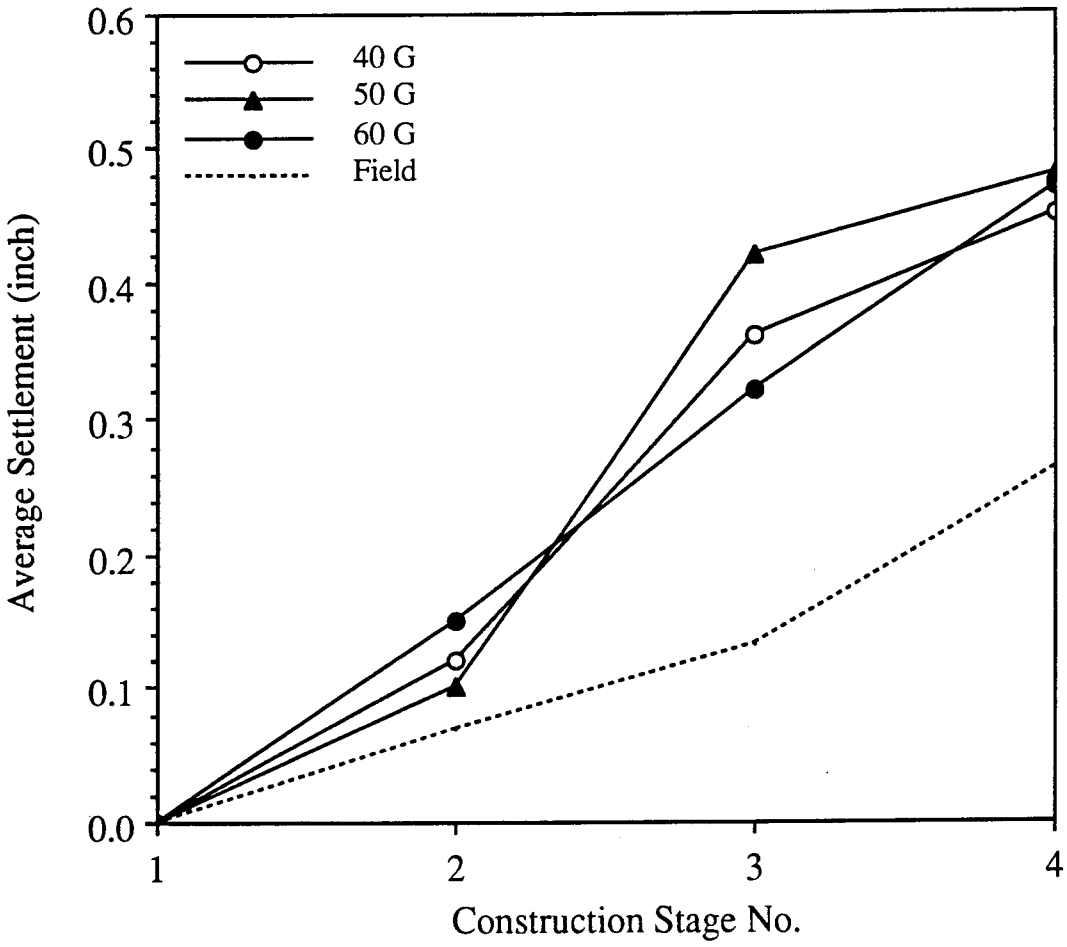

Figure 6.2 Centrifuge Test Results for Panel "A/B" Footing (Bridge A)

Table 6.2 Comparison of Centrifuge Test Results with Field Settlement and Geotechnical Formula Predictions for Panel "A/B" Footing (Bridge A)

Construction Stage No.	Average Settlement of Panel A/B Footing (inch) :										
	Field	Centrifuge Tests			Geotechnical Prediction Methods						
		40G	50G	60G	Burland	D'Appolonia	Hough	Peck-Bazaraa	Terzaghi-Peck	Schmertmann	Ave.
1	0.00	0.00	0.00	0.00	0.00	0.00	0.00	0.00	0.00	0.00	0.00
2	0.07	0.12	0.10	0.15	0.31	0.06	0.08	0.10	0.31	0.25	0.19
3	0.13	0.36	0.42	0.32	0.63	0.12	0.15	0.21	0.63	1.02	0.46
4	0.26	0.45	0.48	0.47	0.80	0.16	0.18	0.27	0.80	1.43	0.47

Table 6.3 Comparison of Centrifuge Test Results with Field Settlement and Geotechnical Formula Predictions for Abutment No. 1 Footing (Bridge B)

Construction Stage No.	Average Settlement of Abutment No. 1 Footing (inch)									
	Field	Centrifuge Tests		Geotechnical Prediction Methods						
		50G	60G	Burland	D'Appolonia	Hough	Peck-Bazaraa	Terzaghi-Peck	Schmertmann	Ave.
1	0.00	0.00	0.00	0.00	0.00	0.00	0.00	0.00	0.00	0.00
2	0.13	0.13	0.13	0.06	0.03	0.06	0.02	0.06	0.02	0.04
3	0.54	0.17	0.18	0.07	0.04	0.08	0.03	0.07	0.07	0.06
4	0.57	0.43	0.48	0.20	0.10	0.20	0.09	0.20	0.56	0.23
5	0.61	0.50	0.56	0.25	0.29	0.25	0.12	0.26	0.78	0.33

twice as much as the field settlement in each construction stage. According to these centrifuge test results, the third construction stage induced more settlement than the other stages. In the field, the fourth construction staged induced more settlement than the other stages. In the field, the fourth construction stage had the largest impact on the settlement performance. According to Table 6.2, the centrifuge results turned out to be on the intermediate level between lower values predicted by D'Appolonia, Hough, and Peck-Bazaraa methods and higher values predicted by Burland, Terzaghi-Peck, and Schmertmann methods.

6.3 Centrifuge Modeling of Bridge B Foundations

The centrifuge modeling of Abutment No. 1 and Central Pier of Bridge B structure was carried out in a similar manner. Two models in scaling factors of 1/40 and 1/50 were prepared for Abutment No. 1, and only one 50 G model was constructed for modeling Central Pier foundation. A total of twenty tests were performed for Abutment No. 1 footing, and only three tests were conducted with the Central Pier foundation model. Figure 6.3 presents the centrifuge test results of the Abutment No. 1 model. For this structure, the construction stages are defined as: 1 = footing construction; 2 = construction of abutment wall or pier columns/cap; 3 = placement of girder beams; 4 = backfilling; 5 = completion of composite deck construction. Agreement between the centrifuge model behavior and the field settlement was excellent up to the second construction stage and relatively good at the end of the fifth construction stage. However, a large difference was introduced when the third stage was simulated. The laboratory test results showed that contribution of the fourth stage was the most significant, while in the field, the third stage induced more settlement. Table 6.3 summarizes for Abutment No. 1 footing results from the field monitoring, applications of

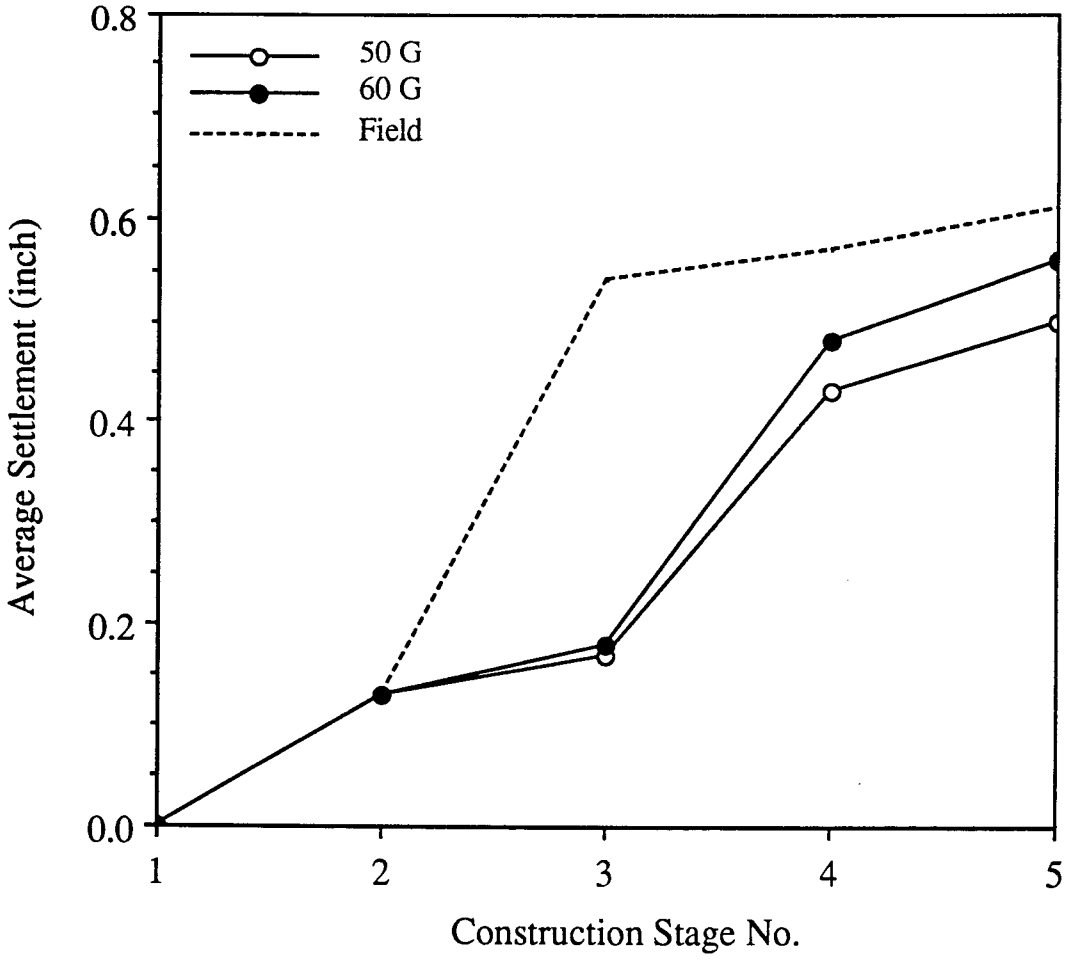

Figure 6.3 Centrifuge Test Results for Abutment No. 1 Footing (Bridge B)

the geotechnical methods, and the laboratory centrifuge tests. Figure 6.4 shows settlement behavior of the Central Pier model. For this structure, the major construction stages are: 1 = footing construction; 2 = construction of abutment wall or pier columns/cap; 3 = backfilling behind abutment wall; 4 = placement of girder beams; and, 5 = completion of composite deck construction. Similar to the case for Panel "A" footing of Bridge A, the centrifuge model settlement was larger than the actual for any construction stage. Both the field and laboratory performance data showed that the second stage induced a little more settlement than the other stages on this foundation.

6.4 Centrifuge Modeling of Bridge C Footing

Field behavior of the footing for Bridge C footing was simulated using three model scales at 40 G, 45 G, and 50 G. Numbers of tests performed were two with the 40 G model, two with the 45 G model, and nine with the 50 G model. Figure 6.5 compares average settlement responses of these three models. The construction stages are defined as: 1 = footing construction; 2 = placement of box culvert sections; 3 = backfilling next to and over box culvert; and 4 = paving. The 50 G model experienced substantially higher settlement than the other two under the last two stages. This was due to some difficulty experienced in controlling the moisture content and dry density of the soil. If the average response is computed among the three models, it is found to match the field settlement relatively well. Both the field and laboratory performance results agreed to indicate that the second stage induced more settlement than the other stages.

Table 6.4 summarizes for each construction stage average settlement based on the field observation, centrifuge modeling, and the geotechnical formulas. According to this table, a similarity existed between the 45 G model behavior and the predictions by Hough method.

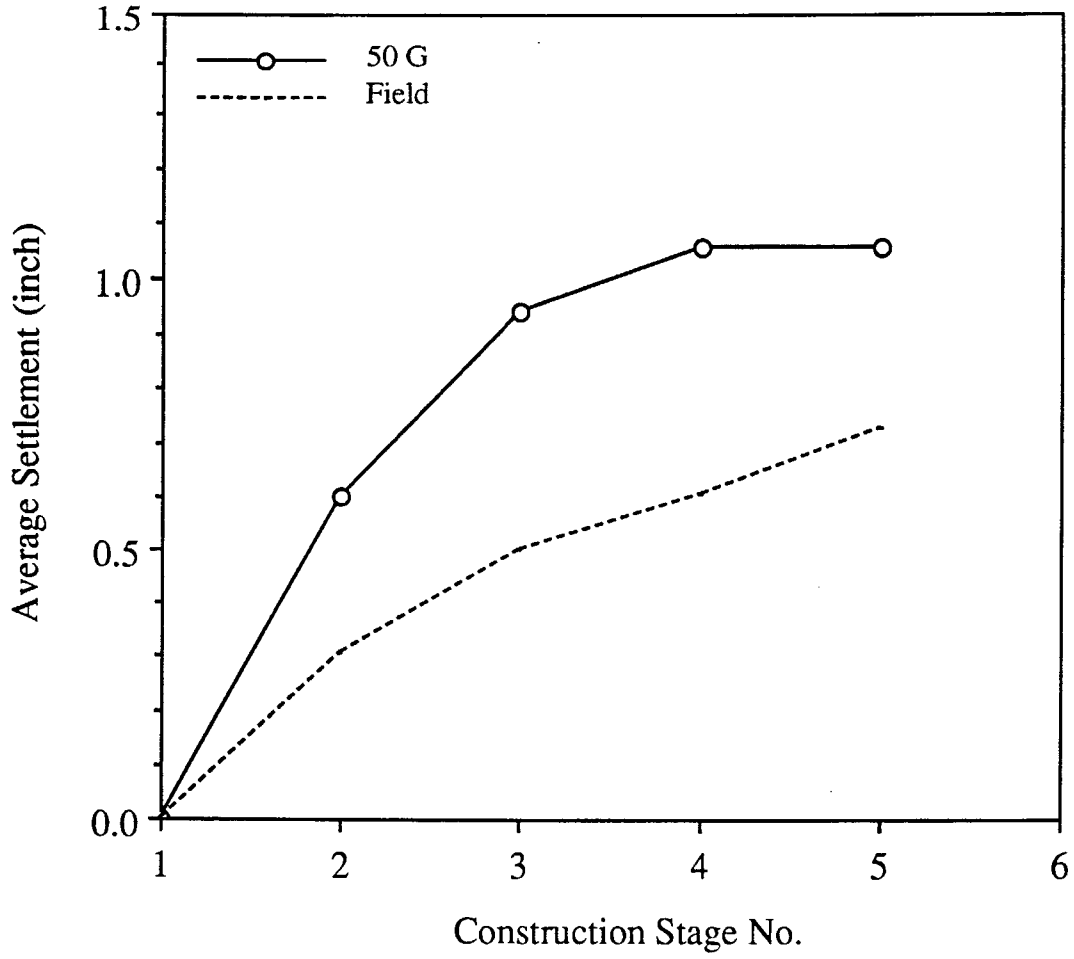

Figure 6.4 Centrifuge Test Results for Central Pier Foundation (Bridge B)

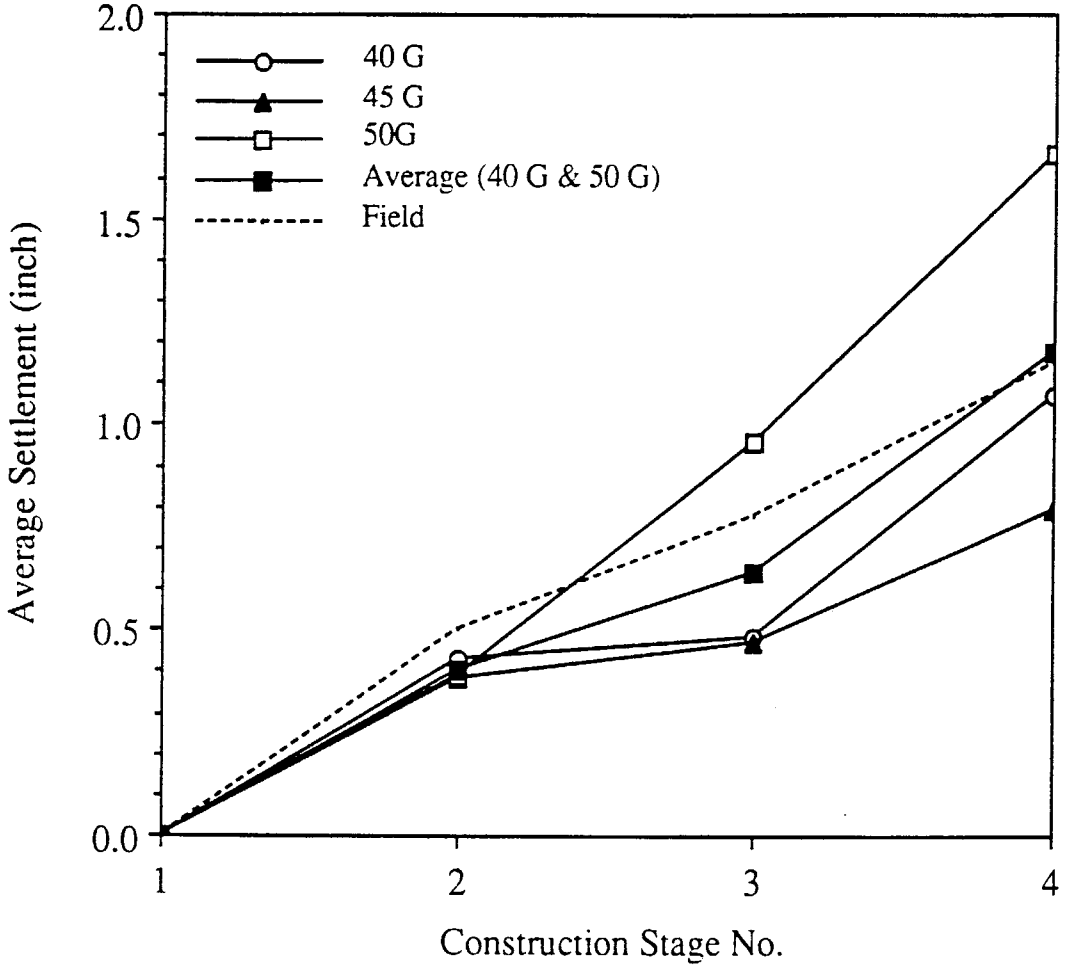

Figure 6.5 Centrifuge Test Results for West Footing (Bridge C)

Table 6.4 Comparison of Centrifuge Test Results with Field Settlement and Geotechnical Formula Predictions for Bridge C (Box Culvert) Footing

Construction Stage No.	Average Settlement of Box Culvert Footing (inch)									
	Field	Centrifuge Tests			Geotechnical Prediction Methods					
		40G	45G	50G	Burland	D'Appolonia	Hough	Peck-Bazaraa	Terzaghi-Peck	Schmertmann
1	0.00	0.00	0.00	0.00	0.00	0.00	0.00	0.00	0.00	0.00
2	0.49	0.43	0.38	0.39	0.04	0.02	0.33	0.10	0.16	0.21
3	0.71	0.48	0.47	0.96	0.19	0.07	0.46	0.15	0.23	0.33
4	1.05	1.07	0.79	1.66	0.37	0.13	0.79	0.30	0.48	0.69

6.5 Centrifuge Modeling of Bridge D Footing

Field behavior of the Pier 3 (Phase I) footing was simulated using three model scales at 40 G, 50 G, and 60 G. Soil samples obtained from the zone under this footing was dried, sieved, rewetted, and compacted in three lifts inside the model container to the average field moisture and dry density conditions. Numbers of tests performed were five with the 40 G model, four with the 50 G model, and three with the 60 G model. Under each load increment corresponding to construction stage, the load was maintained for a period computed from the actual duration in the field using the scaling relation. At the start and end of the loading period, the LVDT readings were taken to record settlements due to both elastic and plastic deformations. Figure 6.6 compares typical settlement responses of these three models relative to the average field settlement through the construction increments. Construction stages in the figure are defined as: 1 = footing construction; 2 = columns/cap construction; 3 = backfilling over footing; 4 = placement of composite beams; 5 = completion of deck construction; and 6 = service load application. Each curve in the figure was identified by the scaling factor (40 G, 50 G, 60 G) and loading time (i = immediate upon loading; T = after the time equivalent to the duration in the field). Some fluctuations were observed among the centrifuge test results because of small variations in the properties of the soil layers. Immediate settlement of the 50 G and 60 G models remained less than the field settlement throughout the stages. Settlements of all the models became larger than the field values after the fourth stage. The overall best fit to the field curve was exhibited by the average immediate settlement performance of the 40 G scale model footing.

Table 6.5 summarizes for each construction stage average settlement based on the field observation, centrifuge modeling, and the geotechnical formulas. According to the data presented

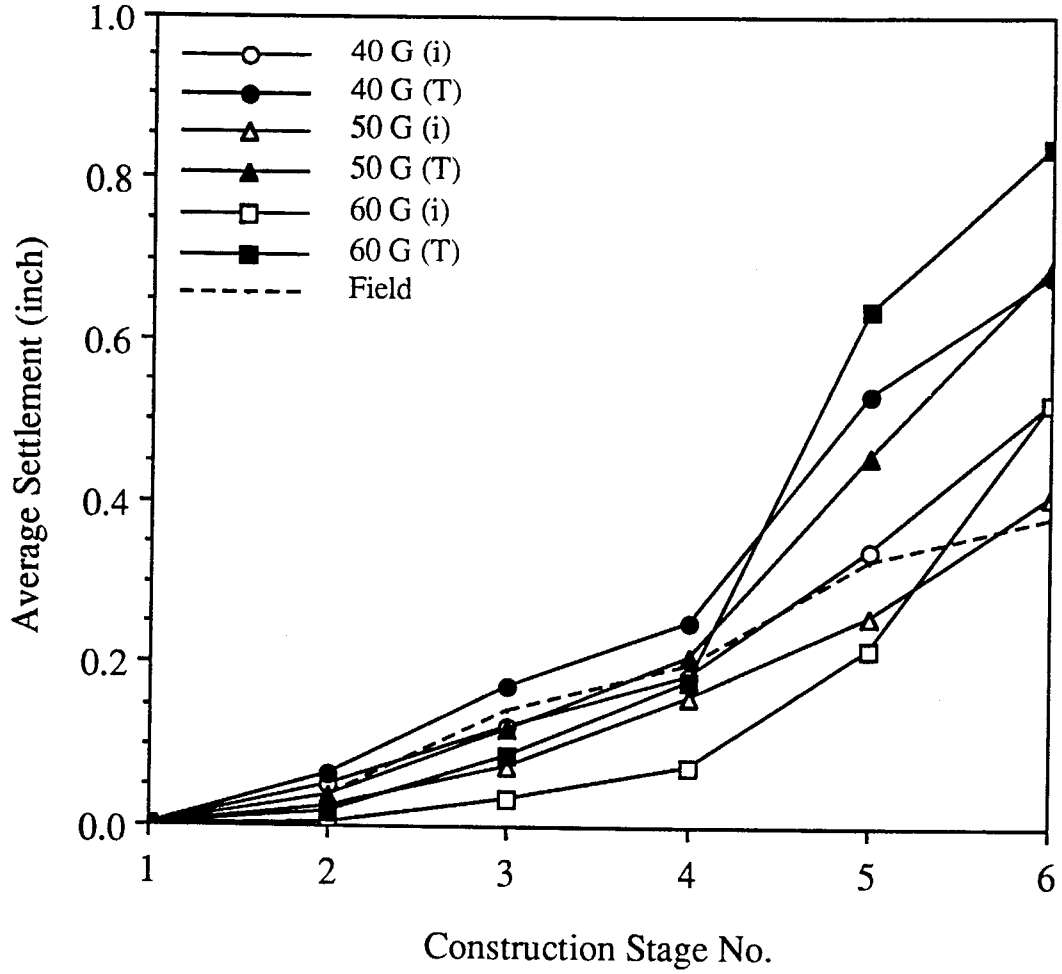

Figure 6.6 Centrifuge Test Results for Pier 3 (Phase I) Footing (Bridge D)

Table 6.5 Comparison of Centrifuge Test Results with Field Settlement and Theoretical Predictions for Pier 3-North Footing (Bridge D)

Construction Stage No.	Average Settlement of Pier 3 Footing (inch) :					
	Field	Centrifuge Tests			Theoretical Predictions	
		40G	50G	60G	Elastic Only	Elastic + Consolidation
1	0.00	0.00	0.00	0.00	0.00	0.00
2	0.04	0.06	0.03	0.02	0.02	0.08
3	0.14	0.17	0.12	0.09	0.03	0.12
4	0.20	0.25	0.21	0.18	0.09	0.30
5	0.33	0.53	0.45	0.64	0.10	0.54
6	0.38	0.68	0.69	0.83	0.11	0.70

in the table, the theoretical predictions overpredicted the field settlement behavior more than any of the centrifuge model results, especially under later construction stages.

6.6 Centrifuge Modeling of Bridge E Footing

Field behavior of the Pier 3 (Phase I) footing was simulated using three model scales at 37.5 G, 55 G, and 62.5 G. The soil sampled from the Pier 3 area was dried, sieved through No. 4 sieve, moistened, and then placed in lifts to match the field dry density and moisture content. The soil was compacted in two layers to more closely simulate the actual field conditions. Table 6.6 presents thickness, unit weight, and moisture content data for each of these soil layers. Numbers of tests performed were two per each scale model. Under each load increment corresponding to construction stage, the load was maintained for a period equivalent to the actual time elapsed in the field before taking the LVDT readings. Figure 6.7 compares typical settlement responses of these three models. Construction stages in the figure are set as: 1 = footing construction; 2 = columns/cap construction; 3 = backfilling; 4 = placement of box beams; and 5 = completion of composite deck construction. Average test results were similar among the three models. The fourth stage induced more settlement than any other. In the field, effects due to Construction Stage Nos. 2 and 4 were equally larger than those of the other two stages. Table 6.7 summarizes for each construction stage average settlement based on the field observation, centrifuge modeling, and the geotechnical formulas. In this case, the theoretical predictions were neither superior nor inferior to the centrifuge test results, being very similar to the typical behavior of the centrifuge model.

Table 6.6 Soil Layers Prepared for Centrifuge Model Tests (Bridge E)

Scaling Scaling Factor	Unit Weight (pcf)	Lower Soil Layer		Upper Soil Layer	
		Thickness	Moisture	Thickness	Moisture
37.5	132.4	2.205 in.	12.0%	1.920"	22.0%
55	132.4	2.705 in.	12.0%	1.420"	22.0%
62.5	132.4	2.877 in.	12.0%	1.248"	22.0%

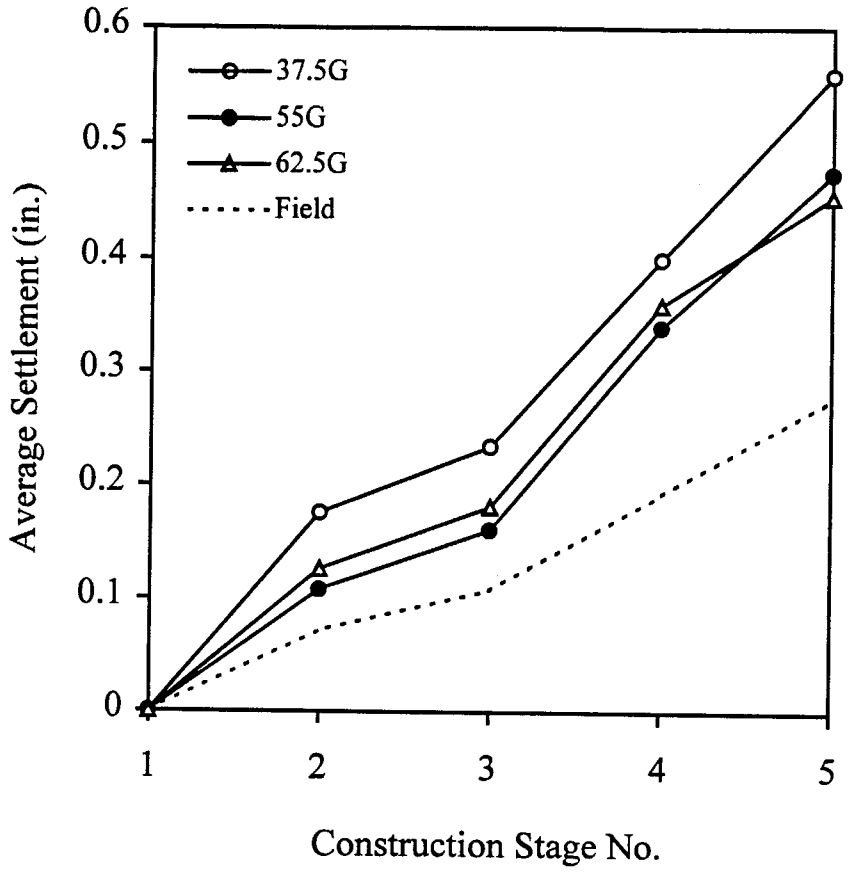

Figure 6.7 Centrifuge Test Results for Pier 3 Footing (Bridge E)

Table 6.7 Comparison of Centrifuge Test Results with Field Settlement and Theoretical Predictions for Phase I - Pier 3 Footing (Bridge E)

Construction Stage No.	Average Settlement of Pier 3 Footing (inch) :					
	Field	Centrifuge Tests			Theoretical Predictions	
		37.5G	55G	62.5G	Elastic Only	Elastic + Consolidation
1	0.00	0.00	0.00	0.00	0.00	0.00
2	0.07	0.18	0.11	0.13	0.10	0.11
3	0.11	0.23	0.16	0.18	0.18	0.20
4	0.19	0.40	0.34	0.36	0.30	0.34
5	0.28	0.40	0.34	0.36	0.41	0.48

Chapter 7

Concluding Remarks

7.1 Summary

This study was highly recommended by the Federal Highway Administration (FHWA) to establish field performance data on spread footings supporting highway bridges. In this study, performance of spread footings of five highway bridge structures located in Ohio were monitored in the field during construction stages and under service load conditions. Factors in evaluating the performance were overall settlement, tilting of abutment wall/pier column, and pressure distribution under the footings. Settlement monitoring points, tilting measurement stations, and earth contact pressure cells were installed on selected foundations to obtain performance data in the field. The performance of these structures was also examined through centrifuge modeling technique in the laboratory. For the footings resting on cohesionless soils, settlement estimations made by six selected geotechnical methods (Burland method, D'Appolonia method, Haugh method, Peck-Bazaraa method, Terzaghi-Peck method, and Schmertmann method) were compared against the field and laboratory performance results. For the footings resting on cohesive soils, the standard methods based on elastic theory and Terzaghi's consolidation theory were applied, and their predicted values were evaluated in light of the field data.

The five bridge structures differed significantly in terms of basic design features, such as the number of span, maximum span dimension, combined bearing area, and others. Foundations of the first three bridges (Bridges A through C) rested on cohesionless soils. In contrast, Bridges D and E had their footings supported by cohesive soils.

Bridge A was a single-span, composite steel bridge structure, with a reinforced concrete deck.

It was constructed over Nelson road as part of the I-670 interstate highway construction, connecting the downtown to a major airport in the east part of the city of Columbus, Franklin County. Its spread footing/wall was a cantilever retaining wall type without any counterfort.

Bridge B was a two-span bridge and supported by two large abutment/wingwall structures at the ends and by a pier foundation in the center. Each span was about 124 feet from bearing to bearing, and the width of the bridge deck was about 57 feet The bridge was constructed to carry U.S. Rt. 68 over U.S. Rt. 35 as a part of a major extension project for U.S. Rt. 35 just south of the city of Xenia in Greene County. The two major foundations of Bridge B were a cantilever type with large-size stepping side walls arranged 90 degrees from the abutment face.

Bridge C, constructed on U.S. Rt. 39 just west of the city of Dover in Tuscarawas County, was a three-sided, flat-topped, concrete box culvert structure. The spread-footing-supported box culvert was installed replacing the old bridge to provide drainage way for the Brandywine Creek.

Bridge D was constructed in two phases over I-75 interstate highway in Butler County, Ohio. It was a six-span, composite deck bridge structure. Overall bridge length and deck width were 414.7 feet and 72 feet, respectively. The longest span was 76.3 feet in length. The two abutments were supported by H-piles. Among twenty-five spread footings, fifteen were pre-existing small, square footings from the previous bridge structure.

Bridge E was the longest structure (670 feet), having a total of nine spans. It was constructed in two phases at St. Rt. 32, over Consolidation Rail and St. Rt. 35, in Hamilton County, Ohio. Overall deck width and the longest span were 54 feet and 86.2 feet, respectively. Phase I foundations were all spread footings, but Phase II foundations were spread footings with drilled pier shafts integrated on the north side.

Subsurface soil conditions at the Bridge A through C sites were relatively similar. Bearing soil strata comprised of cohesionless soils classified typically as AASHTO A-2, A-3, and A-4. Plasticity index was generally less than 4. The SPT N-value was slightly less than 20 at the base of the footings and reached more than 100 from depths 20 feet to 30 feet below the footings in the Bridge A construction area. Under abutment foundations of Bridge B, the N-value was mostly 50 or higher. For Bridge C, the value increased with depth from below 20 to as much as 40.

Soils encountered at the Bridge D and E sites were mostly classified as AASHTO A-6 or A-7. Other soil types were also found in a few isolated regions - A-4 a below Pier 3 (Bridge D), and A-1 and A-2 below Pier 2, forward abutment, and rear abutment (Bridge E). Depth to bedrock was relatively uniform and less than 7 feet at the Bridge D site (this is contrary to what the boring logs indicated), while the bedrock depth varied widely from 9 feet to more than 95 feet in the Bridge E construction area. The SPT N-value at the Bridge D site ranged from about 40 to 60 at the foundation level to 100+ in the weathered rock. At the Bridge E site, the SPT N-value was typically about 20 to 30 at the foundation level and increased gradually with the depth.

Comprehensive field monitoring of spread footings supported highway bridge performance was feasible, utilizing current instrumentation and measurement techniques, such as vibrating wire pressure cells, servo-accelerometer tilting sensor device, and optical level surveying method.

7.2 Conclusions

Through the field monitoring work it was found that:

1) Overall, the current study demonstrated that spread footings could be used successfully to support the highway bridge structures both on cohesionless and cohesive soils, provided that

subsurface soils were favorable (free of unsuitable materials, no high groundwater table, moderately over-consolidated).

2) The settlement results obtained from the five bridges were within the previously reported range. No spread footing experienced average overall settlement of 2 inches or more prior to the service load application. According to Ref. [23], overall settlement of spread footings supported highway bridges resting on cohesionless soil ranged from 0.02 to 2.72 inches with an average total of 0.61 inches. And, typically about 70% of the total settlement occurs prior to placement of the bridge deck structure. In the current study, average of all the maximum settlement values was 0.66 inch; however, the post deck settlement observed was in some cases a little higher than 30%.

3) No reliable data were previously available on magnitudes and variations of contact pressure during construction under spread footings supported highway bridges. In the study reported by Gifford, et al., [23], their pressure cell readings turned out to be so erratic that they could not provide any meaningful insights. In the current study, maximum contact pressure under the footings was typically less than 40 psi (2.9 tsf). Agreement between the field values and theoretical predictions (based on Rankine's theory) was generally good, and some cells did indicate stress redistribution taking place during construction due to changes in magnitude and location of resultant force.

4) The abutment wall rotation detected at the five sites were within $\pm$ 0.3 degree, which is comparable with the previously reported range of 0.23 degree toward backfill to 0.12 degree away from backfill.

5) Both magnitude and direction of abutment wall tilting due to backfilling behind the wall

appeared to be influenced largely by the geometry of the foundation and rigidity of the wall-to-foundation connection. Backfilling operations behind the abutment wall (Bridge A) induced tilting away from the backfill, and backfilling taking place in front of the abutment wall lead to negligible degree of tilting. Almost no measurable tilting was observed on the abutment walls of Bridge B, which had counterforts perpendicularly attached to the front footing/wall. Walls of three-sided box culvert structure, grouted in the key foundations, showed a tendency to rotate toward the backfill during backfilling. The rear abutment wall of Bridge E rotated slightly toward the backfill.

6) The actual abutment wall tilting agreed very well with predictions by an empirical tilting estimation formula for only Panel "A" abutment of Bridge A. In most of the other cases examined, the field tilting responses were underestimated by the formula. No tilting of the abutment wall was taken at the Bridge D site.

7) Daily variations in air temperature seemed to have little effect on abutment wall tilting.

8) Tilting of the pier columns were also within $\pm$ 0.3 degree. Since they were typically backfilled under relatively shallow soil cover, effect of backfilling on tilting of the columns was negligible. Tilting of the pier structures appeared to be induced by variations in the span dimensions and spatial variability in the properties of the bearing soil layers.

9) According to the field data obtained at the Bridge E site, tilting of the pier columns in the transverse direction was about the same order of magnitude as that in the longitudinal direction.

10) Comparisons between predictions by six selected geotechnical settlement estimation methods and the field settlement performance at the first three bridge sites (Bridge A through C)

resulted in the following conclusions:

- None of the six methods was successful in predicting the actual field settlement accurately for all the three bridge structures.
- Burland and Terzaghi-Peck methods yielded very similar settlement estimates which were too high for Bridge A and too low for Bridges B and C.
- Schmertmann method resulted in the largest settlement estimate among the six methods, which was only satisfactory only for Bridge C.
- D'Appolonia method consistently underestimated the actual field settlement.
- Based on the three cases addressed in this study, the method proposed by Hough appears to be the most consistent in estimating the actual settlement with relatively good accuracies.

11) Comparisons between theoretical predictions and field settlement data for Bridges D and E lead to the following conclusions:

- Settlement of a footing on cohesive soils can be estimated reasonably accurately by combining elastic theory and consolidation theory. A great care is needed to set the values of the parameters. It is highly recommended that some laboratory tests be performed on relatively undisturbed soil sample. The theoretical estimate tends to be on the conservative side (larger than the actual settlement in the field).

12) Comparisons among the predictions by settlement estimation methods, the field settlement behaviors, and the centrifuge model behaviors resulted in the following conclusions:

- Settlement rate of the centrifuge models was about twice as large as the actual for Panel "A" footing of Bridge A and Central Pier foundation of Bridge B. Closer

agreement between the centrifuge test and field results was observed for Abutment No. 1 footing of Bridge B, west footing of Bridge C, and Pier 3-North footing of Bridge D.

- Overall, the centrifuge model results were superior to the theoretical estimate. However, there still remains a difficulty in accurately simulating complex subsoil conditions accurately in the model basket.

7.3 Implementation and Recommendation

1) Better QC/QA program must be implemented during the initial subsurface exploration stage. In the current project, large discrepancies existed between the boring logs and the actual field conditions for at least one of the project sites.

2) When estimating the settlement of spread footings on sand, several methods based on different concepts must be applied. Depending on only one method may lead to an unrealistic prediction.

3) Comprehensive laboratory testing should be performed on relatively undisturbed soil samples to determine engineering properties whenever spread footing is selected to support the highway bridge structure.

REFERENCES

1. Wahls, H.E. (1983). "Shallow Foundations for Highway Structures." National Cooperative Research Program Synthesis of Highway Practice, No. 107, Transportation Research Board, National Research Council, Washington, DC, 38 pp.

2. Terzaghi, K. and Peck, R.B. (1967). "Soil Mechanics in Engineering Practice." John Wiley and Sons, Inc., New York.

3. Peck, R.B., Hanson, W.E. and Thornburn, T.H. (1974). "Foundation Engineering." Second Edition, John Wiley and Sons, Inc., New York.

4. Hough, B.K. (1959). "Compressibility as the Basis for Soil Bearing Value." Journal of Soil Mechanics and Foundation Division, The American Society of Civil Engineers, Vol. 85, No. SM4, pp. 11-39.

5. Alpan, I. (1964). "Estimating the Settlement of Foundations on Sands." Civil Engineering and Public Works Review, pp. 14-15.

6. Gibbs, E.J. and Holtz, W.G. (1957). "Research on Determining the Density of Sands by Spoon Penetration Testing." Proceedings of 4th International Conference on Soil Mechanics and Foundation Engineering, Vol. 1, London, pp. 35-39.

7. DeBeer, E.E. (1965). "Bearing Capacity and Settlement of Shallow Foundations on Sand." Proceedings, Symposium on Bearing Capacity and Settlement of Foundations, Duke University, Durham, NC.

8. Meyerhof, G.G. (1965). "Shallow Foundations." Journal of Soil Mechanics and Foundation Division, The American Society of Civil Engineers, Vol. 91, No. SM2, pp. 21-31.

9. Peck, R.B. and Bazaraa, A.R.S. (1969). Discussion of "Settlement of Spread Footings on Sand" by D'Appolonia, D'Appolonia, and Brissette, Journal of Soil Mechanics and Foundation Division, The American Society of Civil Engineers, May.

10. Bazaraa, A.R.S. (1967). "Use of the Standard Penetration Test for Estimating Settlements of Shallow Foundations on Sand." Ph.D. Thesis Presented to the University of Illinois at Urbana, IL.

11. D'Appolonia, D.J., D'Appolonia, E., and Brissette, R.F. (1968). "Settlement of Spread Footings on Sand." Journal of the Soil Mechanics and Foundations Division, The American Society of Civil Engineers, Vol. 94, March, pp. 735-761.

12. D'Appolonia, D.J., D'Appolonia, E., and Brissette, R.F. (1970). "Settlement of Spread Footings on Sand (Closure)." Journal of Soil Mechanics and Foundation Division, The American Society of Civil Engineers, Vol. 96, No. SM2, March, pp 754-761.

13. Schmertmann, J.H. (1970). "Static Cone to Compute Static Settlement Over Sand." Journal of Soil Mechanics and Foundation Division. The American Society of Civil Engineers, Vol. 96, No. SM3, pp. 1011-1043.

14. Leonards, G.A. and Frost, J.D. (1988). "Settlement of Shall Foundations on Granular Soils." Journal of Soil Mechanics and Foundation Division, The American Society of Civil Engineers, Vol. 114, No. 7, pp. 791-809.

15. Oweis, I.S. (1979). "Equivalent Linear Model for Predicting Settlement of Sand Bases." Journal of Geotechnical Engineering Division, The American Society of Civil Engineers, Vol. 115, No. 12, December.

16. Burland, J.B. and Burbridge, M.C. (1984). "Settlement of Foundation on Sand and Gravel." Institution of Civil Engineers - Glasgow and West of Scotland Association.

17. Bowles, J.E. (1987). "Elastic Foundation Settlement on Sand Deposits." Journal of Geotechnical Engineering Division, The American Society of Civil Engineers, Vol. 113, No. 8, pp. 846-860.

18. Steinbrenner, W. (1934). "Tafeln zur Setzungsberechnung." Die Strasse, Vol. 1, October, pp. 121-124.

19. Keene, P. (1978). "Tolerable Movements of Bridge Foundations." Transportation Research Record 678, Washington, DC, pp. 1-6.

20. Walkinshaw, J.L. (1978). "Survey of Bridge Movements in the Western United States." Transportation Research Record 678, Washington, DC, pp. 6-11.

21. Grover, R.A. (1978). "Movements of Bridge Abutments and Settlements of Approach Pavements in Ohio." Transportation Research Record 678, Washington, DC, pp 12-17.

22. Bozozuk, M. (1978). "Bridge Foundations Move." Transportation Research Record 678, Washington, DC, pp. 17-21.

23. Gifford, D.G., Wheeler, J.R., Kraemer, S.R., and McKown, A.F. (1978). "Spread Footings for Highway Bridges." FHWA/RD-86/185, Final Report to Federal Highway Administration, Washington, DC, 229 pp.

24. DiMillio, A.F. (1982). "Performance of Highway Bridge Abutments Supported by Spread Footings on Compacted Fill." FHWA/RD-81/184, Federal Highway Administration, Washington, DC, 55 pp.

25. Moulton, L.K., Ganga Rao, H.V.S., and Halvorson, G.T. (1982). "Tolerable Movement Criteria for Highway Bridges." Vol. I, Interim Report, FHWA-RD-81-162, Federal Highway Administration, Washington, DC, 117 pp.

26. Baus, R.L. (1992). "Spread Footing Performance Evaluation in South Carolina." Report No. F92-102, Final Report for a Project Sponsored by the South Carolina Department of Highways and Public Transportation in Cooperation with the Federal Highway Administration, F92-102, Columbia, SC.

27. Gemperline, D.G. (1987). "Centrifuge Modeling of Shallow Foundations." Geotechnical Special Publication No. 17 - "Soil Properties Evaluation from Centrifugal Models and Field Performance." The American Society of Civil Engineers, pp. 45-70, New York.

28. Ovesen, N.K. (1975). "Centrifugal Testing Applied to Bearing Capacity Problems of Footings on Sand." Geotechnique, Vol. 25, No. 2, pp. 394-401.

29. Cenepa, Y, Garnier, J., Amar, S., and Corte, J.F. (1988). "Comparison Between Field and Centrifuge Model Tests on Shallow Foundations." Centrifuge 88, Balkema, Rotterdam, pp. 322-324.

30. Pu, J.L. and Ko, H.Y. (1988). "Experimental Determination of Bearing Capacity in Sand by Centrifuge Footing Tests." Centrifuge 88, Balkema, Rotterdam, pp. 293-299.

31. Fujii, N. Kusakabe, O., Keto, H., and Maeda, Y. (1988). "Bearing Capacity of a Footing with an Uneven Base on Slope: Direct Comparison of Prototype and Centrifuge Model Behavior." Centrifuge 88, Balkema, Rotterdam, pp. 301-306.

32. GEOKON, Inc. (1984). "Instructional Manual: Model 4800E/C Total Pressure Cell." New Hampshire, 15 pp.

33. Slope Indicator Co. (1984). "Instructional Manual: TILTMETER Model 50322 and 50344." Seattle, WA, 20+ pp.

34. Bowles, J.E. (1988). "Foundation Analysis and Design," Fourth Edition, McGraw-Hill Book Company, New York, 1004 pp.

35. Tettinek, W. and Matl, F. (1953). "A Contribution to Calculating the Inclination of Eccentrically Loaded Foundations," Proceedings of the Third International Conference on Soil Mechanics and Foundation Engineering, Vol. 1, pp 1-8.

36. Taylor, P.W. (1967). "Design of Spread Footings for Earthquake Loadings," Proceedings of the Fifth Australia-New Zealand Conference on Soil Mechanics and Foundation Engineering, pp. 221-229.

37. Cheney, R.S. and Chassie, R.G. (1982). "Soils and Foundation Workshop Manual." Federal Highway Administration Report, Washington, DC.

38. Janbu, N. Bjerrum, L., and Kjaernsli, B. (1971). "Veilendning Ved Losning Av Fundamenteringsoppgaver." Publication No. 16, Norwegion Geotechnical Institute, Oslo, Norway.

39. Das, B.M. (1994). "Principles of Geotechnical Engineering." Third Edition, PWS Publishing Company, Boston, MA, 672 pp.

40. Nagaraj, T. and Murty, B.R.S. (1985). "Prediction of the Preconsolidation Pressure and Recompression Index of Soils." Geotechnical Testing Journal, American Standards for Testing and Materials, Vol. 8, No. 4, pp. 199-202.

41. Rendon-Herrero, O. (1983). "Universal Compression Index Equation." Discussion, Journal of Geotechnical Engineering Division, The American Society of Civil Engineers, Vol. 109, No. 10.

APPENDIX A :

SOIL BORING DATA

Table A.1 Summary of Soil Boring Log Data - Boring F-1 (Bridge A)

Depth Below Footing Base (ft.)	SPT-N Value	Visual Description of Soil	AASHTO Soil Classification	PI Value	Moisture Content (%)
0.0	11	Fine to coarse sand & fine gravel	NT	NT	10
1.5	11	Fine gravel, some silt, little sand, trace coarse gravel, trace clay	A-2-4	NT	12
9.5	18	Fine to coarse sand and fine to coarse gravel, trace silt	NT	NT	8
10.5	30	Clayey silt, some fine to coarse sand, little fine gravel	A-4a	3	11
17.2	30	Clayey silt, little fine to coarse sand, trace fine gravel	A-4b	4	10
19.5	+100	Silt, some fine to coarse sand, little clay, trace fine gravel	NT	NT	9
28.5	+100	Clayey silt, some fine to coarse sand, trace fine gravel	A-4a	15	10
37.0	38	Fine to coarse sand and fine gravel, trace silt	NT	NT	18

Table A.2 Summary of Soil Boring Log Data - Boring F-2 (Bridge A)

Depth Below Footing Base (ft.)	SPT-N Value	Visual Description of Soil	AASHTO Soil Classification	PI Value	Moisture Content (%)
0.0	15	Brown fine to coarse gravel and fine to coarse sand, little silt	A-1b	3	10
3.0	10 11	Brown fine to coarse gravel, little silt, little fine to coarse sand, trace clay	Visual	NT	13
5.5	29	Brown fine to coarse sand and fine gravel , trace silt	Visual	NT	12
9.5		Brown and gray fine gravel, little fine to coarse sand, little silt	Visual	NT	10
11.0	+100	Cobble	Visual	NT	
11.5	27 48 60	Gray clayey silt, some fine to coarse sand, little fine gravel, few sand seams	A-4a	2	12
20.5	+100	Cobble	Visual	NT	
21.0	+100	Gray clayey silt, some fine to coarse sand, trace fine gravel	A-4a	4	8

(Notes) 1. Bottom of boring at the depth of 26.2 ft. below the bottom of footing.
2. Perched groundwater encountered at a depth 9.5 ft. below the bottom of the footing.

Table A.3 Summary of Soil Boring Log Data - Boring F-3 (Bridge A)

Depth Below Footing Base (ft.)	SPT-N Value	Visual Description of Soil	AASHTO Soil Classification	PI Value	Moisture Content (%)
0.0	9	Brown fine gravel, some clayey silt, some fine to coarse sand	A-2-4	2	13
2.0	11				11
4.5	19				11
7.0	18				11
9.5	24	Gray clayey silt, some fine to coarse sand, trace fine gravel	Visual		11
12.0	38	Gray silt, some fine to coarse sand, trace fine gravel	A-4-b	6	12
14.5	36				
17.0	73	Gray clayey silt, some fine to coarse sand, trace fine gravel	Visual		14
19.5	+100	Gray silt, some fine to coarse sand, little clay, trace fine gravel	Visual	5	10
24.5	100				9
29.5	+100	Gray clayey silt, some fine to coarse sand, trace fine gravel	A-4-a		11
34.5	72			4	10
39.5	46	Gray to black fine gravel, some fine to coarse sand, little clayey silt	A-2-4	NP	11

(Notes) 1. Bottom of boring at the depth of 41 ft. below the bottom of footing.
2. Perched groundwater encountered at a depth 7.5 ft. above the bottom of the footing.

Table A.4 Summary of Soil Boring Log Data - Boring F-6 (Bridge A)

Depth Below Footing Base (ft.)	SPT-N Value	Visual Description of Soil	AASHTO Soil Classification	PI Value	Moisture Content (%)
1.0	15	Brown fine to coarse sand, some fine to coarse gravel, little clayey silt	A-1b	NT	11
3.5 6.0 8.5	14 10 14	Brown fine to coarse gravel, some fine to coarse sand, trace clay	Visual	NT	11 10 14
11.0	19	Brown fine to coarse sand and fine to coarse gravel, some clayey silt	Visual	NT	11
13.5	31	Gray clayey silt, little sand, trace fine gravel	Visual	NT	9
16.0	47	Gray silt, trace fine to coarse sand, trace clay, trace fine gravel	A-4b	2	16
18.5 21.0	54 97	Gray silt, some fine to coarse sand, little clay, trace fine gravel	A-4b	NT 2	11 9
26.0 31.0 36.0	66 88 100	Gray clayey silt, some fine to coarse sand, little fine gravel	Visual Visual A-4a	NT NT 5	10 10 11
41.0	63	Gray and brown fine to coarse sand and fine to coarse gravel, trace silt	Visual	NT	10

(Notes) 1. Bottom of boring at the depth of 42.5 ft. below the bottom of footing.
2. Perched groundwater encountered at a depth 9.0 ft. above the bottom of the footing.

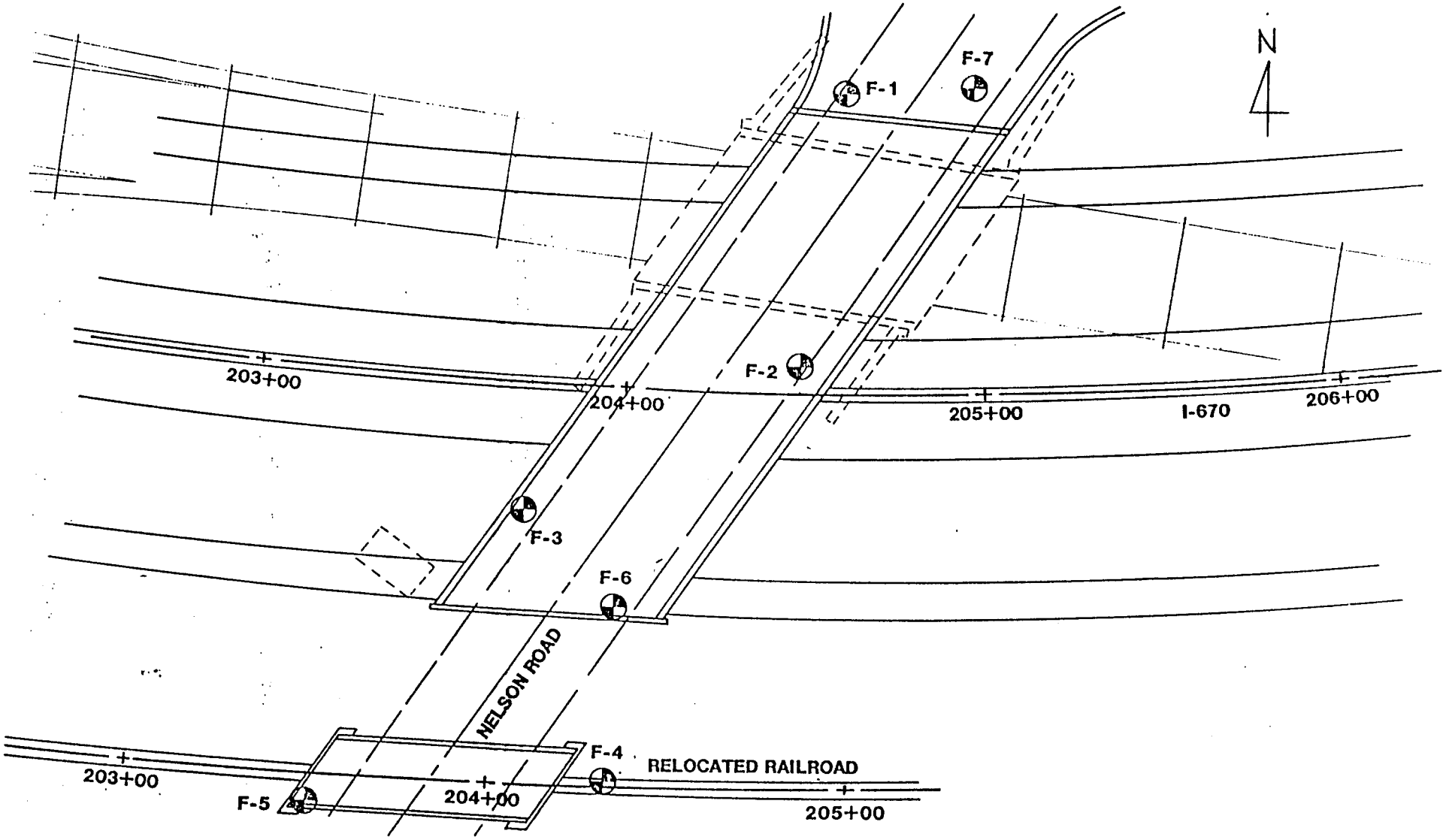

Figure A.1 Boring Location Plan (Bridge A)

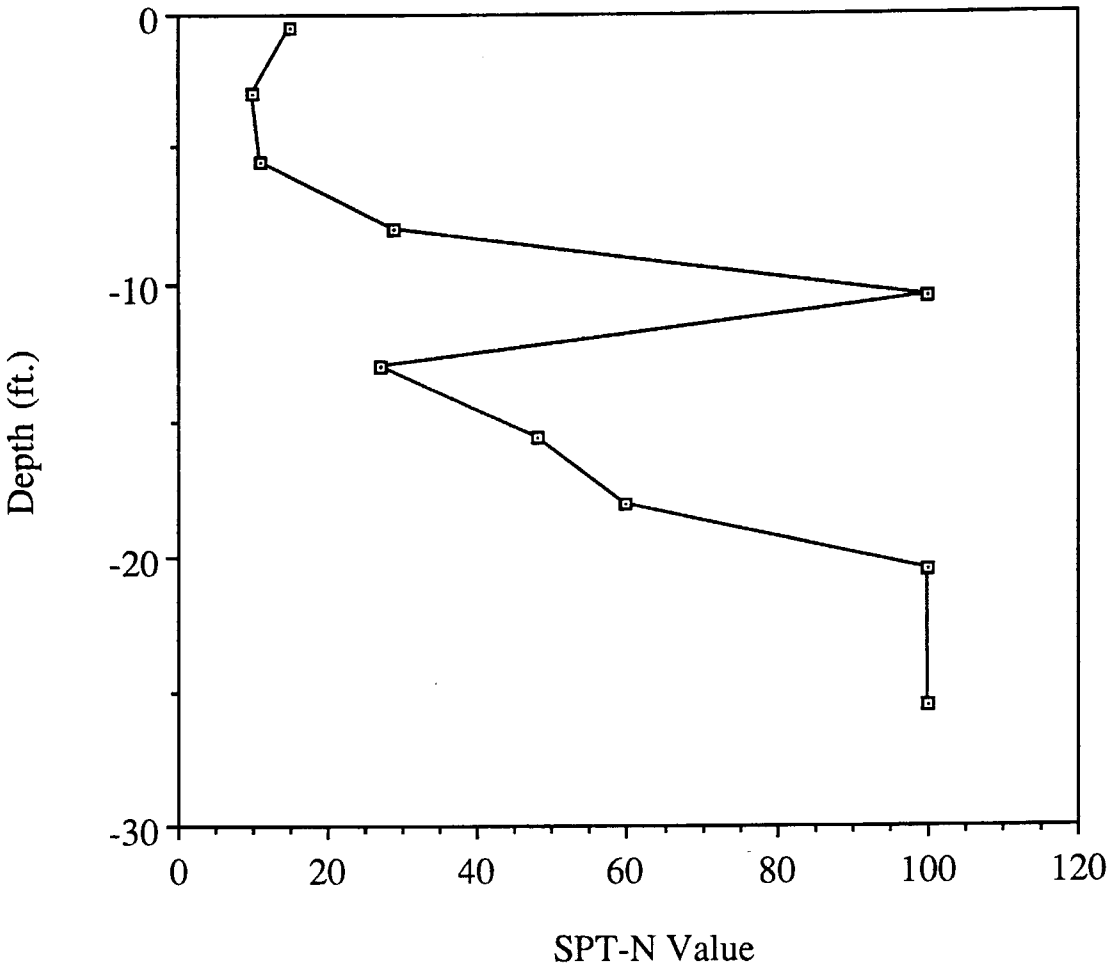

Figure A.2 Variations of SPT-N Value with Depth Below Footing at Boring F-2 (Bridge A)

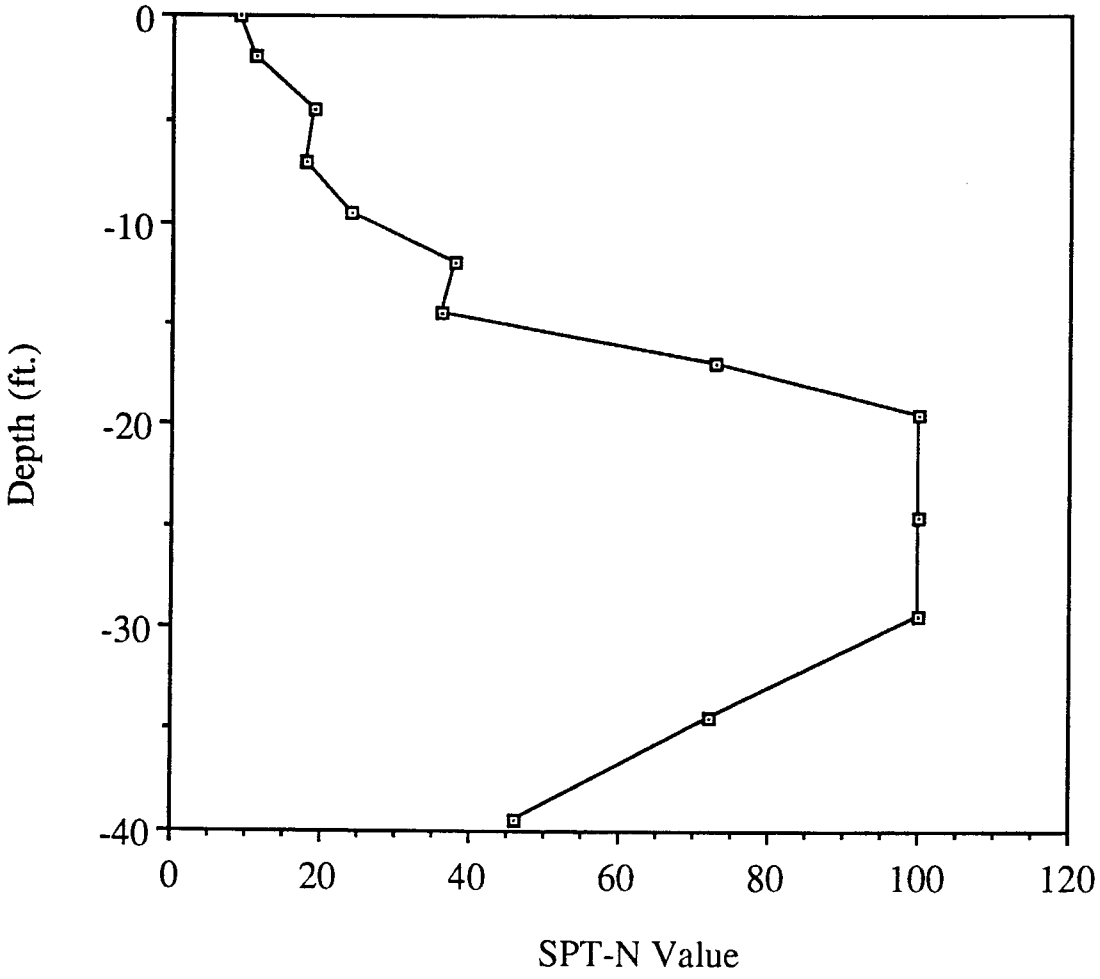

Figure A.3 Variations of SPT-N Value with Depth Below Footing at Boring F-3 (Bridge A)

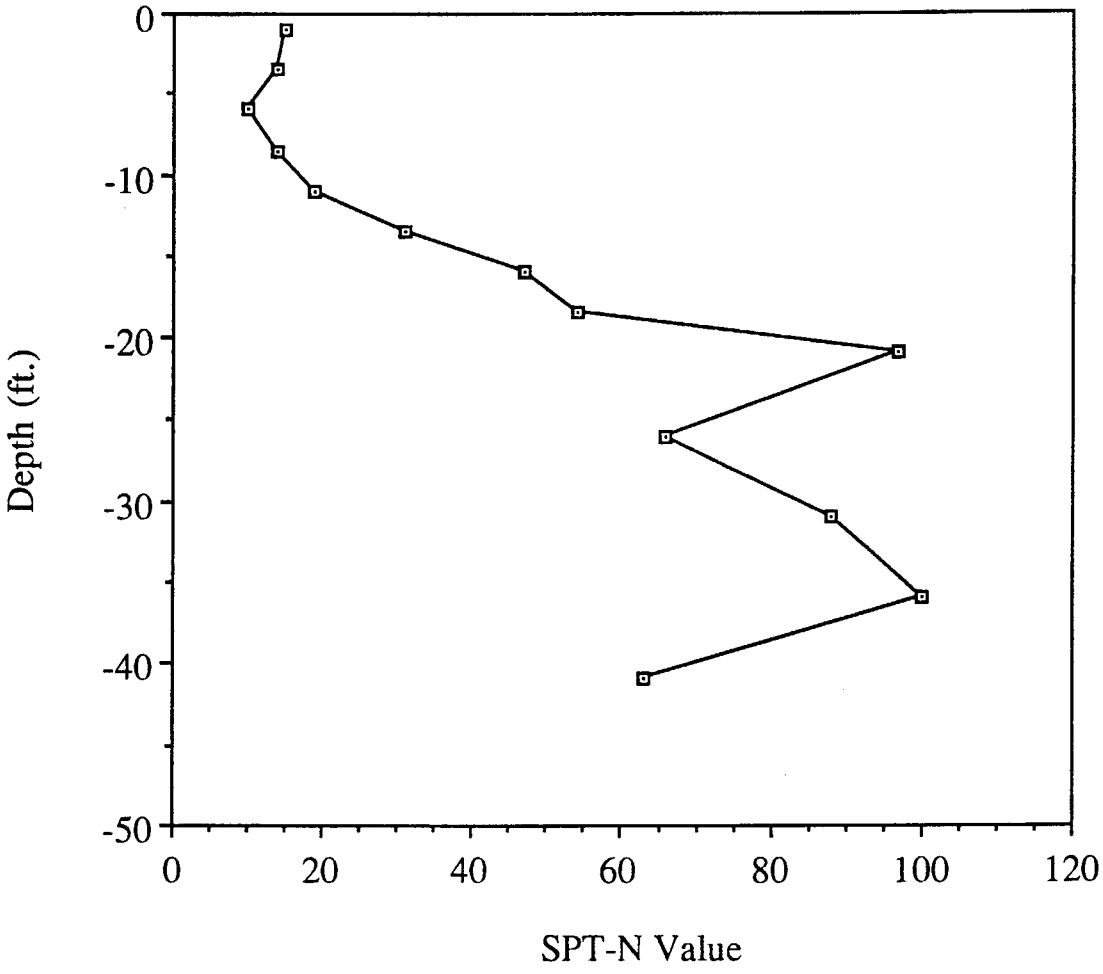

Figure A.4 Variations of SPT-N Value with Depth Below Footing at Boring F-6 (Bridge A)

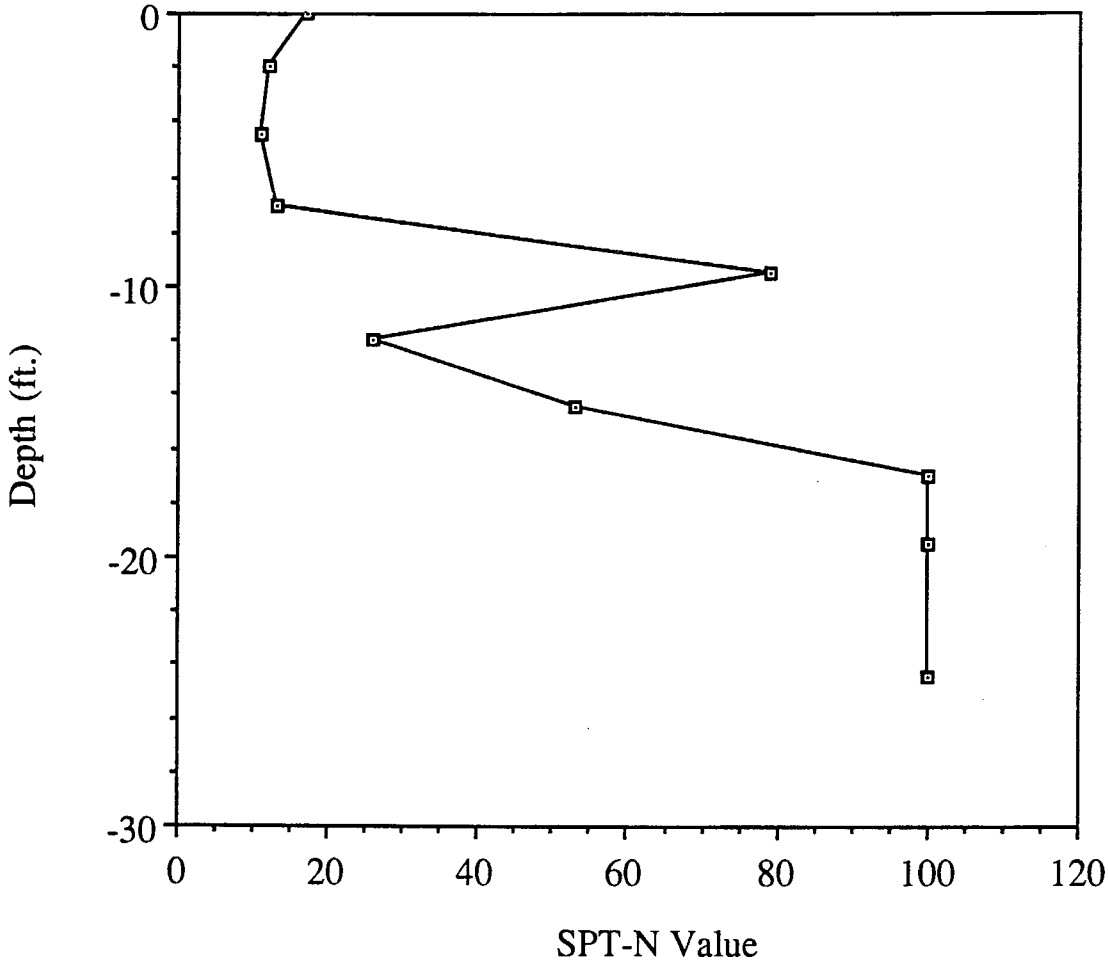

Figure A.5 Variations of SPT-N Value with Depth Below Footing at Boring F-7 (Bridge A)

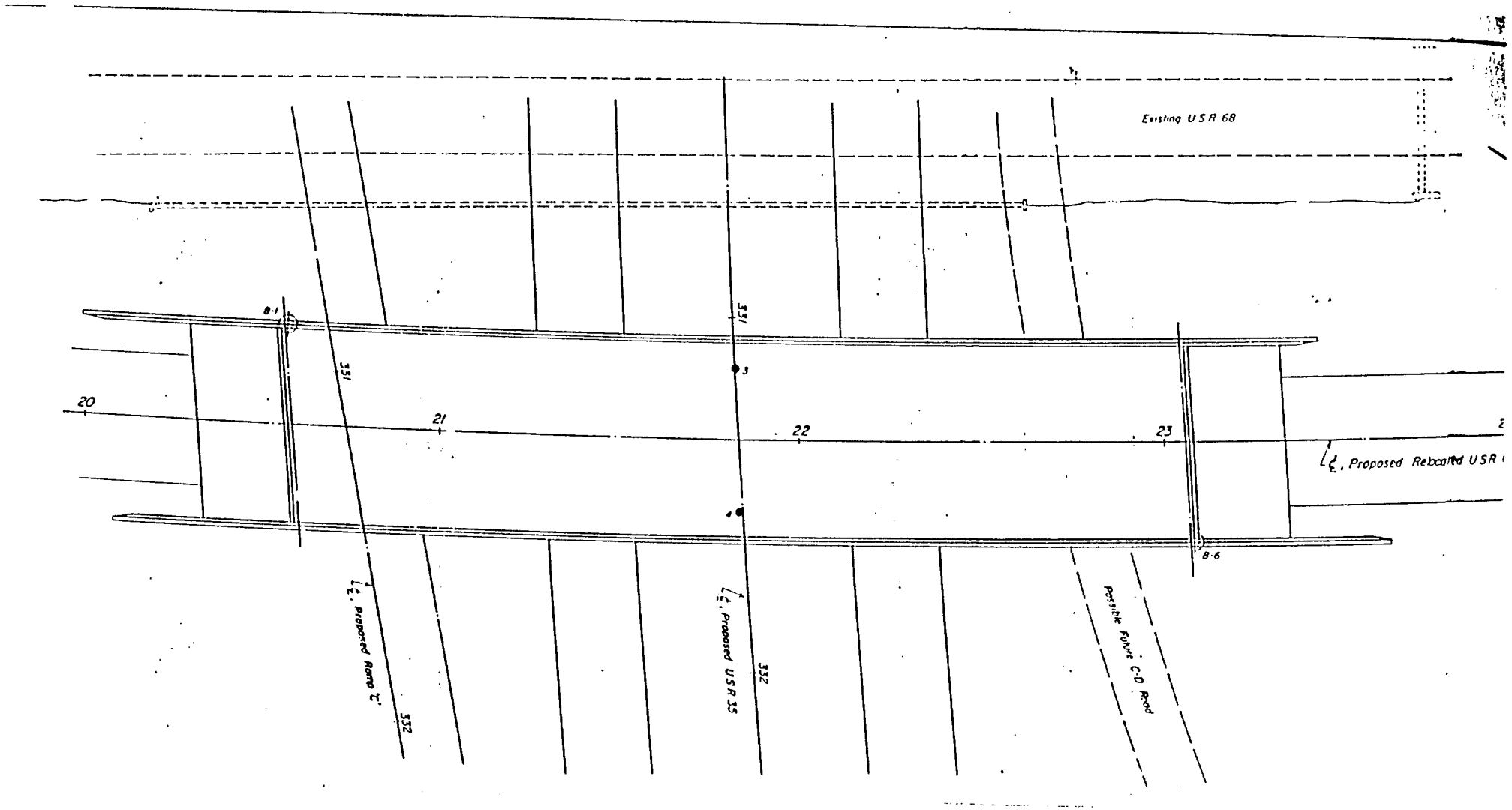

Figure A.6 Boring Location Plan (Bridge B)

Table A.5. Summary of Soil Boring Log Data - Boring B-1 (Bridge B)

Depth Below Footing Base (ft.)	SPT-N Value	Visual Description of Soil	AASHTO Soil Classification	PI Value	Moisture Content (%)
0.0	49	Brown silty gravelly sand	A-1b	3	13
4.5	50	Gray gravelly clay	A-6a	13	11
8.5	67	Brown-gray sandy silt	A-4a	6	11
14.5	45	Brown-gray sandy clay	A-6a	18	23

(Notes) 1. Bottom of boring at the depth of 15 ft. below the bottom of footing.
2. Perched ground water table encountered at a depth 24 ft. above the bottom of the footing.

Table A.6 Summary of Soil Borung Log Data - Boring B-6 (Bridge B)

Depth Below Footing Base	SPT-N Value	Visual Description of Soil	AASHTO Soil Classification	PI Value	Moisture Content (%)
0.0	34	Brown-gray gravelly sandy silt	A-4a	6	13
0.91 m (3.0 ft.)	40			5	17
2.59 m (8.5 ft.)	64	Brown-gray sandy silt	A-4a	5	12
3.96 m (13.0 ft.)	+100			6	12
5.49 m (18.0 ft.)	+100	Brown sandy silt	A-4a	6	10
6.86 m (22.5 ft.)	+100	Brown sandy clay	A-6a	11	10
8.53 m (28.0 ft.)	+100			11	11

(Notes) 1. Bottom of boring at the depth of 8.84 m (29 ft.) below the bottom of footing.
2. Perched ground water table encountered at a depth 5.18 m (17 ft.) above the bottom of the footing.

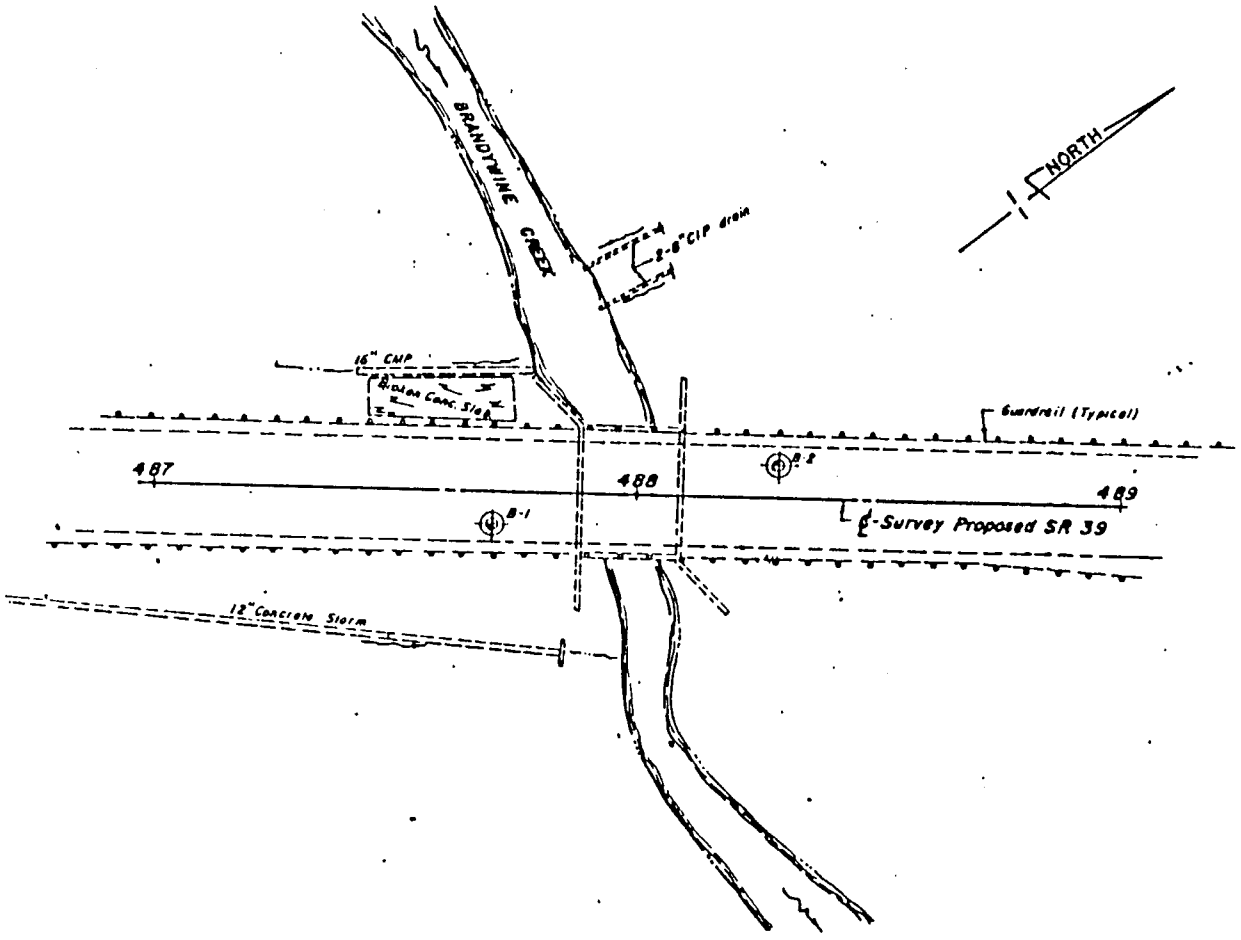

Figure A.7 Boring Location Plan (Bridge C)

Table A.7 Summary of Soil Boring Log Data - Boring B-1 (Bridge C)

Depth Below Footing Base (ft.)	SPT-N Value	Visual Description of Soil	AASHTO Soil Classification	PI Value	Moisture Content (%)
0.0	10	Gray silty sand	A-3a	NP	25
2.7	22 6 9 14	Gray silt	A-4b	NP	22 29 26 24
19.7	10	Gray sandy silt	A-4a	NP	21
24.7	10	Gray silty sand	A-3a	NP	24
29.7	24	Gray sandy silt	A-4a	NP	23
34.7	38	Gray gravelly sandy silt	A-4a	NP	10
39.7	30	Gray sandy silt	A-4a	NP	15

(Notes) 1. Bottom of boring at the depth of 41 ft. below the bottom of footing.
2. Ground water table encountered at a depth 6.3 ft. above the bottom of the footing.

Table A.8 Summary of Soil Boring Log Data - Boring B-2 (Bridge C)

Depth Below Footing Base (ft.)	SPT-N Value	Visual Description of Soil	AASHTO Soil Classification	PI Value	Moisture Content (%)
0.0	14	Gray sandy silt	A-4a	NP	22
3.0	13 11	Gray silt	A-4b	NP	18 25
8.0	20	Gray sandy silt	A-4a	NP	25
10.0	20 13	Brown silt	A-4b	NP	26 25
20.0	11 15	Gray silt	A-4b	NP	28 26
30.0	21 21 38 40	Gray sandy silt	A-4a	NP	27 19 8 11

(Notes) 1. Bottom of boring at the depth of 46 ft. below the bottom of footing.
2. Ground water table encountered at a depth 6. ft. above the bottom of the footing.

Table A.9 Summary of Soil Boring Log Data - Boring B1 (Bridge D)

Depth Below Footing Base (ft.)	SPT-N Value	Visual Description of Soil	AASHTO Soil Classification	PI Value	Moisture Content (%)
0.0	60	Brown sandy, gravelly clay with cobbles	A-6B	21	14
		(the same as above.)	A-6A	14	14
0.5	100+	Gray sandy, gravelly clay with cobbbles	A-6A	13	16
2.5	100+	Gray weathered clay shale			13

(Notes) 1. Bottom of boring at 14.7 ft. below the footing base elevation.
2. No groundwater table was encountered in the bore hole.

Table A.10 Summary of Soil Boring Log Data - Boring B2 (Bridge D)

Depth Below Footing Base (ft.)	SPT-N Value	Visual Description of Soil	AASHTO Soil Classification	PI Value	Moisture Content (%)
0.0		Brown gravelly clay	A-6A	14	18
1.2	100+	Brown clayey, sandy gravel	A-6A	13	23
3.2	100+	Gray weathered clay shale			11

(Notes) 1. Bottom of boring at 8.7 ft. below the footing base elevation.
2. No groundwater table was encountered in the bore hole.

Table A.11 Summary of Soil Boring Log Data - Boring B3 (Bridge D)

Depth Below Footing Base (ft.)	SPT-N Value	Visual Description of Soil	AASHTO Soil Classification	PI Value	Moisture Content (%)
0.0	30	Brown silty, sandy gravel	A-4A	8	11
2.0	57	Brown sandy, gravelly silt	A-4A	8	8
4.0		(the same as above.)	A-4A	8	14
7.0	52	Brown gravelly, sandy silt	A-4A	8	11
9.0	44	Gray sandy, gravelly silt	A-4A	8	11
11.0	41	Gray gravelly, sandy silt	A-4A	8	10
13.0	32	Brown silty, gravelly sand	A-3A	5	16
15.5	100+	Gray weathered, clay shale			11

(Notes) 1. Bottom of boring at 18.2 ft. below the footing base elevation.
2. No groundwater table was encountered in the bore hole.

Table A.12 Summary of Soil Boring Log Data - Boring B4 (Bridge D)

Depth Below Footing Base (ft.)	SPT-N Value	Visual Description of Soil	AASHTO Soil Classification	PI Value	Moisture Content (%)
0.0	34	Brown sandy, gravelly clay	A-6A	13	10
1.6	100+	Brown gravelly clay	A-6B	16	12
3.6		Brown sandy, gravelly clay	A-6B	18	12
7.6	73	Dark gray organic calyey silt	A-4B	7	23
9.6		Gray sandy clay	A-6A	13	16
12.6	37	Gray sandy, gravelly silt	A-4A	9	11
17.6	47	Brown and gray sandy, gravelly clay	A-6A	14	14
20.1	34	Brown sandy, gravelly clay	A-6B	24	11

(Notes) 1. Bottom of boring at 20.1 ft. below the footing base elevation.
2. No groundwater table was encountered in the bore hole.

Table A.13 Summary of Soil Boring Log Data - Boring B5 (Bridge D)

Depth Below Footing Base (ft.)	SPT-N Value	Visual Description of Soil	AASHTO Soil Classification	PI Value	Moisture Content (%)
0.0	37	Brown sandy, gravelly clay	A-6A	13	12
1.9	47	Brown gravelly clay	A-6B	16	7
3.9	36	Brown sandy, gravelly clay	A-6B	16	13
6.9	32	(the same as above.)	A-4B	17	15
8.9	24	Dark gray organic silty clay	A-6B	17	17
10.9	27	Brown and gray silty clay	A-6B	16	17
13.9	47	Brown and gray gravelly, sandy clay	A-7-6	21	17
16.9	60	Brown and gray gravelly, sandy silt	A-4A	8	10
19.3	100+	Brown and gray silty, sandy gravel	A-4A	9	13

(Notes) 1. Bottom of boring at 19.3 ft. below the footing base elevation.
2. No groundwater table was encountered in the bore hole.

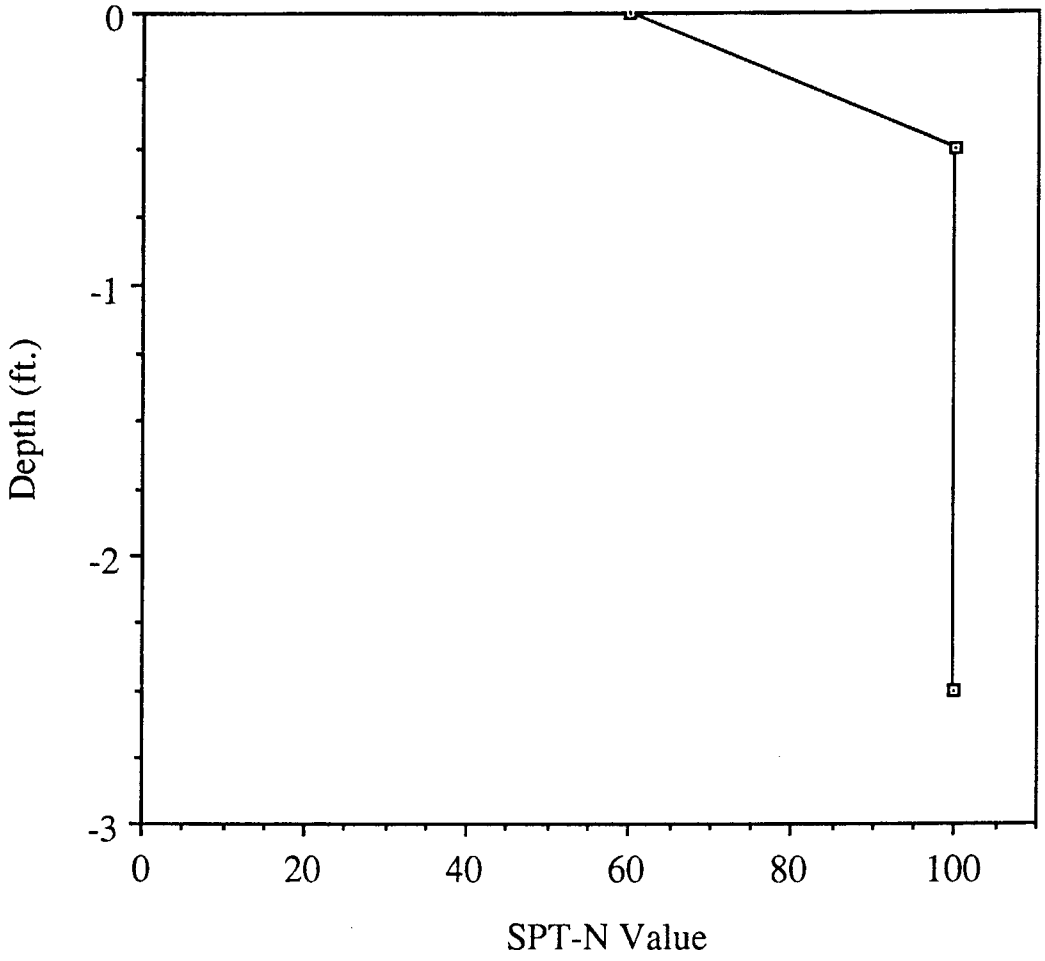

Figure A.8 Variations of SPT-N Value with Depth Below Footing at Boring B1 (Bridge D)

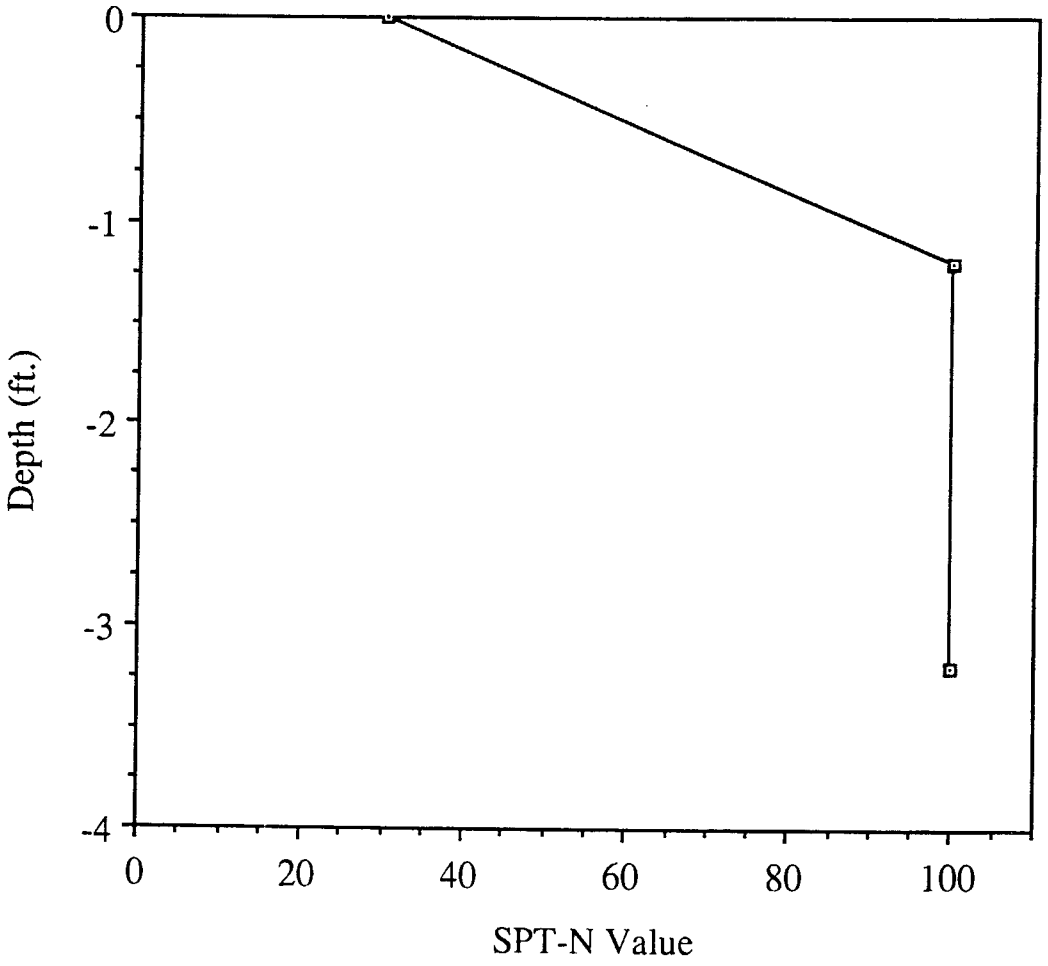

Figure A.9 Variations of SPT-N Value with Depth Below Footing at Boring B2 (Bridge D)

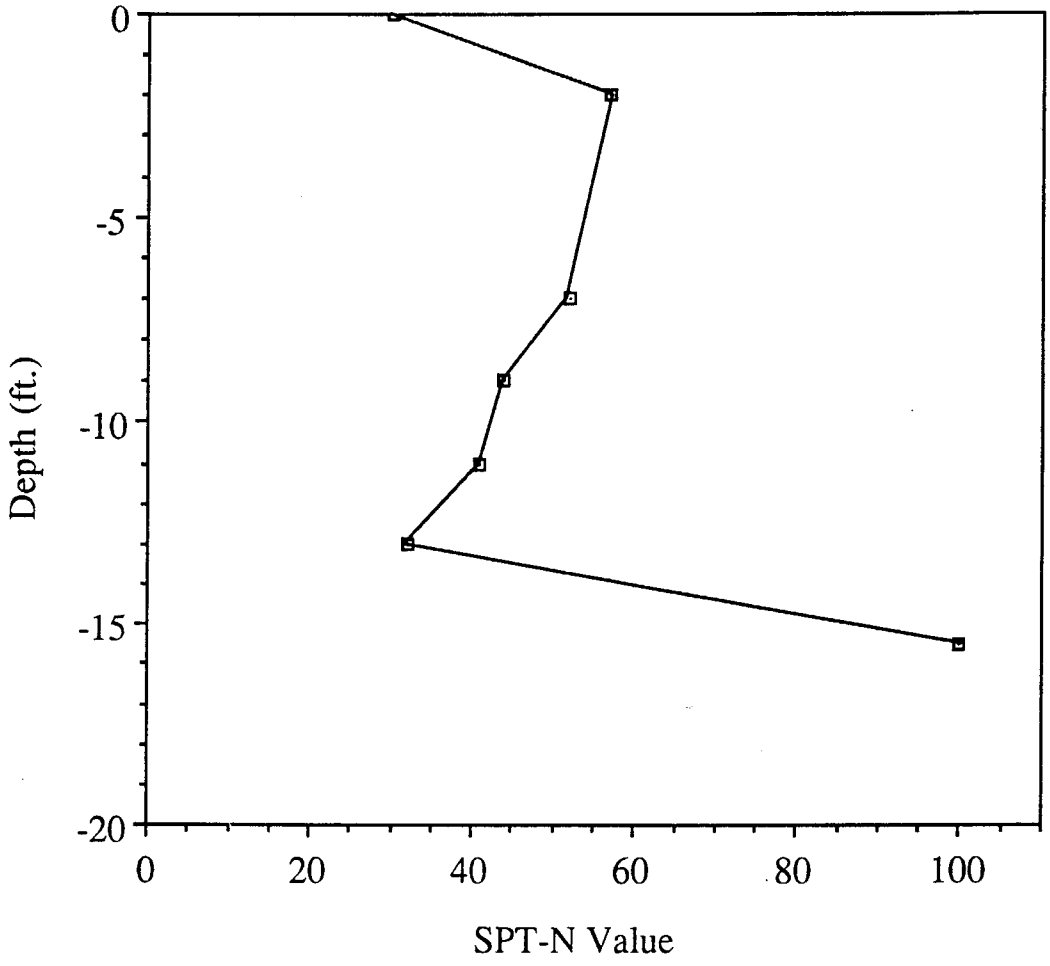

Figure A.10 Variations of SPT-N Value with Depth Below Footing at Boring B3 (Bridge D)

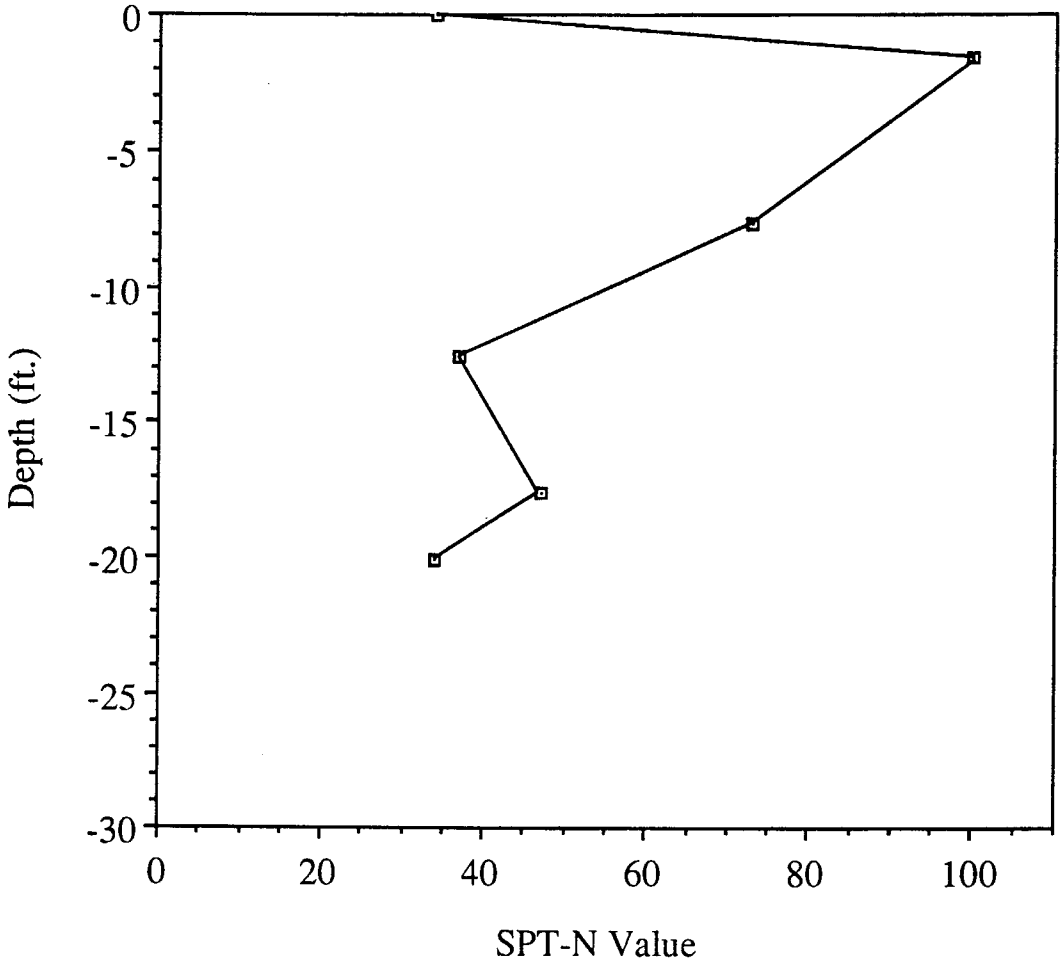

Figure A.11 Variations of SPT-N Value with Depth Below Footing at Boring B4 (Bridge D)

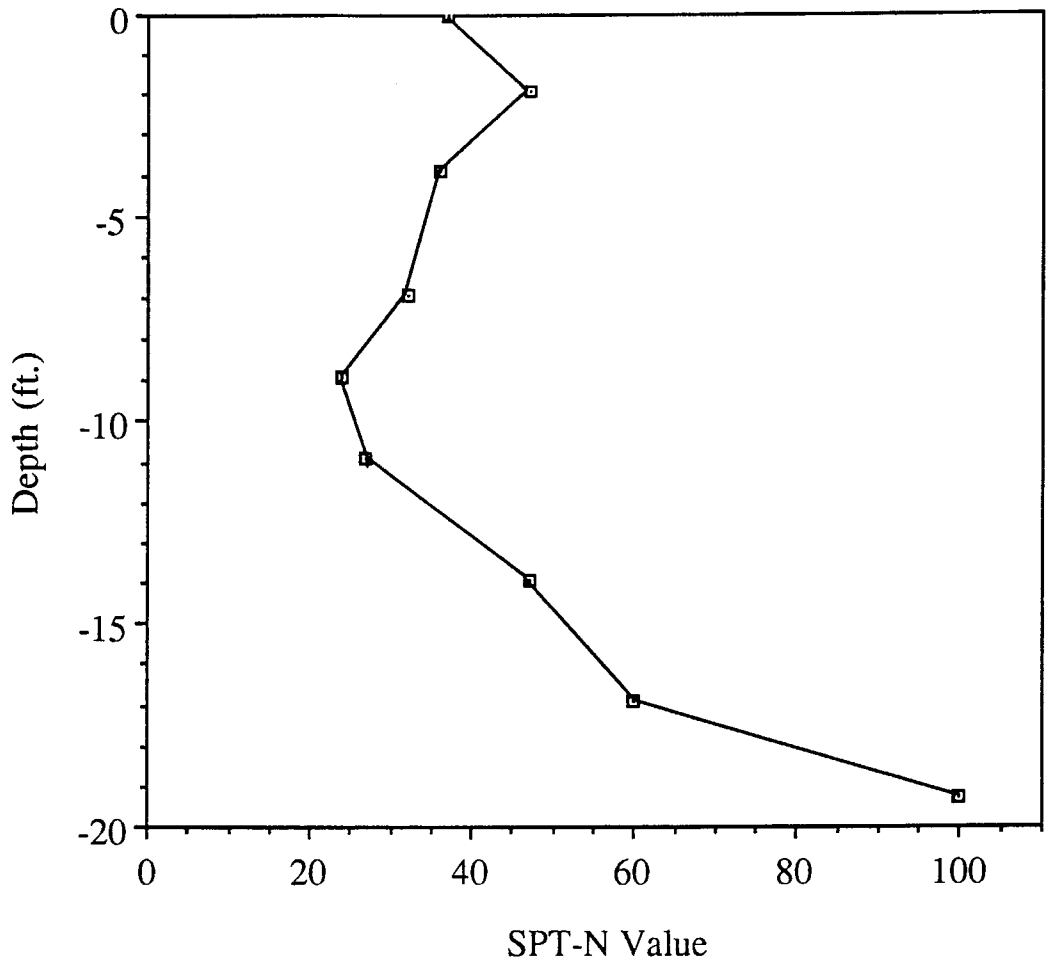

Figure A.12 Variations of SPT-N Value with Depth Below Footing at Boring B5 (Bridge D)

Table A.14 Summary of Soil Boring Log Data - Boring H1 (Bridge E)

Depth Below Footing Base (ft.)	SPT-N Value	Visual Description of Soil	AASHTO Soil Classification	PI Value	Moisture Content (%)
0.0	10	Brown fine to coarse sand, silty clay	A-2-7	25	18
1.5	56	Brown fine to coarse gravel	A-1-b	25	13
4.0	90	Brown silt and clay	A-7-6	23	17
6.5	100+	Brown silty clay	A-7-6	23	13
9.0	100+	Gray weathered shale			10
19.0	100+	Brown weathered sandstone			16
24.0	100+	Brown weathered sandstone			

(Notes) 1. Bottom of Boring at 9.0 ft. below the footing base elevation.

2. No groundwater table was encountered in the bore hole.

Table A.15 Summary of Soil Boring Log Data - Boring H2 (Bridge E)

Depth Below Footing Base (ft.)	SPT-N Value	Visual Description of Soil	AASHTO Soil Classification	PI Value	Moisture Content (%)
0.0	12	Brown clayey silt	A-6a	19	21
1.0	89	Brown silty clay	A-7-6	27	19
9.0	100+	Gray weathered shale			12

(Notes) 1. Bottom of Boring at 9.0 ft. below the footing base elevation.

2. No groundwater table was encountered in the bore hole.

Table A.16 Summary of Soil Boring Log Data - Boring H3 (Bridge E)

Depth Below Footing Base (ft.)	SPT-N Value	Visual Description of Soil	AASHTO Soil Classification	PI Value	Moisture Content (%)
0.0	9	Brown and green clayey silt	A-7-6	22	21
9.0	66	Brown clayey silt	A-6b	21	18
11.0	30	Brown fine to coarse gravel	A-1-b	21	12
15.0	85	Brown fine to coarse gravel	A-2-4	16	6
17.0	100+	Gray weathered shale			22

(Notes) 1. Bottom of Boring at 15.0 ft. below the footing base elevation.

2. No groundwater table was encountered in the bore hole.

Table A.17 Summary of Soil Boring Log Data - Boring H4 (Bridge E)

Depth Below Footing Base (ft.)	SPT-N Value	Visual Description of Soil	AASHTO Soil Classification	PI Value	Moisture Content (%)
0.0	31	Brown clayey silt	A-6b	18	22
4.0	20	Brown clayey silt	A-2-6	18	19
6.0	19	Brown fine to coarse gravel	A-1-a		11
31.0	100+	Gray and green weathered shale			15
36.3	100+	Gray weathered shale			10

(Notes) 1. Bottom of Boring at 31.0 ft. below the footing base elevation.

2. No groundwater table was encountered in the bore hole.

Table A.18 Summary of Soil Boring Log Data - Boring H6 (Bridge E)

Depth Below Footing Base (ft.)	SPT-N Value	Visual Description of Soil	AASHTO Soil Classification	PI Value	Moisture Content (%)
0.0	20	Brown silt and clay	A-7-6	24	23
9.0	8	Brown silt and clay	A-6a	18	24
14.0	35	Brown fine gravel and sand	A-1-b	18	12
54.0	16	Gray clayey silt	A-7-6	17	25
59.0	57	Gray clayey silt	A-6b	17	25

(Notes) 1. Bottom of Boring at 59.0 ft. below the footing base elevation.

2. No groundwater table was encountered in the bore hole.

Table A.19 Summary of Soil Boring Log Data - Boring H7 (Bridge E)

Depth Below Footing Base (ft.)	SPT-N Value	Visual Description of Soil	AASHTO Soil Classification	PI Value	Moisture Content (%)
0.0	22	Brown clayey silt		20	18
1.5	15	Brown clayey silt	A-6a	20	25
9.0	8	Brown clayey silt	A-6b	22	28
11.5	31	Brown fine to coarse gravel	A-1-a		10

(Notes) 1. Bottom of Boring at 45.0 ft. below the footing base elevation.

2. No groundwater table was encountered in the bore hole.

Table A.20 Summary of Soil Boring Log Data - Boring H8 (Bridge E)

Depth Below Footing Base (ft.)	SPT-N Value	Visual Description of Soil	AASHTO Soil Classification	PI Value	Moisture Content (%)
0.0	11	Brown clayey silt	A-6b	19	22
9.0	14	Brown clayey silt	A-6a	22	25
12.5	77	Brown fine to coarse gravel	A-1-a	19	7
24.0	37	Brown fine to coarse gravel	A-1-a		11
44.0	14	Brown fine to coarse sand	A-1-b		13
49.0	13	Gray clayey silt	A-6a	18	25

(Notes) 1. Bottom of Boring at 49.0 ft. below the footing base elevation.

2. No groundwater table was encountered in the bore hole.

Table A.21 Summary of Soil Boring Log Data - Boring H9 (Bridge E)

Depth Below Footing Base (ft.)	SPT-N Value	Visual Description of Soil	AASHTO Soil Classification	PI Value	Moisture Content (%)
0.0	21	Brown silt and clay	A-7-6	24	19
1.5	13	Gray clayey silt	A-6b	18	21
4.0	6	Gray clayey silt	A-7-6	19	23
12.5	16	Brown fine gravel	A-1-a		9

(Notes) 1. Bottom of Boring at 45.5 ft. below the footing base elevation.

2. Water encountered at 27.5 feet below footing.

Table A.22 Summary of Soil Boring Log Data - Boring H10 (Bridge E)

Depth Below Footing Base (ft.)	SPT-N Value	Visual Description of Soil	AASHTO Soil Classification	PI Value	Moisture Content (%)
0.0	12	Brown clayey silt	A-7-6	22	22
4.0	6	Brown clayey silt	A-6b	19	24
6.5	26	Brown silt	A-4b		25
9.0	30	Brown fine to coarse gravel	A-1-a		9
29.0	32	Brown fine to coarse sand	A-1-b		11
44.0	40	Brown fine sand	A-3		21
49.0	34	Gray clayey silt	A-7-6		25

(Notes) 1. Bottom of Boring at 49.0 ft. below the footing base elevation.

2. No groundwater table was encountered in the bore hole.

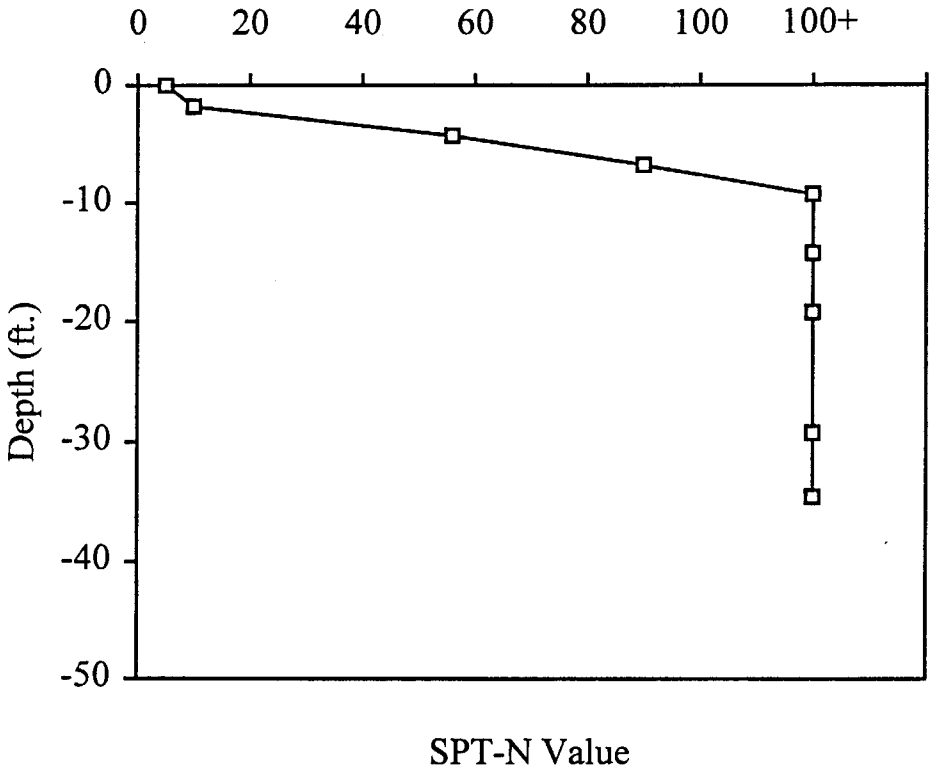

A.13 Variations of SPT-N Value with Depth Below Footing at Boring H-1 (Bridge E)

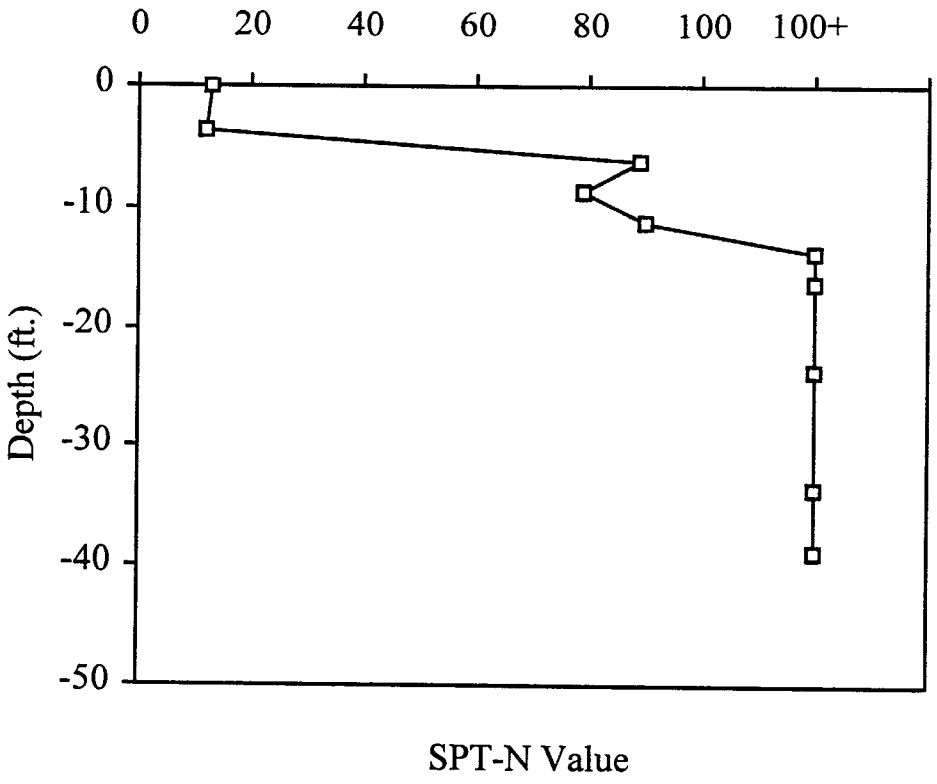

A.14 Variations of SPT-N Value with Depth Below Footing at Boring H-2 (Bridge E)

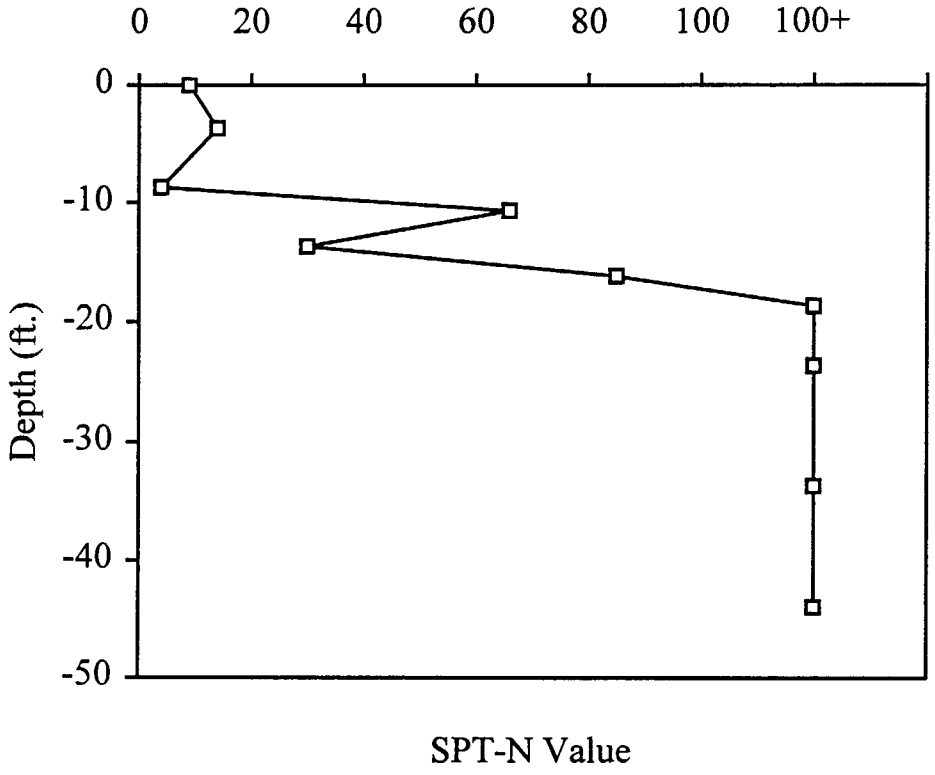

A.15 Variations of SPT-N Value with Depth Below Footing at Boring H-3 (Bridge E)

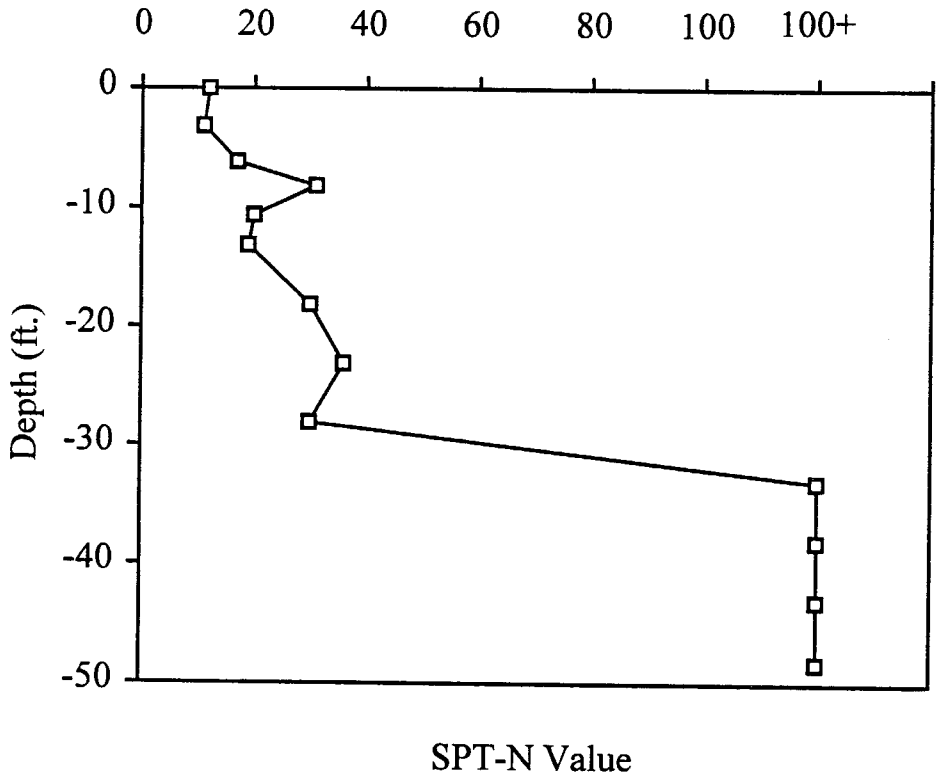

A.16 Variations of SPT-N Value with Depth Below Footing at Boring H-4 (Bridge E)

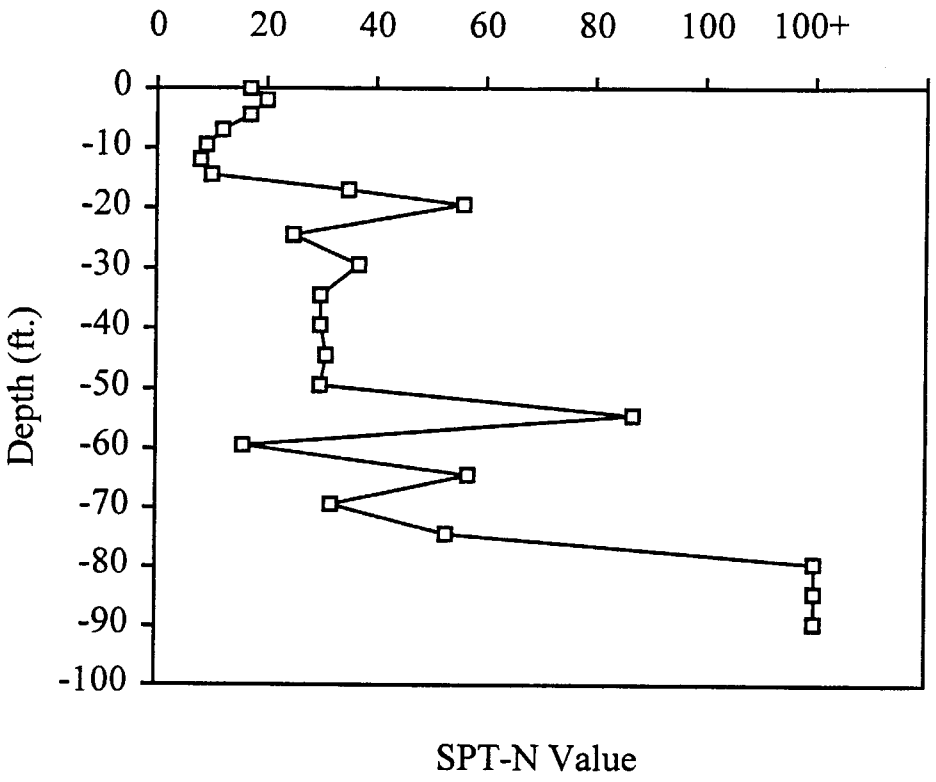

A.17 Variations of SPT-N Value with Depth Below Footing at Boring H-6 (Bridge E)

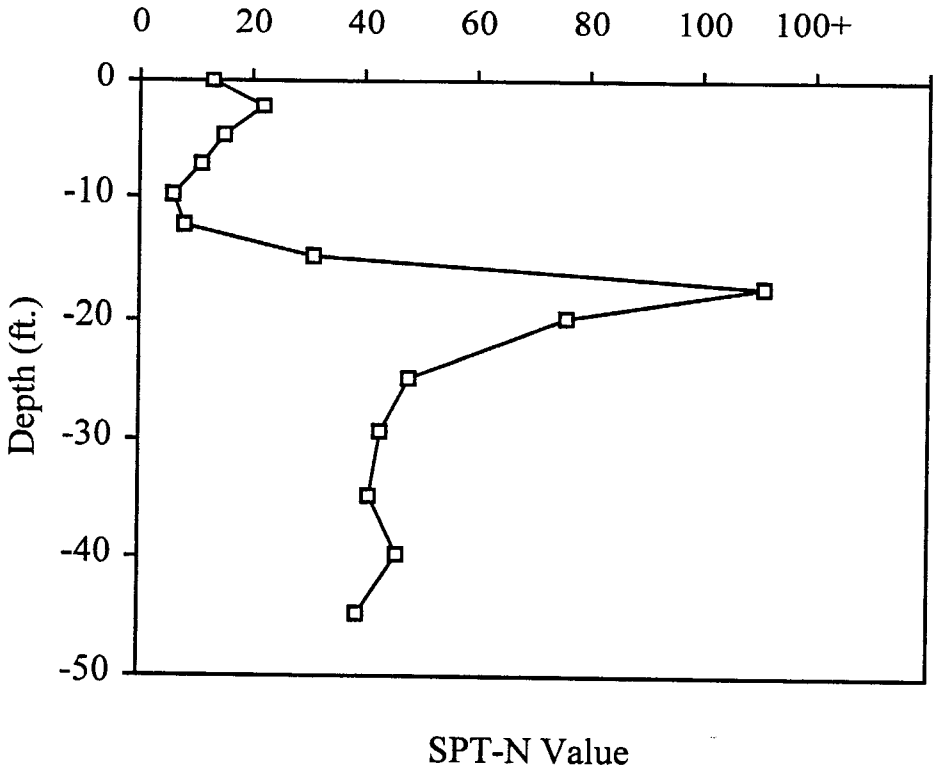

A.18 Variations of SPT-N Value with Depth Below Footing at Boring H-7 (Bridge E)

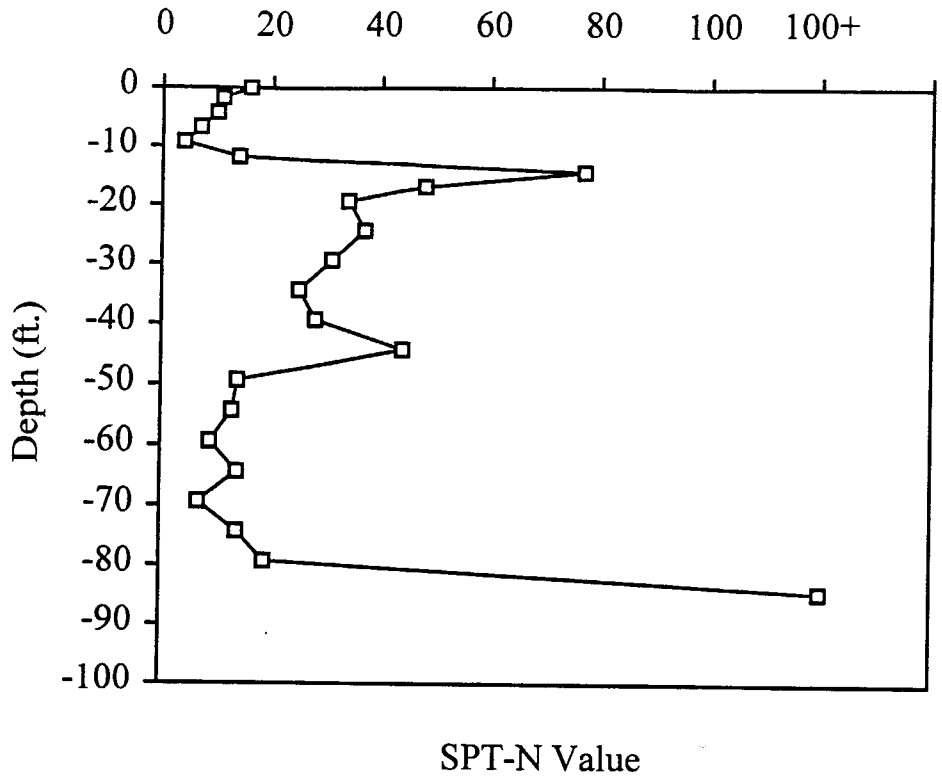

A.19 Variations of SPT-N Value with Depth Below Footing at Boring H-8 (Bridge E)

Notes on Boring Locations (Bridges D and E) :

Bridge D : Boring B-1 located near Pier 1-North footing construction area.

Boring B-2 located near Pier 2-South footing construction area.

Boring B-3 located near Pier 3-North footing construction area.

Boring B-4 located near Pier 4-South footing construction area.

Boring B-5 located near Pier 5-North footing construction area.

Bridge E : Boring H-1 located near Rear Abutment construction area.

Boring H-2 located near Pier 1 construction area.

Boring H-3 located near Pier 2 construction area.

Boring H-4 located near Pier 3 construction area.

Boring H-6 located near Pier 5 construction area.

Boring H-7 located near Pier 6 construction area.

Boring H-8 located near Pier 7 construction area.

Boring H-9 located near Pier 8 construction area.

Boring H-10 located near Forward Abutment construction area.

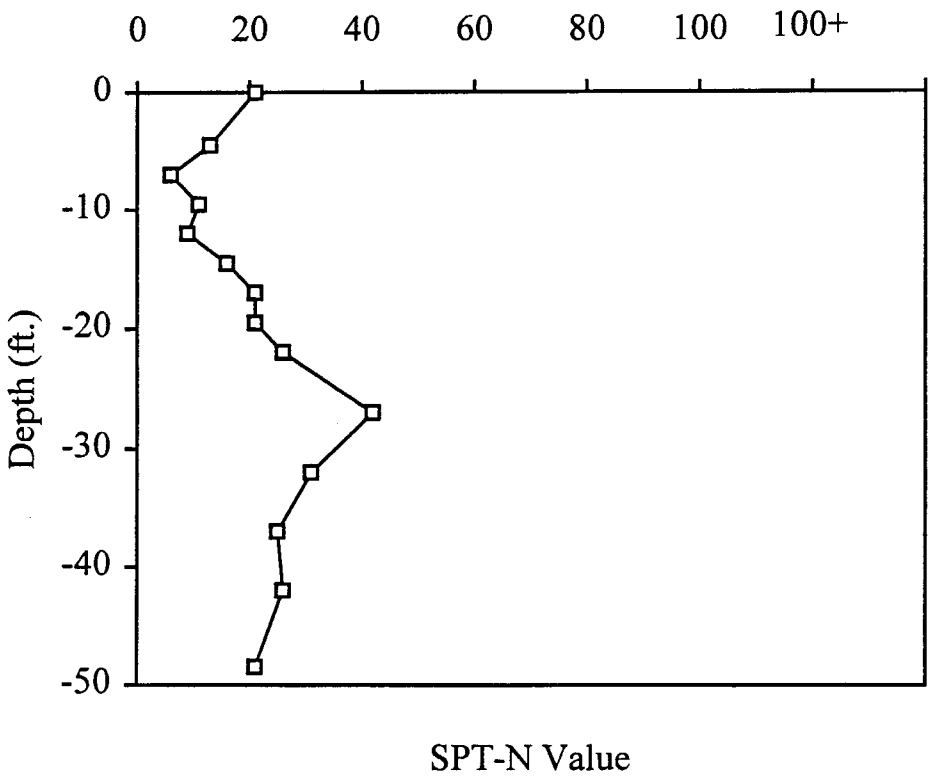

A.20 Variations of SPT-N Value with Depth Below Footing at Boring H-9 (Bridge E)

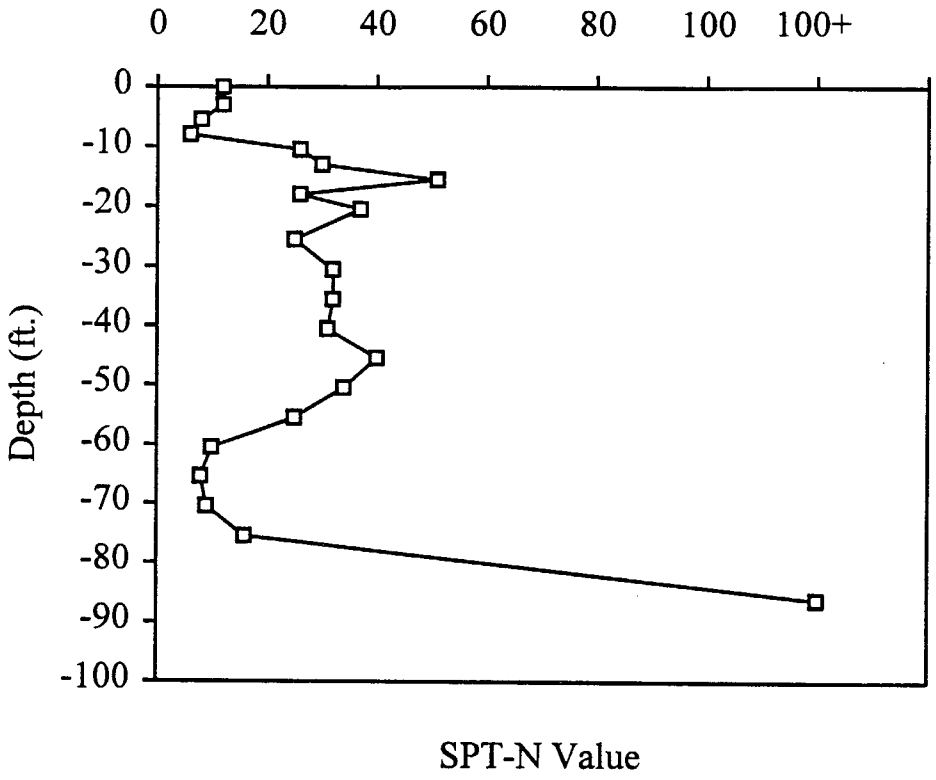

A.21 Variations of SPT-N Value with Depth Below Footing at Boring H-10 (Bridge E)

APPENDIX B :

ADDITIONAL PLOTS
(BRIDGE E)

Date	No of days	Construction Stages	Settlement (inches)		
			RAS1	RAS2	RASC
1-Apr	0	Footing (I)	0.000	0.000	0.000
7-Apr	6		0.036	0.036	0.072
14-Apr	13		0.012	0.060	0.132
26-Apr	25	Wall (I)	0.108	0.132	0.192
13-May	42		0.108	0.108	0.180
24-May	53	Backfilling over Footing and Wall (I)	0.132	0.120	0.204
22-Jun	82	Beam (I)	0.720		
12-Jul	102		0.816		
29-Jul	119	Deck and Parapet (I)	0.876		
12-Aug	133		0.924		
1-Sep	153		1.044		
18-Sep	170	Footing (II)	1.104		
25-Sep	177	Wall (II)	1.152		
2-Oct	184		1.188		
16-Oct	198	Backfilling over Footing (II)	1.152		
6-Nov	219	Beam, Backfilling Wall (II)	1.212		
23-Mar	356	Deck and Parapet (II)	1.368		
16-Jun	441		1.356		
29-Sep	546		1.392		

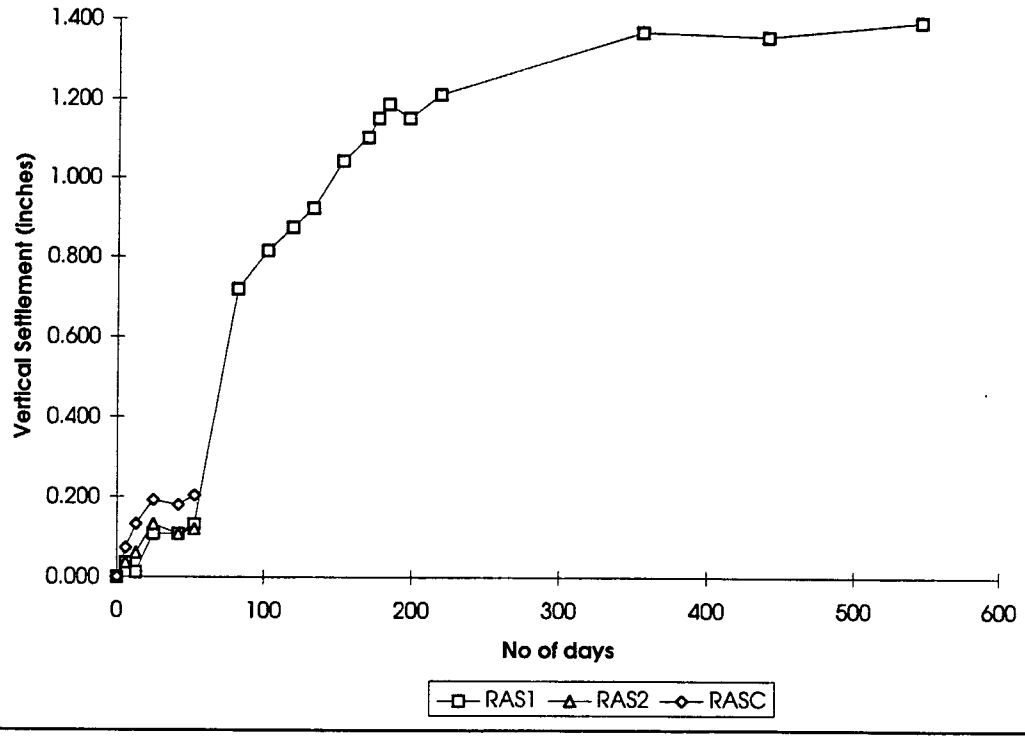

Figure B.1 Settlement of Rear Abutment - Phase I Foundation (Bridge E)

Date	No of days	Construction Stages	Settlement (inches)		
			RAS1	RAS2	RASC
10-Sep	0	Footing (II)	0.000	0.000	0.000
18-Sep	8		0.000	0.036	0.108
25-Sep	15	Wall (II)	0.036	0.048	0.120
2-Oct	22		0.024	0.036	0.108
16-Oct	36	Backfilling over Footing (II)		0.096	
6-Nov	57	Beam, Backfilling Wall (II)		0.180	
5-Dec	86		0.264	0.204	0.300
23-Mar	194	Deck and Parapet (II)	0.312	0.264	0.384
29-Sep	384		0.288	0.336	0.420

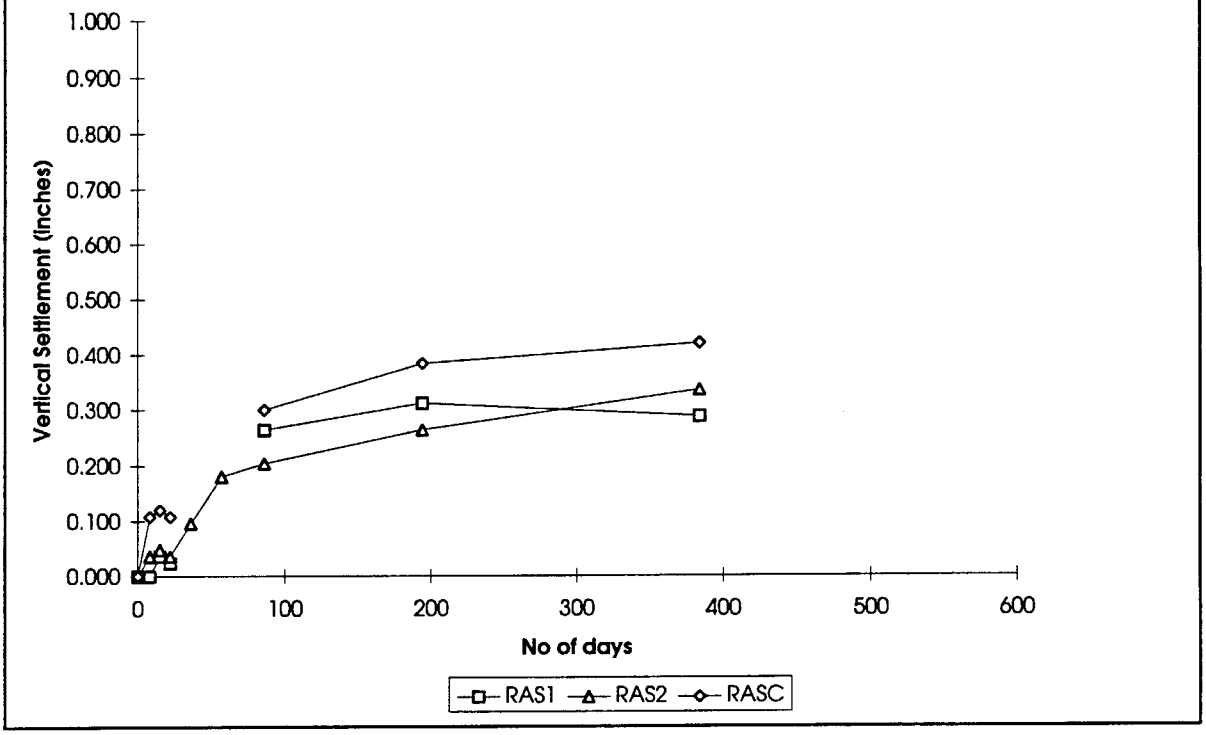

Figure B.2 Settlement of Rear Abutment - Phase II Foundation (Bridge E)

Date	No of days	Construction Stages	Settlement (inches)				
			P1S1	P1S2	P1S3	P1S4	P1SC
7-Apr	0	Footing (I)	0.000	0.000	0.000	0.000	
14-Apr	7	Column (I)	0.012		0.000		0.000
26-Apr	19	Backfilling over Footing (I)		0.144			
13-May	36	Pier Cap (I)		0.192			0.120
24-May	47		0.144	0.132	0.132	0.120	0.192
22-Jun	76	Beam (I)		0.492	0.528	0.456	
12-Jul	96			0.492	0.552	0.504	0.492
29-Jul	113	Deck & Parapet (I)		0.588	0.612	0.552	0.540
12-Aug	127			0.636	0.756	0.624	0.636
1-Sep	147			0.696	0.732	0.660	0.636
10-Sep	156			0.732	0.768	0.768	0.720
18-Sep	164	Footing (II)		0.684	0.744	0.696	0.672
25-Sep	171	Column (II)			0.720	0.696	0.648
2-Oct	178	Pier Cap (II)		0.708	0.744	0.756	0.708
16-Oct	192	Backfilling over Footing (II)		0.672	0.756	0.756	0.684
6-Nov	213	Beam (II)		0.708	0.696	0.708	0.672
23-Mar	350	Deck & Parapet (II)		0.792	0.744	0.744	
16-Jun	435			0.792	0.768	0.732	
29-Sep	540		0.768	0.816	0.744	0.756	

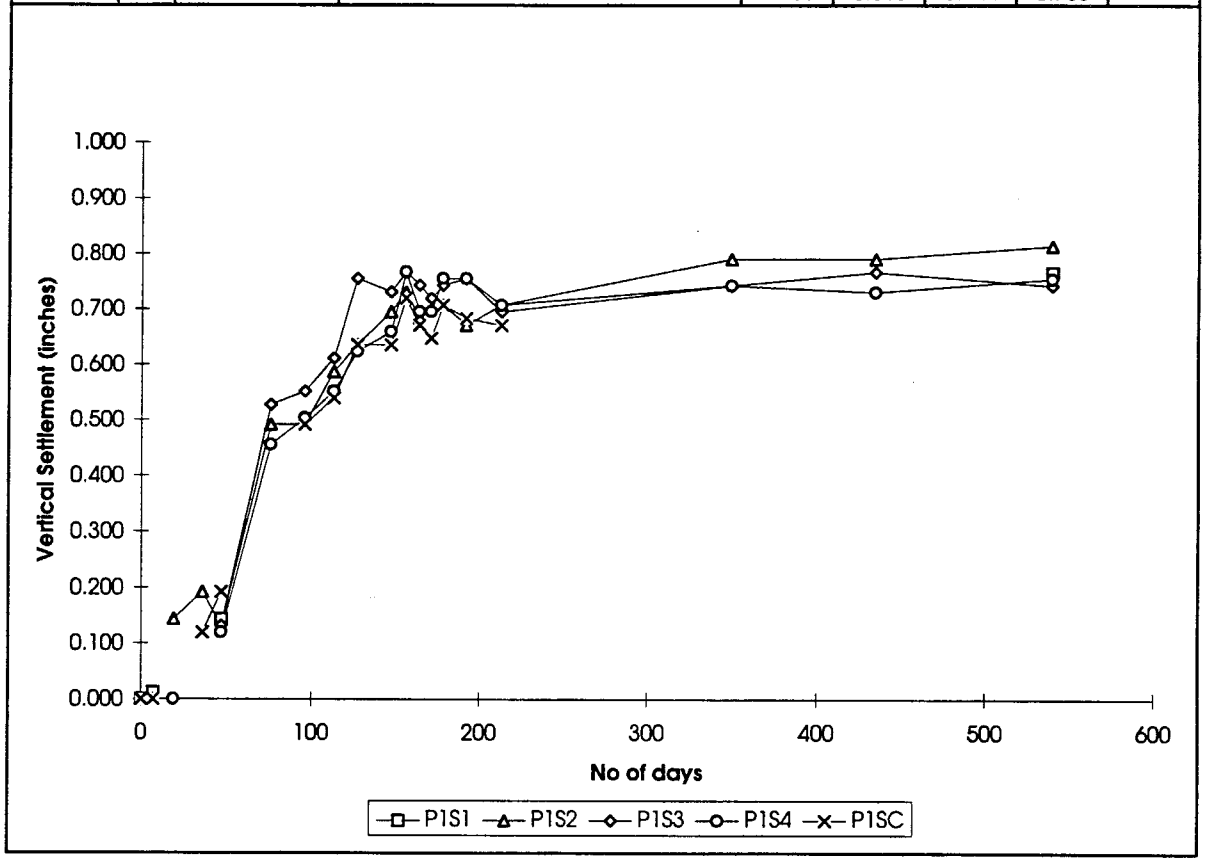

Figure B.3 Settlement of Pier 1 - Phase I Foundation (Bridge E)

Date	No of days	Construction Stages	Settlement (inches)				
			P1S1	P1S2	P1S3	P1S4	P1SC
18-Sep	0	Footing (II)	0.000	0.000	0.000	0.000	0.000
2-Oct	14	Column, Pier Cap (II)	0.036	0.012	0.168	0.108	0.132
16-Oct	28			0.168	0.156	0.108	
6-Nov	49	Beam, Backfilling over Footing (II)	0.054		0.456	0.432	0.228
5-Dec	78				0.552	0.480	0.264
23-Mar	186	Deck and Parapet (II)				0.804	0.348
29-Sep	376			0.144	0.636	0.768	0.408

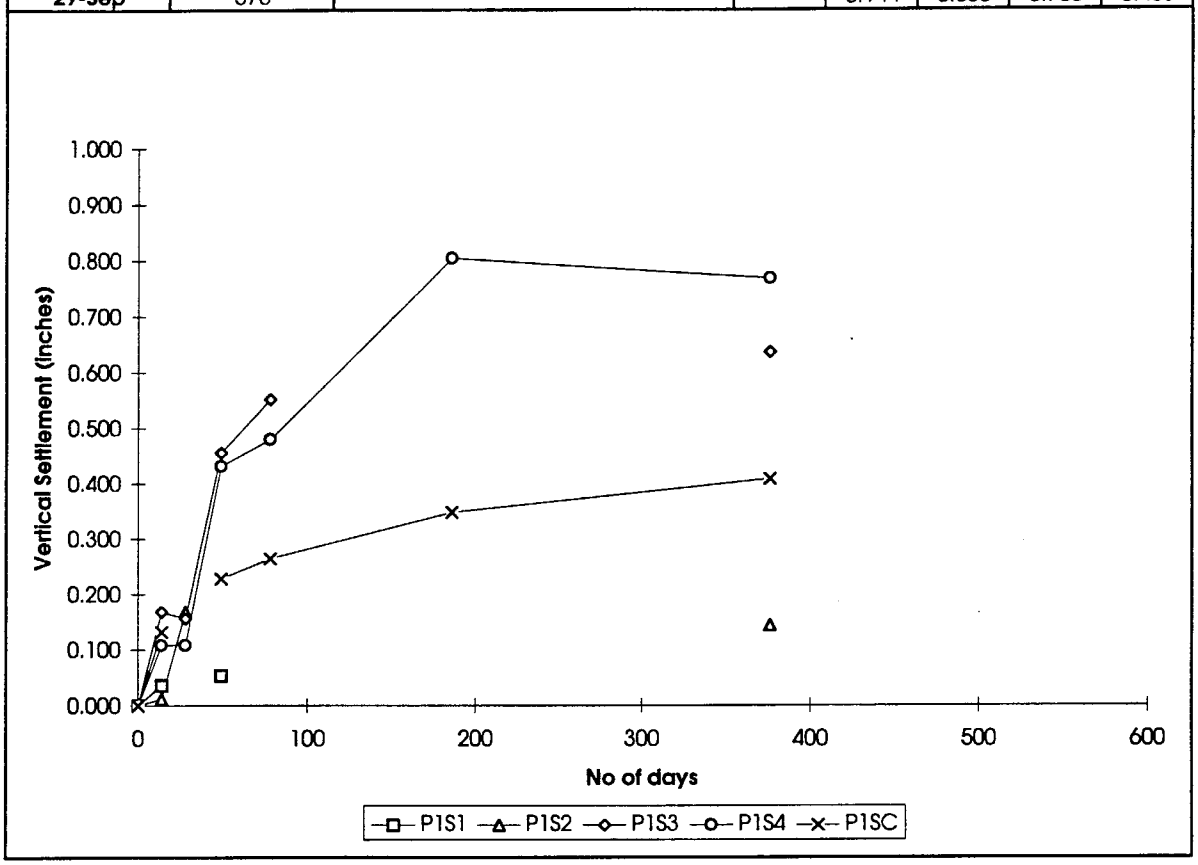

Figure B.4 Settlement of Pier 1 - Phase II Foundation (Bridge E)

Date	No of days	Construction Stages	Settlement (inches)
			P2SC
12-Aug	0	Phase I done	0.000
18-Sep	37	Footing, Column, Pier Cap (II)	0.084
25-Sep	44	Backfilling over Footing (II)	0.084
2-Oct	51		0.132
16-Oct	65		0.168
23-Mar	223	Beam, Deck and Parapet (II)	0.216
16-Jun	308		0.276

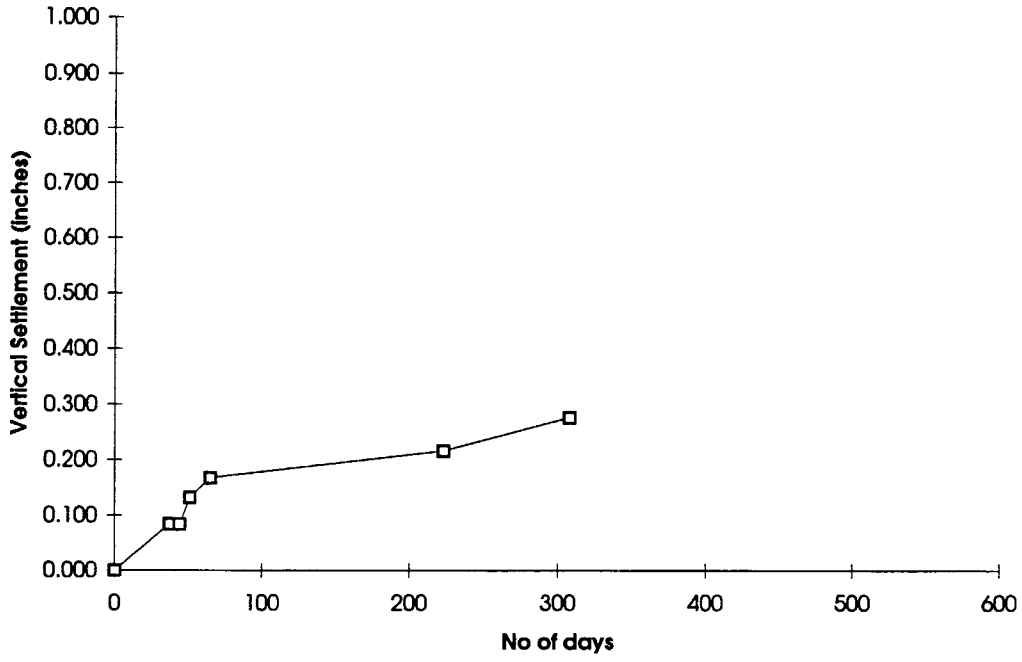

Figure B.5 Settlement of Pier 2 - Phase I Foundation (Bridge E)

Date	No of days	Construction Stages	Settlement (inches)
			P2SC
10-Sep	0	Footing, Column (II)	0.000
18-Sep	8	Pier Cap, Backfilling over Footing (II)	0.072
25-Sep	15		0.060
2-Oct	22		0.120
16-Oct	36		0.096
6-Nov	57	Beam (II)	0.216
5-Dec	86		0.264
23-Mar	194	Deck and Parapet (II)	0.240
29-Sep	384		0.420

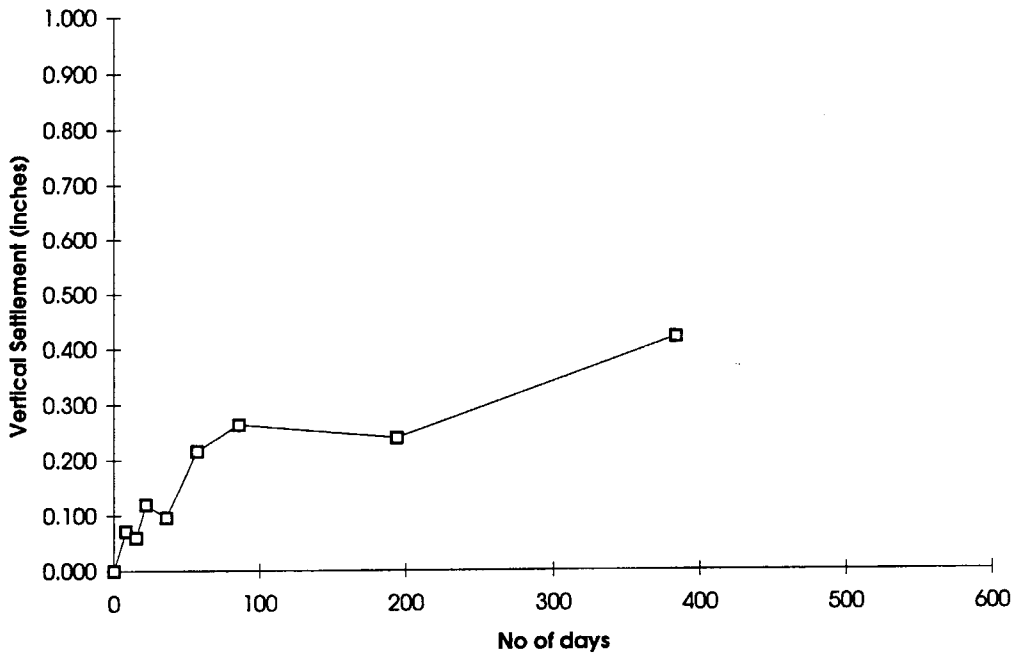

Figure B.6 Settlement of Pier 2 - Phase II Foundation (Bridge E)

Date	No of days	Construction Stages	Settlement (inches)				
			P3S1	P3S2	P3S3	P3S4	P3SC
29-Mar	0	Footing (I)	0.000	0.000	0.000	0.000	
1-Apr	3		0.012	0.000	0.000	0.036	0.000
7-Apr	9		0.036	0.000	0.000	0.000	0.012
26-Apr	28	Wall (I)		0.072			
13-May	45	Backfilling (I)		0.108			
24-May	56		0.132	0.144	0.072	0.192	0.096
22-Jun	85	Beam (I)	0.240	0.192	0.144	0.264	0.180
12-Jul	105		0.312	0.240	0.192		0.240
29-Jul	122	Deck and Parapet (I)	0.336	0.276	0.216	0.276	0.312
12-Aug	136		0.324	0.240	0.204	0.300	0.264
1-Sep	156			0.312		0.420	
10-Sep	165			0.312			0.372
18-Sep	173	Footing (II)		0.396		0.516	0.432
25-Sep	180			0.372			0.432
2-Oct	187	Wall, Backfilling over Footing (II)		0.336			0.420
16-Oct	201			0.444		0.420	0.420
6-Nov	222	Beam (II)		0.396	0.252	0.360	0.396
23-Mar	359	Deck and Parapet (II)	0.516	0.372	0.300		
16-Jun	444		0.696		0.444		
29-Sep	549		0.756	0.504	0.420		

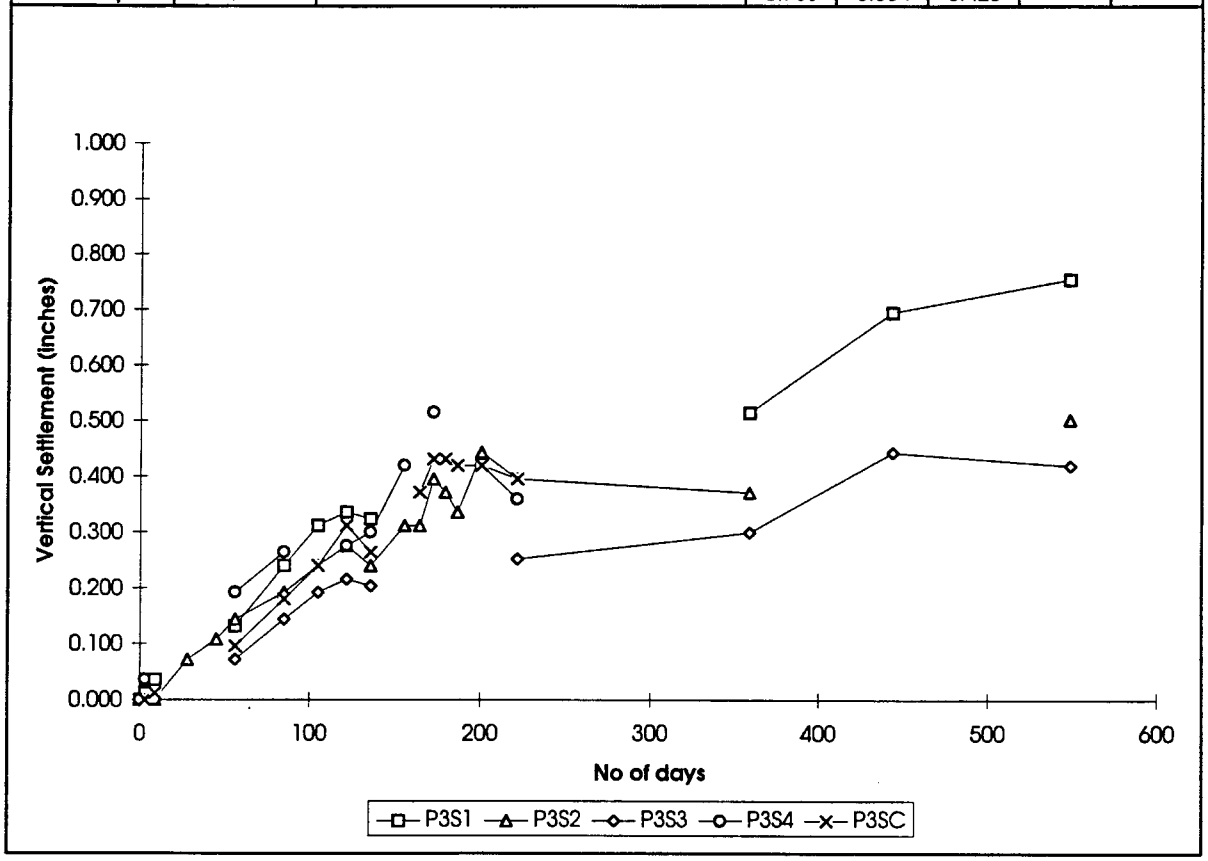

Figure B.7 Settlement of Pier 3 - Phase I Foundation (Bridge E)

Date	No of days	Construction Stages	Settlement (inches)				
			P3S1	P3S2	P3S3	P3S4	P3SC
18-Sep	0	Footing (II)	0.000	0.000	0.000	0.000	0.000
25-Sep	7		0.024		0.012		0.024
2-Oct	14	Wall, Backfilling over Footing (II)	0.084	0.072	0.072	0.048	0.072
16-Oct	28				0.120	0.192	0.156
6-Nov	49	Beam (II)			0.120	0.192	0.180
5-Dec	78			0.168	0.144	0.144	0.252
23-Mar	186	Deck and Parapet (II)	0.228				0.312
29-Sep	376		0.300	0.252			0.480

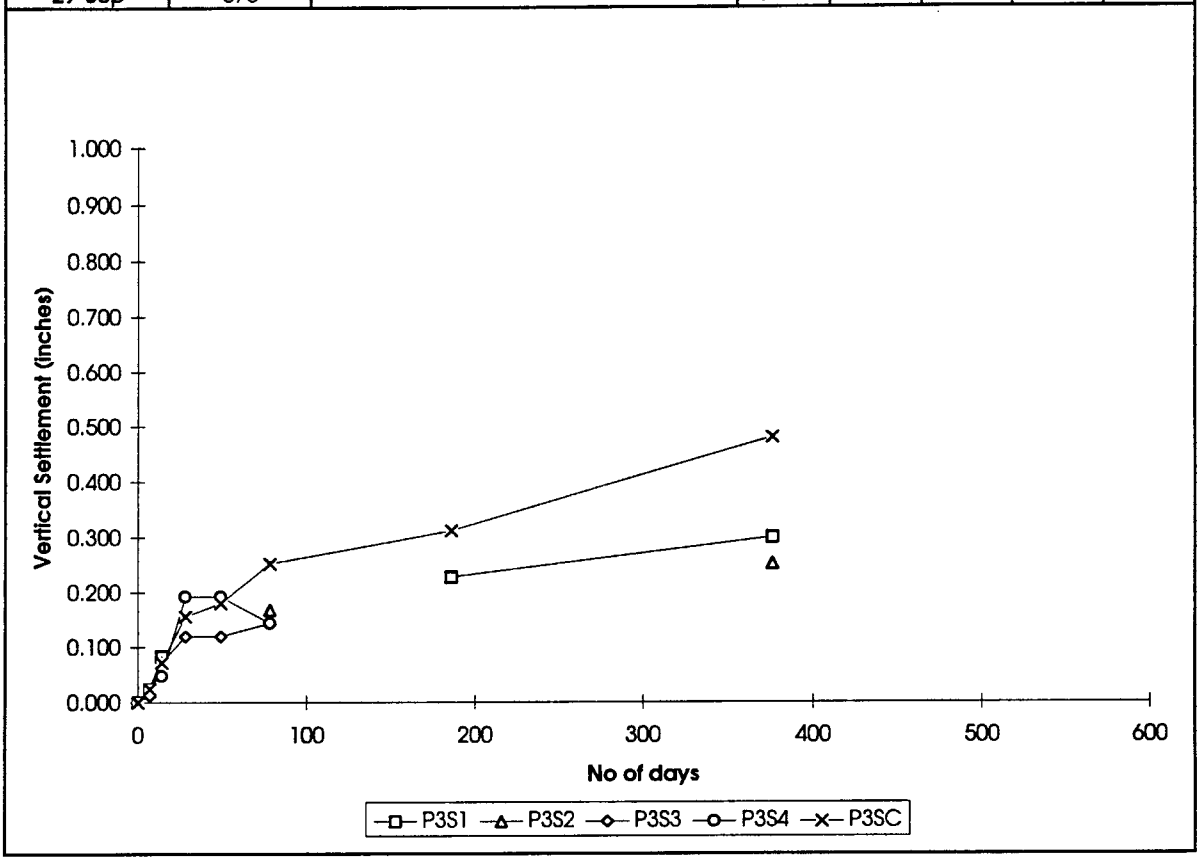

Figure B.8 Settlement of Pier 3 - Phase II Foundation (Bridge E)

Date	No of days	Construction Stages	Settlement (inches)
			P4SC
29-Mar	0	Footing (I)	0.000
1-Apr	3		0.012
7-Apr	9		0.036
14-Apr	16		0.048
26-Apr	28		0.048
13-May	45	Wall (I)	0.144
24-May	56	Backfilling over Footing (I)	0.228
22-Jun	85	Beam (I)	0.300
12-Jul	105		0.312
29-Jul	122	Deck and Parapet (I)	0.468
1-Sep	156	Footing (II)	0.480
2-Oct	187	Wall, Backfilling over Footing (II)	0.480
16-Oct	201		0.528
6-Nov	222	Beam (II)	0.480
23-Mar	359	Deck and Parapet (II)	0.480
16-Jun	444		0.612
29-Sep	549		0.576

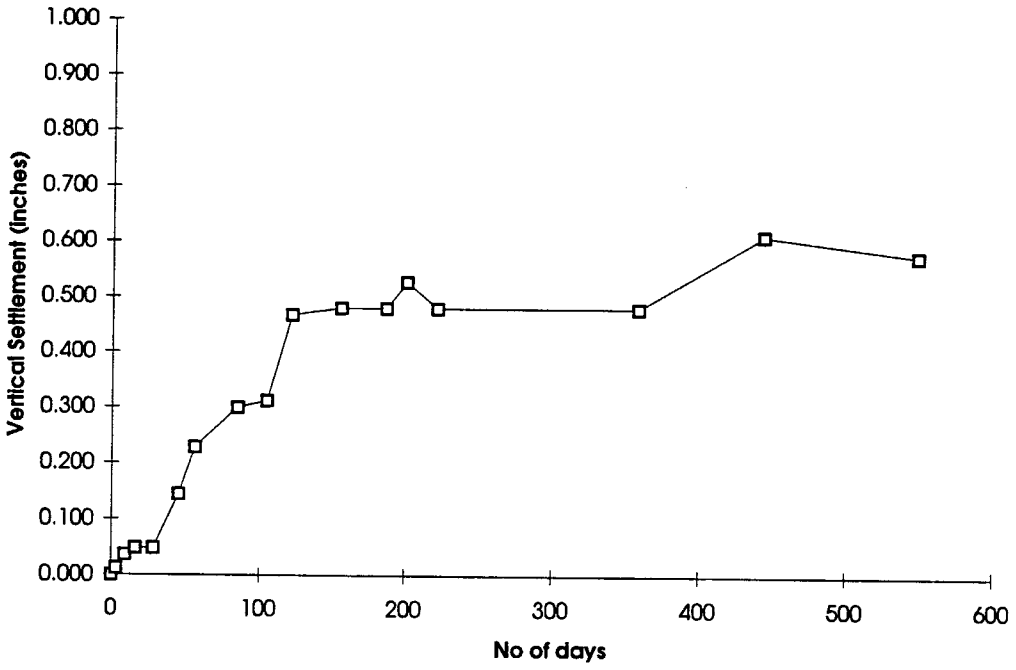

Figure B.9 Settlement of Pier 4 - Phase I Foundation (Bridge E)

Date	No of days	Construction Stages	Settlement (inches)
			P4SC
10-Sep	0	Footing (II)	0.000
18-Sep	8	Wall, Backfilling over Footing (II)	0.000
2-Oct	22		0.012
6-Nov	57	Beam (II)	0.024
5-Dec	86		0.048
23-Mar	194	Deck and Parapet (II)	0.120
29-Sep	384		0.132

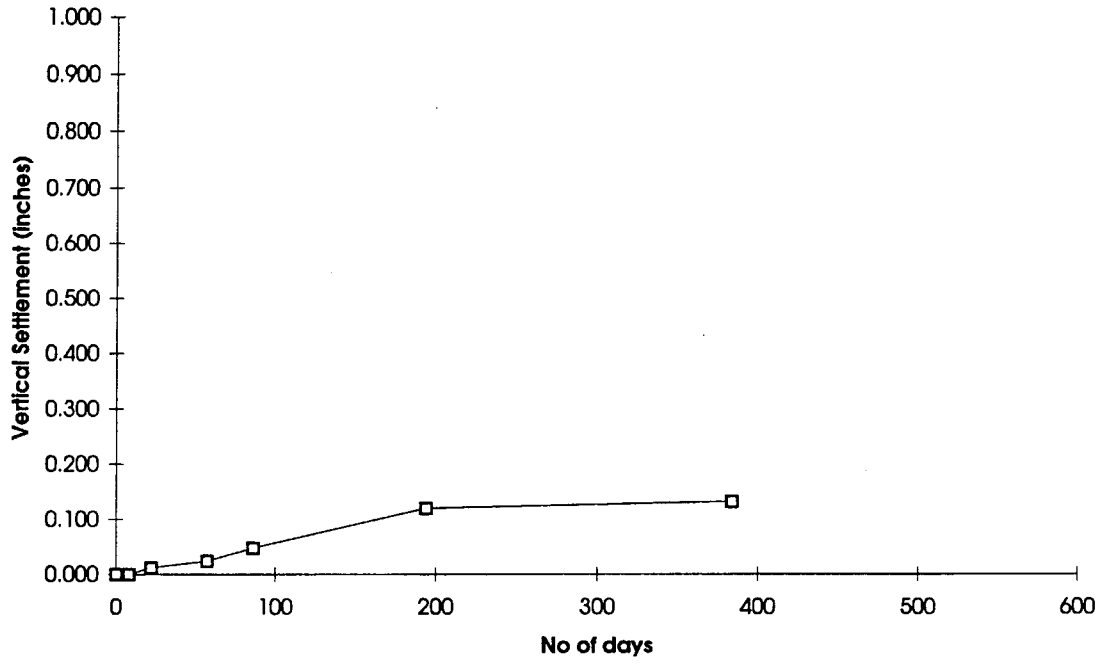

Figure B.10 Settlement of Pier 4 - Phase II Foundation (Bridge E)

Date	No of days	Construction Stages	Settlement (inches)
			P5SC
29-Mar	0	Footing, Column (I)	0.000
1-Apr	3		0.036
7-Apr	9	Backfilling over Footing (I)	0.072
14-Apr	16	Pier Cap (I)	0.072
26-Apr	28		0.084
13-May	45		0.108
24-May	56		0.108
22-Jun	85		0.132
12-Jul	105	Beam (I)	0.156
6-Nov	222	Phase II done	0.192

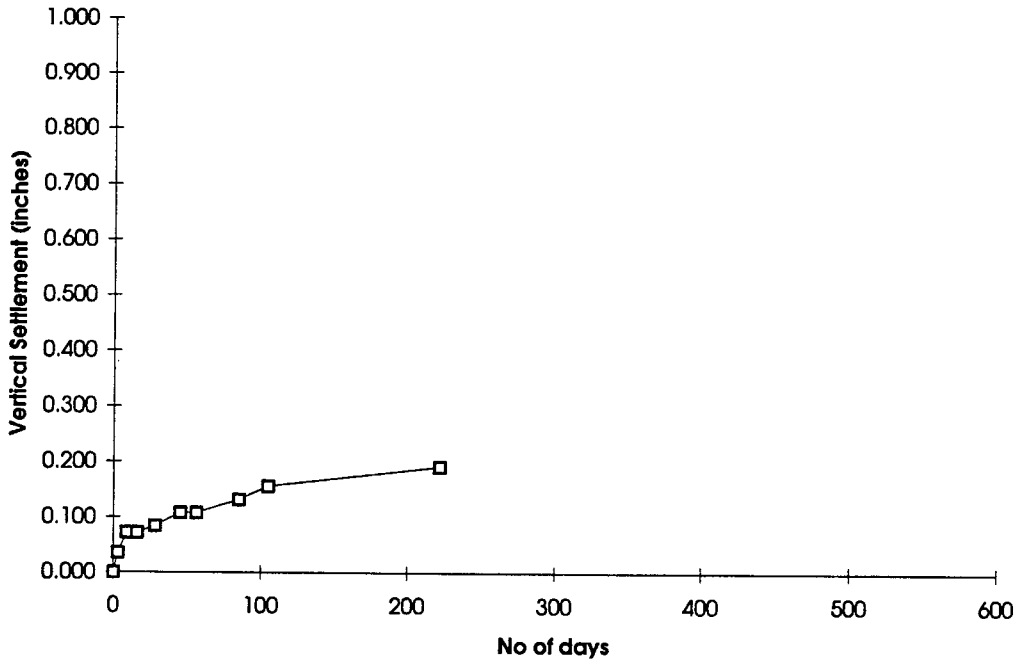

Figure B.11 Settlement of Pier 5 - Phase I Foundation (Bridge E)

Date	No of days	Construction Stages	Settlement (inches)
			P5SC
1-Sep	0	Footing, Column (II)	0.000
10-Sep	9	Pier Cap (II)	0.024
18-Sep	17	Backfilling over Footing (II)	0.036
25-Sep	24		0.072
2-Oct	31		0.084
16-Oct	45	Beam (II)	0.108
6-Nov	66		0.096
23-Mar	203	Deck and Parapet (II)	0.108

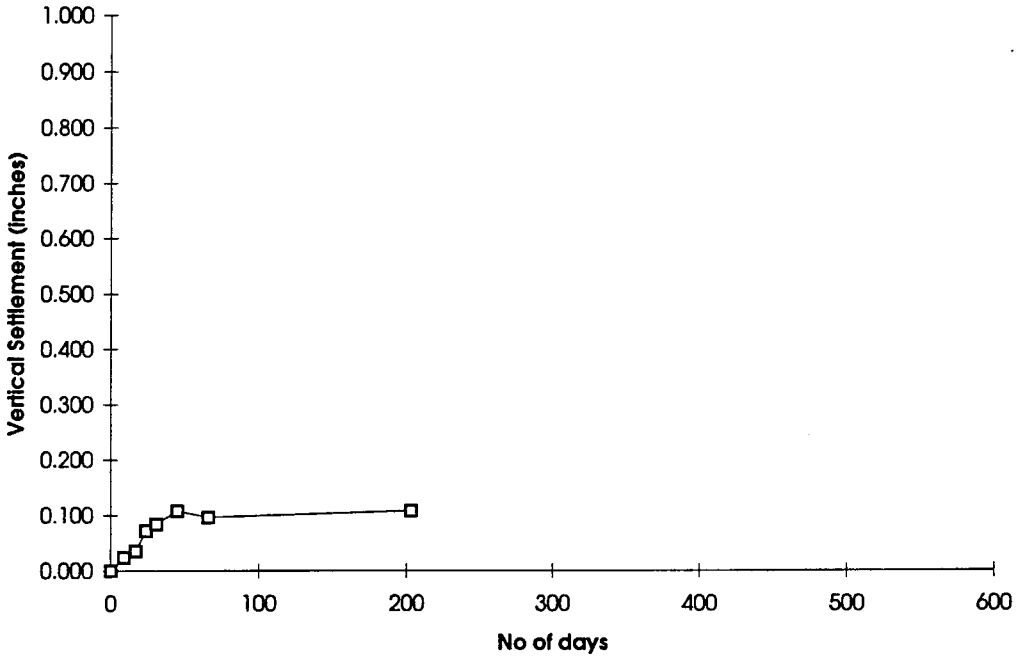

Figure B.12 Settlement of Pier 5 - Phase II Foundation (Bridge E)

Date	No of days	Construction Stages	Settlement (inches)				
			P6S1	P6S2	P6S3	P6S4	P6SC
22-Mar	0	Footing (I)	0.000	0.000	0.000	0.000	
29-Mar	7		0.000	-0.036	-0.012	0.000	
1-Apr	10		-0.012	-0.024	-0.036	-0.024	0.000
7-Apr	16	Column (I)	0.072	0.060	0.036	0.048	0.084
14-Apr	23		0.120	0.084	0.096	0.096	0.120
26-Apr	35	Pier Cap, Backfilling over Footing (I)	0.084		0.084	0.096	0.120
13-May	52		0.156		0.204	0.096	0.168
24-May	63		0.156		0.180	0.132	0.180
22-Jun	92		0.180		0.228	0.132	0.192
12-Jul	112	Beam (I)	0.276		0.300		0.240
29-Jul	129	Deck and Parapet (I)	0.336				0.360
12-Aug	143		0.384				0.240
1-Sep	163	Footing (II)	0.420				0.336
18-Sep	180	Column (II)	0.456				0.384
25-Sep	187	Backfilling over Footing (II)	0.432				0.408
2-Oct	194		0.384				0.324
16-Oct	208	Beam (II)	0.396		0.348	0.216	0.372
6-Nov	229		0.312				0.288
23-Mar	366	Deck and Parapet (II)	0.324			0.204	0.264
16-Jun	451		0.456			0.336	0.372
29-Sep	556		0.384	0.372		0.264	0.336

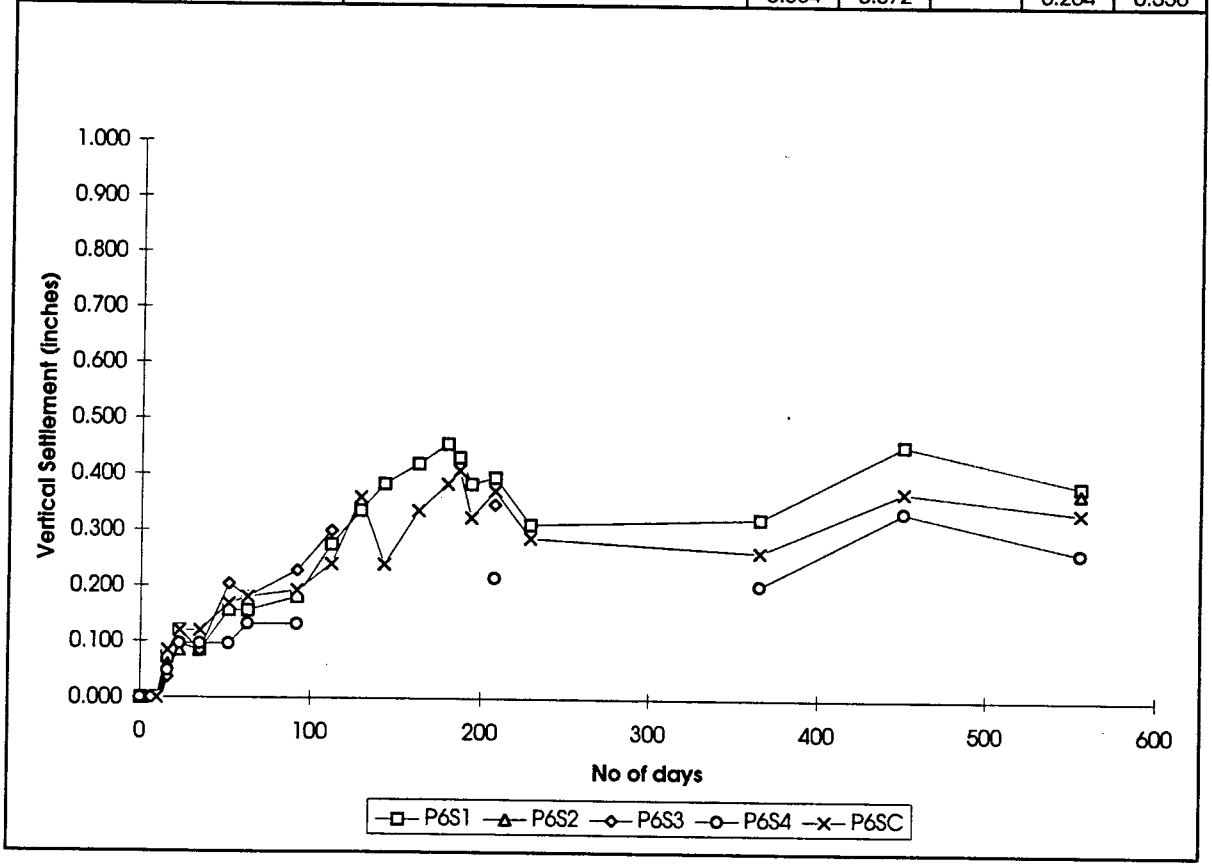

Figure B.13 Settlement of Pier 6 - Phase I Foundation (Bridge E)

Date	No of days	Construction Stages	Settlement (inches)				
			P6S1	P6S2	P6S3	P6S4	P6SC
1-Sep	0	Footing (II)	0.000	0.000	0.000	0.000	0.000
18-Sep	17	Column (II)	0.072	0.048	0.096	0.060	0.096
25-Sep	24	Backfilling over Footing (II)	0.132			0.156	0.096
2-Oct	31		0.216	0.108		0.192	0.168
16-Oct	45	Beam (II)	0.240	0.120	0.252	0.204	0.252
5-Dec	95		0.204		0.264	0.216	0.216
23-Mar	203	Deck and Parapet (II)		0.168	0.372	0.336	0.288
16-Jun	288		0.216		0.384	0.324	0.276
5-Aug	338		0.228		0.372	0.324	0.276
29-Sep	393		0.252		0.384	0.312	0.288

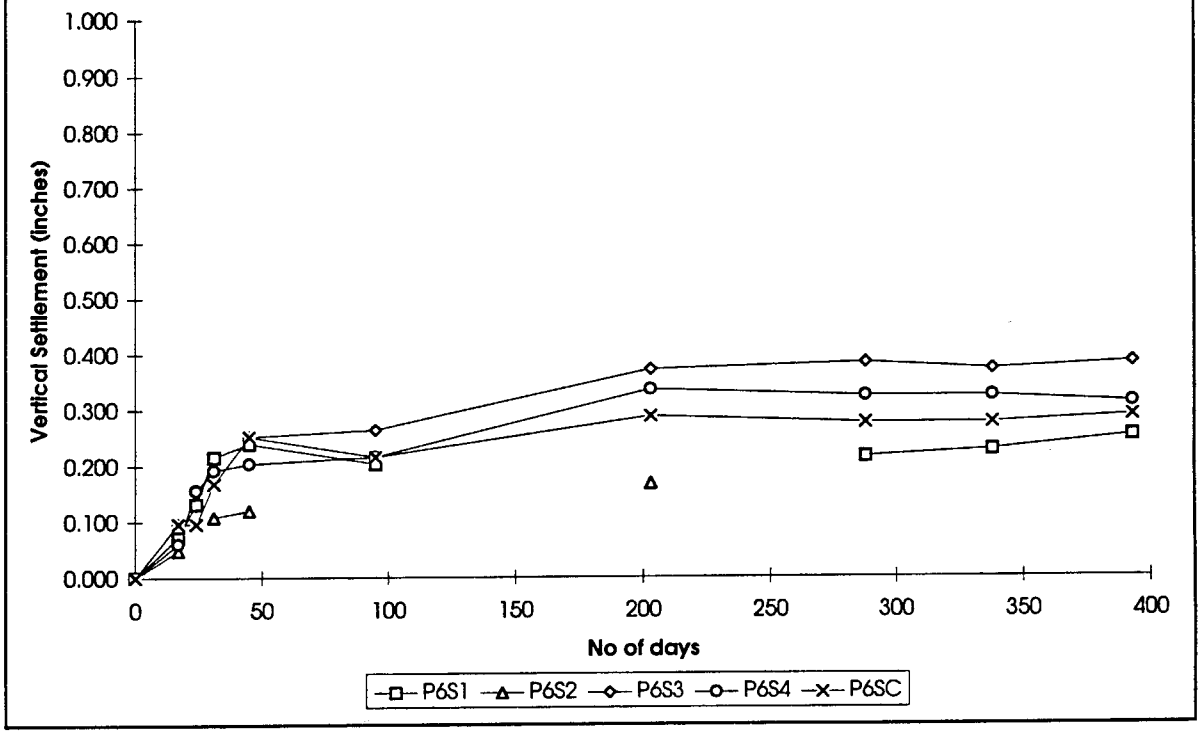

Figure B.14 Settlement of Pier 6 - Phase II Foundation (Bridge E)

Date	No of days	Construction Stages	Settlement (inches)
			P7SC
22-Mar	0	Footing (I)	0.000
29-Mar	7		0.000
1-Apr	10		0.000
7-Apr	16	Column (I)	0.072
14-Apr	23		0.132
13-May	52	Pier Cap, Backfilling over Footing (I)	0.180
24-May	63		0.204
22-Jun	92		0.216
12-Jul	112	Beam (I)	0.264
29-Jul	129	Deck and Parapet (I)	0.360
1-Sep	163	Footing (II)	0.372
10-Sep	172		0.360
25-Sep	187	Column, Pier Cap, Backfilling (II)	0.408
16-Oct	208		0.432
6-Nov	229	Beam (II)	0.420

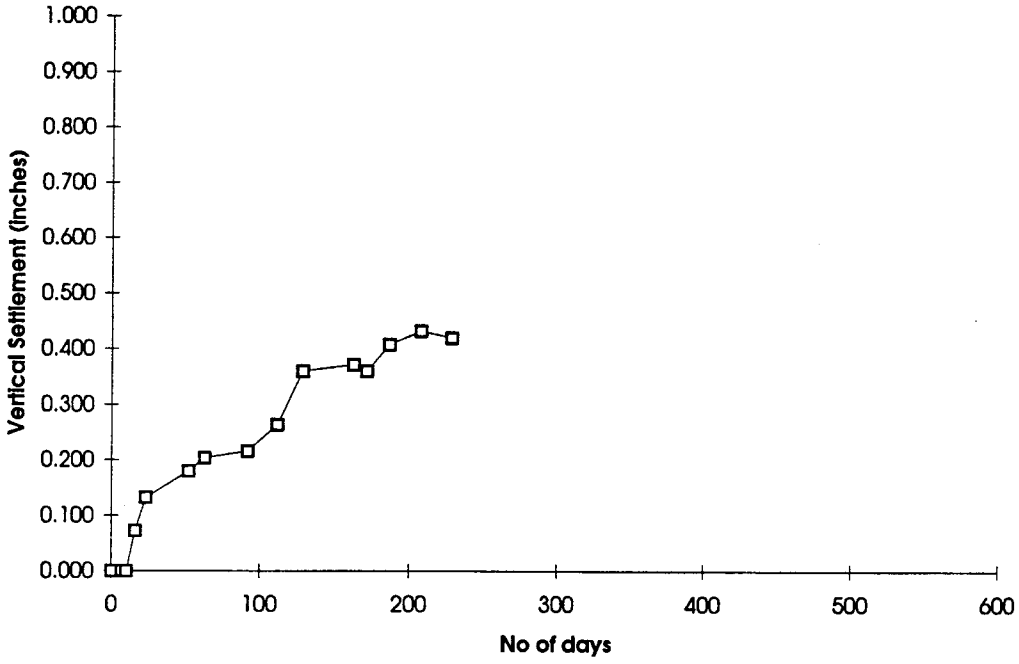

Figure B.15 Settlement of Pier 7 - Phase I Foundation (Bridge E)

Date	No of days	Construction Stages	Settlement (inches)
			P7SC
1-Sep	0	Footing (II)	0.000
10-Sep	9		0.096
18-Sep	17	Column (II)	0.120
25-Sep	24	Pier Cap, Backfilling over Footing (II)	0.120
2-Oct	31		0.156
6-Nov	66	Beam (II)	0.168
5-Dec	95		0.228

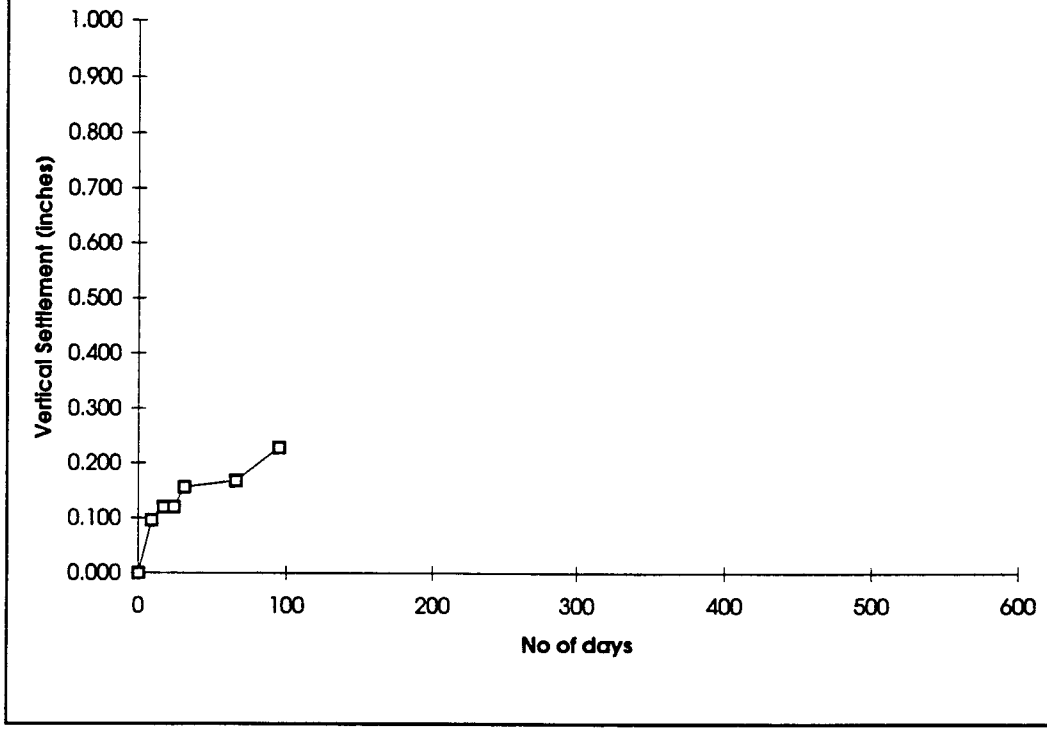

Figure B.16 Settlement of Pier 7 - Phase II Foundation (Bridge E)

Date	No of days	Construction Stages	Settlement (inches)				
			P8S1	P8S2	P8S3	P8S4	P8SC
22-Mar	0	Footing, Column (I)	0.000	0.000	0.000	0.000	
29-Mar	7		0.000	0.012	0.000	-0.012	
1-Apr	10		-0.036	-0.012	0.012	-0.036	
14-Apr	23	Pier Cap (I)	0.144	0.132	0.204		0.000
26-Apr	35	Backfilling over Footing (I)	0.264	0.108	0.216	0.096	0.156
13-May	52		0.360	0.156	0.276	0.252	0.252
24-May	63		0.336	0.204	0.312	0.216	0.276
22-Jun	92		0.324	0.192	0.288	0.192	0.276
12-Jul	112	Beam (I)	0.372	0.348	0.432	0.600	0.564
29-Jul	129	Deck and Parapet (I)	0.588	0.408	0.528		0.672
12-Aug	143			0.324	0.468		
1-Sep	163	Footing (II)		0.384	0.480		0.672
10-Sep	172	Column (II)		0.396	0.552		
18-Sep	180	Pier Cap, Backfilling over Footing (II)	0.480	0.432	0.576		
25-Sep	187		0.468	0.396	0.528		
16-Oct	208	Beam (II)		0.456			
6-Nov	229			0.432			
23-Mar	366	Deck and Parapet (II)		0.468			
16-Jun	451			0.444			
29-Sep	556		0.540	0.468			

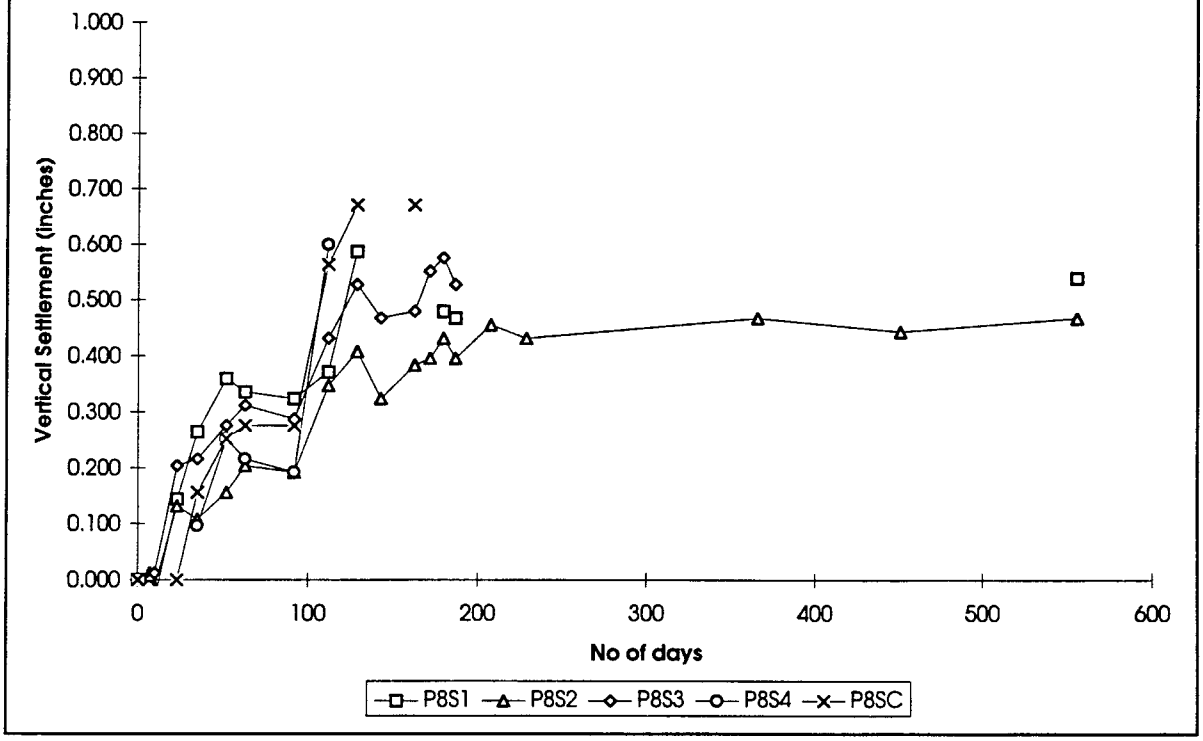

Figure B.17 Settlement of Pier 8 - Phase I Foundation (Bridge E)

Date	No of days	Construction Stages	Settlement (inches)				
			P8S1	P8S2	P8S3	P8S4	P8SC
1-Sep	0	Footing (II)	0.000	0.000	0.000	0.000	0.000
18-Sep	17	Column, Pier Cap, Backfilling (II)	0.000	0.024	0.168	0.108	0.084
25-Sep	24		0.012	0.060		0.096	0.096
2-Oct	31			0.048		0.108	0.096
16-Oct	45	Beam (II)		0.108	0.276	0.216	
5-Dec	95		0.228	0.108		0.216	0.216
23-Mar	203	Deck and Parapet (II)				0.312	0.252
16-Jun	288					0.324	0.252
5-Aug	338			0.168			
29-Sep	393			0.156		0.300	0.264

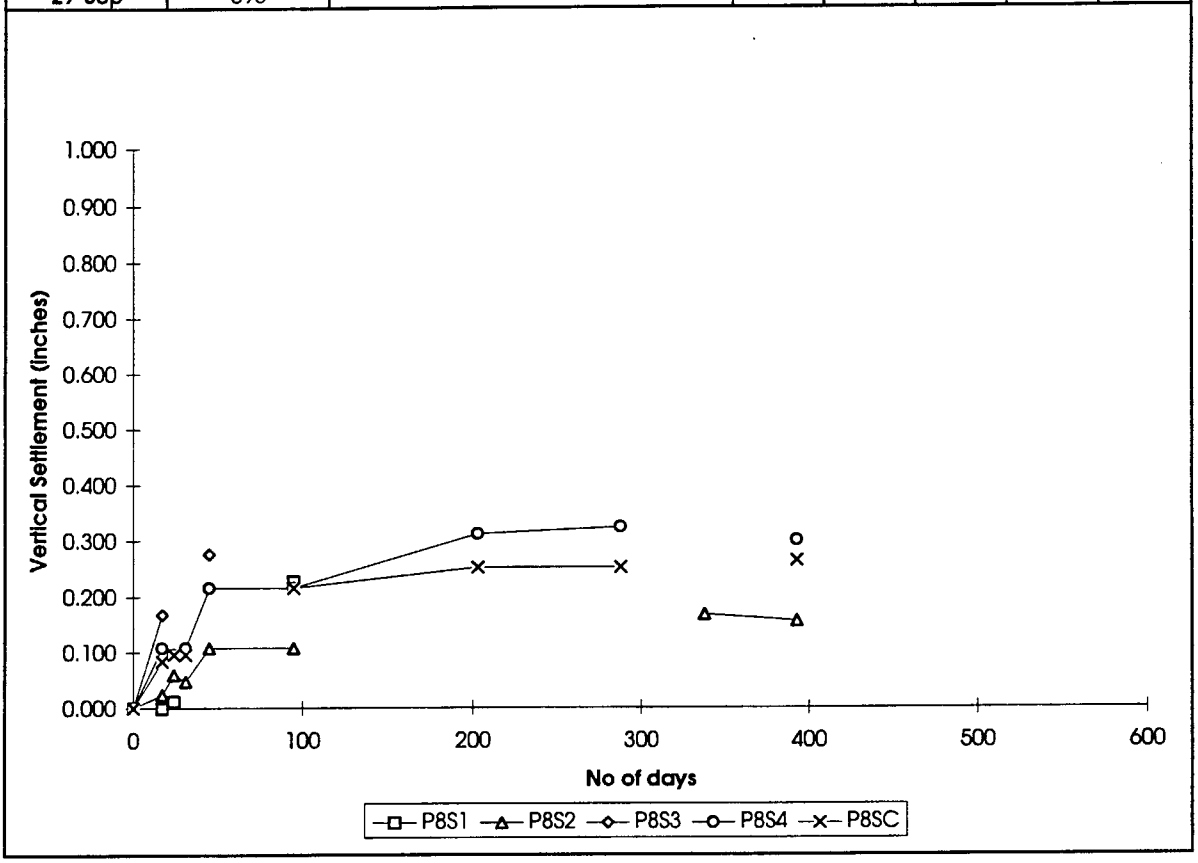

Figure B.18 Settlement of Pier 8 - Phase II Foundation (Bridge E)

Date	No of days	Construction Stages	Settlement (inches)		
			FAS1	FAS2	FASC
22-Mar	0	Footing (I)	0.000	0.000	
29-Mar	7	Wall (I)	0.012	0.036	
1-Apr	10		0.012	0.000	0.000
7-Apr	16		0.072	0.072	0.084
14-Apr	23		0.084	0.084	0.084
26-Apr	35			0.096	0.096
13-May	52			0.144	0.180
24-May	63		0.240	0.192	0.204
22-Jun	92	Backfilling over Footing, Wall (I)	0.288	0.192	0.240
29-Jul	129	Beam, Deck and Parapet (I)	0.480	0.276	0.432
1-Sep	163	Footing (II)		0.300	
25-Sep	187	Wall , Backfilling over Footing, Wall (II)		0.336	0.468
16-Oct	208	Beam (II)		0.348	0.504
16-Jun	451	Deck and Parapet (II)		0.408	0.612
29-Sep	556			0.372	0.588

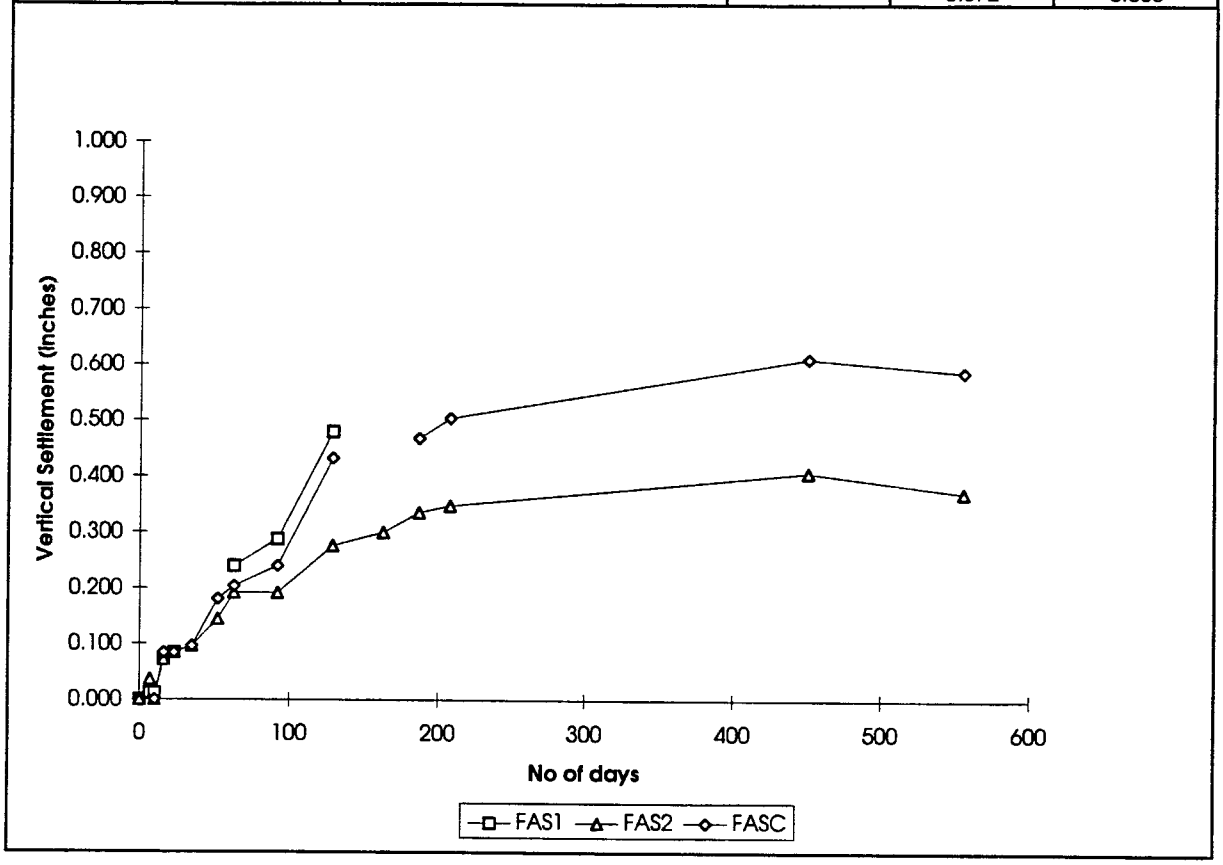

Figure B.19 Settlement of Forward Abutment - Phase I Foundation (Bridge E)

Date	No of days	Construction Stages	Settlement (inches)		
			FAS1	FAS2	FASC
1-Sep	0	Footing (II)	0.000	0.000	0.000
18-Sep	17	Wall (II)	0.012	0.084	0.036
25-Sep	24	Backfilling over Footing (II)		0.108	
2-Oct	31		0.048	0.132	0.120
16-Oct	45	Beam (II)	0.084	0.156	0.144
5-Dec	95	Backfilling Wall (II)	0.096	0.240	0.144
23-Mar	203	Deck and Parapet (II)	0.108	0.288	0.264
16-Jun	288			0.324	0.240
29-Sep	393		0.120		0.252

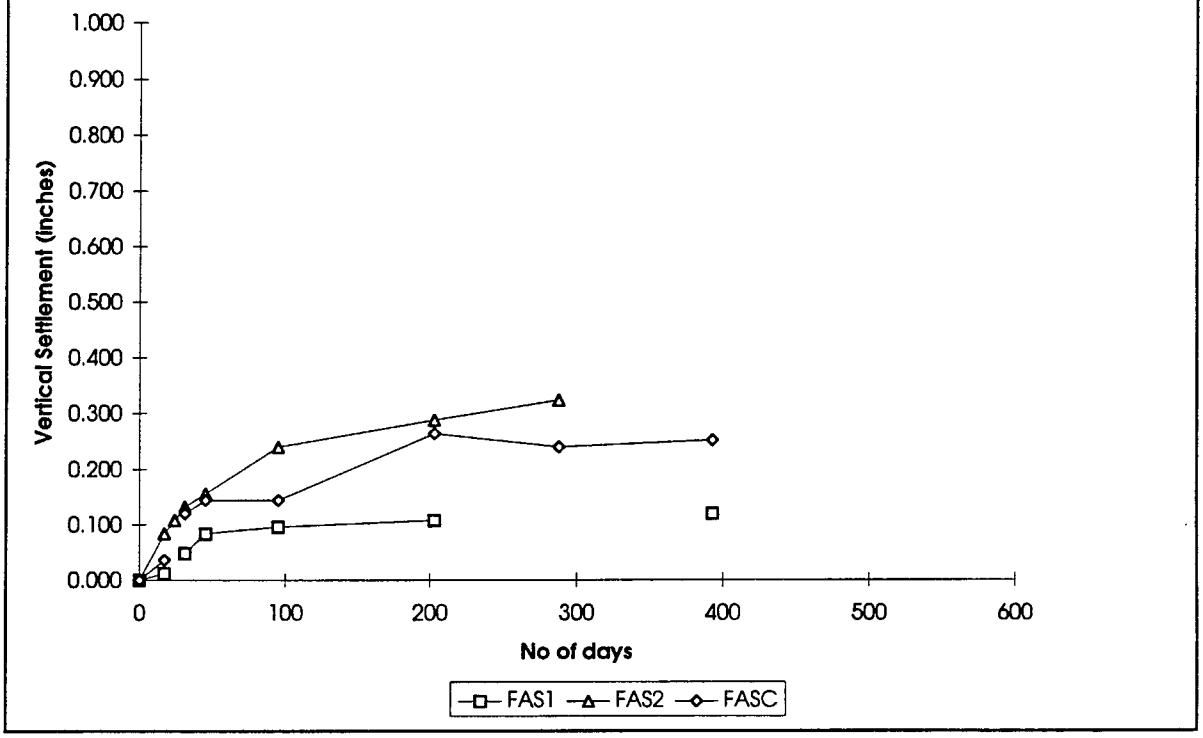

Figure B.20 Settlement of Forward Abutment - Phase II Foundation (Bridge E)

Date	No of days	Construction Stages	Pressure (tsf)		
			Heel	Toe	Key
1-Apr	0	Footing (I)	0.31	0.42	0.42
7-Apr	6		0.49	0.45	0.68
14-Apr	13		0.42	0.45	0.58
26-Apr	25	Wall (I)	0.58	0.64	0.84
13-May	42		0.70	0.75	1.12
24-May	53	Backfilling over Footing and Wall (I)	0.69	0.78	1.16
22-Jun	82	Beam (I)	1.23	1.27	3.43
12-Jul	102		1.27	1.30	3.83
29-Jul	119	Deck and Parapet (I)	1.38	1.39	4.26
12-Aug	133		1.41	1.41	4.34
1-Sep	153		1.43	1.47	4.73
18-Sep	170	Footing (II)	1.40	1.37	4.57
25-Sep	177	Wall (II)	1.52	1.49	4.97
2-Oct	184		1.46	0.31	4.82
16-Oct	198	Backfilling over Footing (II)	1.46	0.02	4.81
6-Nov	219	Beam, Backfilling Wall (II)	1.61	0.04	5.16
23-Mar	356	Deck and Parapet (II)	1.53	0.00	4.90
16-Jun	441		1.59	0.03	5.12
29-Sep	546		1.66	0.08	5.20

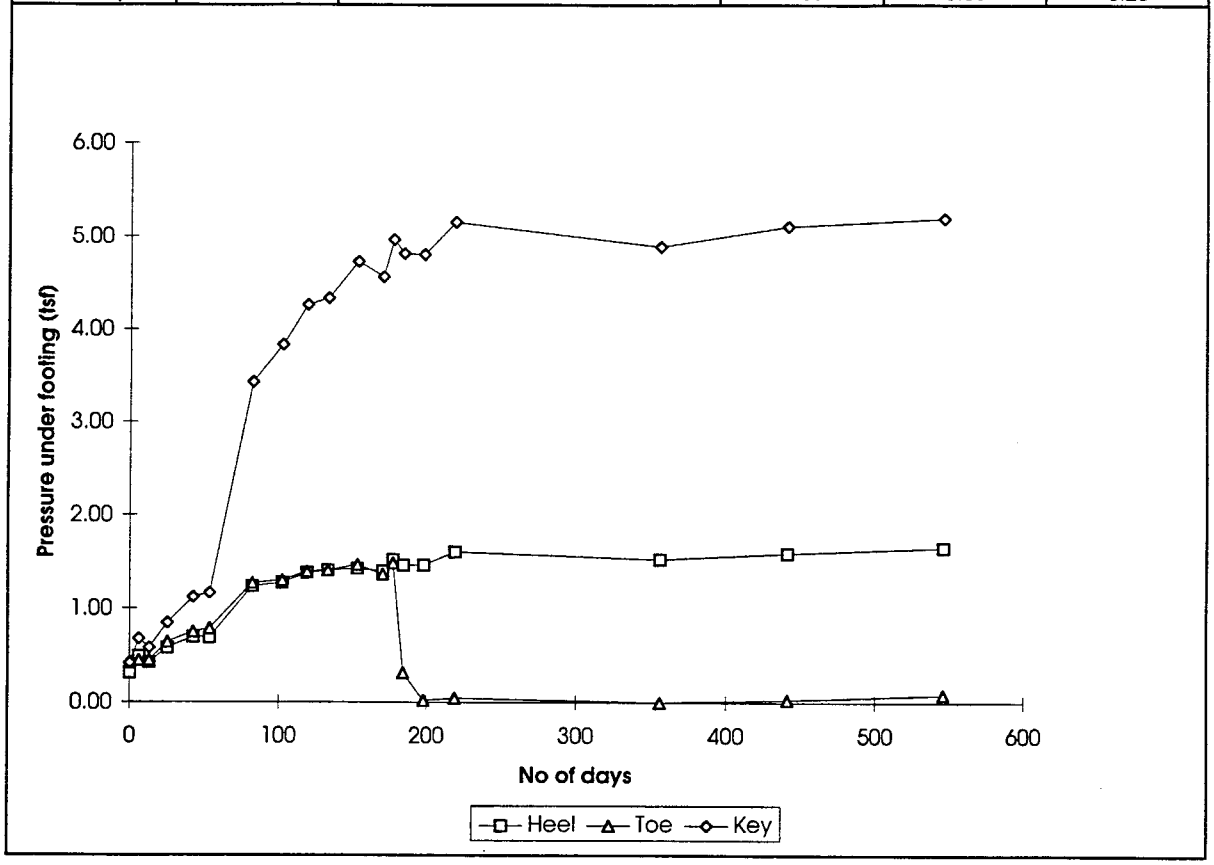

Figure B.21 Pressure under Rear Abutment - Phase I Foundation (Bridge E)

Date	No of days	Construction Stages	Pressure (tsf)			
			NW	NE	SW	SE
7-Apr	0	Footing (I)	0.22	0.54	0.32	0.36
14-Apr	7	Column (I)	0.19	0.53	0.35	0.88
26-Apr	19	Backfilling over Footing (I)	0.39	0.99	0.64	1.40
13-May	36	Pier Cap (I)	0.43	1.12	0.67	1.44
24-May	47		0.44	1.14	0.67	1.42
22-Jun	76	Beam (I)	1.11	2.46	1.52	2.66
12-Jul	96		1.12	2.49	1.52	2.73
29-Jul	113	Deck & Parapet (I)	1.30	2.73	1.85	3.24
12-Aug	127		1.40	2.86	1.88	3.29
1-Sep	147		1.44	3.09	1.79	3.38
10-Sep	156		1.42	3.00	1.80	3.31
18-Sep	164	Footing (II)	1.50	3.10	1.80	3.27
25-Sep	171	Column (II)	1.46	3.09	1.77	3.30
2-Oct	178	Pier Cap (II)	1.44	3.02	1.78	3.26
16-Oct	192	Backfilling over Footing (II)	1.39	3.03	1.75	3.27
6-Nov	213	Beam (II)	1.32	2.92	1.77	3.17
23-Mar	350	Deck & Parapet (II)	1.38	2.86	1.79	3.09
16-Jun	435		1.63	3.21	2.02	3.35
29-Sep	540		1.47	3.15	1.83	3.24

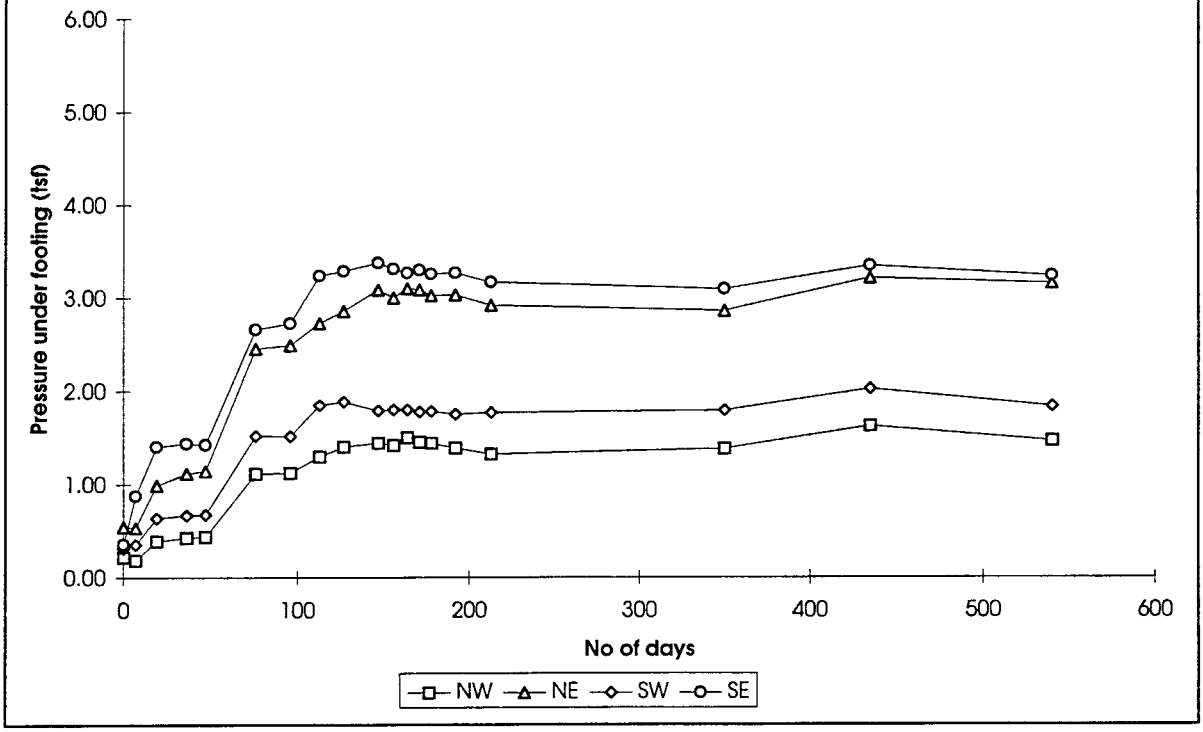

Figure B.22 Pressure under Pier 1 - Phase I Foundation (Bridge E)

Date	No of days	Construction Stages	Pressure (tsf)			
			NE	NW	SE	SW
29-Mar	0	Footing (I)	0.26	0.34	0.32	0.31
1-Apr	3		0.24	0.33	0.32	0.31
7-Apr	9		0.24	0.35	0.31	0.31
26-Apr	28	Wall (I)	0.44	0.67	0.55	
13-May	45	Backfilling (I)	0.46	0.69	0.55	
24-May	56		0.46	0.69	0.57	0.87
22-Jun	85	Beam (I)	0.71	0.96	0.78	1.32
12-Jul	105		0.74	0.95	0.82	1.37
29-Jul	122	Deck and Parapet (I)	0.85	1.00	0.99	1.52
12-Aug	136		0.91	1.04	1.02	1.53
1-Sep	156		0.56	1.04	1.04	1.53
10-Sep	165		0.58	1.01	1.06	1.52
18-Sep	173	Footing (II)	0.61	0.99	1.03	1.49
25-Sep	180		0.65	1.02		1.45
2-Oct	187	Wall, Backfilling over Footing (II)	0.74			1.52
16-Oct	201		0.90	1.14		1.66
6-Nov	222	Beam (II)	0.92	1.08		1.60
23-Mar	359	Deck and Parapet (II)	0.93			1.51
16-Jun	444		1.02		1.14	1.48
29-Sep	549		1.06		1.10	1.57

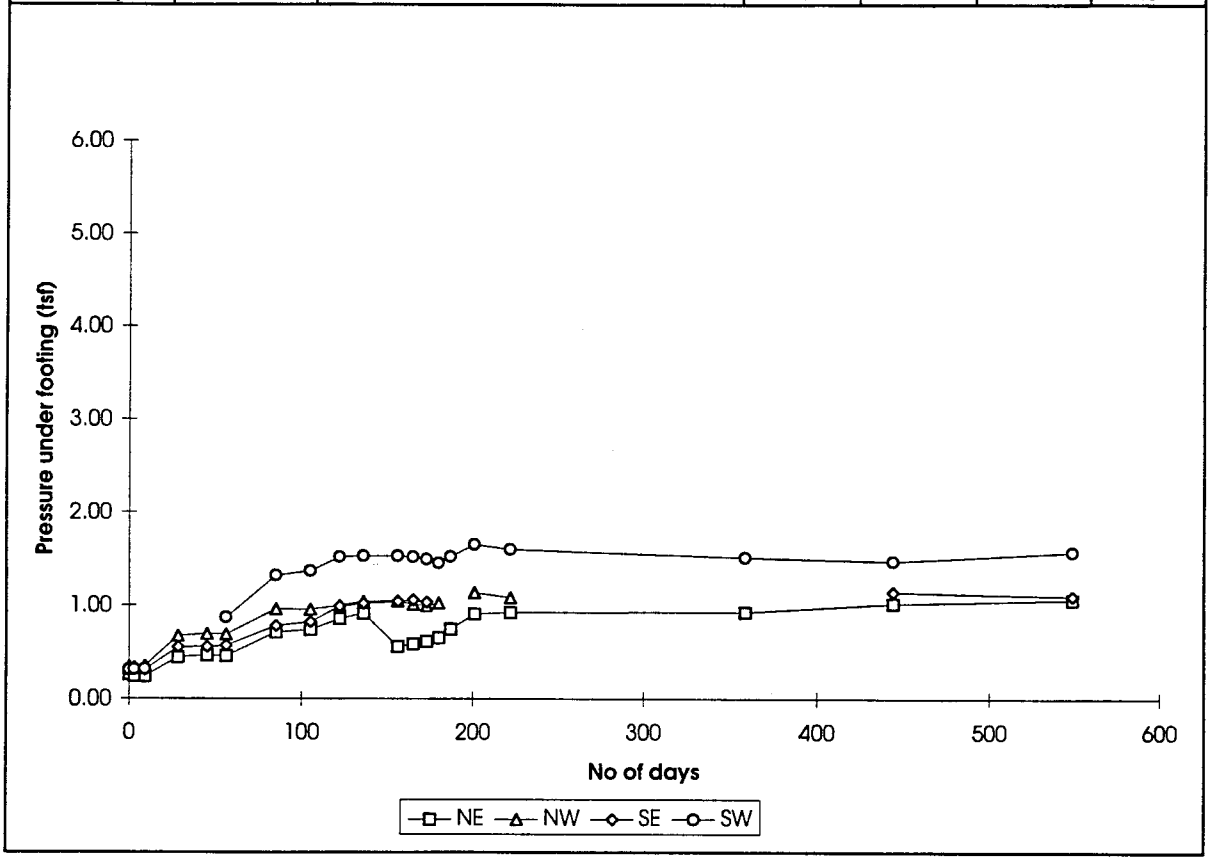

Figure B.23 Pressure under Pier 3 - Phase I Foundation (Bridge E)

Date	No of days	Construction Stages	Pressure (tsf)	
			SC	NC
22-Mar	0	Footing (I)	0.48	0.46
29-Mar	7		0.41	0.42
1-Apr	10		0.42	0.42
7-Apr	16	Column (I)	0.52	0.59
14-Apr	23		0.48	0.53
26-Apr	35	Pier Cap, Backfilling over Footing (I)	0.74	0.82
13-May	52		0.73	0.81
24-May	63		0.72	0.80
22-Jun	92		0.77	0.85
12-Jul	112	Beam (I)	1.18	1.37
29-Jul	129	Deck and Parapet (I)	1.41	1.57
12-Aug	143		1.40	1.69
1-Sep	163	Footing (II)	1.43	1.75
18-Sep	180	Column (II)	1.37	1.72
25-Sep	187	Backfilling over Footing (II)	1.38	1.76
2-Oct	194		1.37	1.74
16-Oct	208	Beam (II)	1.38	1.72
6-Nov	229		1.27	1.75
23-Mar	366	Deck and Parapet (II)	1.18	1.86
16-Jun	451		1.36	1.90
29-Sep	556		1.38	1.84

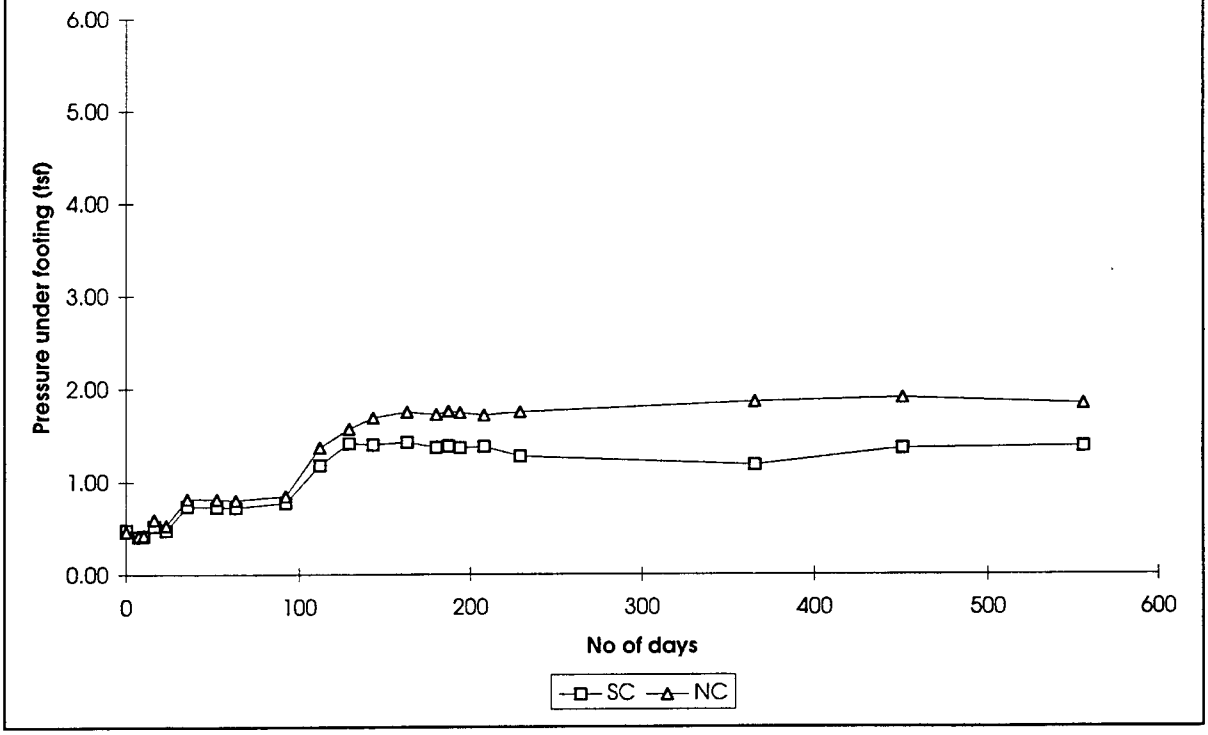

Figure B.24 Pressure under Pier 6 - Phase I Foundation (Bridge E)

Date	No of days	Construction Stages	Pressure (tsf)			
			NW	SW	NE	SE
22-Mar	0	Footing, Column (I)	0.12	0.00	0.24	0.00
29-Mar	7		0.16	0.04	0.31	0.04
1-Apr	10		0.16	0.03	0.31	0.03
14-Apr	23	Pier Cap (I)	0.26	0.05	0.36	0.06
26-Apr	35	Backfilling over Footing (I)	0.26	0.01	0.45	0.02
13-May	52		0.27	0.01	0.45	0.03
24-May	63		0.27	0.00	0.45	0.02
22-Jun	92		0.28	0.00	0.46	0.02
12-Jul	112	Beam (I)	0.55		0.78	0.07
29-Jul	129	Deck and Parapet (I)	0.72	0.01	0.94	0.13
12-Aug	143		0.76	0.01	1.00	0.11
1-Sep	163	Footing (II)	0.86	0.03	0.99	0.11
10-Sep	172	Column (II)	0.82	0.01	1.01	0.10
18-Sep	180	Pier Cap, Backfilling over Footing (II)	0.85	0.01	1.01	0.09
25-Sep	187		0.91	0.01	1.01	0.09
16-Oct	208	Beam (II)	0.95	0.02	1.03	0.12
6-Nov	229		0.97	0.01	1.06	0.10
23-Mar	366	Deck and Parapet (II)	0.96	0.01	1.09	0.10
16-Jun	451		1.03	0.02	1.15	0.12
29-Sep	556		1.05	0.01	1.11	0.12

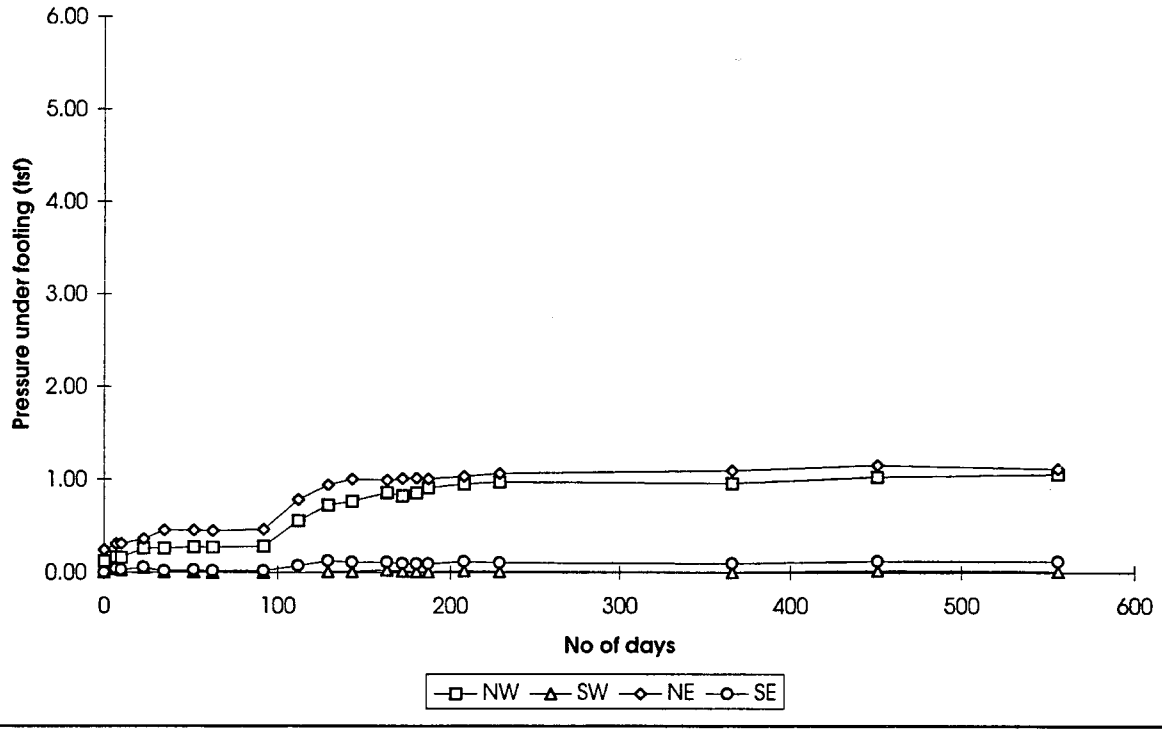

Figure B.25 Pressure under Pier 8 - Phase I Foundation (Bridge E)

Date	No of days	Construction Stages	Pressure (tsf)		
			Heel	Key	Toe
22-Mar	0	Footing (I)	0.0792	0.07704	0.03096
29-Mar	7	Wall (I)	0.07992	0.02736	0.04104
1-Apr	10		0.0922	0.02664	0
7-Apr	16		0.1116	0.03816	0.018
14-Apr	23		0.09288	0	0.00432
26-Apr	35		0.09432	0.01008	0.01512
13-May	52		0.1555	0.02736	0.0288
24-May	63		0.2635	0.05184	0.05328
22-Jun	92	Backfilling over Footing, Wall (I)	0.31176	0.0756	0.09288
29-Jul	129	Beam, Deck and Parapet (I)	0.40176	0.09864	0.21168
1-Sep	163	Footing (II)		0.12024	0.24552
25-Sep	187	Wall , Backfilling over Footing, Wall (II)	0.46368	0.10584	0.24552
16-Oct	208	Beam (II)	0.28512	0.0342	0.2772
16-Jun	451	Deck and Parapet (II)	0.24984	0.12024	0.39456
29-Sep	556		0.30456		0.37656

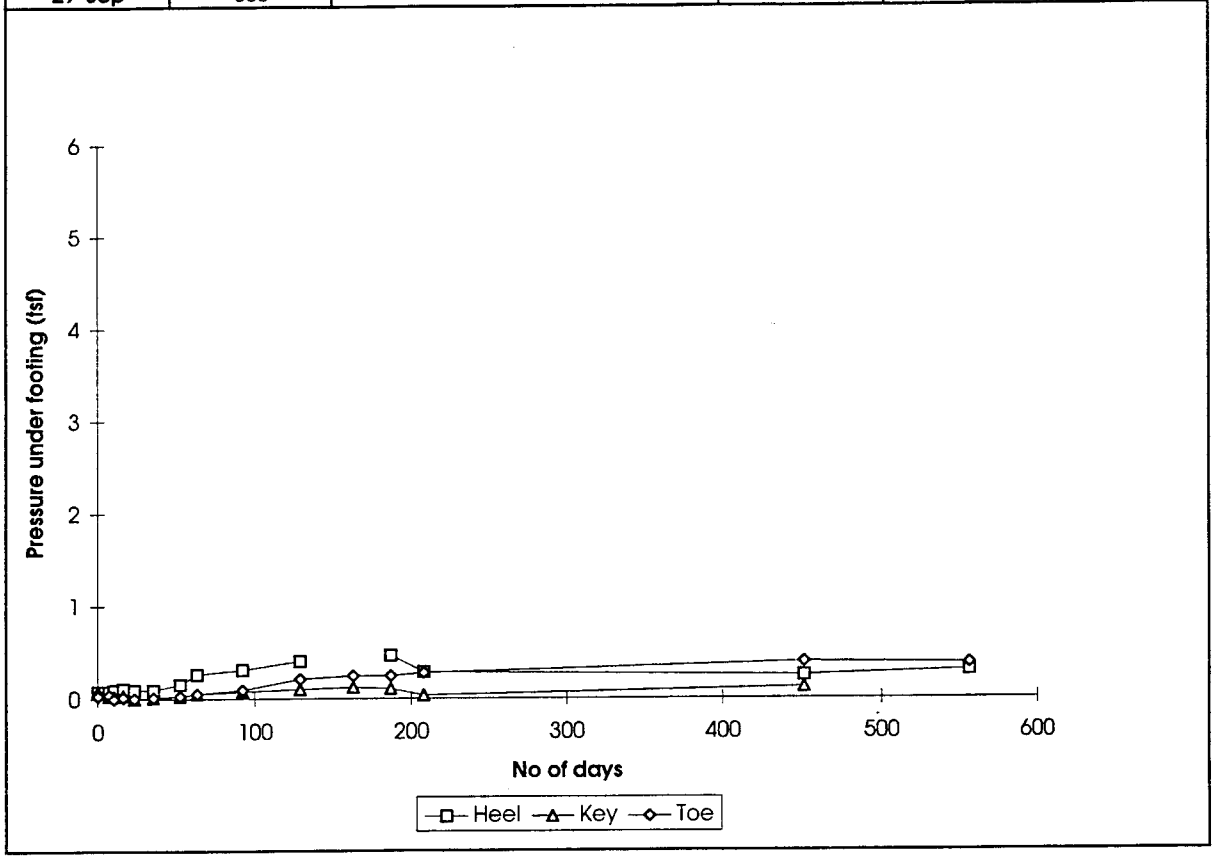

Figure B.26 Pressure under Forward Abutment - Phase I Foundation (Bridge E)

Date	No of days	Construction Stages	Tilting (degree)			
			Longitudinal Direction		Transverse Direction	
			North	South	North	South
14-Apr	0	Footing, Column, Pier Cap (I)	0.0000	0.0000	0.0000	0.0000
26-Apr	12	Backfilling over Footing (I)	0.0158	0.0122	0.0015	-0.0072
13-May	29		0.0143	-0.0194	0.0036	0.0759
24-May	40		0.0100	-0.0222	0.0072	0.0681
22-Jun	69		0.0086	-0.0244	0.0029	0.0695
12-Jul	89	Beam (I)	0.0115	0.0000	0.0108	-0.0079
12-Aug	120	Deck and Parapet (I)	0.0129	-0.0222	-0.0057	0.0581
1-Sep	140	Footing (II)	-0.0115	0.0015	0.0029	0.0244
10-Sep	149	Column (II)	0.0065	-0.0251	0.0022	0.0695
18-Sep	157	Pier Cap, Backfilling over Footing (II)	0.0036	-0.0265	0.0007	0.0674
25-Sep	164		-0.0008	-0.0322	0.0022	0.0681
16-Oct	185	Beam (II)		-0.0452	-0.0007	0.0659
6-Nov	206		-0.0423	-0.0337	0.0165	0.0810
23-Mar	343	Deck and Parapet (II)		-0.0365	0.0115	0.0681
16-Jun	428		0.0086	-0.0358	0.0179	0.0731
5-Aug	478			-0.0215		0.0774

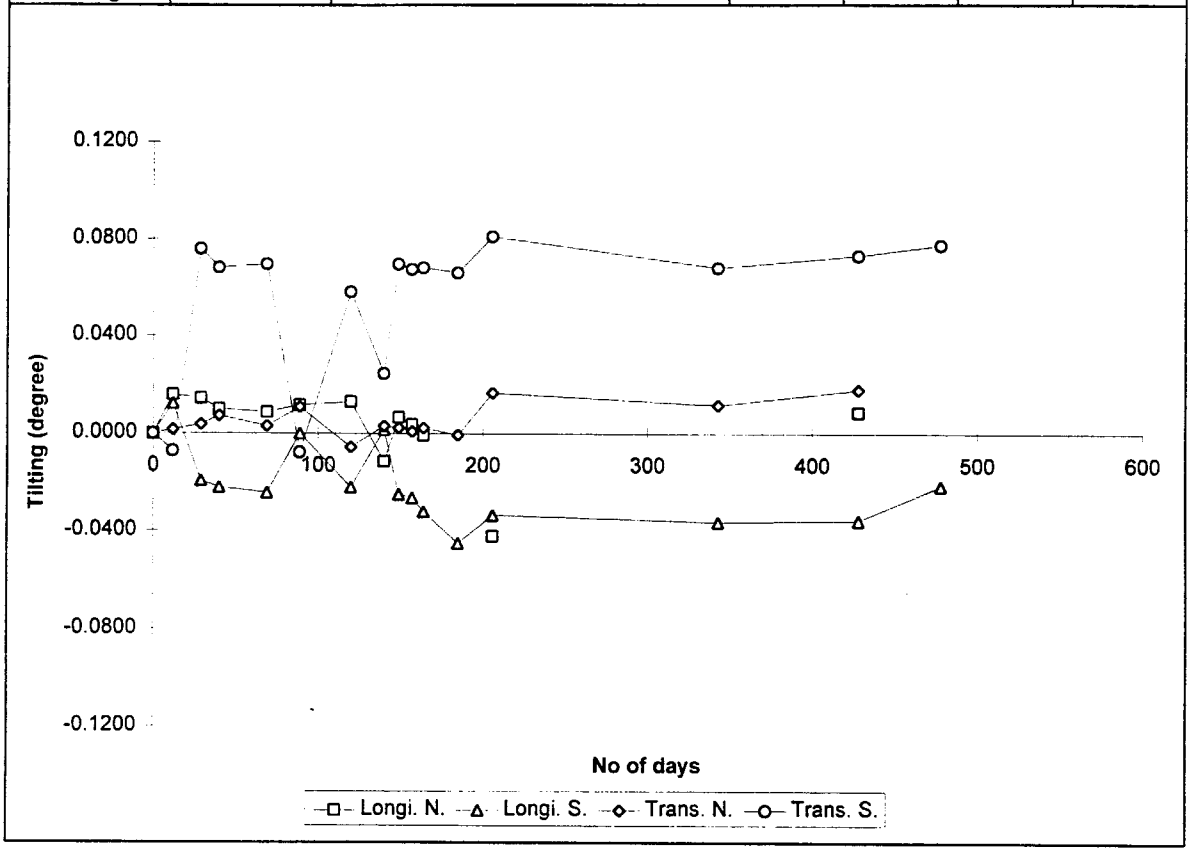

Figure B.27 Tilting of Pier 8 - Phase I Columns (Bridge E)

Date	No of days	Construction Stages	Tilting (degree)			
			Longitudinal Direction		Transverse Direction	
			North	South	North	South
26-Apr	0	Footing, Column, Pier Cap (I)	0.0000	0.0000	0.0000	0.0000
13-May	17	Backfilling over Footing (I)	-0.0057	-0.0201	-0.0007	0.0745
24-May	28		-0.0079	-0.0208	0.0072	0.0702
22-Jun	57	Beam (I)	-0.0172	-0.0294	0.0201	0.0602
12-Jul	77		-0.0014	0.0000	0.0222	0.0122
12-Aug	108	Deck and Parapet (I)	-0.0229	-0.0329	0.0301	0.0537
1-Sep	128		-0.0014	0.0079	0.0301	-0.0043
10-Sep	137		-0.0093	-0.0215	0.0251	0.0666
18-Sep	145	Footing (II)	-0.0043	-0.0150	0.0222	0.0673
25-Sep	152	Column (II)	0.0029	-0.0064	0.0179	0.0673
2-Oct	159	Pier Cap (II)	-0.0057	0.0050	0.0093	-0.0107
16-Oct	173	Backfilling over Footing (II)	0.0014	-0.0086	0.0244	0.0702
6-Nov	194	Beam (II)	0.0000	-0.0043	0.0286	0.0630
23-Mar	331	Deck and Parapet (II)	0.0064	-0.0021	0.0251	0.0716
16-Jun	416		-0.0050	-0.0115	0.0193	0.0709
5-Aug	466		-0.0086	-0.0122	0.0143	0.0602
29-Sep	521		0.0057	0.0000	0.0186	0.0845

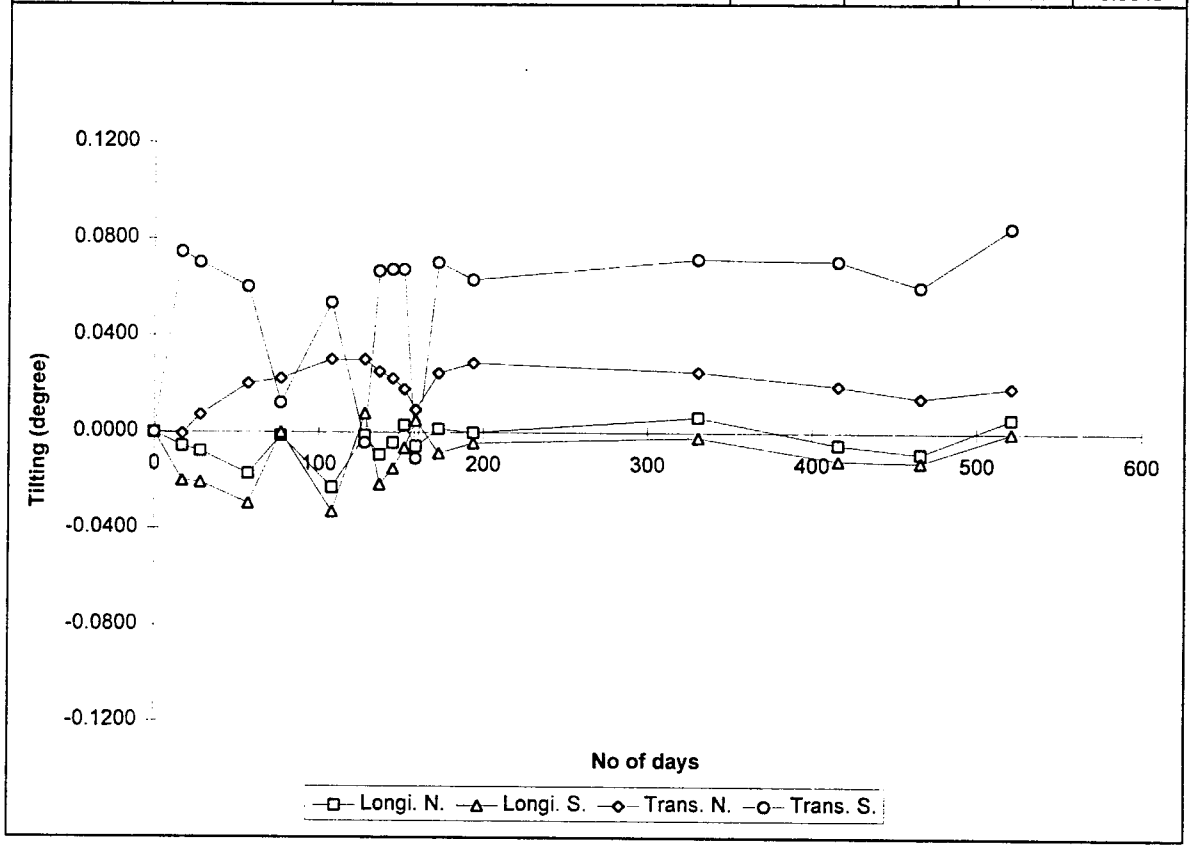

Figure B.28 Tilting of Pier 1 - Phase I Columns (Bridge E)

Date	No of days	Construction Stages	Tilting (degree)	
			Longitudinal Direction	
			North	South
14-Apr	0	Footing, Column (I)	0.0000	0.0000
26-Apr	12	Pier Cap, Backfilling over Footing (I)	0.0000	-0.0036
13-May	29		-0.0279	-0.0495
24-May	40		-0.0351	-0.0373
22-Jun	69		-0.0323	-0.0423
12-Jul	89	Beam (I)	-0.0501	-0.0194
12-Aug	120	Deck and Parapet (I)	-0.0287	-0.0408
10-Sep	149		-0.0344	-0.0466
18-Sep	157	Footing, Column (II)	-0.0344	-0.0416
25-Sep	164	Backfilling over Footing (II)	-0.0344	-0.0437
16-Oct	185	Beam (II)	-0.0344	-0.0458
6-Nov	206		-0.0344	-0.0451
23-Mar	343	Deck and Parapet (II)	-0.0373	-0.0451
16-Jun	428		-0.0301	-0.0408
29-Sep	533		-0.0423	-0.0544

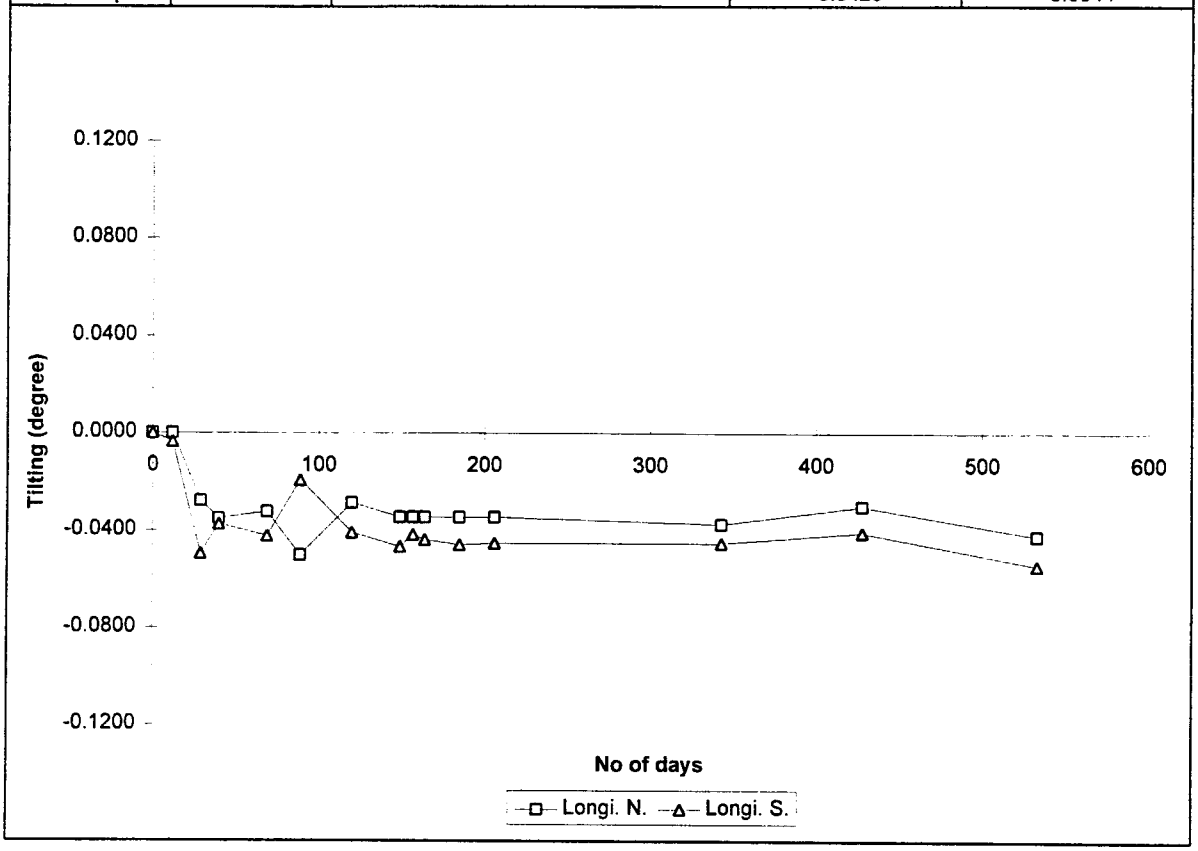

Figure B.29 Tilting of Pier 6 - Phase I Columns (Bridge E)

Date	No of days	Construction Stages	Tilting (degree)
			Longitudinal direction
26-Apr	0	Footing, Wall (I)	0.0000
13-May	17	Backfilling over Footing (I)	0.0559
24-May	28		0.0494
22-Jun	57	Beam (I)	-0.0029
12-Jul	77		0.0100
12-Aug	108	Deck and Parapet (I)	-0.0086
1-Sep	128		0.0093
10-Sep	137		-0.0057
18-Sep	145	Footing (II)	-0.0172
25-Sep	152		-0.0222
2-Oct	159	Wall, Backfilling over Footing (II)	-0.0158
16-Oct	173		-0.0315
6-Nov	194	Beam (II)	-0.0344
23-Mar	331	Deck and Parapet (II)	-0.0415
16-Jun	416		-0.0372
5-Aug	466		-0.0408
29-Sep	521		-0.0673

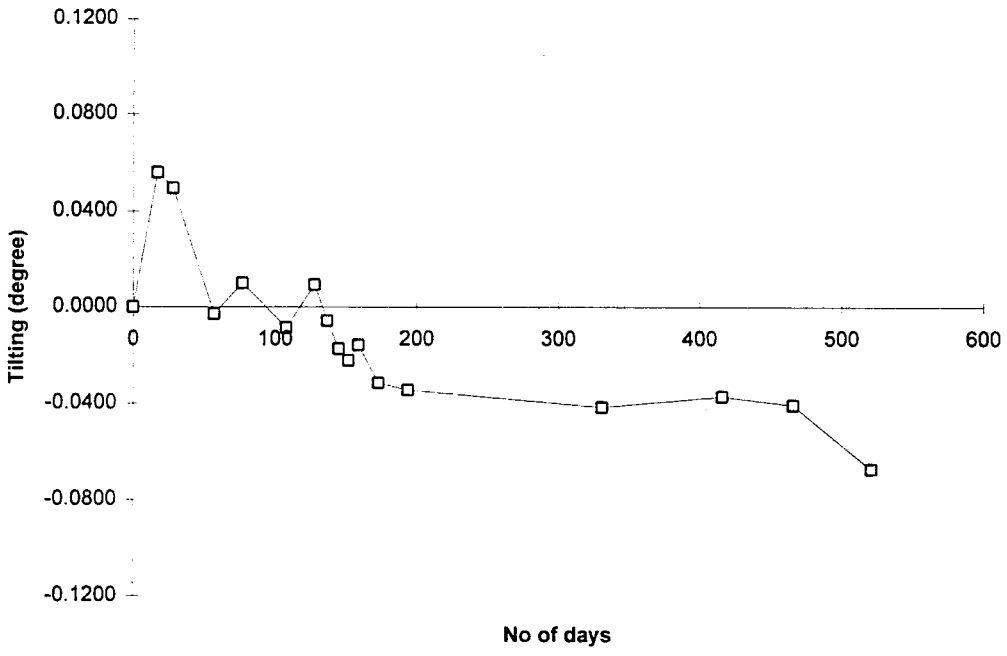

Figure B.30 Tilting of Pier 3 - Phase I Wall (Bridge E)

Date	No of days	Construction Stages	Tilting (degree)
			Longitudinal direction
13-May	0	Footing, Wall (I)	0.0000
24-May	11	Backfilling over Footing and Wall (I)	-0.0043
22-Jun	40	Beam (I)	0.0387
12-Jul	60		0.0473
12-Aug	91	Deck and Parapet (I)	0.0645
1-Sep	111		0.0738
10-Sep	120		0.0695
18-Sep	128	Footing (II)	0.0723
25-Sep	135	Wall (II)	0.0652
2-Oct	142		0.0988
16-Oct	156	Backfilling over Footing (II)	0.0659
6-Nov	177	Beam, Backfilling Wall (II)	0.0759
23-Mar	314	Deck and Parapet (II)	0.0795
16-Jun	399		0.0795
5-Aug	449		0.0695
29-Sep	504		0.0723

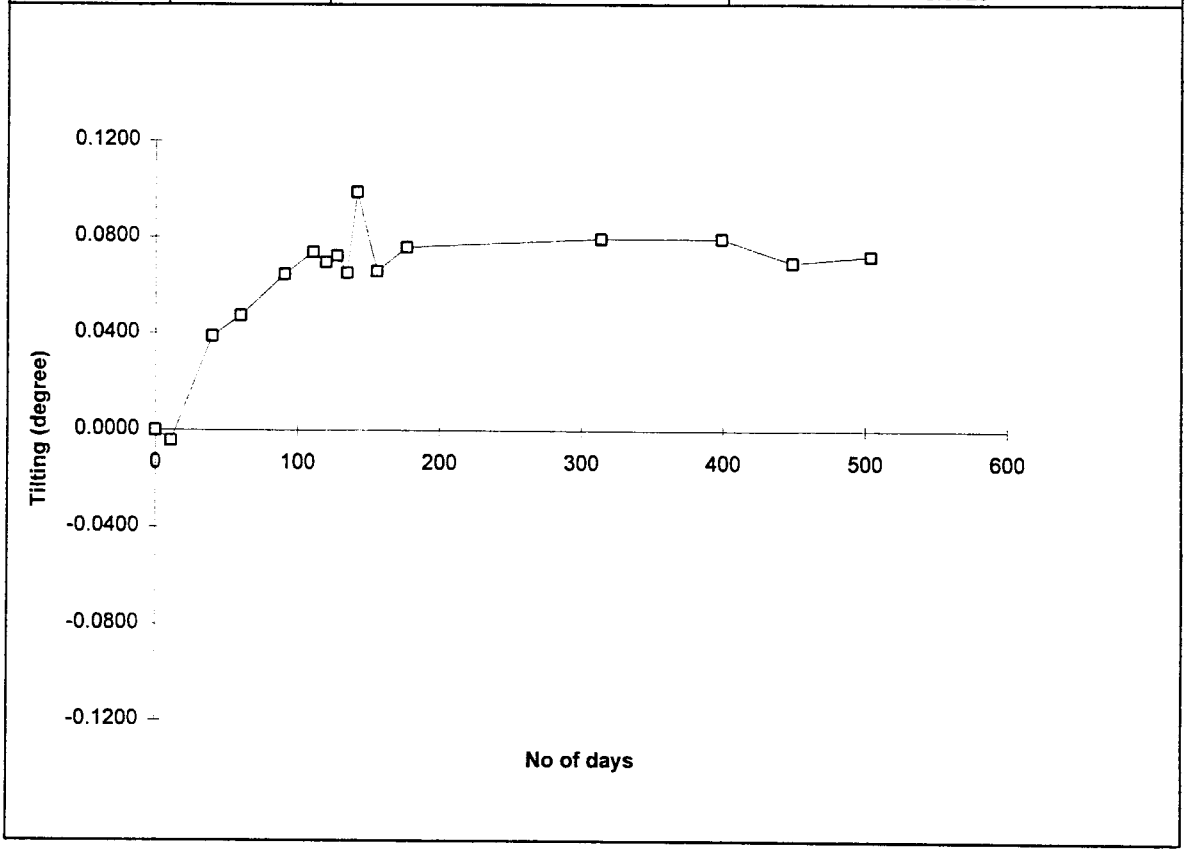

Figure B.31 Tilting of Rear Abutment - Phase I (Bridge E)

Date	No of days	Construction Stages	Tilting (degree)
			Longitudinal direction
14-Apr	0	Footing, Wall (I)	0.0000
26-Apr	12		0.0036
13-May	29		0.0143
24-May	40	Backfilling over Footing and Wall (I)	0.0244
22-Jun	69		0.0365
12-Jul	89	Beam (I)	0.0373
12-Aug	120	Deck and Parapet (I)	0.0279
1-Sep	140	Footing (II)	0.0416
10-Sep	149		0.0315
18-Sep	157	Wall (II)	0.0322
25-Sep	164	Backfilling over Footing (II)	0.0351
2-Oct	171		0.0279
16-Oct	185	Beam (II)	0.0337
6-Nov	206		0.0229
23-Mar	343	Backfilling Wall, Deck and Parapet (II)	0.0394
16-Jun	428		0.0287
5-Aug	478		0.0372
29-Sep	533		0.0480

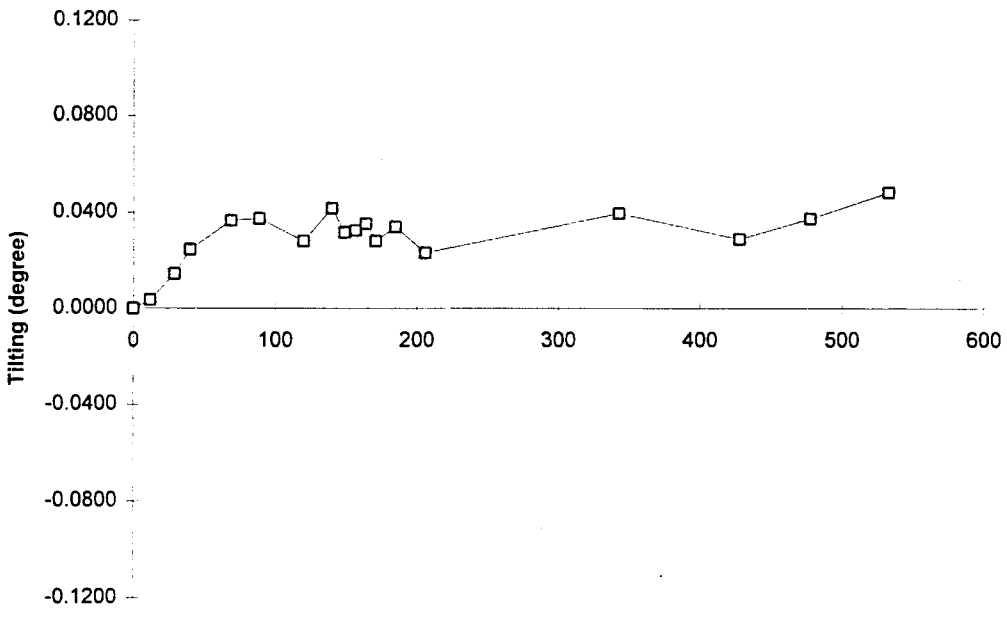

Figure B.32 Tilting of Forward Abutment - Phase I (Bridge E)

Date	No of days	Construction Stages	Tilting (degree)
			Longitudinal direction
2-Oct	0	Footing, Wall (II)	0.0000
16-Oct	14	Backfilling over Footing (II)	-0.0150
6-Nov	35	Beam, Backfilling Wall (II)	0.0100
5-Dec	64		0.0100
23-Mar	172	Deck and Parapet (II)	0.0179
16-Jun	257		0.0158
5-Aug	307		0.0186

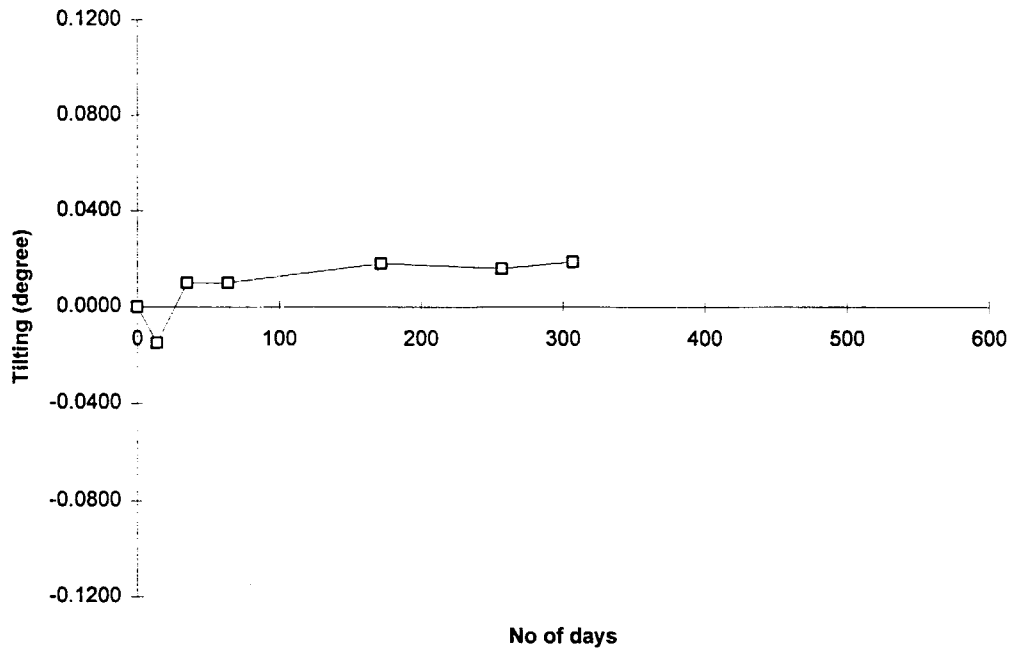

Figure B.33 Tilting of Rear Abutment - Phase II (Bridge E)

Date	No of days	Construction Stages	Tilting (degree)
			Longitudinal direction
2-Oct	0	Footing, Wall (II)	0.0000
16-Oct	14	Beam, Backfilling over Footing (II)	-0.0745
6-Nov	35		-0.0881
23-Mar	172	Backfilling Wall, Deck and Parapet (II)	-0.1017
16-Jun	257		-0.1024
5-Aug	307		-0.0917
29-Sep	362		-0.1146

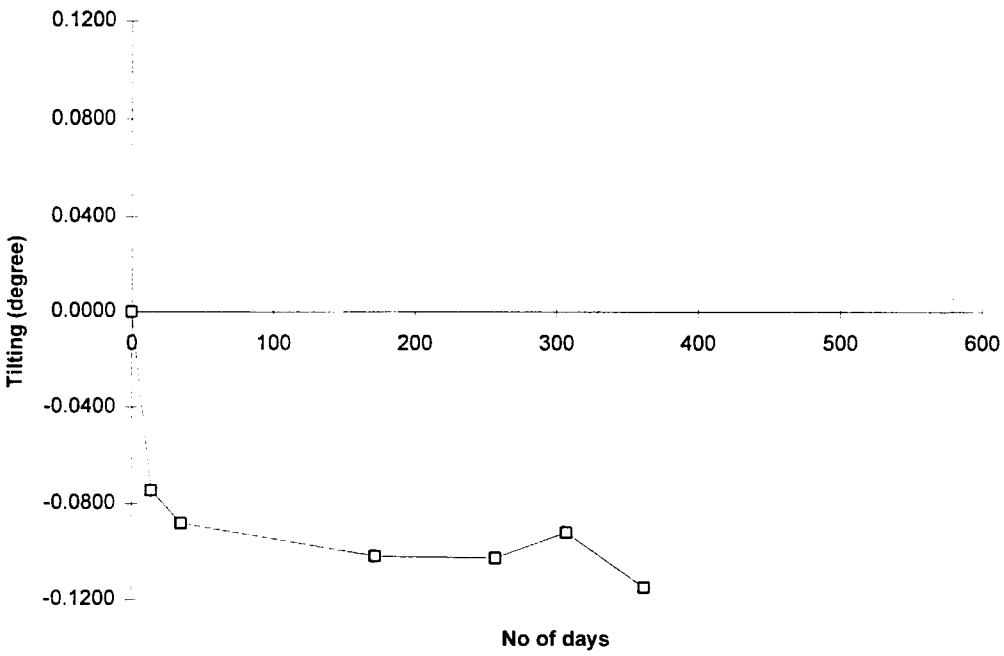

Figure B.34 Tilting of Forward Abutment - Phase II (Bridge E)

Date	No of days	Construction Stages	Settlement (inches)		
			Field Data	Theoretical Data	
				1*	2**
4/1/94	0	Footing (I)	0.00	0.00	0.00
4/26/94	25	Wall (I)	0.11	0.12	0.13
5/24/94	53	Backfilling over Footing and Wall (I)	0.13	0.19	0.21
6/22/94	82	Beam (I)	0.72	0.25	0.29
7/29/94	119	Deck and Parapet (I)	0.88	0.30	0.35
9/29/94	181		1.04	0.30	0.37
11/29/94	242		1.21	0.30	0.39
3/29/95	362		1.37	0.30	0.41
9/29/95	546		1.39	0.30	0.42

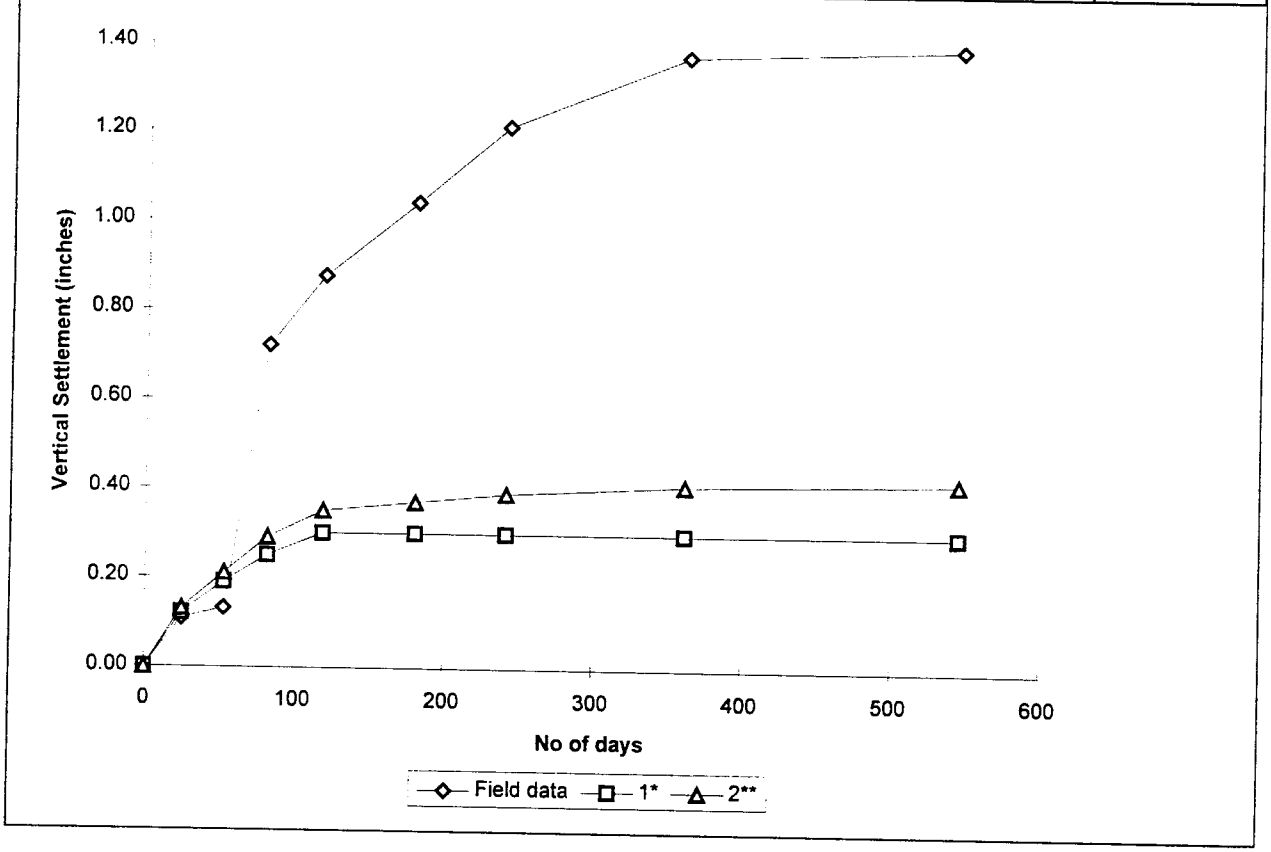

Figure B.35 Comparison Settlement data of Rear Abutment - Phase I Foundation (Bridge E)

* Elastic Settlement Only

**Elastic and Partial Consolidation Settlement

Date	No of days	Construction Stages	Settlement (inches)		
			Field Data	Theoretical Data	
				1*	2**
4/7/94	0	Footing (I)	0.00	0.00	0.00
4/14/94	7	Column (I)	0.01	0.02	0.03
4/26/94	19	Backfilling over Footing (I)	0.14	0.06	0.07
5/13/94	36	Pier Cap (I)	0.19	0.07	0.09
6/22/94	76	Beam (I)	0.49	0.25	0.28
7/29/94	113	Deck and Parapet (I)	0.59	0.39	0.46
11/29/94	236		0.71	0.39	0.53
3/29/95	356		0.79	0.39	0.57
9/29/95	540		0.82	0.39	0.61

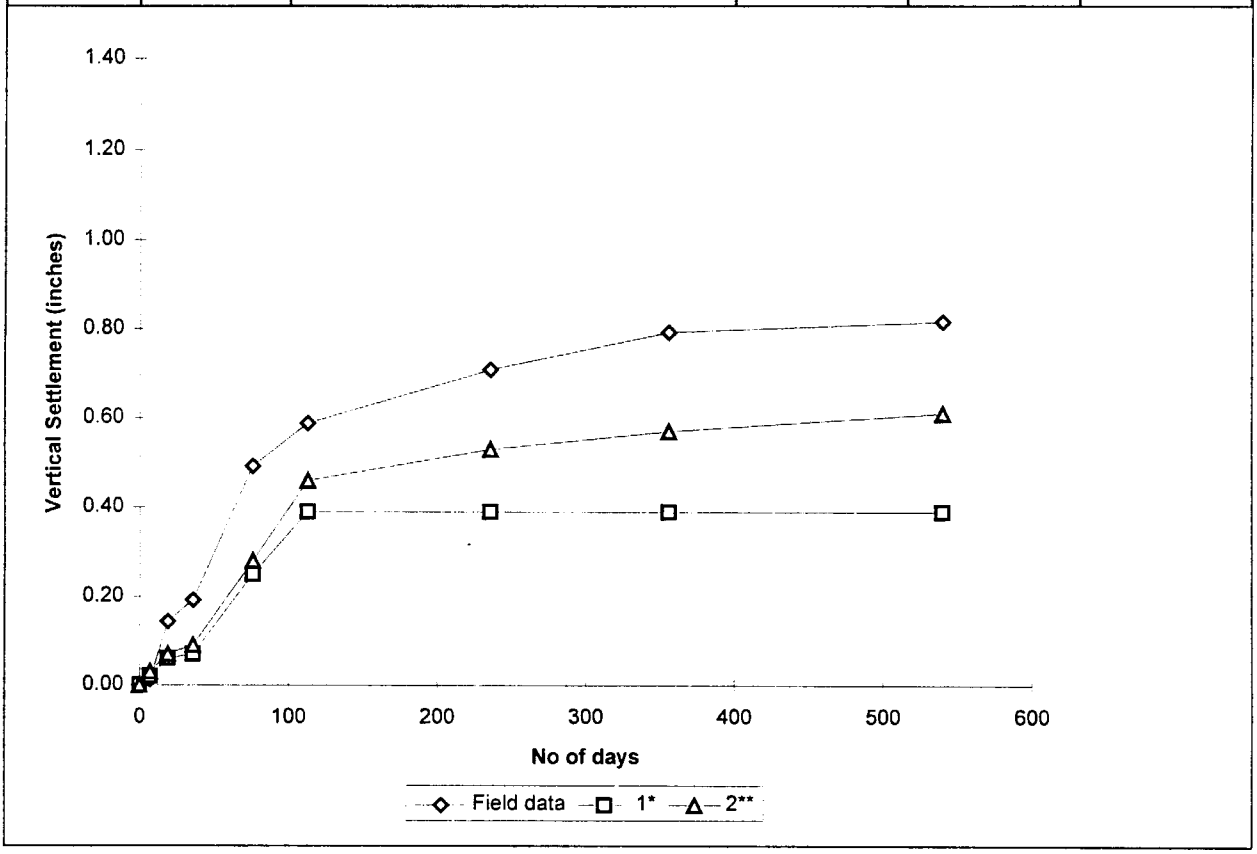

Figure B.36 Comparison Settlement data of Pier 1 - Phase I Foundation (Bridge E)

* Elastic Settlement Only

**Elastic and Partial Consolidation Settlement

Date	No of days	Construction Stages	Settlement (inches)		
			Field Data	Theoretical Data	
				1*	2**
3/29/94	0	Footing (I)	0.00	0.00	0.00
4/26/94	28	Wall (I)	0.07	0.10	0.12
5/13/94	45	Backfilling over Footing (I)	0.11	0.18	0.21
6/22/94	85	Beam (I)	0.19	0.30	0.36
7/29/94	122	Deck and Parapet (I)	0.28	0.41	0.50
9/29/94	184		0.31	0.41	0.54
11/29/94	245		0.40	0.41	0.57
3/29/95	365		0.37	0.41	0.60
9/29/95	549		0.50	0.41	0.63

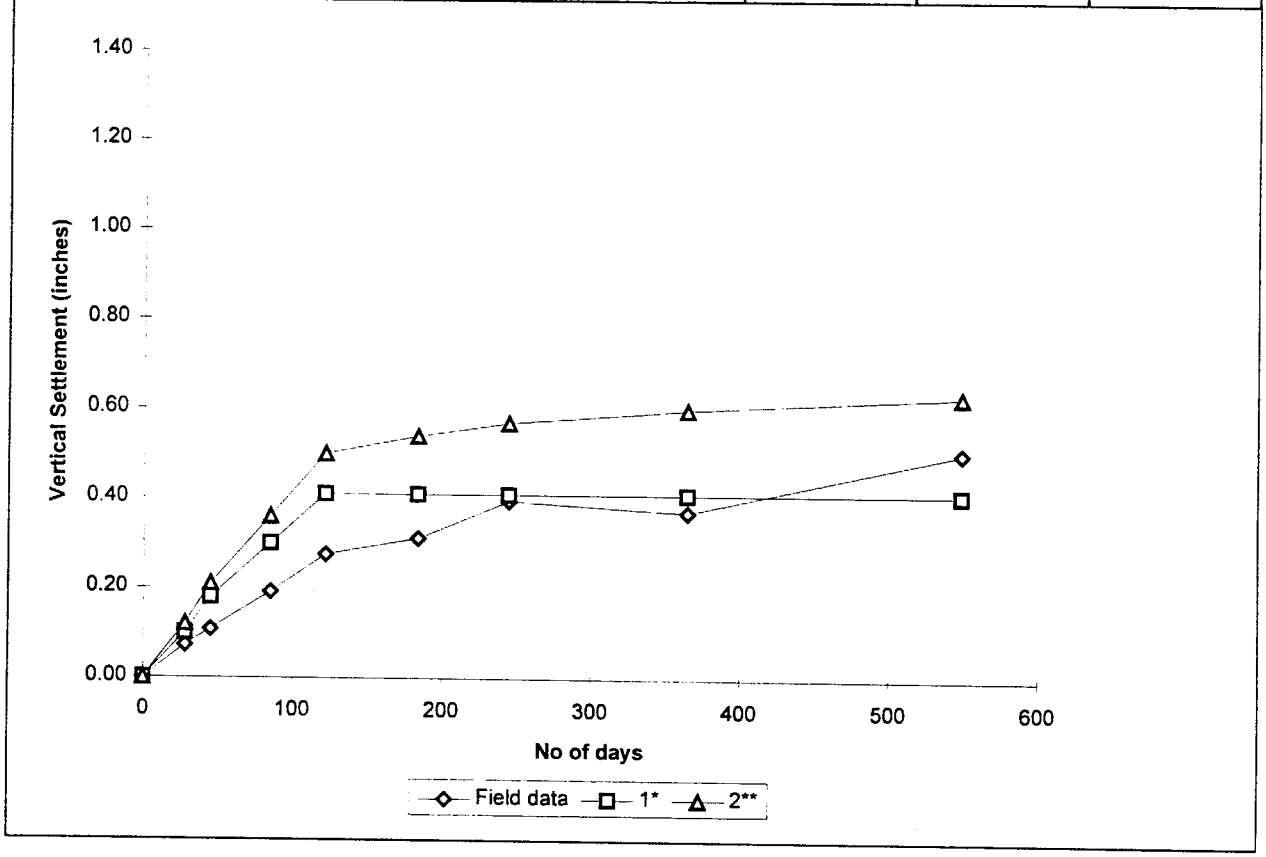

Figure B.37 Comparison Settlement data of Pier 3 - Phase I Foundation (Bridge E)

* Elastic Settlement Only

**Elastic and Partial Consolidation Settlement

Date	No of days	Construction Stages	Settlement (inches)		
			Field Data	Theoretical Data	
				1*	2**
3/29/94	0	Footing (I)	0.00	0.00	0.00
5/13/94	45	Wall (I)	0.14	0.13	0.16
5/24/94	56	Backfilling over Footing (I)	0.23	0.18	0.22
6/22/94	85	Beam (I)	0.30	0.30	0.36
7/29/94	122	Deck and Parapet (I)	0.47	0.43	0.53
9/29/94	184		0.48	0.43	0.59
11/29/94	245		0.48	0.43	0.63
3/29/95	365		0.48	0.43	0.67
9/29/95	549		0.58	0.43	0.71

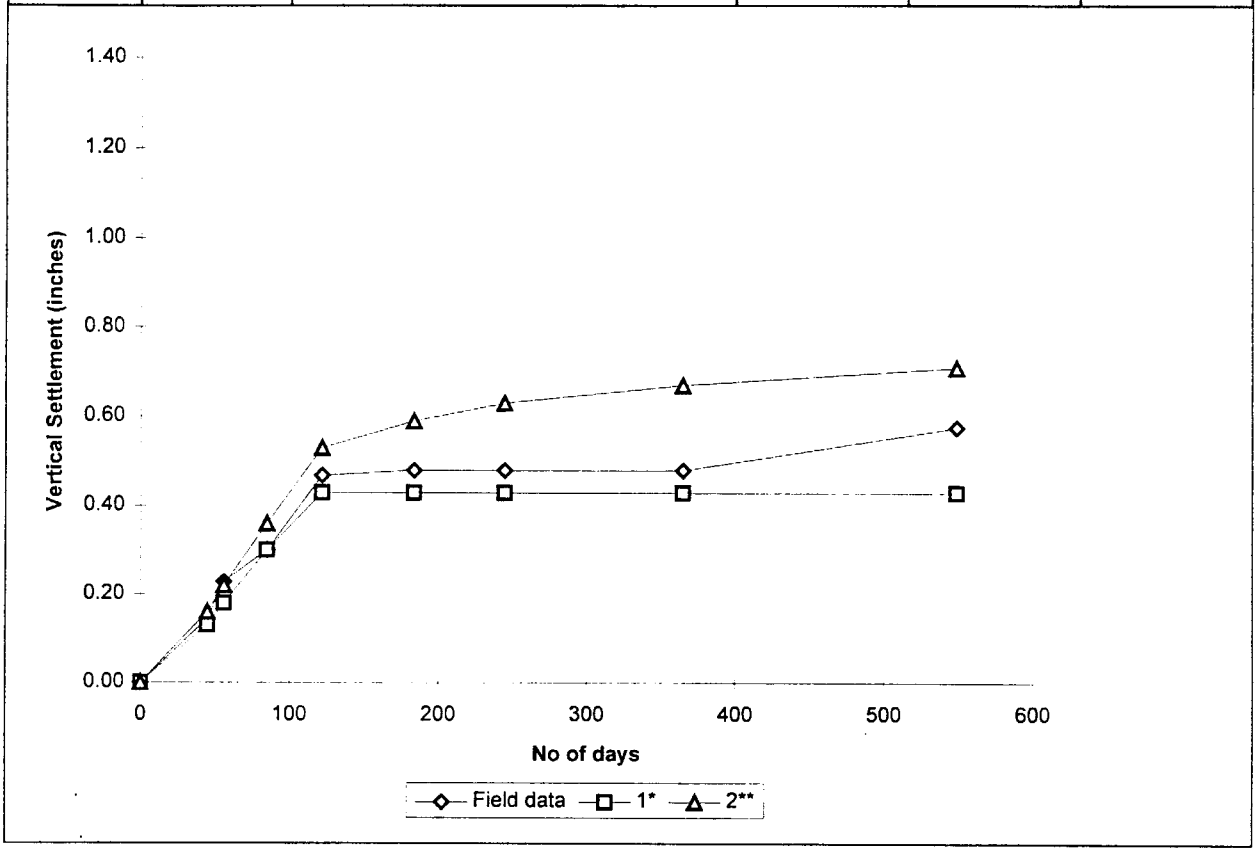

Figure B.38 Comparison Settlement data of Pier 4 - Phase I Foundation (Bridge E)

* Elastic Settlement Only

**Elastic and Partial Consolidation Settlement

Date	No of days	Construction Stages	Settlement (inches)		
			Field Data	Theoretical Data	
				1*	2**
3/29/94	0	Footing, Column (I)	0.00	0.00	0.00
4/7/94	9	Backfilling over Footing (I)	0.07	0.04	0.05
4/14/94	16	Pier Cap (I)	0.07	0.07	0.09
7/12/94	105	Beam (I)	0.16	0.18	0.26
7/29/94	122	Deck and Parapet (I)		0.26	0.37
9/29/94	184			0.26	0.43
11/29/94	245		0.19	0.26	0.48
3/29/95	365			0.26	0.53
9/29/95	549			0.26	0.59

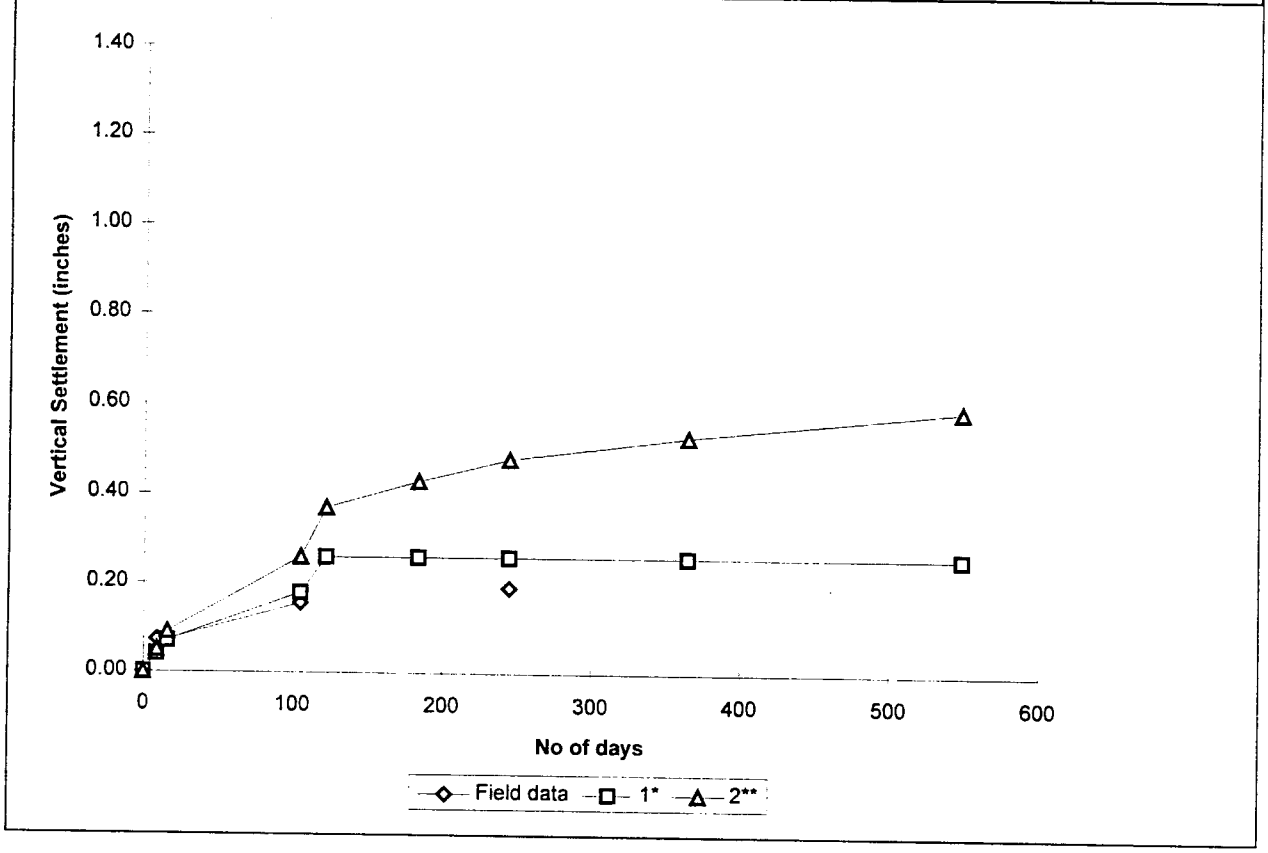

Figure B.39 Comparison Settlement data of Pier 5 - Phase I Foundation (Bridge E)

* Elastic Settlement Only

**Elastic and Partial Consolidation Settlement

Date	No of days	Construction Stages	Settlement (inches)		
			Field Data	Theoretical Data	
				1*	2**
3/22/94	0	Footing (I)	0.00	0.00	0.00
4/7/94	16	Column (I)	0.07	0.01	0.03
4/26/94	35	Pier Cap, Backfilling (I)	0.08	0.07	0.10
7/12/94	112	Beam (I)	0.28	0.17	0.25
7/29/94	129	Deck and Parapet (I)	0.34	0.26	0.38
9/29/94	191		0.43	0.26	0.45
11/29/94	252		0.31	0.26	0.49
3/29/95	372		0.32	0.26	0.55
9/29/95	556		0.38	0.26	0.60

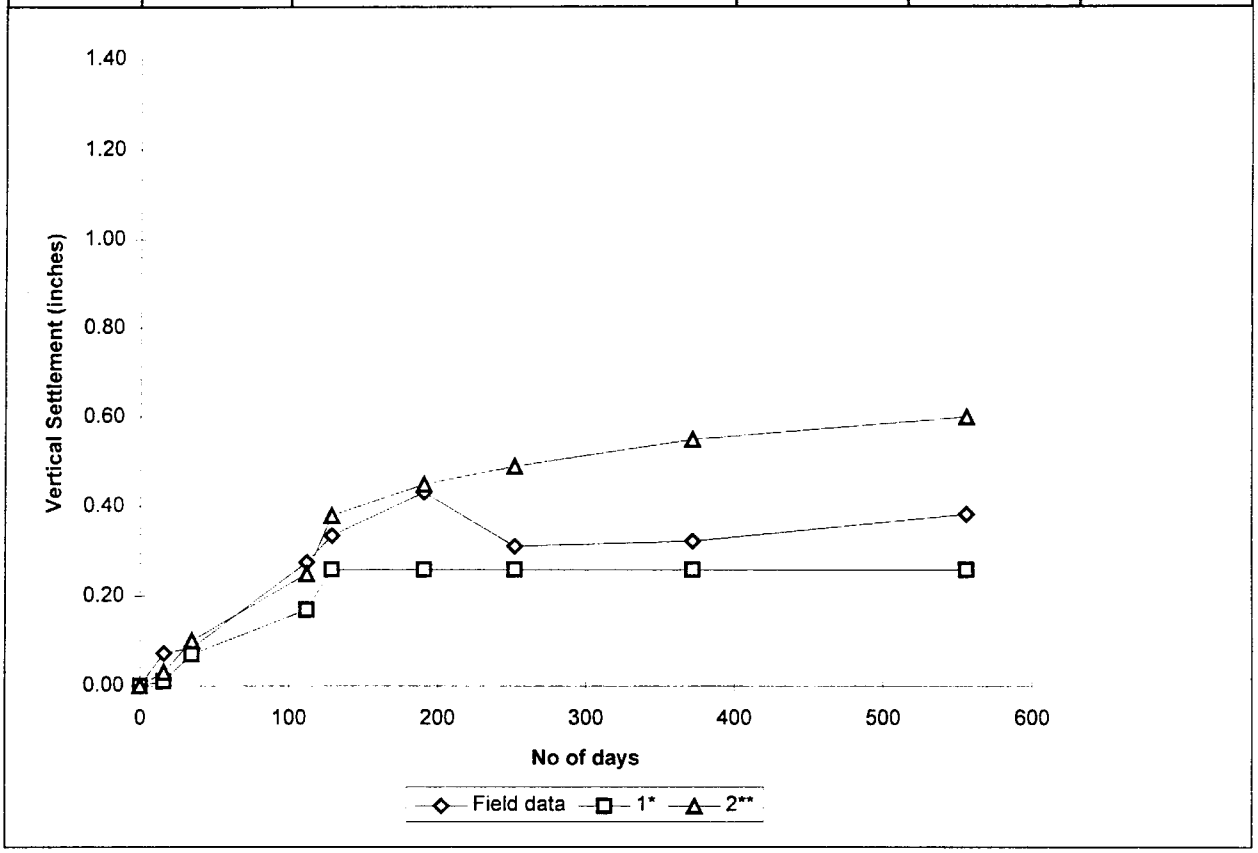

Figure B.40 Comparison Settlement data of Pier 6 - Phase I Foundation (Bridge E)

* Elastic Settlement Only

**Elastic and Partial Consolidation Settlement

Date	No of days	Construction Stages	Settlement (inches)		
			Field Data	Theoretical Data	
				1*	2**
3/22/94	0	Footing (I)	0.00	0.00	0.00
4/7/94	16	Column (I)	0.07	0.02	0.04
5/13/94	52	Pier Cap, Backfilling (I)	0.18	0.07	0.11
7/12/94	112	Beam (I)	0.26	0.21	0.29
7/29/94	129	Deck and Parapet (I)	0.36	0.33	0.44
9/29/94	191		0.37	0.33	0.53
11/29/94	252		0.42	0.33	0.57
3/29/95	372			0.33	0.63
9/29/95	556			0.33	0.68

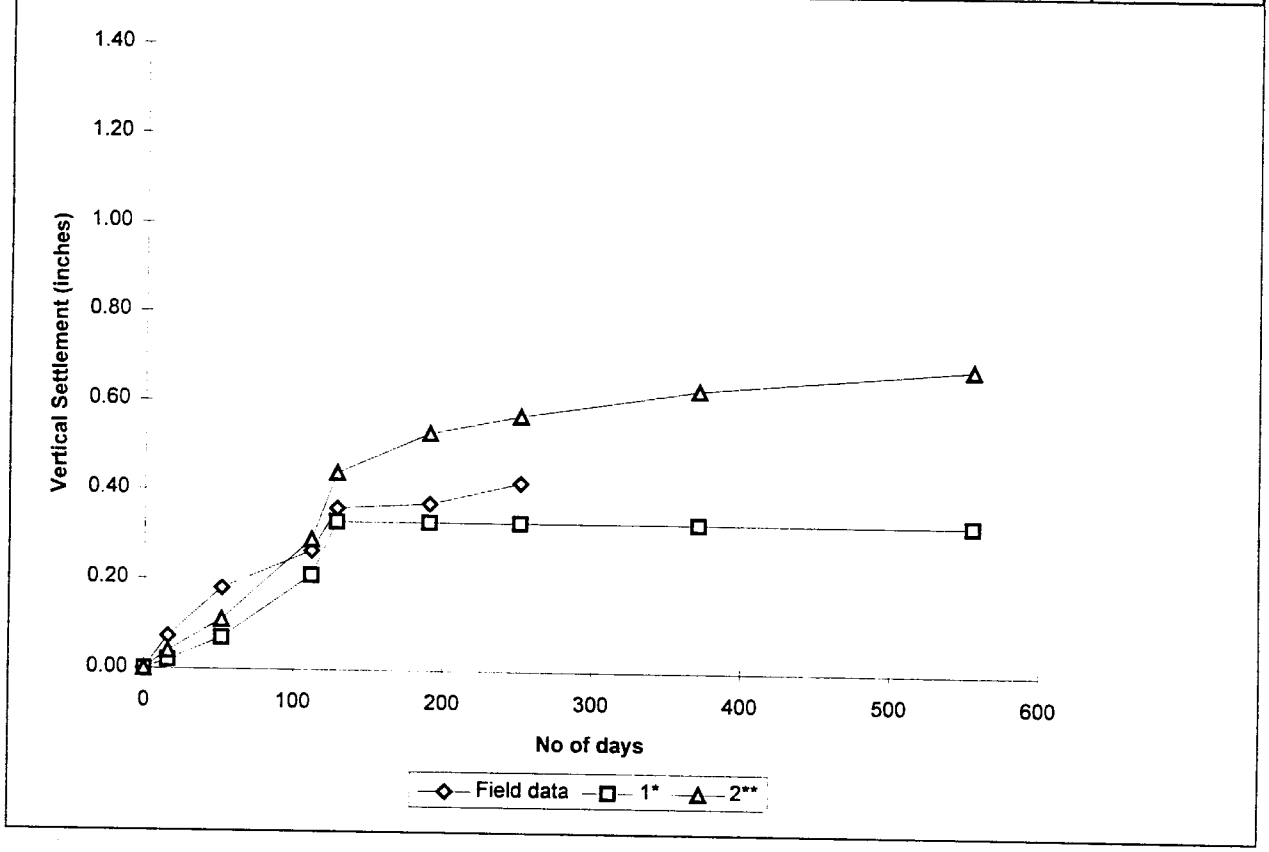

Figure B.41 Comparison Settlement data of Pier 7 - Phase I Foundation (Bridge E)

* Elastic Settlement Only

**Elastic and Partial Consolidation Settlement

Date	No of days	Construction Stages	Settlement (inches)		
			Field Data	Theoretical Data	
				1*	2**
3/22/94	0	Footing, Column (I)	0.00	0.00	0.00
4/14/94	23	Pier Cap (I)	0.13	0.03	0.05
4/26/94	35	Backfillling over Footing (I)	0.11	0.07	0.09
7/12/94	112	Beam (I)	0.35	0.19	0.26
7/29/94	129	Deck and Parapet (I)	0.41	0.27	0.36
9/29/94	191		0.40	0.27	0.43
11/29/94	252		0.43	0.27	0.47
3/29/95	372		0.47	0.27	0.52
9/29/95	556		0.47	0.27	0.58

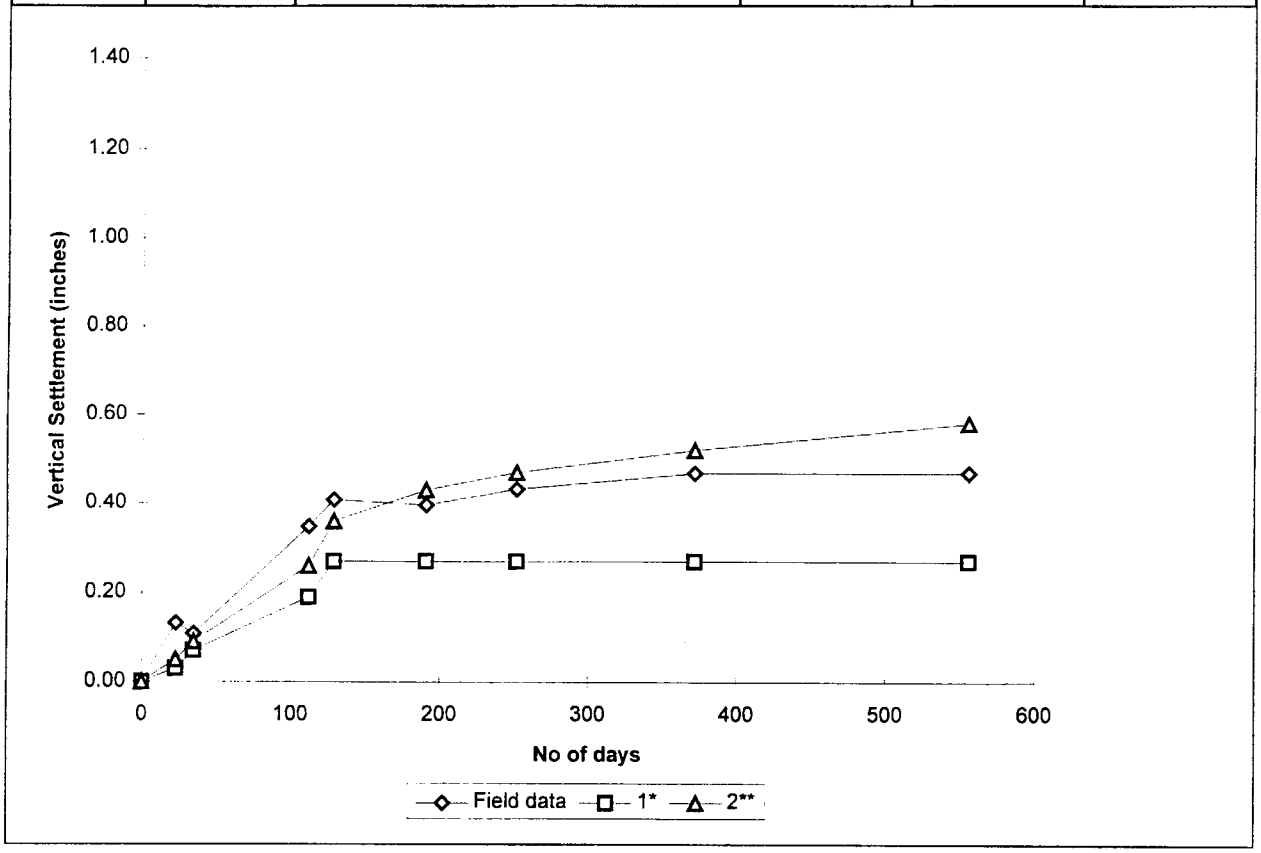

Figure B.42 Comparison Settlement data of Pier 8 - Phase I Foundation (Bridge E)

* Elastic Settlement Only

**Elastic and Partial Consolidation Settlement

Date	No of days	Construction Stages	Settlement (inches)		
			Field Data	Theoretical Data	
				1*	2**
3/22/94	0	Footing (I)	0.00	0.00	0.00
3/29/94	7	Wall (I)	0.04	0.07	0.08
6/22/94	92	Backfilling over Footing (I)	0.19	0.10	0.17
7/29/94	129	Beam, Deck and Parapet (I)	0.28	0.17	0.26
9/29/94	191		0.34	0.17	0.30
11/29/94	252			0.17	0.32
3/29/95	372			0.17	0.36
9/29/95	556		0.37	0.17	0.38

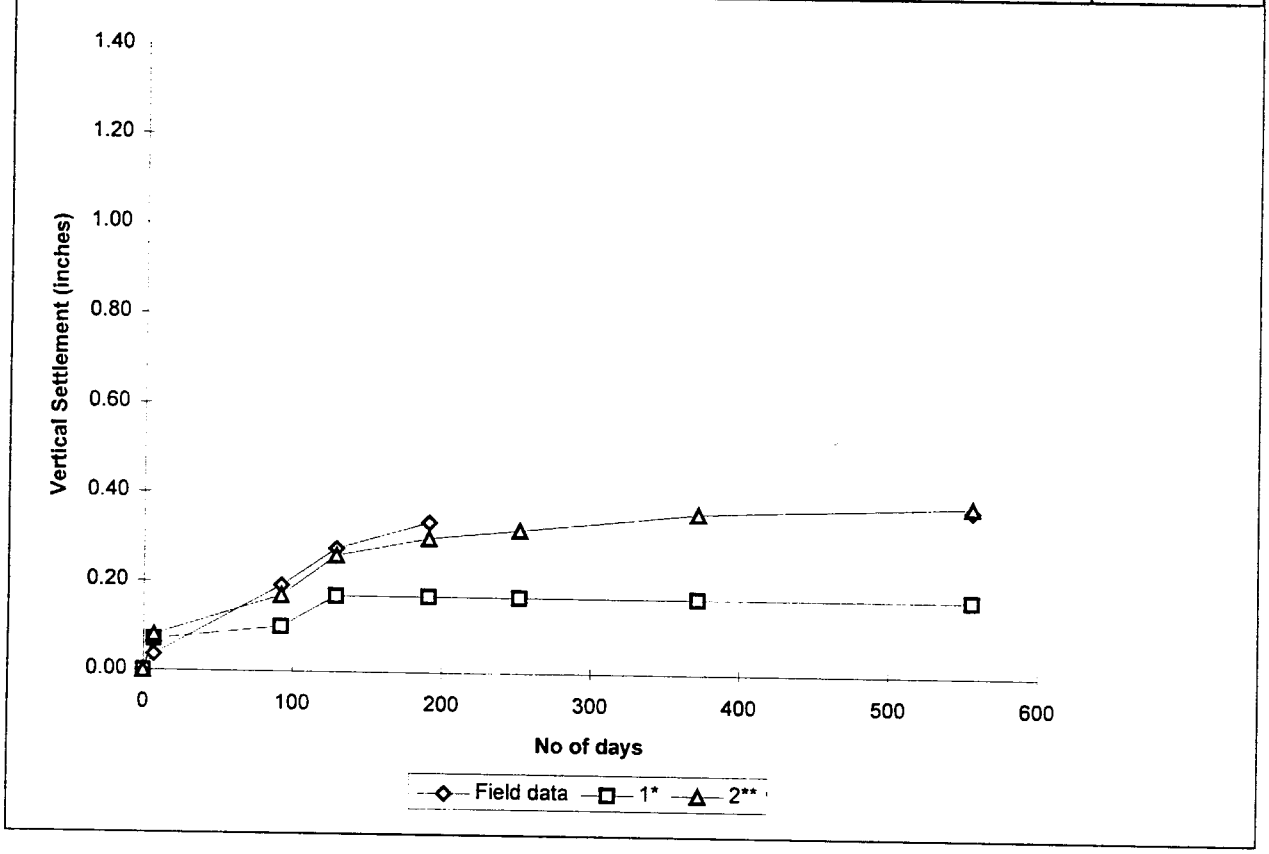

Figure B.43 Comparison Settlement data of Forward Abutment - Phase I Foundation (Bridge E)

* Elastic Settlement Only

**Elastic and Partial Consolidation Settlement

Date	No of days	Construction Stages	Settlement (inches)		
			Field Data	Theoretical Data	
				1*	2**
9/10/94	0	Footing (II)	0.00	0.00	0.00
9/25/94	15	Wall (II)	0.05	0.12	0.13
10/16/94	36	Backfilling over Footing (II)	0.10	0.19	0.21
11/6/94	57	Beam, Backfilling Wall (II)	0.18	0.25	0.28
3/23/95	194	Deck and Parapet (II)	0.26	0.30	0.37
5/23/95	255			0.30	0.38
7/23/95	316			0.30	0.39
9/23/95	378		0.34	0.30	0.40
11/23/95	439			0.30	0.40

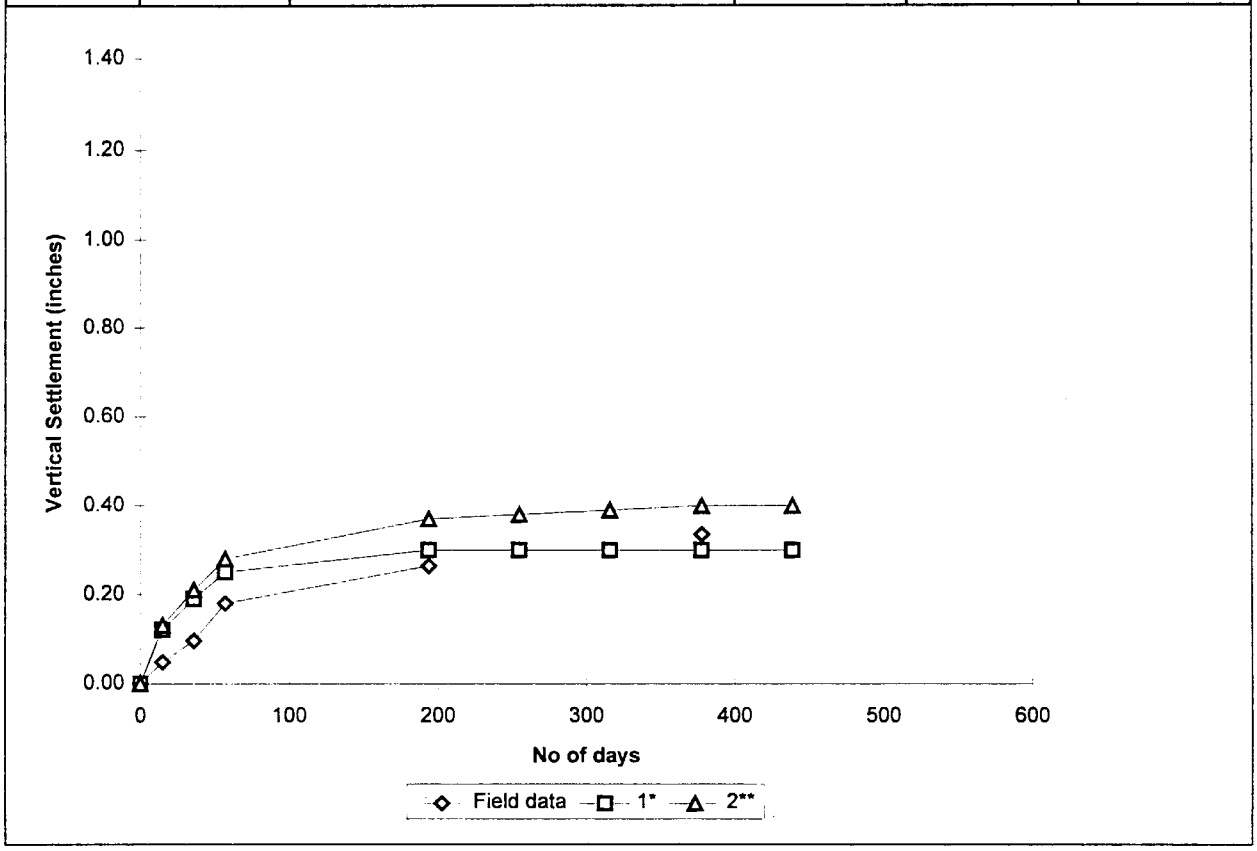

Figure B.44 Comparison Settlement data of Rear Abutment - Phase II Foundation (Bridge E)

* Elastic Settlement Only

**Elastic and Partial Consolidation Settlement

Date	No of days	Construction Stages	Settlement (inches)		
			Field Data	Theoretical Data	
				1*	2**
9/18/94	0	Footing (II)	0.00	0.00	0.00
10/2/94	14	Column, Pier Cap (II)	0.11	0.09	0.10
11/6/94	49	Beam, Backfilling over Footing (II)	0.43	0.33	0.36
3/23/95	186	Deck and Parapet (II)	0.80	0.52	0.62
5/29/95	253			0.52	0.66
7/29/95	314			0.52	0.68
9/29/95	376		0.77	0.52	0.70
11/29/95	437			0.52	0.72
1/29/96	498			0.52	0.73

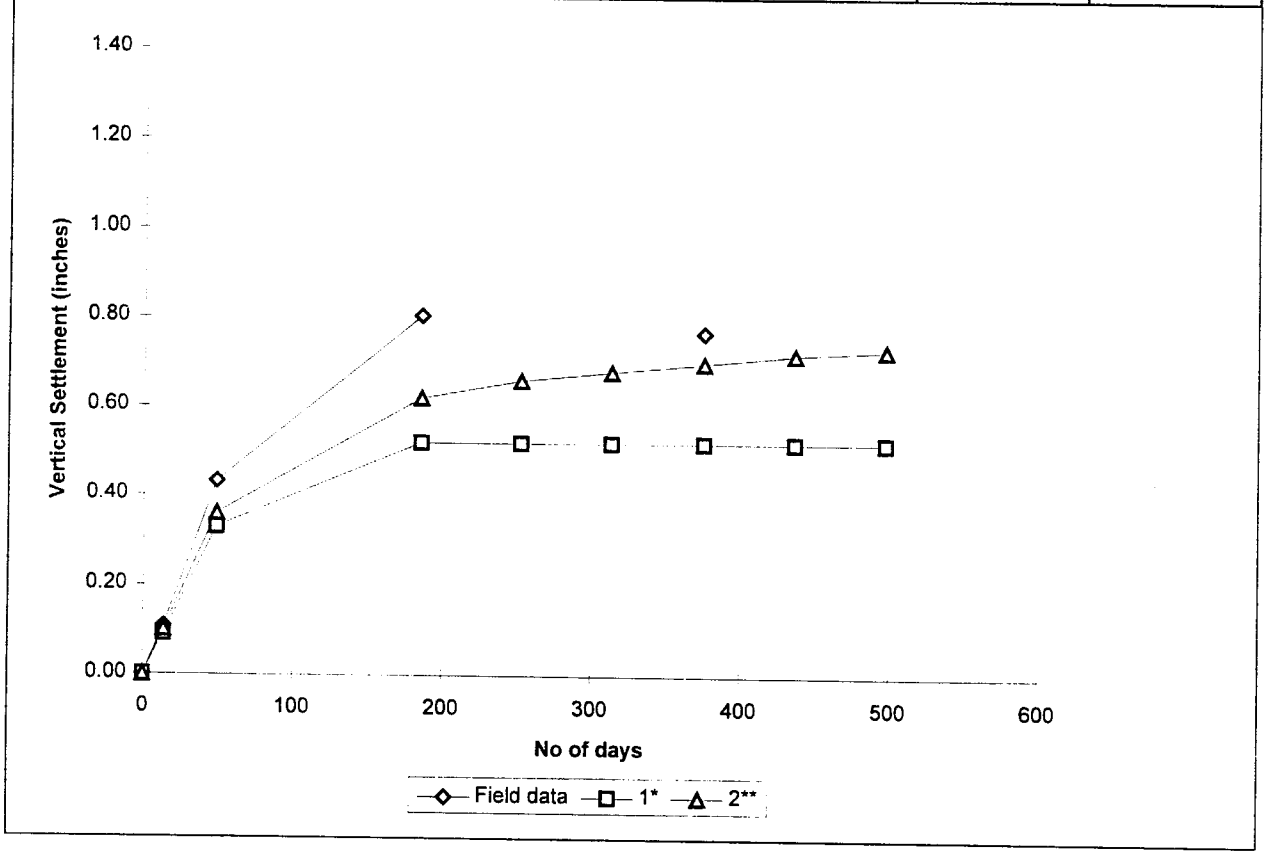

Figure B.45 Comparison Settlement data of Pier 1 - Phase II Foundation (Bridge E)

* Elastic Settlement Only

**Elastic and Partial Consolidation Settlement

Date	No of days	Construction Stages	Settlement (inches)		
			Field Data	Theoretical Data	
				1*	2**
9/10/94	0	Footing, Column (II)	0.00	0.00	0.00
9/18/94	8	Pier Cap, Backfilling (II)	0.07	0.10	0.11
11/6/94	57	Beam (II)	0.22	0.33	0.38
3/23/95	194	Deck and Parapet (II)	0.24	0.52	0.69
5/29/95	261			0.52	0.75
7/29/95	322			0.52	0.78
9/29/95	384		0.42	0.52	0.81
11/29/95	445			0.52	0.82
1/29/96	506			0.52	0.84

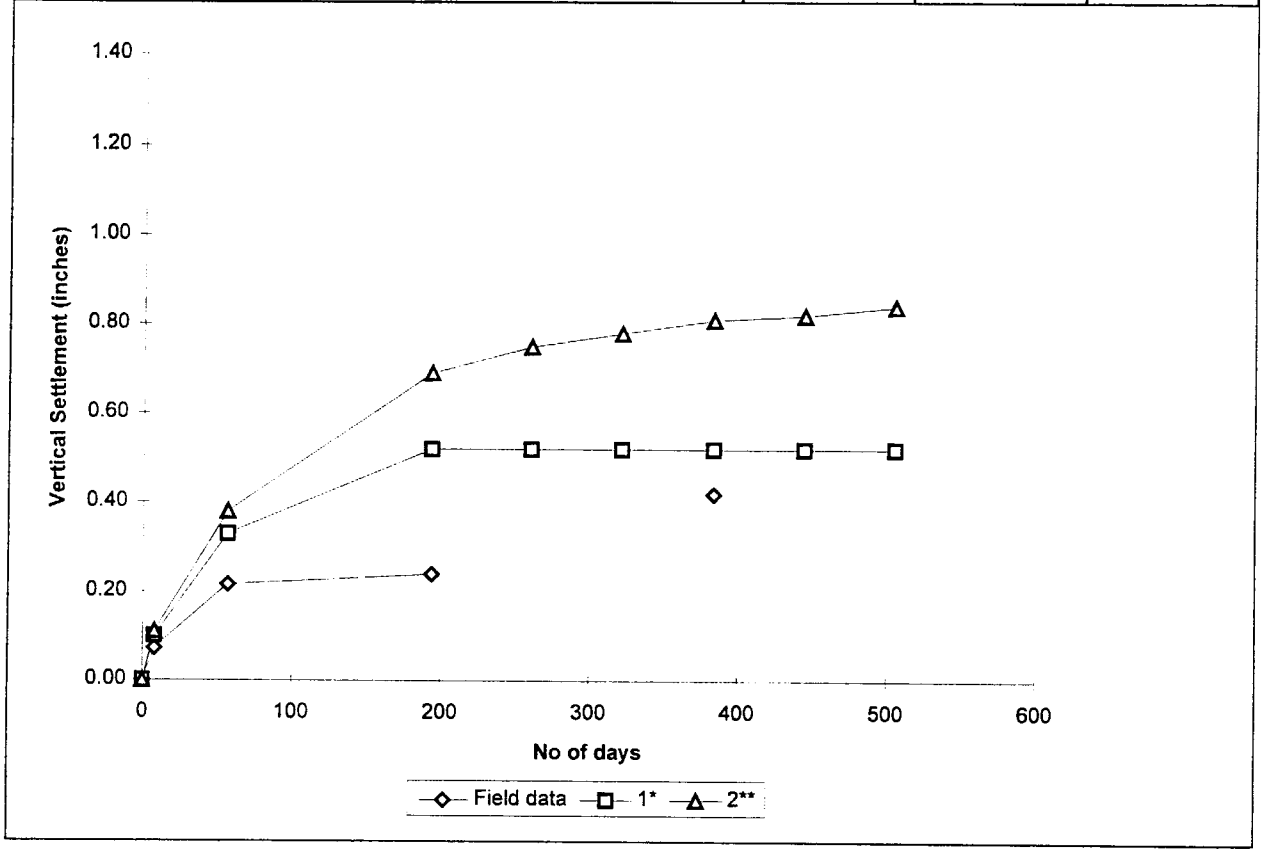

Figure B.46 Comparison Settlement data of Pier 2 - Phase II Foundation (Bridge E)

* Elastic Settlement Only

**Elastic and Partial Consolidation Settlement

Date	No of days	Construction Stages	Settlement (inches)		
			Field Data	Theoretical Data	
				1*	2**
9/18/94	0	Footing (II)	0.00	0.00	0.00
10/2/94	14	Wall, Backfilling over Footing (II)	0.07	0.25	0.27
11/6/94	49	Beam (II)	0.18	0.43	0.50
3/23/95	186	Deck and Parapet (II)	0.31	0.60	0.79
5/29/95	253			0.60	0.85
7/29/95	314			0.60	0.88
9/29/95	376		0.48	0.60	0.90
11/29/95	437			0.60	0.92
1/29/96	498			0.60	0.93

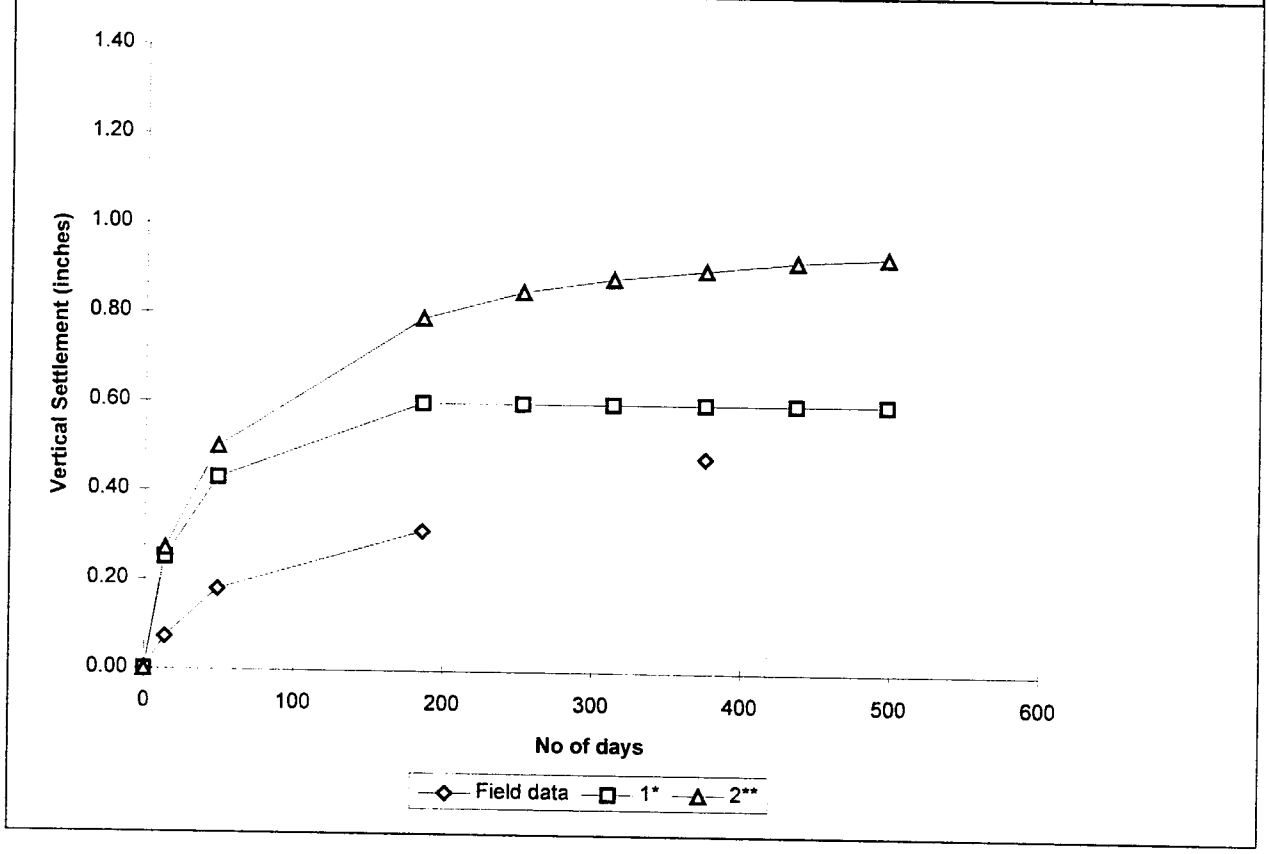

Figure B.47 Comparison Settlement data of Pier 3 - Phase II Foundation (Bridge E)

* Elastic Settlement Only

**Elastic and Partial Consolidation Settlement

Date	No of days	Construction Stages	Settlement (inches)		
			Field Data	Theoretical Data	
				1*	2**
9/10/94	0	Footing (II)	0.00	0.00	0.00
9/18/94	8	Wall, Backfilling over Footing (II)	0.00	0.18	0.19
11/6/94	57	Beam (II)	0.02	0.30	0.38
3/23/95	194	Deck and Parapet (II)	0.12	0.43	0.63
5/29/95	261			0.43	0.69
7/29/95	322			0.43	0.72
9/29/95	384		0.13	0.43	0.75
11/29/95	445			0.43	0.76
1/29/96	506			0.43	0.78

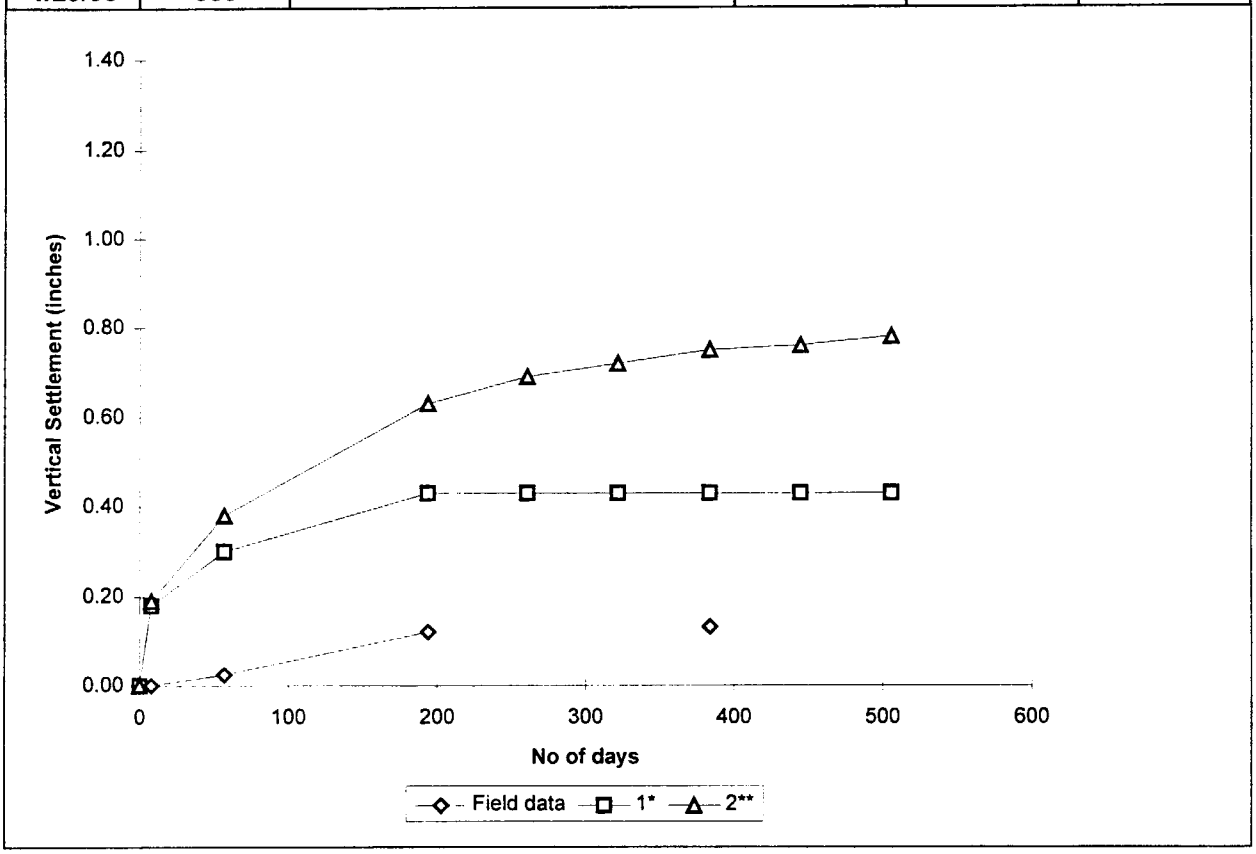

Figure B.48 Comparison Settlement data of Pier 4 - Phase II Foundation (Bridge E)

* Elastic Settlement Only

**Elastic and Partial Consolidation Settlement

Date	No of days	Construction Stages	Settlement (inches)		
			Field Data	Theoretical Data	
				1*	2**
9/1/94	0	Footing, Column (II)	0.00	0.00	0.00
9/10/94	9	Pier Cap (II)	0.02	0.04	0.05
9/18/94	17	Backfilling over Footing (II)	0.04	0.10	0.12
10/16/94	45	Beam (II)	0.11	0.22	0.27
3/23/95	203	Deck and Parapet (II)	0.11	0.32	0.49
5/23/95	264			0.32	0.54
7/23/95	325			0.32	0.58
9/23/95	387			0.32	0.60
11/23/95	448			0.32	0.62

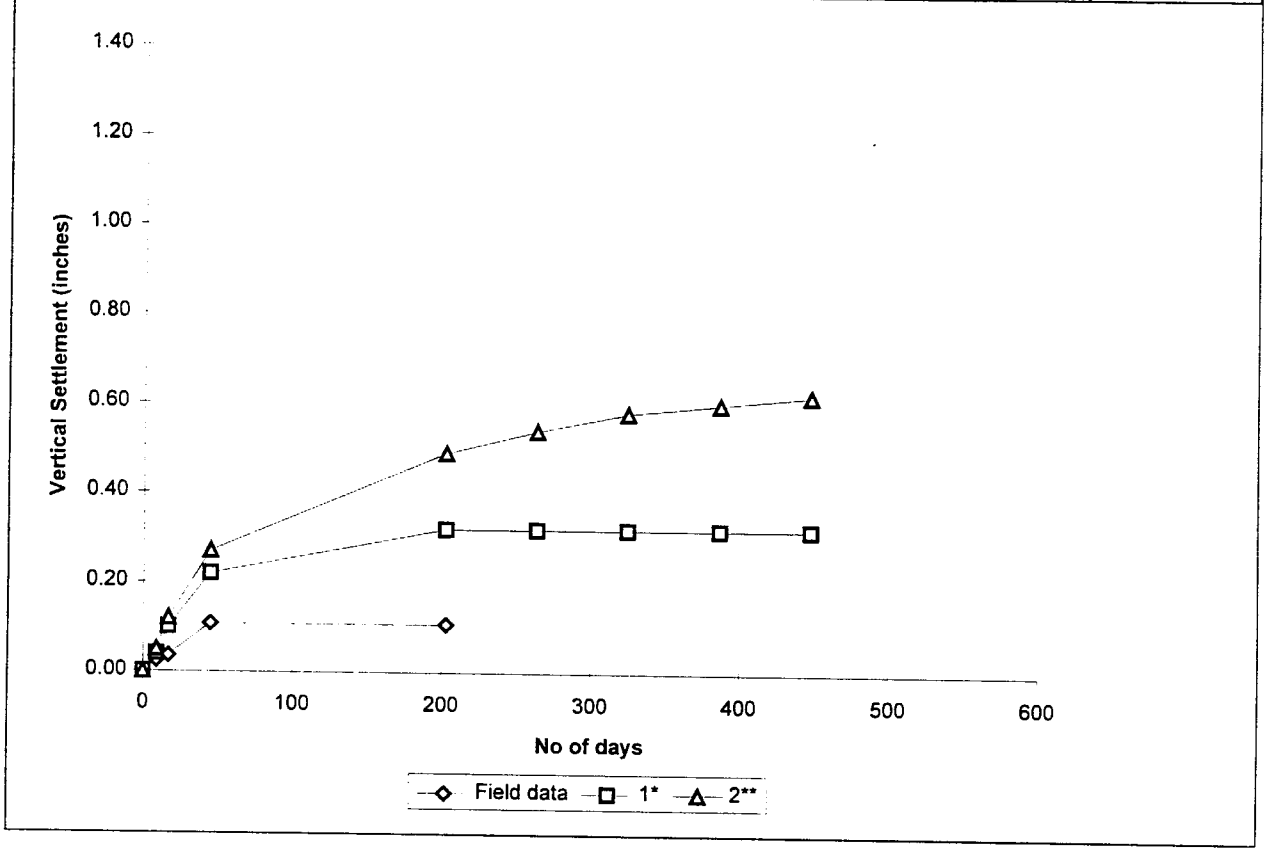

Figure B.49 Comparison Settlement data of Pier 5 - Phase II Foundation (Bridge E)

* Elastic Settlement Only

**Elastic and Partial Consolidation Settlement

Date	No of days	Construction Stages	Settlement (inches)		
			Field Data	Theoretical Data	
				1*	2**
9/1/94	0	Footing (II)	0.00	0.00	0.00
9/18/94	17	Column (II)	0.10	0.02	0.04
9/25/94	24	Pier Cap, Backfilling over Footing (II)	0.10	0.09	0.12
10/16/94	45	Beam (II)	0.25	0.22	0.27
3/23/95	203	Deck and Parapet (II)	0.29	0.31	0.50
5/23/95	264			0.31	0.55
7/23/95	325			0.31	0.58
9/23/95	387		0.29	0.31	0.61
11/23/95	448			0.31	0.63

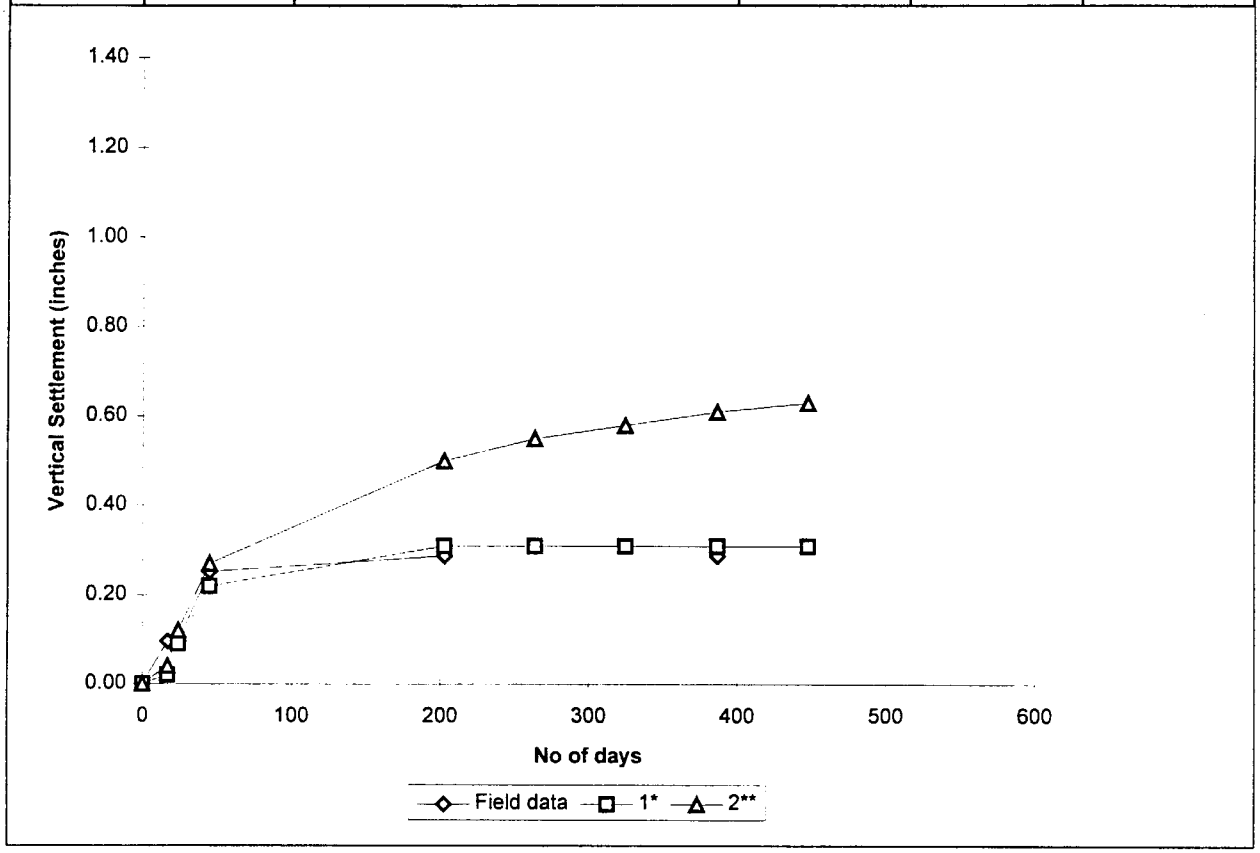

Figure B.50 Comparison Settlement data of Pier 6 - Phase II Foundation (Bridge E)

* Elastic Settlement Only

**Elastic and Partial Consolidation Settlement

Date	No of days	Construction Stages	Settlement (inches)		
			Field Data	Theoretical Data	
				1*	2**
9/1/94	0	Footing (II)	0.00	0.00	0.00
9/18/94	17	Column (II)	0.12	0.02	0.04
9/25/94	24	Pier Cap, Backfilling over Footing (II)	0.12	0.08	0.11
11/6/94	66	Beam (II)	0.17	0.20	0.26
3/23/95	203	Deck and Parapet (II)		0.29	0.48
5/23/95	264			0.29	0.53
7/23/95	325			0.29	0.57
9/23/95	387			0.29	0.59
11/23/95	448			0.29	0.61

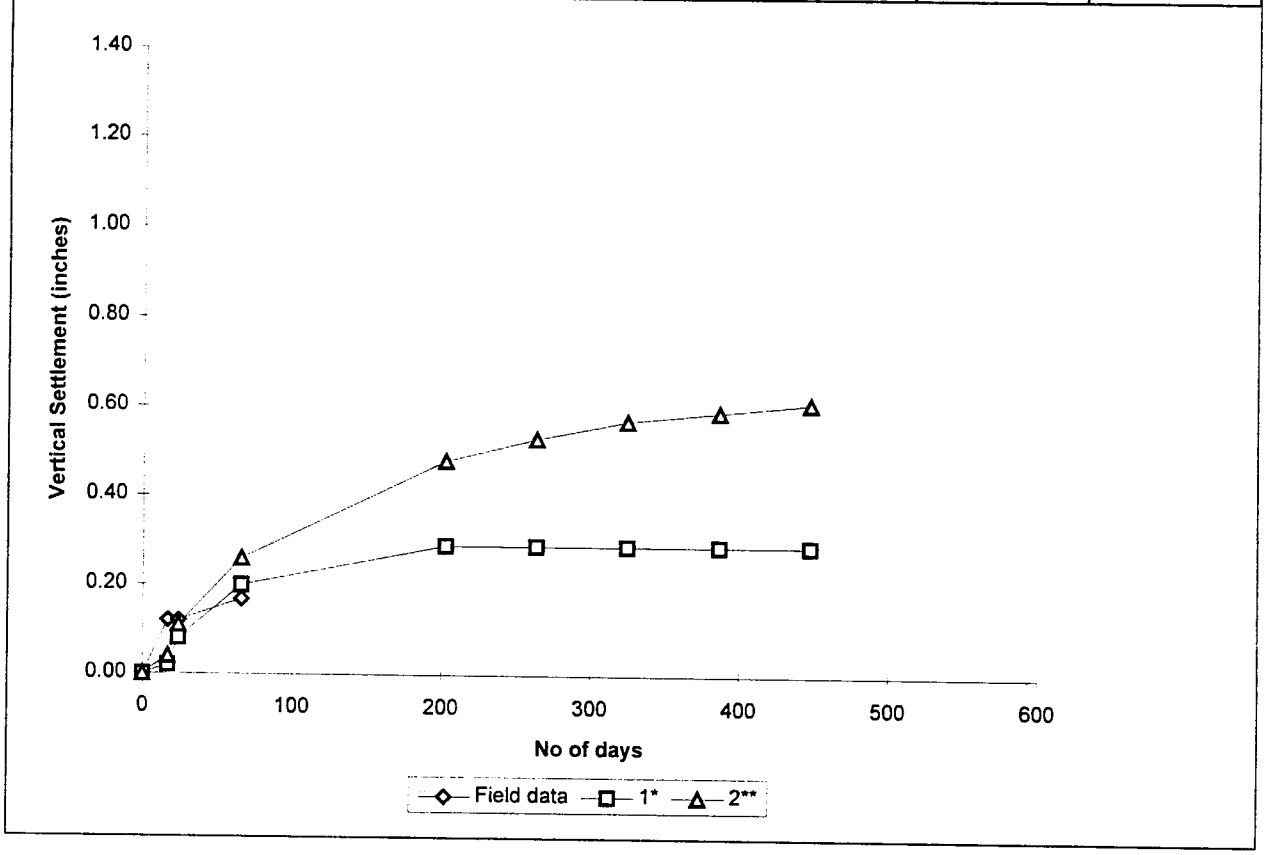

Figure B.51 Comparison Settlement data of Pier 7 - Phase II Foundation (Bridge E)

* Elastic Settlement Only

**Elastic and Partial Consolidation Settlement

Date	No of days	Construction Stages	Settlement (inches)		
			Field Data	Theoretical Data	
				1*	2**
9/1/94	0	Footing (II)	0.00	0.00	0.00
9/18/94	17	Column, Pier Cap, Backfilling (II)	0.11	0.09	0.10
10/16/94	45	Beam (II)	0.22	0.23	0.27
3/23/95	203	Deck and Parapet (II)	0.31	0.33	0.49
5/29/95	270			0.33	0.54
7/29/95	331			0.33	0.56
9/29/95	393		0.30	0.33	0.59
11/29/95	454			0.33	0.61
1/29/96	515			0.33	0.62

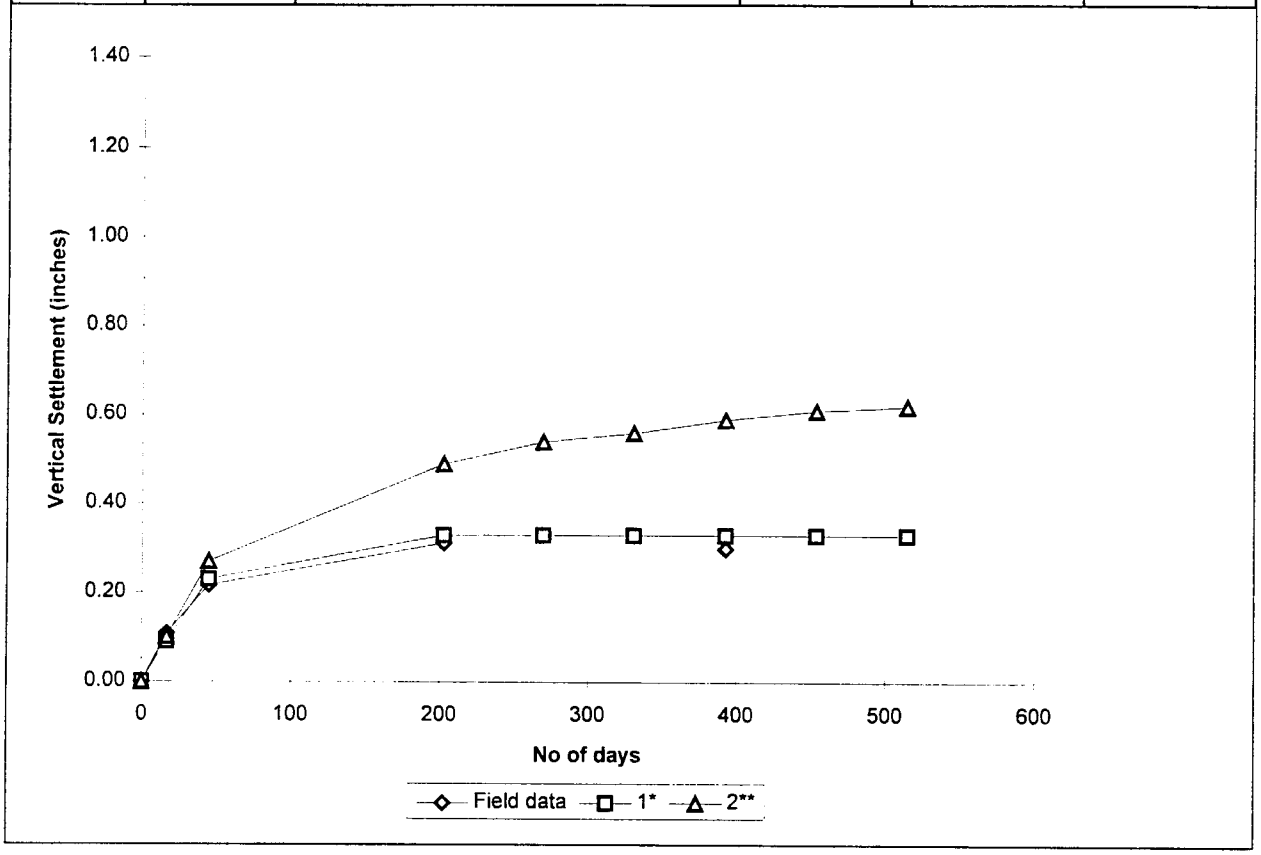

Figure B.52 Comparison Settlement data of Pier 8 - Phase II Foundation (Bridge E)

* Elastic Settlement Only

**Elastic and Partial Consolidation Settlement

Date	No of days	Construction Stages	Settlement (inches)		
			Field Data	Theoretical Data	
				1*	2**
9/1/94	0	Footing (II)	0.00	0.00	0.00
9/18/94	17	Wall (II)	0.08	0.07	0.09
9/25/94	24	Backfilling over Footing (II)	0.11	0.10	0.13
10/16/94	45	Beam (II)	0.16	0.14	0.19
3/23/95	203	Deck and Parapet (II)	0.29	0.18	0.32
5/23/95	264			0.18	0.35
7/23/95	325			0.18	0.36
9/23/95	387			0.18	0.38
11/23/95	448			0.18	0.39

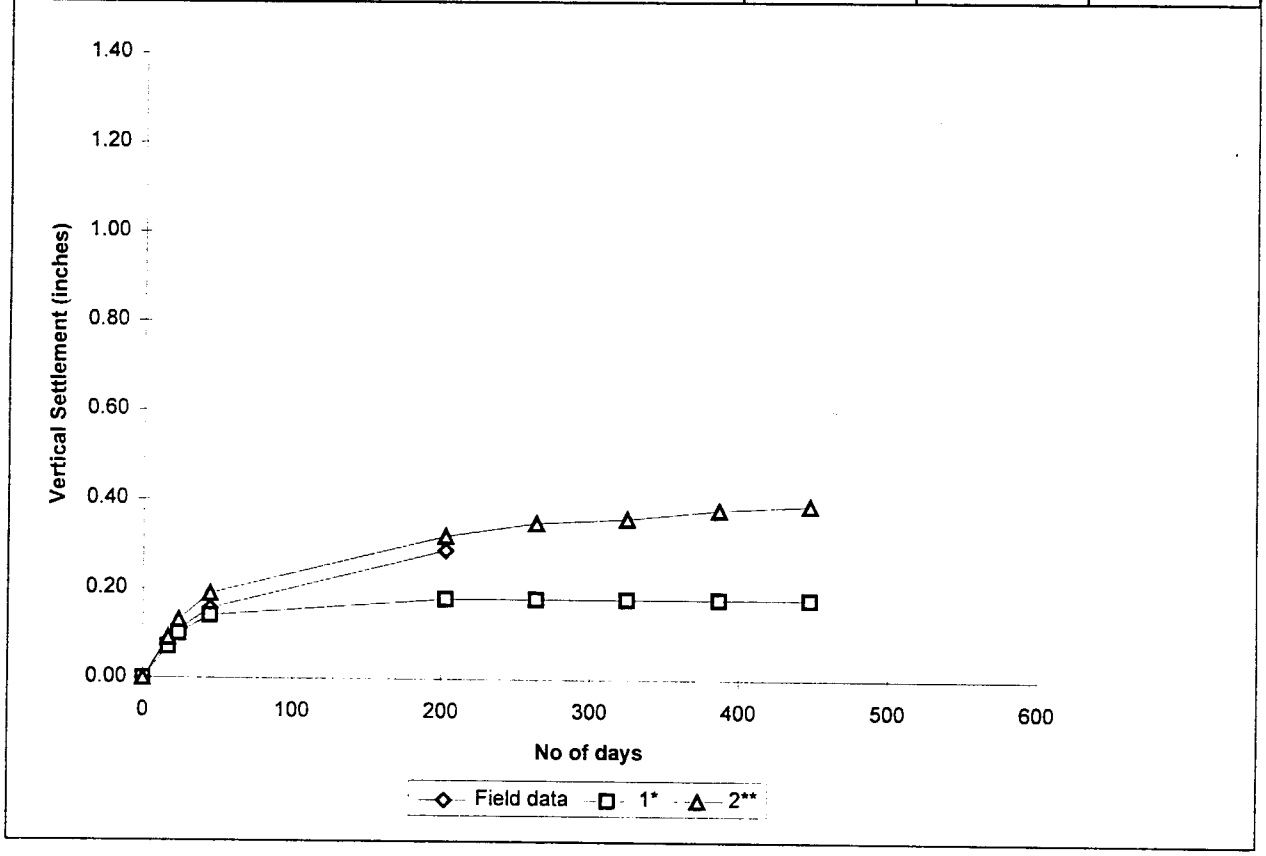

Figure B.53 Comparison Settlement data of Forward Abutment - Phase II Foundation (Bridge E)

* Elastic Settlement Only

**Elastic and Partial Consolidation Settlement

Date	No of days	Construction Stages	Pressure (tsf)					
			Field Data			Theoretical Data		
			Heel	Toe	Key	Heel	Toe	Key
1-Apr	0	Footing (I)	0.31	0.42	0.42	0.24	0.23	0.30
26-Apr	25	Wall (I)	0.58	0.64	0.84	0.56	0.55	0.56
24-May	53	Backfilling over Footing and Wall (I)	0.69	0.78	1.16	1.82	0.69	1.25
22-Jun	82	Beam (I)	1.23	1.27	3.43	2.23	0.94	1.59
29-Jul	119	Deck and Parapet (I)	1.38	1.39	4.26	2.55	1.13	1.84

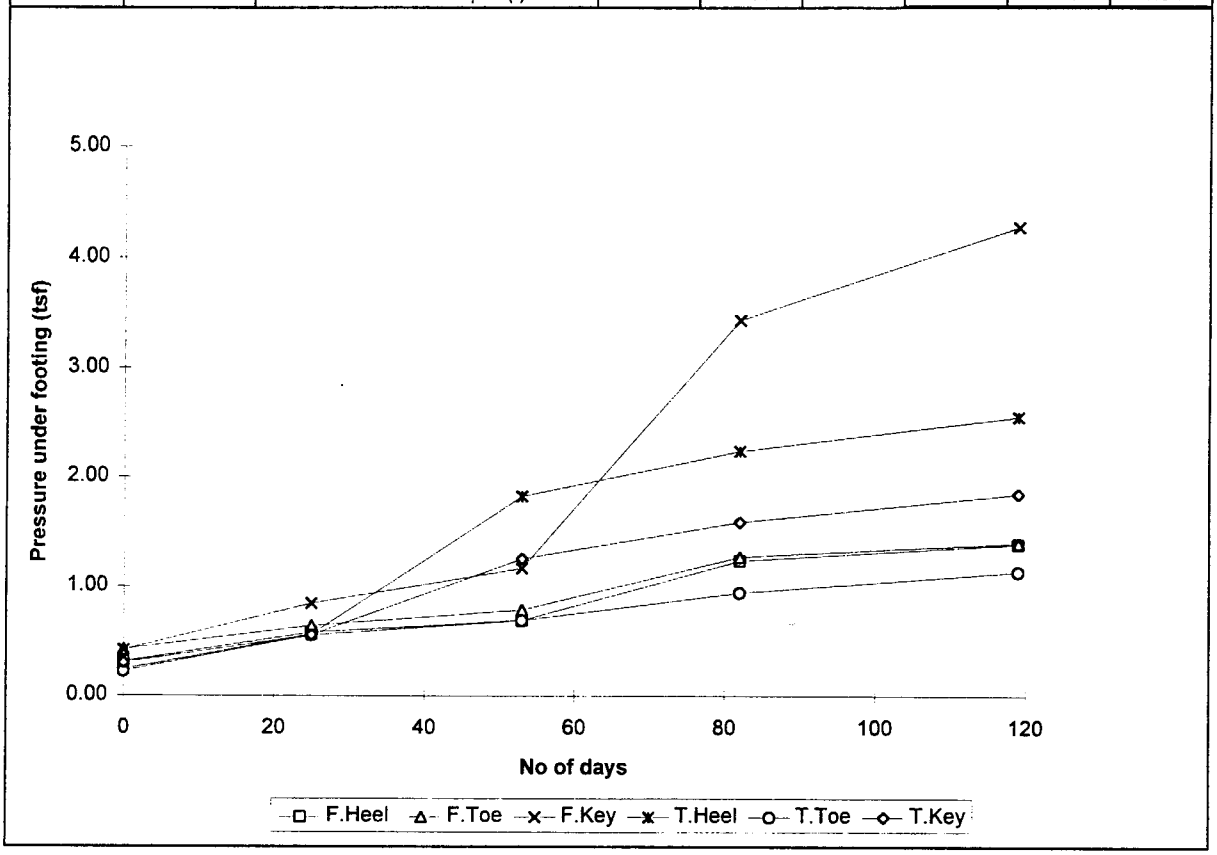

Figure B.54 Comparison Pressure under Rear Abutment - Phase I Foundation (Bridge E)

Date	No of days	Construction Stages	Pressure (tsf)				
			NW	NE	SW	SE	Theoretical
7-Apr	0	Footing (I)	0.22	0.54	0.32	0.36	0.23
14-Apr	7	Column (I)	0.19	0.53	0.35	0.88	0.29
26-Apr	19	Backfilling over Footing (I)	0.39	0.99	0.64	1.40	0.50
13-May	36	Pier Cap (I)	0.43	1.12	0.67	1.44	0.58
22-Jun	76	Beam (I)	1.11	2.46	1.52	2.66	1.51
29-Jul	113	Deck and Parapet (I)	1.30	2.73	1.85	3.24	2.22

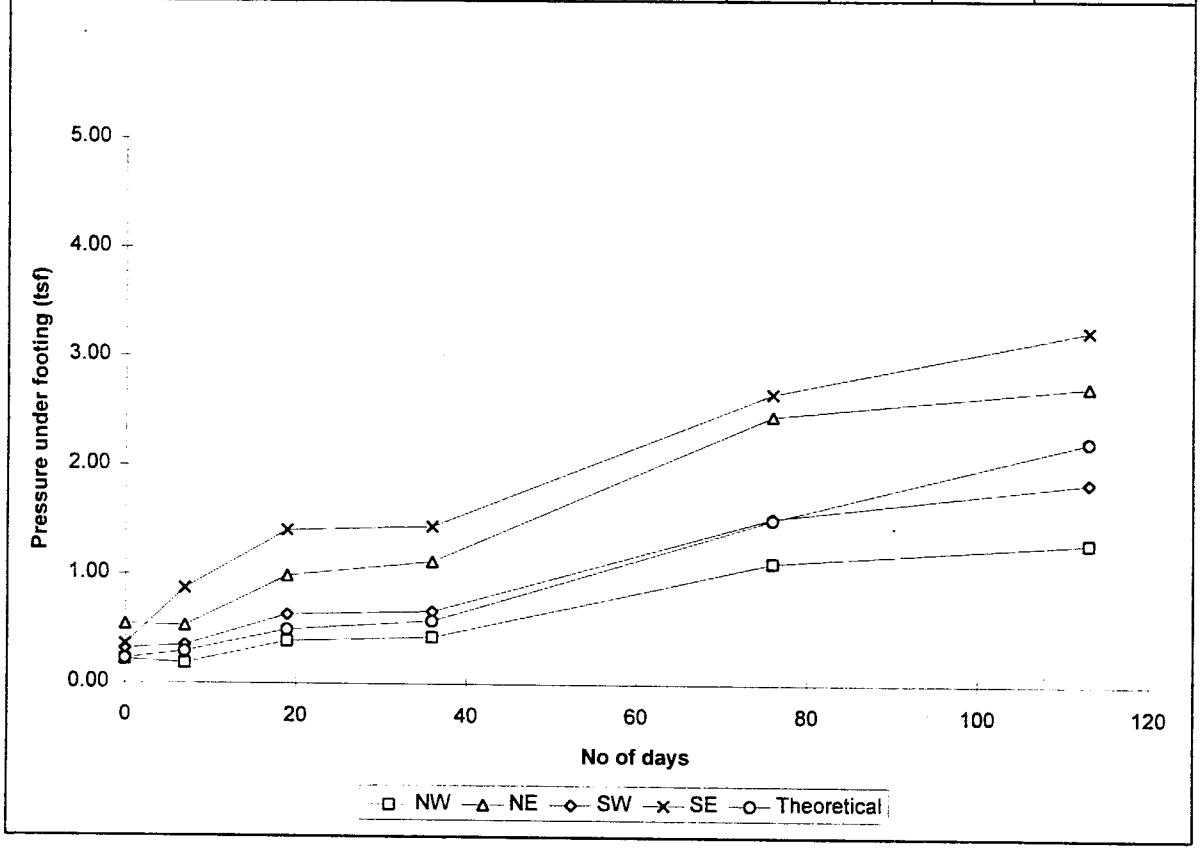

Figure B.55 Comparison Pressure data under Pier 1 - Phase I Foundation (Bridge E)

Date	No of days	Construction Stages	Pressure (tsf)				
			NE	NW	SE	SW	Theoretical
29-Mar	0	Footing (I)	0.26	0.34	0.32	0.31	0.30
26-Apr	28	Wall (I)	0.44	0.67	0.55		0.63
13-May	45	Backfilling over Footing (I)	0.46	0.69	0.55		0.86
22-Jun	85	Beam (I)	0.71	0.96	0.78	1.32	1.27
29-Jul	122	Deck and Parapet (I)	0.85	1.00	0.99	1.52	1.63

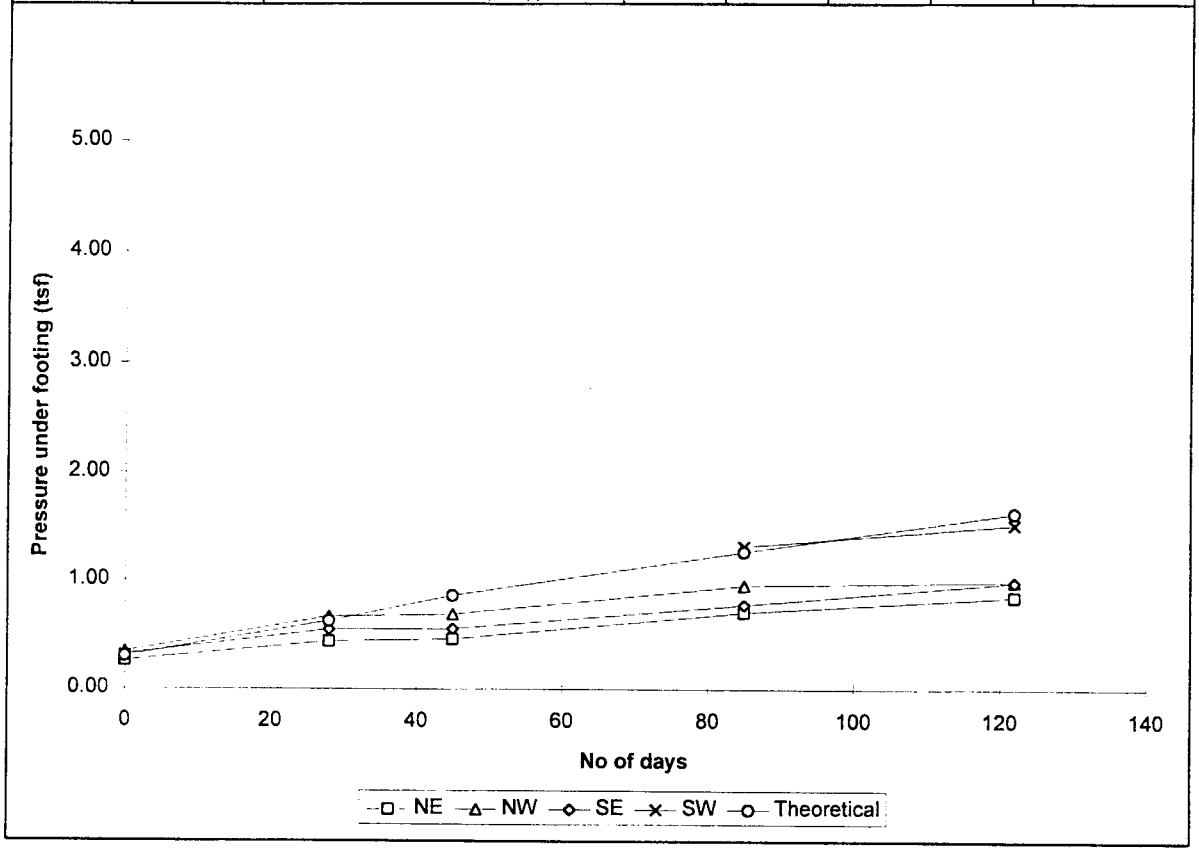

Figure B.56 Comparison Pressure data under Pier 3 - Phase I Foundation (Bridge E)

Date	No of days	Construction Stages	Pressure (tsf)		
			South	North	Theoretical
22-Mar	0	Footing (I)	0.48	0.46	0.23
7-Apr	16	Column (I)	0.52	0.59	0.30
26-Apr	35	Pier Cap, Backfilling over Footing (I)	0.74	0.82	0.55
12-Jul	112	Beam (I)	1.18	1.37	1.05
29-Jul	129	Deck and Parapet (I)	1.41	1.57	1.43

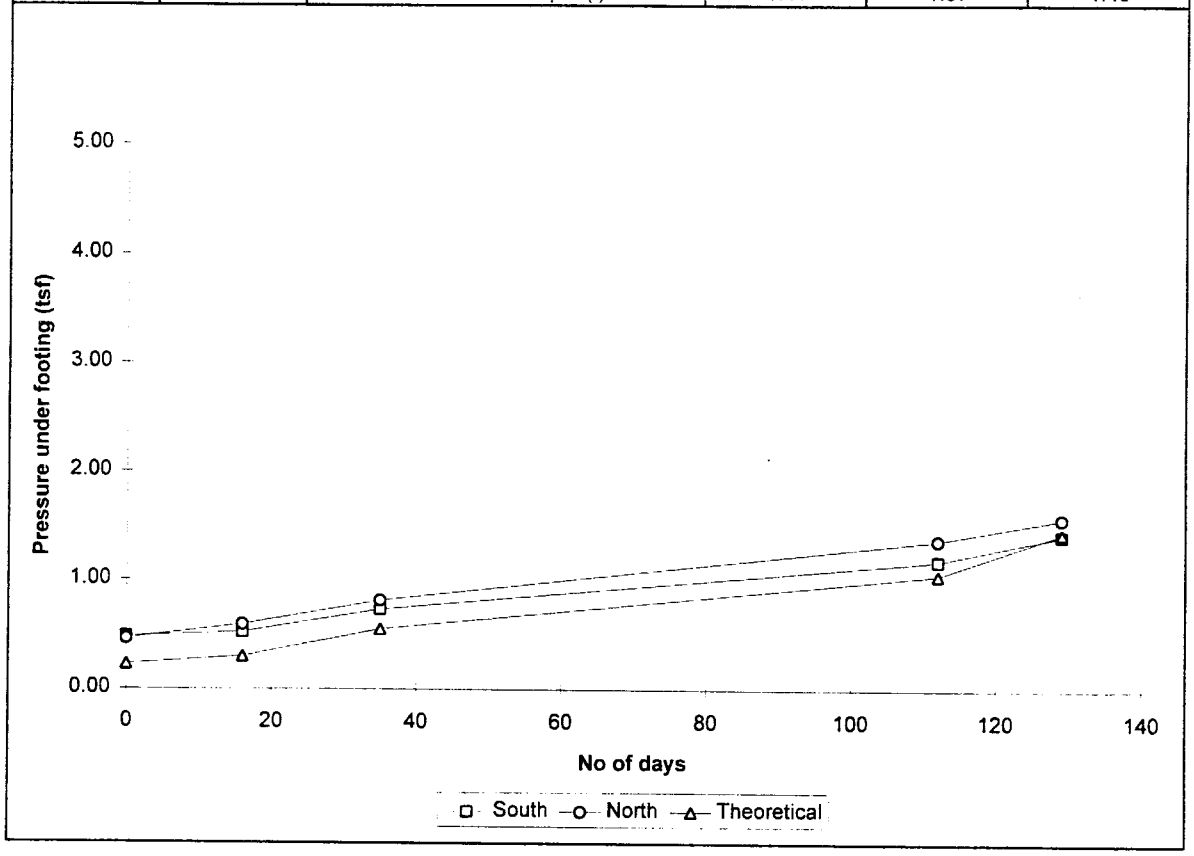

Figure B.57 Comparison Pressure data under Pier 6 - Phase I Foundation (Bridge E)

Date	No of days	Construction Stages	Pressure (tsf)				
			NW	SW	NE	SE	Theoretical
22-Mar	0	Footing, Column (I)	0.12	0.00	0.24	0.00	0.29
14-Apr	23	Pier Cap (I)	0.26	0.05	0.36	0.06	0.38
26-Apr	35	Backfilling over Footing (I)	0.26	0.01	0.45	0.02	0.57
12-Jul	112	Beam (I)	0.55		0.78	0.07	1.16
29-Jul	129	Deck and Parapet (I)	0.72	0.01	0.94	0.13	1.60

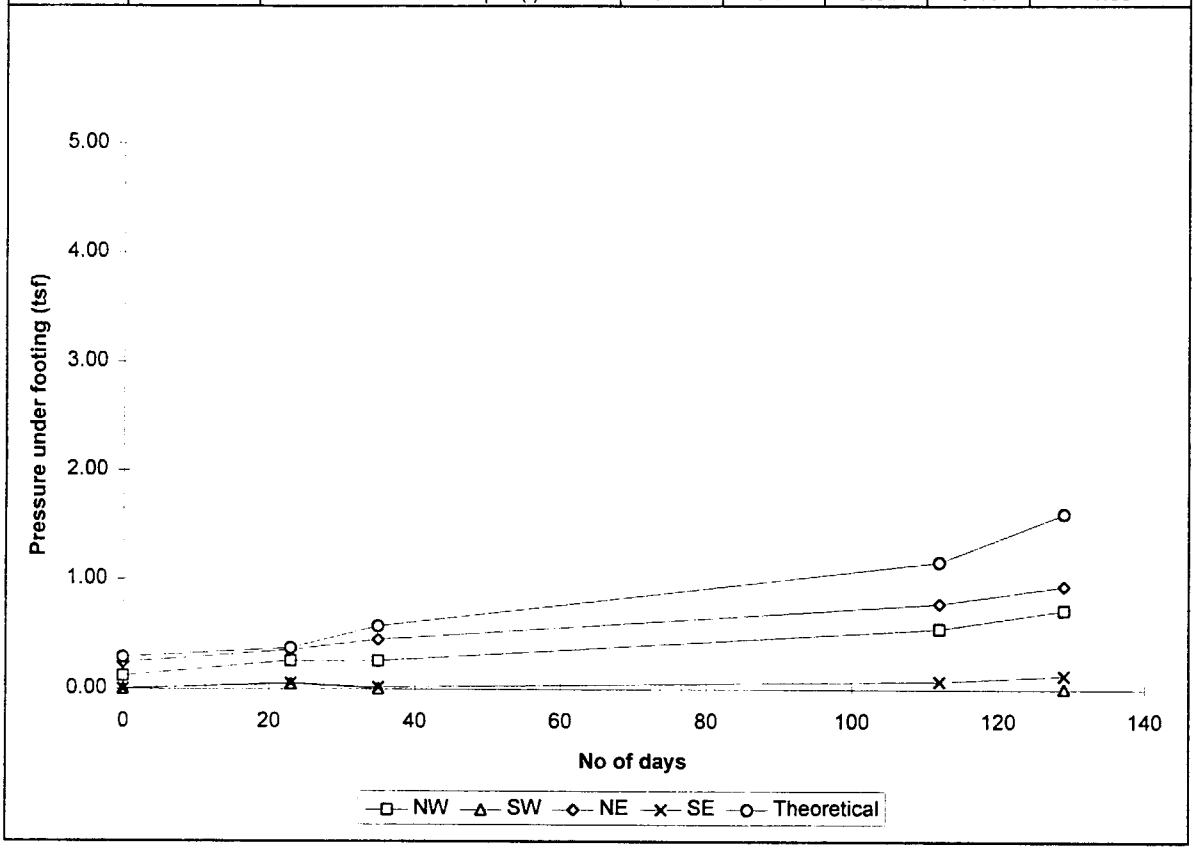

Figure B.58 Comparison Pressure data under Pier 8 - Phase I Foundation (Bridge E)

Date	No of days	Construction Stages	Pressure (tsf)					
			Field Data			Theoretical Data		
			Heel	Key	Toe	Heel	Key	Toe
22-Mar	0	Footing (I)	0.08	0.08	0.03	0.24	0.30	0.23
29-Mar	7	Wall (I)	0.08	0.03	0.04	0.44	0.46	0.48
22-Jun	92	Backfilling over Footing, Wall (I)	0.31	0.08	0.09	0.99	1.00	1.01
29-Jul	129	Beam, Deck and Parapet (I)	0.40	0.10	0.21	1.50	1.47	1.44

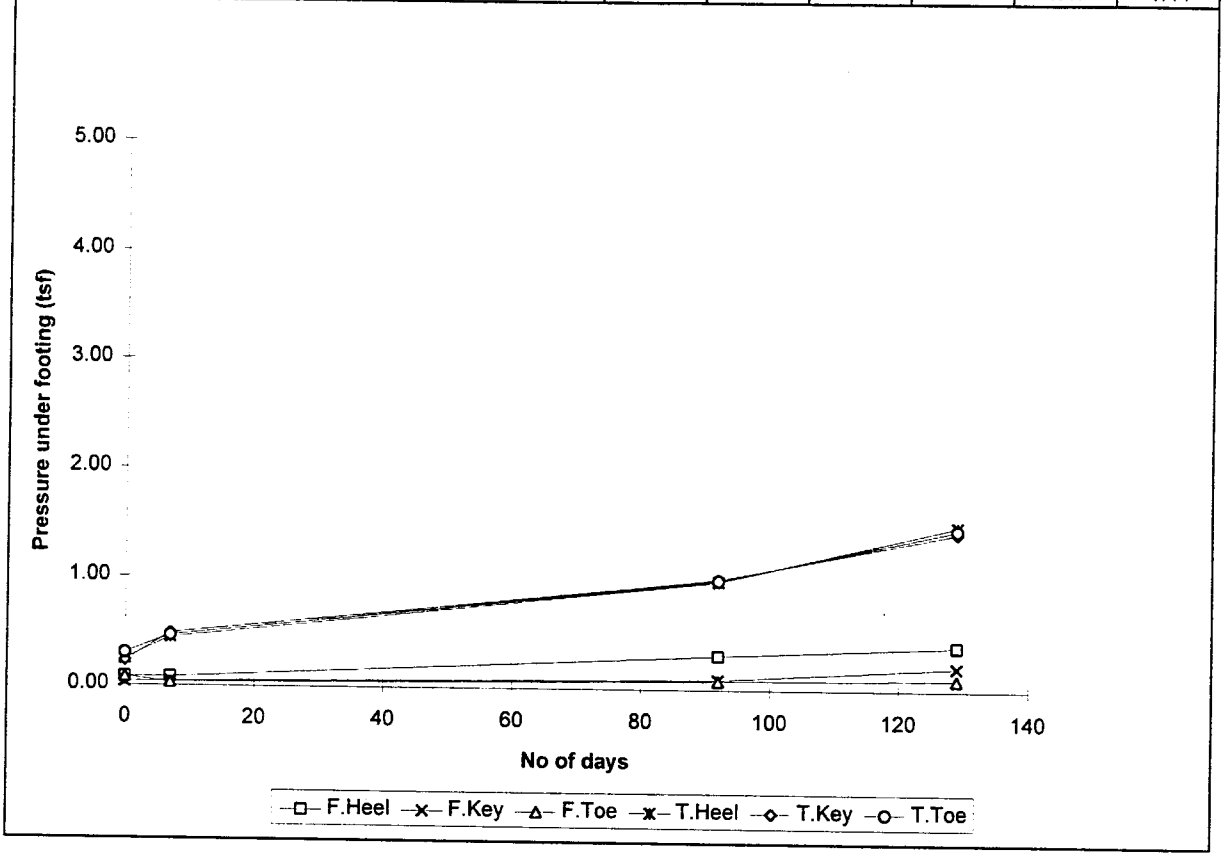

Figure B.59 Comparison Pressure under Forward Abutment - Phase I Foundation (Bridge E)

Date	No of days	Construction Stages	Tilting (degree)	
			Longitudinal Direction	
			Field	Theoretical
13-May	0	Footing, Wall (I)	0.0000	0.0000
24-May	11	Backfilling over Footing (I)	-0.0043	-0.0556
22-Jun	40	Beam (I)	0.0387	-0.0634
12-Aug	91	Deck and Parapet (I)	0.0645	-0.0695

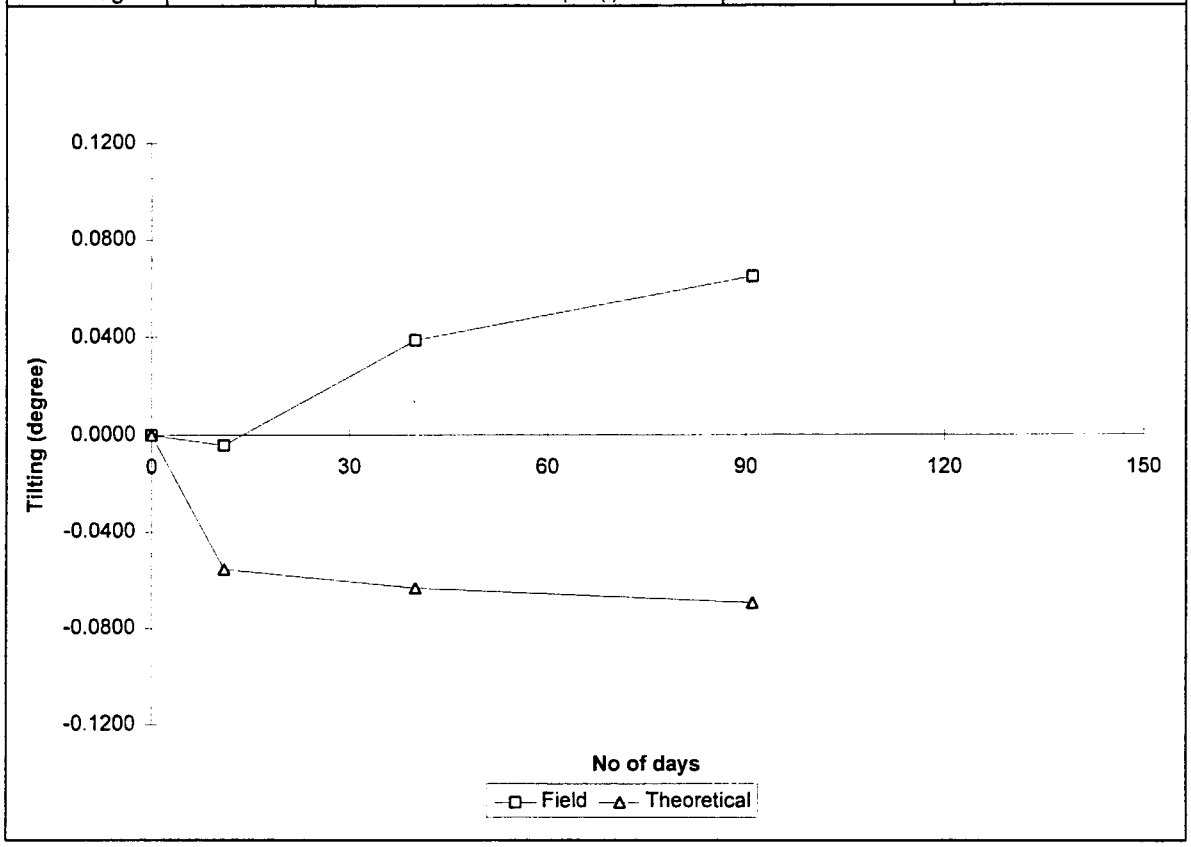

Figure B.60 Comparison Tilting data of Rear Abutment - Phase I (Bridge E)

Date	No of days	Construction Stages	Tilting (degree)		
			Longitudinal Direction		
			North	South	Theoretical
26-Apr	0	Footing, Column, Pier Cap (I)	0.0000	0.0000	0.0000
13-May	17	Backfilling over Footing (I)	-0.0057	-0.0201	0.0000
22-Jun	57	Beam (I)	-0.0172	-0.0294	-0.0003
12-Aug	108	Deck and Parapet (I)	-0.0229	-0.0329	-0.0002

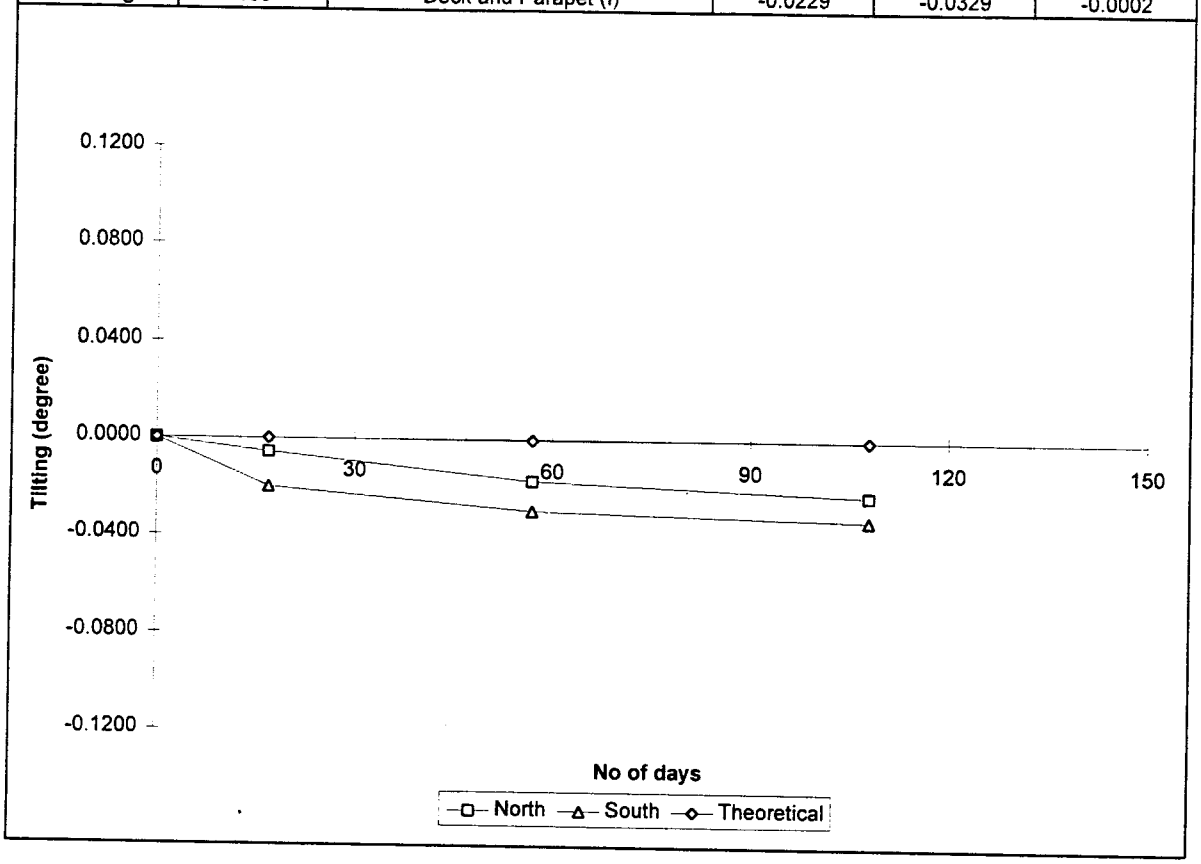

Figure B.61 Comparison Tilting data of Pier 1 - Phase I Columns (Bridge E)

Date	No of days	Construction Stages	Tilting (degree)	
			Longitudinal Direction	
			Field	Theoretical
26-Apr	0	Footing, Wall (I)	0.0000	0.0000
13-May	17	Backfilling over Footing (I)	0.0559	0.0000
22-Jun	57	Beam (I)	-0.0029	-0.0025
12-Aug	108	Deck and Parapet (I)	-0.0086	-0.0019

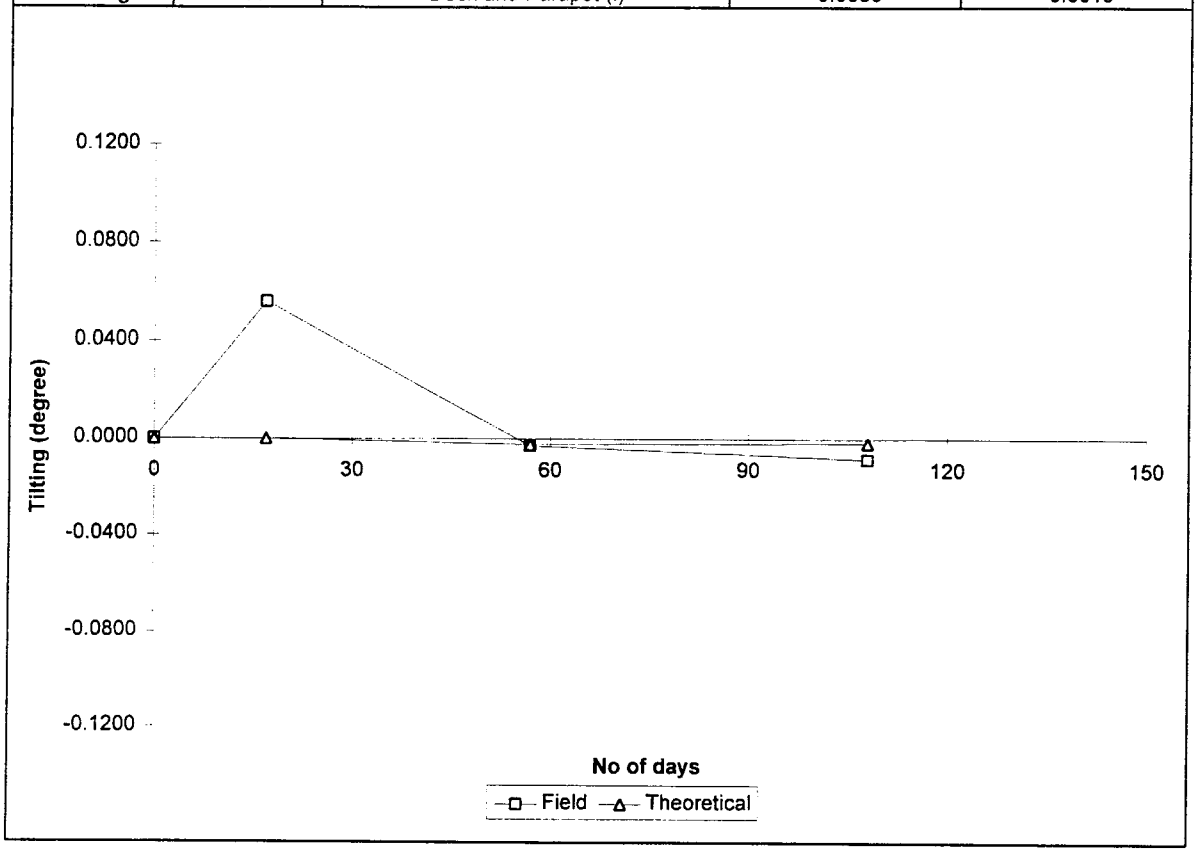

Figure B.62 Comparison Tilting data of Pier 3 - Phase I Columns (Bridge E)

Date	No of days	Construction Stages	Tilting (degree)		
			Longitudinal Direction		
			North	South	Theoretical
14-Apr	0	Footing, Column (I)	0.0000	0.0000	0.0000
26-Apr	12	Pier Cap, Backfilling over Footing (I)	0.0000	-0.0036	0.0000
12-Jul	89	Beam (I)	-0.0501	-0.0194	-0.0040
12-Aug	120	Deck and Parapet (I)	-0.0287	-0.0408	-0.0070

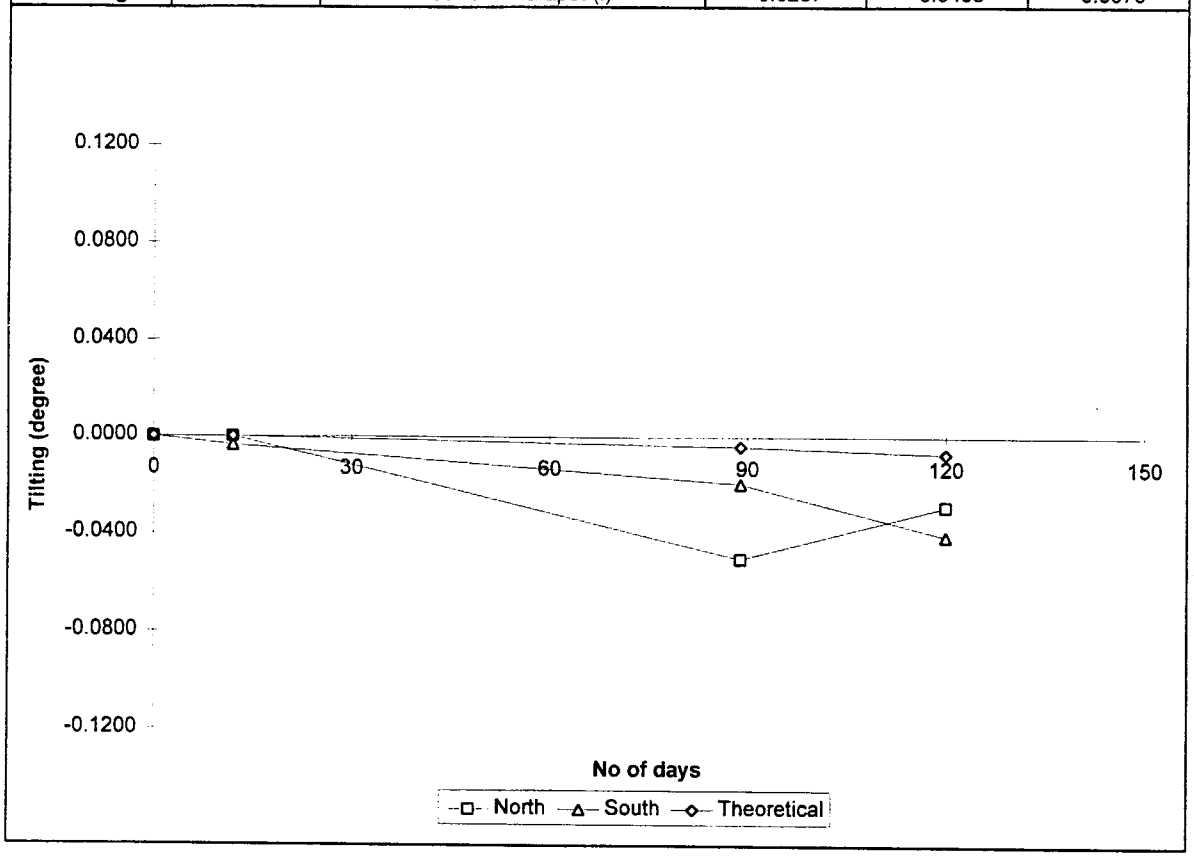

Figure B.63 Comparison Tilting data of Pier 6 - Phase I Columns (Bridge E)

Date	No of days	Construction Stages	Tilting (degree)		
			Longitudinal Direction		
			North	South	Theoretical
14-Apr	0	Footing, Column, Pier Cap (I)	0.0000	0.0000	0.0000
26-Apr	12	Backfilling over Footing (I)	0.0158	0.0122	0.0000
12-Jul	89	Beam (I)	0.0115	0.0000	0.0050
12-Aug	120	Deck and Parapet (I)	0.0129	-0.0222	0.0090

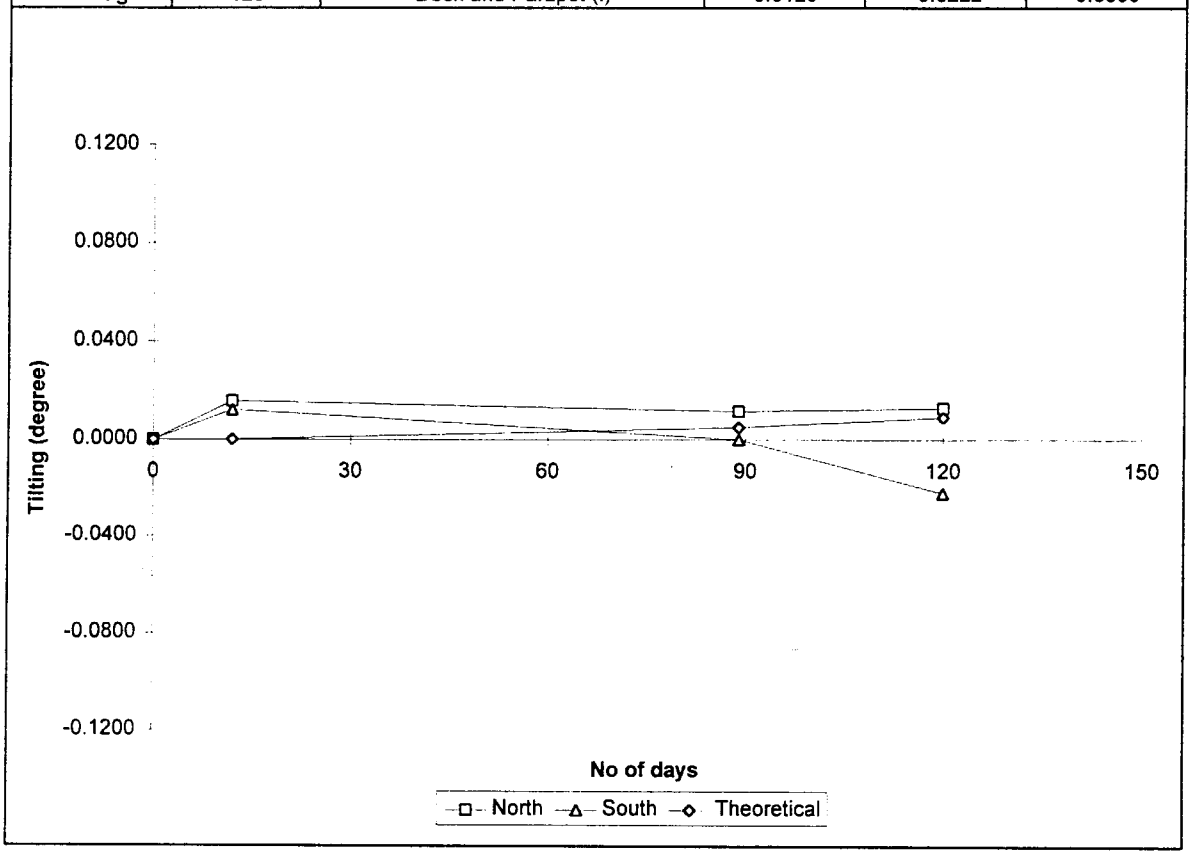

Figure B.64 Comparison Tilting data of Pier 8 - Phase I Columns (Bridge E)

Date	No of days	Construction Stages	Tilting (degree)	
			Longitudinal Direction	
			Field	Theoretical
14-Apr	0	Footing, Wall (I)	0.0000	0.0000
24-May	40	Backfilling over Footing (I)	0.0244	-0.0640
12-Jul	89	Beam (I)	0.0373	-0.0710
12-Aug	120	Deck and Parapet (I)	0.0279	-0.0790

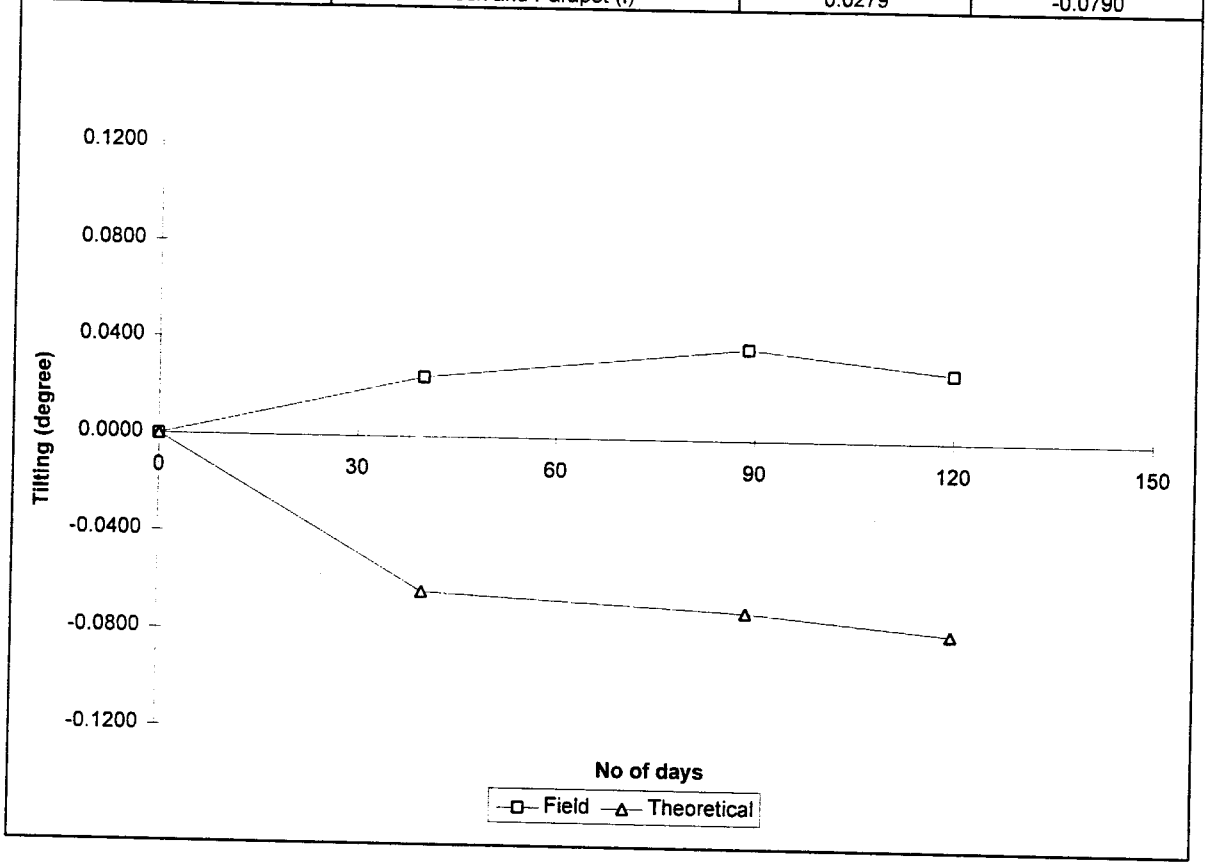

Figure B.65 Comparison Tilting data of Forward Abutment - Phase I (Bridge E)

Date	No of days	Construction Stages	Tilting (degree)	
			Longitudinal Direction	
			Field	Theoretical
2-Oct	0	Footing, Wall (II)	0.0000	0.0000
16-Oct	14	Backfilling over Footing (II)	-0.0150	-0.0556
6-Nov	35	Beam, Backfilling Wall (II)	0.0100	-0.0634
23-Mar	172	Deck and Parapet (II)	0.0179	-0.0695

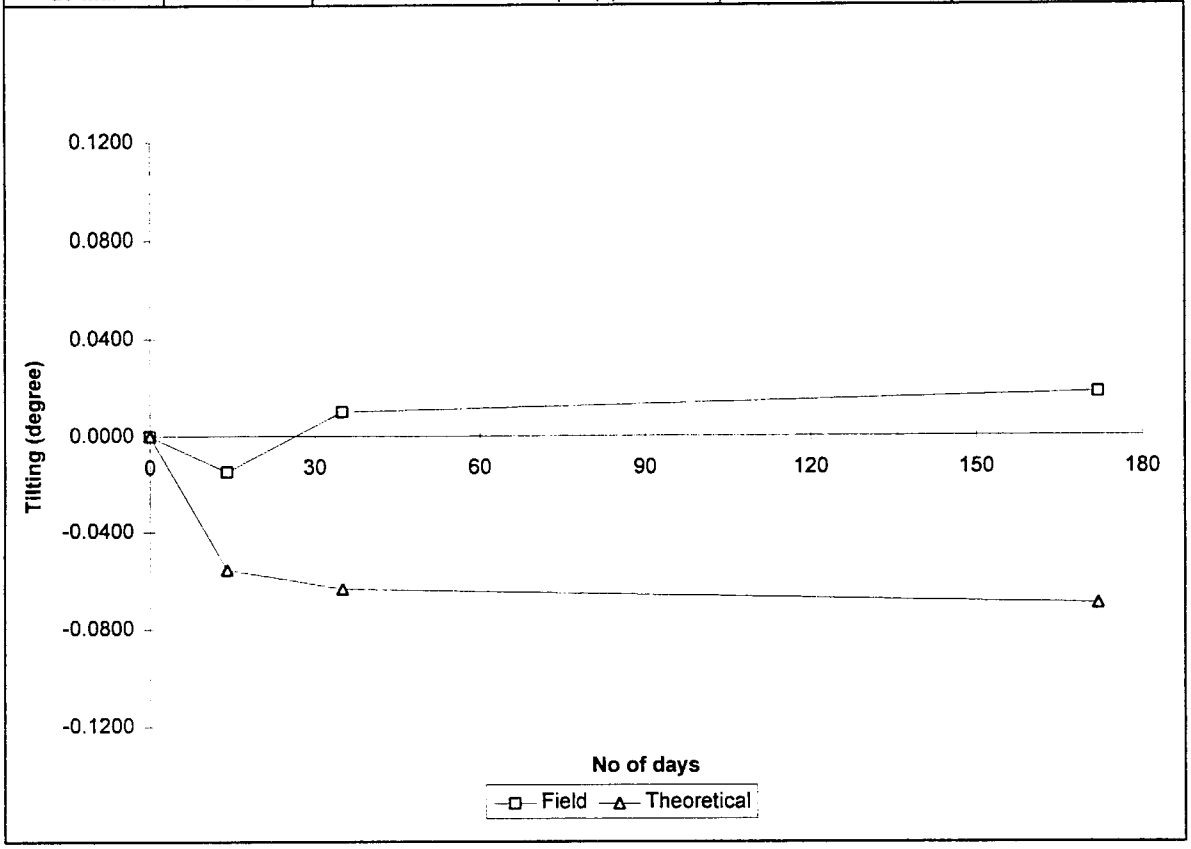

Figure B.66 Comparison Tilting data of Rear Abutment - Phase II (Bridge E)

Date	No of days	Construction Stages	Tilting (degree)	
			Longitudinal Direction	
			Field	Theoretical
2-Oct	0	Footing, Wall (II)	0.0000	0.0000
16-Oct	14	Beam, Backfilling over Footing (II)	-0.0745	-0.0710
23-Mar	172	Backfilling Wall, Deck and Parapet (II)	-0.1017	-0.0790

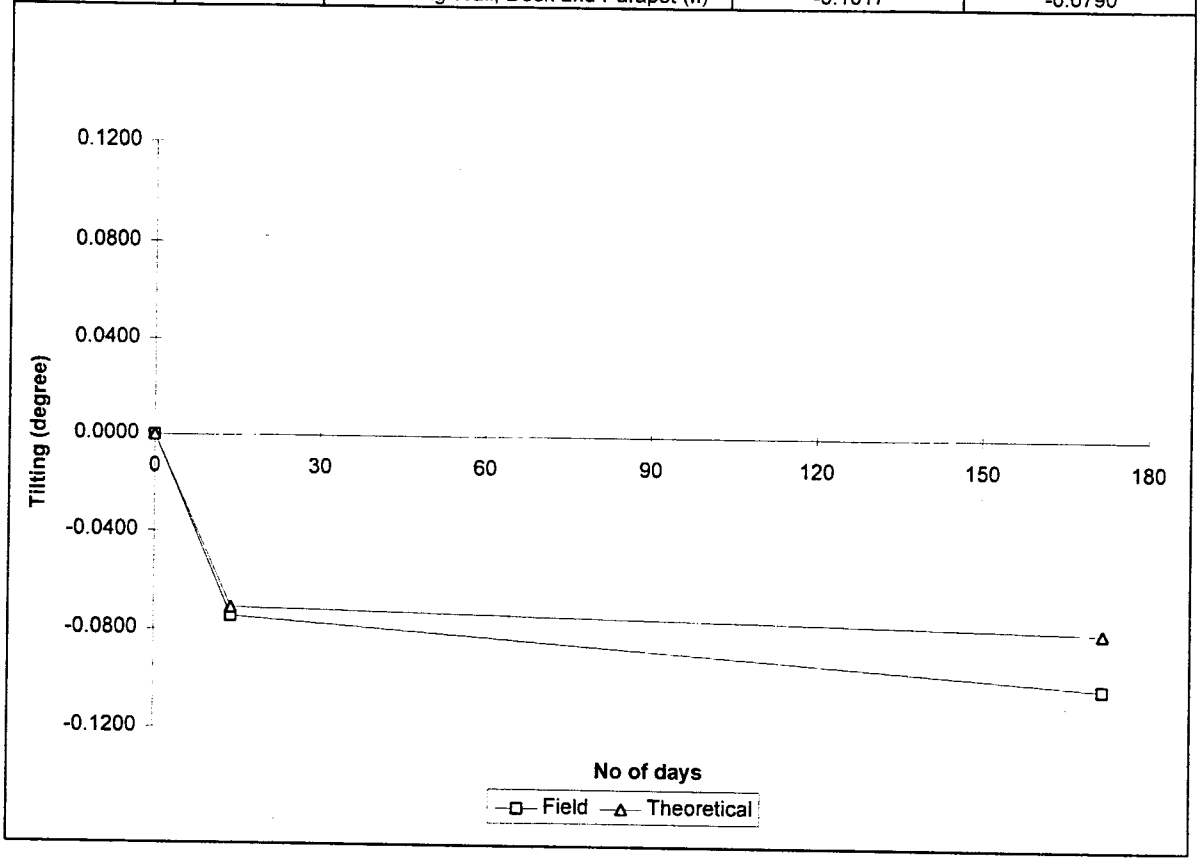

Figure B.67 Comparison Tilting data of Forward Abutment - Phase II (Bridge E)